TALYS-2.0

Simulation of nuclear reactions

Arjan Koning, Stephane Hilaire, Stephane Goriely

s

About the author

Arjan Koning is a nuclear physicist with a Masters Degree in Theoretical physics at the Univ. of Amsterdam, a PhD in the Natural Sciences on Multi-step direct reactions at the Univ. of Groningen, and a Professorship at the Univ. of Uppsala on theoretical nuclear reactions.

Arjan is currently Head of the Nuclear Data Section at the IAEA in Vienna. Before that, he has worked at ECN/NRG Petten, the Netherlands, on nuclear reaction data for science and technology, and as guest scientist at CEA/Bruyères-le-Châtel and Los Alamos National Laboratory on the development and computational implementation of nuclear reaction models. He has led several students to PhD degrees, has coordinated and chaired various international nuclear data projects such as the OECD/NEA JEFF and WPEC projects, and has advised governments and international organisations on nuclear research and development. Among his scientific accomplishments are innovations in nuclear reaction physics, especially for the optical model and pre-equilibrium reactions, the TALYS nuclear model code, Total Monte Carlo uncertainty propagation and the TENDL nuclear data library. As of 2024, his h-index is 58 with more than 23 000 citations.

Although Arjan is currently in a managerial role, he aims to keep his scientific creativity alive by maintaining and extending TALYS plus all products that emerge from that. Pleas from his friends to also spend time on other things are sometimes honoured.

Preface

TALYS is a nuclear reaction program with the objective to provide a complete and accurate simulation of nuclear reactions up to energies of 200 MeV, through an optimal combination of reliable nuclear models, flexibility and user-friendliness. TALYS can be used for the analysis of basic nuclear reaction experiments or to generate nuclear data for applications.

The idea to make TALYS was born in 1998, when I was visiting CEA Bruyères-le-Châtel and we decided to implement our combined knowledge of nuclear reactions into one single software package. Since then, virtually all TALYS development has taken place at NRG Petten, the Netherlands, CEA Bruyères-le-Châtel, France, University Libre, Brussels, and in recent years at the IAEA in Vienna.

After 20 years, thousands of users, and more than 6000 publications in which TALYS is used, I found it time to produce an entirely new version of the code, rewritten in Fortran-95. At the same time, this entirely new tutorial is made available, with a more logical structure than the old TALYS manual.

Like most scientific projects, TALYS is always under development. Nevertheless, at certain moments in time, we freeze a well-defined version of TALYS and subject it to extensive verification and validation procedures. You are now reading the tutorial which applies to both TALYS-1.97, the last version in the row of TALYS-1.xx codes, and version 2.0, which employs more modern Fortran specifications. The plan is to only continue development of the TALYS-2 series after this release.

This part of my work I consider as truly open source: I try to minimize the difference between what I know and what I provide to others. At the start of my career, that meant releasing all knowledge in publications. Nowadays, that means releasing all knowledge in publications and in software, if possible quality-assured, retraceable and user-friendly. I aim to do that and I have spent a significant amount of my available time recycling software of myself and others, and the tutorial, to produce something that is hopefully sustainable.

As a PhD student, and also later, I worked myself through theory books of authors like my professor Hans Weidenmüller, Peter Hodgson (who pushed my early career) and Ray Satchler and

I wondered whether I would once be in the position to write a similar book. It did not happen, other priorities prevailed and being employed for my whole career by research and international organisations instead of a university did not help either (for that particular book that is, for the rest I don't complain). Still, one could read this tutorial as a sort of modern nuclear physics "book". Many essential nuclear models will be discussed, with the extra feature (compared to old-style text books) that they are all accompanied with TALYS sample cases and illustrations.

License, contact and reference

As mentioned on the first page and in the source code, TALYS falls in the category of MIT License software.

In addition to the MIT *terms* I have a *request*:

- When TALYS is used for your reports, publications, etc., please make a proper reference to the code. At the moment this is:
  A.J. Koning, S. Hilaire, S. Goriely, *TALYS: modeling of nuclear reactions*, Eur. Phys. J. A 59, 131 (2023). https://doi.org/10.1140/epja/s10050-023-01034-3
- The webpage for TALYS is **nds.iaea.org/talys**.

Acknowledgements

Contents

III   **Part Three: Reference Guide**

IV	Part Four: Miscellaneous

Part One: TALYS General

1. Introduction

TALYS is a computer program for the analysis and prediction of nuclear reactions. The basic objective behind its construction is the simulation of nuclear reactions that involve neutrons, photons, protons, deuterons, tritons, ^{3}He- and alpha-particles, in the eV - 200 MeV energy range and for target nuclides of mass 12 and heavier. To achieve this, we have implemented a suite of nuclear reaction models into a single code system. This enables us to evaluate nuclear reactions from the resonance range up to intermediate energies.

There are two main purposes of TALYS, which are strongly connected. First, it is a *nuclear physics* tool that can be used for the analysis of nuclear reaction experiments. The interplay between experiment and theory gives us insight in the fundamental interaction between particles and nuclei, and precise measurements enable us to constrain our models. In return, when the resulting nuclear models are believed to have sufficient predictive power, they can give an indication of the reliability of measurements. The many sample cases we present throughout this tutorial confirm that this software project would be nowhere without the existing (and future) experimental database.

After the nuclear physics stage comes the second function of TALYS, namely as a *nuclear data* tool: Either in a default mode, when no measurements are available, or after fine-tuning the adjustable parameters of the various reaction models using available experimental data, TALYS can *generate* nuclear data for all open reaction channels, on a user-defined energy and angle grid. The nuclear data libraries that are constructed with these calculated and experimental results provide essential information for existing and new nuclear technologies. Important applications that rely directly or indirectly on data generated by nuclear reaction simulation codes like TALYS are: conventional and innovative nuclear power reactors, transmutation of radioactive waste, fusion reactors, accelerator applications, homeland security, medical isotope production, radiotherapy, single-event upsets in microprocessors, oil-well logging, geophysics and astrophysics.

In its first decade, the development of TALYS used to follow the "first completeness, then quality" principle. With this, we certainly never suggested that we use toy models to arrive at some quick and dirty results since several reaction mechanisms coded in TALYS are based on theoretical

models whose implementation is only possible with the current-day computer power. It rather means that, in our quest for completeness, we try to divide our effort equally among all nuclear reaction types. The precise description of *all* possible reaction channels in a single calculational scheme is such an enormous task that we have chosen, to put it bluntly, not to devote several years to the theoretical research and absolutely perfect implementation of one particular reaction channel which accounts for only a few millibarns of the total reaction cross section. Instead, we aim to enhance the quality of TALYS equally over the whole reaction range and always search for the largest shortcoming that remains after the last improvement. We now think that "completeness and quality" has been accomplished for several important parts of the program. The reward of this approach is that with TALYS we can cover the whole path from fundamental nuclear reaction models to the creation of complete data libraries for nuclear applications, with the obvious side note that the implemented nuclear models will always need to be upgraded using better physics. An additional long-term aim is full transparency of the implemented nuclear models, in other words, an *understandable* source program, and a modular coding structure.

The idea to construct a computer program that gives a simultaneous prediction of many nuclear reaction channels, rather than a very detailed description of only one or a few reaction channels, is not new. Well-known examples of all-in-one codes from the past century are GNASH [1], ALICE [2], STAPRE [3], and EMPIRE [4]. They have been, and are still, extensively used, not only for academical purposes but also for the creation of the nuclear data libraries that exist around the world. EMPIRE is still maintained and extended by the original authors, whereas various local versions of GNASH, ALICE and STAPRE exist around the world, all with different extensions and improvements. TALYS is newer in the sense that it has been written completely from scratch in the 21st century (with the exception of one very essential module, the coupled-channels code ECIS), using a consistent set of programming procedures.

As specific features of the TALYS package we mention

- In general, an exact implementation of many of the latest nuclear models for direct, compound, pre-equilibrium and fission reactions.
- A continuous, smooth description of reaction mechanisms over a wide energy and mass range. A safe statement is that these limits are 0.001- 200 MeV and $12 < A < 339$, but it is formally possible to go beyond that.
- Completely integrated optical model and coupled-channels calculations by the ECIS-06 code [5].
- Incorporation of recent optical model parameterisations for many nuclei, both phenomenological (optionally including dispersion relations) and microscopical.
- Total and partial cross sections, energy spectra, angular distributions, double-differential spectra and recoils.
- Discrete and continuum photon production cross sections.
- Excitation functions for residual nuclide production, including isomeric cross sections.
- An exact modeling of exclusive channel cross sections, e.g. $(n, 2np)$, spectra, and recoils.
- Automatic reference to nuclear structure parameters as masses, discrete levels, resonances, level density parameters, deformation parameters, fission barrier and gamma-ray parameters, generally from the IAEA Reference Input Parameter Library [6].
- Various width fluctuation models for binary compound reactions and, at higher energies, multiple Hauser-Feshbach emission until all reaction channels are closed.
- Various phenomenological and microscopic level density models.
- Various fission models to predict cross sections and fission fragment and product yields, neutron multiplicities and prompt fission neutron and gamma spectra.
- Models for pre-equilibrium reactions, and multiple pre-equilibrium reactions up to any order.
- Generation of parameters for the unresolved resonance range.

- Reconstruction of resonance range into pointwise cross sections using tabulated resonance parameters.
- Astrophysical reaction rates using Maxwellian averaging.
- Option to start with an excitation energy distribution instead of a projectile-target combination, helpful for coupling TALYS with intranuclear cascade codes or fission fragment studies.
- Use of systematics if an adequate theory for a particular reaction mechanism is not yet available or implemented, or simply as a predictive alternative for more physical nuclear models.
- Medical isotope production yields as a function of accelerator energy and beam current.
- Output files for automatic generation of nuclear data in ENDF-6 format using the TEFAL program.
- Flexible input and output to enable automatic optimization to experimental data and generation of covariance data by the TASMAN program.
- A transparent source program.
- Input/output communication that is easy to use and understand.
- An extensive tutorial.
- A large collection of sample cases.

The central message is that we always provide a complete set of answers for a nuclear reaction, for all open channels and all associated cross sections, spectra, angular distributions, etc. It depends on the current status of nuclear reaction theory, and our ability to implement that theory, whether these answers are generated by sophisticated physical methods or by a simpler empirical approach. With TALYS, a complete set of cross sections can already be obtained with minimal effort, through a four-line input file of the type:

```
projectile  n
element     Fe
mass        56
energy      14.
```

which, if you are only interested in reasonably good answers for the most important quantities, will give you all you need. If you want to be more specific on nuclear models, their parameters and the level of output, you simply add some of the close to 400 keywords that can be specified in TALYS. We thus do not ask you to understand the precise meaning of all these keywords: you can make your input file as simple or as complicated as you want. Let us immediately stress that we realize the danger of this approach. This ease of use may give the obviously false impression that one gets a *good* description of *all* the reaction channels, with minimum reaction specification, as if we would have solved virtually all nuclear reaction problems (in which case we would have been famous). Unfortunately, nuclear physics is not that simple. Clearly, many types of nuclear reactions are very difficult to model properly and can not be expected to be covered by simple default values. Moreover, other nuclear reaction codes may outperform TALYS on particular tasks because they were specifically designed for one or a few reaction channels. In this light, the sample cases spread out over this tutorial are very important, as it contains many sample cases which should give the user an idea of what TALYS can do. We wish to mention that the above sketched method for handling input files was born out of frustration: We have encountered too many computer codes containing an implementation of beautiful physics, but with an unnecessary high threshold to use the code (if you could compile and run it at all), since its input files are supposed to consist of a large collection of mixed, and correlated, integer and real values, for which values *must* be given, forcing the user to first read the entire manual, which often does not exist.

1.1 What TALYS can not do

It maybe helpful to already restrict any extreme expectations in this Introduction. Yes, there are several important things in nuclear physics and nuclear data which TALYS can not handle. If TALYS can not do it, then either we have developed other software to take care of it, or it falls outside the scope of the physics included in TALYS, and software by other people should be used. Some of the restrictions of TALYS are the following

- The heaviest particle is an alpha-particle. Hence, TALYS is not (yet) a heavy-ion code.
- TALYS does not produce complete nuclear data libraries for technological applications. Another software package, TEFAL, which processes the output of TALYS, takes care of that.
- TALYS only provides the central values for a prediction. Full uncertainty quantification, based on random input parameter variation and leading to complete covariance matrices and more general probability distributions for all the output of TALYS, is handled by a program called TASMAN.
- Resonance reactions are not modeled. This is the domain of R-matrix theory and its more or less approximate versions and is handled by codes like SAMMY, REFIT or CONRAD. TALYS does however reconstruct cross sections from resonance parameters.
- Light-nuclide physics, as implemented in R-matrix codes. TALYS is in essence a statistical model code, and that statistics starts to break down for systems with less than 20 nucleons.
- In terms of a complete nuclear reaction output, what is missing is a high-quality prediction of the average number of fission neutrons and the prompt fission neutron spectra. For this, separate codes, TAFIS and TANES, respectively, are available.
- An explicit microscopic treatment of stripping and pick-up mechanism for e.g. (d,p) reactions is not included. There are a few codes, like FRESCO and DEUTACS, which handle that.

1.2 From TALYS-1.96 to TALYS-1.97/TALYS-2.0

Until now, a new official version of TALYS is released every 2 years. For some users, it may be useful to see what has been added to the code since the last release. In Part IV the entire development of TALYS is summarized.

On December 30, 2021 the eight official version of the code, TALYS-1.96, was released. Since then, the code has undergone changes that fall in the usual two categories: significant extensions and corrections that may affect a large part of the user community, and several small bug fixes. As appendix to this tutorial, we add the full log file of changes since the release of TALYS-1.96. Here we list the most important updates:

- The option to read in tables with optimal parameters for several reaction channels. Using the **fit y** keyword one obtains a description of experimental data as good as an automated optimization procedure (with TASMAN) gives. Results are often, but not always, good.
- All separate output files of TALYS are now in YANDF format (Yet Another Nuclear Data Format) as detailed in an appendix in this tutorial. This means that every output file a reaction is completely described by the metadata at the top of the file, allowing more automated processing of TALYS results.
- We added the possibility to have particle decay from a discrete level. For some strange reason, this was never enabled in TALYS: discrete levels could only decay by gamma's. Now, if the energy of the discrete level is above the minimum separation energy (often neutron, proton of alpha) a Hauser-Feshbach calculation is invoked.
- Further refinement of the evaporation of excited fission fragments, per fragment pair, after

which TALYS calculated the fission product yield as well as all neutron observables such as nu(A), nubar, PFNS etc. Currently, three models for excited fission fragments are included: HF3D, GEF, SPY and 4D-Langevin.

For TALYS-1.97/2.0 the following new keywords were introduced: **fit**, see page 365, **ngfit**, see page 366, **nffit**, see page 367, **nnfit**, see page 368, **nafit**, see page 369, **pnfit**, see page 375, **dnfit**, see page 373, **anfit**, see page 372, **gnfit**, see page 374, **macsfit**, see page 370, **gamgamfit**, see page 371, **ftableadjust**, see page 446, **Cbarrier**, see page 643, **Risomer**, see page 361, **Rspincutpreeq**, see page 597, **WFCfactor**, see page 580, **equispec**, see page 328, **densfile**, see page 404, **outall**, see page 693, **source**, see page 342, **user**, see page 341, **format**, see page 343, while the possibilities of **rotational**, see page 543, **Cfermi**, see page 421, **Ufermi**, see page 422, **gnorm**, see page 429, were changed or extended.

1.3 How to use this tutorial

Although we would be honored if you would read this tutorial from the beginning to the end, we can imagine that not all parts are necessary, relevant or suitable to you, so here is a short overview.

1. Part I: TALYS general. This gives a global introduction of TALYS, including
    Chapter 2: Installation guide.
    Chapter 3: The general rules for the input file.
    Chapter 4: A general discussion of nuclear reactions and the types of observables that can be obtained.
    Chapter 5: A description of the various nuclear structure parameters that are used.
2. Part II: TALYS nuclear models for nuclear structure and reactions. This covers
    Chapter 6: Nuclear masses and deformations
    Chapter 7: Discrete levels
    Chapter 8: Level densities
    Chapter 9: Reactions involving photons
    Chapter 10: Optical model
    Chapter 11: Direct reactions
    Chapter 12: Pre-equilibrium reactions
    Chapter 13: Compound reactions
    Chapter 14: Multiple emission
    Chapter 15: Fission
    Chapter 16: Thermal reactions
    Chapter 17: Populated initial nucleus
    Chapter 18: Astrophysical reaction rates
    Chapter 19: Medical isotope production
    Chapter 20: Verification and validation, sample cases and output
3. Part III: Reference Guide. A description of all keywords
4. Part IV: Miscellaneous items, like the historical development of TALYS, outlook and the bibliography.

2. Installation and getting started

2.1 The TALYS package

In what follows we assume TALYS will be installed on a Linux or MacOS operating system. The total TALYS package is in the *talys/* directory and contains the following directories and files:

- *LICENSE* is the license file,
- *README.md* outlines the contents of the package,
- *code_build* and *path_change* are scripts that take care of the installation,
- *source/* contains the source code of TALYS: Fortran subroutines,
- *structure/* contains the nuclear structure database in various subdirectories. See Chapter 5 for more information,
- *doc/* contains the documentation: this manual in pdf format and the description of ECIS-06.
- *samples/* contains the input and output files of the sample cases.

In total, you will need about 6 Gb of free disk space to install TALYS. This rather large amount of memory is almost completely due to microscopic level density, radial density, gamma and fission tables in the nuclear structure database. The code has so far been tested by us on various Unix/Linux systems, so we can not guarantee that it works on all operating systems, although we know that some users have easily installed TALYS under Windows. The only machine dependencies we can think of are the directory separators '/' we use in pathnames that are hardwired in the code. If there is any dependence on the operating system, the associated statements can be altered in the subroutine *machine.f*. Also, the output of the execution time in *timer.f* may be machine dependent. The rest of the code should work on any computer.

TALYS has been tested for the gfortran and Intel compilers.

2.2 Installation

The installation of TALYS is straightforward. You can download TALYS via either git

- **git clone https://github.com/arjankoning1/talys.git**

or by getting the tar file

- from **https://nds,iaea.org/talys/talys.tar**
- **tar zxf talys.tar**

We here provide the necessary steps to do the installation, For a Unix/Linux/MacOs system, the installation is expected to be handled by the *code_build* script, as follows

- edit *code_build* and set the first two variables if necessary: the name of your compiler and its flags.
- **code_build talys**

An alternative installation option is

- **cd talys/source**
- **make**

If this does not work for some reason, we here provide the necessary steps to do the installation manually. For a Unix/Linux or MacOs system, the following steps should be taken:

- **cd talys/source**
- Ensure that TALYS can read the nuclear structure database. This is done in subroutine *machine.f*. If *code_build* has not already replaced the path name in *machine.f90*, do it yourself. We think this is the only machine dependence of TALYS. Apart from a few trivial warning messages for *ecis06t.f*, we expect no complaints from the compiler.
- **gfortran -c *.f *.f90**
- **gfortran *.o -o talys**
- **mv talys ../bin**

The above commands represent the standard compilation options. Consult the manual of your compiler to get an enhanced performance with optimization flags enabled. The only restriction for compilation is that *ecis06t.f* should *not* be compiled in double precision.

2.3   Verification

If TALYS is installed, testing the sample cases is the logical next step. The *samples/* directory contains the script *verify* that runs all the test cases. Each sample case has its own subdirectory, which contains a subdirectory *org/*, where we stored the input files and **our** calculated results, obtained with the gfortran compiler on MacOs Catalina. It also contains a subdirectory *new/*, where we have stored the input files only and where the *verify* script will produce **your** output files. A full description of the keywords used in the input files is given in Part III. The sample cases are scattered over this tutorial. Note that in each subdirectory a file with differences with our original output is created.

Should you encounter error messages upon running TALYS, like *'killed'* or *'segmentation fault'*, then probably the memory of your processor is not large enough. In the TALYS-1.9xx version, edit *talys.cmb* and reduce the value of **memorypar**. In TALYS-2 edit *A0_talys_mod* for this.

2.4   Getting started

If you have created your own working directory with an input file named e.g. *talys.inp*, then a TALYS calculation can easily be started with:

talys < talys.inp > talys.out

where the names *talys.inp* and *talys.out* are not obligatory: you can use any name for these files.

2.5 Other material: Lecture videos and TALYSworld

We will try to keep track of useful collections of educational material for TALYS. In October 2023, a one-week TALYS course was held at ICTP Trieste, which was entirely video recorded. At https://indico.ictp.it/event/10221/other-view?view=ictptimetable you will find lectures about the models implemented in TALYS, the relation to nuclear reaction measurements and a primary on the installation of the code.

For basic use, you do not even need to install TALYS. Marco Verpelli and I have created a GUI at IAEA, which we called TALYSworld, that enables to run TALYS online. All keywords can be specified and after hitting the 'Run' button a direct comparison with experimental cross sections for all reaction channels becomes available on your screen. This tool can be found at

https://nds.iaea.org/relnsd/talys/talys.html

3. Input description

For people who want to go straight to work and will not wait for sample cases later in this tutorial, we give the most important input rules here. For the communication between TALYS and its users, we have constructed an input/output method which shields beginners from all the possible options for nuclear model parameters that can be specified in TALYS, while enabling at the same time maximal flexibility for experienced users.

An input file of TALYS consists of keywords and their associated values. We have devoted the entire part III of this tutorial to the input possibilities with the Reference Guide, but let us illustrate the use of the input by the following example. It represents a minimum input file for TALYS:

```
projectile n
element    al
mass       27
energy     14.
```

This input file represents the simplest question that can be asked to TALYS: if a ^{27}Al nucleus is hit by 14 MeV neutrons, what happens? Behind this simple input file, however, there are more than a few hundred default values for the various nuclear models, parameters, output flags, etc., that you may or may not be interested in. When you use a minimal input file like the one above, you leave it to the authors of TALYS to choose all the parameters and models for you, as well as the level of detail of the output file. If you want to use specific nuclear models other than the default, adjust parameters or want to have more specific information in the output file(s), more keywords are required. Obviously, more keywords means more flexibility and, in the case of adequate use, better results, though often at the expense of increasing the level of phenomenology. In this Chapter, we will give the basic rules that must be obeyed when constructing an input file for TALYS, while part III specifies all the keywords, which have been categorised in several groups.

3.1 Basic input rules

Theoretically, it would be possible to make the use of TALYS completely idiot-proof, i.e. to prevent the user from any input mistakes that possibly can be made and to continue a calculation with "assumed" values after a typo or incomplete information. Although we have invested a relatively large effort in the user-friendliness of TALYS, we have not taken such safety measures to the extreme limit and ask at least some minimal responsibility from the user. Once you have accepted that, only very little effort is required to work with the program. Successful execution of TALYS can be expected if you remember the following simple rules and possibilities of the input file:

1. One input line contains one keyword. Usually it is accompanied by only one value, as in the simple example given above, but some keywords for model parameters need to be accompanied by indices (usually Z and A) on the same line.
2. A keyword and its value(s) *must* be separated by at least 1 blank character.
3. The keywords can be given in arbitrary order. If, by mistake, you use the same keyword more than once in an input file, the value of the last one in the input file will be adopted. This does not of course hold for keywords which are labeled with different Z and A indices, see the beginning of Section 35.
4. All characters can be given in either lowercase or uppercase.
5. A keyword *must* be accompanied by a value. (There is one exception, the **rotational** keyword). To use default values, the keywords should simply be left out of the input file.
6. An input line starting with a # in column 1 is neglected by TALYS. This is helpful for including comments in the input file or to temporarily deactivate keywords.
7. A minimal input file always consists of 4 lines and contains the keywords **projectile**, **element**, **mass** and **energy**. These 4 keywords *must* be given in any input file.

As an example of rules 2, 3, 4 and 6, it can be seen that the following input file is completely equivalent to the one given in the beginning of this Chapter:

```
# Equivalent input file
energy               14.
projectile n
mass 27
Element AL
#outbasic y
```

In the following erroneous input file, only the first 2 lines are correct, while rules 2 and 5 are violated in the other lines.

```
 projectile n
element al
mass27
energy
```

In cases like this, the execution will be stopped and TALYS will give an appropriate error message for the first encountered problem. We like to believe that we have covered all such cases and that it is impossible to let TALYS crash (at least with our compilers, see also Chapter 20), but you are of course invited to prove and let us know about the contrary (Sorry, no cash rewards). Typing errors in the input file will be spotted by TALYS, e.g. if you write **projjectile n**, it will tell you the keyword is not in our list.

3.2 Basic input

The four-line input file given above was an example of a minimum input file for TALYS. In general, you probably want to be more specific, as in the following example:

```
projectile   n
element      nb
mass         93
energy       energies
Ltarget      1
relativistic n
widthmode    2
outinverse   y
a 41 93 13.115
a 41 94 13.421
```

which will simulate the reaction of a neutron incident on ^{93}Nb, for a number of incident energies given in the file *energies*, with the target in its first excited state (**Ltarget 1**, a 16-year isomer), using non-relativistic kinematics, the HRTW-model for width fluctuation corrections (**widthmode 2**) in the compound nucleus calculation, with the particle transmission coefficients and inverse reaction cross sections written on the output file (**outinverse y**) and with user-defined level density parameters **a** for ^{93}Nb and ^{94}Nb.

In Part III, we will explain all the possible keywords. We have classified them according to their meaning and importance. For each keyword, we give an explanation, a few examples, the default value, and the theoretically allowed numerical range. As the input file above shows, there is usually one value per keyword. Often, however, in cases where several residual nuclides are involved, nuclear model parameters differ from nuclide to nuclide. Then, the particular nuclide under consideration must also be given in the input line. In general, for these model parameters, we read keyword, *Z*, *A*, a physical value and sometimes a possible further index (e.g. the fission barrier, index for the giant resonance, etc.), all separated by blanks. As the example above shows for the level density parameter *a*, the same keyword can appear more than once in an input file, to cover several different nuclides. Again, remember that all such keywords, if you don't specify them, have a default value from either the nuclear structure and model parameter database or from systematics. The usual reason to change them is to fit experimental data, to use new information that is not yet in the TALYS database, or simply because the user may not agree with our default values. A final important point to note is that some keywords induce defaults for other keywords. This may seem confusing, but in practice this is not so. As an example, for a ^{56}Fe target the **fission** keyword is automatically disabled whereas for ^{232}Th it is by default enabled. Hence, the default value of the **fission** keyword is mass dependent. In the input description, you will find a few similar cases. Anyway, you can always find all adopted default values for all parameters at the top of the *output* file, see which values have been set by the user or by default, and overrule them in a new input file.

Since TALYS-1.96, it is also possible to give the Z,A relative to the compound nucleus. TALYS is not supposed to work for target nuclides up to mass 4, which enabled us to make use of the Z, A indices to give the relative compound nucleus Z, A equivalent to the real Z, A of the nucleus. Hence, the last two lines in the input file above can also be entered as

```
a 0 1 13.115
a 0 0 13.421
```

where the first keyword is for the target nucleus and the second for the compound nucleus. This feature is especially helpful for automated TALYS scripts in which e.g. only a keyword for the

compound nucleus is to be varied, since that one can always be specified by '0 0', without having to look up the Z and A of the compound nucleus.

3.2.1 Energy-dependent parameter adjustment

TALYS contains hundreds of parameters and most of them are energy-independent. They are ingredients of phenomenological models which have been constructed with, indeed, energy-independent parameters. The OMP parameter r_V, or the height of the fission barrier, **fisbar** are examples. There are two reasons to deviate from this. First, since these models are a phenomenological representation of reality, there is no strict law that these parameters should be energy-independent. Suppose for example that one tries to use a simple Hill-Wheeler expression to approximate fission paths coming from microscopic analyses, which are supposedly built on a better physical basis. Heights and widths of the fission barriers which are dependent on (in this case, excitation) energy will probably emerge. Then, one may want to use those in calculations.

A second reason is that if physically adequate models fail to fit experimental data, such energy-dependent adjustment can be invoked as a last resort. As long as the deviation from the original model is not too large, unpleasant surprises in the various reaction channels are avoided.

To accommodate this, no less that 80 TALYS keywords (parameters) now have the possibility to be extended with such an energy-dependence.

On the input line, we read the usual keyword and its energy-independent value. If a local variation is required, one adds (1) 4 extra parameters, or (2) a filename, to the input line. With either method a multiplication factor deviating from 1 can be given, as a function of energy. The 4 extra parameters, Ea, Eb, Em and D, drive the following multiplication function

$$
\begin{aligned}
f(E) & = 1 + D' \frac{(E - E_a)^N}{(E - E_a)^N + (C - E_a)^N}, \text{if } E < E_m \\
& = 1 + D' \frac{(E_b - E)^N}{(E_b - E)^N + (C - E_b)^N}, \text{if } E \geq E_m
\end{aligned}
\tag{3.1}
$$

where N is currently fixed to 4, and

$$
D' = (D - 1)(1 + \frac{1}{2}^N)
\tag{3.2}
$$

and

$$
\begin{aligned}
C & = E_a + \frac{1}{2}(E_m - E_a), \text{if } E < E_m \\
C & = E_m + \frac{1}{2}(E_b - E_m), \text{if } E \geq E_m
\end{aligned}
\tag{3.3}
$$

An input line would then look as follows:

```
keyword value(s) Ea Eb Em D
```

This means the following: the parameter has a constant value for all energies *outside* the begin energy Ea and end energy Eb. The multiplication function changes smoothly from Ea until Em, and at Em the deviation from the constant value has reached its maximum value D. Between Em and Eb the function changes in the opposite direction until the constant value is reached again at Eb. To ensure some smoothness, Eq. (3.1) was adopted from the KD03 OMP expression for $W_V(E)$. An example for the real volume radius of the optical model is

```
rvadjust n 1. 0.4 3. 1.7 1.02
```

Local parameter adjustment

Figure 3.1: Local adjustment of the r_v parameter for ^{93}Nb.

Suppose we use this input line for neutrons on ^{93}Nb. The default value for r_v is 1.215 fm. We do not change this globally, hence the parameter value 1. Next, we change r_v between 0.4 and 3 MeV with the top (D is positive in this case) at 1.7 MeV. The result is presented in figure rv. One may use several segments, i.e. several input lines, with such local deviations in the same input file, as long as the energy ranges do not overlap (TALYS tests this).

The other option is to use a table with multiplication factors, e.g.

```
rvadjust n myfile.adj
```

where *myfile.adj* looks e.g. as follows

```
0.0  1.
0.4. 1.
1.7  1.1
3.0  1.
200  1.
```

which will simply produces a triangle with top at 1.7 MeV. For such simple cases, the use of Eq. (3.1) may be better.

The latter option may be interesting if one manages to fit, in some nuclear structure study, a phenomelogical prescription available in TALYS to a more complex microscopic description of a nuclear process. For example, maybe a JLM OMP can be simulated by a Woods-Saxon OMP with energy dependent parameters, or a microscopic fission model by a Hill-Wheeler model with energy dependent fission parameters. The resulting fit can then be used as input file to TALYS.

The energy-dependent adjustment is currently possible for the following keywords.

- Optical model: **avadjust, avdadjust, avsoadjust, awadjust, awdadjust, awsoadjust, d1adjust, d2adjust, d3adjust, lv1adjust, lvadjust, lvsoadjust, lw1adjust, lwadjust, lwsoadjust, rcadjust, rvadjust, rvdadjust, rvsoadjust, rwadjust, rwdadjust, rwsoadjust,**

tjadjust, v1adjust, v2adjust, v3adjust, v4adjust, vso1adjust, vso2adjust, w1adjust, w2adjust, w3adjust, w4adjust, wso1adjust, wso2adjust,adepthcor, aradialcor

- Level density: **ctable, krotconstant, ptable, rspincut, rspincutff, s2adjust**
- Gamma-ray strength function: **sgr, sgradjust, spr, spradjust, egr, egradjust, wtable, wtableadjust, epr, epradjust, etable, ftable, ggr, ggradjust, gnorm, gpr, gpradjust**
- Pre-equilibrium: **cbreak, cknock, cstrip, m2constant**
- Fission: **fisbar, fisbaradjust, fishw, fishwadjust, bdamp, bdampadjust, betafiscor, betafiscoradjust, vfiscor, vfiscoradjust**

In a previous version of TALYS, this local adjustment was only applicable for the optical model parameters, with a different muliplication function, see e.g. **rvadjustF** on page 529. The latter keywords are now considered obsolete.

4. Nuclear reactions: General approach

An outline of the general theory and modeling of nuclear reactions can be given in many ways. A common classification is in terms of time scales: short reaction times are associated with direct reactions and long reaction times with compound nucleus processes. At intermediate time scales, pre-equilibrium processes occur. An alternative, more or less equivalent, classification can be given with the number of intranuclear collisions, which is one or two for direct reactions, a few for pre-equilibrium reactions and many for compound reactions, respectively. As a consequence, the coupling between the incident and outgoing channels decreases with the number of collisions and the statistical nature of the nuclear reaction theories increases with the number of collisions. Figs. 4.1 and 4.2 explain the role of the different reaction mechanisms during an arbitrary nucleon-induced reaction in a schematic manner. They will all be discussed in this manual.

This distinction between nuclear reaction mechanisms can be obtained in a more formal way by means of a proper division of the nuclear wave functions into open and closed configurations, as detailed for example by Feshbach's many contributions to the field. This is the subject of several textbooks and will not be repeated here. When appropriate, we will return to the most important theoretical aspects of the nuclear models in TALYS in Part II.

When discussing nuclear reactions in the context of a computer code, as in this manual, a different starting point is more appropriate. We think it is best illustrated by Fig. 4.3. A particle incident on a target nucleus will induce several *binary* reactions which are described by the various competing reaction mechanisms that were mentioned above. The end products of the binary reaction are the emitted particle and the corresponding recoiling residual nucleus. In general this is, however, not the end of the process. A total nuclear reaction may involve a whole sequence of residual nuclei, especially at higher energies, resulting from multiple particle emission. All these residual nuclides have their own separation energies, optical model parameters, level densities, fission barriers, gamma strength functions, etc., that must properly be taken into account along the reaction chain. The implementation of this entire reaction chain forms the backbone of TALYS. The

Nuclear Reaction Mechanisms   **Particle Spectra**
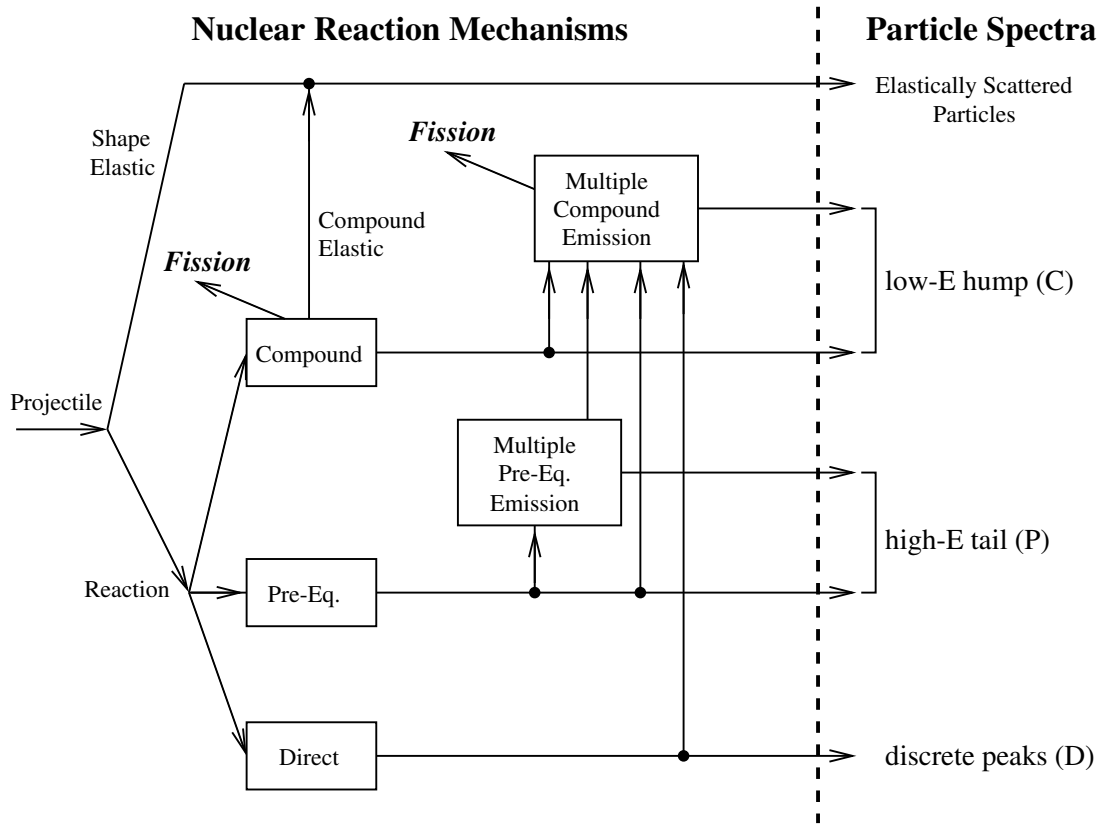
Figure 4.1: The role of direct, pre-equilibrium and compound processes in the description of a nuclear reaction and the outgoing particle spectra. The C, P and D labels correspond to those in Fig. 4.2

program has been written in a way that enables a clear and easy inclusion of all possible nuclear model ingredients for any number of nuclides in the reaction chain. Of course, in this whole chain the target and primary compound nucleus have a special status, since they are subject to *all* reaction mechanisms, i.e. direct, pre-equilibrium, compound and fission and, at low incident energies, width fluctuation corrections in compound nucleus decay. Also, at incident energies below a few MeV, only binary reactions take place and the target and compound nucleus are often the only two nuclei involved in the whole reaction. Historically, it is for the binary reactions that most of the theoretical methods have been developed and refined, mainly because their validity, and their relation with nuclear structure, could best be tested with exclusive measurements. In general, however, Fig. 4.3 should serve as the illustration of a total nuclear reaction at any incident energy. The projectile, in this case a neutron, and the target $(Z_C, N_C - 1)$ form a compound nucleus (Z_C, N_C) with a total energy

$$E^{tot} = E_{CM} + S_n(Z_{CN}, N_{CN}) + E_x^0, \tag{4.1}$$

where E_{CM} is the incident energy in the CM frame, S_n is the neutron separation energy of the compound nucleus, and E_x^0 the excitation energy of the target (which is usually zero, i.e. representing the ground state). The compound nucleus is described by a range of possible spin (J) and parity (Π) combinations, which for simplicity are left out of Fig. 4.3. From this state, transitions to all open channels may occur by means of direct, pre-equilibrium and compound processes. The
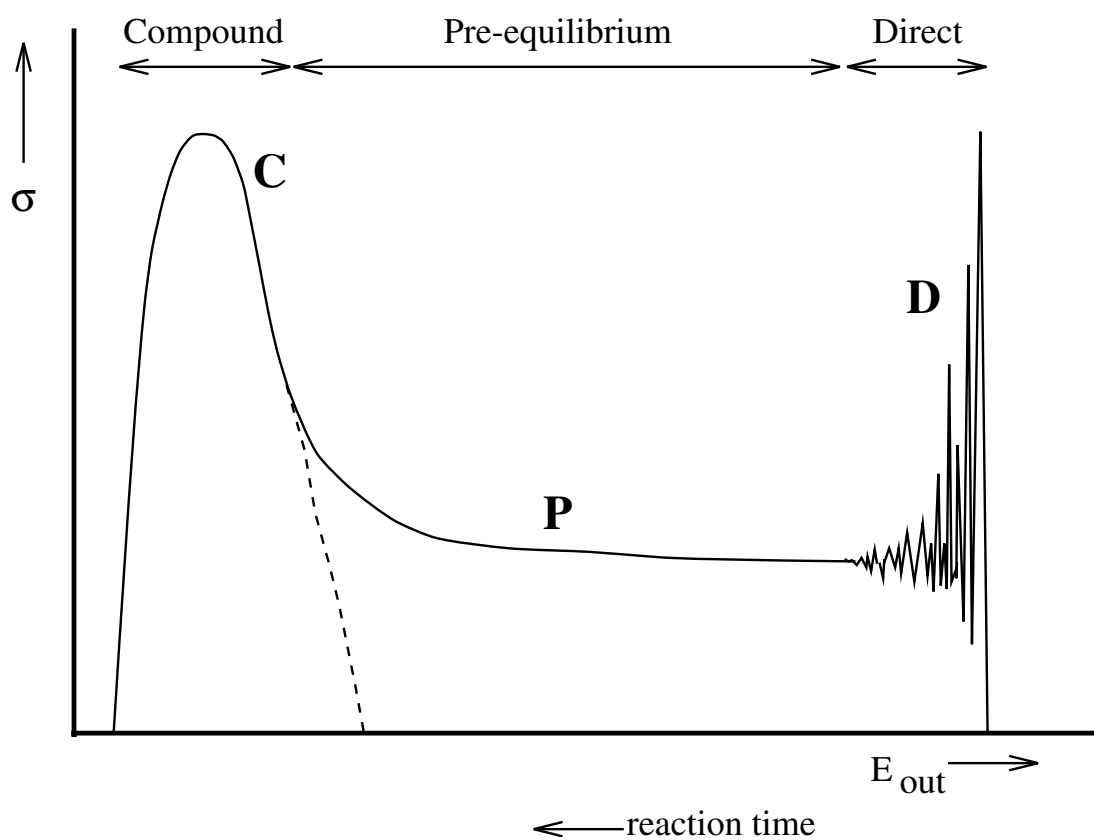
Figure 4.2: Schematical drawing of an outgoing particle spectrum. The energy regions to which direct (D), pre-equilibrium (P) and compound (C) mechanisms contribute are indicated. The dashed curve distinguishes the compound contribution from the rest in the transitional energy region.

residual nuclei formed by these binary reactions may be populated in the discrete level part and in the continuum part of the available excitation energy range. In Fig. 4.3, we have only drawn three binary channels, namely the $(Z_C, N_C - 1)$, $(Z_C - 1, N_C)$ and $(Z_C - 1, N_C - 1)$ nuclei that result from binary neutron, proton and deuteron emission, respectively. Each nucleus is characterized by a separation energy per possible ejectile. If the populated residual nucleus has a maximal excitation energy $E_x^{max}(Z, N)$ that is still above the separation energies for one or more different particles for that nucleus, further emission of these particles may occur and nuclei with lower Z and N will be populated. At the end of the nuclear reaction (left bottom part of Fig. 4.3), all the reaction population is below the lowest particle separation energy, and the residual nucleus $(Z_C - z, N_C - n)$ can only decay to its ground or isomeric states by means of gamma decay. In a computer program, the continuum must be discretized in excitation energy (E_x) bins. We can take these bins equidistant or non-equidistant (the default), although we already want to stress the important fact here that the *emission* energy grid for the outgoing particles is non-equidistant in TALYS. After the aforementioned binary reaction, every continuum excitation energy bin will be further depleted by means of particle emission, gamma decay or fission. Computationally, this process starts at the initial compound nucleus and its highest energy bin, i.e. the bin just below $E_x^{max}(Z_C, N_C) = E^{tot}$, and subsequently in order of decreasing energy bin/level, decreasing N and decreasing Z. Inside each continuum bin, there is an additional loop over all possible J and Π, whereas for each discrete level, J and Π have unique values. Hence, a bin/level is characterized by the set $\{Z, N, E_x, J, \Pi\}$ and by means of gamma or particle emission, it can decay into all accessible $\{Z', N', E_{x'}, J', \Pi'\}$ bins/levels. In this way, the whole reaction chain is followed until all bins and levels are depleted and thus all channels are closed. In the process, all particle production cross sections and residual production cross sections are accumulated to their final values.

We will now zoom in on the various parts of Fig. 4.3 to describe the various stages of the reaction, depending on the incident energy, and we will mention the nuclear reaction mechanisms that apply.

4.1 Reaction mechanisms

In the projectile energy range between 1 keV and several hundreds of MeV, the importance of a particular nuclear reaction mechanism appears and disappears upon varying the incident energy. We will now describe the particle decay scheme that typically applies in the various energy regions. Because of the Coulomb barrier for charged particles, it will be clear that the discussion for low energy reactions usually concerns incident neutrons. In general, however, what follows can be generalized to incident charged particles. The energy ranges mentioned in each paragraph heading are just meant as helpful indications, which apply for a typical medium mass nucleus.

4.1.1 Low energies

Elastic scattering and capture (E < 0.2 MeV)

If the energy of an incident neutron is below the excitation energy of the first inelastic level, and if there are no (n, p), etc. reactions that are energetically possible, then the only reaction possibilities are elastic scattering, neutron capture and, for fissile nuclides, fission. At these low energies, only the $(Z_C, N_C - 1)$ and (Z_C, N_C) nuclides of Fig. 4.3 are involved, see Fig. 4.4. First, the shape (or direct) elastic scattering cross section can directly be determined from the optical model, which will be discussed in Section 10. The compound nucleus, which is populated by a reaction population equal to the reaction cross section, is formed at one single energy $E^{tot} = E_x^{max}(Z_C, N_C)$ and a range
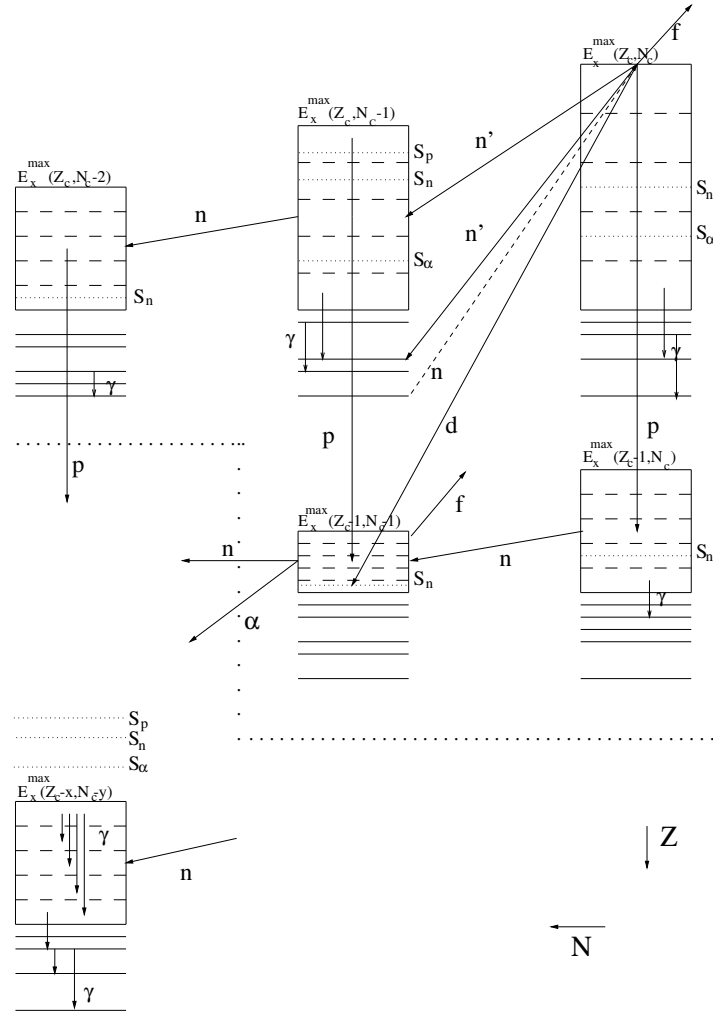
Figure 4.3: Neutron-induced reaction. The dashed arrow represents the incident channel, while the continuous arrows represent the decay possibilities. E_x^{max} denotes the maximal possible excitation energy of each nucleus and S_k is the particle separation energy for particle k. For each nucleus a few discrete levels are drawn, together with a few continuum energy bins. Spin and parity degrees of freedom are left out of this figure for simplicity. Fission is indicated by an f.
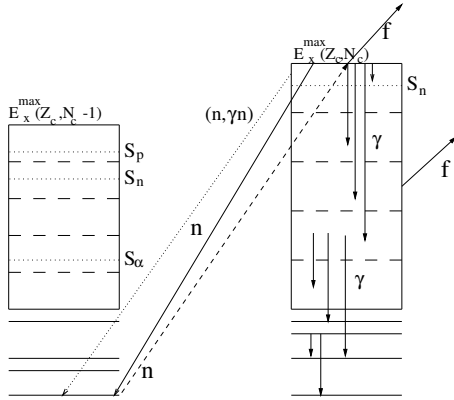
Figure 4.4: Neutron-induced reaction at low energy. The dashed arrow represents the incident channel, while the continuous arrows represents the elastic channel. The only possibilities are elastic scattering and capture of the neutron in the compound nucleus, with subsequent decay to the ground state or an isomeric state of the compound nucleus. A small part of the population may decay to the target nucleus by means of the $(n, \gamma n)$ channel (dotted arrow). For fissile nuclei, fission may be another open channel.

of J, Π-values. This compound nucleus either decays by means of compound elastic scattering back to the initial state of the target nucleus, or by means of neutron capture, after which gamma decay follows to the continuum and to discrete states of the compound nucleus. The competition between the compound elastic and capture channels is described by the compound nucleus theory, which we will discuss in Section 13. To be precise, the elastic and capture processes comprise the first *binary* reaction. To complete the description of the total reaction, the excited (Z_C, N_C) nucleus, which is populated over its whole excitation energy range by the primary gamma emission, must complete its decay. The highest continuum bin is depleted first, for all J and Π. The subsequent gamma decay increases the population of the lower bins, before the latter are depleted themselves. Also, continuum bins that are above the neutron separation energy S_n of the compound nucleus contribute to the feeding of the $(n, \gamma n)$ channel. This results in a weak continuous neutron spectrum, even though the elastic channel is the only true binary neutron channel that is open. The continuum bins and the discrete levels of the compound nucleus are depleted one by one, in decreasing order, until the ground or an isomeric state of the compound nucleus is reached by subsequent gamma decay. If a nuclide is fissile, fission may compete as well, both from the initial compound state $E_x^{max}(Z_C, N_C)$ and from the continuum bins of the compound nucleus, the latter resulting in a $(n, \gamma f)$ cross section. Both contributions add up to the so called first-chance fission cross section.

Inelastic scattering to discrete states (0.2 < E < 4 MeV)

At somewhat higher incident energies, the first inelastic channels open up, see Fig. 4.5. Reactions to these discrete levels have a compound and a direct component. The former is again described by the compound nucleus theory, while the latter is described by the Distorted Wave Born Approximation (DWBA) for spherical nuclei and by coupled-channels equations for deformed nuclei, see Section 11. When the incident energy crosses an inelastic threshold, the compound inelastic contribution rises rapidly and predominates, whereas the direct component increases more gradually. Obviously, the elastic scattering, capture and fission processes described in the previous subsection also apply here. In addition, there is now gamma decay to an isomeric state or the ground state in the target nucleus after inelastic scattering. When there are several, say 10, inelastic levels open to decay,
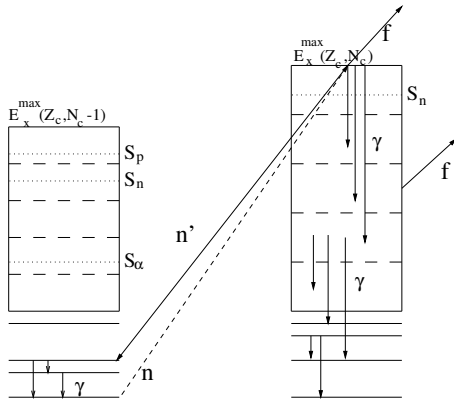
Figure 4.5: Neutron-induced reaction at somewhat higher energy. The dashed arrow represents the incident channel, while the continuous arrows represent the decay possibilities. In addition to the possibilities sketched in the previous figure, there is now inelastic scattering followed by gamma decay in the target nucleus.

the compound contribution to each individual level is still significant. However, the effect of the width fluctuation correction on the compound cross section is already small in this case, as will be outlined in Section 13.

4.1.2 High energies

Pre-equilibrium reactions (E > 4 MeV)

At higher incident energies, inelastic cross sections to both the discrete states and the continuum are possible, see Fig. 4.3. Like reactions to discrete states, reactions to the continuum also have a compound and a direct-like component. The latter are usually described by pre-equilibrium reactions which, by definition, include direct reactions to the continuum. They will be discussed in Section 12. Also non-elastic channels to other nuclides, through charge-exchange, e.g. (n, p), and transfer reactions, e.g. (n, α), generally open up at these energies, and decay to these nuclides can take place by the same direct, pre-equilibrium and compound mechanisms. Again, the channels described in the previous subsections also apply here. In addition, gamma decay to ground and isomeric states of all residual nuclides occurs. When many channels open up, particle decay to individual states (e.g. compound elastic scattering) rapidly becomes negligible. For the excitation of a discrete state, the direct component now becomes predominant, since that involves no statistical competition with the other channels. At about 15 MeV, the *total* compound cross section, i.e. summed over all final discrete states and the excited continuum, is however still larger than the summed direct and pre-equilibrium contributions.

Multiple compound emission (E > 8 MeV)

At incident energies above about the neutron separation energy, the residual nuclides formed after the first binary reaction contain enough excitation energy to enable further decay by compound nucleus particle emission or fission. This gives rise to multiple reaction channels such as $(n, 2n)$, (n, np), etc. For higher energies, this picture can be generalized to many residual nuclei, and thus more complex reaction channels, as explained in the introduction of this Chapter, see also Fig. 4.3. If fission is possible, this may occur for all residual nuclides, which is known as multiple chance fission. All excited nuclides will eventually decay to their isomeric and ground states.

Multiple pre-equilibrium emission (E > 40 MeV)

At still higher incident energies, above several tens of MeV, the residual nuclides formed after binary emission may contain so much excitation energy that the presence of further *fast* particles inside the nucleus becomes possible. These can be imagined as strongly excited particle-hole pairs resulting from the first binary interaction with the projectile. The residual system is then clearly non-equilibrated and the excited particle that is high in the continuum may, in addition to the first emitted particle, also be emitted on a short time scale. This so-called multiple pre-equilibrium emission forms an alternative theoretical picture of the intra-nuclear cascade process, whereby now not the exact location and momentum of the particles is followed, but instead the total energy of the system and the number of particle-hole excitations (exciton number). In TALYS, this process can be generalized to any number of multiple pre-equilibrium stages in the reaction by keeping track of all successive particle-hole excitations, see Section 14.2. For these incident energies, the binary compound cross section becomes small: the non-elastic cross section is almost completely exhausted by primary pre-equilibrium emission. Again, Fig. 4.3 applies.

Sample case 4.1 **All results for 14 MeV n + ^{93}Nb**

We have included 9 different versions of this sample case, in order to give an impression of the various types of information that can be retrieved from TALYS. Most, but not all, output options will be described, while the remainder will appear in the other sample cases. We have chopped the sample output after column 80 to let it fit within this manual. We suggest to consult the output files in the *samples/* directory for the full results. Note that in later versions of TALYS, more and more output is no longer given in the main large output file, but in separate output files with the results per reaction channel etc.

Case a: The simplest input file

The first sample problem concerns the simplest possible TALYS calculation. Consider the following input file that produces the results for a 14 MeV neutron on ^{93}Nb:

```
#
# n-Nb093-14MeV-general
#
# General
#
projectile n
element nb
mass 93
energy 14.
```

This input file called *input* can simply be run as follows:

talys < talys.inp > talys.out

An output file of TALYS consists of several blocks. Whether these blocks are printed or not depends on the status of the various keywords that were discussed in Chapter 3. By default, the so-called main output is always given (through the default **outmain y**), and we discuss this output in the present sample case. For a single incident energy, a default calculation gives the

most important cross sections only. "Most important" is obviously subjective, and probably every user has an own opinion on what should always appear by default in the output. We will demonstrate in the other sample problems how to extract all information from TALYS. The output file starts with a display of the version of TALYS you are using, the name of the authors, and the Copyright statement. Also the physics dimensions used in the output are given:

```
    TALYS-2.0 (Version: December 29, 2023)

 Copyright (C) 2023  A.J. Koning, S. Hilaire and S. Goriely

 Dimensions - Cross sections: mb, Energies: MeV, Angles: degrees
```

The next output block begins with:

```
########## USER INPUT ##########
```

Here, the first section of the output is a print of the keywords/input parameters. This is done in two steps: First, in the block

```
USER INPUT FILE

#
# n-nb093-14mev
#
# general
#
projectile n
element nb
mass 93
energy 14.
```

an exact copy of the input file as given by the user is returned. Next, in the block

```
USER INPUT FILE + DEFAULTS

Keyword           Value   Variable     Explanation

#
# Four main keywords
#
projectile          n     ptype0       type of incident particle
element             Nb     Starget      symbol of target nucleus
mass                93     mass         mass number of target nucleus
energy            14.000 eninc          incident energy in MeV
#
# Basic physical and numerical parameters
#
ejectiles g n p d t h a   outtype      outgoing particles
.............
```

a table with all keywords is given, not only the ones that you have specified in the input file, but also all the defaults that are set automatically. The corresponding Fortran variables are also printed, together with a short explanation of their meaning. This table can be helpful as a guide to change further input parameters for a next run. You may also copy and paste the block directly into your next input file.

In the next output block

```
########## BASIC REACTION PARAMETERS ##########

Projectile            : neutron     Mass in a.m.u.      :   1.008665
Target                :  93Nb       Mass in a.m.u.      :  92.906378

Included channels:
                  gamma
                  neutron
                  proton
                  deuteron
                  triton
                  helium-3
                  alpha

1 incident energy (LAB):

    14.000

Q-values for binary reactions:

Q(n,g):  7.22755
Q(n,n):  0.00000
Q(n,p):  0.69112
Q(n,d): -3.81879
Q(n,t): -6.19635
Q(n,h): -7.72313
Q(n,a):  4.92559
```

we print the main parameters that characterize the nuclear reaction: the projectile, target and their masses and the outgoing particles that are included as competitive channels. The incident energy or range of incident energies in the LAB system is given together with the binary reaction Q-values.

The block with final results starts with

```
########## RESULTS FOR E=  14.00000 ##########

 Energy dependent input flags

 Width fluctuations (flagwidth)          : n
 Unresolved resonance parameters (flagurr) : n
 Preequilibrium (flagpreeq)              : y
 Multiple preequilibrium (flagmulpre)    : n
 Number of continuum excitation energy bins: 40
```

with no further information for the present sample case since no further output was requested. When all nuclear model calculations are done, the most important cross sections are summarized in the main part of the output, in which we have printed the center-of-mass energy, the main (total) cross sections. the inclusive binary cross sections $\sigma_{n,k}^{inc,bin}$, see Eq. (4.19), the total particle production cross sections $\sigma_{n,xn}$ of Eq. (4.20) and the multiplicities Y_n of Eq. (4.22), and the residual production cross sections. The latter are given first per produced nuclide and isomer. Next, nuclides with the same mass are summed to give mass yield curves. Also, the sum over all the residual cross sections is compared with the non-elastic cross section. Obviously, these two values should be approximately equal.

```
########### REACTION SUMMARY FOR E=  14.00000 ###########


Center-of-mass energy:   13.849


1. Total (binary) cross sections


Total           = 3.98195E+03
  Shape elastic   = 2.21132E+03
  Reaction        = 1.77063E+03
    Compound elastic= 6.02817E-04
    Non-elastic    = 1.77063E+03
      Direct          = 3.09942E+01
      Pre-equilibrium = 4.19247E+02
      Giant resonance = 5.69210E+01
      Compound non-el = 1.26347E+03
    Total elastic   = 2.21132E+03


2. Binary non-elastic cross sections (non-exclusive)


gamma   = 2.79389E+00
neutron = 1.69529E+03
proton  = 3.85805E+01
deuteron= 4.96449E+00
triton  = 1.81757E-01
helium-3= 7.29505E-10
alpha   = 2.88177E+01


3. Total particle production cross sections


gamma   = 2.21097E+03    Multiplicity= 1.24869E+00
neutron = 3.08736E+03    Multiplicity= 1.74365E+00
proton  = 4.10702E+01    Multiplicity= 2.31953E-02
deuteron= 4.96449E+00    Multiplicity= 2.80380E-03
triton  = 1.81757E-01    Multiplicity= 1.02651E-04
helium-3= 7.29505E-10    Multiplicity= 4.12003E-13
alpha   = 2.93826E+01    Multiplicity= 1.65944E-02


4. Residual production cross sections


  a. Per isotope
```

```
  Z   A  nuclide    total     level   isomeric   isomeric    lifetime
                 cross section       cross section  ratio

  41  94 ( 94Nb) 1.19960E+00    0    5.71296E-01  0.47624
                                1    6.28304E-01  0.52376   3.75800E+02 sec.
  41  93 ( 93Nb) 3.14864E+02    0    2.77770E+02  0.88219
                                1    3.70943E+01  0.11781   5.08700E+08 sec.
  40  93 ( 93Zr) 2.97680E+01    0    2.97680E+01  1.00000
  41  92 ( 92Nb) 1.37917E+03    0    8.65640E+02  0.62765
                                1    5.13527E+02  0.37235   8.77000E+05 sec.
  40  92 ( 92Zr) 1.62764E+01    0    1.62764E+01  1.00000
  40  91 ( 91Zr) 1.81764E-01    0    1.81764E-01  1.00000
  39  90 ( 90Y ) 2.63291E+01    0    1.25952E+01  0.47837
                                2    1.37340E+01  0.52163   1.14800E+04 sec.
  39  89 ( 89Y ) 3.05343E+00    0    1.27030E+00  0.41602
                                1    1.78314E+00  0.58398   1.56600E+01 sec.


  b. Per mass


  A  cross section


  94 1.19960E+00
  93 3.44632E+02
  92 1.39544E+03
  91 1.81764E-01
  90 2.63291E+01
  89 3.05343E+00


Total residual production cross section:  1770.8403320
Non-elastic cross section              :  1770.6293945
```

At the end of the output, the total calculation time is printed, followed by a message that the
calculation has been successfully completed:

```
Execution time:  0 hours  0 minutes  2.23 seconds
```

```
 The TALYS team congratulates you with this successful calculation.
```

Case b: Discrete state cross sections and spectra

As a first extension to the simple input/output file given above, we will request the output of
cross sections per individual discrete level. Also, the cumulated angle-integrated and double-
differential particle spectra are requested. This is obtained with the following input file:

```
#
# n-Nb093-14MeV-spectra
#
# General
#
projectile n
element nb
mass 93
```

```
energy 14.
#
# Output
#
outdiscrete y
outspectra y
ddxmode 2
filespectrum n p a
fileddxa n 30.
fileddxa n 60.
fileddxa a 30.
fileddxa a 60.
```

In addition to the information printed for case 1a, the cross sections per discrete state for each binary channel are given, starting with the (n, γ) channel,

```
 5. Binary reactions to discrete levels and continuum


   (n,g)   cross sections:


 Inclusive:


 Level Energy    E-out     J/P       Direct    Compound     Total     Origin


   0   0.00000  21.07609   6.0+    0.00000    0.00000    0.00000    Preeq
   1   0.04089  21.03519   3.0+    0.00000    0.00000    0.00000    Preeq
   2   0.05871  21.01738   4.0+    0.00000    0.00000    0.00000    Preeq
   3   0.07867  20.99742   7.0+    0.00169    0.00000    0.00169    Preeq

 ...........................
```

after which the inelastic cross section to every individual discrete state of the target nucleus is printed, including the separation in direct and compound, see Eq. (4.16). These are summed, per contribution, to the total discrete inelastic cross section, see Eq. (4.15). To these cross sections, the continuum inelastic cross sections of Eq. (4.17) are added to give the total inelastic cross section (4.14). Finally, the $(n, \gamma n)$ cross section is also printed. This output block looks as follows

```
 Inelastic cross sections:


 Inclusive:


 Level Energy    E-out     J/P       Direct    Compound     Total     Origin


   1   0.03077  13.81777   0.5-    0.00000    0.00013    0.00013    Preeq
   2   0.68679  13.16175   1.5-    0.00000    0.00025    0.00025    Preeq
   3   0.74395  13.10459   3.5+    3.27713    0.00049    3.27762    Direct
   4   0.80882  13.03972   2.5+    0.03425    0.00037    0.03463    Direct
   5   0.81032  13.03822   2.5-    2.45130    0.00036    2.45166    Direct
   6   0.94980  12.89874   6.5+    5.68166    0.00066    5.68232    Direct
   7   0.97000  12.87854   1.5-    0.00000    0.00025    0.00025    Preeq
   8   0.97891  12.86963   5.5+    4.86351    0.00063    4.86414    Direct
```

```
 9    1.08268   12.76586    4.5+      4.03323     0.00057     4.03379     Direct
10    1.12709   12.72145    2.5+      0.03389     0.00037     0.03426     Direct
11    1.28426   12.56428    2.5-      0.03374     0.00035     0.03409     Direct
12    1.29000   12.55854    0.5-      0.32985     0.00012     0.32997     Direct
13    1.29722   12.55132    4.5+      0.05613     0.00056     0.05669     Direct
14    1.31550   12.53304    2.5+      0.00809     0.00036     0.00846     Direct
15    1.33504   12.51350    8.5+      2.96128     0.00061     2.96189     Direct
                                     ---------   ---------   ---------
Discrete  Inelastic:                  23.76406     0.00609    23.77015
Continuum Inelastic:                 420.88937  1250.63110  1671.52051
                                     ---------   ---------   ---------
Total     Inelastic:                 444.65344  1250.63721  1695.29114

(n,gn) cross section:      1.59155
```

This is repeated for the (n, p) and other channels,

```
  (n,p)   cross sections:

Inclusive:

Level Energy     E-out     J/P        Direct     Compound      Total     Origin

  0   0.00000   14.54008    2.5+      0.33518     0.00026     0.33544     Preeq
  1   0.26682   14.27326    1.5+      1.11920     0.00017     1.11937     Preeq
  2   0.94709   13.59299    0.5+      0.78153     0.00008     0.78161     Preeq
  3   0.94980   13.59028    4.5+      0.08114     0.00037     0.08151     Preeq
.........................
```

The last column in these tables specifies the origin of the direct contribution to the discrete state. "Direct" means that this is obtained with coupled-channels, DWBA or, as in this case, weak coupling, whereas "Preeq" means that the pre-equilibrium cross section is collapsed onto the discrete states, as an approximate method for more exact direct reaction approaches for charge-exchange and pick-up reactions. We note here that the feature of calculating, and printing, the inelastic cross sections for a specific state is of particular interest in the case of excitations, i.e. to obtain this particular cross section for a whole range of incident energies. This will be handled in another sample case.

Since **outspectra y** was specified in the input file, the composite particle spectra for the continuum are also printed. Besides the total spectrum, the division into direct (i.e. smoothed collective effects and giant resonance contributions), pre-equilibrium, multiple pre-equilibrium and compound is given. First we give the photon spectrum,

```
7. Composite particle spectra

Spectra for outgoing gamma

 Energy    Total       Direct     Pre-equil.  Mult. preeq  Compound

  0.001 2.56193E+00 0.00000E+00 2.56817E-13 0.00000E+00 2.56193E+00
  0.002 3.46083E+00 0.00000E+00 2.44734E-12 0.00000E+00 3.46083E+00
```

```
   0.005 6.22649E+00 0.00000E+00 3.40708E-11 0.00000E+00 6.22649E+00
   0.010 1.13850E+01 0.00000E+00 2.57561E-10 0.00000E+00 1.13850E+01
   0.020 2.14177E+01 0.00000E+00 1.94665E-09 0.00000E+00 2.14177E+01
   0.050 5.15819E+01 0.00000E+00 2.71071E-08 0.00000E+00 5.15819E+01
.........................
```

followed by the neutron spectrum

```
Spectra for outgoing neutron

  Energy    Total       Direct     Pre-equil.  Mult. preeq  Compound

   0.001 2.54285E+01 7.90143E-03 9.56260E-02 0.00000E+00 2.53250E+01
   0.002 5.08020E+01 7.91399E-03 1.44361E-01 0.00000E+00 5.06497E+01
   0.005 1.34561E+02 7.95178E-03 2.71935E-01 0.00000E+00 1.34281E+02
   0.010 1.87795E+02 8.01513E-03 4.87956E-01 0.00000E+00 1.87299E+02
   0.020 2.26559E+02 8.14321E-03 9.81582E-01 0.00000E+00 2.25569E+02
.........................
```

and the spectra for the other outgoing particles. Depending on the value of **ddxmode**, the double-differential cross sections are printed as angular distributions or as spectra per fixed angle. For the present sample case, **ddxmode 2**, which gives

```
 9. Double-differential cross sections per outgoing angle

 DDX for outgoing neutron   at   0.000 degrees

   E-out     Total       Direct     Pre-equil. Mult. preeq   Compound

   0.001 2.02749E+00 1.54078E-03 1.06465E-02 0.00000E+00 2.01530E+00
   0.002 4.04819E+00 1.54323E-03 1.60730E-02 0.00000E+00 4.03057E+00
   0.005 1.07176E+01 1.55060E-03 3.02802E-02 0.00000E+00 1.06857E+01
   0.010 1.49607E+01 1.56295E-03 5.43443E-02 0.00000E+00 1.49048E+01
   0.020 1.80612E+01 1.58792E-03 1.09360E-01 0.00000E+00 1.79502E+01
..............................
```

followed by the other angles and other particles. A final important feature of the present input file is that some requested information has been written to separate output files, i.e. besides the standard output file, TALYS also produces the ready-to-plot files

```
aspec014.000.tot
nspec014.000.tot
pspec014.000.tot
```

containing the angle-integrated neutron, proton and alpha spectra, and

```
addx030.0.deg
addx060.0.deg
nddx030.0.deg
nddx060.0.deg
```

containing the double-differential neutron and alpha spectra at 30 and 60 degrees. All these separate output files are in YANDF format, e.g. the (n,xp) emission spectrum of *pspec014.000.tot* looks as follows

```
# header:
#   title: Nb93(n,xp) emission spectrum at  1.400000E+01 MeV
#   source: TALYS-2.0
#   user: Arjan Koning
#   date: 2023-12-12
#   format: YANDF-0.1
# target:
#   Z: 41
#   A: 93
#   nuclide: Nb93
# reaction:
#   type: (n,xp)
#   ENDF_MF: 6
#   ENDF_MT: 5
#   E-incident [MeV]:  1.400000E+01
#   E-average [MeV]:  8.456717E+00
# datablock:
#   quantity: emission spectrum
#   columns: 7
#   entries: 151
##    E-out            xs          Direct      Preequilibrium Multiple preeq
##    [MeV]          [mb/MeV]      [mb/MeV]       [mb/MeV]        [mb/MeV]
   2.000000E-01   2.678184E-30   0.000000E+00   2.678184E-30   0.000000E+00
   3.000000E-01   3.599347E-23   0.000000E+00   3.599347E-23   0.000000E+00
   4.000000E-01   5.176781E-19   0.000000E+00   5.176781E-19   0.000000E+00
   5.000000E-01   3.460652E-16   0.000000E+00   3.460652E-16   0.000000E+00
...........................
```

Case c: Exclusive channels and spectra

As another extension of the simple input file we can print the exclusive cross sections at one incident energy and the associated exclusive spectra. This is accomplished with the input file

```
#
# n-Nb093-14MeV-general-exclusive
#
# General
#
projectile n
element nb
mass 93
energy 14.
#
# Output
#
channels y
outspectra y
```

Contrary to the previous sample case, in this case no double-differential cross sections or results per separate file are printed (since it only concerns one incident energy). The exclusive cross sections are given in one table, per channel and per ground or isomeric state. It is checked whether the exclusive cross sections add up to the non-elastic cross section. Note that this sum rule, Eq. (4.25), is only expected to hold if we include enough exclusive channels in the calculation. If **maxchannel 4**, this equality should always hold for incident energies up to 20 MeV. This output block looks as follows:

```
 6. Exclusive cross sections


6a. Total exclusive cross sections


    Emitted particles      cross section reaction          level      isomeric
  n   p   d   t   h   a                                               cross section
  0   0   0   0   0   0    1.19960E+00  (n,g)
                                                             0       5.71296E-01
                                                             1       6.28304E-01
  1   0   0   0   0   0    3.13448E+02  (n,n')
                                                             0       2.76520E+02
                                                             1       3.69274E+01
  0   1   0   0   0   0    2.97658E+01  (n,p)
  0   0   1   0   0   0    4.96449E+00  (n,d)
  0   0   0   1   0   0    1.81764E-01  (n,t)
  0   0   0   0   0   1    2.63285E+01  (n,a)
                                                             0       1.25948E+01
                                                             2       1.37337E+01
  2   0   0   0   0   0    1.37899E+03  (n,2n)
                                                             0       8.65528E+02
                                                             1       5.13465E+02
  1   1   0   0   0   0    1.13115E+01  (n,np)
  1   0   0   0   0   1    3.05339E+00  (n,na)
                                                             0       1.27026E+00
                                                             1       1.78312E+00
  0   1   0   0   0   1    5.03111E-06  (n,pa)


 Absorption cross section                 :    62.44013


 Sum over exclusive channel cross sections:  1769.24536
 (n,gn) + (n,gp) +...(n,ga) cross sections:     1.59452
 Total                                     :  1770.83984
 Non-elastic cross section                 :  1770.62939
```

Note that the (n,np) and (n,d) cross sections add up to the residual production cross section for ^{92}Zr, as given in the first sample case.

Since **outspectra y**, for each exclusive channel the spectrum per outgoing particle is given. This output block begins with:

```
 6b. Exclusive spectra


     Emitted particles      cross section reaction        gamma cross section
```

```
   n   p   d   t   h   a
   1   0   0   0   0   0    3.26664E+02  (n,n')              1.00870E+03


 Outgoing spectra


 Energy  gamma          neutron     proton      deuteron    triton      helium-3


 0.001 4.06619E+00 2.14250E-03 0.00000E+00 0.00000E+00 0.00000E+00 0.00000E+00
 0.002 4.08311E+00 4.22497E-03 0.00000E+00 0.00000E+00 0.00000E+00 0.00000E+00
 0.005 4.13354E+00 1.04500E-02 0.00000E+00 0.00000E+00 0.00000E+00 0.00000E+00
 0.010 4.21777E+00 2.08288E-02 0.00000E+00 0.00000E+00 0.00000E+00 0.00000E+00
 0.020 4.38694E+00 4.16553E-02 0.00000E+00 0.00000E+00 0.00000E+00 0.00000E+00
 0.050 4.92328E+00 1.04608E-01 0.00000E+00 0.00000E+00 0.00000E+00 0.00000E+00
 0.100 6.46225E+00 2.10358E-01 0.00000E+00 0.00000E+00 0.00000E+00 0.00000E+00
.................................
     Emitted particles      cross section reaction      gamma cross section
   n   p   d   t   h   a
   1   1   0   0   0   0    1.06861E+01  (n,np)              1.97965E+01


 Outgoing spectra


 Energy  gamma          neutron     proton      deuteron    triton      helium-3


 0.001 6.35050E-02 1.87485E-01 0.00000E+00 0.00000E+00 0.00000E+00 0.00000E+00
 0.002 6.94942E-02 3.74836E-01 0.00000E+00 0.00000E+00 0.00000E+00 0.00000E+00
 0.005 8.74445E-02 9.36836E-01 0.00000E+00 0.00000E+00 0.00000E+00 0.00000E+00
 0.010 1.17368E-01 1.88679E+00 0.00000E+00 0.00000E+00 0.00000E+00 0.00000E+00
 0.020 1.77238E-01 3.89497E+00 0.00000E+00 0.00000E+00 0.00000E+00 0.00000E+00
 0.050 3.57037E-01 6.03595E+00 0.00000E+00 0.00000E+00 0.00000E+00 0.00000E+00
 0.100 6.57333E-01 8.96107E+00 0.00000E+00 0.00000E+00 0.00000E+00 0.00000E+00
 0.200 1.58990E+00 1.04045E+01 0.00000E+00 0.00000E+00 0.00000E+00 0.00000E+00
 0.300 1.88712E+00 9.88185E+00 0.00000E+00 0.00000E+00 0.00000E+00 0.00000E+00
 0.400 2.01034E+00 9.03657E+00 0.00000E+00 0.00000E+00 0.00000E+00 0.00000E+00
 0.500 1.41701E+00 8.28305E+00 0.00000E+00 0.00000E+00 0.00000E+00 0.00000E+00
 0.600 5.68786E+00 7.59201E+00 0.00000E+00 0.00000E+00 0.00000E+00 0.00000E+00
 0.700 8.64822E+00 6.60600E+00 0.00000E+00 0.00000E+00 0.00000E+00 0.00000E+00
 0.800 4.28359E+00 5.86945E+00 0.00000E+00 0.00000E+00 0.00000E+00 0.00000E+00
 0.900 2.37448E+00 5.09628E+00 0.00000E+00 0.00000E+00 0.00000E+00 0.00000E+00
 1.000 2.20641E+00 4.19745E+00 1.23263E-07 0.00000E+00 0.00000E+00 0.00000E+00
.................................
```

Note, as explained in Section 4.3.2, that the (n,np) channel is characterized by both a neutron and a proton spectrum.

Case d: Nuclear structure

It is possible to have all the nuclear structure information in the output file. The simplest way is to set **outbasic y**, which means that about everything that can be printed, will be printed. This may be a bit overdone if one is only interested in e.g. discrete levels or level densities. If the keywords **outlevels** and/or **outdensity** are set to **y**, discrete level and level density information will always be given for the target nucleus and the primary compound nucleus. With **outgamma y**, photon

strength function information is also given. If we would set, in addition, **outpopulation y**, this info will also be given for all the other residual nuclides that are reached in the reaction chain. The input file for this sample case is

```
#
# General
#
projectile n
element nb
mass 93
energy 14.
#
# Output
#
outlevels y
outdensity y
outgamma y
```

In addition to the output of case 1a, the separation energies for the six light particles are printed.

```
 NUCLEAR STRUCTURE INFORMATION FOR Z= 41 N= 52 ( 93Nb)


 Mass in a.m.u.     :  92.906373


 Separation energies:


 Particle        S


 neutron      8.83087
 proton       6.04279
 deuteron    12.45297
 triton      13.39009
 helium-3    15.64713
 alpha        1.92655
```

In the next output block, the discrete level scheme is printed for the first levels. The discrete level info contains level number, energy, spin, parity, branching ratios and lifetimes of possible isomers. It is also indicated whether the spin (J) or parity (P) of a level is experimentally known or whether a value was assigned to it (see Section 7.1). The "string" of the original ENSDF database is also given, so that the user can learn about possible alternative choices for spin and parity. This output block begins with:

```
 Discrete levels of Z= 41 N= 52 ( 93Nb)


 Number  Energy Spin Parity  Branching Ratio (%) Lifetime(sec) Assignment       ENSDF


   0      0.0000  4.5    +
   1      0.0308  0.5    -                                     5.087E+08
                                   --->  0   100.0000
   2      0.6868  1.5    -
```

```
                                    ---> 1  100.0000
   3      0.7440  3.5    +
                                    ---> 0  100.0000
   4      0.8088  2.5    +
                                    ---> 3    2.1580
                                    ---> 0   97.8420
.....................................
```

Since **outdensity y**, we print all the level density parameters that are involved in the main output file. Note also that, since **outdensity y** by default implies **filedensity y**, the files *ld041093.tot* and *ld041094.tot* have been created in YANDF format. They contain all level density parameters and a comparison between cumulated discrete levels and the integrated level density. discussed in Section 8: the level density parameter at the neutron separation energy $a(S_n)$, the experimental and theoretical average resonance spacing D_0, the asymptotic level density parameter $\tilde{a}$, the shell damping parameter γ, the pairing energy Δ, the shell correction energy δW, the matching energy E_x, the last discrete level, the levels for the matching problem, the temperature T, the back-shift energy E_0, the discrete state spin cut-off parameter σ and the spin cut-off parameter at the neutron separation energy. Next, we print a table with the level density parameter a, the spin cut-off parameter and the level density itself, all as a function of the excitation energy. The file **ld041093.tot** looks as follows:

```
# header:
#   title: Nb93 level density
#   source: TALYS-2.0
#   user: Arjan Koning
#   date: 2023-12-12
#   format: YANDF-0.1
# residual:
#   Z: 41
#   A: 93
#   nuclide: Nb93
# parameters:
#   ldmodel keyword: 1
#   level density model: Gilbert-Cameron
#   Collective enhacement: n
#   a(Sn) [MeV^-1]:  1.233156E+01
#   asymptotic a [MeV^-1]:  1.224515E+01
#   shell correction [MeV]:  1.037895E-01
#   damping gamma:  9.559104E-02
#   pairing energy [MeV]:  1.244342E+00
#   adjusted pairing shift [MeV]:  0.000000E+00
#   separation energy [MeV]:  8.830873E+00
#   discrete spin cutoff parameter:  1.165425E+01
#   spin cutoff parameter(Sn):  2.095789E+01
#   matching energy [MeV]:  7.615608E+00
#   temperature [MeV]:  8.670035E-01
#   E0 [MeV]: -1.345862E+00
#   Nlow: 5
#   Ntop: 15
#   ctable:  1.000000E-20
```

```
#    ptable:  1.000000E-20
# observables:
#    experimental D0 [eV]:  0.000000E+00
#    experimental D0 unc. [eV]:  0.000000E+00
#    theoretical D0 [eV]:  7.795445E+01
#    Chi-2 D0:  0.000000E+00
#    C/E D0:  0.000000E+00
#    Frms D0:  0.000000E+00
#    Erms D0:  0.000000E+00
#    Chi-2 per level:  1.128847E-01
#    Frms per level:  1.030749E+00
#    Erms per level:  1.005810E+00
#    average deviation per level:  7.030114E-02
# datablock:
#    quantity: level density
#    columns: 6
#    entries: 100
##       E             Level       N_cumulative       Total LD          a
##     [MeV]             []             []           [MeV^-1]        [MeV^-1]
    9.498000E-01        6          7.096463E+00     1.628955E+01     1.236664E+01
    9.700000E-01        7          7.429368E+00     1.667353E+01     1.236664E+01
    9.789100E-01        8          7.578694E+00     1.684576E+01     1.236664E+01
    1.082680E+00        9          9.434585E+00     1.898762E+01     1.236664E+01
    1.127090E+00       10          1.029970E+01     1.998556E+01     1.236664E+01
    1.284260E+00       11          1.373884E+01     2.395769E+01     1.236641E+01
    1.290000E+00       12          1.387682E+01     2.411683E+01     1.236638E+01
....................................
```

With **outgamma y** the gamma-ray information is printed. First, all relevant parameters are given: the total radiative width Γ_Γ, the s-wave resonance spacing D_0, the s-wave strength function S_0 and the normalization factor for the gamma-ray strength function. Second, we print the giant resonance information. For each multipolarity, we print the strength of the giant resonance σ_0, its energy and its width. Next, the gamma-ray strength function and transmission coefficients for this multipolarity and as a function of energy are printed. This output block begins with:

```
########## GAMMA STRENGTH FUNCTIONS, TRANSMISSION COEFFICIENTS AND CROSS SEC

 Gamma-ray information for Z= 41 N= 53 ( 94Nb)


 S-wave strength function parameters:


 Exp. total radiative width=   0.14500 eV +/- 0.01000 Theor. total radiative
                                                      Theor. total radiative
                                                      Theor. total radiative
 Exp. D0                   =     80.00 eV +/-   10.00 Theor. D0
                                                      Theor. D1

 Theor. S-wave strength f. =  15.47386E-4
 Average resonance energy  =     10000.00 eV
```

```
 Incident energy: E[MeV]=  14.000

 Gamma-ray strength function model for E1: IAEA-CRP SMLO 2019 Tables

 Gamma-ray strength function model for M1: IAEA GSF CRP (2018)

 Adjustable parameters for E1: etable=   0.00000 ftable=   1.00000 wtable=

 Inclusion of an E1 upbend C x U*/ (1+exp(E-eta)) with  C=  0.00E+00 eta=

 Inclusion of an M1 upbend C exp(-F*|beta2|) exp(-eta*E) with C=  3.50E-0

 Normalized gamma-ray strength functions and transmission coefficients for l= 1

 Giant resonance parameters :

 sigma0(M1) =    1.322        sigma0(E1) = 192.148    PR: sigma0(M1) =    0.066
      E(M1) =    8.441            E(E1) =   16.523    PR:      E(M1) =    3.174
  gamma(M1) =    4.000        gamma(E1) =    5.515    PR:  gamma(M1) =    1.500
      k(M1) =    8.67373E-08      k(E1) =    8.67373E-08


      E        f(M1)          f(E1)          T(M1)          T(E1)


    0.001  1.79672E-08  1.56975E-09  1.12891E-16  2.65817E-17
    0.002  1.79538E-08  1.57089E-09  9.02457E-16  2.12748E-16
    0.005  1.79122E-08  1.57435E-09  1.40682E-14  3.32861E-15
    0.010  1.78432E-08  1.58011E-09  1.12112E-13  2.66879E-14
    0.020  1.77059E-08  1.59153E-09  8.89998E-13  2.14444E-13
    0.050  1.73010E-08  1.62634E-09  1.35881E-11  3.39519E-12
...................................
```

which is repeated for each *l*-value. Finally, the photoabsorption cross section is printed:

```
Photoabsorption cross sections

  E [MeV]    xs [mb]


  1.000000E-03   2.559201E-04
  2.000000E-03   6.118469E-04
  5.000000E-03   1.377138E-03
  1.000000E-02   2.647125E-03
  2.000000E-02   5.166643E-03
  5.000000E-02   1.256542E-02
...................................
```

Since we put in this input file the keyword **filepsf y** detailed PSF information is also available in separate output files. For example **psf041094.E1** reads as follows:

```
# header:
#   title: Nb94 photon strength function
#   source: TALYS-2.0
#   user: Arjan Koning
```

```
#    date: 2023-12-12
#    format: YANDF-0.1
# residual:
#    Z: 41
#    A: 94
#    nuclide: Nb94
# parameters:
#    strength keyword: 9
#    PSF model: IAEA-CRP SMLO 2019 Tables
#    radiation type: E1
# observables:
#    experimental Gamma_gamma [eV]:  1.450000E-01
#    experimental Gamma_gamma unc. [eV]:  1.000000E-02
#    theoretical Gamma_gamma [eV]:  1.236158E-01
#    C/E Gamma_gamma:  8.525231E-01
# datablock:
#    quantity: photon strength function
#    columns: 2
#    entries: 86
##       E              f(E1)
##     [MeV]             []
   1.000000E-03   1.569746E-09
   2.000000E-03   1.570894E-09
   5.000000E-03   1.574351E-09
   1.000000E-02   1.580114E-09
   2.000000E-02   1.591526E-09
.......................................
```

Case e: Detailed pre-equilibrium information

The single- and double-differential spectra have already been covered in sample 1b. In addition to this, the contribution of the pre-equilibrium mechanism to the spectra and cross sections can be printed in more detail with the **outpreequilibrium** keyword. With the input file

```
#
# n-Nb093-14MeV-preeq
#
# General
#
projectile n
element nb
mass 93
energy 14.
#
# Output
#
outpreequilibrium y
outspectra y
ddxmode 2
```

we obtain, in addition to the aforementioned output blocks, a detailed outline of the pre-equilibrium model used, in this case the default: the two-component exciton model. First, the

parameters for the exciton model are printed, followed by the matrix elements as a function of the exciton number:

```
 ########## PRE-EQUILIBRIUM ##########

 ++++++++++ TWO-COMPONENT EXCITON MODEL ++++++++++

 1. Matrix element for E=  21.076

 Constant for matrix element :   1.000
 p-p ratio for matrix element:   1.000
 n-n ratio for matrix element:   1.500
 p-n ratio for matrix element:   1.000
 n-p ratio for matrix element:   1.000

 p(p) h(p) p(n) h(n)     M2pipi      M2nunu      M2pinu      M2nupi

   0    0    1    0     2.63420E-05 3.95131E-05 2.63420E-05 2.63420E-05
   0    0    2    1     1.08884E-04 1.63327E-04 1.08884E-04 1.08884E-04
   1    1    1    0     1.08884E-04 1.63327E-04 1.08884E-04 1.08884E-04
   0    0    3    2     1.76643E-04 2.64964E-04 1.76643E-04 1.76643E-04
   1    1    2    1     1.76643E-04 2.64964E-04 1.76643E-04 1.76643E-04
.....................................
```

Next, the emission rates are printed: first as function of particle type and particle-hole number, and in the last column summed over particles:

```
 2. Emission rates or escape widths

 A. Emission rates ( /sec)

 p(p) h(p) p(n) h(n)     gamma       neutron      proton      deuteron     triton

   0    0    1    0     2.16570E+18 0.00000E+00 0.00000E+00 0.00000E+00 0.00000E+0
   0    0    2    1     5.29285E+17 1.63578E+21 0.00000E+00 0.00000E+00 0.00000E+0
   1    1    1    0     5.58040E+17 8.15540E+20 2.32728E+20 2.79804E+19 0.00000E+0
   0    0    3    2     1.26381E+17 4.52770E+20 0.00000E+00 0.00000E+00 0.00000E+0
   1    1    2    1     1.08464E+17 3.04371E+20 1.11136E+19 3.36637E+18 9.21406E+1
.....................................
```

Also, the alternative representation in terms of the escape widths, see Eqs. (12.51) and (12.52), is given,

```
 B. Escape widths (MeV)

 p(p) h(p) p(n) h(n)     gamma       neutron      proton      deuteron     triton

   0    0    1    0     1.42549E-03 0.00000E+00 0.00000E+00 0.00000E+00 0.00000E+0
   0    0    2    1     3.48382E-04 1.07669E+00 0.00000E+00 0.00000E+00 0.00000E+0
   1    1    1    0     3.67309E-04 5.36798E-01 1.53184E-01 1.84170E-02 0.00000E+0
   0    0    3    2     8.31858E-05 2.98019E-01 0.00000E+00 0.00000E+00 0.00000E+0
```

```
1    1    2    1     7.13921E-05 2.00341E-01 7.31511E-03 2.21578E-03 6.06481E-0
2    2    1    0     9.92804E-05 8.90114E-02 1.26899E-02 1.26325E-03 0.00000E+0
.....................................
```

The internal transition rates such as those of Eq. (12.17) and the associated damping and total
widths are given next,

```
 3. Internal transition rates or damping widths, total widths

 A. Internal transition rates ( /sec)

 p(p) h(p) p(n) h(n)     lambdapiplus   lambdanuplus    lambdapinu      lambdanup

 0    0    1    0     1.45456E+21     1.74977E+21     0.00000E+00     0.00000E+0
 0    0    2    1     3.18197E+21     3.67047E+21     0.00000E+00     1.62232E+2
 1    1    1    0     1.74347E+21     3.78846E+21     1.30118E+20     0.00000E+0
 0    0    3    2     3.26507E+21     3.59251E+21     0.00000E+00     7.12888E+2
 1    1    2    1     2.35211E+21     3.64486E+21     1.72552E+20     2.29011E+2
.....................................
```

The lifetimes, $t(p,h)$ of Eq. (12.40) and the depletion factors $D_{p,h}$ of Eq. (12.41), are printed
next,

```
 4. Lifetimes
 p(p) h(p) p(n) h(n)       Strength

  0    0    1    0       3.11867E-22
  0    0    2    1       6.41109E-23
  1    1    1    0       6.88639E-23
  0    0    3    2       3.09624E-23
  1    1    2    1       7.50433E-23
  2    2    1    0       2.43181E-23
.....................................
```

The partial state densities are printed for the first particle-hole combinations as a function of
excitation energy. We also print the exciton number-dependent spin distributions and their sum,
to see whether we have exhausted all spins. This output block is as follows

```
 ++++++++++ PARTIAL STATE DENSITIES ++++++++++

 Particle-hole state densities

   Ex   P(n=3)   gp     gn                           Configuration p(p) h(p)
                           1 1 0 0   0 0 1 1   1 1 1 0   1 0 1 1   2 1 0 0

 1.000  0.000  2.733  3.533 7.471E+00 1.248E+01 9.728E+00 1.139E+01 0.000E+00
 2.000  0.000  2.733  3.533 1.494E+01 2.497E+01 4.559E+01 5.633E+01 8.212E+00
 3.000  0.000  2.733  3.533 2.241E+01 3.745E+01 1.078E+02 1.354E+02 2.627E+01
 4.000  0.000  2.733  3.533 2.988E+01 4.994E+01 1.965E+02 2.486E+02 5.453E+01
 5.000  0.000  2.733  3.533 3.736E+01 6.242E+01 3.116E+02 3.959E+02 9.301E+01
 6.000  0.000  2.733  3.533 4.483E+01 7.491E+01 4.530E+02 5.774E+02 1.417E+02
```

```
.....................................
 Particle-hole spin distributions

   n      J= 0        J= 1        J= 2        J= 3        J= 4        J= 5

   1  1.7785E-02  4.3554E-02  4.8369E-02  3.6832E-02  2.1025E-02  9.3136E-03
   2  6.3683E-03  1.7261E-02  2.3483E-02  2.4247E-02  2.0773E-02  1.5284E-02
   3  3.4812E-03  9.7603E-03  1.4208E-02  1.6237E-02  1.5926E-02  1.3878E-02
   4  2.2659E-03  6.4613E-03  9.7295E-03  1.1698E-02  1.2277E-02  1.1642E-02
   5  1.6234E-03  4.6764E-03  7.1862E-03  8.9070E-03  9.7354E-03  9.7128E-03
.....................................
```

We print a table with the pre-equilibrium cross sections per stage and outgoing energy, for each outgoing particle. At the end of each table, we give the total pre-equilibrium cross sections per particle. Finally the total pre-equilibrium cross section summed over outgoing particles is printed,

```
 ++++++++++ TOTAL PRE-EQUILIBRIUM CROSS SECTIONS ++++++++++

 Pre-equilibrium cross sections for gamma

    E       Total        p=1         p=2         p=3         p=4         p=5

  0.001 2.2249E-13 9.1810E-14 5.0384E-14 3.8551E-14 4.1750E-14 0.0000E+00 0.000
  0.002 2.1767E-12 8.9578E-13 4.9358E-13 3.7794E-13 4.0941E-13 0.0000E+00 0.000
  0.005 2.9926E-11 1.2218E-11 6.8126E-12 5.2280E-12 5.6681E-12 0.0000E+00 0.000
  0.010 2.2566E-10 9.0941E-11 5.1690E-11 3.9811E-11 4.3221E-11 0.0000E+00 0.000
  0.020 1.7108E-09 6.7253E-10 3.9631E-10 3.0739E-10 3.3461E-10 0.0000E+00 0.000
  0.050 2.4211E-08 8.9017E-09 5.7581E-09 4.5550E-09 4.9961E-09 0.0000E+00 0.000
  0.100 1.7108E-07 5.7425E-08 4.1833E-08 3.4050E-08 3.7774E-08 0.0000E+00 0.000
.....................................
 19.000 1.3505E-01 1.3040E-01 4.3802E-03 2.6369E-04 4.8448E-06 0.0000E+00 0.000
 19.500 1.2227E-01 1.1875E-01 3.4007E-03 1.2338E-04 6.6196E-07 0.0000E+00 0.000
 20.000 1.1171E-01 1.0895E-01 2.7321E-03 3.1776E-05 0.0000E+00 0.0000E+00 0.000
 21.000 0.0000E+00 0.0000E+00 0.0000E+00 0.0000E+00 0.0000E+00 0.0000E+00 0.000
 22.000 0.0000E+00 0.0000E+00 0.0000E+00 0.0000E+00 0.0000E+00 0.0000E+00 0.000

         1.2864E+00 1.1291E+00 1.2096E-01 2.6279E-02 1.0140E-02 0.0000E+00 0.000

 Integrated:    1.28644


 Pre-equilibrium cross sections for neutron

    E       Total        p=1         p=2         p=3         p=4         p=5

  0.001 9.4598E-02 0.0000E+00 2.6248E-02 2.5416E-02 2.0231E-02 1.4060E-02 8.642
  0.002 1.4281E-01 0.0000E+00 3.9637E-02 3.8373E-02 3.0539E-02 2.1220E-02 1.304
  0.005 2.6901E-01 0.0000E+00 7.4728E-02 7.2301E-02 5.7513E-02 3.9941E-02 2.453
  0.010 4.8271E-01 0.0000E+00 1.3428E-01 1.2979E-01 1.0316E-01 7.1572E-02 4.391
  0.020 9.7103E-01 0.0000E+00 2.7090E-01 2.6131E-01 2.0733E-01 1.4358E-01 8.790
```

```
....................................
17.500 2.5293E-01 0.0000E+00 0.0000E+00 0.0000E+00 0.0000E+00 0.0000E+00 0.000
18.000 0.0000E+00 0.0000E+00 0.0000E+00 0.0000E+00 0.0000E+00 0.0000E+00 0.000
18.500 0.0000E+00 0.0000E+00 0.0000E+00 0.0000E+00 0.0000E+00 0.0000E+00 0.000
19.000 0.0000E+00 0.0000E+00 0.0000E+00 0.0000E+00 0.0000E+00 0.0000E+00 0.000

       2.6727E+01 0.0000E+00 0.0000E+00 0.0000E+00 1.0326E-02 1.1088E-02 4.974


Integrated:    26.72690


Total pre-equilibrium cross section:   415.82114
```

Sample case 4.2 Case f: Discrete direct cross sections and angular distributions

More specific information on the characteristics of direct reactions can be obtained with the
following input file,

```
#
# n-Nb093-14MeV-discrete
#
# General
#
projectile n
element nb
mass 93
energy 14.
#
# Output
#
outdiscrete        y
outangle           y
outlegendre        y
outdirect          y
outspectra         y
```

Now we obtain, through **outdirect y**, the direct cross sections from inelastic collective scattering
and giant resonances. The output block begins with

```
++++++++++ DIRECT CROSS SECTIONS ++++++++++

Direct inelastic cross sections

Level  Energy   E-out     J/P   Cross section  Def. par.

  3    0.74395  13.10459  3.5+     3.27713      B  0.04108
  4    0.80882  13.03972  2.5+     0.03425      B  0.00586
  5    0.81032  13.03822  2.5-     2.45130      B  0.03558
  6    0.94980  12.89874  6.5+     5.68166      B  0.05434
  8    0.97891  12.86963  5.5+     4.86351      B  0.05031
```

```
   9   1.08268  12.76586    4.5+     4.03323    B  0.04593
....................................


 Discrete direct inelastic cross section:    23.76406   Level 1- 30
 Collective cross section in continuum  :    32.30161
```

which for the case of ^{93}Nb gives the results of the weak-coupling model. For every level, the angular distribution is given, since **outangle y** was specified:

```
 Direct inelastic angular distributions

 Angle Ex= 0.744   Ex= 0.809   Ex= 0.810   Ex= 0.950   Ex= 0.979   Ex= 1.083
       JP= 3.5+    JP= 2.5+    JP= 2.5-    JP= 6.5+    JP= 5.5+    JP= 4.5+


   0.0 1.00425E+00 1.58216E-03 7.50804E-01 1.73829E+00 1.48762E+00 1.23259E+00
   2.0 1.00116E+00 1.59623E-03 7.48488E-01 1.73292E+00 1.48303E+00 1.22878E+00
   4.0 9.92237E-01 1.63798E-03 7.41812E-01 1.71744E+00 1.46977E+00 1.21779E+00
   6.0 9.78514E-01 1.70633E-03 7.31535E-01 1.69357E+00 1.44933E+00 1.20082E+00
....................................
```

The table with total giant resonance results is given next,

```
 ++++++++++ GIANT RESONANCES ++++++++++

       Cross section   Exc. energy Emis. energy   Width     Deform. par.

 GMR  :     0.00000    16.37500    -2.52646     3.00000     0.02645
 GQR  :     0.00000    14.34671    -0.49817     4.14092     0.14236
 LEOR :    24.61940     6.84228     7.00626     5.00000     0.15971
 HEOR :     0.00000    25.38264   -11.53410     7.36250     0.13210

 Total:    24.61940
```

followed, since **outspectra y**, by the associated spectra,

```
 Giant resonance spectra

  Energy   Total      GMR        GQR        LEOR       HEOR      Collective

   0.001 7.7214E-03 0.0000E+00 0.0000E+00 7.7214E-03 0.0000E+00 0.0000E+00
   0.002 7.7337E-03 0.0000E+00 0.0000E+00 7.7337E-03 0.0000E+00 0.0000E+00
   0.005 7.7706E-03 0.0000E+00 0.0000E+00 7.7706E-03 0.0000E+00 0.0000E+00
   0.010 7.8325E-03 0.0000E+00 0.0000E+00 7.8325E-03 0.0000E+00 0.0000E+00
   0.020 7.9577E-03 0.0000E+00 0.0000E+00 7.9577E-03 0.0000E+00 0.0000E+00
   0.050 8.3441E-03 0.0000E+00 0.0000E+00 8.3441E-03 0.0000E+00 0.0000E+00
....................................
```

The total, i.e. direct + compound cross section per discrete level of each residual nucleus was already described for sample 1b. In addition, we have now requested the angular distributions and the associated Legendre coefficients. First, the angular distribution for elastic scattering,

separated by direct and compound contribution, is given. Since **outlegendre y** it is given first in terms of Legendre coefficients. This output block begins with:

```
8. Discrete state angular distributions


8a1. Legendre coefficients for elastic scattering

  L         Total           Direct          Compound         Normalized

  0       1.75971E+02     1.75971E+02       4.71035E-05       7.95776E-02
  1       1.55728E+02     1.55728E+02       0.00000E+00       7.04232E-02
  2       1.39720E+02     1.39720E+02       1.86062E-06       6.31840E-02
  3       1.21488E+02     1.21488E+02       0.00000E+00       5.49390E-02
  4       1.02659E+02     1.02659E+02       3.25580E-07       4.64241E-02
...................................
```

where the final column means division of the Legendre coefficients by the cross section. This is followed by the associated angular distribution. This output block begins with:

```
8a2. Elastic scattering angular distribution

Angle         Total           Direct          Compound

  0.0       6.69554E+03     6.69554E+03       6.12260E-05
  2.0       6.62134E+03     6.62134E+03       6.11570E-05
  4.0       6.40317E+03     6.40317E+03       6.09526E-05
  6.0       6.05390E+03     6.05390E+03       6.06204E-05
  8.0       5.59369E+03     5.59369E+03       6.01725E-05
 10.0       5.04824E+03     5.04824E+03       5.96247E-05
 12.0       4.44657E+03     4.44657E+03       5.89949E-05
...................................
```

Next, the Legendre coefficients for inelastic scattering to each discrete level, separated by the direct and compound contribution, is given. This output block begins with:

```
8b1. Legendre coefficients for inelastic scattering

   Level  1

  L         Total           Direct          Compound         Normalized

  0       5.43660E-04     5.33254E-04       1.04057E-05       7.95775E-02
  1       1.86109E-04     1.86109E-04       0.00000E+00       2.72415E-02
  2       6.20916E-05     6.21244E-05      -3.27812E-08       9.08857E-03
  3       1.66523E-05     1.66523E-05       0.00000E+00       2.43746E-03
  4      -1.37214E-05    -1.35853E-05      -1.36110E-07      -2.00846E-03
  5      -1.90397E-05    -1.90397E-05       0.00000E+00      -2.78691E-03
  6      -1.61471E-05    -1.61584E-05       1.12224E-08      -2.36352E-03
...................................
```

which is also followed by the associated angular distributions. This output block begins with:

```
8b2. Inelastic angular distributions

   Level  1

 Angle        Total            Direct         Compound

   0.0     1.07320E-03     1.06392E-03     9.28143E-06
   2.0     1.07540E-03     1.06611E-03     9.28519E-06
   4.0     1.08196E-03     1.07266E-03     9.29647E-06
   6.0     1.09280E-03     1.08348E-03     9.31533E-06
   8.0     1.10774E-03     1.09840E-03     9.34185E-06
  10.0     1.12646E-03     1.11708E-03     9.37618E-06
  12.0     1.14844E-03     1.13902E-03     9.41848E-06
.....................................
```

Finally, the same is given for the (n, p) and the other channels.

Case g: Discrete gamma-ray production cross sections
The gamma-ray intensity for each mother and daughter discrete level appearing in the reaction can be obtained with the following input file,

```
#
# n-Nb093-14MeV-gamma
#
# General
#
projectile n
element nb
mass 93
energy 14.
#
# Output
#
outgamdis           y
```

For all discrete gamma-ray transitions, the intensity is printed. For each nucleus, the initial level and the final level is given, the associated gamma energy and the cross section. This output block begins with:

```
10. Gamma-ray intensities

 Nuclide:  94Nb

    Initial level            Final level      Gamma Energy  Cross section

 no.  J/Pi    Ex          no.  J/Pi    Ex

  2   4.0+  0.0587  --->  1    3.0+  0.0409     0.01780      2.11853E-01
  3   6.0+  0.0787  --->  0    6.0+  0.0000     0.07867      2.12745E-01
  4   5.0+  0.1134  --->  0    6.0+  0.0000     0.11340      8.56884E-02
```

```
   4   5.0+  0.1134  --->  2   4.0+  0.0587    0.05470    3.36955E-02
   5   2.0-  0.1403  --->  1   3.0+  0.0409    0.09941    2.43882E-01
   6   2.0-  0.3016  --->  5   2.0-  0.1403    0.16126    5.42965E-02
   7   4.0+  0.3118  --->  2   4.0+  0.0587    0.25311    5.48060E-02
.................................
```

When we discuss multiple incident energy runs in the other sample cases, we will see how the excitation functions for gamma production cross sections per level are accumulated and how they can be written to separate files for easy processing.

Case h: The full output file

In this sample case we print basically everything that can be printed in the main output file for a single-energy reaction on a non-fissile nucleus. The input file is

```
#
# n-Nb093-14MeV-full
#
# General
#
projectile n
element nb
mass 93
energy 14.
#
# Output
#
outbasic            y
outpreequilibrium   y
outspectra          y
outangle            y
outlegendre         y
ddxmode             2
outgamdis           y
partable            y
```

resulting in an output file that contains all nuclear structure information, all partial results, and moreover all intermediate results of the calculation, as well as results of intermediate checking. Note that basically all flags in the "Output" block on top of the output file are set to **y**, the only exceptions being irrelevant for this sample case. In addition to the output that is already described, various other output blocks are present. First, since **outbasic y** automatically means **outomp y**, a block with optical model parameters is printed. The optical model parameters for all included particles are given as a function of incident energy. This output block begins with:

```
 ######### OPTICAL MODEL PARAMETERS ##########

          neutron   on   93Nb

  Energy    V     rv    av    W     rw    aw    Vd    rvd   avd   Wd    rwd   awd

   0.001  51.02 1.215 0.663  0.14 1.215 0.663  0.00 1.274 0.534  3.32 1.274 0.53
```

```
   0.002  51.02 1.215 0.663   0.14 1.215 0.663   0.00 1.274 0.534   3.32 1.274 0.53
   0.005  51.02 1.215 0.663   0.14 1.215 0.663   0.00 1.274 0.534   3.32 1.274 0.53
   0.010  51.02 1.215 0.663   0.14 1.215 0.663   0.00 1.274 0.534   3.33 1.274 0.53
   0.020  51.02 1.215 0.663   0.14 1.215 0.663   0.00 1.274 0.534   3.33 1.274 0.53
.................................
```

In the next part, we print general quantities that are used throughout the nuclear reaction calculations, such as transmission coefficients and inverse reaction cross sections. The transmission coefficients as a function of energy are given for all particles included in the calculation. Depending upon whether **outtransenergy y** or **outtransenergy n**, the transmission coefficient tables will be grouped per energy or per angular momentum, respectively. The latter option may be helpful to study the behavior of a particular transmission coefficient as a function of energy. The default is **outtransenergy n**, leading to the following output block,

```
 ########## TRANSMISSION COEFFICIENTS AND INVERSE REACTION CROSS SECTIONS ######

 Transmission coefficients for incident neutron  at   0.00101 MeV

   L   T(L-1/2,L)   T(L+1/2,L)    Tav(L)

   0  0.00000E+00  8.82145E-03  8.82145E-03
   1  1.45449E-04  2.56136E-04  2.19240E-04

 Transmission coefficients for incident neutron  at   0.00202 MeV

   L   T(L-1/2,L)   T(L+1/2,L)    Tav(L)

   0  0.00000E+00  1.24534E-02  1.24534E-02
   1  4.11628E-04  7.24866E-04  6.20454E-04
   2  2.55785E-08  1.88791E-08  2.15588E-08

 Transmission coefficients for incident neutron  at   0.00505 MeV

   L   T(L-1/2,L)   T(L+1/2,L)    Tav(L)

   0  0.00000E+00  1.96205E-02  1.96205E-02
   1  1.62890E-03  2.86779E-03  2.45483E-03
   2  2.52135E-07  1.86214E-07  2.12582E-07
.................................
```

which is repeated for each included particle type. Next, the (inverse) reaction cross sections is given for all particles on a LAB energy grid. For neutrons also the total elastic and total cross section on this energy grid is printed for completeness. This output block begins with:

```
 Total cross sections for neutron

    E         total       reaction    elastic   OMP reaction

  0.00101  1.1594E+04  6.2369E+03  5.3566E+03  6.2369E+03
  0.00202  1.0052E+04  4.7092E+03  5.3430E+03  4.7092E+03
```

```
   0.00505  8.8645E+03  3.5518E+03  5.3127E+03  3.5518E+03
   0.01011  8.4660E+03  3.1918E+03  5.2741E+03  3.1918E+03
   0.02022  8.4357E+03  3.2208E+03  5.2148E+03  3.2208E+03
   0.05054  8.9304E+03  3.8249E+03  5.1055E+03  3.8249E+03
   0.10109  9.6344E+03  4.5808E+03  5.0536E+03  4.5808E+03
   0.20217  1.0198E+04  5.0370E+03  5.1609E+03  5.0370E+03
   0.30326  1.0068E+04  4.7878E+03  5.2799E+03  4.7878E+03
   0.40434  9.6390E+03  4.3377E+03  5.3013E+03  4.3377E+03
   0.50543  9.1158E+03  3.8893E+03  5.2264E+03  3.8893E+03
   0.60651  8.5881E+03  3.5056E+03  5.0825E+03  3.5056E+03
   0.70760  8.0915E+03  3.1968E+03  4.8946E+03  3.1968E+03
 ...................................
```

The final column "OMP reaction" gives the reaction cross section as obtained from the optical model. This is not necessary the same as the adopted reaction cross section of the middle column, since sometimes (especially for complex particles) this is overruled by systematics, see the **sysreaction** keyword, (p. 545). For the incident energy, we separately print the OMP parameters, the transmission coefficients and the shape elastic angular distribution,

```
+++++++++ OPTICAL MODEL PARAMETERS FOR INCIDENT CHANNEL ++++++++++

         neutron  on  93Nb

 Energy   V    rv    av    W     rw    aw    Vd   rvd   avd   Wd   rwd   awd

  14.000  46.11 1.215 0.663  0.98 1.215 0.663  0.00 1.274 0.534  6.84 1.274 0.53

 Optical model results

 Total cross section    : 3.9819E+03 mb
 Reaction cross section: 1.7706E+03 mb
 Elastic cross section : 2.2113E+03 mb

 Transmission coefficients for incident neutron  at   14.000 MeV

  L    T(L-1/2,L)    T(L+1/2,L)    Tav(L)

  0  0.00000E+00  7.46404E-01  7.46404E-01
  1  8.02491E-01  7.78050E-01  7.86197E-01
  2  7.77410E-01  8.08483E-01  7.96054E-01
  3  7.75550E-01  6.94249E-01  7.29092E-01
  4  9.15115E-01  9.53393E-01  9.36381E-01
  5  6.01374E-01  6.19435E-01  6.11226E-01
  6  7.00430E-01  4.72026E-01  5.77443E-01
  7  1.15102E-01  1.90743E-01  1.55444E-01
  8  1.59959E-02  1.88919E-02  1.75291E-02
  9  2.36267E-03  2.49532E-03  2.43249E-03
 10  3.55525E-04  3.61442E-04  3.58625E-04
 11  5.38245E-05  5.39431E-05  5.38864E-05
 12  8.20113E-06  8.17260E-06  8.18630E-06
 13  1.26174E-06  1.25428E-06  1.25788E-06
```

```
 Shape elastic scattering angular distribution

 Angle    Cross section

   0.0      6.69554E+03
   2.0      6.62134E+03
   4.0      6.40317E+03
   6.0      6.05390E+03
   8.0      5.59369E+03
  10.0      5.04824E+03
  12.0      4.44657E+03
  14.0      3.81867E+03
  16.0      3.19323E+03
  18.0      2.59561E+03
  20.0      2.04638E+03
.....................................
```

At some point during a run, TALYS has performed the direct reaction calculation and the
pre-equilibrium calculation. A table is printed which shows the part of the reaction population
that is left for the formation of a compound nucleus. Since the pre-equilibrium cross sections are
calculated on an emission energy grid, there is always a small numerical error when transferring
these results to the excitation energy grid. The pre-equilibrium spectra are therefore normalized.
The output block looks as follows

```
 ########## POPULATION CHECK ##########

 Particle Pre-equilibrium Population

 gamma          1.28644       1.27794
 neutron      428.71729     410.91696
 proton        25.24361      25.20203
 deuteron       3.50197       3.49032
 triton         0.09480       0.09451
 helium-3       0.00000       0.00000
 alpha         26.72690      26.64193


 ++++++++++ Normalization of reaction cross section ++++++++++

 Reaction cross section            : 1770.63000 (A)
 Sum over T(j,l)                   : 1770.62537 (B)
 Compound nucleus formation c.s. : 1243.46240 (C)
 Ratio C/B                         :    0.70227
```

After the compound nucleus calculation, the results from the binary reaction are printed. First, the
binary cross sections for the included outgoing particles are printed, followed by, if **outspectra
y**, the binary emission spectra. If also **outcheck y**, the integral over the emission spectra is
checked against the cross sections. The printed normalization factor has been applied to the
emission spectra. This output block begins with:

```
########## BINARY CHANNELS ###########


++++++++++ BINARY CROSS SECTIONS ++++++++++


gamma     channel to Z= 41 N= 53 ( 94Nb): 2.23665E+00
neutron   channel to Z= 41 N= 52 ( 93Nb): 1.68950E+03
proton    channel to Z= 40 N= 53 ( 93Zr): 3.79183E+01
deuteron  channel to Z= 40 N= 52 ( 92Zr): 1.04112E+01
triton    channel to Z= 40 N= 51 ( 91Zr): 6.70826E-01
helium-3  channel to Z= 39 N= 52 ( 91Y ): 2.35820E-08
alpha     channel to Z= 39 N= 51 ( 90Y ): 2.98966E+01


Binary emission spectra

 Energy    gamma         neutron       proton        deuteron      triton        helium-3

  0.001 1.14462E-06 1.89788E+00 0.00000E+00 0.00000E+00 0.00000E+00 0.00000E+0
  0.002 2.28923E-06 3.74165E+00 0.00000E+00 0.00000E+00 0.00000E+00 0.00000E+0
  0.005 5.72311E-06 9.25456E+00 0.00000E+00 0.00000E+00 0.00000E+00 0.00000E+0
  0.010 1.14464E-05 1.84461E+01 0.00000E+00 0.00000E+00 0.00000E+00 0.00000E+0
  0.020 2.28940E-05 3.68901E+01 0.00000E+00 0.00000E+00 0.00000E+00 0.00000E+0
  0.050 5.72550E-05 9.26411E+01 0.00000E+00 0.00000E+00 0.00000E+00 0.00000E+0
  0.100 1.14633E-04 1.86293E+02 0.00000E+00 0.00000E+00 0.00000E+00 0.00000E+0
  0.200 2.30055E-04 3.28686E+02 2.64905E-30 1.35926E-43 0.00000E+00 0.00000E+0
  0.300 7.48114E-04 4.14446E+02 3.56019E-23 9.99027E-34 9.03852E-41 0.00000E+0
  0.400 1.81798E-03 4.97986E+02 5.12047E-19 1.48517E-27 3.14528E-33 0.00000E+0
  0.500 2.88939E-03 5.48371E+02 3.42302E-16 1.47275E-23 2.43692E-28 0.00000E+0
  0.600 3.96241E-03 5.39365E+02 4.07677E-14 1.28871E-20 9.22918E-25 0.00000E+0
  0.700 5.03710E-03 5.29973E+02 1.64259E-12 2.45195E-18 5.46266E-22 0.00000E+0
...................................
++++++++++ CHECK OF INTEGRATED BINARY EMISSION SPECTRA ++++++++++

            Continuum cross section  Integrated spectrum  Compound normalizatio

gamma              2.19555E+00          2.19555E+00          1.00011E+00
neutron            1.66025E+03          1.64343E+03          1.01805E+00
proton             3.43220E+01          3.43220E+01          1.00226E+00
deuteron           3.51689E+00          3.51689E+00          1.02829E+00
triton             9.54471E-02          9.54471E-02          1.01145E+00
helium-3           2.86109E-10          2.86109E-10          0.00000E+00
alpha              2.86177E+01          2.86176E+01          9.99189E-01
```

Since **outpopulation y**, the population that remains in the first set of residual nuclides after binary emission is printed,

```
++++++++++ POPULATION AFTER BINARY EMISSION ++++++++++


Population of Z= 41 N= 53 ( 94Nb) after binary gamma    emission: 2.23665E+00
Maximum excitation energy:  21.076 Discrete levels: 10 Continuum bins: 40 Conti


bin    Ex    Popul.    J= 0.0-   J= 0.0+   J= 1.0-   J= 1.0+   J= 2.0-   J= 2.0
```

```
 0    0.000 3.206E-07 0.000E+00 0.000E+00 0.000E+00 0.000E+00 0.000E+00 0.000E+
 1    0.041 1.889E-07 0.000E+00 0.000E+00 0.000E+00 0.000E+00 0.000E+00 0.000E+
 2    0.059 2.525E-07 0.000E+00 0.000E+00 0.000E+00 0.000E+00 0.000E+00 0.000E+
 3    0.079 1.528E-03 0.000E+00 0.000E+00 0.000E+00 0.000E+00 0.000E+00 0.000E+
 4    0.113 3.443E-03 0.000E+00 0.000E+00 0.000E+00 0.000E+00 0.000E+00 0.000E+
 5    0.140 1.051E-02 0.000E+00 0.000E+00 0.000E+00 0.000E+00 1.051E-02 0.000E+
 6    0.302 9.579E-03 0.000E+00 0.000E+00 0.000E+00 0.000E+00 9.579E-03 0.000E+
 7    0.312 1.818E-03 0.000E+00 0.000E+00 0.000E+00 0.000E+00 0.000E+00 0.000E+
 8    0.334 4.717E-03 0.000E+00 0.000E+00 0.000E+00 0.000E+00 0.000E+00 0.000E+
 9    0.396 6.486E-03 0.000E+00 0.000E+00 0.000E+00 0.000E+00 0.000E+00 0.000E+
10    0.450 3.014E-03 0.000E+00 0.000E+00 0.000E+00 0.000E+00 0.000E+00 0.000E+
11    0.708 3.665E-02 2.036E-04 1.520E-04 1.592E-03 1.152E-03 3.293E-03 2.540E-
12    1.224 5.702E-02 2.592E-04 1.935E-04 2.065E-03 1.494E-03 4.428E-03 3.415E-
...................................
```

where in this case bins 0-10 concern discrete levels and bins 11-50 concern continuum bins.

After this output of the binary emission, we print for each nuclide in the decay chain the population as a function of excitation energy, spin and parity *before* it decays. This loop starts with the initial compound nucleus and the nuclides formed by binary emission. When all excitation energy bins of the nucleus have been depleted, the final production cross section (per ground state/isomer) is printed. The feeding from this nuclide to all its daughter nuclides is also given. If in addition **outspectra y**, the emission spectra for all outgoing particles from this nucleus are printed. At high incident energies, when generally **multipreeq y**, the result from multiple pre-equilibrium emission is printed (not included in this output). If **outcheck y**, it is checked whether the integral over the emission spectra from this nucleus is equal to the corresponding feeding cross section. This output block begins with:

```
 ########## MULTIPLE EMISSION ##########

 Population of Z= 41 N= 53 ( 94Nb) before decay: 3.58813E+00
Maximum excitation energy:  21.076 Discrete levels: 10 Continuum bins: 40 Conti

 bin    Ex    Popul.    J= 0.0    J= 1.0    J= 2.0    J= 3.0    J= 4.0    J= 5.0

 0    0.000 1.050E-06 0.000E+00 0.000E+00 0.000E+00 0.000E+00 0.000E+00 0.000E+
 1    0.041 6.181E-07 0.000E+00 0.000E+00 0.000E+00 6.181E-07 0.000E+00 0.000E+
 2    0.059 8.266E-07 0.000E+00 0.000E+00 0.000E+00 0.000E+00 8.266E-07 0.000E+
 3    0.079 1.525E-03 0.000E+00 0.000E+00 0.000E+00 0.000E+00 0.000E+00 0.000E+
 4    0.113 3.436E-03 0.000E+00 0.000E+00 0.000E+00 0.000E+00 0.000E+00 3.436E-
 5    0.140 1.049E-02 0.000E+00 0.000E+00 1.049E-02 0.000E+00 0.000E+00 0.000E+
 6    0.302 9.558E-03 0.000E+00 0.000E+00 9.558E-03 0.000E+00 0.000E+00 0.000E+
 7    0.312 1.814E-03 0.000E+00 0.000E+00 0.000E+00 0.000E+00 1.814E-03 0.000E+
 8    0.334 4.706E-03 0.000E+00 0.000E+00 0.000E+00 4.706E-03 0.000E+00 0.000E+
 9    0.396 6.472E-03 0.000E+00 0.000E+00 0.000E+00 6.472E-03 0.000E+00 0.000E+
10    0.450 3.008E-03 0.000E+00 0.000E+00 0.000E+00 3.008E-03 0.000E+00 0.000E+
11    0.708 3.657E-02 1.517E-04 1.150E-03 2.536E-03 3.531E-03 3.593E-03 2.702E-
12    1.224 5.693E-02 1.939E-04 1.497E-03 3.419E-03 5.023E-03 5.489E-03 4.513E-
13    1.739 6.580E-02 1.843E-04 1.443E-03 3.395E-03 5.210E-03 6.036E-03 5.335E-
14    2.255 7.347E-02 1.744E-04 1.381E-03 3.323E-03 5.274E-03 6.390E-03 5.973E-
```

```
.....................................
 Emitted flux per excitation energy bin of Z= 41 N= 53 ( 94Nb):


bin    Ex       gamma          neutron       proton       deuteron      triton       heli

   0    0.000 0.00000E+00 0.00000E+00 0.00000E+00 0.00000E+00 0.00000E+00 0.00000
   1    0.041 0.00000E+00 0.00000E+00 0.00000E+00 0.00000E+00 0.00000E+00 0.00000
   2    0.059 2.11853E-01 0.00000E+00 0.00000E+00 0.00000E+00 0.00000E+00 0.00000
   3    0.079 2.12745E-01 0.00000E+00 0.00000E+00 0.00000E+00 0.00000E+00 0.00000
   4    0.113 1.19384E-01 0.00000E+00 0.00000E+00 0.00000E+00 0.00000E+00 0.00000
   5    0.140 2.43882E-01 0.00000E+00 0.00000E+00 0.00000E+00 0.00000E+00 0.00000
   6    0.302 5.42965E-02 0.00000E+00 0.00000E+00 0.00000E+00 0.00000E+00 0.00000
.....................................
 Emission cross sections to residual nuclei from Z= 41 N= 53 ( 94Nb):


gamma     channel to Z= 41 N= 53 ( 94Nb): 2.66180E+00
neutron   channel to Z= 41 N= 52 ( 93Nb): 1.05107E+00
proton    channel to Z= 40 N= 53 ( 93Zr): 1.67352E-03
deuteron  channel to Z= 40 N= 52 ( 92Zr): 1.07608E-06
triton    channel to Z= 40 N= 51 ( 91Zr): 2.06095E-08
helium-3  channel to Z= 39 N= 52 ( 91Y ): 1.07027E-16
alpha     channel to Z= 39 N= 51 ( 90Y ): 4.69800E-04


Emission spectra from Z= 41 N= 53 ( 94Nb):


 Energy   gamma          neutron       proton       deuteron      triton       helium-3

   0.001 1.14218E-02 5.11503E-03 0.00000E+00 0.00000E+00 0.00000E+00 0.00000E+0
   0.002 1.19276E-02 1.10501E-02 0.00000E+00 0.00000E+00 0.00000E+00 0.00000E+0
   0.005 1.34434E-02 3.25383E-02 0.00000E+00 0.00000E+00 0.00000E+00 0.00000E+0
   0.010 1.59698E-02 7.24291E-02 0.00000E+00 0.00000E+00 0.00000E+00 0.00000E+0
   0.020 2.10227E-02 1.27402E-01 0.00000E+00 0.00000E+00 0.00000E+00 0.00000E+0
   0.050 4.45166E-02 2.33433E-01 0.00000E+00 0.00000E+00 0.00000E+00 0.00000E+0
.....................................
 ++++++++++ CHECK OF INTEGRATED EMISSION SPECTRA ++++++++++


           Cross section   Integrated spectrum  Average emission energy

gamma         2.66180E+00      2.66180E+00            1.776
neutron       1.05107E+00      1.05107E+00            1.174
proton        1.67352E-03      1.67334E-03            5.377
deuteron      1.07608E-06      7.97929E-07            5.635
triton        2.06095E-08      0.00000E+00            0.000
helium-3      1.07027E-16      0.00000E+00            0.000
alpha         4.69800E-04      4.69563E-04           10.831


Final production cross section of Z= 41 N= 53 ( 94Nb):


Total       : 1.18344E+00
Ground state: 5.75062E-01
Level  1    : 6.08379E-01
```

Note that once a new nucleus is encountered in the reaction chain, all nuclear structure information for that nucleus is printed as well.

Case i: No output at all

It is even possible to have an empty output file. With the following input file,

```
#
# General
#
projectile n
element nb
mass 93
energy 14.
#
# Output
#
outmain n
```

it is specified that even the main output should be suppressed. The sample output file should be empty. This can be helpful when TALYS is invoked as a subroutine from other programs and the output from TALYS is not required (if the communication is done e.g. through shared arrays or subroutine variables). We have not yet used this option ourselves. ■

4.2 Cross section definitions

In TALYS, cross sections for reactions to all open channels are calculated. Although the types of most of these partial cross sections are generally well known, it is appropriate to define them for completeness. This section concerns basically the book-keeping of the various cross sections, including all the sum rules they obey. The particular nuclear models that are needed to obtain them are described in Part II. Thus, we do not yet give the definition of cross sections in terms of more fundamental quantities. Unless otherwise stated, we use incident neutrons as example in what follows and we consider only photons (γ), neutrons (n), protons (p), deuterons (d), tritons (t), helium-3 particles (h) and alpha particles (α) as competing particles. Also, to avoid an overburdening of the notation and the explanation, we will postpone the competition of fission to the last section of this Chapter.

4.2.1 Total cross sections

The most basic nuclear reaction calculation is that with the optical model, which will be explained in more detail in Section 10. Here, it is sufficient to summarize the relations that can be found in many nuclear reaction textbooks, namely that the optical model yields the *reaction cross section* σ_{reac} and, in the case of neutrons, the *total cross section* σ_{tot} and the *shape-elastic cross section* $\sigma_{shape-el}$. They are related by

$$\sigma_{tot} = \sigma_{shape-el} + \sigma_{reac}. \tag{4.2}$$

If the elastic channel is, besides shape elastic scattering, also fed by compound nucleus decay, the latter component is a part of the reaction cross section and is called the *compound elastic cross section* $\sigma_{comp-el}$. With this, we can define the *total elastic cross section* σ_{el},

$$\sigma_{el} = \sigma_{shape-el} + \sigma_{comp-el}, \tag{4.3}$$

and the *non-elastic cross section* σ_{non-el},

$$\sigma_{non-el} = \sigma_{reac} - \sigma_{comp-el}, \tag{4.4}$$

so that we can combine these equations to give

$$\sigma_{tot} = \sigma_{el} + \sigma_{non-el}. \tag{4.5}$$

The last equation contains the quantities that can actually be measured in an experiment. We also note that the competition between the many compound nucleus decay channels ensures that $\sigma_{comp-el}$ rapidly diminishes for incident neutron energies above a few MeV, in which case σ_{non-el} becomes practically equal to σ_{reac}.

A further subdivision of the outcome of a nuclear reaction concerns the breakdown of σ_{non-el}: this cross section contains all the partial cross sections. For this we introduce the exclusive cross sections, from which all other cross sections of interest can be derived.

4.2.2 Exclusive cross sections

In this manual, we call a cross section *exclusive* when the outgoing channel is precisely specified by the type and number of outgoing particles (+ any number of photons). Well-known examples are the inelastic or (n, n') cross section and the $(n, 2n)$ cross section, which corresponds with two, *and only* two, neutrons (+ accompanying photons) in the outgoing channel. We denote the *exclusive cross section* as $\sigma^{ex}(i_n, i_p, i_d, i_t, i_h, i_\alpha)$, where i_n stands for the number of outgoing neutrons, etc. In this notation, where the incident particle is assumed implicit, e.g. the $(n, 2np)$ cross section is given by $\sigma^{ex}(2, 1, 0, 0, 0, 0)$, for which we will also use the shorthand notation $\sigma_{n,2np}$. For a non-fissile nucleus, the sum over all exclusive cross sections is equal to the non-elastic cross section

$$\sigma_{non-el} = \sum_{i_n=0}^{\infty} \sum_{i_p=0}^{\infty} \sum_{i_d=0}^{\infty} \sum_{i_t=0}^{\infty} \sum_{i_h=0}^{\infty} \sum_{i_\alpha=0}^{\infty} \sigma^{ex}(i_n, i_p, i_d, i_t, i_h, i_\alpha), \tag{4.6}$$

provided we impose that $\sigma^{ex}(1, 0, 0, 0, 0, 0)$ is the exclusive *inelastic* cross section $\sigma_{n,n'}$, i.e. it does not include shape- or compound elastic scattering.

The precise calculation of exclusive cross sections and spectra is a complicated book-keeping problem which, to our knowledge, has not been properly documented. We will describe the exact formalism here. In what follows we use quantities with a prime for daughter nuclides and quantities without a prime for mother nuclides in a decay chain. Consider an excitation energy bin or discrete level E_x in a nucleus (Z, N). Let $P(Z, N, E_x)$ represent the population of this bin/level before it decays. Let $s_k(Z, N, E_x, E_{x'})$ be the part of the population that decays from the (Z, N, E_x) bin/level to the residual $(Z', N', E_{x'})$ bin/level, whereby (Z, N) and (Z', N') are connected through the particle type k, with the index k running from γ-rays up to α-particles. With these definitions, we can link the various residual nuclides while keeping track of all intermediate particle emissions. A special case for the population is the initial compound nucleus (Z_C, N_C), which contains all the initial reaction population at its total excitation energy E_x^{max} (projectile energy + binding energy), i.e.

$$P(Z_C, N_C, E_x^{max}) = \sigma_{non-el}, \tag{4.7}$$

while all other population bins/levels are zero. For the initial compound nucleus, $s_k(Z_C, N_C, E_x^{max}, E_{x'})$ represents the binary feeding to the excitation energy bins of the first set of residual nuclides. This term generally consists of direct, pre-equilibrium and compound components.

The population of any bin in the decay chain is equal to the sum of the decay parts for all particles that can reach this bin from the associated mother bins, i.e.

$$P(Z',N',E_{x'}(i')) = \sum_{k=\gamma,n,p,d,t,h,\alpha} \sum_i s_k(Z,N,E_x(i),E_{x'}(i')), \tag{4.8}$$

where the sum over i runs over discrete level and continuum energy bins in the energy range from $E_{x'}(i') + S_k$ to $E_x^{max}(Z,N)$, where S_k is the separation energy of particle k so that the sum only includes decay that is energetically allowed, and $E_x^{max}(Z,N)$ is the maximum possible excitation energy of the (Z,N) nucleus. Note again that the particle type k determines (Z,N).

To obtain the exclusive cross sections, we need to start with the initial compound nucleus and work our way down to the last nucleus that can be reached. First, consider a daughter nucleus (Z',N') somewhere in the reaction chain. We identify all exclusive channels $(i_n,i_p,i_d,i_t,i_h,i_\alpha)$ that lead to this residual (Z',N') nucleus, i.e. all channels that satisfy

$$i_n + i_d + 2i_t + i_h + 2i_\alpha = N_C - N'$$
$$i_p + i_d + i_t + 2i_h + 2i_\alpha = Z_C - Z'. \tag{4.9}$$

For each of these channels, the *inclusive* cross section per excitation energy bin S is equal to the sum of the feeding from all possible mother bins, i.e.

$$S(i_n,i_p,i_d,i_t,i_h,i_\alpha,E_{x'}(i')) = \sum_{k=\gamma,n,p,d,t,h,\alpha} \sum_i \frac{s_k(Z,N,E_x(i),E_{x'}(i'))}{P(Z,N,E_x(i))}$$
$$\times \quad S(i_n - \delta_{nk}, i_p - \delta_{pk}, i_d - \delta_{dk}, i_t - \delta_{tk}, i_h - \delta_{hk}, i_\alpha - \delta_{\alpha k}, E_x(i)), \tag{4.10}$$

where we introduce Kronecker delta's, with characters as subscript, as

$$\delta_{nk} \quad = \quad 1 \text{ if } k = n \text{ (neutron)}$$
$$= \quad 0, \text{ otherwise} \tag{4.11}$$

and similarly for the other particles. Note that S is still inclusive in the sense that it is not yet depleted for further decay. The summation runs over the excitation energies of the mother bin from which decay into the $E_{x'}(i')$ bin of the residual nucleus is energetically allowed. Feeding by gamma decay from bins above the $(Z',N',E_{x'}(i'))$ bin is taken into account by the $k = \gamma$ term, in which case all of the Kronecker delta's are zero.

With Eq. (4.7) as initial condition, the recursive procedure is completely defined. For a fixed nucleus, Eq. (4.10) is calculated for all excitation energy bins, in decreasing order, until the remaining population is in an isomeric or the ground state of the nucleus. When there is no further decay possible, the exclusive cross section per ground state/isomer, numbered by i, can be identified,

$$\sigma_i^{ex}(i_n,i_p,i_d,i_t,i_h,i_\alpha) = S(i_n,i_p,i_d,i_t,i_h,i_\alpha,E_i). \tag{4.12}$$

The total exclusive cross section for a particular channel is then calculated as

$$\sigma^{ex}(i_n,i_p,i_d,i_t,i_h,i_\alpha) = \sum_{i=0,isomers} \sigma_i^{ex}(i_n,i_p,i_d,i_t,i_h,i_\alpha). \tag{4.13}$$

The procedure outlined above automatically sorts and stores all exclusive cross sections, irrespective of the order of particle emission within the reaction chain. For example, the (n,np) and (n,pn) channels are automatically added. The above formalism holds *exactly* for an arbitrary number of emitted particles.

We stress that keeping track of the excitation energy E_x throughout this formalism is essential to get the exact exclusive cross sections for two reasons:

(i) the exact determination of the branching ratios for exclusive isomeric ratios. The isomeric ratios for different exclusive reactions that lead to the same residual product, e.g. (n,np) and (n,d), both leading to $(Z_C - 1, N_C - 1)$, are generally different from each other and thus also from the isomeric ratios of the total residual product. Hence, it would be an approximation to apply isomeric branching ratios for residual products, obtained after the full reaction calculation, a posteriori on the exclusive channels. This is avoided with our method,

(ii) the exclusive spectra, which we will explain in Section 4.3.2.

Suppose one would only be interested in the total exclusive cross sections of Eq. (4.13), i.e. neither in the exclusive isomeric ratios, nor in the exclusive spectra. Only in that case, a simpler method would be sufficient. Since only the total reaction population that decays from nucleus to nucleus needs to be tracked, the total exclusive cross section for a certain channel is easily determined by subtracting the total ongoing flux from the total feeding flux to this channel. This is described in e.g. Section II.E.f of the GNASH manual [1]. We note that the exact treatment of TALYS does not require a large amount of computing time, certainly not when compared with more time-expensive parts of the full calculation.

When TALYS computes the binary reaction models and the multiple pre-equilibrium and Hauser-Feshbach models, it stores both $P(Z, N, E_x)$ (through the *popexcl* array) and $s_k(Z, N, E_x, E_{x'})$ (through the *feedexcl* array) for all residual nuclei and particles. This temporary storage enables us to first complete the full reaction calculation, including all its physical aspects, until all channels are closed. Then, we turn to the exclusive cross section and spectra problem afterwards in a separate subroutine: *channels.f*. It is thus considered as an isolated book-keeping problem.

The total number of different exclusive channels rapidly increases with the number of reaction stages. It can be shown that for m outgoing particles (i.e. reaction stages) which can be of k different types, the maximum number of exclusive cross sections is $\binom{m+k-1}{m}$. In general, we include neutrons up to alpha-particles as competing particles, i.e. $k = 6$, giving $\binom{m+5}{m}$ possible exclusive channels, or 6, 21, 56 and 126, respectively, for the first 4 stages. This clarifies why exclusive channels are usually only of interest for only a few outgoing particles (the ENDF format for evaluated data libraries includes reactions up to 4 particles). At higher energies, and thus more outgoing particles, exclusive cross sections loose their relevance and the cross sections per channel are usually accumulated in the total particle production cross sections and residual production cross sections. Certainly at higher energies, this apparent loss of information is no longer an issue, since the observable quantities to which nuclear models can be tested are of a cumulative nature anyway, when many particles are involved.

In TALYS, the cumulated particle production cross sections and residual production cross sections are always *completely* tracked down until all residual nuclides have decayed to an isomer or the ground state, regardless of the incident energy, whereas exclusive cross sections are only tracked up to a user-defined depth. To elucidate this important point we discuss the low and the high energy case. For low energies, say up to 20 MeV, keeping track of the exclusive cross section is important from both the fundamental and the applied point of view. It can be imagined that in a (n,np) measurement both the emitted neutron and proton have been measured in the detector. Hence the cross section is *not* the same as that of an activation measurement of the final residual nucleus, since the latter would also include a contribution from the (n,d) channel. Another example is the $(n,2n)$ channel, distinguished from the (n,n') or the general (n,xn) cross section, which is of importance in some integral reactor benchmarks. If, on the other hand, we encounter in the literature a cross section of the type $^{120}\text{Sn}(p,7p18n)^{96}\text{Ru}$, we can be sure that the residual product ^{96}Ru was measured and not the indicated number of neutrons and protons in a detector.

The $(p, 7p18n)$ symbol merely represents the number of neutron and proton units, while other light ions are generally included in the emission channel. Hence, for high energies the outcome of a nuclear reaction is usually tracked in parallel by two sets of quantities: the $(proj, xn), \ldots (proj, x\alpha)$ particle production cross sections and spectra, and the residual production cross sections. These will be exactly defined in the next sections.

4.2.3 Binary cross sections

Some of the exclusive channels need, and get, more attention than others. The exclusive binary cross sections, for reactions that are characterized by one, and only one, particle out, are special in the sense that they comprise both discrete and continuous energy transitions. Inelastic scattering can occur through both direct collective and compound transitions to the first few excited levels and through pre-equilibrium and compound reactions to the continuum. Let us assume that for a target nucleus the basic structure properties (spin, parity, deformation parameters) of the first N levels are known. Then, the *inelastic cross section*, $\sigma_{n,n'}$ is the sum of a *total discrete inelastic cross section* $\sigma_{n,n'}^{disc}$ and a *continuum inelastic cross section* $\sigma_{n,n'}^{cont}$

$$\sigma_{n,n'} = \sigma_{n,n'}^{disc} + \sigma_{n,n'}^{cont}, \tag{4.14}$$

where $\sigma_{n,n'}^{disc}$ is the sum over the inelastic cross sections for all the individual discrete states

$$\sigma_{n,n'}^{disc} = \sum_{i=1}^{N} \sigma_{n,n'}^{i}. \tag{4.15}$$

A further breakdown of each term is possible by means of reaction mechanisms. The inelastic cross section for each individual state i has a direct and a compound contribution:

$$\sigma_{n,n'}^{i} = \sigma_{n,n'}^{i,direct} + \sigma_{n,n'}^{i,comp}, \tag{4.16}$$

where the direct component comes from DWBA or coupled-channels calculations. Similarly, for the inelastic scattering to the continuum we can consider a pre-equilibrium and a compound contribution

$$\sigma_{n,n'}^{cont} = \sigma_{n,n'}^{PE} + \sigma_{n,n'}^{cont,comp}. \tag{4.17}$$

The set of definitions (4.14-4.17) can be given in a completely analogous way for the other binary channels $\sigma_{n,p}$, i.e. $\sigma^{ex}(0,1,0,0,0,0)$, $\sigma_{n,d}$, $\sigma_{n,t}$, $\sigma_{n,h}$ and $\sigma_{n,\alpha}$. For the depletion of the reaction population that goes into the pre-equilibrium channels, which will be discussed in Section 12, it is helpful to define here the *total discrete direct cross section*,

$$\sigma^{disc,direct} = \sum_{i} \sum_{k=n',p,d,t,h,\alpha} \sigma_{n,k}^{i,direct}. \tag{4.18}$$

Finally, we also consider an alternative division for the non-elastic cross section. It is equal to the sum of the *inclusive* binary cross sections

$$\sigma_{non-el} = \sum_{k=\gamma,n',p,d,t,h,\alpha} \sigma_{n,k}^{inc,bin}, \tag{4.19}$$

where again at the present stage of the outline we do not consider fission and ejectiles heavier than α-particles. This is what we actually use in the inclusive nuclear reaction calculations. With the direct, pre-equilibrium and compound models, several residual nuclides can be formed after the binary reaction, with a total population per nucleus that is equal to the terms of Eq. (4.19). The residual nuclides then decay further until all channels are closed. Note that $\sigma^{inc,bin}$ is not a "true" cross section in the sense of a quantity for a final combination of a product and light particle(s).

4.2.4 Total particle production cross sections

Especially for incident energies higher than about 10 MeV, it is appropriate to define the composite or *total neutron production cross section*, $\sigma_{n,xn}$. It can be expressed in terms of the exclusive cross sections as follows

$$\sigma_{n,xn} = \sum_{i_n=0}^{\infty} \sum_{i_p=0}^{\infty} \sum_{i_d=0}^{\infty} \sum_{i_t=0}^{\infty} \sum_{i_h=0}^{\infty} \sum_{i_\alpha=0}^{\infty} i_n \sigma^{ex}(i_n, i_p, i_d, i_t, i_h, i_\alpha), \tag{4.20}$$

i.e. in the more common notation,

$$\sigma_{n,xn} = \sigma_{n,n'} + 2\sigma_{n,2n} + \sigma_{n,np} + 2\sigma_{n,2np} + ... \tag{4.21}$$

Again, $\sigma_{n,xn}$ is not a true cross section since the incident and outgoing channels are not exactly defined by its individual reaction components. (Contrary to our definition, in some publications $\sigma_{n,xn}$ is used to indicate activation measurements of a whole string of isotopes (e.g. $^{202-208}$Pb) in which case x is a number that varies case by case. In our work, this is called an exclusive cross section). The *neutron multiplicity*, or *yield*, Y_n is defined as

$$Y_n = \frac{\sigma_{n,xn}}{\sigma_{non-el}}. \tag{4.22}$$

Similarly, the *total proton production cross section*, $\sigma_{n,xp}$ is defined as

$$\sigma_{n,xp} = \sum_{i_n=0}^{\infty} \sum_{i_p=0}^{\infty} \sum_{i_d=0}^{\infty} \sum_{i_t=0}^{\infty} \sum_{i_h=0}^{\infty} \sum_{i_\alpha=0}^{\infty} i_p \sigma^{ex}(i_n, i_p, i_d, i_t, i_h, i_\alpha), \tag{4.23}$$

and the proton multiplicity, or yield, Y_p is defined as

$$Y_p = \frac{\sigma_{n,xp}}{\sigma_{non-el}}, \tag{4.24}$$

and similarly for the other particles. We note that we do not, in practice, use Eq. (4.20) to calculate the composite particle production cross section. Instead, we first calculate the inclusive binary cross section of Eq. (4.19) and then, during the depletion of each residual nucleus by further decay we directly add the reaction flux, equal to the $s_k(Z, N, E_x, E_{x'})$ term of Eq. (4.8), to $\sigma_{n,xn}$, $\sigma_{n,xp}$, etc. This procedure has already been sketched in the multiple decay scheme at the beginning of this Chapter. In the output of TALYS, we include Eq. (4.20) only as a numerical check. For a few outgoing particles Eq. (4.20) should exactly hold. For higher energies and thus more outgoing particles (typically more than 4, see the **maxchannel** (p. 318) keyword) the exclusive cross sections are no longer tracked by TALYS and Eq. (4.20) can no longer be expected to hold numerically. Remember, however, that we always calculate the total particle production cross sections, irrespective of the number of outgoing particles, since we continue the multiple emission calculation until all residual nuclides are in their isomeric or ground states.

> **Sample case 4.3** **Excitation functions: ^{208}Pb (n,n'), (n,2n), (n,p) etc**
> Often we are not interested in only one incident energy, but in excitation functions of the cross sections. If more than one incident energy is given in the file specified by the **energy** keyword, it is helpful to have the results, for each type of cross section, in a table as a function of incident energy. TALYS will first calculate all quantities that remain equal for all incident energy calculations, such as the transmission coefficients. Next, it will calculate the results for each incident energy. When the calculation for the last incident energy has been completed, the cross sections are collected and printed as excitation functions in the output if **outexcitation y** (which is the default if there is more than one incident energy). Moreover, we can provide the

results in separate files: one file per reaction channel. Consider the following input file

```
#
# n-Pb208-xs
#
# General
#
projectile n
element pb
mass 208
energy energies
#
# Parameters
#
Rgamma 2.2
gn 81 208 9.4
gp 81 208 6.2
optmodfileN 82 n-Pb208.omp
#
# Output
#
channels y
filechannels y
filetotal y
fileresidual y
outdiscrete y
```

which provides all partial cross sections for neutrons incident on ^{208}Pb for 46 incident energies, from 1 to 30 MeV, as given in the file *energies* that is present in this sample case directory. In the main output file, first the results per incident energy are given. At the end of the output file, there is an output block that begins with:

```
########## EXCITATION FUNCTIONS ###########
```

and in the 1.xx versions of TALYS we then printed all the excitation functions in the output file. However, for plotting data, or processing into ENDF-6 data files, it is more practical to have the data in individual output files and we no longer repeat them in the main output file (unless you put **outall y**). Note that, since **filechannels y**, several files with names as e.g. *xs200000.tot* have been created in your working directory. These files contain the entire excitation function per reaction channel. Besides these exclusive cross sections, residual production cross section files are produced (**fileresidual y**). Note that for this reaction, *rp082207.tot* and *xs200000.tot* obviously have equal contents.

We illustrate this sample case with various comparisons with measurements. Since **filetotal y**, a file *total.tot* is created with, among others, the total cross section. The resulting curves are shown in Figs. 4.6 and 4.7.   ■

The most important cumulative cross sections cross sections as a function of incident energy

are given in *all.tot*. This output file begins with:

```
# header:
#   title: Pb208(n,all) general cross sections [mb]
#   source: TALYS-2.0
#   user: Arjan Koning
#   date: 2023-12-14
#   format: YANDF-0.1
# target:
#   Z: 82
#   A: 208
#   nuclide: Pb208
# reaction:
#   type: (n,all)
# datablock:
#   quantity: cross section
#   columns: 11
#   entries: 46
##      MeV         Non-elastic       Elastic          Total        Compound elast.
##      [mb]          [mb]             [mb]             [mb]             [mb]
    1.000000E+00   1.217163E+00    4.836003E+03    4.837220E+03    1.726403E+03
    1.200000E+00   1.414917E+00    4.780395E+03    4.781810E+03    1.818645E+03
    1.400000E+00   1.646118E+00    4.939614E+03    4.941260E+03    1.947554E+03
.....................................
```

Next, the binary cross sections are available in *binary.tot*:

```
# header:
#   title: Pb208(n,bin) cross section - binary
#   source: TALYS-2.0
#   user: Arjan Koning
#   date: 2023-12-14
#   format: YANDF-0.1
# target:
#   Z: 82
#   A: 208
#   nuclide: Pb208
# reaction:
#   type: (n,bin)
# datablock:
#   quantity: cross section
#   columns: 8
#   entries: 46
##       E           gamma           neutron          proton          deuteron
##     [MeV]          [mb]             [mb]             [mb]             [mb]
    1.000000E+00   8.779958E-01    0.000000E+00    0.000000E+00    0.000000E+00
    1.200000E+00   1.068442E+00    0.000000E+00    0.000000E+00    0.000000E+00
    1.400000E+00   1.290755E+00    0.000000E+00    0.000000E+00    0.000000E+00
    1.600000E+00   1.549974E+00    0.000000E+00    0.000000E+00    0.000000E+00
    1.800000E+00   1.866545E+00    0.000000E+00    0.000000E+00    0.000000E+00
.....................................
```

The total particle production cross sections are printed in e.g. *gprod.tot*,

```
# header:
#   title: Pb208(n,xg) cross section
#   source: TALYS-2.0
#   user: Arjan Koning
#   date: 2023-12-14
#   format: YANDF-0.1
# target:
#   Z: 82
#   A: 208
#   nuclide: Pb208
# reaction:
#   type: (n,xg)
#   ENDF_MF: 3
#   ENDF_MT: 202
# datablock:
#   quantity: cross section
#   columns: 3
#   entries: 46
##       E              xs          Multiplicity
##     [MeV]           [mb]             []
   1.000000E+00    1.022519E+00    8.400836E-01
   1.200000E+00    1.262476E+00    8.922617E-01
   1.400000E+00    1.551970E+00    9.428056E-01
   1.600000E+00    1.896921E+00    9.935793E-01
   1.800000E+00    2.324284E+00    1.045839E+00
   2.000000E+00    2.850885E+00    1.098516E+00
.....................................
```

and similar for *nprod.tot*, etc. The output of the residual production cross sections are in e.g. *rp081206.tot*,

```
# header:
#   title: Pb208(n,x)Tl206 cross section
#   source: TALYS-2.0
#   user: Arjan Koning
#   date: 2023-12-14
#   format: YANDF-0.1
# target:
#   Z: 82
#   A: 208
#   nuclide: Pb208
# reaction:
#   type: (n,x)
#   Q-value [MeV]: -6.373698E+00
#   E-threshold [MeV]:  6.404610E+00
#   ENDF_MF: 6
#   ENDF_MT: 5
# residual:
#   Z: 81
```

```
#   A: 206
#   nuclide: Tl206
#   mass [amu]:  2.059761E+02
# datablock:
#   quantity: cross section
#   columns: 2
#   entries: 46
##        E              xs
##      [MeV]           [mb]
   1.000000E+00    0.000000E+00
.....................................
   1.400000E+01    0.000000E+00
   1.500000E+01    1.556446E-03
   1.600000E+01    1.065114E-02
   1.700000E+01    4.880429E-02
   1.800000E+01    1.548131E-01
   1.900000E+01    3.705726E-01
   2.000000E+01    7.212246E-01
   2.200000E+01    1.773993E+00
   2.400000E+01    3.246034E+00
   2.600000E+01    5.406227E+00
   2.800000E+01    9.282149E+00
   3.000000E+01    1.677222E+01
.....................................
```

The exclusive reaction cross sections are in e.g. *xs100000.tot*,

```
# header:
#   title: Pb208(n,n')Pb208 cross section
#   source: TALYS-2.0
#   user: Arjan Koning
#   date: 2023-12-14
#   format: YANDF-0.1
# target:
#   Z: 82
#   A: 208
#   nuclide: Pb208
# reaction:
#   type: (n,n')
#   Q-value [MeV]:  0.000000E+00
#   E-threshold [MeV]:  2.627202E+00
# residual:
#   Z: 82
#   A: 208
#   nuclide: Pb208
# datablock:
#   quantity: cross section
#   columns: 4
#   entries: 46
##        E              xs          gamma xs     xs/res.prod.xs
##      [MeV]           [mb]           [mb]             []
   1.000000E+00    0.000000E+00    0.000000E+00    0.000000E+00
```

```
1.200000E+00    0.000000E+00    0.000000E+00    0.000000E+00
1.400000E+00    0.000000E+00    0.000000E+00    0.000000E+00
1.600000E+00    0.000000E+00    0.000000E+00    0.000000E+00
1.800000E+00    0.000000E+00    0.000000E+00    0.000000E+00
2.000000E+00    0.000000E+00    0.000000E+00    0.000000E+00
2.200000E+00    0.000000E+00    0.000000E+00    0.000000E+00
2.400000E+00    0.000000E+00    0.000000E+00    0.000000E+00
2.600000E+00    0.000000E+00    0.000000E+00    0.000000E+00
2.800000E+00    3.161401E+02    3.161401E+02    9.986830E-01
3.000000E+00    5.137026E+02    5.137026E+02    9.990581E-01
3.200000E+00    6.628177E+02    6.628177E+02    9.991065E-01
3.400000E+00    8.731140E+02    1.010644E+03    9.992927E-01
3.600000E+00    1.069874E+03    1.409531E+03    9.993466E-01
3.800000E+00    1.258737E+03    1.863202E+03    9.993635E-01
4.000000E+00    1.441710E+03    2.406890E+03    9.993697E-01
................................
```

4.2.5 Residual production cross sections

We can define another important type of derived cross section using the exclusive cross section, namely the residual production cross section σ_{prod}. All exclusive cross sections with the same number of neutron and proton units in the outgoing channel sum up to the same residual nucleus production cross section for the final nucleus (Z,N), i.e.

$$\sigma_{prod}(Z,N) = \sum_{i_n=0}^{\infty} \sum_{i_p=0}^{\infty} \sum_{i_d=0}^{\infty} \sum_{i_t=0}^{\infty} \sum_{i_h=0}^{\infty} \sum_{i_\alpha=0}^{\infty} \sigma^{ex}(i_n,i_p,i_d,i_t,i_h,i_\alpha)\delta_N\delta_Z, \qquad (4.25)$$

where the Kronecker delta's are defined by

$$\begin{aligned} \delta_N &= & 1 \text{ if } i_n+i_d+2i_t+i_h+2i_\alpha = N_C-N \\ &= & 0 \text{ otherwise} \\ \delta_Z &= & 1 \text{ if } i_p+i_d+i_t+2i_h+2i_\alpha = Z_C-Z \\ &= & 0 \text{ otherwise,} \end{aligned} \qquad (4.26)$$
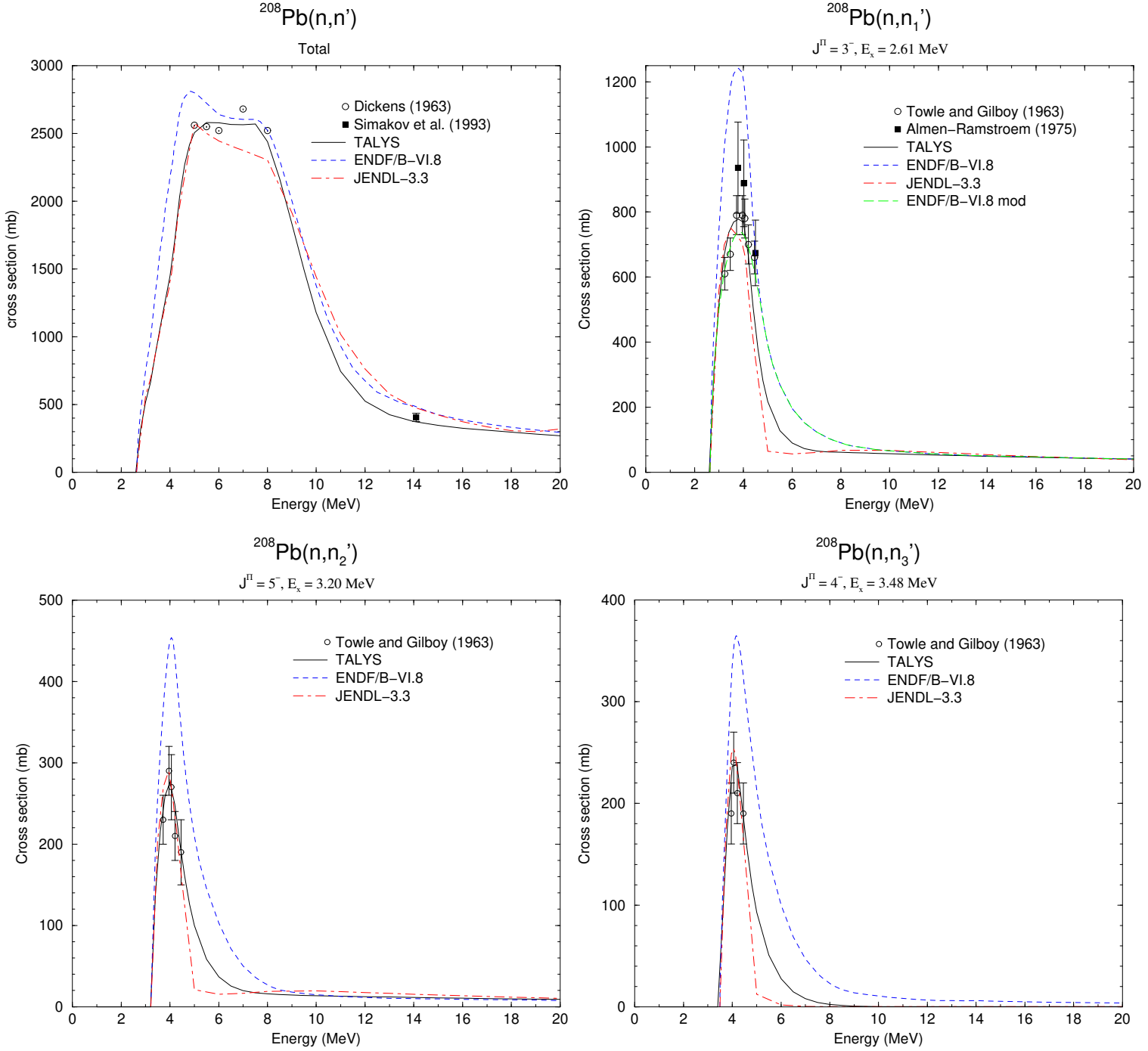
where the first compound nucleus that is formed from the projectile and target nucleus is denoted by (Z_C,N_C). As an example, consider the $n+\,^{56}\text{Fe} \rightarrow \,^{54}\text{Mn} +x$ reaction. The exclusive cross sections that add up to the ^{54}Mn production cross section are $\sigma_{n,2np}, \sigma_{n,nd}$, and $\sigma_{n,t}$, or $\sigma^{ex}(2,1,0,0,0,0), \sigma^{ex}(1,0,1,0,0,0)$, and $\sigma^{ex}(0,0,0,1,0,0)$, respectively.

Since all exclusive cross sections contribute to the residual production cross section for one nuclide (Z,N) only, Eq. (4.6) automatically implies

$$\sigma_{non-el} = \sum_Z \sum_N \sigma_{prod}(Z,N). \qquad (4.27)$$

Similar to Eq. (4.13), Eq. (4.25) is separated per isomer

$$\sigma_{prod,i}(Z,N) = \sum_{i_n=0}^{\infty} \sum_{i_p=0}^{\infty} \sum_{i_d=0}^{\infty} \sum_{i_t=0}^{\infty} \sum_{i_h=0}^{\infty} \sum_{i_\alpha=0}^{\infty} \sigma_i^{ex}(i_n,i_p,i_d,i_t,i_h,i_\alpha)\delta_N\delta_Z, \qquad (4.28)$$

Figure 4.6: Partial cross sections for neutrons incident on ^{208}Pb.
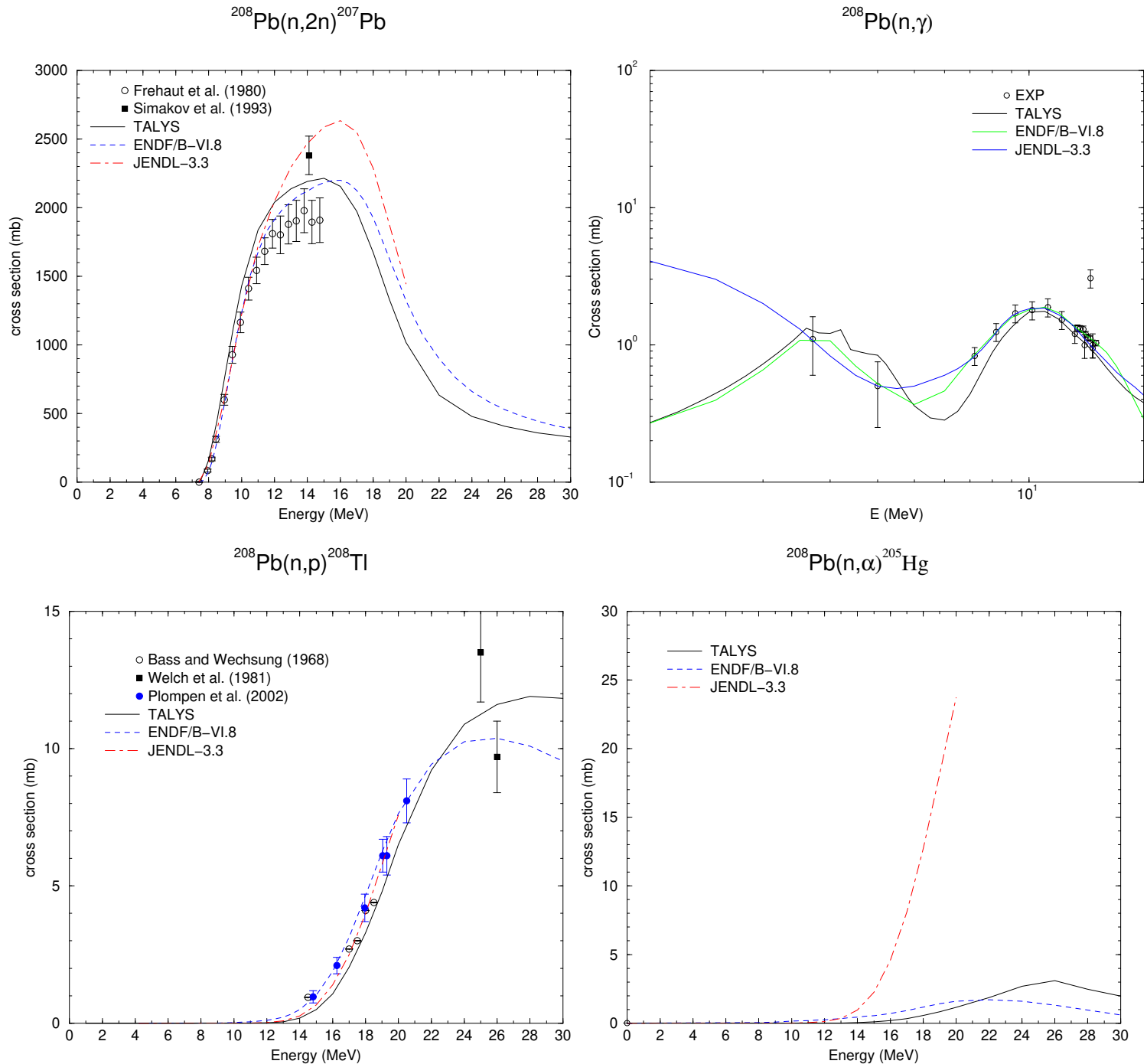
Figure 4.7: Partial cross sections for neutrons incident on ^{208}Pb.

and the equivalent of Eq. (4.13) is

$$\sigma_{prod}(Z,N) = \sum_{i=0,isomers} \sigma_{prod,i}(Z,N). \qquad (4.29)$$

Also here, we do not calculate σ_{prod} and $\sigma_{prod,i}$ using Eqs. (4.25) and (4.28), although optionally TALYS includes it as a numerical check in the output for residual nuclides close to the target. Analogous to the total particle production, we determine the residual production cross section, for both the isomers and the ground state, after the complete decay of each nucleus by means of an inclusive calculation.

Sample case 4.4 **Residual production cross sections for protons on Fe**
In this sample case, we calculate the residual production cross sections for protons on ^{nat}Fe for incident energies up to 100 MeV. A calculation for a natural target is launched, meaning that successive TALYS calculations for each isotope are performed, after which the results are weighted with the natural abundance. We restrict ourselves to a calculation with all nuclear model parameters set to their default values. The following input file is used:

```
#
# p-Fe000-rp
#
# General
#
projectile p
element fe
mass 0
energy energies
#
# Output
#
fileresidual     y
```

The file *energies* contains 24 incident energies between 1 and 100 MeV. Obviously, this sample case can be extended to more incident energies, e.g. up to 200 MeV, by simply adding numbers to the *energies* file. In that case, we recommend to include more energy bins in the calculation, (e.g. **bins 80**) to avoid numerical fluctuations, although this will inevitably take more computer time. Note that we have enabled the **fileresidual** keyword, so that a separate cross sections file for each final product is produced. The results from the files *rp027056.tot*, *rp027055.tot*, *rp025054.tot* and *rp025052.tot* are presented, together with experimental data, in Fig. 4.8.
As an example, the file *rp025052.tot* looks as follows.

```
# header:
#   title: Fe0(p,x)Mn52 cross section
#   source: TALYS-2.0
#   user: Arjan Koning
#   date: 2023-12-11
#   format: YANDF-0.1
# target:
#   Z: 26
```

```
#    A: 0
#    nuclide: Fe0
# reaction:
#    type: (p,x)
#    ENDF_MF: 6
#    ENDF_MT: 5
# residual:
#    Z: 25
#    A: 52
#    nuclide: Mn52
# datablock:
#    quantity: cross section
#    columns: 2
#    entries: 24
##       E              xs
##     [MeV]          [mb]
   1.000000E+00   0.000000E+00
....................
   1.600000E+01   0.000000E+00
   1.800000E+01   1.777641E-03
   2.000000E+01   4.415140E-01
   2.500000E+01   2.496402E+01
   3.000000E+01   3.582130E+01
   3.500000E+01   3.283743E+01
   4.000000E+01   2.765386E+01
   4.500000E+01   2.235001E+01
   5.000000E+01   1.994102E+01
   6.000000E+01   4.507320E+01
   7.000000E+01   6.835677E+01
   8.000000E+01   7.106861E+01
   9.000000E+01   6.800709E+01
   1.000000E+02   6.312850E+01
```

Sample case 4.5 **Gamma-ray intensities:** ^{208}**Pb**$(n,n\gamma)$ **and** ^{208}**Pb**$(n,2n\gamma)$

This feature could simply have been included in the sample case on excitation functions for ^{208}Pb, but in order not to overburden the description of that sample case we include it here. With the input file

```
#
# n-Pb208-nngamma
#
# General
#
projectile n
element pb
mass 208
energy energies
```
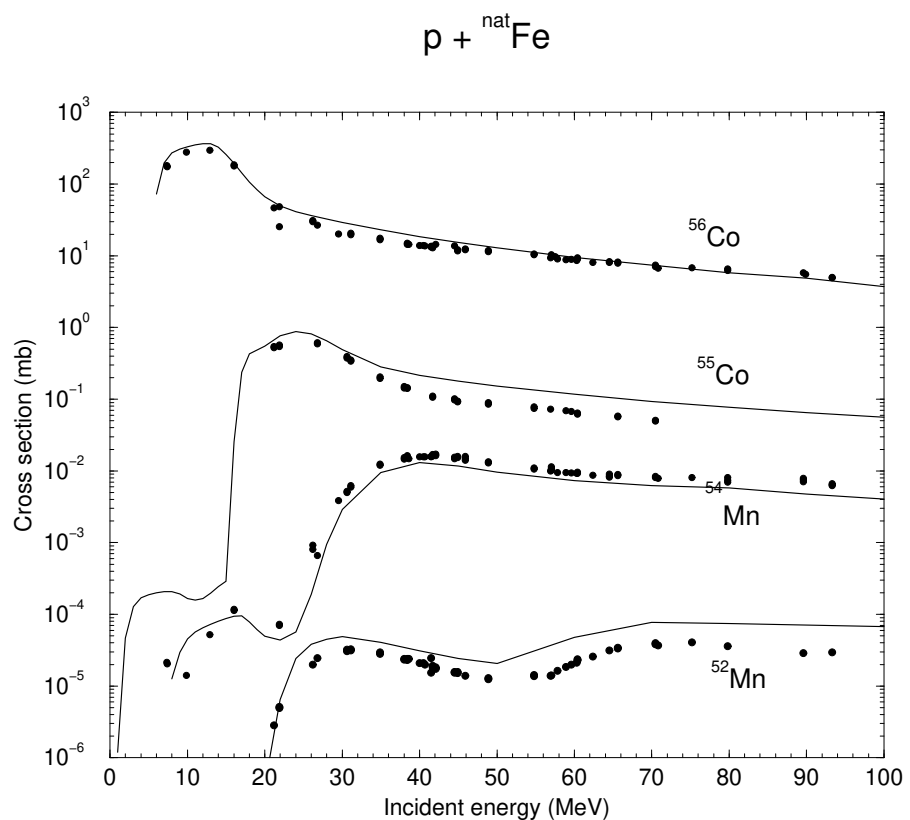
Figure 4.8: Residual production cross sections for protons incident on ^{nat}Fe. Experimental data are obtained from [7].

```
#
# Parameters
#
isomer 1.e-4
maxZ 0
Rgamma 2.2
optmodfileN 82 n-Pb208.omp
#
# Output
#
channels y
filechannels y
fileresidual y
outgamdis y
```

all discrete gamma lines are printed and stored in separate files. To avoid the production of too many data files, we have put **maxZ 0** so that only the gamma-ray production files for Pb-chain are created. Also, we include a special OMP with the file *pb.omp* and we set **isomer 1.e-4** to allow for gamma decay of some rather short-lived levels. Experimental data exists for the ^{208}Pb$(n, n'\gamma)$ cross section for level 1 to level 0 and the ^{208}Pb$(n, 2n'\gamma)$ cross section for level 2 to level 0 and for level 1 to level 0. These data have been plotted together with the results of the calculated files *gam082208L01L00.tot*, *gam082207L02L00.tot* and *gam082207L01L00.tot*, in Fig. 4.9.

Here are the contents of *gam082207L01L00.tot* as an example:

```
# header:
#   title: Pb208(n,xg_1-0)Pb207 gamma-ray production cross section
#   source: TALYS-2.0
#   user: Arjan Koning
#   date: 2023-12-11
#   format: YANDF-0.1
# target:
#   Z: 82
#   A: 208
#   nuclide: Pb208
# reaction:
#   type: (n,xg_1-0)
#   Q-value [MeV]: -7.937571E+00
#   E-threshold [MeV]:  7.976068E+00
#   level:
#     number: 1
#     energy [MeV]:  5.696980E-01
#     spin:  2.500000E+00
#     parity: -1
#     level:
#       number: 0
#       energy [MeV]:  0.000000E+00
#       spin:  5.000000E-01
#       parity: -1
```

```
#   gamma energy [MeV]:  5.696980E-01
# residual:
#   Z: 82
#   A: 207
#   nuclide: Pb207
# datablock:
#   quantity: gamma-ray production cross section
#   columns: 2
#   entries: 67
##       E              xs
##     [MeV]           [mb]
   1.000000E-11   0.000000E+00
.................................
   7.500000E+00   0.000000E+00
   8.000000E+00   3.859060E-01
   8.500000E+00   9.522382E+01
   9.000000E+00   3.090241E+02
   9.500000E+00   5.028625E+02
   1.000000E+01   6.213652E+02
   1.100000E+01   7.397191E+02
   1.200000E+01   7.665779E+02
   1.300000E+01   7.781571E+02
   1.400000E+01   7.736282E+02
...................
```

4.3 Spectra and angular distributions

In addition to cross sections, TALYS also predicts energy spectra, angular distributions and energy-angle distributions.

4.3.1 Discrete angular distributions

The elastic angular distribution $\frac{d\sigma^{el}}{d\Omega}$ has a direct and a compound component:

$$\frac{d\sigma^{el}}{d\Omega} = \frac{d\sigma^{shape-el}}{d\Omega} + \frac{d\sigma^{comp-el}}{d\Omega}, \tag{4.30}$$

where the shape-elastic part comes directly from the optical model while the compound part comes from compound nucleus theory, namely Eq. (13.8). An analogous relation holds for inelastic scattering to a single discrete state i

$$\frac{d\sigma^i_{n,n'}}{d\Omega} = \frac{d\sigma^{i,direct}_{n,n'}}{d\Omega} + \frac{d\sigma^{i,compound}_{n,n'}}{d\Omega}, \tag{4.31}$$

where the direct component comes from DWBA or coupled-channels calculations. For charge exchange, we can write

$$\frac{d\sigma^i_{n,p}}{d\Omega} = \frac{d\sigma^{i,direct}_{n,p}}{d\Omega} + \frac{d\sigma^{i,compound}_{n,p}}{d\Omega} \tag{4.32}$$

and analogous expressions can be written for the other binary reactions (n,d), etc.
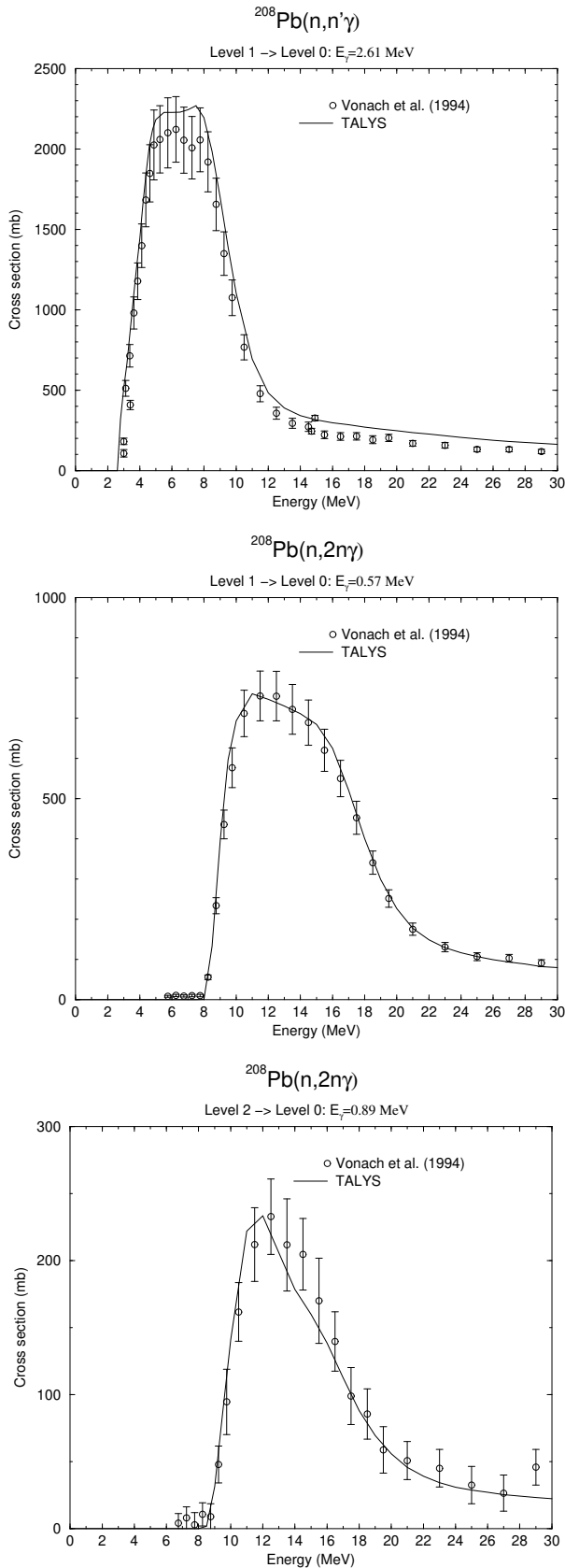
Figure 4.9: Gamma-ray production lines for a few transitions in ^{208}Pb(n,n') and ^{208}Pb(n,2n) reactions. The experimental data are from [8].

Of course, the integration over solid angle of every angular distribution defined here must be equal to the corresponding cross section, e.g.

$$\sigma_{n,n'}^{i,direct} = \int d\Omega \frac{d\sigma_{n,n'}^{i,direct}}{d\Omega}. \tag{4.33}$$

In the output of TALYS, we use a representation in terms of outgoing angle and one in terms of Legendre coefficients, i.e. Eq. (4.30) can also be written as

$$\frac{d\sigma^{el}}{d\Omega} = \sum_L (C_L^{shape-el} + C_L^{comp-el}) P_L(\cos\Theta), \tag{4.34}$$

where P_L are Legendre polynomials. For inelastic scattering we have

$$\frac{d\sigma_{n,n'}^i}{d\Omega} = \sum_L (C_L^{i,direct} + C_L^{i,comp}) P_L(\cos\Theta), \tag{4.35}$$

and similarly for the other binary channels. The Legendre expansion is required for the storage of the results in ENDF data libraries.

4.3.2 Exclusive spectra

An exclusive spectrum is not only specified by the exact number of emitted particles, but also by their outgoing energies.

In TALYS, exclusive spectra are calculated in the same loops that take care of the exclusive cross sections. The inclusive continuum spectra are obtained by taking the derivative of the inclusive cross sections per excitation energy of Eq. (4.10) with respect to the outgoing particle energy $E_{k'}$,

$$E_{k'} = E_x - E_{x'}(i') - S_{k'}, \tag{4.36}$$

where $S_{k'}$ is the separation energy for outgoing particle k'. Note that since the inclusive cross section per excitation energy S depends on $E_{k'}$ via s_k, the product rule of differentiation applies to Eq. (4.10). Therefore, the inclusive spectrum per excitation energy for an outgoing particle k' of a given $(i_n, i_p, i_d, i_t, i_h, i_\alpha)$ channel is

$$\frac{dS}{dE_{k'}}(i_n, i_p, i_d, i_t, i_h, i_\alpha, E_{x'}(i')) = \sum_{k=\gamma,n,p,d,t,h,\alpha} \sum_i$$
$$[\frac{s_k(Z, N, E_x(i), E_{x'}(i'))}{P(Z, N, E_x(i))} \frac{dS}{dE_{k'}}(i_n - \delta_{nk}, i_p - \delta_{pk}, i_d - \delta_{dk}, i_t - \delta_{tk}, i_h - \delta_{hk}, i_\alpha - \delta_{\alpha k}, E_x(i))$$
$$+ \quad \delta_{kk'} \frac{ds_k(Z, N, E_x(i), E_{x'}(i'))}{dE_{k'}} \frac{S(i_n - \delta_{nk}, i_p - \delta_{pk}, i_d - \delta_{dk}, i_t - \delta_{tk}, i_h - \delta_{hk}, i_\alpha - \delta_{\alpha k}, E_x(i))}{P(Z, N, E_x(i))}], \tag{4.37}$$

where, as initial condition, the derivatives of $s_k(Z_C, N_C, E_x^{max}, E_{x'}(i'))$ are the binary emission spectra. The first term on the right-hand side corresponds to the spectrum of the feeding channel and the second term denotes the contribution of the last emitted particle. The calculation of Eq. (4.37) can be done simultaneously with the exclusive cross section calculation, i.e. we follow exactly the same recursive procedure. The final exclusive spectrum for outgoing particle k' is given by

$$\frac{d\sigma^{ex}}{dE_{k'}}(i_n, i_p, i_d, i_t, i_h, i_\alpha) = \sum_{i=0,isomers} \frac{dS}{dE_{k'}}(i_n, i_p, i_d, i_t, i_h, i_\alpha, E_i), \tag{4.38}$$

The terms on the right hand side are the exclusive spectra per ground state or isomer. The latter naturally result from our method, even though only the total exclusive spectra of the left hand side are of interest.

We stress that for a given $(i_n, i_p, i_d, i_t, i_h, i_\alpha)$ channel, Eq. (4.37) is calculated for *every* outgoing particle k' (i.e. n, p, d, t, h and α). Hence, e.g. the $(n, 2np\alpha)$ channel is characterized by only one exclusive cross section, $\sigma_{n,2np\alpha}$, but by three spectra, one for outgoing neutrons, protons and alpha's, respectively, whereby all three spectra are constructed from components from the first up to the fourth particle emission (i.e. the α can have been emitted in each of the four stages). In practice, this means that all spectra have a first order pre-equilibrium component (and for higher energies also higher order pre-equilibrium components), and a compound component from multiple emission. Upon integration over outgoing energy, the exclusive cross sections may be obtained,

$$\sigma^{ex}(i_n, i_p, i_d, i_t, i_h, i_\alpha) = \frac{1}{i_n + i_p + i_d + i_t + i_h + i_\alpha} \sum_{k'=n,p,d,t,h,\alpha} \int dE_{k'} \frac{d\sigma^{ex}}{dE_{k'}}(i_n, i_p, i_d, i_t, i_h, i_\alpha). \quad (4.39)$$

4.3.3 Binary spectra

Similar to the cross sections, the exclusive spectra determine various other specific spectra of interest. The exclusive *inelastic spectrum* is a special case of Eq. (4.38)

$$\frac{d\sigma_{n,n'}}{dE_{n'}} = \frac{d\sigma^{ex}}{dE_{n'}}(1,0,0,0,0,0). \quad (4.40)$$

Since Eq. (4.37) represents an energy spectrum, it includes by definition only continuum transitions, i.e. it does not include the binary reactions to discrete states. Hence, upon integration, Eq. (4.40) only gives the continuum inelastic cross section of Eq. (4.14):

$$\sigma_{n,n'}^{cont} = \int dE_{n'} \frac{d\sigma_{n,n'}}{dE_{n'}}. \quad (4.41)$$

Similar relations hold for the binary (n,p), (n,d), (n,t), (n,h) and (n,α) spectra. The contributions to the binary spectra generally come from pre-equilibrium and continuum compound spectra.

4.3.4 Total particle production spectra

Similar to the total particle production cross sections, the *composite* or *total neutron spectrum* can be expressed in terms of exclusive spectra as follows

$$\frac{d\sigma_{n,xn}}{dE_{n'}} = \sum_{i_n=0}^{\infty} \sum_{i_p=0}^{\infty} \sum_{i_d=0}^{\infty} \sum_{i_t=0}^{\infty} \sum_{i_h=0}^{\infty} \sum_{i_\alpha=0}^{\infty} \frac{d\sigma^{ex}}{dE_{n'}}(i_n, i_p, i_d, i_t, i_h, i_\alpha), \quad (4.42)$$

i.e. in the other notation,

$$\frac{d\sigma_{n,xn}}{dE_{n'}} = \frac{d\sigma_{n,n'}}{dE_{n'}} + \frac{d\sigma_{n,2n}}{dE_{n'}} + \frac{d\sigma_{n,np}}{dE_{n'}} + \frac{d\sigma_{n,2np}}{dE_{n'}} + ... \quad (4.43)$$

Similar relations hold for the (n,xp), etc. spectra. Note that, in contrast with Eq. (4.20), the multiplicity is already implicit in the exclusive spectra.

Again, in practice we do not use Eq. (4.42) to calculate the composite spectra but instead add the $ds_k(Z, N, E_x, E_{x'})/dE_{k'}$ term that appears in Eq. (4.37) to the composite spectra while depleting all nuclides in an inclusive calculation. We do use Eq. (4.42) as a numerical check in the case of a

few outgoing particles. Finally, integration of the total neutron spectrum and addition of the binary discrete cross section gives the total particle production cross section

$$\sigma_{n,xn} = \int dE_{n'} \frac{d\sigma_{n,xn}}{dE_{n'}} + \sigma_{n,n'}^{disc}, \tag{4.44}$$

and similarly for the other particles.

Sample case 4.6 Inelastic spectra at 20 MeV: Direct + Preeq + GR + Compound

For pre-equilibrium studies, it may be worthwhile to distinguish between the various components of the emission spectrum. This was already mentioned in sample case (1c). As an extra sample case, we compare the calculated ^{209}Bi(n,xn) spectrum at 20 MeV with experimental data. This is accomplished with the following input file,

```
#
# n-Bi209-spec
#
# General
#
projectile n
element bi
mass 209
energy 20.
#
# Parameters
#
ddxmode 2
filespectrum n
```

The various components of the spectrum, and the total, as present in the file *nspec020.000.tot*, are plotted in Fig. 4.10.   ∎

4.3.5 Double-differential cross sections

The generalization of the exclusive spectra to angular dependent cross sections is done by means of the exclusive double-differential cross sections

$$\frac{d^2\sigma^{ex}}{dE_{k'}d\Omega}(i_n, i_p, i_d, i_t, i_h, i_\alpha), \tag{4.45}$$

which are obtained by either physical models or systematics. Integration over angles yields the exclusive spectrum

$$\frac{d\sigma^{ex}}{dE_{k'}}(i_n, i_p, i_d, i_t, i_h, i_\alpha) = \int d\Omega \frac{d^2\sigma^{ex}}{dE_{k'}d\Omega}(i_n, i_p, i_d, i_t, i_h, i_\alpha). \tag{4.46}$$

The other relations are analogous to those of the spectra, e.g. the inelastic double-differential cross section for the continuum is

$$\frac{d^2\sigma_{n,n'}}{dE_{n'}d\Omega} = \frac{d^2\sigma^{ex}}{dE_{n'}d\Omega}(1,0,0,0,0,0), \tag{4.47}$$
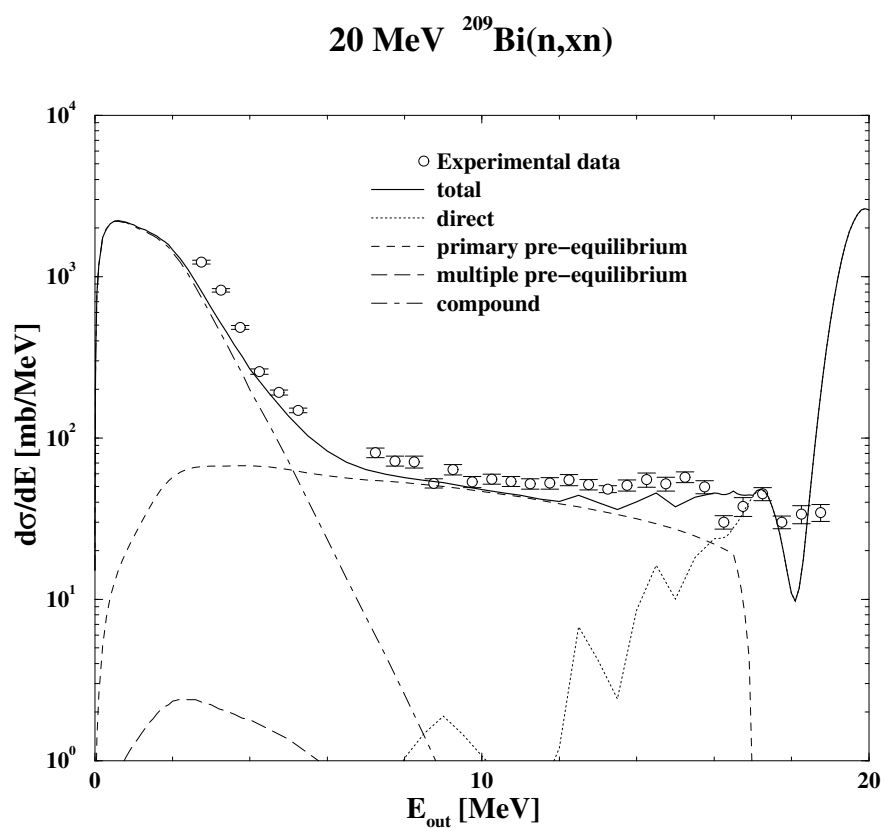
20 MeV ^{209}Bi(n,xn)

Figure 4.10: ^{209}Bi (n,xn) spectrum at 20 MeV. Experimental data are obtained from [9].

and the total neutron double-differential cross section can be expressed as

$$\frac{d^2\sigma_{n,xn}}{dE_{n'}d\Omega} = \sum_{i_n=0}^{\infty} \sum_{i_p=0}^{\infty} \sum_{i_d=0}^{\infty} \sum_{i_t=0}^{\infty} \sum_{i_h=0}^{\infty} \sum_{i_\alpha=0}^{\infty} \frac{d^2\sigma^{ex}}{dE_{n'}d\Omega}(i_n,i_p,i_d,i_t,i_h,i_\alpha). \tag{4.48}$$

For the *exclusive* calculation, the angular information is only tracked for the first particle emission. The reason is that for incident energies up to about 20 to 30 MeV, only the first emitted particle deviates from an isotropic angular distribution. Multiple compound emission to the continuum is essentially isotropic. The isotropic contribution to the exclusive double-differential spectrum is then simply determined by the part of the corresponding cross section that comes from Hauser-Feshbach decay. At higher incident energies, where the approximation of only one forward-peaked particle becomes incorrect, the interest in exclusive spectra, or for that matter, the computational check of Eq. (4.48), is no longer there. The presence of multiple pre-equilibrium emission at energies above several tens of MeV requires that we include angular information for every emitted particle in the *total* double-differential cross section, i.e. the left-hand side of Eq. (4.48). Again, this is all tracked correctly in the full inclusive calculation.

4.4 Fission cross sections

For clarity, we have kept the fission channel out of the discussion so far. The generalization to a picture in which fission is possible is however not too difficult. For fissile nuclides, the first expression that needs generalization is that of the non-elastic cross section expressed as a sum of exclusive cross sections, Eq. (4.6). It should read

$$\sigma_{non-el} = \sum_{i_n=0}^{\infty} \sum_{i_p=0}^{\infty} \sum_{i_d=0}^{\infty} \sum_{i_t=0}^{\infty} \sum_{i_h=0}^{\infty} \sum_{i_\alpha=0}^{\infty} \sigma^{ex}(i_n,i_p,i_d,i_t,i_h,i_\alpha) + \sigma_f, \tag{4.49}$$

where the *total fission* cross section σ_f is the sum over exclusive fission cross sections

$$\sigma_f = \sum_{i_n=0}^{\infty} \sum_{i_p=0}^{\infty} \sum_{i_d=0}^{\infty} \sum_{i_t=0}^{\infty} \sum_{i_h=0}^{\infty} \sum_{i_\alpha=0}^{\infty} \sigma_f^{ex}(i_n,i_p,i_d,i_t,i_h,i_\alpha), \tag{4.50}$$

where $\sigma_f^{ex}(i_n,i_p,i_d,i_t,i_h,i_\alpha)$ represents the cross section for fissioning *after* the emission of i_n neutrons, i_p protons, etc. Well-known special cases are $\sigma_{n,f} = \sigma_f^{ex}(0,0,0,0,0,0)$, $\sigma_{n,nf} = \sigma_f^{ex}(1,0,0,0,0,0)$ and $\sigma_{n,2nf} = \sigma_f^{ex}(2,0,0,0,0,0)$, which are also known as first-chance, second-chance and third-chance fission cross section, respectively. Eq. (4.50) is more general in the sense that it also includes cases where particles other than neutrons can be emitted before the residual nucleus fissions, e.g. (n,npf), which may occur at higher incident energies.

The generalization of the non-elastic cross section of Eq. (4.19) is

$$\sigma_{non-el} = \sum_{k=\gamma,n',p,d,t,h,\alpha} \sigma_{n,k}^{inc,bin} + \sigma_f^{bin}, \tag{4.51}$$

where σ_f^{bin} represents fission from the initial compound state (i.e. excluding $(n,\gamma f)$ processes).

Analogous to Eq. (4.25), we can define a cross section for each fissioning residual product

$$\sigma_{prod}^{fis}(Z,N) = \sum_{i_n=0}^{\infty} \sum_{i_p=0}^{\infty} \sum_{i_d=0}^{\infty} \sum_{i_t=0}^{\infty} \sum_{i_h=0}^{\infty} \sum_{i_\alpha=0}^{\infty} \sigma_f^{ex}(i_n,i_p,i_d,i_t,i_h,i_\alpha)\delta_N\delta_Z. \tag{4.52}$$

At higher energies, the meaning of $\sigma_{prod}^{fis}(Z,N)$ is more relevant than the exclusive fission cross sections. Consequently, for the total fission cross section we have

$$\sigma_f = \sum_Z \sum_N \sigma_{prod}^{fis}(Z,N). \tag{4.53}$$

What remains to be explained is how σ_f^{ex} is computed. First, we need to add to Eq. (4.8) a term we denote by $s_f(Z,N,E_x(i))$, which is the part of the population that fissions from the $(Z,N,E_x(i))$ bin. Hence, for fissile nuclides we have

$$P(Z,N,E_x(i)) = s_f(Z,N,E_x(i)) + \sum_{k=\gamma,n,p,d,t,h,\alpha} \sum_i s_k(Z,N,E_x(i),E_{x'}(i')). \tag{4.54}$$

where in this case the sum over i runs over discrete levels and continuum bins from 0 to $E_x(i) - S_k$. The exclusive fission cross section σ_f^{ex} is

$$\sigma_f^{ex}(i_n,i_p,i_d,i_t,i_h,i_\alpha) = \sum_i \frac{s_f(Z,N,E_x(i))}{P(Z,N,E_x(i))} S(i_n,i_p,i_d,i_t,i_h,i_\alpha,E_x(i)). \tag{4.55}$$

where i runs from 0 to $E_x^{max}(Z,N)$. The rest of the calculation of the exclusive particle cross section proceeds exactly as before. Eq. (4.10) is now automatically depleted from the fission cross section (4.55), in the sense that the s_k terms alone, summed over γ and particles only, no longer add up to the population P.

Finally, the exclusive fission cross sections are also accompanied by spectra. For example, the first two neutrons emitted in the $(n,2nf)$ channel (third-chance fission) are described by an outgoing neutron spectrum. The exclusive spectrum of outgoing particle k' in a fission channel is

$$\frac{d\sigma_f^{ex}}{dE_{k'}}(i_n,i_p,i_d,i_t,i_h,i_\alpha) = \sum_i \frac{s_f(Z,N,E_x(i))}{P(Z,N,E_x(i))} \frac{dS}{dE_{k'}}(i_n,i_p,i_d,i_t,i_h,i_\alpha), \tag{4.56}$$

while the exclusive particle spectra are again described by Eq. (4.37). For double-differential spectra, the usual generalization holds. We also repeat here that the total (observable) fission cross section is always calculated by letting reaction population go into the fission channel from each (Z,N,E_x,J,Π) channel until all nuclides have ended up in their ground or isomeric state, irrespective of the user request for an exclusive channel calculation.

Sample case 4.7 **Fission cross sections: n + ^{232}Th: WKB approach**

It is well known that a systematic approach for fission is difficult to achieve. It is possible to obtain very satisfactory fits to fission data with TALYS, but at the expense of using many adjustable input parameters. We are performing extensive model calculations to bring somewhat more structure in the collection of fitting parameters. In the meantime, we include here a sample case for the description of the fission cross section of ^{232}Th. This sample case shows the WKB approximation to calculate fission transmission coefficients as outlined in Ref. [10] and Ref. [11]. It can be invoked with the keyword **fismodel 5**.

We use the following input file,

```
#
# n-Th232-fisaa-wkb
#
# General
#
projectile n
```

```
element     Th
mass        232
ltarget     000
energy      energies
maxlevelstar    30
partable y
bins 40
ejectiles g n
#
# do not use best parameters from database
#
best n
#
# set multi-preequilibrium switch lower for actinides
#
multipreeq 6.
#
# output of extra channels
#
channels y
filechannels y
outfission y
#
# reduce output for activation-only calculation
#
outspectra n
outangle n
ddxmode 0
outdiscrete n
maxrot 2
strength 9
strengthm1 3
ngfit y
upbend y
ldmodel 5
fismodel 5
fispartdamp y
hbstate n
class2 n
ecissave y
eciscalc y
inccalc y
outdiscrete y
riplrisk y
#
```

```
# Current variables of TASMAN Run:  2509
#
ctable          90 233    1.35146 1
ptable          90 233 -1.94808E+00 1
ctable          90 233 -9.41013E-01 2
ptable          90 233    1.01594 2
ctable          90 233    3.16960 3
ptable          90 233 -1.14439E+00 3
betafiscor      90 233    1.04349
vfiscor         90 233    0.71170
ctable          90 232    0.32630 1
ptable          90 232    2.77492 1
ctable          90 232    8.34473 2
ptable          90 232 -6.59883E+00 2
ctable          90 232    0.69898 3
ptable          90 232    0.75241 3
betafiscor      90 232    0.50505
vfiscor         90 232    0.84379
ctable          90 231  5.77646E-02 1
ptable          90 231 -2.67866E+00 1
ctable          90 231 -3.61946E+00 2
ptable          90 231 -2.25936E+00 2
ctable          90 231 -2.85851E+00 3
ptable          90 231    2.66753 3
betafiscor      90 231    1.58614
vfiscor         90 231    1.62104
ctable          90 230 -3.18402E+00 1
ptable          90 230 -4.20179E+00 1
ctable          90 230    1.13153 2
ptable          90 230 -5.43220E-01 2
ctable          90 230    1.01315 3
ptable          90 230 -2.80603E+00 3
betafiscor      90 230    1.66138
vfiscor         90 230    1.71450
```

The above parameters are the usual ones to be adjusted to get good agreement with experimental data: level density and fission parameters for the ground state or on top of the barriers. The resulting file *fission.tot* is plotted together with experimental data in Fig. 4.11.

Due to the presence of **outfission y** in the input file, all nuclear structure related to the fission process is given in the output for the target and the compound nucleus

```
 Fission information for Z= 90 N=142 (232Th)

 Number of fission barriers       :  3
 Correction factor betafiscor:   0.505
 Correction factor vfiscor   :   0.844
```

```
Adjustable factor betafiscoradjust:   1.000
Adjustable factor vfiscoradjust   :   1.000


Parameters for fission barrier  1


Type of axiality                   :  3
Height of fission barrier 1        :    4.098
Width of fission barrier 1         :    1.103
Rtransmom                          :    0.600
Moment of inertia                  :   87.657
Number of head band transition states:  0
Start of continuum energy          :    0.000
.................
Parameters for fission barrier  2


Type of axiality                   :  1
Height of fission barrier 2        :    5.804
Width of fission barrier 2         :    1.032
Rtransmom                          :    1.000
Moment of inertia                  :  154.212
Number of head band transition states:  0
Start of continuum energy          :    0.000
.............
```

Moreover, the corresponding fission transmission coefficients are printed for all excitation energies encountered in the calculation

```
Fission transmission coefficients for Z= 90 N=143 (233Th) and an excitation

   J      T(J,-)      T(J,+)    Gamma(J,-)  Gamma(J,+)   tau(J,-)    tau(J,+)

  0.5   0.00000E+00 0.00000E+00 0.00000E+00 0.00000E+00 0.00000E+00 0.00000E+00
  1.5   0.00000E+00 0.00000E+00 0.00000E+00 0.00000E+00 0.00000E+00 0.00000E+00
  2.5   0.00000E+00 0.00000E+00 0.00000E+00 0.00000E+00 0.00000E+00 0.00000E+00
  3.5   0.00000E+00 0.00000E+00 0.00000E+00 0.00000E+00 0.00000E+00 0.00000E+00
  4.5   0.00000E+00 0.00000E+00 0.00000E+00 0.00000E+00 0.00000E+00 0.00000E+00
  5.5   0.00000E+00 0.00000E+00 0.00000E+00 0.00000E+00 0.00000E+00 0.00000E+00
  6.5   0.00000E+00 0.00000E+00 0.00000E+00 0.00000E+00 0.00000E+00 0.00000E+00
.............
```

The fission information for all residual nuclides can be obtained in the output file as well by adding *outpopulation y* to the input file.

As an exercise, the user may want to try to adjust the first fission barrier of ^{232}Th to get a better fit of the second chance fission cross section.   ■

4.5 Recoils

4.5.1 Qualitative analysis

In a nuclear reaction code, the calculations are usually performed in the center of mass (CM) frame, while the experimental data are obtained in the Laboratory (LAB) frame. It is therefore necessary

^{232}Th(n,f)
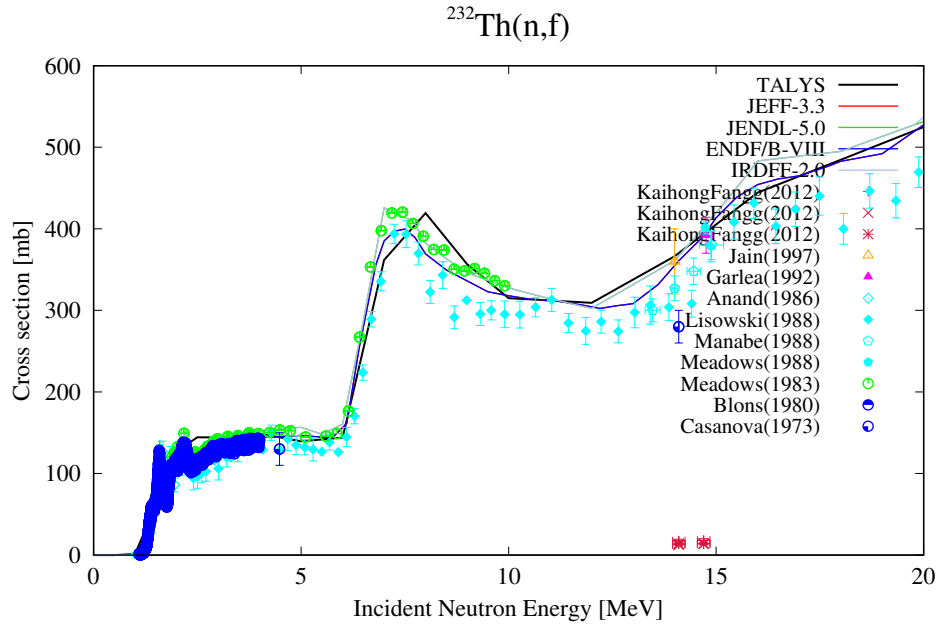
Figure 4.11: Neutron induced fission cross section of ^{232}Th compared with experimental data.

to perform a transformation either by (i) expressing the experimental data in the CM frame or by (ii) expressing the CM model results in the LAB frame. Of course, the cross sections are the same in both frames, but the spectra are certainly different. The best example is given by the elastic peak in an emission spectrum which is a Dirac delta peak in the CM frame and rather looks like a Gaussian when measured experimentally. The reason for this, apart from the fact that the projectile beam is not perfectly mono-energetic, is that the composite system has a velocity in the LAB frame before decay occurs. Consequently if one considers the emission of an ejectile with a well defined energy in the CM frame, the ejectile energy in the LAB frame will not be unique because of all the CM emission angles. More precisely, a maximum ejectile energy will be obtained when the emission occurs at $0°$, and a minimum will be obtained at $180°$, together with all the intermediate situations. Dealing with this situation is simple if only one nucleus decays, but if two particles are sequentially emitted, the first emission probabilities create a velocity distribution of the residual nuclei in the LAB frame. One must first loop over these velocities before one can compute the secondary emission.

4.5.2 General method

As mentioned in section 4.2.2, in TALYS each nucleus that can decay is described by an array $P(Z,N,E_x)$ which gives the population in a bin/level with excitation energy E_x of the nucleus (Z,N). A special case is the initial compound nucleus which contains all the initial reaction population at its total excitation energy E_x^{max}. For the kinematics of the binary reactions, it is necessary to keep track of the velocities and moving directions of these nuclei in the LAB frame, so that we can reconstruct the LAB spectra from the decays in the CM frame. We therefore have to add in principle three dimensions to the P array. The first one to keep track of the recoil energy, and the two other ones for the emission angles. However, such book-keeping would become very time consuming, especially for high energies.

Hence, we only take into account the recoil energies and the usual Θ angle and define another

array $P_{rec}(Z,N,E_x,E_r,\Theta_r)$ which indicates the fraction of the total population $P(Z,N,E_x)$ moving with the kinetic energy E_r in the direction Θ_r with respect to the beam direction in the LAB frame. Obviously,

$$P(Z,N,E_x) = \sum_{E_r\ bins} \sum_{\Theta_r\ bins} P_{rec}(Z,N,E_x,E_r,\Theta_r). \tag{4.57}$$

Again, the initial compound nucleus (Z_C,N_C) is a special one. Its kinetic energy E_r^0 in the LAB frame is unique and is given by

$$E_r^0 = \sqrt{(E_p^2 + 2M_pE_p + M_C^2)} - M_C, \tag{4.58}$$

where E_p is the projectile kinetic energy in the LAB, M_p the projectile mass and M_C the compound nucleus mass, and it moves in the beam direction (i.e. $0°$). Before any emission is calculated, the initial reaction population is stored in the array element $P_{rec}(Z_c,N_c,E_x^{max},E_r^0,0)$. As explained before, the population of the residual nuclei bins are calculated by looping over all possible ejectiles, emission energies and angles in the CM frame. Therefore, each time we decay from a mother bin to a residual bin, we know exactly what fraction of the total bin population is emitted in a given CM (energy,angle) bin. We then simply couple the CM emission energies and angles with the CM kinetic energy and moving direction in the LAB frame to determine simultaneously the ejectile double-differential spectrum in the LAB and the residual nucleus population in the corresponding LAB (energy,angle) bin. This may seem simple from a qualitative point of view, it is however not trivial to implement numerically and can be time consuming.

4.5.3 Quantitative analysis

From now on, for simplicity, we assume that the kinematics of the binary reactions can be considered as a classical process, i.e. we exclude γ decay and relativistic kinematics in the recoil calculation. We here consider the emission of a given ejectile from a given energy bin i of the decaying nucleus (Z,N) which moves with a given velocity v_{cm} (or kinetic energy E_{cm}) in the direction Θ_{cm} with respect to the beam direction. The total population that is going to decay is $P(Z,N,E_i)$ and the fraction of this population moving with the velocity v_{cm} in the direction Θ_{cm} is given by $P_{rec}(Z,N,E_i,E_{cm},\Theta_{cm})$. We can determine the total emitted flux for a given emission energy and a given emission angle in the CM frame. In practice, we rather decay from a initial bin to a residual bin in a given angular bin in the CM frame. If recoil effects are neglected we directly derive from such a decay an energy bin $[E_{low}^{CM},E_{up}^{CM}]$ and an angular bin $[\Theta_{low}^{CM},\Theta_{up}^{CM}]$ in which the total flux Φ_{ej}^{CM} is emitted. Accounting for recoil effects requires an intermediate step to share the available energy ΔE (difference between the energy bins of the initial nucleus and final nucleus) among the ejectile with mass m_{ej} and the residual nucleus with mass M_R.

To do this, we use the classical relation

$$\vec{v}_{ej}^{LAB} = \vec{v}_{cm} + \vec{v}_{ej}^{CM}, \tag{4.59}$$

which connects the LAB velocity $\vec{v}_{ej}^{LAB}$ of the ejectile with its velocity $\vec{v}_{ej}^{CM}$ in the CM frame and the CM frame velocity $\vec{v}_{cm}$. We need to connect $\vec{v}_{ej}^{CM}$ with ΔE.

This can be done upon writing

$$\Delta E = \frac{1}{2}m_{ej}(\vec{v}_{ej}^{CM})^2 + \frac{1}{2}M_R(\vec{v}_R^{CM})^2, \tag{4.60}$$

where $\overrightarrow{v}_R^{CM}$ is the residual nucleus velocity in the CM frame, and using the relation

$$m_{ej}\,\overrightarrow{v}_{ej}^{CM} + m_R\,\overrightarrow{v}_R^{CM} = \overrightarrow{0}. \tag{4.61}$$

Combining (4.60) and (4.61) yields

$$v_{ej}^{CM} = \sqrt{2\frac{M_R}{m_{ej}(m_{ej}+M_R)}\Delta E}, \tag{4.62}$$

which reduces to the classical relation

$$v_{ej}^{CM} = \sqrt{\frac{2\Delta E}{m_{ej}}}, \tag{4.63}$$

if recoil effects are neglected (i.e. in the limit $M_R \rightarrow +\infty$).

Once this connection is established, Eq. (4.59) is used to determine the velocity and angle of both the emitted light particle and the residual nucleus by simple projections on the LAB axis.

Hence, given a decay situation in the CM frame, we can reconstruct both the energy and angle of emission in the LAB frame. We now have to determine the link between the double-differential decay characteristics in both frames. The solution is well known (see Ref. [12] for instance) and consists of using a Jacobian which accounts for the modification of an elementary solid angle $d\Omega$ in the CM frame when going into the LAB frame. However, in TALYS we have to employ another method because we do not generally calculate decays for well defined energies and angles but rather for a given energy bin and angular bin. Moreover, since we do not account for the azimuthal angle, we may also encounter some problems when calculating recoil for secondary emission. Indeed, only the first binary process has the azimuthal symmetry with respect to the beam direction.

4.5.4 The recoil treatment in TALYS

The way the double-differential spectra are calculated by TALYS in the LAB frame from those obtained in the CM frame is illustrated in Fig. 4.12. As stressed in Chapter 4, the emission energy grid for the outgoing particles is non-equidistant. Moreover, one has to keep in mind that the total flux $\Phi(i,j)$ in an energy-angular bin (i,j) is connected with the double differential cross section $xs(i,j)$ by

$$\Phi(i,j) = xs(i,j)\Delta E(i)\Delta cos\Theta(j). \tag{4.64}$$

Consequently, it is appropriate to locate the grid points using an energy-cosine grid. As an example, in Fig. 4.12, we consider the decay in the CM bin defined by the energy interval $[2,3]$ and the cosine interval $[0.25, 0.5]$ (black region). We assume that the decay occurs from a composite system moving with a kinetic energy of 1 MeV in the direction $45°$ with respect to the initial beam direction. The mass of the ejectile is assumed to be $m_e = 1$ arb.unit, and that of the composite system 20 arb.unit. In that case, the region reached by the ejectile is a slightly deformed trapezoid (gray region) which covers several bins. Therefore, if the emitted flux is located in a single bin in the CM, it must be distributed over several bins when going to the LAB frame. This is the key problem to be solved in TALYS. To solve this problem, we need to make assumptions to be able (i) to calculate the area covered in the LAB frame (gray region) and (ii) the way this global area is distributed over the bins it partially covers. The assumption made in TALYS consists of neglecting the deformation of the boundaries of the grey area and assuming this area to be a trapezoid. In other words, we make

20 MeV n + ^{28}Si: recoil spectrum
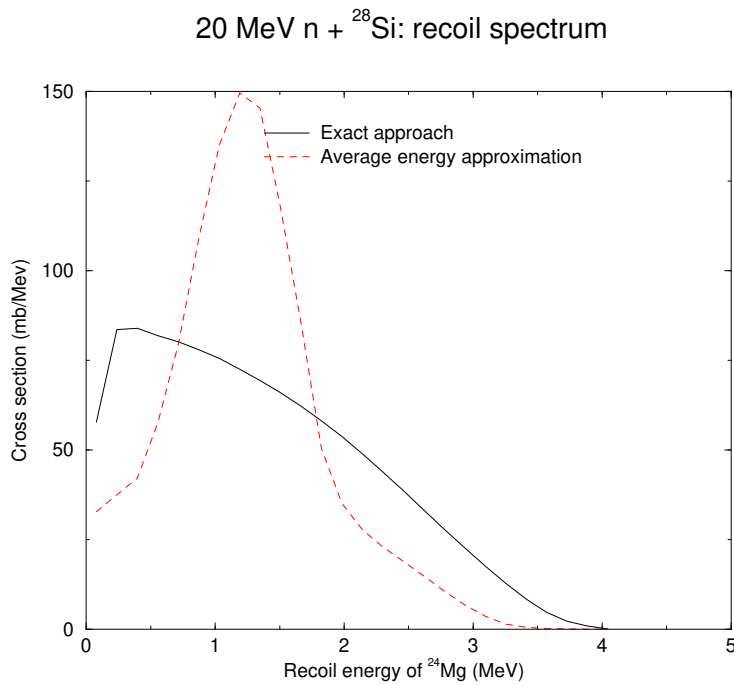
Figure 4.12: CM and LAB double-differential spectra in TALYS.

the assumption that a triangle in the CM frame is transformed into a triangle when going in the LAB. This is helpful since the area of a triangle is given by a simple analytic expression as function of the coordinates of the summits of the triangle. Therefore, we divide the starting CM bins into two triangles to determine the two triangles obtained in the LAB frame. With such a method, the whole problem can be solved and the decay calculated in the CM frame can be transformed to the LAB frame without any further approximations.

However, in practice, coupling the angular direction (in the LAB) of the nucleus that decays with the ejectile emission angle in the CM frame, while neglecting the azimuthal angle, gives double differential ejectile spectra in the LAB which are generally not correct. In fact, we believe that it is better not to account for the angular distribution of the decaying nucleus unless both Θ and ϕ are explicitly treated. Fortunately, the final angular distribution of the recoiling nucleus is seldom of interest.

4.5.5 Method of average velocity

As mentioned above, we do not loop over the angular distribution of the decaying nucleus. This is equivalent to replacing the array $P_{rec}(Z,N,E_i,E_r,\Theta_r)$ by $P_{rec}(Z,N,E_i,E_r)$. Then, we only have to keep track of the velocities of the nucleus that is going to decay, i.e. we have to loop over the E_r bins to reconstruct both the ejectile and residual nuclei spectra. Another approximation that we have implemented as an option with **recoilaverage y** (p. 325), consists of using an average velocity before this reconstruction, a method first applied by Chadwick et al. [13, 14]. This approach avoids the loop over the E_r bins altogether and reduces the calculation time. However, for high energies, this might be too crude an approximation.

4.5.6 Approximative recoil correction for binary ejectile spectra

Maybe you are not interested in a full recoil calculation, but merely want to correct the outgoing particle spectra for the recoil of the nucleus. In that case you may use the following method which is implemented in TALYS for just that purpose and which is outlined below.

The assumptions are made that (*i*) only binary emission takes place, and that (*ii*) emission only occurs under 0°. Hence, this approximation is basically expected to be valid for angle-integrated spectra only. The CM to LAB conversion of the ejectile spectra takes under these conditions the following simple form:

$$E_{ej}^{lab} = \frac{M_R}{M_C} \Delta E + \frac{m_{ej} M_p}{M_C^2} E_p + 2 \sqrt{\frac{m_{ej} M_R M_p}{M_C^3} E_p \Delta E}, \tag{4.65}$$

in which E_{ej}^{lab} is the LAB ejectile energy. This correction is applied to the *full* ejectile spectrum including the multiple emission contributions. Hence, the approximation is rather crude. It saves, however, a lot of computer time. Since the high-energy tail originates completely from binary emission, this tail is correctly converted to the LAB system. Furthermore, the correction is small at low energies where the largest contributions from multiple emission reside.

Sample case 4.8 **Recoils: 20 MeV n + ^{28}Si**

In this sample case, we calculate the recoils of the residual nuclides produced by 20 MeV neutrons incident on ^{28}Si reaction. Two methods are compared.

Case a: "Exact" approach

In the exact approach, each excitation energy bin of the population of each residual nucleus is described by a full distribution of kinetic recoil energies. The following input file is used

```
#
# n-Si028-recoil-exact
#
# General
#
projectile n
element si
mass 28
energy 20.
#
# Parameters
#
m2constant 0.70
sysreaction p d t h a
spherical y
#
# Output
#
recoil y
filerecoil y
```

```
#
# General
#
projectile n
element si
mass 28
energy 20.
#
# Parameters
#
m2constant 0.70
sysreaction p d t h a
spherical y
#
# Output
#
recoil y
filerecoil y
```

For increasing incident energies, this calculation becomes quickly time-expensive. The recoil calculation yields separate files with the recoil spectrum per residual nucleus, starting with *rec*, followed by the Z, A and incident energy, e.g. *rec012024spec020.000.tot*. Also following additional output block is printed:

```
 8. Recoil spectra

 Recoil Spectrum for  29Si

  Energy    Cross section

   0.018 0.00000E+00
   0.053 0.00000E+00
   0.088 0.00000E+00
....................................
   0.676 3.21368E+00
   0.720 3.22112E+00
   0.763 3.21215E+00
   0.807 3.10619E+00
   0.851 2.60156E+00
   0.894 2.30919E-01

 Integrated recoil spectrum      :  1.04358E+00
 Residual production cross section:  9.71110E-01
```

Case b: Approximative approach
As an approximation, each excitation energy bin of the population of each residual nucleus is described by a an average kinetic recoil energy. For this, we add one line to the input file above,

```
recoilaverage y
```

The results, together with those of case (a), are compared in Fig. 4.12. ∎

5. Nuclear structure and model parameters

5.1 General setup of the database

We have aimed to unify the nuclear structure and model parameter database of TALYS as much as possible. In the *talys/structure/* directory you can find the *masses/, abundance/, levels/, fission/, resonances/, deformation/, optical/, thermal/, gamma/, density/, decay/ integral/* and *best/* subdirectories. Most subdirectories contain about 100 files, where each individual file points to a nuclear element and has the name *zZZZ* where ZZZ is the charge number of the element. One file contains the info for all the isotopes of one element. For example, the file *talys/structure/levels/final/Fe.lev* contains the discrete levels of all Fe (Z=26) isotopes. As you will see below, the chemical symbol is always present in the file itself, allowing an easy search. Every directory has this same substructure and also the formats in which the data are stored have been kept uniform as much as possible.

The nuclear structure database has been created from a collection of "raw" data files, which for a large part come from the Reference Input Parameter Library RIPL [6], that we used as a basis for TALYS.

5.2 Integral validation library

Since all excitation functions are available in TALYS after a run with many incident energies, it is relatively easy to calculate production or reaction rates for various applications. This is for example done for astrophysics and medical isotope production. Another possibility is to calculate the so called effective cross section for integral activation measurements, by folding the excitation functions by an experimental flux. In *talys/structure/flux*, we have stored more than 40 spectra, coming from the EASY package [15, 16], which have been used in past activation benchmarks. Also the effective cross sections are stored, allowing direct comparison with experimental data.

5.3 Decay data library

For medical isotope production, the decay paths to the produced isotopes need to be known. Therefore, in *talys/structure/decay* we have stored the JEFF-3.1.1 Radioactive Decay Data File in the usual element by element files.

5.4 Best TALYS input parameters

We have created the possibility to store the "best" set of model input parameters per nuclide. This is a helpful feature to ensure reproducibility of earlier obtained results, i.e. a nuclear reaction analysis with TALYS is stored in the best possible way (rather than scattered over input files in several working directories). Theoretically, a complete collection of best TALYS input parameter files would enable a high-quality description of nuclear reactions on all nuclides simultaneously (when used e.g. in a script to produce a complete nuclear data library), especially if the work is divided among more than a few persons. One would thus be able to get the best possible results with a seemingly default input file. The only requirement is that the keyword **best y** (p. 306) is set in the input file. All adjusted optical model, level density etc. parameters are stored in the *talys/structure/best* directory. As subdirectories, full isotope names should be used in the format (a1,i3.3) or (a2,i3.3), depending on the element symbol. Furthermore, the first character of the Symbol should be in upper case. In other words, valid examples of subdirectories are *Yb174/*, *F019/*, *Be009/*, and *U235*. For the sets of best parameters in these subdirectories, we use filenames *zZZZaAAAS.best* where ZZZ and AAA are the Z and A of the nuclide in i3.3 format, and S is the particle symbol (g, n, p, d, t, h,or a). This strict naming procedure is required for software that uses TALYS for nuclear data evaluation purposes. As an example, we show the best parameters for neutrons incident on ^{80}Se as present in the file *talys/structure/best/Se080/n-Se080.talys*,

```
#
# General
#
ldmodel 2
m2constant 0.9
#
# (n,tot), (n,el), (n,inl)
#
rvadjust n 1. 0.01 1. 0.5 0.99
rvadjust n 1. 10. 5.5 1.02
#
# (n,p), (n,2n), (n,np)
#
rvadjust p 1.04
avadjust p 1.04
gnadjust 34 81 0.90
gpadjust 34 81 0.90
tadjust 34 80 1.15
#
# (n,a)
#
rvadjust a 1.05
avadjust a 1.05
Cstrip a 1.00
Cknock a 1.00
aadjust      32  77 1.10
#
```

TALYS

Input:
* Keywords, eg:
`projectile n`
`element fe`
`mass 56`
`energy 14.`

Optional loops
* Incident
  energies

* Natural
  isotopes

Optical Model:
* Phenomenology
  local / global

Nucl. Structure:
* Abundancies
* Discrete levels
* Deformations
* Masses
* Level density par.
* Resonance par.
* Fission barrier par.
* Thermal XS
* Microscopic LD
* Prescission shapes

Direct reaction:
* Spherical OM
* DWBA
* Rotational CC
* Vibrational CC
* Giant resonances
* Weak–coupling

Preequilibrium:
* Exciton model
  – 2–component
* p–h LD phenom.
  – surface effects
* Kalbach systematics
  – angular distribution
  – cluster emission
* γ–ray emission

Compound:
* Width fluctuations
  – Moldauer
  – GOE triple integr.
  – HRTW
* Hauser–Feshbach
* Fission competition
  – isotopic yields
* γ–ray emission
* GC+ Ignatyuk

Multiple emission:
* Exciton (any order)
* Hauser–Feshbach
* Fission competition
  – isotopic yields
* γ–ray cascade
* All flux depleted
* Exclusive channels
* Recoils

Output:
*File 'output'
  defined by
  keywords

*Dedicated
  files with
  spectra, ...

ENDF:
* transport libs
* activation libs

Figure 5.1: Nuclear models in TALYS
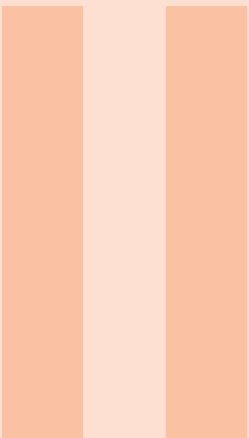
```
# (n,g)
ldmodelCN 1
#
#
# Other: Isomers, (n,d), (n,t), (n,h) etc.
#
```

If we use **best y**, the above set of keywords will automatically be added to the TALYS input file This directory is also the best place to store other TALYS input files such as files with tabular optical model parameters. They need to be copied to the working directory when the **best y** option is used. It is also possible to create alternative "best" database under *talys/structure* with a different collection of best input files. These can then be invoked with **bestpath** (p. 337).

Fig. 5.1 gives an overview of the nuclear models that are included in TALYS. They can generally be categorized into optical, direct, pre-equilibrium, compound and fission models, all driven by a comprehensive database of nuclear structure and model parameters. We will first describe the optical model and the various models for direct reactions that are used. Next, we give an outline of the various pre-equilibrium models that are included. Then, we describe compound nucleus models for both binary and multiple emission, and level densities, which are important ingredients of pre-equilibrium and compound models. Finally, we give an outline of the fission models.

Part Two: Nuclear Models

In this part of the tutorial, all nuclear models which are implemented in TALYS are described. This includes nuclear structure databases, which contains properties such as masses, discrete levels, level densities, fission barriers, etc., to nuclear reaction models such as the optical model and models for direct, compound, pre-equilibrium and fission reactions.

The set up in each Chapter follows the same consistent structure:

- **Outline of the model.** The nuclear models are explained to a reasonable depth. In general we restrict ourselves to the physical aspects and equations which are actually implemented in TALYS. We try to give as many relevant references as possible for more detailed information.

- **Options.** All TALYS keywords relevant to the Chapter under consideration are briefly mentioned. A full description of the keywords is given in Part III, the reference guide.

- **Implementation.** We give a short description on the implementation in terms of databases and also the subroutines which take care of the modelling.

- **Sample cases.** We aim to give you practical advice on how to use TALYS while we explain the nuclear models. That means that sample cases are scattered throughout this Part, when they matter most.

6. Nuclear masses and deformations

6.1 Nuclear masses

At the level of nuclear physics that is relevant to TALYS, the mass can be considered as the most basic property of the nucleus, and directly affects all the outcomes of a nuclear reaction calculation. For a start, separation energies and Q-values are directly dependent on the masses of the involved nuclides, and determine whether certain reactions can take place or not. The nuclear community has invested a lot of effort to compile experimental nuclear masses in data tables, and simultaneously theoretical nuclear structure models have been developed to predict masses and other properties of the nucleus.

In TALYS, we use both the real mass M in atomic mass units ($amu = 931.49386$ MeV) and the mass excess $\Delta M = (M - A) * amu$ in MeV from the mass tables. The latter are retrieved for a more precise calculation of separation energies. For example, the neutron separation energy of a nucleus (Z,N) is

$$S_n(Z,N) = M(Z,N-1) - M(Z,N) + M(n) \tag{6.1}$$

but we have actually implemented

$$S_n(Z,N) = \Delta M(Z,N-1) - \Delta M(Z,N) + \Delta M(n) \tag{6.2}$$

where $\Delta M(n)$ is the neutron mass excess and similarly for the other light particles,

For reaction Q-values one needs the masses of two nuclides. The Q-value is the difference between two separation energies,

$$Q(a,b) = S_a(Z,N) - S_b(Z,N) \tag{6.3}$$

If for only one of the two masses the experimental mass excess is known, at the edge of the experimental mass table, we take two *theoretical* mass excesses to calculate the Q-value, for

consistency. TALYS uses various different choices for theoretical nuclear masses, which can all be invoked when experimental masses are not available.

6.1.1   Experimental nuclear masses

The most recent generally used Atomic Mass Evaluation is AME2020 [17], which is the successor of the well-known Audi-Wapstra mass table, and this is the default in TALYS. Obviously, around the valley of stability we need to use experimentally determined masses and can not afford to deviate from this, especially if we want to reproduce experimental reaction data and be credible when providing data for nuclear applications. There are currently about 3550 nuclides for which the mass has been measured.

6.1.2   Theoretical nuclear masses

Theoretical masses are needed outside the range where measurements have been performed and sometimes exhibit an interesting dispersion, especially when applied in nuclear reaction models. The options we have included are:

- The latest version of the Skyrme-Hartree-Fock-Bogoliubov nuclear mass model by Goriely and Pearson [18]. This is the default,
- The Gogny-Hartree-Fock-Bogoliubov nuclear mass model by Goriely et al. [19],
- The Finite-Range Droplet Macroscopic (FRDM) model by Möller et al. [20],
- The Duflo-Zuker mass formula [21], included as a subroutine in TALYS. This is used if a nuclide is even outside the mass tables, or can be used simply as an interesting alternative.

Options 6.1.1 Enough flexibility has been built in for varying the nuclear masses. First of all, **massmodel** (p. 346) can be used to change the theoretical mass model, **expmass** (p. 347) to disable the experimental mass table altogether (i.e. discard AME2020), while the keywords **massnucleus** (p. 350) and **massexcess** (p. 351) can be used to directly change individual masses in the user input.

It is possible that we find future mass models so important that we add them to the database of the official TALYS version. Until that time, you can add your own mass table by adding a subdirectory to *talys/structure/masses/* and extend the range of values for **massmodel**. It is then your responsibility that the files have exactly the same structure as those of the standard four mass models. Hence, if you create e.g. a new mass table called *talys/structure/masses/moller2020/* with the correct files and file structure inside (i.e. that of **massmodel 1**, **2** or **3**, you can invoke that in the input with **massdir moller2020** (p. 349).

Implementation 6.1.1 All the mass models have been processed into our database and are stored in the *talys/structure/masses/* directory. We have provided 4 subdirectories, *audi/* for AME2020, *hfb/* for Skyrme-Hartree-Fock-Bogoliubov, *hfbd1m/* for Gogny-Hartree-Fock-Bogoliubov and *frdm/* for the FRDM model.

As an example, below are masses of Fe-isotopes as given in file *masses/audi/Fe.mass*. We have stored Z, A, mass (*amu*), mass excess (MeV), nuclear symbol with the format (2i4,2f12.6,42x,i4,a2).

```
  26  45   45.015467   14.408000                                          45Fe
  26  46   46.001299    1.210000                                          46Fe
  26  47   46.992346   -7.130000                                          47Fe
  26  48   47.980667  -18.008575                                          48Fe
```

```
26  49    48.973429   -24.750730                                            49Fe
26  50    49.962988   -34.476460                                            50Fe
```

All nuclear masses are read in *masses.f90*. First, it is checked whether an experimental value for the mass exists. If not, it reads the masses from one of the theoretical mass tables or resorts to the Duflo-Zuker formula, which is programmed in *duflo.f90*. Once all masses have been read, *separation.f90* calculates the separation energies for all nuclides and particles of interest. Next, the program returns to *nuclides.f90* where the Q-values are calculated.

Fundamental constants such as amu, masses and mass excesses of light particles, e.g. $\Delta M(n)$, are all stored in *constants.f90*.

Sample case 6.1 Mass models: n + ^{132}Sn.

This sample case illustrates the use of different mass models. We calculate neutron-induced reactions on ^{132}Sn as a function of incident energy for the default mass model (AME2020), which for this reaction provides experimental masses, the 3 different theoretical mass tables, and the Duflo-Zuker formula. The following input file is used for the default run,

```
#
# General
#
projectile n
element Sn
mass 132
energy 8. 20. 1.
```

while for the other cases we use

```
#
# General
#
projectile n
element Sn
mass 132
energy 8. 20. 1.
expmass n
massmodel 0
```

where **massmodel 0** activates the Duflo-Zuker formula, and another 3 runs with only the last line changed into **massmodel 1**, **2** and **3**, respectively.

Fig. 9.1 displays the different (n,p) cross sections, as obtained in files *rp049132.tot*. ∎

6.2 Deformation parameters

Deformation parameters are used at various places in TALYS. First of all, as input to OMP calculations for deformed nuclides, by means of the coupled-channels (for strong deformations) or DWBA (for weak deformations) formalism. This require values for (at least) β_2 and for rotational nuclides also β_4 and β_6. In addition, deformation parameters are used for the estimation of moments of inertia, which enter some level density models .

Options 6.2.1 The **beta2** (p. 348) is available to manually change the deformation parameter β_2.

Implementation 6.2.1 For the 3 directories with theoretical masses, the ground state deformation parameters β_2 and β_4 are given in the data files. The parameters in the *hfb/* directory are used by default for deformed nuclides. Moreover, the ground state spin and parity (for *hfb/* and *hfbd1m/*, not for *frdm/*) as estimated by the HFB model are given. As an example, below are the masses of some of the Fe-isotopes as given in file *masses/hfb/Fe.mass*. We have stored Z, A, mass (*amu*), mass excess (MeV), β_2, β_4, ground state spin and parity, nuclear symbol with the format (2i4,2f12.6,2f8.4,20x,f4.1,i2,i4,a2).

```
26   42    42.055503    51.701000   0.3200   0.0400                        0.0 1   42Fe
26   43    43.041632    38.780000   0.2700   0.0300                        0.5 1   43Fe
26   44    44.026225    24.428000  -0.2100   0.0400                        0.0 1   44Fe
26   45    45.014192    13.220000  -0.1800   0.0300                        1.5 1   45Fe
26   46    45.999931    -0.064000  -0.1100   0.0200                        0.0 1   46Fe
26   47    46.992187    -7.278000  -0.0900   0.0200                        3.5-1   47Fe
26   48    47.979358   -19.228000   0.1800   0.0700                        0.0 1   48Fe
```

6.3   Isotopic abundances

We have included the possibility to evaluate nuclear reactions for natural elements. The abundances are taken from RIPL[6] (which are equal to those of the Nuclear Wallet Cards from Brookhaven National Laboratory). If **mass 0** (p. 292), a TALYS calculation is performed for each isotope, after which the results are averaged with the isotopic abundance as weight.

Options 6.3.1 By default, the abundances are taken from the tables mentioned above. However, it may be useful to do TALYS calculations for enriched targets. For that purpose, the **abundance** (p. 333) keyword is available to create the isotopic target composition of your own choice.

Implementation 6.3.1 In *abundance.f90* the abundances are read. Note that for natural targets, there is a loop over all core subroutines of TALYS, in *talysloops.f90*, for each isotope, after which all results are properly averaged with the abundances as weight in *natural.f90*.

The isotopic abundances are stored in the *talys/structure/abundance/* directory. As an example, below are the isotopic abundances for Fe from the file *abundance/Fe.abun*. For each isotope, we have stored Z, A, its abundance, its uncertainty (not used in TALYS), nuclear symbol with the format (2i4,f11.6,f10.6,45x,i4,a2).

```
26   54     5.845000   0.035000                                             54Fe
26   56    91.754000   0.036000                                             56Fe
26   57     2.119000   0.010000                                             57Fe
26   58     0.282000   0.004000                                             58Fe
```

7. Discrete levels

7.1 Discrete level file

Besides global properties like the mass and deformation of the nucleus, the discrete level scheme is essential for nuclear reaction simulations, as it is important for both direct and compound nuclear reactions. The most important examples are the discrete levels to be included for coupled-channels or DWBA calculations, Hauser-Feshbach decay in which the transition to each discrete level competes with all other channels, validation of the low-energy part of the level density and the gamma-ray decay from higher to lower discrete levels in residual nuclides. For the current capabilities of TALYS, we require for each discrete level the

- sequence number
- energy
- spin
- parity
- half life, especially when large (isomers)
- number of level branchings for gamma decay
- branching ratios to lower levels
- electron conversion coefficients

Ideally, this information would all be available from measurements, and a good example of an extensive experimental discrete level compilation and evaluation can be found in the ENSDF and NUBASE databases. These databases are the source for the RIPL database for discrete levels. Unfortunately, to have only measured discrete level data is not enough for TALYS, or any nuclear model code. The level scheme needs to be complete, i.e. for each discrete level all values of the above list need to be present, so that Hauser-Feshbach decay and gamma-ray cascade can be properly calculated.

Whenever information was missing in RIPL, it has been added to the TALYS discrete level files

with educated guesses.

For nuclides far away from the valley of stability, the discrete level database has been completed with the HFB ground state estimates for spin and parity from the mass database of [19], so that at lest discrete level and mass databases span the same range of nuclides.

Each discrete level should always have a spin and parity. Often, the measured level scheme is complete in terms of levels and energies up to a certain level number, but the spin may not be specified. All one can do then is to assign the spin and maximize the likelihood that it is correct. For that, a histogram is made of the measured spins of all levels up to the level with unknown spin. Next, this histogram is compared with a Fermi gas spin distribution,

$$R_F(E_x, J) = \frac{2J+1}{2\sigma^2} \exp\left[-\frac{(J+\frac{1}{2})^2}{2\sigma^2}\right]. \tag{7.1}$$

where

$$\sigma^2 = \left(0.83 A^{0.26}\right)^2 \tag{7.2}$$

gives a reasonable estimate [22] for discrete levels with energies up to a few MeV. The spin assigned to the level is that of the bin with measured spin values which has the largest underestimation of the theoretical spin distribution. Hence, for multiple levels with unknown spins the final distribution of measured + assigned spins will approach the theoretical one. A similar procedure is followed for unknown parities, we assign the parity which leads to a more equal parity distribution for all levels up to that level.

In addition an assignment procedure needs to be followed for branching ratios of levels to lower levels. Omission of branching ratios for a certain level, e.g. because they have not been measured, would mean that there is no gamma decay from that level and the reaction flux would be tied up there. In a Hauser-Feshbach calculation scheme, this would lead to an underestimation of the cross section which is determined by the feeding of higher levels to the ground state or an isomer. For assignment of branching ratios we make use of the photon strength function (PSF), which will be discussed in more detail later. For each mother level Ml, the probability of decay to a daughter level D is given by magnetic (M) or electric (E) radiation, with E1 and M1 as the strongest transitions. the gamma energy is

$$E_\gamma = E(M) - E(D),$$
$$l = J(M) - J(D),$$
$$P' = P(M) - P(D) \tag{7.3}$$

leading to the transmission coefficient

$$T_{X\ell}(E_\gamma) = 2\pi \overleftarrow{f_{X\ell}}(E_\gamma) E_\gamma^{2\ell+1}. \tag{7.4}$$

$$Br(D) = T_{X\ell}(E_\gamma, l, P') / \sum_{i=1}^{M} T_{X\ell}(E_\gamma, l, P') \tag{7.5}$$

Finally, the electron conversion coefficient estimates what fraction of the decay goes to electron conversion and the gamma-ray intensity. It is specified when the branching ratio is experimentally known, in other cases we keep it at a value of 0.001.

Spin, parity and branching ratio assignment have an impact of various observables. First of all, the isomeric ration, i.e. the division of the cross section between the ground state and an isomer, but also on gamma-ray intensities accompanying reactions, such as e.g. (n,n'γ) cross section. For the latter, in addition the electron conversion coefficient is important to assign the proper amount of the level decay to gamma emission.

Options 7.1.1 There are three versions of the discrete level database, and the **disctable** (p. 358) keyword allows to choose between them. The default choice is the RIPL-3 database, but with using theoretical level densities to extend any discrete level sequence to at least 100 levels. Moreover, unknown spins, parities and branching ratios are always assigned a value, based on the simple statistical rules mentioned above. We know discrete levels exist, measured or not, and including them should at least give a more realistic prediction of the discrete lines in a gamma-ray spectrum. Another options is the "pure" RIPL database, based on measurements only, which means that the last known discrete level may have a rather low sequence number, and in Hauser-Feshbach calculations is then directly followed by the continuum described by the level density. The third option is a purely theoretical database, i.e all discrete levels come from level density estimates, which may be used for interesting studies on the predictive power of Hauser-Feshbach calculations. With **branch** (p. 360) the branching ratios of the discrete level database can be overruled.

Implementation 7.1.1 The discrete level schemes are in the *talys/structure/levels/* directory. We have transformed it to a format that corresponds with that of the other parameter files in our database. Also, we filled in some omissions, repaired several errors and added some information necessary for Hauser-Feshbach calculations as explained above. For consistency, we have included discrete levels for all nuclides that are present in the (theoretical) mass database.

As an example, below are the first discrete levels of ^{93}Nb as given in file *final/Nb.lev*. We have stored Z, A, total number of lines for this isotope, number of levels for this isotope, nuclear symbol with the format (2i4,2i5,56x,i4,a2). There is a loop over the levels in which we first read the level number, level energy in MeV, spin, parity, number of gamma-ray branchings, lifetime, spin assignment character, parity assignment character, original ENSDF string with the format (i4,f11.6,f6.1,3x,i2,i3,19x,e9.3,1x,2a1,a18). If the spin of a level does not come from the original file but instead is assigned in RIPL or by us, we place a 'J' in column 59. Analogously, an assigned parity is denoted by a 'P' in column 60. Note also that we have retained the original ENSDF string in columns 61-78. This string indicates the possible choices for spins and parities. If TALYS produces odd results for a nuclear reaction, a possible cause could be the wrong assignment of spin or parity. Columns 59 and 60 and the ENSDF string will reveal whether there are other possibilities that can be (and maybe should have been) adopted. For each level, there may be an inner loop over the number of gamma-ray branchings, and for each branching we read the number of the level to which the gamma-ray decay takes place and the corresponding branching ratio and electron-conversion factor. If a branching ratio has been assigned by us, a 'B' is placed in column 58. The format for this line is (29x,i3,f10.6,e10.3,5x,a1).

```
 41  93  394  126                                                      93Nb
  0   0.000000   4.5   1  0                                            9/2+
  1   0.030770   0.5  -1  1                        5.090E+08           1/2-
                         0  1.000000 1.690E+05
  2   0.686790   1.5  -1  1                        2.800E-13           3/2-
```

```
                                              1   1.000000 1.870E-03
       3    0.743950    3.5    1   1                        5.100E-13                          7/2+
                                              0   1.000000 1.410E-03
       4    0.808820    2.5    1   2                        6.160E-12                          5/2+
                                              3   0.021580 7.670E-01
                                              0   0.978420 1.200E-03
       5    0.810320    2.5   -1   2                        1.000E-12                          5/2-
                                              2   0.000000 1.273E-01
                                              1   1.000000 1.310E-03
       6    0.949800    6.5    1   1                        4.360E-12                         13/2+
                                              0   1.000000 8.120E-04
       7    0.970000    1.5   -1   2                                    J                1/2-,3/2-
                                              4   0.500000 0.000E+00       B
                                              2   0.500000 0.000E+00       B
       8    0.978910    5.5    1   1                        2.580E-13                         11/2+
                                              0   1.000000 7.690E-04
       9    1.082680    4.5    1   3                        2.800E-12                          9/2+
                                              8   0.073863 2.044E-01
                                              3   0.687527 9.110E-03
                                              0   0.238610 6.080E-04
      10    1.127090    1.5    1   1                                    J                3/2,5/2,7/2
                                              4   1.000000 1.050E-02
```

For nuclides for which no experimental information was available, the string 'HFB' has been added as a comment to denote that the information comes from structure calculations.

There is a directory *levels/spectn* with spectroscopic factors for the direct capture process.

7.2 Deformation parameters

Options 7.2.1 The complexity of the coupling scheme can be steered by the **maxrot** (p. 549) for the number of included levels from the rotational band and **maxband** (p. 550) for the number of included vibrational levels.

Implementation 7.2.1 Deformation parameters, lengths and coupling schemes for coupled channels calculations are stored in directory *talys/structure/deformation/*. They are strongly linked to the discrete level file. For each isotope, we first write Z, A, number of levels, type of collectivity, the type of parameter, nuclear symbol with the format (3i4,3x,a1,3x,a1,54x,i4,a2). The type of parameter can be D (deformation length δ_L) or B (deformation parameter β_L). The type of collectivity can be S (spherical), V (vibrational), R (rotational) and A (asymmetric rotational). Next, we read for each level the number of the level corresponding to that of the discrete level database, the type of collectivity per level, the number of the vibrational band, multipolarity, magnetic quantum number, phonon number of the level, deformation parameter(s) with the format (i4,3x,a1,4i4,4f9.4). The type of collectivity per level can be either D (DWBA), V (vibrational) or R (rotational). In the case of levels that belong to a rotational band, only the level number and an 'R' are given. For the first level of the rotational band, the deformation parameter β_2 (and, if present, β_4 and β_6) can be given. If these β parameters are not given they are retrieved from the *talys/structure/mass/* directory. In certain cases, the deformation parameters have been adjusted to fit data. In those cases, they are added to the coupling schemes. Also, for the first level of a vibrational band the deformation parameter is given. The vibration-rotational model

is thus invoked if within the rotational model also states belonging to a vibrational band can be specified. The level of complexity of rotational or vibrational-rotational calculations can be specified with the **maxrot** (p. 549) and **maxband** (p. 550) keywords. For weakly coupled levels that can be treated with DWBA, the level number, a 'D' and the deformation parameter is given.

As an example, below are the deformation parameters for some even Ca isotopes, taken from *Fe.def*. This file ensures that for a reaction on ^{40}Ca, a coupled-channels calculation with a vibrational model will automatically be invoked. Levels 2 (3^- at 3.737 MeV, with $\delta_3 = 1.34$), 3 (2^+ at 3.904 MeV, with $\delta_2 = 0.36$), 4 (5^- at 4.491 MeV, with $\delta_5 = 0.93$), will all be coupled individually as one-phonon states. There is an option to enforce a spherical OMP calculation through **spherical y** (p. 542) in the input, In that case all levels will be treated with DWBA. The table below reveals that for the other Ca-isotopes the direct calculation will always be done with DWBA, but with deformation parameters β_L instead of deformation lengths δ_L.

```
20   40   4   V   D                                                    40Ca
 0   V   0
 2   V   1   3           1   1.34000
 3   V   2   2           1   0.36000
 4   V   3   5           1   0.93000
20   42   3   S   B                                                    42Ca
 0   V   0
 1   D                       0.24700
 9   D                       0.30264
20   44   3   S   B                                                    44Ca
 0   V   0
 1   D                       0.25300
 8   D                       0.24012
20   46   3   S   B                                                    46Ca
 0   V   0
 1   D                       0.15300
 6   D                       0.20408
20   48   3   S   B                                                    48Ca
 0   V   0
 1   D                       0.10600
 4   D                       0.23003
```

As a second example, below is the info for ^{238}U from the *U.def* file. The basis for the coupling scheme is a rotational model with deformation lengths $\delta_2 = 1.546$ and $\delta_4 = 0.445$, in which levels 1, 2, 3, 4, 7 and 22 can be coupled. In practice, we would include at least levels 1 and 2 (and if the results are important enough also levels 3 and 4) as rotational levels. There are 5 vibrational bands which can be included. By default we include no vibrational bands in a rotational model, but if e.g. **maxband 1** in the input, the levels 5, 6, 8 and 13 would be included with deformation length $\delta_3 = 0.9$.

```
92  238  23   R   D                                                   238U
 0   R   0                   1.54606   0.44508
 1   R   0
 2   R   0
 3   R   0
 4   R   0
```

```
    5    V    1    3    0        0.90000
    6    V    1
    7    R    0
    8    V    1
    9    V    2    4    0        0.20000
   10    V    3    3    1        0.10000
   11    V    3
   12    V    2
   13    V    1
   14    V    4    2    0        0.10000
   15    V    3
   16    V    4
   17    V    2
   21    V    5    2    2        0.10000
   22    R    0
   23    V    5
   25    V    4
   31    V    5
```

Finally, we note that in principle all level numbers in the *deformation/* database need to be re-checked if a new discrete level database (see the previous Section) is installed. It is however unlikely that new low-lying levels will be discovered for nuclides for which the coupling scheme is given.

8. Level densities

In statistical models for predicting cross sections, nuclear level densities are used at excitation energies where discrete level information is not available or incomplete. We use several models for the level density in TALYS, which range from phenomenological analytical expressions to tabulated level densities derived from microscopic models. The complete details for phenomenological models can be found in Koning et al. [22].

To set the notation, we first give some general definitions. The *level density* $\rho(E_x, J, \Pi)$ corresponds to the number of nuclear levels per MeV around an excitation energy E_x, for a certain spin J and parity Π. The *total level density* $\rho^{\text{tot}}(E_x)$ corresponds to the total number of levels per MeV around E_x, and is obtained by summing the level density over spin and parity:

$$\rho^{\text{tot}}(E_x) = \sum_J \sum_\Pi \rho(E_x, J, \Pi). \tag{8.1}$$

The nuclear levels are degenerate in M, the magnetic quantum number, which gives rise to the *total state density* $\omega^{\text{tot}}(E_x)$ which includes the $2J+1$ states for each level, i.e.

$$\omega^{\text{tot}}(E_x) = \sum_J \sum_\Pi (2J+1)\rho(E_x, J, \Pi). \tag{8.2}$$

When level densities are given by analytical expressions they are usually factorized as follows

$$\rho(E_x, J, \Pi) = P(E_x, J, \Pi)R(E_x, J)\rho^{\text{tot}}(E_x), \tag{8.3}$$

where $P(E_x, J, \Pi)$ is the parity distribution and $R(E_x, J)$ the spin distribution. In all but two level density models in TALYS (**ldmodel 5,6**) (p. 378), the parity equipartition is assumed, i.e.

$$P(E_x, J, \Pi) = \frac{1}{2}, \tag{8.4}$$

However, in our programming, we have accounted for the possibility to adopt non-equal parities, such as e.g. in the case of microscopic level density tables.

8.1 Effective level density

We first describe the simplest expressions that are included in TALYS for level densities. We here use the term "effective" to denote that the nuclear collective effects are not explicitly considered, but instead are effectively included in the level density expression.

8.1.1 The Fermi Gas Model

Arguably the best known analytical level density expression is that of the Fermi Gas model (FGM). It is based on the assumption that the single particle states which construct the excited levels of the nucleus are equally spaced, and that collective levels are absent. For a two-fermion system, i.e. distinguishing between excited neutrons and protons, the total Fermi gas state density reads

$$\omega_F^{\text{tot}}(E_x) = \frac{\sqrt{\pi}}{12} \frac{\exp\left[2\sqrt{aU}\right]}{a^{1/4}U^{5/4}}, \tag{8.5}$$

with U defined by

$$U = E_x - \Delta, \tag{8.6}$$

where the energy shift Δ is an empirical parameter which is equal to, or for some models closely related to, the pairing energy which is included to simulate the known odd-even effects in nuclei. The underlying idea is that Δ accounts for the fact that pairs of nucleons must be separated before each component can be excited individually. In practice, Δ plays an important role as adjustable parameter to reproduce observables, and its definition can be different for the various models we discuss here. Eq. (8.5) indicates that throughout this manual we will use both the *true* excitation energy E_x, as basic running variable and for expressions related to discrete levels, and the *effective* excitation energy U, mostly for expressions related to the continuum.

Eq. (8.5) also contains the level density parameter a, which theoretically is given by $a = \frac{\pi^2}{6}(g_\pi + g_\nu)$, with g_π (g_ν) denoting the spacing of the proton (neutron) single particle states near the Fermi energy. In practice a is determined, through Eq. (8.5), from experimental information of the specific nucleus under consideration or from global systematics. In contemporary analytical models, it is energy-dependent. This will be discussed in more detail below.

Under the assumption that the projections of the total angular momentum are randomly coupled, it was derived by Ericson [23] that the Fermi gas level density is

$$\rho_F(E_x, J, \Pi) = \frac{1}{2} \frac{2J+1}{2\sqrt{2\pi}\sigma^3} \exp\left[-\frac{(J+\frac{1}{2})^2}{2\sigma^2}\right] \frac{\sqrt{\pi}}{12} \frac{\exp\left[2\sqrt{aU}\right]}{a^{1/4}U^{5/4}}, \tag{8.7}$$

where the first factor $\frac{1}{2}$ represents the aforementioned equiparity distribution and σ^2 is the spin cut-off parameter, which represents the width of the angular momentum distribution. It depends on excitation energy and will also be discussed in more detail below. Eq. (8.7) is a special case of the factorization of Eq. (8.3), with the Fermi gas spin distribution given by,

$$R_F(E_x, J) = \frac{2J+1}{2\sigma^2} \exp\left[-\frac{(J+\frac{1}{2})^2}{2\sigma^2}\right]. \tag{8.8}$$

Summing $\rho_F(E_x, J, \Pi)$ over all spins and parities yields for the total Fermi gas level density

$$\rho_F^{\text{tot}}(E_x) = \frac{1}{\sqrt{2\pi}\sigma} \frac{\sqrt{\pi}}{12} \frac{\exp\left[2\sqrt{aU}\right]}{a^{1/4}U^{5/4}}, \tag{8.9}$$

which is, through Eq. (8.5), related to the total Fermi gas state density as

$$\rho_F^{\text{tot}}(E_x) = \frac{\omega_F^{\text{tot}}(E_x)}{\sqrt{2\pi}\sigma}. \tag{8.10}$$

These equations show that ρ_F^{tot} and ρ_F are determined by three parameters, a, σ and Δ. The first two of these have specific energy dependencies that will now be discussed separately, while we postpone the discussion of Δ to the Section on the various specific level density models.

In the Fermi gas model, the level density parameter a can be derived from D_0, the average s-wave level spacing at the neutron separation energy S_n, which is usually obtained from the available experimental set of s-wave resonances. The following equation can be used:

$$\frac{1}{D_0} = \sum_{J=|I-\frac{1}{2}|}^{J=I+\frac{1}{2}} \rho_F(S_n, J, \Pi), \tag{8.11}$$

where I is the spin of the target nucleus. From this equation, the level density parameter a can be extracted by an iterative search procedure.

In the TALYS-output, all quantities of interest are printed, if requested.

8.1.2 The level density parameter a

The formulae described above may suggest a nuclide-specific constant value for the level density parameter a, and the first level density analyses spanning an entire range of nuclide, see Gilbert et al, Dilg et al, and Baba et al [24, 25, 26] indeed treated a as a parameter independent of energy. Later, Ignatyuk et al. [27] recognized the correlation between the parameter a and the shell correction term of the liquid-drop component of the mass formula. They argued that a more realistic level density is obtained by assuming that the Fermi gas formulae outlined above are still valid, but that energy-dependent shell effects should be effectively included through an energy dependent expression for a. This expression takes into account the presence of shell effects at low energy and their disappearance at high energy in a phenomenological manner. It reads,

$$a = a(E_x) = \tilde{a}\left(1 + \delta W \frac{1 - \exp[-\gamma U]}{U}\right). \tag{8.12}$$

Here, $\tilde{a}$ is the asymptotic level density value one would obtain in the absence of any shell effects, i.e. $\tilde{a} = a(E_x \longrightarrow \infty)$ in general, but also $\tilde{a} = a(E_x)$ for all E_x if $\delta W = 0$. The damping parameter γ determines how rapidly $a(E_x)$ approaches $\tilde{a}$. Finally, δW is the shell correction energy. The absolute magnitude of δW determines how different $a(E_x)$ is from $\tilde{a}$ at low energies, while the sign of δW determines whether $a(E_x)$ decreases or increases as a function of E_x.

The asymptotic value $\tilde{a}$ is given by the smooth form

$$\tilde{a} = \alpha A + \beta A^{2/3}, \tag{8.13}$$

where A is the mass number, while the following systematical formula for the damping parameter is used,

$$\gamma = \frac{\gamma_1}{A^{\frac{1}{3}}} + \gamma_2. \tag{8.14}$$

In Eqs. (8.13)-(8.14), α, β and $\gamma_{1,2}$ are global parameters that have been determined to give the best average level density description over a whole range of nuclides. They are given in Table 8.1, where also the average pairing correction δ_{global} is given. Also, $\gamma_2 = 0$ by default.

Model	α	β	γ_1	δ_{global}
BFM effective	0.0722396	0.195267	0.410289	0.173015
BFM collective	0.0381563	0.105378	0.546474	0.743229
CTM effective	0.0692559	0.282769	0.433090	0.
CTM collective	0.0207305	0.229537	0.473625	0.
GSM effective	0.110575	0.0313662	0.648723	1.13208
GSM collective	0.0357750	0.135307	0.699663	-0.149106

Table 8.1: Global level density parameters for the phenomenological models

We define δW, expressed in MeV, as the difference between the experimental mass of the nucleus M_{exp} and its mass according to the spherical liquid-drop model mass M_{LDM} (both expressed in MeV),

$$\delta W = M_{\text{exp}} - M_{\text{LDM}}. \tag{8.15}$$

For the real mass we take the value from the AME2020 experimental mass compilation [17]. Following Mengoni and Nakajima [28], for M_{LDM} we take the formula by Myers and Swiatecki [29]:

$$
\begin{aligned}
M_{\text{LDM}} &= M_n N + M_H Z + E_{\text{vol}} + E_{\text{sur}} + E_{\text{coul}} + \delta \\
M_n &= 8.07144 \text{ MeV} \\
M_H &= 7.28899 \text{ MeV} \\
E_{\text{vol}} &= -c_1 A \\
E_{\text{sur}} &= c_2 A^{2/3} \\
E_{\text{coul}} &= c_3 \frac{Z^2}{A^{1/3}} - c_4 \frac{Z^2}{A} \\
c_i &= a_i \left[1 - \kappa \left(\frac{N-Z}{A} \right)^2 \right], \quad i = 1,2 \\
a_1 &= 15.677 \text{ MeV} \\
a_2 &= 18.56 \text{ MeV} \\
\kappa &= 1.79 \\
c_3 &= 0.717 \text{ MeV} \\
c_4 &= 1.21129 \text{ MeV} \\
\delta &= -\frac{11}{\sqrt{A}} \quad \text{even} - \text{even} \\
&= 0 \quad \text{odd} \\
&= \frac{11}{\sqrt{A}} \quad \text{odd} - \text{odd}.
\end{aligned}
\tag{8.16}
$$

Eq. (8.12) should in principle be applied at all excitation energies, unless a different level density prescription is used at low energies, as e.g. for the CTM. Therefore, a helpful extra note for practical calculations is that for small excitation energies, i.e. $E_x \leq \Delta$, the limiting value of Eq. (8.12) is given by its first order Taylor expansion

$$\lim_{E_x - \Delta \to 0} a(E_x) = \tilde{a} \left[1 + \gamma \delta W \right]. \tag{8.17}$$

From now on, wherever the level density parameter a appears in the formalism, we implicitly assume the form (8.12) for $a(E_x)$.

It is important to define the order in which the various parameters of Eq. (8.12) are calculated in TALYS, because they can be given as an adjustable parameter in the input file, they can be known from experiment or they can be determined from systematics.

If the level density parameter at the neutron separation energy $a(S_n)$ is *not* known from an experimental D_0 value, we use the above systematical formulae for the global level density parameters. In this case, all parameters in Eq. (8.12) are defined and $a(E_x)$ can be completely computed at any excitation energy. However, for several nuclei $a(S_n)$ can be derived from an experimental D_0 value through Eq. (8.11), and one may want to use this information. In TALYS, this occurs when an input value for $a(S_n)$ is given and when **asys n** is set, meaning that instead of using the systematical formulae (8.13)-(8.15) the resonance parameter database is used to determine level density parameters. If we want to use this "experimental" $a(S_n)$ we are immediately facing a constraint: Eq. (8.12) gives the following condition that must be obeyed

$$a(S_n) = \tilde{a}\left[1 + \delta W \frac{1 - \exp(-\gamma(S_n - \Delta))}{S_n - \Delta}\right] \tag{8.18}$$

This means also that $a(S_n), \tilde{a}, \delta W$ and γ cannot *all* be given simultaneously in the input, since it would lead to inconsistency. In the case of an experimental $a(S_n)$, at least another parameter must be re-adjusted. The asymptotic level density parameter $\tilde{a}$ is the first choice. This is not as strange as it seems at first sight. Even though the values for δW depend strongly on the particular theoretical mass model and are merely adopted to reproduce the global trend of shell effects for various regions of the nuclide chart, we do not alter them when going from a global to a local model. Likewise, we feel that it is dangerous to adjust γ_1 merely on the basis of discrete level information and the mean resonance spacing at the neutron separation energy, since its presence in the exponent of Eq. (8.12) may lead to level density values that deviate strongly from the global average at high energy.

Hence, if $a(S_n)$ is given, and also γ and δW are given in the input or from tables then the asymptotic level density parameter $\tilde{a}$ is automatically obtained from

$$\tilde{a} = a(S_n)/\left[1 + \delta W \frac{1 - \exp(-\gamma(S_n - \Delta))}{S_n - \Delta}\right] \tag{8.19}$$

Other choices can however be forced with the input file. If $a(S_n)$, $\tilde{a}$ and δW are given while γ is not given in the input, γ is eliminated as a free parameter and is obtained by inverting Eq. (8.18),

$$\gamma = -\frac{1}{S_n - \Delta} \ln\left[1 - \frac{S_n - \Delta}{\delta W}\left(\frac{\tilde{a}}{a(S_n)} - 1\right)\right] \tag{8.20}$$

If δW is the only parameter not given in the input, it is automatically determined by inverting Eq. (8.18),

$$\delta W = \frac{(S_n - \Delta)\left(\frac{a(S_n)}{\tilde{a}} - 1\right)}{1 - \exp(-\gamma(S_n - \Delta))} \tag{8.21}$$

All this flexibility is not completely without danger. Since both δW and $a(S_n)$ are independently derived from experimental values, it may occur that Eq. (8.20) poses problems. In particular, δW may have a sign opposite to $[a(S_n) - \tilde{a}]$. In other words, if the argument of the natural logarithm is not between 0 and 1, our escape route is to return to Eq. (8.14) for γ and to readjust δW through Eq. (8.21).

The recipe outlined above represents a full-proof method to deal with all the parameters of Eq. (8.12), i.e. it always gives a reasonable answer since we are able to invert the Ignatyuk formula

in all possible ways. We emphasize that in general, consistent calculations are obtained with Eqs. (8.15), (8.13), (8.14), and when available, a specific $a(S_n)$ value from the tables. The full range of possibilities of parameter specification for the Ignatyuk formula is summarized in Table 8.2. The reason to include all these parameter possibilities is simple: fitting experiments. Moreover, these variations are not as unphysical as they may seem: Regardless of whether they are derived from experimental data or from microscopic nuclear structure models, the parameters $a(S_n), \tilde{a}, \delta W$ and γ always have an uncertainty. Hence, as long as the deviation from their default values is kept within bounds, they can be helpful fitting parameters.

Table 8.2: Specification of parameter handling for Ignatyuk formula

Input	Calculation
- (Default)	γ: Eq. (8.14), $\tilde{a}$: Eq. (8.13) or Eq. (8.19), δW: Eq. (8.15), $a(S_n)$: Eq. (8.18)
$a(S_n), \gamma, \tilde{a}, \delta W$	TALYS-Error: Conflict
$a(S_n)(\text{table}), \gamma, \tilde{a}, \delta W$	$a(S_n)$: Eq. (8.18) (Input overruled)
$\gamma, \tilde{a}, \delta W$	$a(S_n)$: Eq. (8.18)
$\gamma, \tilde{a}$	δW: Eq. (8.15), $a(S_n)$: Eq. (8.18)
$\gamma, \delta W$	$\tilde{a}$: Eq. (8.13), $a(S_n)$: Eq. (8.18)
$\tilde{a}, \delta W$	γ: Eq. (8.14), $a(S_n)$: Eq. (8.18)
γ	$\tilde{a}$: Eq. (8.13), δW: Eq. (8.15), $a(S_n)$: Eq. (8.18)
$\tilde{a}$	γ: Eq. (8.14), δW: Eq. (8.15), $a(S_n)$: Eq. (8.18)
δW	γ: Eq. (8.14), $\tilde{a}$: Eq. (8.13), $a(S_n)$: Eq. (8.18)
$a(S_n)$	γ: Eq. (8.20) or (8.14), $\tilde{a}$: Eq. (8.19), δW: Eq. (8.15) or (8.21)
$a(S_n), \tilde{a}, \delta W$	γ: Eq. (8.20)
$a(S_n), \delta W$	$\tilde{a}$: Eq. (8.19) γ: Eq. (8.20)
$a(S_n), \tilde{a}$	δW: Eq. (8.15), γ: Eq. (8.20) or γ: Eq. (8.14), δW: Eq. (8.21)
$a(S_n), \gamma$	δW: Eq. (8.15), $\tilde{a}$: Eq. (8.19)
$a(S_n), \gamma, \delta W$	$\tilde{a}$: Eq. (8.19)
$a(S_n), \gamma, \tilde{a}$	δW: Eq. (8.21)

8.1.3 The spin cut-off parameter

The spin cut-off parameter σ^2 represents the width of the angular momentum distribution of the level density. The general expression for the continuum is based on the observation that a nucleus possesses collective rotational energy that can not be used to excite the individual nucleons. In this picture, one can relate σ^2 to the (undeformed) moment of inertia of the nucleus I_0 and the thermodynamic temperature t,

$$t = \sqrt{\frac{U}{a}}. \tag{8.22}$$

Indeed, an often used expression is $\sigma^2 = \sigma_\parallel^2 = I_0 t$, where the symbol $\sigma_\parallel^2$ designates the parallel spin cut-off parameter, obtained from the projection of the angular momentum of the single-particle states on the symmetry axis. However, it has has been observed from microscopic level density studies that the quantity σ^2/t is not constant as argued by Goriely and Hilaire [30, 31], but instead

shows marked shell effects, similar to the level density parameter a. To take that effect into account we follow Goriely and Mughabghab [30, 32] and adopt the following expression,

$$\sigma^2 = \sigma_{\parallel}^2 = \sigma_F^2(E_x) = I_0 \frac{a}{\tilde{a}} t, \tag{8.23}$$

with $\tilde{a}$ from Eq. (8.13) and

$$I_0 = \frac{\frac{2}{5} m_0 R^2 A}{(\hbar c)^2}, \tag{8.24}$$

where $R = 1.2 A^{1/3}$ is the radius, and m_0 the neutron mass in amu. This gives

$$\sigma_F^2(E_x) = 0.01389 \frac{A^{5/3}}{\tilde{a}} \sqrt{aU}. \tag{8.25}$$

On average, the $\sqrt{aU}/\tilde{a}$ has the same energy- and mass-dependent behaviour as the temperature $\sqrt{U/a}$. The differences occur in the regions with large shell effects. Eq. (8.25) can be altered by means of **Rspincut** (p. 401).

Analogous to the level density parameter, we have to account for low excitation energies for which Eq. (8.25) is not defined ($E_x \le \Delta$) or less appropriate. This leads us to an alternative method to determine the spin cut-off parameter, namely from the spins of the low-lying discrete levels. Suppose we want to determine this discrete spin cut-off parameter σ_d^2 in the energy range where the total level density agrees well with the discrete level sequence, i.e. from a lower discrete level N_L with energy E_L to an upper level N_U with energy E_U. It can be derived that

$$\sigma_d^2 = \frac{1}{3 \sum_{i=N_L}^{N_U} (2J_i + 1)} \sum_{i=N_L}^{N_U} J_i(J_i + 1)(2J_i + 1). \tag{8.26}$$

where J_i is the spin of discrete level i. Reading these spins from the discrete level file readily gives the value for σ_d^2. In TALYS, σ_d^2 can be used on a nucleus-by-nucleus basis, when discrete levels are known. For cases where either Eqs. (8.25) or (8.26) are not applicable, e.g. because there are no discrete levels and $U = E_x - P$ is negative, we take the systematical formula

$$\sigma^2 = \left(0.83 A^{0.26}\right)^2 \tag{8.27}$$

which gives a reasonable estimate for energies in the order of 1-2 MeV.

The final functional form for $\sigma^2(E_x)$ is a combination of Eqs. (8.25) and (8.26). Defining $E_d = \frac{1}{2}(E_L + E_U)$ as the energy in the middle of the $N_L - N_U$ region, we assume σ_d^2 is constant up to this energy and can then be linearly interpolated to the expression given by Eq. (8.25). We choose the matching point to be the neutron separation energy S_n of the nucleus under consideration, i.e.

$$
\begin{aligned}
\sigma^2(E_x) \quad &= \quad \sigma_d^2 &&\text{for } 0 \le E_x \le E_d \\
&= \quad \sigma_d^2 + \frac{E_x - E_d}{S_n - E_d}(\sigma_F^2(S_n) - \sigma_d^2) &&\text{for } E_d \le E_x \le S_n \\
&= \quad \sigma_F^2(E_x) &&\text{for } E_x \ge S_n.
\end{aligned}
\tag{8.28}
$$

Analogous to the level density parameter a, from now on we implicitly assume the energy dependence for $\sigma^2(E_x)$ whenever σ^2 appears in the formalism.

8.1.4 Constant Temperature Model

In the Constant Temperature Model (CTM), as introduced by Gilbert and Cameron [24], the excitation energy range is divided into a low energy part from 0 MeV up to a matching energy E_M, where the so-called constant temperature law applies and a high energy part above E_M, where the Fermi gas model applies. Hence, for the total level density we have

$$
\begin{aligned}
\rho^{\text{tot}}(E_x) & = \rho_T^{\text{tot}}(E_x), \quad \text{if } E_x \leq E_M, \\
& = \rho_F^{\text{tot}}(E_x), \quad \text{if } E_x \geq E_M,
\end{aligned}
\tag{8.29}
$$

and similarly for the level density

$$
\begin{aligned}
\rho(E_x, J, \Pi) & = \frac{1}{2} R_F(E_x, J) \rho_T^{\text{tot}}(E_x), \quad \text{if } E_x \leq E_M, \\
& = \rho_F(E_x, J, \Pi), \qquad\quad \text{if } E_x \geq E_M.
\end{aligned}
\tag{8.30}
$$

Note that the spin distribution of Eq. (8.8) is also used in the constant temperature region, including the low-energy behaviour for the spin cut-off parameter as expressed by Eq. (8.28).

For the Fermi gas expression, we use the effective excitation energy $U = E_x - \Delta^{\text{CTM}}$, where the energy shift is given by

$$
\Delta^{CTM} = \chi \frac{12}{\sqrt{A}},
\tag{8.31}
$$

with

$$
\begin{aligned}
\chi & = 0, \quad \text{for odd} - \text{odd}, \\
& = 1, \quad \text{for odd} - \text{even}, \\
& = 2, \quad \text{for even} - \text{even}.
\end{aligned}
\tag{8.32}
$$

Note that by default no adjustable pairing shift parameter is used in the CTM. In TALYS, the number 12 in the enumerator of Eq. (8.31) can be altered using **pairconstant** (p. 419). This also applies to the other level density models.

For low excitation energy, the CTM is based on the experimental evidence that the cumulated histogram $N(E_x)$ of the first discrete levels can be well reproduced by an exponential law of the type

$$
N(E_x) = \exp\left(\frac{E_x - E_0}{T}\right),
\tag{8.33}
$$

which is called the constant temperature law. The nuclear temperature T and E_0 are parameters that serve to adjust the formula to the experimental discrete levels. Accordingly, the constant temperature part of the total level density reads

$$
\rho_T^{\text{tot}}(E_x) = \frac{dN(E_x)}{dE_x} = \frac{1}{T} \exp\left(\frac{E_x - E_0}{T}\right).
\tag{8.34}
$$

For higher energies, the Fermi gas model is more suitable and the total level density is given by Eq. (8.9). The expressions for ρ_T^{tot} and ρ_F^{tot} have to be matched at a matching energy E_M where they, and their derivatives, are identical. First, continuity requires that

$$
\rho_T^{\text{tot}}(E_M) = \rho_F^{\text{tot}}(E_M).
\tag{8.35}
$$

Inserting Eq. (8.34) in this equation directly leads to the condition

$$E_0 = E_M - T \ln \left[T \rho_F^{\text{tot}}(E_M) \right].$$ (8.36)

Second, continuity of the derivatives requires that

$$\frac{d\rho_T^{\text{tot}}}{dE_x}(E_M) = \frac{d\rho_F^{\text{tot}}}{dE_x}(E_M).$$ (8.37)

Inserting Eq. (8.34) in this equation directly leads to the condition

$$\frac{\rho_T^{\text{tot}}(E_M)}{T} = \frac{d\rho_F^{\text{tot}}}{dE_x}(E_M),$$ (8.38)

or

$$\frac{1}{T} = \frac{d \ln \rho_F^{\text{tot}}}{dE_x}(E_M).$$ (8.39)

In principle, for all Fermi gas type expressions, including the energy dependent expressions for a, σ^2, K_{rot} etc., Eq. (8.39) could be elaborated analytically, but in practice we use a numerical approach to allow any level density model to be used in the matching problem. For this, we determine the inverse temperature of Eq. (8.39) numerically by calculating ρ_F^{tot} on a sufficiently dense energy grid.

The matching problem gives us two conditions, given by Eqs. (8.36) and (8.39), with three unknowns: T, E_0 and E_M. Hence, we need another constraint. This is obtained by demanding that in the discrete level region the constant temperature law reproduces the experimental discrete levels, i.e. ρ_T^{tot} needs to obey

$$N_U = N_L + \int_{E_L}^{E_U} dE_x \rho^{\text{tot}}(E_x),$$ (8.40)

or, after inserting Eq. (8.34),

$$N_U = N_L + \left(\exp[\frac{E_U}{T}] - \exp[\frac{E_L}{T}] \right) \exp[\frac{-E_0}{T}].$$ (8.41)

The combination of Eqs. (8.36), (8.39) and (8.41) determines T, E_0 and E_M. Inserting Eq. (8.36) in Eq. (8.41) yields:

$$T \rho_F^{\text{tot}}(E_M) \exp[\frac{-E_M}{T}] \left(\exp[\frac{E_U}{T}] - \exp[\frac{E_L}{T}] \right) + N_L - N_U = 0,$$ (8.42)

from which E_M can be solved by an iterative procedure with the simultaneous use of the tabulated values given by Eq. (8.39). The levels N_L and N_U are chosen such that $\rho_T(E_x)$ gives the best description of the observed discrete states and are stored in the nuclear structure database. For nuclides for which no, or not enough, discrete levels are given we rely on empirical formula for the temperature. For the effective model,

$$T = -0.22 + \frac{9.4}{\sqrt{A(1 + \gamma \delta W)}}$$ (8.43)

and for the collective model

$$T = -0.25 + \frac{10.2}{\sqrt{A(1 + \gamma \delta W)}}$$ (8.44)

where γ is taken from Eq. (8.14) and Table 8.1. Next, we directly obtain E_M from Eq. (8.39) and E_0 from Eq. (8.36). Again, Eqs. (8.43) and (8.44) were obtained by fitting all individual values of the nuclides for which sufficient discrete level information exists. In a few cases, the global expression for T leads to a value for E_M which is clearly off scale. In that case, we resort to empirical expressions for the matching energy. For the effective model

$$E_M = 2.33 + 253/A + \Delta^{CTM}, \tag{8.45}$$

and for the collective model

$$E_M = 2.67 + 253/A + \Delta^{CTM}, \tag{8.46}$$

after which we obtain T from Eq. (8.39).

8.1.5 The Back-shifted Fermi gas Model

In the Back-shifted Fermi gas Model (BFM) of Dilg et al [25], the pairing energy is treated as an adjustable parameter and the Fermi gas expression is used all the way down to 0 MeV. Hence for the total level density we have

$$\rho_F^{\mathrm{tot}}(E_x) = \frac{1}{\sqrt{2\pi}\sigma} \frac{\sqrt{\pi}}{12} \frac{\exp\left[2\sqrt{aU}\right]}{a^{1/4}U^{5/4}}, \tag{8.47}$$

and for the level density,

$$\rho_F(E_x, J, \Pi) = \frac{1}{2} \frac{2J+1}{2\sqrt{2\pi}\sigma^3} \exp\left[-\frac{(J+\frac{1}{2})^2}{2\sigma^2}\right] \frac{\sqrt{\pi}}{12} \frac{\exp\left[2\sqrt{aU}\right]}{a^{1/4}U^{5/4}}, \tag{8.48}$$

respectively. These expressions, as well as the energy-dependent expressions for a and σ^2, contain the effective excitation energy $U = E_x - \Delta^{\mathrm{BFM}}$, where the energy shift is given by

$$\Delta^{BFM} = \chi \frac{12}{\sqrt{A}} + \delta, \tag{8.49}$$

with

$$\begin{aligned}
\chi &= -1, \text{for odd} - \text{odd}, \\
&= 0, \text{ for odd} - \text{even}, \\
&= 1, \text{ for even} - \text{even}, \tag{8.50}
\end{aligned}$$

and δ an adjustable parameter to fit experimental data per nucleus.

A problem of the original BFM, which may have hampered its use as the default level density option in nuclear model analyses, is the divergence of Eqs. (8.47)-(8.48) when U goes to zero. A solution to this problem has been provided by Grossjean and Feldmeier [33], has been put into a practical form by Demetriou and Goriely [34], and is adopted in TALYS. The expression for the total BFM level density is

$$\rho_{\mathrm{BFM}}^{\mathrm{tot}}(E_x) = \left[\frac{1}{\rho_F^{\mathrm{tot}}(E_x)} + \frac{1}{\rho_0(t)}\right]^{-1}, \tag{8.51}$$

where ρ_0 is given by

$$\rho_0(t) = \frac{\exp(1)}{24\sigma} \frac{(a_n + a_p)^2}{\sqrt{a_n a_p}} \exp(4a_n a_p t^2), \tag{8.52}$$

where $a_n = a_p = a/2$ and t is given by Eq. (8.22).

With the usual spin distribution, the level density reads

$$\rho_{\text{BFM}}(E_x, J, \Pi) = \frac{1}{2} \frac{2J+1}{2\sigma^2} \exp\left[-\frac{(J+\frac{1}{2})^2}{2\sigma^2}\right] \rho_{\text{BFM}}^{\text{tot}}(E_x). \qquad (8.53)$$

In sum, there are two adjustable parameters for the BFM, a and δ.

8.1.6 The Generalized Superfluid Model

The Generalized Superfluid Model (GSM) takes superconductive pairing correlations into account according to the Bardeen-Cooper-Schrieffer theory. The phenomenological version of the model, by Ignatyuk et al. [35, 36] is characterized by a phase transition from a superfluid behaviour at low energy, where pairing correlations strongly influence the level density, to a high energy region which is described by the FGM. The GSM thus resembles the CTM to the extent that it distinguishes between a low energy and a high energy region, although for the GSM this distinction follows naturally from the theory and does not depend on specific discrete levels that determine a matching energy. Instead, the model automatically provides a constant temperature-like behaviour at low energies. For the level density expressions, it is useful to recall the general formula for the total level density,

$$\rho^{\text{tot}}(E_x) = \frac{1}{\sqrt{2\pi}\sigma} \frac{e^S}{\sqrt{D}}, \qquad (8.54)$$

where S is the entropy and D is the determinant related to the saddle-point approximation. For the GSM this expression has two forms: one below and one above the so called critical energy U_c.

For energies below U_c, the level density is described in terms of thermodynamical functions defined *at U_c*, which is given by

$$U_c = a_c T_c^2 + E_{\text{cond}}. \qquad (8.55)$$

Here, the critical temperature T_c is

$$T_c = 0.567\Delta_0, \qquad (8.56)$$

where the pairing correlation function is given by

$$\Delta_0 = \frac{12}{\sqrt{A}}. \qquad (8.57)$$

This correlation function also determines the condensation energy E_{cond}, which characterizes the decrease of the superfluid phase relative to the Fermi gas phase. It is given by the expression

$$E_{\text{cond}} = \frac{3}{2\pi^2} a_c \Delta_0^2, \qquad (8.58)$$

where the critical level density parameter a_c is given by the iterative equation

$$a_c = \tilde{a}\left[1 + \delta W \frac{1 - \exp(-\gamma a_c T_c^2)}{a_c T_c^2}\right], \qquad (8.59)$$

which is easily obtained once $\tilde{a}$, δW and γ are known. Eq. (8.59) indicates that shell effects are again appropriately taken into account. For the determination of the level density we also invoke the expression for the critical entropy S_c,

$$S_c = 2a_c T_c, \qquad (8.60)$$

the critical determinant D_c,

$$D_c = \frac{144}{\pi} a_c^3 T_c^5, \tag{8.61}$$

and the critical spin cut-off parameter σ_c^2,

$$\sigma_c^2 = 0.01389 A^{5/3} \frac{a_c}{\tilde{a}} T_c. \tag{8.62}$$

Now that everything is specified at U_c, we can use the superfluid Equation Of State (EOS) to define the level density below U_c. For this, we define an effective excitation energy

$$U' = E_x + \chi \Delta_0 + \delta, \tag{8.63}$$

where

$$\begin{aligned}
\chi &= 2, \quad \text{for odd} - \text{odd}, \\
&= 1, \quad \text{for odd} - \text{even}, \\
&= 0, \quad \text{for even} - \text{even},
\end{aligned} \tag{8.64}$$

and δ is an adjustable shift parameter to obtain the best description of experimental data per nucleus. Note that the convention for χ is again different from that of the BFM or CTM. Defining

$$\varphi^2 = 1 - \frac{U'}{U_c}, \tag{8.65}$$

then for $U' \leq U_c$ the quantities φ and T obey the superfluid EOS, according to Ignatyuk et al [35],

$$\varphi = \tanh\left(\frac{T_c}{T} \varphi\right), \tag{8.66}$$

which is equivalent to

$$T = 2 T_c \, \varphi \left[\ln \frac{1+\varphi}{1-\varphi}\right]^{-1}. \tag{8.67}$$

The other required functions for $U' \leq U_c$ are the entropy S,

$$S = S_c \frac{T_c}{T}\left(1 - \varphi^2\right) = S_c \frac{T_c}{T} \frac{U'}{U_c}, \tag{8.68}$$

the determinant D,

$$D = D_c \left(1 - \varphi^2\right)\left(1 + \varphi^2\right)^2 = D_c \frac{U'}{U_c}\left(2 - \frac{U'}{U_c}\right)^2, \tag{8.69}$$

and the spin cut-off parameter

$$\sigma^2 = \sigma_c^2 \left(1 - \varphi^2\right) = \sigma_c^2 \frac{U'}{U_c}. \tag{8.70}$$

In sum, the level density can now be specified for the entire energy range. For $U' \leq U_c$, the total level density is given by

$$\rho_{\text{GSM}}^{\text{tot}}(E_x) = \frac{1}{\sqrt{2\pi}\sigma} \frac{e^S}{\sqrt{D}}, \tag{8.71}$$

using Eqs. (8.68)-(8.70). Similarly, the level density is

$$\rho_{\text{GSM}}(E_x, J, \Pi) = \frac{1}{2} R_F(E_x, J) \rho_{\text{GSM}}^{\text{tot}}(E_x). \tag{8.72}$$

For $U' \geq U_c$ the FGM applies, though with an energy shift that is different from the pairing correction of the CTM and BFM. The total level density is

$$\rho_{\text{GSM}}^{\text{tot}}(E_x) = \frac{1}{\sqrt{2\pi}\sigma} \frac{\sqrt{\pi}}{12} \frac{\exp\left[2\sqrt{aU}\right]}{a^{1/4}U^{5/4}}, \tag{8.73}$$

where the effective excitation energy is defined by $U = E_x - \Delta^{GSM}$, with

$$\Delta^{GSM} = E_{\text{cond}} - \chi\Delta_0 - \delta. \tag{8.74}$$

The spin cut-off parameter in the high-energy region reads

$$\sigma^2 = I_0 \frac{a}{\tilde{a}} \sqrt{\frac{U}{a}}, \tag{8.75}$$

and I_0 is given by Eq. (8.24). The level density is given by

$$\rho_{\text{GSM}}(E_x, J, \Pi) = \frac{1}{2} R_F(E_x, J) \rho_{\text{GSM}}^{\text{tot}}(E_x). \tag{8.76}$$

At the matching energy, i.e., for $E_x' = U_c - \chi\Delta_0 - \delta$, it is easy to verify that Eqs. (8.71) and (8.73) match so that the total level density is perfectly continuous. In sum, there are two adjustable parameters for the GSM, a and δ.

8.2 Collective effects in the level density

All the previously described models do not explicitly account for collective effects. However, it is well known that generally the first excited levels of nuclei result from coherent excitations of the fermions it contains. The Fermi gas model is not appropriate to describe such levels. Nevertheless, the models presented so far can still be applied successfully in most cases since they incorporate collectivity in the level density in an effective way through a proper choice of the energy-dependent level density parameter values.

In some calculations, especially if the disappearance of collective effects with excitation energy plays a role (e.g. in the case of fission), one would like to model the collective effects in more detail. It can be shown that the collective effects may be accounted for explicitly by introducing collective enhancement factors on top of an intrinsic level density $\rho_{F,\text{int}}(E_x, J, \Pi)$. Then the deformed Fermi gas level density $\rho_{F,\text{def}}(E_x, J, \Pi)$ reads

$$\rho_{F,\text{def}}(E_x, J, \Pi) = K_{\text{rot}}(E_x) K_{\text{vib}}(E_x) \rho_{F,\text{int}}(E_x, J, \Pi), \tag{8.77}$$

while the total level densities $\rho_{F,\text{def}}^{\text{tot}}$ and $\rho_{F,\text{int}}^{\text{tot}}$ are related in the same way. K_{rot} and K_{vib} are called the rotational and vibrational enhancement factors, respectively. If K_{rot} and K_{vib} are explicitly accounted for, $\rho_{F,\text{int}}(E_x, J, \Pi)$ should now describe purely single-particle excitations, and can be determined again by using the Fermi gas formula. Obviously, the level density parameter a of $\rho_{F,\text{int}}$ will be different from that of the effective level density described before.

The vibrational enhancement of the level density is approximated, see Capote et al [6], by

$$K_{\text{vib}} = \exp[\delta S - (\delta U/t)], \tag{8.78}$$

where δS and δU are changes in the entropy and excitation energy, respectively, resulting from the vibrational modes and T is the nuclear temperature given by Eq. (8.22). These changes are described by the Bose gas relationships, i.e

$$
\begin{aligned}
\delta S &= \sum_i (2\lambda_i + 1)\Big[(1+n_i)\ln(1+n_i) - n_i \ln n_i\Big], \\
\delta U &= \sum_i (2\lambda_i + 1)\omega_i n_i,
\end{aligned}
\tag{8.79}
$$

where ω_i are the energies, λ_i the multipolarities, and n_i the occupation numbers for vibrational excitations at a given temperature. The disappearance of collective enhancement of the level density at high temperatures can be taken into account by defining the occupation numbers in terms of the equation

$$
n_i = \frac{\exp(-\gamma_i/2\omega_i)}{\exp(\omega_i/T) - 1},
\tag{8.80}
$$

where γ_i are the spreading widths of the vibrational excitations. This spreading of collective excitations in nuclei should be similar to the zero-sound damping in a Fermi liquid, and the corresponding width can be written as

$$
\gamma_i = C(\omega_i^2 + 4\pi^2 T^2).
\tag{8.81}
$$

The value of $C = 0.0075\, A^{1/3}$ was obtained from the systematics of the neutron resonance densities of medium-weight nuclei by Grudzevich et al [37]. We use a modified systematics, see Capote et al [6] which includes shell effects to estimate the phonon energies (in MeV), namely

$$
\omega_2 = 65 A^{-5/6}/(1+0.05\delta W),
\tag{8.82}
$$

for the quadrupole vibrations and

$$
\omega_3 = 100 A^{-5/6}/(1+0.05\delta W),
\tag{8.83}
$$

for the octupole excitations.

An alternative, liquid drop model, estimation of the vibrational collective enhancement factor is given by Iljinov et al. [38]

$$
K_{\text{vib}}(E_x) = \exp\left(0.0555 A^{\frac{2}{3}} t^{\frac{4}{3}}\right).
\tag{8.84}
$$

The **kvibmodel** keyword can be used to choose between these models.

A more important contribution to the collective enhancement of the level density originates from rotational excitations. Its effect is not only much stronger ($K_{\text{rot}} \sim 10 - 100$ whereas $K_{\text{vib}} \sim 3$), but the form for the rotational enhancement depends on the nuclear shape as well. This makes it crucial, among others, for the description of fission cross sections.

The expression for the rotational enhancement factor depends on the deformation, see Capote et al and Junghans et al [6, 39]. Basically, K_{rot} is equal to the perpendicular spin cut-off parameter $\sigma_\perp^2$,

$$
\sigma_\perp^2 = I_\perp t,
\tag{8.85}
$$

with the rigid-body moment of inertia perpendicular to the symmetry axis given by

$$
I_\perp = I_0\left(1 + \frac{\beta_2}{3}\right) = 0.01389 A^{5/3}\left(1 + \frac{\beta_2}{3}\right),
\tag{8.86}
$$

where β_2 is the ground-state quadrupole deformation, which we take from the nuclear structure database. Hence,

$$\sigma_\perp^2 = 0.01389A^{5/3}\left(1+\frac{\beta_2}{3}\right)\sqrt{\frac{U}{a}}. \tag{8.87}$$

For high excitation energies, it is known that the rotational behavior vanishes. To take this into account, it is customary to introduce a phenomenological damping function $f(E_x)$ which is equal to 1 in the purely deformed case and 0 in the spherical case. The expression for the level density is then

$$\begin{aligned} \rho(E_x,J,\Pi) &= [1-f(E_x)]K_{\text{vib}}(E_x)\rho_{F,\text{int}}(E_x,J,\Pi) + f(E_x)\rho_{F,\text{def}}(E_x,J,\Pi) \\ &= K_{\text{rot}}(E_x)K_{\text{vib}}(E_x)\rho_{F,\text{int}}(E_x,J,\Pi) \end{aligned} \tag{8.88}$$

where

$$K_{\text{rot}}(E_x) = \max([\sigma_\perp^2-1]f(E_x)+1,1). \tag{8.89}$$

The function $f(E_x)$ is taken as a combination of Fermi functions,

$$f(E_x) = \frac{1}{1+\exp(\frac{E_x-E_{col}^{g.s.}}{d_{col}^{g.s.}})}, \tag{8.90}$$

which yields the desired property of K_{rot} going to 1 for high excitation energy. Little is known about the parameters that govern this damping, although attempts have been made (see e.g. Hansen et al[40]). We arbitrarily take $E_{col}^{g.s.} = 30$ MeV, $d_{col}^{g.s.} = 5$ MeV.

Finally, these collective enhancement expressions can be applied to the various phenomenological level density models. The CTM formalism can be extended with explicit collective enhancement, i.e. the total level density reads

$$\begin{aligned} \rho^{\text{tot}}(E_x) &= \rho_T^{\text{tot}}(E_x), \quad \text{if } E_x \leq E_M, \\ &= K_{\text{rot}}(E_x)K_{\text{vib}}(E_x)\rho_{F,\text{int}}^{\text{tot}}(E_x), \quad \text{if } E_x \geq E_M, \end{aligned} \tag{8.91}$$

and similarly for the level density $\rho(E_x,J,\Pi)$. Note that the collective enhancement is not applied to the constant temperature region, since collectivity is assumed to be already implicitly included in the discrete levels. The matching problem is completely analogous to that described before, although the resulting parameters E_M, E_0 and T will of course be different.

The BFM can also be extended with explicit collective enhancement, i.e.

$$\rho_{\text{BFM}}^{\text{tot}}(E_x) = K_{\text{rot}}(E_x)K_{\text{vib}}(E_x)\left[\frac{1}{\rho_{F,\text{int}}^{\text{tot}}(E_x)} + \frac{1}{\rho_0(t)}\right]^{-1}, \tag{8.92}$$

and similarly for the level density $\rho(E_x,J,\Pi)$. Finally, the GSM can be extended as follows

$$\rho_{\text{GSM}}^{\text{tot}}(E_x) = K_{\text{rot}}(E_x)K_{\text{vib}}(E_x)\rho_{GSM,\text{int}}^{\text{tot}}(E_x). \tag{8.93}$$

(In fact, the term "general" in the GSM was originally meant for the collective enhancement).

Options 8.2.1 Since phenomenological level densities need to be generated from analytical expressions for the total level density, spin distribution, collective enhancement, shell models, etc. they come with a large number of models and adjustable parameters. First of all, different level density models can be chosen with **ldmodel** (p. 378) The global level density parameters of Eq. (8.13), see table 8.1, can be adjusted with the keywords **alphald** (p. 414), and **betald** (p. 415), and the global shell damping parameter of Eq. (8.14) with **gammashell1** (p. 417)

and **gammashell2** (p. 418). The global pairing correction can be changed with **Pshiftconstant** (p. 400). For a particular nucleus, the level density parameter at the binding energy can be adjusted with **a** (p. 380), the asymptotic level density parameter at infinite excitation energy with **alimit** (p. 382), and the shell damping parameter with **gammald** (p. 25). In addition, we can impose a relative adjustment to the level density parameter a (so we don't need to know its actual value) with **aadjust** (p. 381). One can also choose to use a global model for the level density parameter with **asys** (p. 383). For the CTM, the keywords **T** (p. 394), **Tadjust** (p. 395), **E0** (p. 396), **E0adjust** (p. 397), **Exmatchadjust** (p. 393), **Exmatch** (p. 392), **Nlow** (p. 390), **Ntop** (p. 391), **CTMglobal** (p. 412), are available. The pairing energy can be adjusted with the keywords **pairconstant** (p. 419), **pair** (p. 385), **Pshift** (p. 398), **Pshiftadjust** (p. 399). The user can change the model and parameters for the spin cutoff parameter with **spincutmodel** (p. 409), **Rspincut** (p. 401), **s2adjust** (p. 403), the shell model with **shellmodel** (p. 410), and **deltaW** (p. 384), and vibrational enhancement with **Kvibmodel** (p. 411). Collective enhancement can be enabled or disabled with **colenhance** (p. 407), and further adjustment of collective enhancement can be attained with **colldamp** (p. 408), **Krotconstant** (p. 420), **Ufermi** (p. 422), **Cfermi** (p. 421), For fission level densities, **Rtransmom** (p. 423), **Rclass2mom** (p. 424), are available. The amount of level densities in output files can be steered with **filedensity** (p. 405), **outdensity** (p. 406).

Implementation 8.2.1 Level density parameters are determined in *densitypar.f*.

   The level density parameters are stored in the *talys/structure/density/* directory. First, there are 4 subdirectories, *ground/*, *fission/*, *ph/*, *phjp* for ground state, fission barrier, particle-hole level densities, and spin-parity dependent particle-hole level densities, respectively. In *ground/ctm/*, *ground/bfm/*, and *ground/gsm/*, phenomenological level density parameters are stored. When the level density parameter **a** is given, it is derived from a fit to the D_0 resonance spacing of the RIPL database. As an example, below are the parameters for the Zr-isotopes from *ground/bfm/Zr.ld*. For each isotope, we have stored Z, A, and then for both the effective and explicit collective model N_L, N_U, level density parameter a in MeV^{-1}, and pairing correction in MeV, nuclear symbol. The format is (2i4,2(2i4,2f12.5)4x,i4,a2).

```
 40   86   8   17     0.00000      0.51730    8   17     0.00000      1.04574      86Zr
 40   87   8   26     0.00000      0.15936    8   26     0.00000      0.65313      87Zr
 40   88   5   17     0.00000     -0.04425    5   17     0.00000      0.46704      88Zr
 40   89   2   15     0.00000      0.39230    2   15     0.00000      0.96543      89Zr
 40   90   8   16     0.00000      0.99793    8   16     0.00000      1.80236      90Zr
 40   91   3   17     9.57730      0.40553    3   17     5.13903      1.15428      91Zr
 40   92   3   16     9.94736     -0.03571    3   16     5.00387      0.39829      92Zr
 40   93   8   18    11.07918      0.50929    8   18     5.92169      1.07202      93Zr
 40   94   4   16    12.51538      0.28941    4   16     6.66540      0.60420      94Zr
 40   95   3   18    11.98832      0.83535    3   18     5.97084      1.28803      95Zr
 40   96   3   16     0.00000      0.64799    3   16     0.00000      1.06393      96Zr
 40   98   8   16     0.00000      0.32758    8   16     0.00000      0.67594      98Zr
 40   99   2   21     0.00000     -0.01325    2   21     0.00000      0.26100      99Zr
 40  100   8   17     0.00000     -0.25519    8   17     0.00000      0.00789     100Zr
 40  101   8   15     0.00000     -0.13926    8   15     0.00000      0.17608     101Zr
 40  102   8   17     0.00000     -0.37952    8   17     0.00000     -0.12167     102Zr
```

8.3 Microscopic level densities

Besides the phenomenological models that are used in TALYS, there is also an option to employ more microscopic approaches. For the RIPL database, S. Goriely has calculated level densities from drip line to drip line on the basis of Hartree-Fock calculations [41] for excitation energies up to 150 MeV and for spin values up to $I = 30$. If **ldmodel 4** (p. 378), these tables with microscopic level densities can be read. Moreover, new energy-, spin- and parity-dependent nuclear level densities based on the microscopic combinatorial model have been proposed by Hilaire and Goriely [42]. The combinatorial model includes a detailed microscopic calculation of the intrinsic state density and collective enhancement. The only phenomenological aspect of the model is a simple damping function for the transition from spherical to deformed, see also Eq. (8.88). The calculations make coherent use of nuclear structure properties determined within the deformed Skyrme-Hartree-Fock-Bogoliubov framework. Level densities for more than 8500 nuclei are made available in tabular format, for excitation energies up to 200 MeV and for spin values up to $J = 49$. These level densities are used with **ldmodel 5**.

The most recent option, invoked with **ldmodel 6**, is based on temperature-dependent Hartree-Fock-Bogoliubov calculations using the Gogny force [43].

Since these microscopical level densities, which we will call ρ_{HFM}, have not been adjusted to experimental data, we add adjustment flexibility through a scaling function, i.e.

$$\rho(E_x, J, \pi) = \exp(c\sqrt{E_x - \delta})\rho_{HFM}(E_x - \delta, J, \pi) \tag{8.94}$$

where by default $c = 0$ and $\delta = 0$ (i.e. unaltered values from the tables). The "pairing shift" δ simply implies obtaining the level density from the table at a different energy. The constant c plays a role similar to that of the level density parameter a of phenomenological models. Adjusting c and δ together gives adjustment flexibility at both low and higher energies.

For both microscopic level density models, tables for level densities on top of the fission barriers are automatically invoked for **ldmodel 4, 5** or **6**, when available in the structure database. For nuclides outside the tabulated microscopic database, the default Fermi gas model is used.

Options 8.3.1 For microscopic level density models all characteristics like spin distributions, collective enhancement etc are all intrinsic in the estimation of the level density tables from the theory. Therefore, only a few parameters are available to adjust these tabulated levels densities: the keywords **ctable** (p. 386), **ptable** (p. 388), **cglobal** (p. 425), **pglobal** (p. 426). To study its effect, parity dependence can be enables and disabled with **parity** (p. 413).

Implementation 8.3.1 The two subdirectories *ground/hilaire/* and *ground/goriely/*, contain the tabulated microscopic level densities of Hilaire [42] and Goriely [41], respectively, also present in RIPL. For each isotope, there are first 4 comment lines, indicating the nucleus under consideration. Next, the excitation energy, temperature, number of cumulative levels, total level density, total state density and level density per spin are read in the format (f7.2,7.3,e10.2,31e9.2). Below is an example for the first energies of ^{42}Fe from *ground/goriely/Fe.tab*

```
***********************************************************************
*  Z= 26 A= 42: Total and Spin-dependent Level Density [MeV-1] for Fe 42 *
***********************************************************************
 U[MeV] T[MeV]  NCUMUL    RHOOBS    RHOTOT      J=0       J=1       J=2
   0.25  0.224  1.09E+00 7.33E-01 2.07E+00 2.44E-01 3.39E-01 1.26E-01
   0.50  0.302  1.33E+00 1.17E+00 4.14E+00 2.74E-01 4.83E-01 2.88E-01
```

```
   0.75   0.365   1.71E+00 1.86E+00 7.60E+00 3.45E-01 6.76E-01 4.95E-01
   1.00   0.419   2.29E+00 2.82E+00 1.31E+01 4.33E-01 9.05E-01 7.55E-01
```

Level densities for fission barriers are tabulated in *fission/hilaire/* and *fission/goriely/*. There is an *inner/* and *outer/* subdirectory, for the inner and outer barrier, respectively. Here is an example for the first few energy/spin points of ^{230}U from *fission/goriely/inner/U.ld*. The format is the same as for the ground state, see above.

```
**************************************************************************
*  Z= 92 A=230: Total and Spin-dependent Level Density [MeV-1] at the inner
   saddle point c=  1.24 h=  0.00 a=  0.00 B=  3.80 MeV  *
**************************************************************************
 U[MeV]  T[MeV]  NCUMUL   RHOOBS    RHOTOT     J=0       J=1       J=2
   0.25   0.162   1.11E+00 8.86E-01 5.92E+00 6.44E-02 1.64E-01 1.98E-01
   0.50   0.190   1.51E+00 2.32E+00 1.81E+01 1.19E-01 3.20E-01 4.31E-01
   0.75   0.209   2.56E+00 6.10E+00 5.25E+01 2.54E-01 7.01E-01 9.85E-01
```

In *density/ph/* microscopic particle-hole state densities are stored for 72 two-component ph combinations and 14 one-component ph combinations. The same energy grid and format as for total level densities is used. The particle-hole combinations are denoted as $p_\pi h_\pi p_\nu h_\nu$.

Here is an example for the first few energy/ph points of ^{42}Fe from *density/ph/Fe.ph*.

```
              **************************************************
              *  Z= 26 A= 42 Particle-hole density [MeV-1]  *
              *  Proton  Fermi energy = -49.556 MeV         *
              *  Neutron Fermi energy = -31.217 MeV         *
              **************************************************
 U[MeV]    0010     1000     0011     0020     0110     1001     1010
   0.25 0.00E+00 0.00E+00 0.00E+00 0.00E+00 0.00E+00 0.00E+00 0.00E+00
   0.50 0.00E+00 2.00E+00 0.00E+00 0.00E+00 0.00E+00 4.00E+00 0.00E+00
   0.75 0.00E+00 2.00E+00 0.00E+00 0.00E+00 0.00E+00 4.00E+00 0.00E+00
   1.00 0.00E+00 2.00E+00 0.00E+00 0.00E+00 0.00E+00 8.00E+00 0.00E+00
   1.25 0.00E+00 2.00E+00 0.00E+00 0.00E+00 0.00E+00 8.00E+00 0.00E+00
   1.50 0.00E+00 0.00E+00 0.00E+00 0.00E+00 0.00E+00 4.00E+00 0.00E+00
```

Finally, in *density/phjp/* microscopic particle-hole state densities, dependent on spin and parity, are tabulated for direct capture calculations.

8.4   Average resonance parameters

Neutron average resonance parameters are provided in the *talys/structure/resonances/* directory and stem from the the RIPL-2 database. As an example, below are the parameters for the Fe-isotopes from *resonances/Fe.res*. For each isotope, we have stored Z, A, the experimental s-wave resonance spacing D_0 in keV, its uncertainty, the experimental s-wave strength function S_0 ($\times 10^{-4}$), its uncertainty, the experimental total radiative width in eV and its uncertainty, nuclear symbol. The format is (2i4,2e9.2,2f5.2,2f9.5,20x,i4,a2).

```
  26   55 1.80E+01 2.40E+00 6.90 1.80  1.80000  0.50000                    55Fe
  26   57 2.54E+01 2.20E+00 2.30 0.60  0.92000  0.41000                    57Fe
  26   58 6.50E+00 1.00E+00 4.70 1.10  1.90000  0.60000                    58Fe
  26   59 2.54E+01 4.90E+00 4.40 1.30  3.00000  0.90000                    59Fe
```

Sample case 8.1 **Different level density models : n + ^{99}Tc**

To demonstrate the variety of level density models that we have added recently to TALYS, we include a sample case in which 3 different models are compared. The results are given in Fig. 8.1 for the cumulative number of discrete levels and in Fig.8.2 for the (n,p) cross section.

Case a: Constant Temperature Model

The input file is

```
#
# n-Tc099-ld1
#
# General
#
projectile n
element tc
mass 99
energy energies
#
# Parameters
#
outdensity y
filedensity y
ldmodel 1
```

This is the default calculation: TALYS use the local CTM level density for its calculations

Case b: Back-shifted Fermi gas Model

The input file is

```
#
# n-Tc099-ld2
#
# General
#
projectile n
element tc
mass 99
energy energies
#
# Parameters
#
outdensity y
filedensity y
ldmodel 2
```

Case c: Hartree-Fock Model

The input file is

```
#
# n-Tc099-ld5
#
# General
#
projectile n
element tc
mass 99
energy energies
#
# Parameters
#
outdensity y
filedensity y
ldmodel 5
```

The level density files contain a lot of metadata. For example, *ld043100.tot* looks as follows

```
# header:
#   title: Tc100 level density
#   source: TALYS-2.0
#   user: Arjan Koning
#   date: 2023-12-14
#   format: YANDF-0.1
# residual:
#   Z: 43
#   A: 100
#   nuclide: Tc100
# parameters:
#   ldmodel keyword: 1
#   level density model: Gilbert-Cameron
#   Collective enhacement: n
#   a(Sn) [MeV^-1]:  1.616190E+01
#   asymptotic a [MeV^-1]:  1.336739E+01
#   shell correction [MeV]:  3.021460E+00
#   damping gamma:  9.330641E-02
#   pairing energy [MeV]:  0.000000E+00
#   adjusted pairing shift [MeV]:  0.000000E+00
#   separation energy [MeV]:  6.764404E+00
#   discrete spin cutoff parameter:  8.238095E+00
#   spin cutoff parameter(Sn):  2.342199E+01
#   matching energy [MeV]:  4.445303E+00
#   temperature [MeV]:  6.575356E-01
#   E0 [MeV]: -2.006161E+00
#   Nlow: 8
#   Ntop: 17
#   ctable:  1.000000E-20
#   ptable:  1.000000E-20
# observables:
```
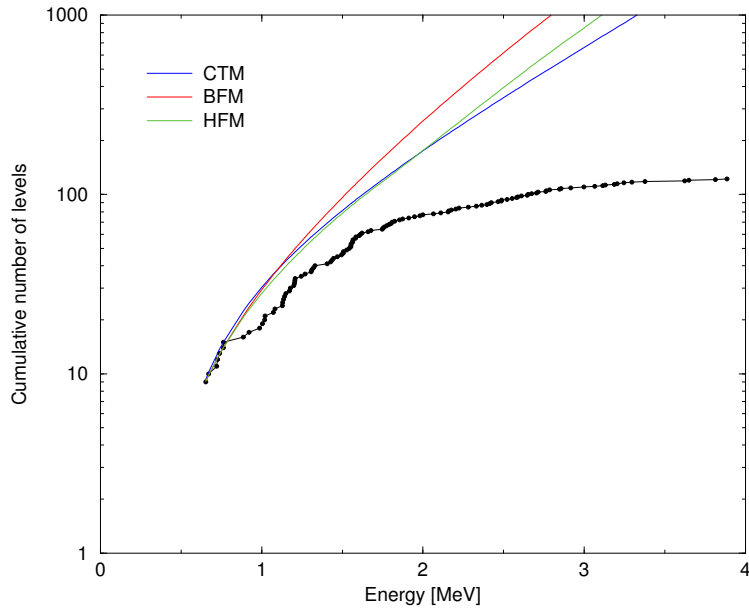
Figure 8.1: Cumulative number of discrete levels of ^{99}Tc for different level density models.

```
#    experimental D0 [eV]:  1.200000E+01
#    experimental D0 unc. [eV]:  1.300000E+00
#    theoretical D0 [eV]:  1.200798E+01
#    Chi-2 D0:  3.767498E-05
#    C/E D0:  1.000665E+00
#    Frms D0:  1.000003E+00
#    Erms D0:  1.000003E+00
#    Chi-2 per level:  4.622709E-02
#    Frms per level:  1.016615E+00
#    Erms per level:  1.000363E+00
#    average deviation per level:  5.333306E-02
# datablock:
#    quantity: level density
#    columns: 6
#    entries: 79
##      E           Level       N_cumulative     Total LD          a
##     [MeV]         []             []           [MeV^-1]       [MeV^-1]
    3.194900E-01     9          9.020750E+00    5.225714E+01    1.708033E+01
    3.351600E-01    10          9.849436E+00    5.351747E+01    1.707764E+01
    3.409800E-01    11          1.016229E+01    5.399327E+01    1.707664E+01
    3.555800E-01    12          1.095939E+01    5.520555E+01    1.707412E+01
    4.006300E-01    13          1.353307E+01    5.912044E+01    1.706639E+01
    4.243600E-01    14          1.496155E+01    6.129303E+01    1.706232E+01
    4.403800E-01    15          1.595550E+01    6.280470E+01    1.705957E+01
    4.542000E-01    16          1.683263E+01    6.413869E+01    1.705721E+01
    4.567900E-01    17          1.699907E+01    6.439182E+01    1.705677E+01
    4.580900E-01    18          1.708286E+01    6.451926E+01    1.705655E+01
.................
```
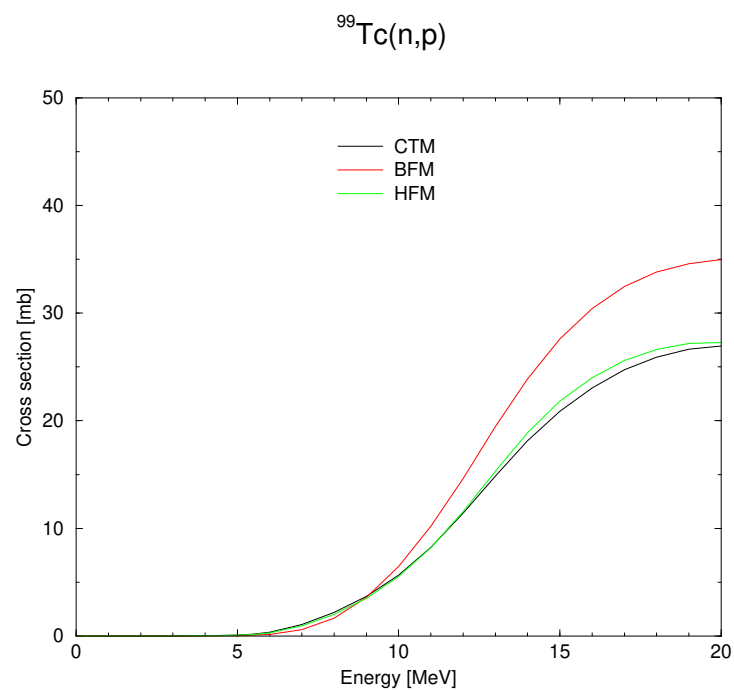
Figure 8.2: ^{99}Tc(n,p) cross section for different level density models.

9. Reactions involving photons

9.1 Photon strength functions and transmission coefficients

Photon strength functions (PSF) are important for the description of any transition involving gamma rays in nuclear reactions. The best known reaction channels which are governed by the PSF are the (n,γ) and (γ,n) reaction channels, but the PSF can be regarded as an important universal entity in reaction modeling since gamma rays in general may accompany emission of any other emitted particle, and gamma transitions occur for both the continuum and discrete levels.

Before we describe the PSF models implemented in TALYS, we first give the basic relations which establish their parameters, constraints and use in reaction models.

The transmission of a gamma ray at an energy E_γ is described by the PSF $f_{X\ell}(E_\gamma)$. Here X denotes either electric (E) or magnetic (M) radiation; and ℓ is the radiation multipolarity. In general, dipole $(\ell = 1)$ radiation dominates over radiation of higher multipolarity for a given ε_γ, e.g. $f_{E1}(E_\gamma) >> f_{E2}(E_\gamma)$. Also E transitions are generally stronger than M transitions for a given multipolarity, i.e. $f_{E1}(E_\gamma) > f_{M1}(E_\gamma)$

One distinguishes between

- upward PSF $\overrightarrow{f_{X\ell}}(E_\gamma)$, related to the cross section for gamma absorption such as for (γ,n) reactions, which is determined for $E_\gamma > S_n$ (the neutron separation energy).
- downward PSF $\overleftarrow{f_{X\ell}}(E_\gamma)$, related to the average width of the gamma decay and thus to (n,γ) reactions, which is determined for $E_\gamma < S_n$.

The essential relation between the photoabsorption cross section and the upward PSF is

$$\sigma_{(\gamma,abs)}(E_\gamma) = \sum_{X\ell} \sigma_{X\ell}(E_\gamma), \tag{9.1}$$

where,

$$\overrightarrow{f_{X\ell}}(E_\gamma) = K_{X\ell} \frac{\sigma_{X\ell}(E_\gamma)}{E_\gamma^{2\ell-1}}, \tag{9.2}$$

and,

$$K_{X\ell} = \frac{1}{(2\ell+1)\pi^2\hbar^2c^2},$$ (9.3)

Eq. (9.2) means that the shape, and parameters, of the PSF is determined by $\sigma_{X\ell}$ summed over all spins and parities. In practice, with other components being negligible near the peak of the PSF, this means that the high-energy part of f_{E1} is determined by the (γ,n) cross section.

The downward PSF is related to the de-excitation of the nucleus. Like the particle transmission coefficients that emerge from the optical model, photon transmission coefficients enter the Hauser-Feshbach model for the determination of the competition between photon emission and emission of other particles. The relation between the photon transmission coefficient and downward PSF is given by

$$T_{X\ell}(E_\gamma) = 2\pi\overleftarrow{f_{X\ell}}(E_\gamma)E_\gamma^{2\ell+1}.$$ (9.4)

The average radiation width Γ_γ may be obtained by integrating the gamma-ray transmission coefficients over the density of final states that may be reached in the first step of the gamma-ray cascade. This leads to the essential relation for the downward PSF,

$$\frac{2\pi\Gamma_\gamma}{D_0} = \sum_J \sum_\Pi \sum_{X\ell} \sum_{I'=|J-\ell|}^{J+\ell} \sum_{\Pi'} \int_0^{S_n} dE_\gamma T_{X\ell}(E_\gamma)\rho(S_n - E_\gamma, I', \Pi')F(X, \Pi', \ell),$$ (9.5)

where D_0 is the average resonance spacing derived from the level density ρ. The J, Π sum is over the compound nucleus states with spin J and parity Π that can be formed with s-wave incident particles, and I', Π' denote the spin and parity of the final states. The multipole selection rules are $F(E, \Pi', \ell) = 1$ if $\Pi = \Pi'(-1)^\ell$, $F(M, \Pi', \ell) = 1$ if $\Pi = \Pi'(-1)^{\ell+1}$, and 0 otherwise. The integral over dE_γ includes a summation over discrete states.

At the same time, $\overleftarrow{f_{X\ell}}(E_\gamma)$ and thus $T_{X\ell}(E_\gamma)$ is strictly related to the (n,γ) cross section just above the resonance range, before the opening of the inelastic channel. Since the transmission coefficient for neutrons is much larger than that of photons, $T_n >> T_\gamma$, the Hauser-Feshbach formula for this energy range can be stated as,

$$\begin{aligned} \sigma(n,\gamma) &= \frac{T_n T_\gamma}{T_n + T_\gamma} \approx T_\gamma \\ &= \sum_J \sum_\Pi \sum_{X\ell} \sum_{I'=|J-\ell|}^{J+\ell} \sum_{\Pi'} \int_0^{S_n} dE_\gamma T_{X\ell}(E_\gamma)\rho(S_n - E_\gamma, I', \Pi')F(X, \Pi', \ell), \end{aligned}$$ (9.6)

Both Γ_γ and (n,γ) cross sections around 30 keV, have been experimentally determined for more than 200 nuclides, and are therefore important observables to constrain the PSF model and its parameters.

The Brink hypothesis assumes the approximate equality of the upward and downward PSF and from now on we will use $f_{X\ell} = \overleftarrow{f_{X\ell}} = \overrightarrow{f_{X\ell}}$ in the notation. Also in TALYS no distinction is made. Hence, the ideal PSF for the whole energy range is thus characterized by a good description of the (γ,n) cross section for $E_\gamma > S_n$ and simultaneously a good description of the (n,γ) cross section governed by $E_\gamma < S_n$, obeying Eqs. (9.5) and (9.6). For the latter low-energy part, the PSF can be fine-tuned by using experimental information from e.g. (p,p') reactions that feed gamma decay just below S_n, also known as the Oslo-method, and also from (γ,γ') reactions.

We have implemented various phenomenological and microscopic models for the photon strength function. We will mention them all, but will put extra emphasis on the preferred phenomenological model, the Simplified Modified Lorentzian Model (SMLO), and the preferred microscopic model, QRPA with Gogny-D1M. These two models were developed and tested during an IAEA CRP on photon strength functions and photonuclear cross sections [44, 45] and are regarded, by us at least, as the two best physical options for PSF, from a physics point of view. After the description of the various PSF models, we will outline how a proper normalization of PSF's to experimental data can be obtained.

9.2 Analytic, Lorentzian models for photon strength functions

The phenomenological models are generally parameterized in terms of Lorentzian forms with giant resonance (GR) parameters:

- $\sigma_{X\ell}$: strength of the giant resonance,
- $E_{X\ell}$: energy of the giant resonance,
- $\Gamma_{X\ell}$: width of the giant resonance.

We note that the PSF sometimes, for deformed nuclei, exhibits two peaks. In that case one often uses a second Lorentzian, and for the phenomenological models the total PSF for $E1$ is then given by

$$f_{X\ell}(E_\gamma) = \sum_{i=1}^{2} f_{X\ell}^i(E_\gamma, \sigma_{E1}^i, E_{E1}^i, \Gamma_{E1}^i) \tag{9.7}$$

9.2.1 Brink-Axel model

The first, and oldest, model is the so-called Brink-Axel option [46, 47], in which a standard Lorentzian form describes the giant dipole resonance shape, i.e.

$$f_{X\ell}(E_\gamma) = K_{X\ell} \frac{\sigma_{X\ell} E_\gamma \Gamma_{X\ell}^2}{(E_\gamma^2 - E_{X\ell}^2)^2 + E_\gamma^2 \Gamma_{X\ell}^2}. \tag{9.8}$$

At present, we use the Brink-Axel option for all multipoles higher than 1. In TALYS, this model can be invoked with **strength 2**.

9.2.2 Kopecky-Uhl model

For $E1$ radiation, an option which has been used as a default for many years in TALYS is the generalized Lorentzian form of Kopecky and Uhl [48],

$$f_{E1}(E_\gamma, T) = K_{E1} \left[\frac{E_\gamma \tilde{\Gamma}_{E1}(E_\gamma)}{(E_\gamma^2 - E_{E1}^2)^2 + E_\gamma^2 \tilde{\Gamma}_{E1}(E_\gamma)^2} + \frac{0.7 \Gamma_{E1} 4\pi^2 T^2}{E_{E1}^5} \right] \sigma_{E1} \Gamma_{E1}, \tag{9.9}$$

where the energy-dependent damping width $\tilde{\Gamma}(E_\gamma)$ is given by

$$\tilde{\Gamma}_{E1}(E_\gamma) = \Gamma_{E1} \frac{E_\gamma^2 + 4\pi^2 T^2}{E_{E1}^2}, \tag{9.10}$$

and T is the nuclear temperature given by Kopecky et al [49]

$$T = \sqrt{\frac{E_n + S_n - \Delta - E_\gamma}{a(S_n)}}, \tag{9.11}$$

where S_n is the neutron separation energy, E_n the incident neutron energy, Δ the pairing correction (see the chapter on level densities) and a the level density parameter at S_n. This model is used with **strength 1**.

9.2.3 Parameters for standard Lorentzian models

For $E1$-transitions, GDR parameters for various individual nuclides exist. These are stored in the nuclear structure database of TALYS. For all $X\ell$ transitions, systematic formulae compiled by Kopecky [6] for the resonance parameters are used. For $E1$ transitions for which no nuclide-specific data exist, we use

$$\sigma_{E1} = 1.2 \times 120NZ/(A\pi\Gamma_{E1}) \text{ mb}, \quad E_{E1} = 31.2A^{-1/3} + 20.6A^{-1/6} \text{ MeV}, \quad \Gamma_{E1} = 0.026E_{E1}^{1.91} \text{ MeV}. \tag{9.12}$$

For $E2$ transitions we use

$$\sigma_{E2} = 0.00014Z^2E_{E2}/(A^{1/3}\Gamma_{E2}) \text{ mb}, \quad E_{E2} = 63.A^{-1/3} \text{ MeV}, \quad \Gamma_{E2} = 6.11 - 0.012A \text{ MeV}. \tag{9.13}$$

For multipole radiation higher than $E2$, we use

$$\sigma_{E\ell} = 8.10^{-4}\sigma_{E(\ell-1)}, \quad E_{E\ell} = E_{E(\ell-1)} \quad \Gamma_{E\ell} = \Gamma_{E(\ell-1)}, \tag{9.14}$$

For $M1$ transitions we use

$$f_{M1} = 1.58e - 9A^{0.47} \text{ at } 7 \text{ MeV}, \quad E_{M1} = 41.A^{-1/3} \text{ MeV}, \quad \Gamma_{M1} = 4 \text{ MeV}, \tag{9.15}$$

where Eq. (9.8) thus needs to be applied at 7 MeV to obtain the σ_{M1} value. For multipole radiation higher than $M1$, we use

$$\sigma_{M\ell} = 8.10^{-4}\sigma_{M(\ell-1)}, \quad E_{M\ell} = E_{M(\ell-1)} \quad \Gamma_{M\ell} = \Gamma_{M(\ell-1)}, \tag{9.16}$$

Pygmy resonances

In addition to the GDR contribution above, we can include Pygmy resonances by adding another contribution of the form (9.8) to the strength function. The Pygmy resonance parameters do not have a default.

9.2.4 Hybrid model

The hybrid model of Goriely [50] (**strength 5**), see also RIPL [6], is a Lorentzian model with energy and temperature dependent width which results in a different type of functional form at low energy than that of Kopecky-Uhl.

9.3 Microscopic models for photon strength functions

There are various microscopic options for $E1$ and $M1$ radiation and the PSF's for these models have been stored as tables. As we will see later, all these tabulated values can be adjusted for fitting purposes.

9.3.1 Skyrme-Hartree-Fock BCS model

Goriely and Khan [51] calculated gamma-ray strength functions according to the Skyrme-Hartree-Fock BCS model with QRPA (**strength 3**) and these are invoked with **strength 3**.

9.3.2 Skyrme-Hartree-Fock-Bogoliubov model

The Skyrme-Hartree-Fock-Bogoliubov model with QRPA by Goriely et al. [52] is implemented as (**strength 4**), see also RIPL [6].

9.3.3 Temperature-dependent Skyrme-Hartree-Fock-Bogoliubov model

The Skyrme-Hartree-Fock-Bogoliubov model with QRPA by Goriely et al. [52] can be extended with temperature dependence and this is implemented as (**strength 6**).

9.3.4 Temperature-dependent Relativistic Mean Field model

The Temperature-dependent RMF model by Daoutidis and Goriely [53] is implemented as (**strength 7**).

9.3.5 Gogny-Hartree-Fock-Bogoliubov model

The Gogny-Hartree-Fock-Bogoliubov model with QRPA by Goriely et al. [54], based on the D1M version of the Gogny force is implemented as (**strength 8**).

Options 9.3.1 The keywords **strength** (p. 430) and **strengthM1** (p. 431) can be used to vary between different PSF models. The strength, width and energy parameters for the phenomenological GR PSF's for each radiation type and multipolarity can be explicitly provided by **sgr** (p. 433), **ggr** (p. 434), **egr** (p. 432), and for Pygmy resonances by **spr** (p. 460), **gpr** (p. 461), **epr** (p. 459). In addition to these nominal values, one may use **sgradjust** (p. 436), **ggradjust** (p. 437), **egradjust** (p. 435), **spradjust** (p. 463), **gpradjust** (p. 464), **epradjust** (p. 462), which all have a default value of 1. to deviate relative to the built-in default value for the GR and PR parameters.

To adjust the PSF normalization according to Eq. (9.5), the **gnorm** (p. 429) and **gamgamadjust** (p. 439) are available. For microscopic PSF models, **etable** (p. 443), and **ftable** (p. 445) are available to adjust tabulated values

Direct capture can be invoked with **racap** (p. 455).

Implementation 9.3.1 GDR parameters are read in *gammapar.f* For E1 radiation, the Giant Dipole Resonance (GDR) parameters, stored in the *talys/structure/gamma/gdr/* directory, originate from the Beijing GDR compilation, as present in the RIPL database. As an example, below are the GDR parameters for the U-isotopes from *U.gdr*. For each isotope, we have stored Z, A, energy E_0 in MeV, strength σ_0 in mb, width of the GDR Γ_0 in MeV and, if present, another energy, strength and width for the second peak, nuclear symbol. The format is (2i4,6f8.2,18x,i4,a2).

```
92 233   11.08  221.00    1.94   13.86  433.00    5.47                   233U
92 234   11.13  371.00    2.26   13.94  401.00    4.46                   234U
92 235   10.90  328.00    2.30   13.96  459.00    4.75                   235U
92 236   10.92  271.00    2.55   13.78  415.00    4.88                   236U
92 238   10.77  311.00    2.37   13.80  459.00    5.13                   238U
```

The other subdirectories contain tabulated PSF's from various microscopic approaches. For example, the second subdirectory *gamma/hbfcs/*, contains the tabulated microscopic gamma ray strength functions of Goriely et al [51], calculated according to Hartree-Fock BCS theory. For each isotope, there is first a line indicating the nucleus under consideration, read in the format

(2(4x,i3)). Next, one line with units is given after which comes a table of excitation energies and strength functions, in the format (f9.3,e12.3). Below is an example for the first energies of ^{110}Ba from *gamma/hfbcs/Ba.psf*

```
 Z=  56 A= 121 Ba
  U[MeV]   fE1[mb/MeV]
    0.100    5.581E-05
    0.200    2.233E-04
    0.300    5.028E-04
    0.400    8.947E-04
    0.500    1.400E-03
    0.600    2.018E-03
    0.700    2.752E-03
    0.800    3.601E-03
```

Similarly *gamma/hbf/*, contains the tabulated microscopic gamma ray strength functions of Goriely et al [52], calculated according to Hartree-Fock QRPA theory. For each isotope, there is first a line indicating the nucleus under consideration, read in the format (2(4x,i3)). Next, one line with units is given after which comes a table of excitation energies and strength functions, in the format (f9.3,e12.3). Below is an example for the first energies of ^{110}Ba from *gamma/hfb/Ba.psf*

```
 Z=  56 A= 110
  U[MeV]   fE1[mb/MeV]
    0.100    8.463E-03
    0.200    9.116E-03
    0.300    9.822E-03
    0.400    1.058E-02
    0.500    1.139E-02
    0.600    1.226E-02
    0.700    1.318E-02
    0.800    1.416E-02
```

Sample case 9.1 **Photonuclear reactions: g + ^{90}Zr**

This sample case illustrates the capabilities of TALYS to simulate photonuclear reactions. We calculate the (γ,n) reaction on ^{90}Zr as a function of incident energy, with default model parameters, and compare the result to experimental data. The following input file is used

```
#
# g-Zr090-xs
#
# General
#
projectile g
element zr
mass 90
energy energies
```

^{90}Zr(γ,xn)
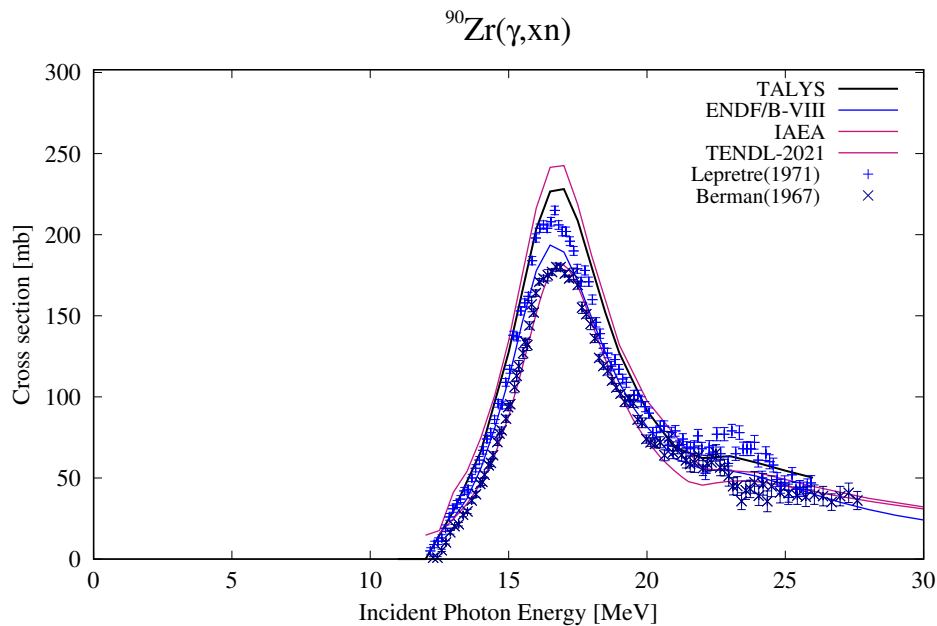
Figure 9.1: Photonuclear reaction on ^{90}Zr. Experimental data are obtained from Berman et al. [55].

Fig. 9.1 displays the resulting production cross section of ^{89}Zr, as obtained in file *rp040089.tot*.
■

Sample case 9.2 Direct neutron capture for n + ^{89}Y

For this sample case we use the input file

```
#
# n-Y089-dircap
#
# General
#
projectile n
element y
mass 89
energy n0-5.grid
#
# Parameters
#
racap y
```

The contribution of the direct capture process can be found in the last column of *total.tot*. ■

9.4 Adjustment of PSF

Regardless of the PSF model which is adopted, it is quite likely that an optimal fit to e.g. $\sigma(n,\gamma)$ or Γ_γ can only be obtained with some adjustment of the PSF. The simple Lorentzian models like

Brink-Axel or Kopecky-Uhl have ready to use parameters for that, but this is not the case for tabulated PSF's coming from microscopic calculations. It is however straightforward to bring all PSF models to the same practical level. If we denote the original, analytical or tabulated, PSF as $f_{E1}(E_\gamma)$ then we can add adjustment flexibility through scaling parameters to obtain the final PSF as follows,

$$f_{E1}^{\text{final}}(E_\gamma) = f^{\text{table}} f_{E1}(E_{E1} + w^{\text{wtable}}(E_\gamma - E_{E1}) + E_{\text{table}}) \tag{9.17}$$

where by default $f^{\text{table}} = 1$, $E_{\text{table}} = 0$, $w^{\text{table}} = 1$, i.e. unaltered values from the original table or function, and E_{E1} is the energy at the middle of the PSF which can be numerically determined. Here, f^{table} scales the entire PSF up or down and for many years this has been the standard parameter in TALYS (called 'gnorm'), inspired by the GNASH code, to adjust the PSF to obtain agreement with experimental (n,γ) cross sections in the fast neutron range. However, it should be considered as unphysical as the (n,γ) cross section is only sensitive to the low-energy tail of the PSF, and a too large adjustment of f^{table} would destroy the agreement of the PSF with (γ,n)-based GDR data near the peak. Moreover, the (n,γ) excitation function may show dubious behavior after such a radical adjustment. The energy shift E_{table} moves the PSF to the left or right and simply implies reading the PSF at a somewhat different energy. The most effective adjustment parameter for (n,γ) cross sections is w^{table}. It leaves the PSF practically untouched near its peak while it has a significant effect below S_n. In addition, since the majority of adjusted values of w^{table} lies within 15% of 1, the resulting PSF is often not in disagreement with measurements for PSF's near S_n. In TALYS, the associated keywords are **ftable** (p. 445), **etable** (p. 443). and **wtable** (p. 447). Note that the adjustment flexibility of the (less physical) phenomenological models is somewhat higher, since in addition one may adjust the parameters for a possible second peak as well. Microscopic PSF's certainly predict such double peaks, but we have to accept the relative position of the two peaks as they come from the tables.

9.5 Renormalization of gamma-ray strength functions

The Γ_γ values are, when available, read from our nuclear structure database.

In the introduction we mentioned the essential relation Eq. (9.5). At sufficiently low incident neutron energies, the average radiative capture width Γ_γ is due entirely to the s-wave interaction, and it is Γ_γ at the neutron separation energy S_n that is often used to normalize gamma-ray transmission coefficients, see Gardner [56]. Referring to Eq. (9.5), the normalization is then carried out as follows

$$\frac{2\pi\Gamma_\gamma}{D_0} = G_{norm} \sum_J \sum_\Pi \sum_{X\ell} \sum_{I'=|J-\ell|}^{J+\ell} \sum_{\Pi'} \int_0^{S_n} dE_\gamma T_{X\ell}(E_\gamma)\rho(S_n - E_\gamma, I', \Pi')f(X,\Pi',\ell), \tag{9.18}$$

i.e. G_{norm} is the normalization factor that enforces the equality (9.5). In practice, the transmission coefficients (9.4) are thus multiplied by G_{norm} before they enter the nuclear reaction calculation. G_{norm} can be specified by the user. The default is the value returned by Eq. (9.18). If $G_{norm} = 1$ is specified, no normalization is carried out and strength functions purely determined from giant resonance parameters are taken. Other values can be entered for G_{norm}, e.g. for fitting of the neutron capture cross section. Normalisation per multipolarity can be performed by adjusting the $\sigma_{X\ell}$ values in the input, see Part III.

9.6 Photoabsorption cross section

TALYS requires an estimate of the photo-absorption cross sections for models for photo-nuclear reactions and for pre-equilibrium gamma-ray emission. Obviously, for low energies this can be directly related to the GDR PSF we have discussed above. However, at higher energies this needs to be complemented by an additional contribution. Following Chadwick et al. [57], a more general expression for the photo-absorption cross section is

$$\sigma_{abs}(E_\gamma) = \sigma_{GDR}(E_\gamma) + \sigma_{QD}(E_\gamma). \tag{9.19}$$

The quasi-deuteron component σ_{QD} is given by

$$\sigma_{QD}(E_\gamma) = L\frac{NZ}{A}\sigma_d(E_\gamma)f(E_\gamma). \tag{9.20}$$

Here, $\sigma_d(E_\gamma)$ is the experimental deuteron photo-disintegration cross section, parameterized as

$$\sigma_d(E_\gamma) = 61.2\frac{(E_\gamma - 2.224)^{3/2}}{E_\gamma^3}, \tag{9.21}$$

for $E_\gamma > 2.224$ MeV and zero otherwise. The so-called Levinger parameter is $L = 6.5$ and the Pauli-blocking function is approximated by the polynomial expression

$$f(E_\gamma) = 8.3714.10^{-2} - 9.8343.10^{-3}E_\gamma + 4.1222.10^{-4}E_\gamma^2 - 3.4762.10^{-6}E_\gamma^3 + 9.3537.10^{-9}E_\gamma^4 \tag{9.22}$$

for $20 < E_\gamma < 140$ MeV,

$$f(E_\gamma) = \exp(-73.3/E_\gamma) \tag{9.23}$$

for $E_\gamma < 20$ MeV, and

$$f(E_\gamma) = \exp(-24.2348/E_\gamma) \tag{9.24}$$

for $E_\gamma > 140$ MeV.

For the Hauser-Feshbach calculations in TALYS, the associated photon transmission coefficients are normalized as follows,

$$T_{X\ell}^{\text{final}}(E_\gamma) = T_{X\ell}(E_\gamma)\frac{\sigma_{abs}(E_\gamma)}{\sigma_{abs}(E_\gamma) - \sigma_{QD}(E_\gamma)}. \tag{9.25}$$

9.7 Direct capture

For light nuclides and (very) neutron-rich nuclides, the direct capture process may have a significant contribution. Therefore, a direct capture model was implemented, to be activated with the **racap** keyword (p. 455). More details may become available in future versions of this manual. For the moment we refer to Xu and Goriely [58].

10. Optical model

The central assumption underlying the optical model is that the complicated interaction between an incident particle and a nucleus can be represented by a complex mean-field potential, which divides the reaction flux into a part covering shape elastic scattering and a part describing all competing non-elastic channels. Solving the Schrödinger equation numerically with this complex potential yields a wealth of valuable information. First, it returns a prediction for the basic observables, namely the elastic angular distribution and polarisation, the reaction and total cross section and, for low energies, the s, p-wave strength functions and the potential scattering radius R'. The essential value of a good optical model is that it can reliably predict these quantities for energies and nuclides for which no measurements exist. Also, the quality of the not directly observable quantities that are provided by the optical model has an equally important impact on the evaluation of the various reaction channels. Well-known examples are transmission coefficients, for compound nucleus and multi-step compound decay, and the distorted wave functions that are used for direct inelastic reactions and for transitions to the continuum that describe statistical multi-step direct reactions. Also, the reaction cross sections that are calculated with the optical model are crucial for the semi-classical pre-equilibrium models.

All optical model calculations are performed by ECIS-06, written by Raynal [5], which is used as a subroutine in TALYS.

10.1 Spherical OMP: Neutrons and protons

The default optical model potentials (OMP) used in TALYS are the local and global parameterisations of Koning and Delaroche [59].

The phenomenological OMP for nucleon-nucleus scattering, $\mathscr{U}$, is defined as:

$$\begin{aligned}
\mathscr{U}(r,E) &= -\mathscr{V}_V(r,E) - i\mathscr{W}_V(r,E) - i\mathscr{W}_D(r,E) \\
&\quad + \mathscr{V}_{SO}(r,E).\mathbf{l}.\sigma + i\mathscr{W}_{SO}(r,E).\mathbf{l}.\sigma + \mathscr{V}_C(r),
\end{aligned} \tag{10.1}$$

where $\mathscr{V}_{V,SO}$ and $\mathscr{W}_{V,D,SO}$ are the real and imaginary components of the volume-central (V), surface-central (D) and spin-orbit (SO) potentials, respectively. E is the LAB energy of the incident particle in MeV. All components are separated in energy-dependent well depths, V_V, W_V, W_D, V_{SO}, and W_{SO}, and energy-independent radial parts f, namely

$$
\begin{aligned}
\mathscr{V}_V(r,E) &= V_V(E)f(r,R_V,a_V), \\
\mathscr{W}_V(r,E) &= W_V(E)f(r,R_V,a_V), \\
\mathscr{W}_D(r,E) &= -4a_D W_D(E)\frac{d}{dr}f(r,R_D,a_D), \\
\mathscr{V}_{SO}(r,E) &= V_{SO}(E)\left(\frac{\hbar}{m_\pi c}\right)^2 \frac{1}{r}\frac{d}{dr}f(r,R_{SO},a_{SO}), \\
\mathscr{W}_{SO}(r,E) &= W_{SO}(E)\left(\frac{\hbar}{m_\pi c}\right)^2 \frac{1}{r}\frac{d}{dr}f(r,R_{SO},a_{SO}).
\end{aligned}
\tag{10.2}
$$

The form factor $f(r,R_i,a_i)$ is a Woods-Saxon shape

$$
f(r,R_i,a_i) = (1+\exp[(r-R_i)/a_i])^{-1},
\tag{10.3}
$$

where the geometry parameters are the radius $R_i = r_i A^{1/3}$, with A being the atomic mass number, and the diffuseness parameters a_i. For charged projectiles, the Coulomb term $\mathscr{V}_C$, as usual, is given by that of a uniformly charged sphere

$$
\begin{aligned}
\mathscr{V}_C(r) &= \frac{Zze^2}{2R_C}\left(3-\frac{r^2}{R_C^2}\right), \quad \text{for } r \le R_C \\
&= \frac{Zze^2}{r}, \quad \text{for } r \ge R_C,
\end{aligned}
\tag{10.4}
$$

with $Z(z)$ the charge of the target (projectile), and $R_C = r_C A^{1/3}$ the Coulomb radius.

The functional forms for the potential depths depend on $(E - E_f)$, where E_f, the Fermi energy in MeV, is defined as the energy halfway between the last occupied and the first unoccupied shell of the nucleus. For incident neutrons,

$$
E_f^n = -\frac{1}{2}[S_n(Z,N)+S_n(Z,N+1)],
\tag{10.5}
$$

with S_n the neutron separation energy for a nucleus with proton number Z and neutron number N, while for incident protons

$$
E_f^p = -\frac{1}{2}[S_p(Z,N)+S_p(Z+1,N)],
\tag{10.6}
$$

with S_p the proton separation energy. We use the mass table of the nuclear structure database to obtain the values of the separation energies.

Our OMP parameterisation for either incident neutrons or protons is

$$
\begin{aligned}
V_V(E) &= v_1[1 - v_2(E - E_f) + v_3(E - E_f)^2 - v_4(E - E_f)^3] \\
W_V(E) &= w_1 \frac{(E - E_f)^2}{(E - E_f)^2 + (w_2)^2} \\
r_V &= \text{constant} \\
a_V &= \text{constant} \\
W_D(E) &= d_1 \frac{(E - E_f)^2}{(E - E_f)^2 + (d_3)^2} \exp[-d_2(E - E_f)] \\
r_D &= \text{constant} \\
a_D &= \text{constant} \\
V_{SO}(E) &= v_{so1} \exp[-v_{so2}(E - E_f)] \\
W_{SO}(E) &= w_{so1} \frac{(E - E_f)^2}{(E - E_f)^2 + (w_{so2})^2} \\
r_{SO} &= \text{constant} \\
a_{SO} &= \text{constant} \\
r_C &= \text{constant},
\end{aligned}
\tag{10.7}
$$

where $E_f = E_f^n$ for incident neutrons and $E_f = E_f^p$ for incident protons. Here E is the incident energy in the LAB system. This representation is valid for incident energies from 1 keV up to 200 MeV. Note that V_V and W_V share the same geometry parameters r_V and a_V, and likewise for the spin-orbit terms.

In general, all parameters appearing in Eq. (10.7) differ from nucleus to nucleus. When enough experimental scattering data of a certain nucleus is available, a so called local OMP can be constructed. TALYS retrieves all the parameters v_1, v_2, etc. of these local OMPs automatically from the nuclear structure and model parameter database, see the next Chapter, which contains the same information as the various tables of Koning and Delaroche [59]. If a local OMP parameterisation is not available in the database, the built-in global optical models are automatically used, which can be applied for any Z, A combination. A flag exists, **localomp** (p. 499) to overrule the local OMP by the global OMP. The global neutron OMP, validated for $0.001 \leq E \leq 200$ MeV and $24 \leq A \leq 209$,

is given by

$$
\begin{aligned}
V_V(E) &= v_1^n[1 - v_2^n(E - E_f^n) + v_3^n(E - E_f^n)^2 - v_4^n(E - E_f^n)^3] \\
W_V(E) &= w_1^n \frac{(E - E_f^n)^2}{(E - E_f^n)^2 + (w_2^n)^2} \\
r_V &= 1.3039 - 0.4054A^{-1/3} \\
a_V &= 0.6778 - 1.487.10^{-4}A \\
W_D(E) &= d_1^n \frac{(E - E_f^n)^2}{(E - E_f^n)^2 + (d_3^n)^2} \exp[-d_2^n(E - E_f^n)] \\
r_D &= 1.3424 - 0.01585A^{1/3} \\
a_D &= 0.5446 - 1.656.10^{-4}A \\
V_{SO}(E) &= v_{so1}^n \exp[-v_{so2}^n(E - E_f^n)] \\
W_{SO}(E) &= w_{so1}^n \frac{(E - E_f^n)^2}{(E - E_f^n)^2 + (w_{so2}^n)^2} \\
r_{SO} &= 1.1854 - 0.647A^{-1/3} \\
a_{SO} &= 0.59,
\end{aligned}
\tag{10.8}
$$

where the units are in fm and MeV and the parameters for the potential depths and E_f^n are given in Table 10.1.

The global proton OMP is given by

$$
\begin{aligned}
V_V(E) &= v_1^p[1 - v_2^p(E - E_f^p) + v_3^p(E - E_f^p)^2 - v_4^p(E - E_f^p)^3] \\
&\quad + \bar{V}_C.v_1^p\left[v_2^p - 2v_3^p(E - E_f^p) + 3v_4^p(E - E_f^p)^2\right] \\
W_V(E) &= w_1^p \frac{(E - E_f^p)^2}{(E - E_f^p)^2 + (w_2^p)^2} \\
r_V &= 1.3039 - 0.4054A^{-1/3} \\
a_V &= 0.6778 - 1.487.10^{-4}A \\
W_D(E) &= d_1^p \frac{(E - E_f^p)^2}{(E - E_f^p)^2 + (d_3^p)^2} \exp[-d_2^p(E - E_f^p)] \\
r_D &= 1.3424 - 0.01585A^{1/3} \\
a_D &= 0.5187 + 5.205.10^{-4}A \\
V_{SO}(E) &= v_{so1}^p \exp[-v_{so2}^p(E - E_f^p)] \\
W_{SO}(E) &= w_{so1}^p \frac{(E - E_f^p)^2}{(E - E_f^p)^2 + (w_{so2}^p)^2} \\
r_{SO} &= 1.1854 - 0.647A^{-1/3} \\
a_{SO} &= 0.59 \\
r_C &= 1.198 + 0.697A^{-2/3} + 12.994A^{-5/3},
\end{aligned}
\tag{10.9}
$$

where the parameters for the potential depths, $\bar{V}_C$ and E_f^p are given in Table 10.2. The functional form of the proton global OMP differs from the neutron global OMP only by the Coulomb correction term in $V_V(E)$.

v_1^n	$= 59.30 - 21.0(N-Z)/A - 0.024A$	MeV
v_2^n	$= 0.007228 - 1.48.10^{-6}A$	MeV^{-1}
v_3^n	$= 1.994.10^{-5} - 2.0.10^{-8}A$	MeV^{-2}
v_4^n	$= 7.10^{-9}$	MeV^{-3}
w_1^n	$= 12.195 + 0.0167A$	MeV
w_2^n	$= 73.55 + 0.0795A$	MeV
d_1^n	$= 16.0 - 16.0(N-Z)/A$	MeV
d_2^n	$= 0.0180 + 0.003802/(1 + \exp[(A - 156.)/8.)])$	MeV^{-1}
d_3^n	$= 11.5$	MeV
v_{so1}^n	$= 5.922 + 0.0030A$	MeV
v_{so2}^n	$= 0.0040$	MeV^{-1}
w_{so1}^n	$= -3.1$	MeV
w_{so2}^n	$= 160.$	MeV
E_f^n	$= -11.2814 + 0.02646A$	MeV

Table 10.1: Potential depth parameters and Fermi energy for the neutron global OMP of Eq. (10.8).

v_1^p	$= 59.30 + 21.0(N-Z)/A - 0.024A$	MeV
v_2^p	$= 0.007067 + 4.23.10^{-6}A$	MeV^{-1}
v_3^p	$= 1.729.10^{-5} + 1.136.10^{-8}A$	MeV^{-2}
v_4^p	$= v_4^n$	MeV^{-3}
w_1^p	$= 14.667 + 0.009629A$	MeV
w_2^p	$= w_2^n$	MeV
d_1^p	$= 16.0 + 16.0(N-Z)/A$	MeV
d_2^p	$= d_2^n$	MeV^{-1}
d_3^p	$= d_3^n$	MeV
v_{so1}^p	$= v_{so1}^n$	MeV
v_{so2}^p	$= v_{so2}^n$	MeV^{-1}
w_{so1}^p	$= w_{so1}^n$	MeV
w_{so2}^p	$= w_{so2}^n$	MeV
E_f^p	$= -8.4075 + 0.01378A$	MeV
$\bar{V}_C$	$= 1.73.Z.A^{-1/3}/r_C$	MeV

Table 10.2: Potential depth parameters and Fermi energy for the proton global OMP of Eq. (10.9). The parameter values for neutrons are given in Table 10.1. $\bar{V}_C$ appears in the Coulomb correction term $\Delta V_C(E)$, of the real central potential.

The spherical optical model described above provides the transmission coefficients, DWBA cross sections, total and elastic cross sections, etc., mentioned in the beginning of this section. For deformed nuclides, strongly coupled collective levels need to be included. This will be explained in Chapter 11 on direct reactions.

10.1.1 Extension to 1 GeV

To be able to predict the total, elastic and non-elastic cross sections up to 1 GeV, the OMP described above has been extended by Koning [60]. It is emphasized here that this was just done to test at which energy the validity of TALYS in predicting other (residual) cross section will fail. We are well aware of the fact that the usual Schrödinger picture of the OMP is valid up to about 180 MeV, and should then be taken over by a Dirac approach. Nevertheless, a functional form was be constructed which leaves all KD03 parameter values below a joining energy E_J, at or around 200 MeV, unaltered while smoothly extending the energy dependence above E_J. This was only applied to the real, V_V, and imaginary, W_V, volume parts of the potential. For that, the KD03 OMP for neutrons below E_J reads [59],

$$
\begin{aligned}
V_V(E) &= v_1^n[1 - v_2^n(E - E_f^n) + v_3^n(E - E_f^n)^2 - v_4^n(E - E_f^n)^3] \\
W_V(E) &= w_1^n \frac{(E - E_f^n)^2}{(E - E_f^n)^2 + (w_2^n)^2},
\end{aligned}
$$

(10.10)

where E_f^n is the Fermi energy. For V_V, we assume that the exponential decrease should continue beyond E_J. After all, the KD03 form of Eq. (10.10) for V_V is just a Taylor expansion of the exponential function, in which we gave ourselves the freedom to alter the individual coefficients v_1, etc. Also, following studies like those of Typel et al. [61] and Chiba et al. [62], we assume that it converges to a negative value V_∞. Hence, the form chosen for $E > E_J$ is

$$
V_V(E) = V_\infty + b . \exp(-c(E - E_f^n)).
$$

(10.11)

We determine the new parameters b and c by calculating the value at $E = E_f^n$, giving

$$
b = V_V(E_f^n) - V_\infty.
$$

(10.12)

Hence,

$$
V_V(E) = V_\infty + (V_V(E_f^n) - V_\infty) \exp(-c(E - E_f^n)).
$$

(10.13)

Next, c can be determined by requiring that the high-energy potential is equal to that of the low energy expression Eq. (10.10) at the joining energy:

$$
V_V(E_J) = V_\infty + (V_V(E_f^n) - V_\infty) \exp(-c(E_J - E_f^n)),
$$

(10.14)

giving

$$
c = -\frac{1}{(E_J - E_f^n)} \log\left(\frac{V_V(E_J) - V_\infty}{V_V(E_f^n) - V_\infty}\right).
$$

(10.15)

For W_V it is expected that at high energies new absorption channels, such as pion production, emerge and that W_V will show another smooth increase as function of energy. Hence, the form of W_V for $E > E_J$ is

$$
W_V(E) = w_3^n \frac{(E - E_f^n)^4}{(E - E_f^n)^4 + (w_4^n)^4} + d,
$$

(10.16)

where we find that a power of 4, instead of the usual 2, gives a better description of experimental data. Also here, a parameter d was added to ensure a value exactly equal to KD03 at E_J, i.e. at $E = E_J$ we have

$$d = W_V(E_J) - w_3^n \frac{(E_J - E_f^n)^4}{(E_J - E_f^n)^4 + (w_4^n)^4} \tag{10.17}$$

In sum, we have the following simple extension of the KD03 OMP for $E > E_J$:

$$
\begin{aligned}
V_V(E) &= V_\infty + (V_V(E_f^n) - V_\infty) \\
&\quad * \exp\left(\frac{E - E_f^n}{E_J - E_f^n} * \log(\frac{V_V(E_J) - V_\infty}{V_V(E_f^n) - V_\infty})\right) \\
W_V(E) &= W_V(E_J) - w_3^n \frac{(E_J - E_f^n)^4}{(E_J - E_f^n)^4 + (w_4^n)^4} \\
&\quad + w_3^n \frac{(E - E_f^n)^4}{(E - E_f^n)^4 + (w_4^n)^4}
\end{aligned}
\tag{10.18}
$$

which joins smoothly with the KD03 expression of Eq. (10.10) for $E < E_J$. The following, preliminary, values were obtained from a fit to neutron total and proton non-elastic cross sections up to 1 GeV:

$$
\begin{aligned}
E_J &= 200. \\
V_\infty &= -30. \\
w_3^n &= 25. - 0.0417A \\
w_4^n &= 250.
\end{aligned}
\tag{10.19}
$$

All parameters can be adjusted with keywords. In Eq. (10.18), $V_V(E_f)$, $V_V(E_J)$ and $W_V(E_J)$ are obtained from Eq. (10.10). The above extension, and parameters, also hold for incident protons.

10.2 Spherical dispersive OMP: Neutrons

The theory of the nuclear optical model can be reformulated in terms of dispersion relations that connect the real and imaginary parts of the optical potential, and we have added an option in TALYS to take them into account. These dispersion relations are a natural result of the causality principle that a scattered wave cannot be emitted before the arrival of the incident wave. The dispersion component stems directly from the absorptive part of the potential,

$$\Delta \mathcal{V}(r,E) = \frac{\mathcal{P}}{\pi} \int_{-\infty}^{\infty} \frac{\mathcal{W}(r,E')}{E' - E} dE', \tag{10.20}$$

where $\mathcal{P}$ denotes the principal value. The total real central potential can be written as the sum of a Hartree-Fock term $\mathcal{V}_{HF}(r,E)$ and the the total dispersion potential $\Delta \mathcal{V}(r,E)$

$$\mathcal{V}(r,E) = \mathcal{V}_{HF}(r,E) + \Delta \mathcal{V}(r,E). \tag{10.21}$$

Since $\mathcal{W}(r,E)$ has a volume and a surface component, the dispersive addition is,

$$
\begin{aligned}
\Delta \mathcal{V}(r,E) &= \Delta \mathcal{V}_V(r,E) + \Delta \mathcal{V}_D(r,E) \\
&= \Delta V_V(E) f(r,R_V,a_V) - 4a_D \Delta V_D(E) \frac{d}{dr} f(r,R_D,a_D)
\end{aligned} \tag{10.22}
$$

where the volume dispersion term is given by

$$
\Delta V_V(E) = \frac{\mathscr{P}}{\pi} \int_{-\infty}^{\infty} \frac{W_V(E')}{E' - E} dE', \tag{10.23}
$$

and the surface dispersion term is given by

$$
\Delta V_D(E) = \frac{\mathscr{P}}{\pi} \int_{-\infty}^{\infty} \frac{W_D(E')}{E' - E} dE'. \tag{10.24}
$$

Hence, the real volume well depth of Eq. (10.2) becomes

$$
V_V(E) = V_{HF}(E) + \Delta V_V(E), \tag{10.25}
$$

and the real surface well depth is

$$
V_D(E) = \Delta V_D(E). \tag{10.26}
$$

In general, Eqs. (10.23)-(10.24) cannot be solved analytically. However, under certain plausible conditions, analytical solutions exist. Under the assumption that the imaginary potential is symmetric with respect to the Fermi energy E_F,

$$
W(E_F - E) = W(E_F + E), \tag{10.27}
$$

where W denotes either the volume or surface term, we can rewrite the dispersion relation as,

$$
\Delta V(E) = \frac{2}{\pi}(E - E_F) \mathscr{P} \int_{E_F}^{\infty} \frac{W(E')}{(E' - E_F)^2 - (E - E_F)^2} dE', \tag{10.28}
$$

from which it easily follows that $\Delta V(E)$ is skew-symmetric around E_F,

$$
\Delta V(E + E_F) = -\Delta V(E - E_F), \tag{10.29}
$$

and hence $\Delta V(E_F) = 0$. This can then be used to rewrite Eq. (10.20) as

$$
\begin{aligned}
\Delta V(E) &= \Delta V(E) - \Delta V(E_F) \\
&= \frac{\mathscr{P}}{\pi} \int_{-\infty}^{\infty} W(E') \left(\frac{1}{E' - E} - \frac{1}{E' - E_F} \right) dE' \\
&= \frac{E - E_F}{\pi} \int_{-\infty}^{\infty} \frac{W(E')}{(E' - E)(E' - E_F)} dE'.
\end{aligned} \tag{10.30}
$$

For the Hartree-Fock term we adopt the usual form for $V_V(E)$ given in Eq. (10.7). The dispersion integrals for the functions for absorption can be calculated analytically and are included as options in ECIS-06. This makes the use of a dispersive optical model parameterization completely equivalent to that of a non-dispersive OMP: the dispersive contributions are calculated automatically once the OMP parameters are given. Upon comparison with a nondispersive parameterization, we find that v_1 is rather different (as expected) and that r_V, a_V, v_2, v_3, w_1 and w_2 are slightly different. We have included dispersive spherical neutron OMP parameterization for about 70 nuclides (unpublished). They can be used with the keyword **dispersion y** (p. 498).

Sample case 10.1 **Different optical models : n + ^{120}Sn**

To demonstrate the variety of optical models that we have added to TALYS, we include a sample case in which 4 OMP's for neutrons on ^{120}Sn are compared. The results are given in Fig. 10.1 for the total cross section and in Fig.10.2 for the total inelastic cross section.

Case a: Koning-Delaroche local potential

The input file is

```
#
# n-Sn120-omp-KD03
#
# General
#
projectile n
element    sn
mass       120
energy     energies
outbasic y
```

This is the default calculation: TALYS will find a local OMP in the structure database and will use it.

Case b: Koning-Delaroche global potential

The input file is

```
#
# n-Sn120-omp-KD03global
#
# General
#
projectile n
element    sn
mass       120
energy     energies
#
# Parameters
#
localomp n
```

Case c: Koning-Delaroche local dispersive potential

The input file is

```
#
# n-Sn120-ompKD03disp
#
# General
#
```

```
projectile n
element    sn
mass       120
energy     energies
#
# Parameters
#
dispersion y
```

Case d: Bauge-Delaroche JLM potential

The input file is

```
#
# n-Sn120-omp-JLM
#
# General
#
projectile n
element    sn
mass       120
energy     energies
#
# Parameters
#
jlmomp y
```

◾

10.3 Spherical OMP: Complex particles

For deuterons, tritons, Helium-3 and alpha particles, we use a simplification of the folding approach of Watanabe [63], see Madland [64]. We take the nucleon OMPs described in the previous section, either local or global, as the basis for these complex particle potentials.

10.3.1 Deuterons

For deuterons, the real central potential depth at incident energy E is

$$V_V^{deuteron}(E) = V_V^{neutron}(E/2) + V_V^{proton}(E/2), \tag{10.31}$$

and similarly for W_V and W_D. For the spin-orbit potential depth we have

$$V_{SO}^{deuteron}(E) = (V_{SO}^{neutron}(E) + V_{SO}^{proton}(E))/2, \tag{10.32}$$

and similarly for W_{SO}. For the radius and diffuseness parameter of the real central potential we have

$$
\begin{aligned}
r_V^{deuteron} &= (r_V^{neutron} + r_V^{proton})/2, \\
a_V^{deuteron} &= (a_V^{neutron} + a_V^{proton})/2,
\end{aligned} \tag{10.33}
$$

and similarly for the geometry parameters of the other potentials.
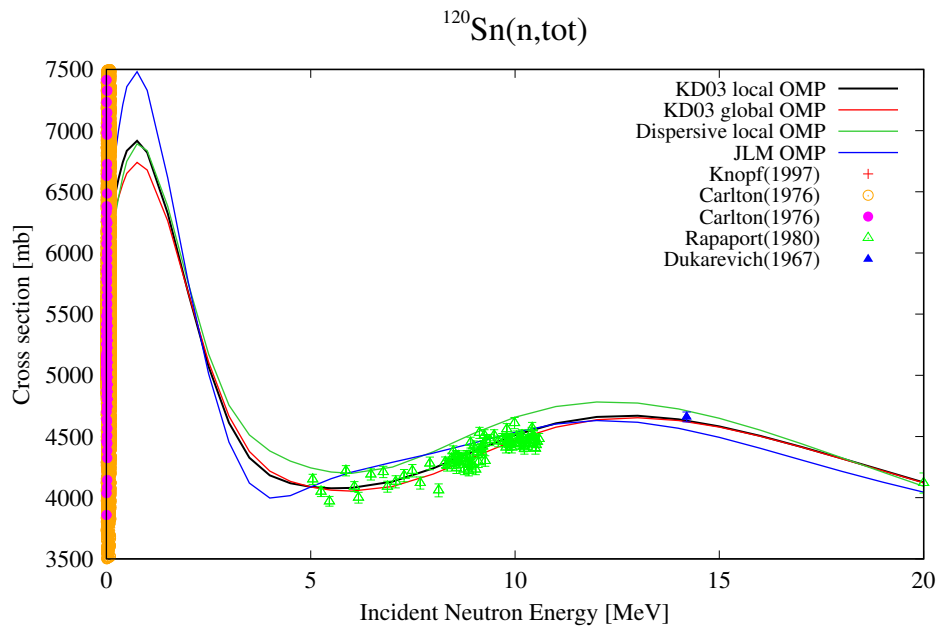
Figure 10.1: Total cross section for neutrons incident on ^{120}Sn for different optical model potentials.
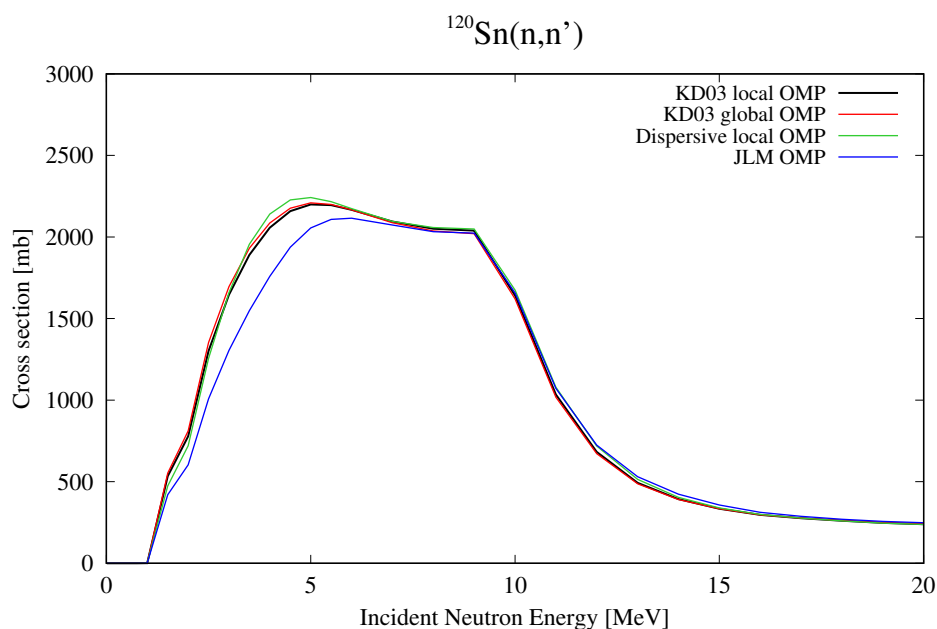
Figure 10.2: Total inelastic cross section for neutrons incident on ^{120}Sn for different optical model potentials.

Note that several of these formulae are somewhat more general than necessary, since the nucleon potentials mostly have geometry parameters, and also potential depths such as V_{SO}, which are equal for neutrons and protons (a_D is an exception). The general formulae above have been implemented to also account for other potentials, if necessary.

We are well aware of the fact that others have constructed specific potentials for deuterons that may outperform the Watanabe-type potential described here. Therefore, we have also added the deuteron potentials of Daehnick et al. [65], Bojowald et al. [66], Han et al. [67], and Haixia An et al. [68] as options.

10.3.2 Tritons

For tritons, the real central potential depth at incident energy E is

$$V_V^{triton}(E) = 2V_V^{neutron}(E/3) + V_V^{proton}(E/3), \tag{10.34}$$

and similarly for W_V and W_D. For the spin-orbit potential depth we have

$$V_{SO}^{triton}(E) = (V_{SO}^{neutron}(E) + V_{SO}^{proton}(E))/6, \tag{10.35}$$

and similarly for W_{SO}. For the radius and diffuseness parameter of the real central potential we have

$$\begin{aligned} r_V^{triton} &= (2r_V^{neutron} + r_V^{proton})/3, \\ a_V^{triton} &= (2a_V^{neutron} + a_V^{proton})/3, \end{aligned} \tag{10.36}$$

and similarly for the geometry parameters of the other potentials.

10.3.3 Helium-3

For Helium-3, the real central potential depth at incident energy E is

$$V_V^{Helium-3}(E) = V_V^{neutron}(E/3) + 2V_V^{proton}(E/3), \tag{10.37}$$

and similarly for W_V and W_D. For the spin-orbit potential depth we have

$$V_{SO}^{Helium-3}(E) = (V_{SO}^{neutron}(E) + V_{SO}^{proton}(E))/6, \tag{10.38}$$

and similarly for W_{SO}. For the radius and diffuseness parameter of the real central potential we have

$$\begin{aligned} r_V^{Helium-3} &= (r_V^{neutron} + 2r_V^{proton})/3, \\ a_V^{Helium-3} &= (a_V^{neutron} + 2a_V^{proton})/3, \end{aligned} \tag{10.39}$$

and similarly for the geometry parameters of the other potentials.

10.3.4 Alpha particles

For alpha's, the real central potential depth at incident energy E is

$$V_V^{alphas}(E) = 2V_V^{neutron}(E/4) + 2V_V^{proton}(E/4), \tag{10.40}$$

and similarly for W_V and W_D. For the spin-orbit potential depth we have

$$V_{SO}^{alphas}(E) = W_{SO}^{alphas}(E) = 0. \tag{10.41}$$

For the radius and diffuseness parameter of the real central potential we have

$$
\begin{aligned}
r_V^{alphas} &= (r_V^{neutron} + r_V^{proton})/2, \\
a_V^{alphas} &= (a_V^{neutron} + a_V^{proton})/2,
\end{aligned}
\tag{10.42}
$$

and similarly for the geometry parameters of the other potentials.

As extra options the alpha potentials by McFadden and Satchler[69] and Demetriou et al [70] are available.

All optical model parameters for complex particles can be altered via adjustable parameters through the **v1adjust** (p. 472) etc. keywords, with which the standard values can be multiplied. Also local energy-dependent adjustment of the geometry is possible as a last resort to fit data.

Options 10.3.1 All phenomenological optical model parameters mentioned in this Chapter can be adjusted. The keywords **rvadjust** (p. 470), **avadjust** (p. 471), **v1adjust** (p. 472), **v2adjust** (p. 473), **v3adjust** (p. 474), **v4adjust** (p. 475), **rwadjust** (p. 476), **awadjust** (p. 477), **w1adjust** (p. 478), **w2adjust** (p. 479), **w3adjust** (p. 480), **w4adjust** (p. 481), **rvdadjust** (p. 482), **avdadjust** (p. 483), **rwdadjust** (p. 484), **awdadjust** (p. 485), **d1adjust** (p. 486), **d2adjust** (p. 487), **d3adjust** (p. 488), **rvsoadjust** (p. 493), **vso1adjust** (p. 489), **vso2adjust** (p. 490), **rwsoadjust** (p. 495), **awsoadjust** (p. 496), **wso1adjust** (p. 491), **wso2adjust** (p. 492), **rcadjust** (p. 497), are available to adjust the standard values that are built-in or given in the input. Dispersive OMP's can be invoked with **dispersion** (p. 498), one can switch between local and global OMP's with **localomp** (p. 499), and distinguish between incident and outgoing channel with **incadjust** (p. 518). As for most parameters, even energy-dependent adjustment of the geometry is possible as a last resort to fit data. Extensions to 1 GeV can be steered with **Vinfadjust** (p. 517) and **Ejoin** (p. 516). One may also provide a particular table of parameters for the KD03 potential by means of the keywords for local parameter files **optmod** (p. 520), **optmodfileN** (p. 521) and **optmodfileP** (p. 522). A full tabulated OMP file can be provided with **ompenergyfile** (p. 335).

Implementation 10.3.1 The optical model parameters are stored in the *talys/structure/optical/* directory. All the parameters are based on one and the same functional form, see Section 10. There are two subdirectories: *neutron/* and *proton/*. For each isotope, optical potential parameters can be given. Per isotope, we have stored *Z*, *A*, number of different optical potentials (2), character to determine coupled-channels potential, nuclear symbol with the format (3i4,3x,a1,58x,i4,a2). On the next line we read the OMP index (1: non-dispersive, 2: dispersive). Fermi energy and reduced Coulomb radius with the format (i4,f7.2,f8.3). On the next 3 lines we read the optical model parameters as defined in Section 10 with the following format

```
(2f8.3,f6.1,f10.4,f9.6,f6.1,f7.1) rv,av,v1,v2,v3,w1,w2
(2f8.3,f6.1,f10.4,f7.2) rvd,avd,d1,d2,d3
(2f8.3,f6.1,f10.4,f7.2,f6.1) rvso,avso,vso1,vso2,wso1,wso2
```

For neutrons, a dispersive potential may also be available. (These potentials have not (yet) been unpublished). In that case, another block of data is given per isotope, but now with an OMP index equal to 2, to denote the parameters for a dispersive potential. As an example, here are the parameters for the Fe-isotopes from *neutron/n-Fe.omp*.

```
 26   54    2                                                    54Fe
  1 -11.34   0.000
  1.186   0.663  58.2     0.0071 0.000019  13.2    78.0
```

```
   1.278    0.536   15.4     0.0223  10.90
   1.000    0.580    6.1     0.0040  -3.1  160.0
   2 -11.34   0.000
   1.215    0.670   54.2     0.0077 0.000022   9.5    88.0
   1.278    0.536   15.4     0.0223  10.90
   1.000    0.580    6.1     0.0040  -3.1  160.0
  26  56    2                                                    56Fe
   1  -9.42   0.000
   1.186    0.663   56.8     0.0071 0.000019  13.0    80.0
   1.282    0.532   15.3     0.0211  10.90
   1.000    0.580    6.1     0.0040  -3.1  160.0
   2  -9.42   0.000
   1.212    0.670   53.2     0.0079 0.000023  10.0    88.0
   1.282    0.532   15.3     0.0211  10.90
   1.000    0.580    6.1     0.0040  -3.1  160.0
```

Sample case 10.2 **Different alpha-particle optical model potentials: alpha + ^{165}Ho**
To demonstrate the variety of (spherical) optical model potentials for alpha-particles available in
TALYS, we include a sample case in which 4 OMPs for alpha-particles on ^{165}Ho are compared.
The results are given in Fig. 10.3 for the (α,n) reaction cross sections within the incident-energy
range of most recent measured data [71] below the Coulomb barrier.

Case a: Watanabe folding approach with Koning-Delaroche nucleon potentials
The input file is

```
#
# a-Ho165-omp1
#
# General
#
projectile a
element Ho
mass 165
energy energies
#
# Model
#
alphaomp 1
#
# Output
#
outomp y
```

where the file energies consists of energies between 7 and 15.5 MeV with 0.5 MeV energy
steps, corresponding to the energy range of the measured data. This is the default calculation.
Fig. 10.3 displays the resulting (α,n) reaction cross sections for the target nucleus 165Ho, as
obtained in the file rp069168.tot.

Case b: McFadden-Satchler (21) potential

The input file, using the alphaomp keyword value of 2, is

```
#
# a-Ho165-omp2
#
# General
#
projectile a
element Ho
mass 165
energy energies
#
# Model
#
alphaomp 2
#
# Output
#
outomp y
```

Case c: Demetriou, Grama and Goriely (70) double folding dispersive potential

The input file, using the alphaomp keyword value of 5, is

```
#
# a-Ho165-omp5
#
# General
#
projectile a
element Ho
mass 165
energy energies
#
# Model
#
alphaomp 5
#
# Output
#
outomp y
```

Case d: Avrigeanu et al. (72) potential

The input file, using the alphaomp keyword additional value of 6, is

^{165}Ho(α,n)^{168}Tm
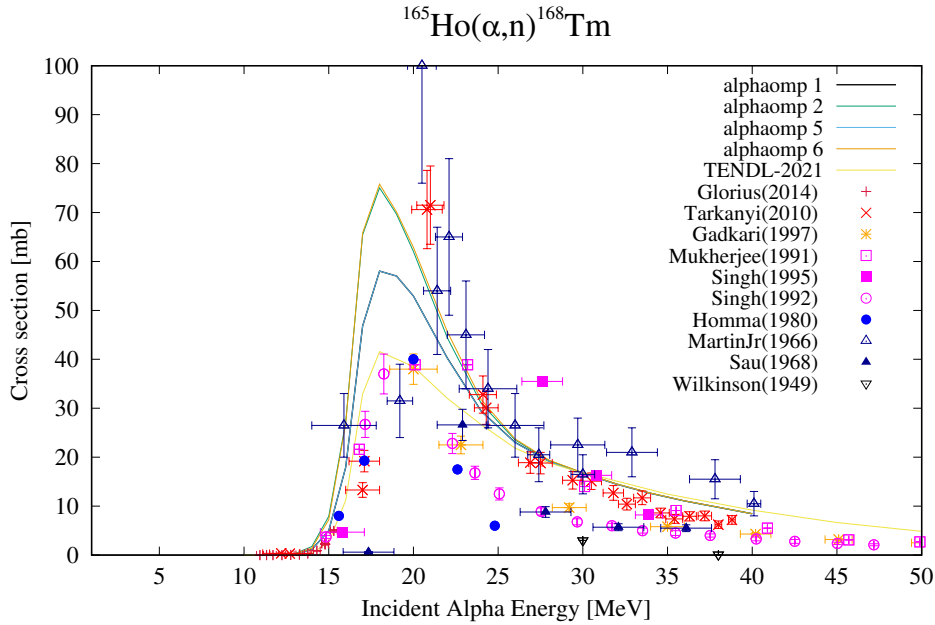
Figure 10.3: ^{165}Ho(α,n)^{168}Tm reaction cross sections for different OMP's.

```
#
# a-Ho165-omp6
#
# General
#
projectile a
element Ho
mass 165
energy energies
#
# Model
#
alphaomp 6
#
# Output
#
outomp y
```

where the file energies consists in addition of energies up to 33 MeV corresponding to all
energy ranges which are considered in Table II of Ref. [72]. ■

10.4 Semi-microscopic optical model (JLM)

Besides the phenomenological OMP, it is also possible to perform TALYS calculations with the
semi-microscopic nucleon-nucleus spherical optical model potential as described by Bauge et
al. [73]. We have implemented Eric Bauge's MOM code [6] as a subroutine to perform so called

Jeukenne-Lejeune-Mahaux (JLM) OMP calculations. The optical model potential of Bauge et al. [73] and its extension to deformed and unstable nuclei has been widely tested [73, 74, 75, 76, 77] and produces predictions from A=30 to 240 and for energies ranging from 10 keV up to 200 MeV. MOM stands for "Modèle Optique Microscopique" in French, or "Microscopic Optical Model" in English. In this version of TALYS, only spherical JLM OMP's are included.

The MOM module reads the radial matter densities from the nuclear structure database and performs the folding of the Nuclear Matter (NM) optical model potential described by Bauge et al. [73] with the densities to obtain a local OMP. This is then put in the ECIS-06 routine to compute observables by solving the Schrödinger equation for the interaction of the projectile with the aforementioned OMP. The OMP's are calculated by folding the target radial matter density with an OMP in nuclear matter based on the Brückner-Hartree-Fock work of Jeukenne, Lejeune and Mahaux [78, 79, 80, 81]. This NM OMP was then phenomenologically altered by Bauge et al. [73, 82] in order to improve the agreement of predicted finite nuclei observables with a large set of experimental data. These improvements consist in unifying the low and high energy parameterizations of the NM interaction in [82], and in studying the energy variations of the potential depth normalization factors [73]. These factors now include non-negligible normalizations of isovector components [73] that are needed in order to account simultaneously for (p,p) and (n,n) elastic scattering as well as (p,n)$_{IAS}$ quasi-elastic scattering. The final NM potential for a given nuclear matter density $\rho = \rho_n - \rho_p$ and asymmetry $\alpha = (\rho_n + \rho_p)/\rho$ reads

$$
\begin{aligned}
U_{NM}(E)_{\rho,\alpha} = \quad & \lambda_V(E)\left[V_0(\tilde{E}) \pm \lambda_{V1}(E)\alpha V_1(\tilde{E})\right] \\
+ \quad & i\lambda_W(E)\left[W_0(\tilde{E}) \pm \lambda_{W1}(E)\alpha W_1(\tilde{E})\right],
\end{aligned}
\tag{10.43}
$$

with E the incident nucleon energy, $\tilde{E} = E - V_c$ (where V_c is the Coulomb field), V_0, V_1, W_0, and W_1 the real isoscalar, real isovector, imaginary isoscalar, and imaginary isovector NM OMP components respectively, and λ_V, λ_{V1}, λ_W, and λ_{W1} the real (isoscalar+isovector), real isovector, imaginary, and imaginary isovector normalization factors respectively. The values of λ_V, λ_{V1}, λ_W, and λ_{W1} given in [73] read

$$
\lambda_V(E) = 0.951 + 0.0008\,\ln(1000E) + 0.00018\,[\ln(1000E)]^2
\tag{10.44}
$$

$$
\begin{aligned}
\lambda_W(E) = \quad & \left[1.24 - \left[1 + e^{\left(\frac{E-4.5}{2.9}\right)}\right]^{-1}\right]\left[1 + 0.06\,e^{-\left(\frac{E-14}{3.7}\right)^2}\right] \\
\times \quad & \left[1 - 0.09\,e^{-\left(\frac{E-80}{78}\right)^2}\right]\left[1 + \left(\frac{E-80}{400}\right)\Theta(E-80)\right]
\end{aligned}
\tag{10.45}
$$

$$
\lambda_{V1}(E) = 1.5 - 0.65\left[1 + e^{\frac{E-1.3}{3}}\right]^{-1}
\tag{10.46}
$$

$$
\begin{aligned}
\lambda_{W1}(E) = \quad & \left[1.1 + 0.44\left[1 + \left(e^{\frac{E-40}{50.9}}\right)^4\right]^{-1}\right] \\
\times \quad & \left[1 - 0.065\,e^{-\left(\frac{E-40}{13}\right)^2}\right]\left[1 - 0.083\,e^{-\left(\frac{E-200}{80}\right)^2}\right].
\end{aligned}
\tag{10.47}
$$

with the energy E expressed in MeV. As stated in [73], in the 20 to 50 MeV range, the uncertainties related to λ_V, λ_{V1}, λ_W, and λ_{W1} are estimated to be 1.5%, 10%, 10%, and 10%, respectively. Outside this energy range, uncertainties are estimated to be 1.5 times larger.

In order to apply the NM OMP to finite nuclei an approximation had to be performed. This is the Local Density Approximation (LDA) where the local value of the finite nucleus OMP is taken to be the NM OMP value for the local finite nucleus density: $U_{FN}(r) = U_{NM}(\rho(r))$. Since this LDA produces potentials with too small rms radii, the improved LDA, which broadens the OMP with a Gaussian form factor (10.48), is introduced. In [82, 73] different prescriptions for the improved Local Density approximation are compared and LDA range parameters are optimized.

$$U_{FN}(r,E) = (t\sqrt{\pi})^{-3} \int \frac{U_{NM}(\rho(r'),E)}{\rho(r')} \exp(-|\vec{r}-\vec{r}'|^2/t_r^2)\rho(r')d\vec{r'}, \tag{10.48}$$

with t the range of the Gaussian form factor. The $t_r = 1.25$ fm and $t_i = 1.35$ fm values were found [73] to be global optimal values for the real and imaginary ranges, respectively.

Finally, since no spin-orbit (SO) potential exists between a nucleon and NM, the Scheerbaum [83] prescription was selected in [82], coupled with the phenomenological complex potential depths $\lambda_{v_{so}}$, and $\lambda_{w_{so}}$. The SO potential reads

$$U_{n(p)}^{so}(r) = (\lambda_{v_{so}}(E) + i\lambda_{v_{so}}(E)) \frac{1}{r}\frac{d}{dr}\left(\frac{2}{3}\rho_{p(n)} + \frac{1}{3}\rho_{n(p)}\right), \tag{10.49}$$

with

$$\lambda_{v_{so}} = 130\exp(-0.013E) + 40 \tag{10.50}$$

and

$$\lambda_{w_{so}} = -0.2(E - 20). \tag{10.51}$$

All JLM OMP parameters can be altered via adjustable parameters through the **lvadjust**, **lwadjust** etc. keywords, with which the standard values can be multiplied.

Options 10.4.1 Choices for JLM-based OMP's are available with **jlmomp** (p. 506) and **jlmmode** (p. 507),**radialfile** (p. 515), **radialmodel** (p. 514), and the associated parameters **lvadjust** (p. 508), **lwadjust** (p. 509), **lv1adjust** (p. 510), **lw1adjust** (p. 511), **lvsoadjust** (p. 512), **lwsoadjust** (p. 513). with which the standard values can be multiplied. For alpha particle OMP's, the **alphaomp** (p. 501), **adepthcor** (p. 503) and **aradialcor** (p. 502) keywords are available, and for deuteron OMP's **deuteronomp** (p. 500).

Implementation 10.4.1 For the calculation of the JLM OMP, both Stephane Goriely and Stephane Hilaire have provided radial matter densities from dripline to dripline. They are stored in *talys/structure/optical/jlm/*. As an example, below are the data of some of the Fe-isotopes as given in file *talys/structure/optical/jlm/goriely/Fe.rad*. First we give Z, A, number of radii (lines), incremental step between radii, all in fm, with the format (2i4,i5,f7.3). Next we give the radius, and the radial densities for different deformations, first for protons and then for neutrons, with the format (f8.3,10(e12.5)),

```
 26   56   200   0.100
  0.100 8.04162E-02 0.00000E+00 0.00000E+00 0.00000E+00 0.00000E+00 9.06018E-02
  0.200 8.02269E-02 0.00000E+00 0.00000E+00 0.00000E+00 0.00000E+00 9.05443E-02
```

```
    0.300 7.98895E-02 0.00000E+00 0.00000E+00 0.00000E+00 0.00000E+00 9.04407E-02
    0.400 7.94588E-02 0.00000E+00 0.00000E+00 0.00000E+00 0.00000E+00 9.03063E-02
    0.500 7.89124E-02 0.00000E+00 0.00000E+00 0.00000E+00 0.00000E+00 9.01315E-02
```

Note that only the spherical components in this database are non-zero. In the files of Hilaire, see *talys/structure/optical/jlm/hilaire/*, there are also deformed components, but they will only become relevant when deformed JLM calculations are included in TALYS.

10.5 Systematics for non-elastic cross sections

Since the reaction cross sections for complex particles as predicted by the OMP have not been tested and rely on a relatively simple folding model, we added a possibility to estimate the non-elastic cross sections from empirical expressions. The adopted *tripathi.f* subroutine that provides this does not coincide with the published expression as given by Tripathi et al. [84], but checking our results with the published figures of Ref. [84] made us decide to adopt this empirical model as an option. We sometimes use it for deuterons up to alpha-particles. A high-quality OMP for complex particles would make this option redundant.

Sample case 10.3 **Local parameter adjustment for n + ^{93}Nb**

```
#
# n-Nb093-adjust
#
# General
#
projectile n
element nb
mass 93
energy 0.2 5. 0.2
outomp y
#
# Local parameter adjustment
#
rvadjust n 1.02 1. 3. 2. 1.10
avadjust n 1.02 1. 3. 2. 0.95


 ######### OPTICAL MODEL PARAMETERS ##########

          neutron  on  93Nb

  Energy    V     rv    av    W     rw    aw    Vd   rvd   avd    Wd   rwd

   0.001  51.02 1.239 0.676  0.14 1.239 0.676  0.00 1.274 0.534  3.32 1.274
   0.002  51.02 1.239 0.676  0.14 1.239 0.676  0.00 1.274 0.534  3.32 1.274
...................
   0.910  50.69 1.239 0.676  0.17 1.239 0.676  0.00 1.274 0.534  3.80 1.274
   1.011  50.66 1.239 0.676  0.18 1.239 0.676  0.00 1.274 0.534  3.85 1.274
```

```
   1.112   50.62 1.240 0.676   0.18 1.239 0.676   0.00 1.274 0.534   3.90 1.274
   1.213   50.58 1.244 0.675   0.18 1.239 0.676   0.00 1.274 0.534   3.95 1.274
   1.314   50.55 1.257 0.671   0.19 1.239 0.676   0.00 1.274 0.534   4.00 1.274
   1.415   50.51 1.282 0.665   0.19 1.239 0.676   0.00 1.274 0.534   4.05 1.274
   1.516   50.47 1.309 0.657   0.20 1.239 0.676   0.00 1.274 0.534   4.10 1.274
   1.617   50.44 1.331 0.651   0.20 1.239 0.676   0.00 1.274 0.534   4.15 1.274
   1.718   50.40 1.346 0.647   0.20 1.239 0.676   0.00 1.274 0.534   4.20 1.274
   1.820   50.37 1.355 0.645   0.21 1.239 0.676   0.00 1.274 0.534   4.24 1.274
   1.921   50.33 1.360 0.643   0.21 1.239 0.676   0.00 1.274 0.534   4.29 1.274
   2.022   50.29 1.363 0.643   0.22 1.239 0.676   0.00 1.274 0.534   4.34 1.274
   2.224   50.22 1.352 0.646   0.22 1.239 0.676   0.00 1.274 0.534   4.43 1.274
   2.426   50.15 1.323 0.653   0.23 1.239 0.676   0.00 1.274 0.534   4.52 1.274
   2.628   50.08 1.270 0.668   0.24 1.239 0.676   0.00 1.274 0.534   4.61 1.274
   2.830   50.00 1.241 0.676   0.25 1.239 0.676   0.00 1.274 0.534   4.70 1.274
   3.033   49.93 1.239 0.676   0.26 1.239 0.676   0.00 1.274 0.534   4.78 1.274
   3.235   49.86 1.239 0.676   0.27 1.239 0.676   0.00 1.274 0.534   4.86 1.274
   3.437   49.79 1.239 0.676   0.28 1.239 0.676   0.00 1.274 0.534   4.95 1.274
.....................
```

Note that outside 1 and 3 MeV both rv and av have their constant values while in between these energies the parameters vary according to the prescription given in Section 3.2.1.   ■

11. Direct reactions

Various models for direct reactions are included in the program: DWBA for (near-)spherical nuclides, coupled-channels for deformed nuclides, the weak-coupling model for odd nuclei, and also a giant resonance contribution in the continuum. In all cases, TALYS drives the ECIS-06 code to perform the calculations. The results are presented as discrete state cross sections and angular distributions, or as contributions to the continuum.

11.1 Deformed nuclei: Coupled-channels

The formalism outlined in the OMP Chapter works, theoretically, for nuclides which are spherical and, in practice, for nuclides which are not too strongly deformed. In general, however, the more general coupled-channels method should be invoked to describe simultaneously the elastic scattering channel and the low-lying states which are, due to their collective nature, strongly excited by inelastic scattering. These collective excitations can be described as the result of static or dynamic deformations, which cause the homogeneous neutron-proton fluid to rotate or vibrate. The associated deformation parameters can be predicted from a (semi-)microscopic model or can be derived from an analysis of the experimental angular distributions.

The coupled-channels formalism for scattering and reaction studies is well known and will not be described in this manual. For a detailed presentation, we refer to Tamura [85]. We will only state the main aspects here to put the formalism into practice. Delaroche et al. [86] and Olsson et al.[87] have been used as guidance, as these papers explain clearly how to translate collective effects of various nuclides into ECIS calculations. In general various different channels, usually the ground state and several inelastic states, are included in a coupling scheme while the associated coupled equations are solved. In ECIS-06, this is done in a so called sequential iterative approach by Raynal [5]. Besides Ref. [5], Carlsson's lecture [88] is also recommended for more insight in the use of the ECIS code.

Various collective models for deformed nuclei exist. Note that the spherical optical model of Eq. (10.2) is described in terms of the nuclear radius $R_i = r_i A^{1/3}$. For deformed nuclei, this expression is generalized to include collective motions. Various models have been implemented in ECIS-06, which enables us to cover many nuclides of interest. We will describe the ones that can be invoked by TALYS. The collective models are automatically applied upon reading the deformation parameter database, see Section 7.2.

11.1.1 Symmetric rotational model

In the symmetric rotational model, the radii of the different terms of the OMP are expressed as

$$R_i = r_i A^{1/3} \left[1 + \sum_{\lambda=2,4,\dots} \beta_\lambda Y_\lambda^0(\Omega) \right], \tag{11.1}$$

where the β_λ's are permanent, static deformation parameters, and the Y functions are spherical harmonics. The quadrupole deformation β_2 plays a leading role in the interaction process. Higher order deformations β_λ (with $\lambda = 4,6,\dots$) are systematically smaller in magnitude than β_2. The inclusion of β_4 and β_6 deformations in coupled-channels calculations produces changes in the predicted observables, but in general, only β_2 and β_4 are important in describing inelastic scattering to the first few levels in a rotational band. For even-even nuclides like ^{184}W and ^{232}Th, the symmetric rotational model provides a good description of the lowest $0^+, 2^+, 4^+$ (and often $6^+, 8+$, etc.) rotational band. The nuclear model and parameter database of TALYS specifies whether a rotational model can be used for a particular nucleus, together with the included levels and deformation parameters. Either a deformation parameter β_λ or a deformation length $\delta_\lambda = \beta_\lambda r_i A^{1/3}$ may be given. The latter one is generally recommended since it has more physical meaning than β_λ and should not depend on incident energy (while r_i may, in some optical models, depend on energy). We take δ_λ equal for the three OMP components V_V, W_V and W_D and take the spin-orbit potential undeformed. The same holds for the vibrational and other collective models.

By default, TALYS uses the global optical model by Soukhovitskii et al. [89] for actinides. For rotational non-fissile nuclides, if no specific potential is specified through one of the various input methods, we take our local or global spherical potential and subtract 15% from the imaginary surface potential parameter d_1, if rotational or vibrational levels are included in the coupling scheme.

11.1.2 Harmonic vibrational model

A vibrational nucleus possesses a spherically symmetric ground state. Its excited states undergo shape oscillations about the spherical equilibrium model. In the harmonic vibrational model, the radii of the different terms of the OMP are expressed as

$$R_i = r_i A^{1/3} \left[1 + \sum_{\lambda\mu} \alpha_{\lambda\mu} Y_\lambda^\mu(\Omega) \right], \tag{11.2}$$

where the $\alpha_{\lambda\mu}$ operators can be related to the coupling strengths β_λ, describing the vibration amplitude with multipolarity λ. Expanding the OMP to first or second order with this radius gives the OMP expressions for the excitation of one-phonon (first order vibrational model) and two-phonon (second order vibrational model) states [5]. For vibrational nuclei, the minimum number of states to couple is two. For even-even nuclei, we generally use the $(0^+, 2^+)$ coupling, where the 2^+ level is a one-quadrupole phonon excitation. The level scheme of a vibrational nucleus (e.g. ^{110}Pd)

often consists of a one-phonon state (2^+) followed by a $(0^+, 2^+, 4^+)$ triplet of two-phonon states. When this occurs, all levels are included in the coupling scheme with the associated deformation length δ_2 (or deformation parameter β_2). If the 3^- and 5^- states are strongly collective excitations, that is when β_3 and β_5 are larger than 0.1, these levels may also be included in the coupling scheme. An example is ^{120}Sn [90], where the low lying $(0^+, 2^+, 3^-, 4^+, 5^-)$ states can all be included as one-phonon states in a single coupling scheme.

Again, if no specific potential is specified through one of the various input methods, we take our local or global spherical potential and subtract 15% from the imaginary surface potential parameter d_1.

11.1.3 Vibration-rotational model

For certain nuclides, the level scheme consists not only of one or more rotational bands, but also of one or more vibrational bands that can be included in the coupling scheme. An example is ^{238}U, where many vibrational bands can be coupled. In Chapter 5 on discrete level information, it is explained how such calculations are automatically performed by TALYS. Depending on the number of levels included, the calculations can be time-consuming.

11.1.4 Asymmetric rotational model

In the asymmetric rotational model, in addition to the spheroidal equilibrium deformation, the nucleus can oscillate such that ellipsoidal shapes are produced. In this model the nucleus has rotational bands built on the statically deformed ground state and on the γ-vibrational state. The radius is now angular dependent,

$$R_i(\Theta) = r_i A^{1/3} \left[1 + \beta_2 \cos \gamma Y_2^0(\Omega) + \sqrt{\frac{1}{2}} \beta_2 \sin \gamma (Y_2^2(\Omega) + Y_2^{-2}(\Omega)) + \beta_4 Y_4^0(\Omega) \right], \quad (11.3)$$

where we restrict ourselves to a few terms. The deformation parameters β_2, β_4 and γ need to be specified. ^{24}Mg is an example of a nucleus that can be analyzed with the asymmetric rotational model. Mixing between bands is not yet automated as an option in TALYS.

> **Options 11.1.1** With **rotational** (p. 543) it is possible to disable a coupled-channel calculation for certain particles. With **autorot** (p. 551, TALYS looks for a coupled levels scheme in its database and automatically starts a coupled channels calculation. Coupled-channels calculations can be disabled with **spherical** (p. 542) Since coupled-channels calculations can be very time consuming, the keywords **ecissave** (p. 546), **inccalc** (p. 548), **eciscalc** (p. 547), are available to re-use ECIS information from the previous run. The complexity of the coupled-levels scheme can be steered with **maxrot** (p. 549) and **maxband** (p. 550).

> **Sample case 11.1** **Coupled-channels rotational model: n + ^{28}Si**
>
> In this sample case, we consider spherical OMP and rotational coupled-channels calculations for the deformed nucleus ^{28}Si.
>
> **Case a: Spherical optical model**
>
> In the first case, we treat ^{28}Si as a spherical nucleus and include the first (2^+), second (4^+) and sixth (3^-) level as weakly coupled levels, i.e. the cross sections are calculated with DWBA. The input file is

```
#
# n-Si028-cc
#
# General
#
projectile n
element si
mass 28
energy energies
#
# Parameters
#
spherical y
#
# Output
#
channels y
filechannels y
```

For the default calculation, TALYS will look in the *deformation/exp* database to see whether a coupling scheme is given. Since this is the case for ^{28}Si, we have to put **spherical y** to enforce a spherical calculation.

Case b: Symmetric rotational model

In the second case, we include the first and second level of the ground state rotational band and the 3^- state in the coupling scheme. This is accomplished with the input file

```
#
# n-Si028-cc-sym
#
# General
#
projectile n
element si
mass 28
energy energies
#
# Output
#
channels y
filechannels y
```

In Fig. 11.1, the calculated total inelastic scattering for cases a and b are plotted. ■

Sample case 11.2 **Coupled-channels vibrational model: n + ^{74}Ge**
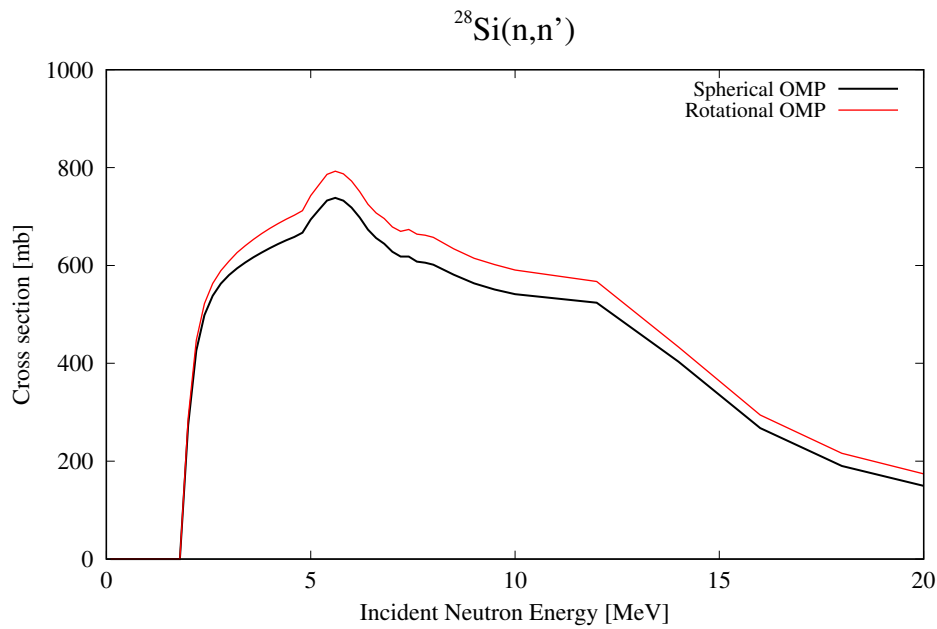
Figure 11.1: Total inelastic neutron scattering off ^{28}Si for a spherical and a deformed OMP.

In this sample case we consider a neutron-induced reaction on the vibrational nucleus ^{74}Ge which consists of a one-phonon state (2^+) followed by a $(0^+, 2^+, 4^+)$ triplet of two-phonon states, and a 3^- phonon state. The coupling scheme as stored in *structure/deformation/exp/z032* is automatically adopted. The following input file is used:

```
#
# n-Ge074-vib
#
# General
#
projectile n
element ge
mass 74
energy energies
#
# Output
#
outexcitation n
outdiscrete y
filediscrete 1
```

In Fig. 11.2, the calculated inelastic scattering to the first discrete state is plotted. ∎
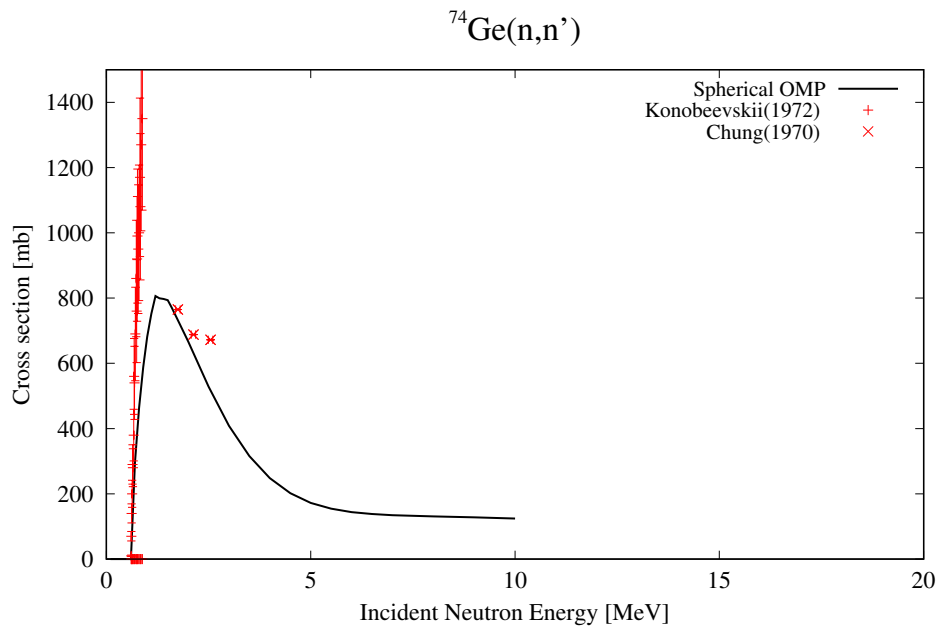
Figure 11.2: Inelastic scattering to the first discrete state of ^{74}Ge.

11.2 Distorted Wave Born Approximation

The Distorted Wave Born Approximation (DWBA) is only valid for small deformations. Until the advent of the more general coupled-channels formalism, it was the commonly used method to describe inelastic scattering, for both weakly and strongly coupled levels. Nowadays, we see DWBA as a first order vibrational model for small deformation, with only a single iteration to be performed for the coupled-channels solution. (See, however Satchler [91] for the exact difference between this so called distorted wave method and DWBA). The interaction between the projectile and the target nucleus is modeled by the derivative of the OMP for elastic scattering times a strength parameter. The latter, the deformation parameter β_λ, is then often used to vary the overall magnitude of the cross section (which is proportional to β_λ^2).

In TALYS, we use DWBA

(a) if a deformed OMP is not available. This applies for the spherical OMPs mentioned in the previous Section, which are all based on elastic scattering observables only. Hence, if we have not constructed a coupled-channels potential, TALYS will automatically use (tabulated or systematical) deformation parameters for DWBA calculations.

(b) if a deformed OMP is used for the first excited states only. For the levels that do not belong to that basic coupling scheme, e.g. for the many states at somewhat higher excitation energy, we use DWBA with (very) small deformation parameters.

Options 11.2.1 By default, OMP calculations will take deformation parameters and coupled level schemes into account, but with **spherical** (p. 542) this can be disabled and turned into a spherical OMP calculation.

Sample case 11.3 **Spherical optical model and DWBA: n + ^{208}Pb**

Three types of optical model calculations are included in the set of sample cases. In this first one, we treat ^{208}Pb as a spherical nucleus and request calculations for the elastic angular distributions and inelastic angular distributions at a few incident energies. This is accomplished with the input file

```
#
# n-Pb208-omp
#
# General
#
projectile n
element pb
mass 208
energy energies
#
# Avoid unnecessary calculations and output
#
ejectiles n
preequilibrium n
compound n
maxZ 0
maxN 0
bins 5
fileresidual n
filetotal n
#
# Output
#
outangle y
fileelastic y
fileangle 1
fileangle 2
```

where the file *energies* consists of the energies 11., 13.7, 20., 22., and 25.7 MeV (for which experimental data exists). The keyword *fileelastic y* has created the files *nn011.000ang.L00*, etc. which contain the elastic scattering angular distribution and are compared with experimental data in Fig. 11.3. With **fileangle 1** and **fileangle 2** we have created the files *nn010.000ang.L01*, etc. with the inelastic scattering angular distribution to the first and second discrete state. These are also plotted in Figs. 11.3. Note that the keywords in the middle block (**ejectiles n** up to **filetotal n**) have been added to avoid a full calculation of all the cross sections. For the present sample case we assume that only elastic scattering and DWBA angular distributions are of interest, so we economize on output options, number of bins, ejectiles and nuclides that can be reached. Obviously, for reliable results for all observables this middle block would have to be deleted. See also sample case (1f) for obtaining more specific information from the output.
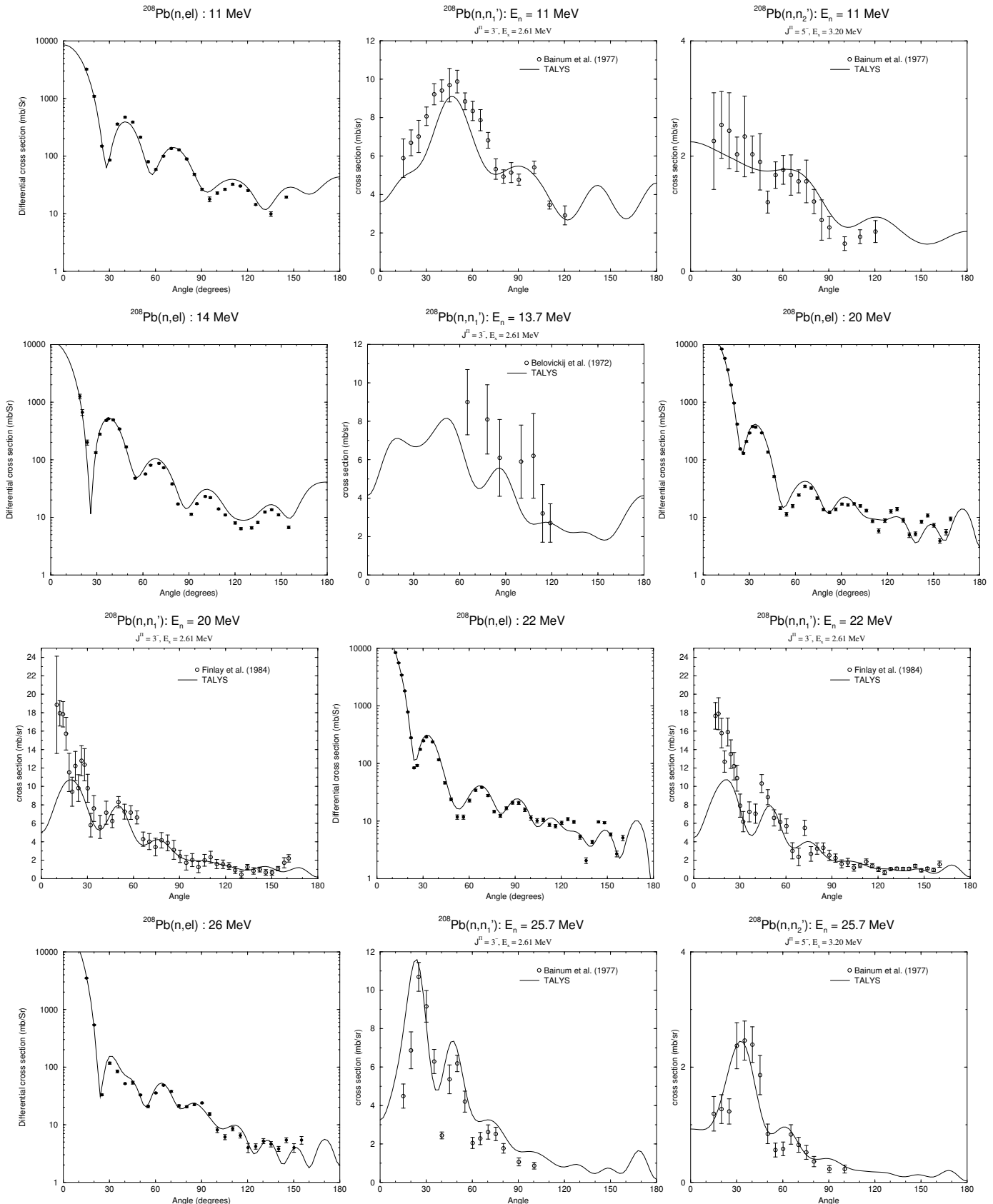
Figure 11.3: Elastic and inelastic scattering angular distributions between 11 and 26 MeV for ^{208}Pb.

11.3 Odd nuclei: Weak coupling

Direct inelastic scattering off odd-A nuclei can be described by the weak-coupling model [92], which assumes that a valence particle or hole interacts only weakly with a collective core excitation. Hence the model implies that the nucleon inelastic scattering by the odd-A nucleus is very similar to that by the even core alone, i.e. the angular distributions have a similar shape. Let L be the spin of the even core state, and J_0 and J the spin of the ground and excited state, respectively, of the odd-A nucleus, resulting from the angular momentum coupling. Then, the spins J of the multiplet states in the odd-A nucleus range from $|L - J_0|$ to $(L + J_0)$. If the strength of the inelastic scattering is characterized by the square of the deformation parameters $\beta_{L,J}^2$, then the sum of all $\beta_{L,J}^2$ or $\sigma(E)$ for the transitions in the odd-A nucleus should be equal to the value β_L^2 or $\sigma(E)$ for the single transition in the even core nucleus:

$$\sum_J \beta_{L,J}^2 = \beta_L^2, \quad \sum_J \sigma_{J_0 \to J} = \sigma_{0 \to L}, \tag{11.4}$$

where the symbol $0 \to L$ indicates a transition between the ground state to the excited state with spin L in the even core nucleus. The deformation parameters $\beta_{L,J}^2$ are now given by

$$\beta_{L,J}^2 = \frac{2J + 1}{(2J_0 + 1)(2L + 1)} \beta_L^2. \tag{11.5}$$

In practice, the DWBA cross sections are calculated for the real mass of the target nucleus and at the exact excitation energies of the odd-A states, but for the even-core spin L and with deformation parameters $\beta_{L,J}$.

We stress that our weak-coupling model is not full-proof. First of all, there are always two choices for the even-even core. The default used in TALYS (by means of the keyword **core -1**) is to use the even-even core obtained by subtracting a nucleon, but the other choice (**core 1**), to obtain the even-even core by adding a nucleon, may sometimes be more appropriate. The next uncertainty is the choice of levels in the odd-A core. We select the levels that are closest to the excitation energy of the even-spin state of the even-even core. Again, this may not always be the most appropriate choice. A future option is to designate these levels manually.

> **Options 11.3.1** With **core** (p. 569), one can choose between the $A - 1$ or $A + 1$ nucleus for the even-even core.

> **Implementation 11.3.1** In *weakcoupling.f90* the strength is distributed over the odd-spin levels.

11.4 Giant resonances

The high-energy part of the continuum spectra are generally described by pre-equilibrium models. These models are essentially of a single-particle nature. Upon inspection of continuum spectra, some structure in the high-energy tail is observed that can not be accounted for by the smooth background of the single-particle pre-equilibrium model. For example, many 14 MeV inelastic neutron spectra show a little hump at excitation energies around 6-10 MeV. This structure is due to collective excitations of the nucleus that are known as giant resonances [93, 94]. We use a macroscopic, phenomenological model to describe giant resonances in the inelastic channel. For each multipolarity, an energy weighted sum rule (EWSR) S_ℓ applies,

$$S_\ell = \sum_i E_{\ell,i} \beta_{\ell,i}^2 = 57.5 A^{-5/3} l(2l + 1) \quad \text{MeV}, \tag{11.6}$$

where $E_{\ell,i}$ is the excitation energy of the i-th state with multipolarity ℓ. The summation includes all the low-lying collective states, for each ℓ, that have already been included in the coupled-channels or DWBA formalism. The EWSR thus determines the remaining collective strength that is spread over the continuum. Our treatment is phenomenological in the sense that we perform a DWBA calculation with ECIS-06 for each giant resonance state and spread the cross section over the continuum with a Gaussian distribution. The central excitation energy for these states and the spreading width is different for each multipolarity and has been empirically determined. For the giant monopole resonance (GMR) EWSR we have

$$S_0 = 23A^{-5/3} \text{ MeV}, \tag{11.7}$$

with excitation energy and width

$$E_{0,GMR} = 18.7 - 0.025A \text{ MeV}, \quad \Gamma_{GMR} = 3 \text{ MeV}. \tag{11.8}$$

The EWSR for the giant quadrupole resonance (GQR) is

$$S_2 = 575A^{-5/3} \text{ MeV}, \tag{11.9}$$

with

$$E_{0,GQR} = 65A^{-1/3} \text{ MeV}, \quad \Gamma_{GQR} = 85A^{-2/3} \text{ MeV}. \tag{11.10}$$

The EWSR for the giant octupole resonance is

$$S_3 = 1208A^{-5/3} \text{ MeV}, \tag{11.11}$$

which has a low-energy (LEOR) and a high-energy (HEOR) component. Following Kalbach [94], we assume

$$S_{3,LEOR} = 0.3S_3, \quad S_{3,HEOR} = 0.7S_3, \tag{11.12}$$

with excitation energy and width

$$E_{0,LEOR} = 31A^{-1/3} \text{ MeV}, \quad \Gamma_{LEOR} = 5 \text{ MeV}, \tag{11.13}$$

and

$$E_{0,HEOR} = 115A^{-1/3} \text{ MeV}, \quad \Gamma_{HEOR} = 9.3 - A/48 \text{ MeV}, \tag{11.14}$$

respectively. We also take as width for the actual Gaussian distribution $\Gamma_{Gauss} = 0.42\Gamma_\ell$.

The contribution from giant resonances is automatically included in the total inelastic cross section. The effect is most noticeable in the single- and double-differential energy spectra.

Options 11.4.1 With **giantresonance** (p. 556) we can disable or enable the giant resonance contribution.

Implementation 11.4.1 In *giant.f90* the Giant Resonance contribution is implemented.

12. Pre-equilibrium reactions

It is now well-known that the separation of nuclear reaction mechanisms into direct and compound is too simplistic. As Fig. 4.2 shows, the cross section as predicted by the pure compound process is too small with respect to measured continuum spectra, and the direct processes described in the previous section only excite the discrete levels at the highest outgoing energies. Furthermore, the measured angular distributions in the region between direct and compound are anisotropic, indicating the existence of a memory-preserving, direct-like reaction process. Apparently, as an intermediate between the two extremes, there exists a reaction type that embodies both direct- and compound-like features. These reactions are referred to as *pre-equilibrium, precompound* or, when discussed in a quantum-mechanical context, *multi-step processes*. Pre-equilibrium emission takes place after the first stage of the reaction but long before statistical equilibrium of the compound nucleus is attained. It is imagined that the incident particle step-by-step creates more complex states in the compound system and gradually loses its memory of the initial energy and direction. Pre-equilibrium processes cover a sizable part of the reaction cross section for incident energies between 10 and (at least) 200 MeV. Pre-equilibrium reactions have been modeled both classically and quantum-mechanically and both are included in TALYS.

12.1 Exciton model

In the exciton model (see Refs. [95, 96, 97] for extensive reviews), the nuclear state is characterized at any moment during the reaction by the total energy E^{tot} and the total number of particles above and holes below the Fermi surface. Particles (p) and holes (h) are indiscriminately referred to as excitons. Furthermore, it is assumed that all possible ways of sharing the excitation energy between different particle-hole configurations with the same exciton number $n = p + h$ have equal a-priori probability. To keep track of the evolution of the scattering process, one merely traces the temporal development of the exciton number, which changes in time as a result of intranuclear
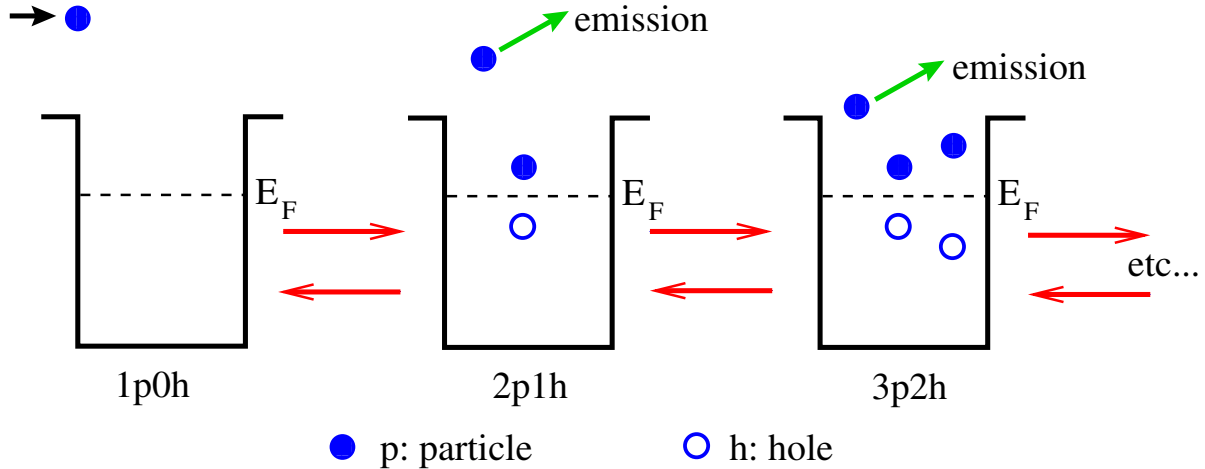
Figure 12.1: Reaction flow in exciton model

two-body collisions. The basic starting point of the exciton model is a time-dependent master equation, which describes the probability of transitions to more and less complex particle-hole states as well as transitions to the continuum (emission). Upon integration over time, the energy-averaged emission spectrum is obtained. These assumptions makes the exciton model amenable for practical calculations. The price to be paid, however, is the introduction of a free parameter, namely the average matrix element of the residual two-body interaction, occurring in the transition rates between two exciton states. When this matrix element is properly parameterized, a very powerful model is obtained.

Qualitatively, the equilibration process of the excited nucleus is imagined to proceed as follows, see Fig. 12.1. After entering the target nucleus, the incident particle collides with one of the nucleons of the Fermi sea, with depth E_F. The formed state with $n = 3$ (2p1h), in the case of a nucleon-induced reaction, is the first that is subject to particle emission, confirming the picture of the exciton model as a compound-like model rather than a direct-like model. Subsequent interactions result in changes in the number of excitons, characterized by $\Delta n = +2$ (a new particle-hole pair) or $\Delta n = -2$ (annihilation of a particle-hole pair) or $\Delta n = 0$ (creation of a different configuration with the same exciton number). In the first stage of the process, corresponding to low exciton numbers, the $\Delta n = +2$ transitions are predominant. Apart from transitions to more complex or less complex exciton states, at any stage there is a non-zero probability that a particle is emitted. Should this happen at an early stage, it is intuitively clear that the emitted particle retains some "memory" of the incident energy and direction: the hypothesis of a fully equilibrated compound nucleus is not valid. This phase is called the pre-equilibrium phase, and it is responsible for the experimentally observed high-energy tails and forward-peaked angular distributions. If emission does not occur at an early stage, the system eventually reaches a (quasi-) equilibrium. The equilibrium situation, corresponding to high exciton numbers, is established after a large number of interactions, i.e. after a long lapse of time, and the system has "forgotten" about the initial state. Accordingly, this stage may be called the compound or evaporation stage. Hence, in principle the exciton model enables to compute the emission cross sections in a unified way, without introducing adjustments between equilibrium and pre-equilibrium contributions. However, in practical cases it turns out that it is simpler and even more accurate to distinguish between a pre-equilibrium and an equilibrium phase and to perform the latter with the usual Hauser-Feshbach formalism. This is the approach followed in TALYS.

Two versions of the exciton model are implemented in TALYS: The default is the two-component model in which the neutron or proton types of particles and holes are followed throughout the reaction. We describe this model first, and then discuss the simpler, and more generally known, one-component model which is also implemented as an option. The following Section contains basically the most important equations of the recent exciton model study of [95].

12.1.1 Two-component exciton model

In the following reaction equations, we use a notation in which p_π (p_v) is the proton (neutron) particle number and h_π (h_v) the proton (neutron) hole number. From this, we define the proton exciton number $n_\pi = p_\pi + h_\pi$ and the neutron exciton number $n_v = p_v + h_v$. From this, we can construct the charge-independent particle number $p = p_\pi + p_v$, the hole number $h = h_\pi + h_v$ and the exciton number $n = n_\pi + n_v$.

The temporal development of the system can be described by a master equation, describing the gain and loss terms for a particular class of exciton states, see [95]. Integrating the master equation over time up to the equilibration time τ_{eq} yields the mean lifetime of the exciton state τ that can be used to calculate the differential cross section [98]. The primary pre-equilibrium differential cross section for the emission of a particle k with emission energy E_k can then be expressed in terms of τ, the composite-nucleus formation cross section σ^{CF}, and an emission rate W_k,

$$
\begin{aligned}
\frac{d\sigma_k^{\mathrm{PE}}}{dE_k} &= \sigma^{\mathrm{CF}} \sum_{p_\pi = p_\pi^0}^{p_\pi^{\max}} \sum_{p_v = p_v^0}^{p_v^{\max}} W_k(p_\pi, h_\pi, p_v, h_v, E_k) \tau(p_\pi, h_\pi, p_v, h_v) \\
&\quad \times \; P(p_\pi, h_\pi, p_v, h_v),
\end{aligned}
\tag{12.1}
$$

where the factor P represents the part of the pre-equilibrium population that has survived emission from the previous states and now passes through the (p_π, h_π, p_v, h_v) configurations, averaged over time. Expressions for all quantities appearing in this expression will be detailed in the rest of this Section. The initial proton and neutron particle numbers are $p_\pi^0 = Z_p$, and $p_v^0 = N_p$, respectively with Z_p (N_p) the proton (neutron) number of the projectile. For any exciton state in the reaction process, $h_\pi = p_\pi - p_\pi^0$ and $h_v = p_v - p_v^0$, so that for primary pre-equilibrium emission the initial hole numbers are $h_\pi^0 = h_v^0 = 0$. For e.g. a neutron-induced reaction, the initial exciton number is given by $n^0 = n_v^0 = 1$ ($0p_\pi 0h_\pi 1p_v 0h_v$), but only pre-equilibrium gamma emission can occur from this state (nucleon emission from this state is essentially elastic scattering and this is already covered by the optical model). Particle emission only occurs from $n = 3$ ($2p1h$) and higher exciton states. We use a hardwired value of $p_\pi^{\max} = p_v^{\max} = 6$ as the upper limit of the summation, see [95]. We use the never-come-back approximation, i.e. throughout the cascade one neglects the interactions that decrease the exciton number, although the adopted solution of Eq. (12.1) does include transitions that convert a proton particle-hole pair into a neutron pair and vice versa. The maximum values $p_\pi^{\max}$ and $p_v^{\max}$ thus entail an automatic separation of the pre-equilibrium population and the compound nucleus population. The latter is then handled by the more adequate Hauser-Feshbach mechanism. We now discuss the various ingredients of Eq. (12.1).

A. Reaction cross sections

The basic feeding term for pre-equilibrium emission is the composite formation cross section σ^{CF}, which is given by

$$
\sigma^{\mathrm{CF}} = \sigma_{\mathrm{reac}} - \sigma_{\mathrm{direct}},
\tag{12.2}
$$

where the reaction cross section σ_{reac} is directly obtained from the optical model and σ_{direct} is the sum of the cross sections for direct reactions to discrete states $\sigma^{disc,direct}$ as defined in Eq. (4.18), and for giant resonances, see Section 11.4.

B. Emission rates and particle-hole state densities

The emission rate W_k has been derived by Cline and Blann [99] from the principle of microreversibility, and can easily be generalized to a two-component version as shown by Dobes and Betak [100]. The emission rate for an ejectile k with relative mass μ_k and spin s_k is

$$
\begin{aligned}
W_k(p_\pi,h_\pi,p_v,h_v,E_k) &= \frac{2s_k+1}{\pi^2\hbar^3}\mu_k E_k \sigma_{k,\text{inv}}(E_k) \\
&\times \frac{\omega(p_\pi-Z_k,h_\pi,p_v-N_k,h_v,E^{\text{tot}}-E_k)}{\omega(p_\pi,h_\pi,p_v,h_v,E^{\text{tot}})},
\end{aligned}
\tag{12.3}
$$

where $\sigma_{k,\text{inv}}(E_k)$ is the inverse reaction cross section, again calculated with the optical model, Z_k (N_k) is the charge (neutron) number of the ejectile and E^{tot} is the total energy of the composite system.

For the particle-hole state density $\omega(p_\pi,h_\pi,p_v,h_v,E_x)$ we use the expression of Běták and Dobeš [100, 101]. Their formula is based on the assumption of equidistant level spacing and is corrected for the effect of the Pauli exclusion principle and for the finite depth of the potential well. The two-component particle-hole state density is

$$
\begin{aligned}
\omega(p_\pi,h_\pi,p_v,h_v,E_x) &= \frac{g_\pi^{n_\pi} g_v^{n_v}}{p_\pi! h_\pi! p_v! h_v! (n-1)!}(U-A(p_\pi,h_\pi,p_v,h_v))^{n-1} \\
&\times f(p,h,U,V),
\end{aligned}
\tag{12.4}
$$

where g_π and g_v are the single-particle state densities, A the Pauli correction, f the finite well function, and $U = E_x - P_{p,h}$ with $P_{p,h}$ Fu's pairing correction [102],

$$
\begin{aligned}
P_{p,h} &= \Delta - \Delta\left[0.996 - 1.76\left(\frac{n}{n_{\text{crit}}}\right)^{1.6}\bigg/\left(\frac{E_x}{\Delta}\right)^{0.68}\right]^2 \\
&\quad \text{if}\quad E_x/\Delta \geq 0.716 + 2.44\left(\frac{n}{n_{\text{crit}}}\right)^{2.17}, \\
&= \Delta \quad \text{otherwise},
\end{aligned}
\tag{12.5}
$$

with

$$
n_{\text{crit}} = 2gT_{\text{crit}}\ln 2,
\tag{12.6}
$$

where $T_{\text{crit}} = 2\sqrt{\Delta/\frac{1}{4}g}/3.5$ and $g = g_\pi + g_v$. The pairing energy Δ for total level densities is given by

$$
\Delta = \chi\frac{12}{\sqrt{A}},
\tag{12.7}
$$

where here A is the mass number and $\chi = 0, 1$ or 2 for odd-odd, odd or even-even nuclei. The Pauli correction term is given by

$$
\begin{aligned}
A(p_\pi,h_\pi,p_v,h_v) &= \frac{[\max(p_\pi,h_\pi)]^2}{g_\pi} + \frac{[\max(p_v,h_v)]^2}{g_v} \\
&\quad - \frac{p_\pi^2+h_\pi^2+p_\pi+h_\pi}{4g_\pi} - \frac{p_v^2+h_v^2+p_v+h_v}{4g_v}.
\end{aligned}
\tag{12.8}
$$

For the single-particle state densities we take

$$g_\pi = Z/15, \qquad g_\nu = N/15, \tag{12.9}$$

which is, through the relationship $g = a\pi^2/6$, in line with the values for our total level density parameter a, see Eq. (8.13), and also provides a globally better description of spectra than the generally adopted $g = A/13$.

The finite well function $f(p,h,E_x,V)$ accounts for the fact that a hole cannot have an energy below that of the bottom of the potential well depth V. It is given by

$$f(p,h,E_x,V) = 1 + \sum_{i=1}^{h} (-1)^i \binom{h}{i} \left[\frac{E_x - iV}{E_x} \right]^{n-1} \Theta(E_x - iV), \tag{12.10}$$

where Θ is the unit step function. Note that f is different from 1 only for excitation energies greater than V. In the original version of Běták and Dobeš, V is given by the depth E_f of the Fermi well. This was generalized by Kalbach [103, 94] to obtain an effective method to include surface effects in the first stage of the interaction, leading to a harder pre-equilibrium spectrum. For the first stage the maximum depth of the hole should be significantly reduced, since in the surface region the potential is shallower than in the interior. This automatically leaves more energy to be adopted by the excited particle, yielding more emission at the highest outgoing energies. We use the following functional form for V in terms of the projectile energy E_p and the mass A,

$$V = 22 + 16 \frac{E_p^4}{E_p^4 + (450/A^{1/3})^4} \text{ MeV for } h = 1 \text{ and incident protons,}$$

$$V = 12 + 26 \frac{E_p^4}{E_p^4 + (245/A^{1/3})^4} \text{ MeV for } h = 1 \text{ and incident neutrons,}$$

$$V = E_f = 38 \text{ MeV for } h > 1, \tag{12.11}$$

see Koning and Duijvestijn [95] for a further justification of this parameterisation.

C. Lifetimes

The lifetime τ of exciton state $(p_\pi, h_\pi, p_\nu, h_\nu)$ in Eq. (12.1) is defined as the inverse sum of the total emission rate and the various internal transition rates,

$$\tau(p_\pi, h_\pi, p_\nu, h_\nu) = [\lambda_\pi^+(p_\pi, h_\pi, p_\nu, h_\nu) + \lambda_\nu^+(p_\pi, h_\pi, p_\nu, h_\nu)$$
$$+ \lambda_{\pi\nu}^0(p_\pi, h_\pi, p_\nu, h_\nu) + \lambda_{\nu\pi}^0(p_\pi, h_\pi, p_\nu, h_\nu) + W(p_\pi, h_\pi, p_\nu, h_\nu)]^{-1}, \tag{12.12}$$

where λ_π^+ (λ_ν^+) is the internal transition rate for proton (neutron) particle-hole pair creation, $\lambda_{\pi\nu}^0$ ($\lambda_{\nu\pi}^0$) is the rate for the conversion of a proton (neutron) particle-hole pair into a neutron (proton) particle-hole pair, and λ_π^- (λ_ν^-) is the rate for particle-hole annihilation. These transition rates will be discussed in Sec. 12.1.1. The total emission rate W is the integral of Eq. (12.3) over all outgoing energies, summed over all outgoing particles,

$$W(p_\pi, h_\pi, p_\nu, h_\nu) = \sum_{k=\gamma,n,p,d,t,h,\alpha} \int dE_k W_k(p_\pi, h_\pi, p_\nu, h_\nu, E_k). \tag{12.13}$$

The final ingredient of the exciton model equation, Eq. (12.1), is the part of the pre-equilibrium population P that has survived emission from all previous steps and has arrived at the exciton state $(p_\pi, h_\pi, p_\nu, h_\nu)$. The expression for P is somewhat more complicated than that of the depletion factor that appears in the one-component exciton model [97]. For two components, contributions

from both particle creation *and* charge exchange reactions need to be taken into account, whereas transitions that do not change the exciton number cancel out in the one-component model.

For the $(p_\pi, h_\pi, p_\nu, h_\nu)$ state, P is given by a recursive relation:

$$
\begin{aligned}
P(p_\pi, h_\pi, p_\nu, h_\nu) = \quad & P(p_\pi - 1, h_\pi - 1, p_\nu, h_\nu)\Gamma_\pi^+(p_\pi - 1, h_\pi - 1, p_\nu, h_\nu) && (A) \\
+ \; & P(p_\pi, h_\pi, p_\nu - 1, h_\nu - 1)\Gamma_\nu^+(p_\pi, h_\pi, p_\nu - 1, h_\nu - 1) && (B) \\
+ \; & [P(p_\pi - 2, h_\pi - 2, p_\nu + 1, h_\nu + 1)\Gamma_\pi'^+(p_\pi - 2, h_\pi - 2, p_\nu + 1, h_\nu + 1) \\
+ \; & P(p_\pi - 1, h_\pi - 1, p_\nu, h_\nu)\Gamma_\nu'^+(p_\pi - 1, h_\pi - 1, p_\nu, h_\nu)] \\
\times \; & \Gamma_{\nu\pi}^0(p_\pi - 1, h_\pi - 1, p_\nu + 1, h_\nu + 1) && (C+D) \\
+ \; & [P(p_\pi, h_\pi, p_\nu - 1, h_\nu - 1)\Gamma_\pi'^+(p_\pi, h_\pi, p_\nu - 1, h_\nu - 1) \\
+ \; & P(p_\pi + 1, h_\pi + 1, p_\nu - 2, h_\nu - 2)\Gamma_\nu'^+(p_\pi + 1, h_\pi + 1, p_\nu - 2, h_\nu - 2)] \\
\times \; & \Gamma_{\pi\nu}^0(p_\pi + 1, h_\pi + 1, p_\nu - 1, h_\nu - 1) && (E+F).
\end{aligned}
$$

$$(12.14)$$

This relation contains 6 distinct feeding terms: (A) creation of a proton particle-hole pair from the $(p_\pi - 1, h_\pi - 1, p_\nu, h_\nu)$ state, (C) creation of a proton particle-hole pair from the $(p_\pi - 2, h_\pi - 2, p_\nu + 1, h_\nu + 1)$ state followed by the conversion of a neutron particle-hole pair into a proton particle-hole pair, and (D) creation of a neutron particle-hole pair from the $(p_\pi - 1, h_\pi - 1, p_\nu, h_\nu)$ state followed by its conversion into a proton particle-hole pair. The three remaining terms (B), (E), and (F) are obtained by changing protons into neutrons and vice versa. The probabilities of creating new proton or neutron particle-hole pairs and for converting a proton (neutron) pair into a neutron (proton) pair are calculated as follows:

$$
\begin{aligned}
\Gamma_\pi^+(p_\pi, h_\pi, p_\nu, h_\nu) &= \lambda_\pi^+(p_\pi, h_\pi, p_\nu, h_\nu)\tau(p_\pi, h_\pi, p_\nu, h_\nu), \\
\Gamma_\nu^+(p_\pi, h_\pi, p_\nu, h_\nu) &= \lambda_\nu^+(p_\pi, h_\pi, p_\nu, h_\nu)\tau(p_\pi, h_\pi, p_\nu, h_\nu), \\
\Gamma_\pi'^+(p_\pi, h_\pi, p_\nu, h_\nu) &= \lambda_\pi^+(p_\pi, h_\pi, p_\nu, h_\nu)\tau'(p_\pi, h_\pi, p_\nu, h_\nu), \\
\Gamma_\nu'^+(p_\pi, h_\pi, p_\nu, h_\nu) &= \lambda_\nu^+(p_\pi, h_\pi, p_\nu, h_\nu)\tau'(p_\pi, h_\pi, p_\nu, h_\nu), \\
\Gamma_{\pi\nu}^0(p_\pi, h_\pi, p_\nu, h_\nu) &= \lambda_{\pi\nu}^0(p_\pi, h_\pi, p_\nu, h_\nu)\tau(p_\pi, h_\pi, p_\nu, h_\nu), \\
\Gamma_{\nu\pi}^0(p_\pi, h_\pi, p_\nu, h_\nu) &= \lambda_{\nu\pi}^0(p_\pi, h_\pi, p_\nu, h_\nu)\tau(p_\pi, h_\pi, p_\nu, h_\nu), \\
\tau'(p_\pi, h_\pi, p_\nu, h_\nu) &= [\lambda_\pi^+(p_\pi, h_\pi, p_\nu, h_\nu) + \lambda_\nu^+(p_\pi, h_\pi, p_\nu, h_\nu) \\
&\quad + W(p_\pi, h_\pi, p_\nu, h_\nu)]^{-1}.
\end{aligned}
$$

$$(12.15)$$

The use of τ' in the probability $\Gamma_\pi'^+$ ($\Gamma_\nu'^+$), to create a new proton (neutron) particle-hole pair preceding an exchange interaction, originates from the approximation that only one exchange interaction is allowed in each pair-creation step. The appropriate lifetime in this case consists merely of pair creation and emission rates, see Kalbach [104].

The initial condition for the recursive equations is

$$
P(p_\pi^0, h_\pi^0, p_\nu^0, h_\nu^0) = 1, \tag{12.16}
$$

after which P can be solved for any configuration.

To calculate the pre-equilibrium spectrum, the only quantities left to determine are the internal transition rates λ_π^+, λ_ν^+, $\lambda_{\pi\nu}^0$ and $\lambda_{\nu\pi}^0$.

D. Internal transition rates

The transition rate λ_π^+ for the creation of a proton particle-hole pair is given by four terms, accounting for p_π, h_π, p_ν and h_ν scattering that leads to a new (p_π, h_π) pair,

$$\lambda_\pi^+(p_\pi, h_\pi, p_\nu, h_\nu) = \frac{1}{\omega(p_\pi, h_\pi, p_\nu, h_\nu, E^{\text{tot}})}$$

$$\left[\int_{L_1^{p\pi}}^{L_2^{p\pi}} \lambda_{\pi\pi}^{1p}(u) \omega(p_\pi - 1, h_\pi, p_\nu, h_\nu, E^{\text{tot}} - u) \omega(1, 0, 0, 0, u) du \right.$$

$$+ \int_{L_1^{h\pi}}^{L_2^{h\pi}} \lambda_{\pi\pi}^{1h}(u) \omega(p_\pi, h_\pi - 1, p_\nu, h_\nu, E^{\text{tot}} - u) \omega(0, 1, 0, 0, u) du$$

$$+ \int_{L_1^{p\nu}}^{L_2^{p\nu}} \lambda_{\nu\pi}^{1p}(u) \omega(p_\pi, h_\pi, p_\nu - 1, h_\nu, E^{\text{tot}} - u) \omega(0, 0, 1, 0, u) du$$

$$+ \left. \int_{L_1^{h\nu}}^{L_2^{h\nu}} \lambda_{\nu\pi}^{1h}(u) \omega(p_\pi, h_\pi, p_\nu, h_\nu - 1, E^{\text{tot}} - u) \omega(0, 0, 0, 1, u) du \right], \tag{12.17}$$

where the first and third term represent particle scattering and the second and fourth term hole scattering. The integration limits correct for the Pauli exclusion principle,

$$\begin{aligned}
L_1^{p\pi} &= A(p_\pi + 1, h_\pi + 1, p_\nu, h_\nu) - A(p_\pi - 1, h_\pi, p_\nu, h_\nu), \\
L_2^{p\pi} &= E^{\text{tot}} - A(p_\pi - 1, h_\pi, p_\nu, h_\nu), \\
L_1^{h\pi} &= A(p_\pi + 1, h_\pi + 1, p_\nu, h_\nu) - A(p_\pi, h_\pi - 1, p_\nu, h_\nu), \\
L_2^{h\pi} &= E^{\text{tot}} - A(p_\pi, h_\pi - 1, p_\nu, h_\nu), \\
L_1^{p\nu} &= A(p_\pi, h_\pi, p_\nu + 1, h_\nu + 1) - A(p_\pi, h_\pi, p_\nu - 1, h_\nu), \\
L_2^{p\nu} &= E^{\text{tot}} - A(p_\pi, h_\pi, p_\nu - 1, h_\nu), \\
L_1^{h\nu} &= A(p_\pi + 1, h_\pi + 1, p_\nu, h_\nu) - A(p_\pi, h_\pi, p_\nu, h_\nu - 1), \\
L_2^{h\nu} &= E^{\text{tot}} - A(p_\pi, h_\pi, p_\nu, h_\nu - 1), \tag{12.18}
\end{aligned}$$

which demands that (a) the minimal energy available to the scattering particle or hole creating a new particle-hole pair equals the Pauli energy of the final state minus the Pauli energy of the inactive particles and holes not involved in the scattering process, and (b) the maximal energy available equals the total excitation energy minus the latter Pauli energy.

The term $\lambda_{\pi\pi}^{1p}(u)$ is the collision probability per unit time for a proton-proton interaction leading to an additional proton particle-hole pair. In general, the corresponding term for a hole is obtained by relating it to the particle collision probability through the accessible state density of the interacting particles and holes,

$$\lambda_{\pi\pi}^{1h}(u) = \lambda_{\pi\pi}^{1p}(u) \frac{\omega(1, 2, 0, 0, u)}{\omega(2, 1, 0, 0, u)}. \tag{12.19}$$

Similarly, $\lambda_{\nu\pi}^{1p}(u)$ is the collision probability per unit time for a neutron-proton interaction leading to an additional proton particle-hole pair, and for the corresponding hole term we have

$$\lambda_{\nu\pi}^{1h}(u) = \lambda_{\nu\pi}^{1p}(u) \frac{\omega(1, 1, 0, 1, u)}{\omega(1, 1, 1, 0, u)}. \tag{12.20}$$

The transition rate for conversion of a proton particle-hole pair into a neutron pair is

$$\lambda_{\pi\nu}^0(p_\pi, h_\pi, p_\nu, h_\nu) = \frac{1}{\omega(p_\pi, h_\pi, p_\nu, h_\nu, E^{\text{tot}})} \int_{L_1^{p\pi}}^{L_2^{p\pi}} \lambda_{\pi\nu}^{1p1h}(u)$$

$$\omega(p_\pi - 1, h_\pi - 1, p_\nu, h_\nu, E^{\text{tot}} - u) \omega(1, 1, 0, 0, u) du, \tag{12.21}$$

with integration limits

$$
\begin{aligned}
L_1^{p\pi} &= A(p_\pi, h_\pi, p_\nu, h_\nu) - A(p_\pi - 1, h_\pi - 1, p_\nu, h_\nu) \\
L_2^{p\pi} &= E^{\text{tot}} - A(p_\pi - 1, h_\pi - 1, p_\nu, h_\nu).
\end{aligned}
\tag{12.22}
$$

The term $\lambda_{\pi\nu}^{1p1h}$ is the associated collision probability. Interchanging π and ν in Eqs. (12.17-12.22) gives the expressions for λ_ν^+, $\lambda_{\nu\nu}^{1h}$, $\lambda_{\pi\nu}^{1h}$ and $\lambda_{\nu\pi}^0$.

We distinguish between two options for the collision probabilities:

D1. Effective squared matrix element

Expressing the transition rate in terms of an effective squared matrix element has been used in many exciton model analyses. Also in TALYS, it is one of the options for our calculations and comparisons with data. The collision probabilities of Eqs. (12.17) and (12.21) are determined with the aid of Fermi's golden rule of time-dependent perturbation theory, which for a two-component model gives

$$
\begin{aligned}
\lambda_{\pi\pi}^{1p}(u) &= \frac{2\pi}{\hbar} M_{\pi\pi}^2 \omega(2, 1, 0, 0, u), \\
\lambda_{\pi\pi}^{1h}(u) &= \frac{2\pi}{\hbar} M_{\pi\pi}^2 \omega(1, 2, 0, 0, u), \\
\lambda_{\nu\pi}^{1p}(u) &= \frac{2\pi}{\hbar} M_{\nu\pi}^2 \omega(1, 1, 1, 0, u), \\
\lambda_{\nu\pi}^{1h}(u) &= \frac{2\pi}{\hbar} M_{\nu\pi}^2 \omega(1, 1, 0, 1, u), \\
\lambda_{\pi\nu}^{1p1h}(u) &= \frac{2\pi}{\hbar} M_{\pi\nu}^2 \omega(0, 0, 1, 1, u),
\end{aligned}
\tag{12.23}
$$

where the relations (12.19)-(12.20) have been applied. Interchanging π and ν gives the expressions for $\lambda_{\nu\nu}^{1p}$, $\lambda_{\nu\nu}^{1h}$, $\lambda_{\pi\nu}^{1p}$, $\lambda_{\pi\nu}^{1h}$, and $\lambda_{\nu\pi}^{1p1h}$. Here, the $M_{\pi\pi}^2$, etc. are average squared matrix elements of the residual interaction, which are assumed to depend on the total energy E^{tot} of the whole composite nucleus only. Such a matrix element thus represents a truly *effective* residual interaction, whereby all individual residual interactions taking place inside the nucleus can be cast into an average form for the squared matrix element to which one assigns a global E^{tot}-dependence a posteriori.

The average residual interaction inside the nucleus is not necessarily the same for like and unlike nucleons. The two-component matrix elements are given, in terms of an average M^2, by

$$
\begin{aligned}
M_{\pi\pi}^2 &= R_{\pi\pi} M^2, \\
M_{\nu\nu}^2 &= R_{\nu\nu} M^2, \\
M_{\pi\nu}^2 &= R_{\pi\nu} M^2, \\
M_{\nu\pi}^2 &= R_{\nu\pi} M^2.
\end{aligned}
\tag{12.24}
$$

In TALYS, we take

$$
R_{\nu\nu} = 1.5, R_{\nu\pi} = R_{\pi\pi} = R_{\pi\nu} = 1.,
\tag{12.25}
$$

which is in line with the, more parameter-free, optical model based exciton model that we describe later. Note that this deviates somewhat from the parameters adopted by Koning and Duijvestijn [95]. The current parameterization gives slightly better performance for cross section excitation functions.

In TALYS, the above parameters are adjustable with Eq. (12.25) as default. The following semi-empirical expression for the squared matrix element has been shown to work for incident energies between 7 and 200 MeV [95]:

$$M^2 = \frac{C_1 A_p}{A^3} \left[7.48 C_2 + \frac{4.62 \times 10^5}{(\frac{E^{\text{tot}}}{n.A_p} + 10.7 C_3)^3} \right].$$ (12.26)

Eq. (12.26) is a generalization of older parameterisations such as given in Refs. [104, 94], which apply in smaller (lower) energy ranges. Here C_1, C_2 and C_3 are adjustable constants that are all equal to 1 by default, and A_p is the mass number of the projectile, which allows generalization for complex-particle reactions. Again, Eq. (12.26) is slightly different (10%) from the expression given in Ref. [95] to allow for better fits of excitation functions.

Finally, for matrix element based transition rates and equidistant particle-hole level densities, the integrals in the transition rates can be approximated analytically [104], giving

$$
\begin{aligned}
\lambda_{\pi+}(p_\pi, h_\pi, p_\nu, h_\nu) &= \frac{2\pi}{\hbar} \frac{g_\pi^2}{2n(n+1)} \frac{[E^{tot} - A(p_\pi + 1, h_\pi + 1, p_\nu, h_\nu)]^{n+1}}{[E^{tot} - A(p_\pi, h_\pi, p_\nu, h_\nu)]^{n-1}} \\
&\times (n_\pi g_\pi M_{\pi\pi}^2 + 2n_\nu g_\nu M_{\pi\nu}^2) f(p+1, h+1, E^{tot}, V) \\
\lambda_{\nu+}(p_\pi, h_\pi, p_\nu, h_\nu) &= \frac{2\pi}{\hbar} \frac{g_\nu^2}{2n(n+1)} \frac{[E^{tot} - A(p_\pi, h_\pi, p_\nu + 1, h_\nu + 1)]^{n+1}}{[E^{tot} - A(p_\pi, h_\pi, p_\nu, h_\nu)]^{n-1}} \\
&\times (n_\nu g_\nu M_{\nu\nu}^2 + 2n_\pi g_\pi M_{\nu\pi}^2) f(p+1, h+1, E^{tot}, V) \\
\lambda_{\pi\nu}(p_\pi, h_\pi, p_\nu, h_\nu) &= \frac{2\pi}{\hbar} M_{\pi\nu}^2 \frac{p_\pi h_\pi}{n} g_\nu^2 f(p, h, E^{tot}, V) \left[\frac{E^{tot} - B_{\pi\nu}(p_\pi, h_\pi, p_\nu, h_\nu)}{E^{tot} - A(p_\pi, h_\pi, p_\nu, h_\nu)} \right]^{n-1} \\
&\times (2[E^{tot} - B_{\pi\nu}(p_\pi, h_\pi, p_\nu, h_\nu)] \\
&+ n|A(p_\pi, h_\pi, p_\nu, h_\nu) - A(p_\pi - 1, h_\pi - 1, p_\nu + 1, h_\nu + 1)|) \\
\lambda_{\nu\pi}(p_\pi, h_\pi, p_\nu, h_\nu) &= \frac{2\pi}{\hbar} M_{\nu\pi}^2 \frac{p_\nu h_\nu}{n} g_\pi^2 f(p, h, E^{tot}, V) \left[\frac{E^{tot} - B_{\nu\pi}(p_\pi, h_\pi, p_\nu, h_\nu)}{E^{tot} - A(p_\pi, h_\pi, p_\nu, h_\nu)} \right]^{n-1} \\
&\times (2[E^{tot} - B_{\nu\pi}(p_\pi, h_\pi, p_\nu, h_\nu)] \\
&+ n|A(p_\pi, h_\pi, p_\nu, h_\nu) - A(p_\pi + 1, h_\pi + 1, p_\nu - 1, h_\nu - 1)|), \quad (12.27)
\end{aligned}
$$

with

$$
\begin{aligned}
B_{\pi\nu}(p_\pi, h_\pi, p_\nu, h_\nu) &= max[A(p_\pi, h_\pi, p_\nu, h_\nu), A(p_\pi - 1, h_\pi - 1, p_\nu + 1, h_\nu + 1)] \\
B_{\nu\pi}(p_\pi, h_\pi, p_\nu, h_\nu) &= max[A(p_\pi, h_\pi, p_\nu, h_\nu), A(p_\pi + 1, h_\pi + 1, p_\nu - 1, h_\nu - 1)]. \quad (12.28)
\end{aligned}
$$

which is also included as an option. The default is however to use the numerical solutions for the internal transition rates. This analytical solution requires a value for M^2 that is 20% larger than that of Eq. (12.26), which apparently is the energy-averaged effect of introducing such approximations.

D2. Collision rates based on the optical model

Instead of modeling the intranuclear transition rate by an average squared matrix element, one may also relate the transition rate to the average imaginary optical model potential depth [95]. The collision probabilities, when properly averaged over all particle-hole configurations as in Eq. (12.17), in principle would yield a parameter free expression for the transition rate.

The average well depth W_i can be obtained by averaging the total imaginary part of the potential $\mathscr{W}$ over the whole volume of the nucleus

$$W_i(E) = \frac{\int \mathscr{W}_i(r,E)\rho(r)dr}{\int \rho(r)dr}, \tag{12.29}$$

where ρ represents the density of nuclear matter for which we take the form factor $f(r,R,a)$ of the volume part of the optical model potential, given by the usual Woods-Saxon shape of Eq. (10.3). The total imaginary potential is given by

$$\mathscr{W}_i(r,E) = \mathscr{W}_{V,i}(E)f(r,R_{V,i},a_{V,i}) - 4a_{D,i}\mathscr{W}_{D,i}(E)\frac{d}{dr}f(r,R_{D,i},a_{D,i}). \tag{12.30}$$

Next, we define an *effective* imaginary optical potential [95] related to nucleon-nucleon collisions in nuclear matter:

$$W_i^{\text{eff}}(E) = C^{\text{omp}}\, W_i(E). \tag{12.31}$$

We use as best overall parameter

$$C^{\text{omp}} = 0.55. \tag{12.32}$$

This parameter can be adjusted with the **M2constant** keyword, which serves as a multiplier for the value given in Eq. (12.32). The collision probabilities are now related as follows to the *effective* imaginary optical potential:

$$
\begin{aligned}
\lambda_{\pi\pi}^{1p}(u) &= \frac{1}{4}\;\frac{2W_p^{\text{eff}}(u-S(p))}{\hbar} \\[2mm]
\lambda_{\pi\pi}^{1h}(u) &= \frac{1}{4}\;\frac{2W_p^{\text{eff}}(u-S(p))}{\hbar}\frac{\omega(1,2,0,0,u)}{\omega(2,1,0,0,u)} \\[2mm]
\lambda_{\nu\pi}^{1p}(u) &= \frac{3}{4}\;\frac{2W_n^{\text{eff}}(u-S(n))}{\hbar} \\[2mm]
\lambda_{\nu\pi}^{1h}(u) &= \frac{3}{4}\;\frac{2W_n^{\text{eff}}(u-S(n))}{\hbar}\frac{\omega(1,1,0,1,u)}{\omega(1,1,1,0,u)} \\[2mm]
\lambda_{\nu\pi}^{1p1h}(u) &= \frac{1}{2}\;\frac{2W_n^{\text{eff}}(u-S(n))}{\hbar},
\end{aligned}
\tag{12.33}
$$

and similarly for the components of λ_ν^+ and $\lambda_{\nu\pi}^0$. The transition rates for the exciton model are then obtained by inserting these terms in Eqs. (12.17) and (12.21). Apart from Eq. (12.32), a parameter-free model is obtained.

12.1.2 One-component exciton model

The one-component exciton model has been made redundant by the more flexible and physically more justified two-component model. Nevertheless, it is included as an option since it connects to many older pre-equilibrium studies and thus may be helpful as comparison. In the one-component exciton model, the pre-equilibrium spectrum for the emission of a particle k at an energy E_k is given by

$$\frac{d\sigma_k^{\text{PE}}}{dE_k} = \sigma^{\text{CF}}\sum_{p=p_0}^{p_{\max}} W_k(p,h,E_k)\tau(p,h), \tag{12.34}$$

where $p_{\max} = 6$ and σ^{CF} are defined as below Eq. (12.1). For the initial particle number p_0 we have $p_0 = A_p$ with A_p the mass number of the projectile. In general, the hole number $h = p - p_0$ in Eq. (12.34), so that the initial hole number is always zero, i.e. $h_0 = 0$ for primary pre-equilibrium emission.

The emission rate W_k is

$$W_k(p,h,E_k) = \frac{2s_k+1}{\pi^2\hbar^3}\mu_k E_k \sigma_{k,\mathrm{inv}}(E_k)\frac{\omega(p-A_k,h,E_{\mathrm{tot}}-E_k)}{\omega(p,h,E^{\mathrm{tot}})}Q_k(p), \tag{12.35}$$

with all quantities explained below Eq. (12.3), and A_k is the mass number of the ejectile and $Q_k(p)$ is a factor accounting for the distinguishability of neutrons and protons [105]

$$\begin{aligned}
Q_k(p) &= \frac{(p-A_k)!}{p!}\left[\sum_{p_\pi=Z_k}^{p-N_k}(\frac{Z}{A})^{n_\pi-Z_k}(\frac{A}{N})^{n_\nu-N_k}\frac{1}{h_\pi!h_\nu!}\frac{1}{(p_\pi-Z_k)!(p_\nu-N_k)!}\right] \\
&\quad / \left[\sum_{p_\pi=Z_k}^{p-N_k}(\frac{Z}{A})^{n_\pi}(\frac{N}{A})^{n_\nu}\frac{1}{p_\pi!p_\nu!h_\pi!h_\nu!}\right].
\end{aligned} \tag{12.36}$$

For gamma's we set $Q_\gamma(p) = 1$.

Finally, $\omega(p,h,E_x)$ is the particle-hole state density for which we use the one-component expression by Běták and Dobeš [101], again corrected for the effect of the Pauli exclusion principle and for the finite depth of the potential well. The one-component particle-hole state density has a simpler form than that of Eq. (12.4),

$$\omega(p,h,E_x) = \frac{g^n}{p!h!(n-1)!}[E_x - A(p,h)]^{n-1}f(p,h,E_x,V), \tag{12.37}$$

where $g = A/15$ is the single-particle state density and

$$A(p,h) = \frac{[max(p,h)]^2}{g} - \frac{p^2+h^2+p+h}{4g}, \tag{12.38}$$

is the Pauli correction factor. The finite well function f is given by Eq. (12.10).

To obtain the lifetimes $\tau(p,h)$ that appear in Eq. (12.34), we first define the total emission rate $W(p,h)$ as the integral of Eq. (12.35) over all outgoing energies, summed over all outgoing particles:

$$W(p,h) = \sum_{k=\gamma,n,p,d,t,h,\alpha}\int dE_k W_k(p,h,E_k). \tag{12.39}$$

As mentioned already, we have implemented the never-come-back solution of the master equation. This is based on the assumption that at the beginning of the cascade one neglects the interactions that decrease the exciton number. Then, for the one-component model the expression for the lifetime is (see e.g. Ref. [97])

$$\tau(p,h) = \frac{1}{\lambda^+(p,h)+W(p,h)}D_{p,h}, \tag{12.40}$$

where $D_{p,h}$ is a depletion factor that accounts for the removal of reaction flux, through emission, by the previous stages

$$D_{p,h} = \prod_{p'=p_0}^{p-1}\frac{\lambda^+(p',h')}{\lambda^+(p',h')+W(p',h')}, \tag{12.41}$$

with again $h' = p' - p_0$. The initial case of Eq. (12.40) is

$$\tau(p_0, h_0) = \frac{1}{\lambda^+(p_0, h_0) + W(p_0, h_0)}. \tag{12.42}$$

To calculate the pre-equilibrium spectrum, the only quantity left to determine is the internal transition rate $\lambda^+(p, h)$ from state (p, h) to state $(p+1, h+1)$. The general definition of $\lambda^+(p, h)$ is

$$
\begin{aligned}
\lambda^+(p, h) \quad &= \quad \frac{1}{\omega(p, h, E^{\text{tot}})} \Big[\int_{L_1^p}^{L_2^p} du \lambda^{1p}(u) \omega(p-1, h, E^{\text{tot}} - u) \omega(1, 0, u) \\
&+ \quad \int_{L_1^h}^{L_2^h} du \lambda^{1h}(u) \omega(p, h-1, E^{\text{tot}} - u) \omega(0, 1, u) \Big].
\end{aligned}
\tag{12.43}
$$

where the two terms account for particle and hole scattering, respectively, and the integration limits

$$
\begin{aligned}
L_1^p \quad &= \quad A(p+1, h+1) - A(p-1, h) \\
L_2^p \quad &= \quad E^{\text{tot}} - A(p-1, h) \\
L_1^h \quad &= \quad A(p+1, h+1) - A(p, h-1) \\
L_2^h \quad &= \quad E^{\text{tot}} - A(p, h-1),
\end{aligned}
\tag{12.44}
$$

correct for the Pauli exclusion principle.

We again distinguish between two options:

1. Effective squared matrix element

The collision probabilities are determined with the aid of Fermi's golden rule of time-dependent perturbation theory, which for the one-component model are

$$
\begin{aligned}
\lambda^{1p}(u) \quad &= \quad \frac{2\pi}{\hbar} M^2 \omega(2, 1, u) \\
\lambda^{1h}(u) \quad &= \quad \frac{2\pi}{\hbar} M^2 \omega(1, 2, u),
\end{aligned}
\tag{12.45}
$$

with M^2 the average squared matrix element of the residual interaction. In the one-component model, "forbidden" transitions are taken into account, so that a squared matrix element smaller than that of Eq. (12.26) of the two-component model is needed to compensate for these transitions. We find that for the one-component model we need to multiply M^2 of Eq. (12.26) by 0.5 to obtain a global comparison with data that is closest to our two-component result, i.e.

$$M^2 = \frac{0.5 C_1 A_p}{A^3} \left[7.48 C_2 + \frac{4.62 \times 10^5}{(\frac{E^{\text{tot}}}{n.A_p} + 10.7 C_3)^3} \right]. \tag{12.46}$$

For completeness, we note that the transition rate can be well approximated by an analytical form as discussed in Refs. [106, 101, 103]. The result is

$$\lambda^+(p, h) = \frac{2\pi}{\hbar} M^2 \frac{g^3}{2(n+1)} \frac{[E^{\text{tot}} - A(p+1, h+1)]^{n+1}}{[E^{\text{tot}} - A(p, h)]^{n-1}} f(p+1, h+1, E^{\text{tot}}, V). \tag{12.47}$$

However, the overall description of experimental data obtained with the one-component model is however worse that that of the two-component model, so we rarely use it.

2. Collision rates based on the optical model

Also in the one-component model the transition rates can be related to the effective nucleon-nucleon interaction $\bar{\sigma}$ and thereby to the imaginary optical potential,

$$
\begin{aligned}
\lambda^{1p}(u) &= \frac{1}{2}\frac{2W^{\text{eff}}(u-S)}{\hbar}\\
\lambda^{1h}(u) &= \frac{1}{2}\frac{2W^{\text{eff}}(u-S)}{\hbar}\frac{\omega(1,2,u)}{\omega(2,1,u)},
\end{aligned}
\tag{12.48}
$$

with S the separation energy of the particle. Since the one-component model makes no distinction between neutron and proton particle-hole pairs, W_V^{eff} is evaluated as follows,

$$
W_i^{\text{eff}}(E) = 0.5 C^{\text{omp}} W_i(E),
\tag{12.49}
$$

analogous to the multiplication with a factor 0.5 for M^2.

Energy width representation

The formalism given above, i.e. Eqs. (12.34), (12.35) and (12.40), forms a representation in which the time appears, i.e. the dimensions of $W(p,h)$ and $\tau(p,h)$ are $[s]^{-1}$ and $[s]$ respectively. An alternative expression for the exciton model that is often used is in terms of energy widths. Since this may be more recognisable to some users we also give it here. The partial escape width $\Gamma_k^{\uparrow}(p,h,E_k)$ is related to the emission rate by

$$
\Gamma_k^{\uparrow}(p,h,E_k) = \hbar W_k(p,h,E_k).
\tag{12.50}
$$

Integrated over energy we have

$$
\Gamma_k^{\uparrow}(p,h) = \hbar W_k(p,h),
\tag{12.51}
$$

and the total escape width is

$$
\Gamma^{\uparrow}(p,h) = \sum_{k=\gamma,n,p,d,t,h,\alpha} \Gamma_k^{\uparrow}(p,h) = \hbar W(p,h).
\tag{12.52}
$$

The damping width $\Gamma^{\downarrow}$ is related to the internal transition rate by

$$
\Gamma^{\downarrow}(p,h) = \hbar \lambda^{+}(p,h).
\tag{12.53}
$$

Defining the total width by

$$
\Gamma^{\text{tot}}(p,h) = \Gamma^{\downarrow}(p,h) + \Gamma^{\uparrow}(p,h),
\tag{12.54}
$$

we can rewrite the exciton model cross section (12.34) as

$$
\frac{d\sigma_k^{\text{PE}}}{dE_k} = \sigma^{\text{CF}} \sum_{p=p_0}^{p_{\max}} \frac{\Gamma_k^{\uparrow}(p,h,E_k)}{\Gamma^{\text{tot}}(p,h)} \left(\prod_{p'=p_0}^{p-1} \frac{\Gamma^{\downarrow}(p',h')}{\Gamma^{\text{tot}}(p',h')} \right).
\tag{12.55}
$$

In the output file of TALYS, the results for the various quantities in both the time and the energy width representation are given.

In sum, the default model used by TALYS is the two-component exciton model with collision probabilities based on the effective squared matrix element of Eq. (12.26).

Options 12.1.1 Pre-equilibrium calculations can be enabled or disabled with the **preequilib-rium** keyword (p. 592).

12.2 Photon exciton model

For pre-equilibrium photon emission, we have implemented the model of Akkermans and Gruppelaar [107]. This model gives a simple but powerful simulation of the direct-semidirect capture process within the framework of the exciton model. Analogous to the particle emission rates, the continuum γ-ray emission rates may be derived from the principle of detailed balance or microscopic reversibility, assuming that only $E1$-transitions contribute. This yields

$$W_\gamma(p,h,E_\gamma) = \frac{E_\gamma^2}{\pi^2\hbar^3 c^2} \frac{\sigma_{\gamma,abs}(E_\gamma)}{\omega(p,h,E^{tot})} \left(\frac{g^2 E_\gamma \omega(p-1,h-1,E_x-E_\gamma)}{g(n-2)+g^2 E_\gamma} + \frac{gn\omega(p,h,E_x-E_\gamma)}{gn+g^2 E_\gamma} \right)$$
(12.56)

where $\sigma_{\gamma,abs}(E_\gamma)$ is the photon absorption cross section of Eq. (9.19). The initial particle-hole configuration in Eq. (12.34) is $n_0 = 1$ ($1p0h$) for photon emission. For "direct" γ-ray emission in nucleon-induced reactions only the second term between brackets ($n = 1$) contributes. The "semi-direct" γ-ray emission ($n = 3$) consists of both terms.

The emission rate (12.56) is included in Eqs. (12.34) and (12.39) so that the pre-equilibrium photon cross section automatically emerges.

For the two-component model, we use

$$W_\gamma(p_\pi,h_\pi,p_\nu,h_\nu,E_\gamma) = \frac{E_\gamma^2}{\pi^2\hbar^3 c^2} \frac{\sigma_{\gamma,abs}(E_\gamma)}{\omega(p_\pi,h_\pi,p_\nu,h_\nu,E^{tot})}$$

$$\times \quad (\frac{g^2 E_\gamma \frac{1}{2} \left[\omega(p_\pi-1,h_\pi-1,p_\nu,h_\nu,E_x-E_\gamma)+\omega(p_\pi,h_\pi,p_\nu-1,h_\nu-1,E_x-E_\gamma) \right]}{g(n-2)+g^2 E_\gamma}$$

$$+ \quad \frac{gn\omega(p_\pi,h_\pi,p_\nu,h_\nu,E_x-E_\gamma)}{gn+g^2 E_\gamma}).$$
(12.57)

Options 12.2.1 The strength of the photonuclear contribution van be steered with **Rgamma** (p. 620).

12.3 Pre-equilibrium spin distribution

Since the exciton model described above does not provide a spin distribution for the residual states after pre-equilibrium emission, a model needs to be adopted that provides the spin population in the continuum in binary reactions. TALYS provides two options for this. The default is to adopt the compound nucleus spin distribution (described in Chapter 13) also for the excited states resulting from pre-equilibrium emission. Another option that has been quite often used in the past is to assign a spin distribution to the particle-hole state density. For that, we adopt the usual decomposition of the state density into a J-dependent part and an energy-dependent part,

$$\rho(p,h,J,E_x) = (2J+1)R_n(J)\omega(p,h,E_x).$$
(12.58)

The function $R_n(J)$ represents the spin distribution of the states in the continuum. It is given by

$$R_n(J) = \frac{2J+1}{\pi^{1/2}n^{3/2}\sigma^3} \exp\left[-\frac{(J+\frac{1}{2})^2}{n\sigma^2} \right],$$
(12.59)

and satisfies, for any exciton number n,

$$\sum_J (2J+1)R_n(J) = 1. \tag{12.60}$$

The used expression for the spin cut-off parameter σ is that by Gruppelaar et al. [108],

$$\sigma^2 = 0.24nA^{\frac{2}{3}}, \tag{12.61}$$

where A is the mass number of the nucleus. Similarly, for the two-component particle-hole level density we have

$$\rho(p_\pi, h_\pi, p_\nu, h_\nu, J, E_x) = (2J+1)R_n(J)\omega(p_\pi, h_\pi, p_\nu, h_\nu, E_x). \tag{12.62}$$

In practice, with this option the residual states formed by pre-equilibrium reactions would be multiplied by R_n a posteriori. There are various arguments to prefer the compound nucleus spin distribution, so we use that default.

▌ **Options 12.3.1** With **preeqspin y** (p. 596) Eq. (12.61) is invoked.

12.4 Continuum stripping, pick-up, break-up and knock-out reactions

For pre-equilibrium reactions involving deuterons, tritons, Helium-3 and alpha particles, a contribution from the exciton model is automatically calculated with the formalism of the previous subsections. It is however well-known that for nuclear reactions involving projectiles and ejectiles with different particle numbers, mechanisms like stripping, pick-up, break-up and knock-out play an important role and these direct-like reactions are not covered by the exciton model. Therefore, Kalbach [109] developed a phenomenological contribution for these mechanisms, which we have included in TALYS. In total, the pre-equilibrium cross section for these reactions is given by the sum of an exciton model (EM), nucleon transfer (NT), and knock-out (KO) contribution:

$$\frac{d\sigma_k^{\text{PE}}}{dE_k} = \frac{d\sigma_k^{EM}}{dE_k} + \frac{d\sigma_k^{NT}}{dE_k} + \frac{d\sigma_k^{KO}}{dE_k} \tag{12.63}$$

where the contribution from the exciton model was outlined in the previous subsection.

12.4.1 Transfer reactions

The general differential cross section formula for a nucleon transfer reaction of the type $A(a,b)B$ is

$$
\begin{aligned}
\frac{d\sigma_{a,b}^{NT}}{dE_b} &= \frac{2s_b+1}{2s_a+1}\frac{A_b}{A_a}\frac{E_b\sigma_{b,inv}(E_b)}{A_a}K\left(\frac{A_a}{E_a+V_a}\right)^{2n}\left(\frac{C}{A_B}\right)^n \\
&\times N_a\left(\frac{2Z_A}{A_A}\right)^{2(Z_a+2)h_\pi+2p_\nu}\omega_{NT}(p_\pi, h_\pi, p_\nu, h_\nu, U)
\end{aligned}
\tag{12.64}
$$

where

$$
\begin{aligned}
C_a &= 5500 \text{ for incident neutrons,} \\
&= 3800 \text{ for incident charged particles,}
\end{aligned}
\tag{12.65}
$$

$$
\begin{aligned}
N_a &= \frac{1}{80E_a} \text{ for pickup,} \\
&= \frac{1}{580\sqrt{E_a}} \text{ for stripping,} \\
&= \frac{1}{1160\sqrt{E_a}} \text{ for exchange.}
\end{aligned}
\tag{12.66}
$$

K is an enhancement factor taking into account the fact that d, t and 3-He are loosely bound:

$$
\begin{aligned}
K &= 12 \ \text{ for } \ (N,\alpha), \\
&= 12 - 11\frac{E_a - 20}{E_a} \ \text{ for } \ (\alpha,N) \ \text{ and } \ E_a > 20, \\
&= 1 \ \text{ otherwise,}
\end{aligned}
\tag{12.67}
$$

where N stands for either neutron or proton. The well depth V_a is set at

$$
V_a = 12.5 A_a \ \text{MeV,}
\tag{12.68}
$$

and represents the average potential drop seen by the projectile between infinity and the Fermi level. The possible degrees of freedom for the reaction are all included in the residual state density $\omega_{NT}(p_\pi, h_\pi, p_\nu, h_\nu, U)$. Since we do not use this model to describe exchange reactions in inelastic scattering, there is no need to sum the various terms of Eq. (12.64) over p_π, as in Ref. [109]. The exciton numbers are automatically determined by the transfer reaction, i.e. $n = |A_a - A_b|$, $n_\pi = h_\pi = |Z_a - Z_b|$, $n_\nu = h_\nu = |N_a - N_b|$, $p_\pi = p_\nu = 0$. The accessible state density that is directly determined by the reaction is $\omega(p_\pi, h_\pi, p_\nu, h_\nu, U)$, given by Eq. (12.4). The total residual state density however also takes into account more complex configurations that can be excited by the transfer reaction. It is given by

$$
\omega_{NT}(p_\pi, h_\pi, p_\nu, h_\nu, U) = \sum_{i=0}^{3} \sum_{j=0}^{3-i} (X_{NT})^{i+j} \omega(p_\pi + i, h_\pi + i, p_\nu + j, h_\nu + j, U)
$$

$$
+ \ \sum_{i=0}^{p_\pi} \sum_{j=0}^{h_\pi} \sum_{k=0}^{p_\nu} \sum_{l=0}^{h_\nu} \omega(p_\pi - i, h_\pi - j, p_\nu - k, h_\nu - l, U) \Theta(i+j+k+l - \frac{1}{2})
\tag{12.69}
$$

The first term allows that up to three particle-hole pairs can be excited in a transfer reaction. The factor X_{NT} represents the probability for exciting such a pair and is given by

$$
X_{NT} = \frac{7\sqrt{E_a/A_a}}{V_1 A_A^2}(p_\nu^2 + p_\pi^2 + h_\nu^2 + 1.5 h_\pi^2)
\tag{12.70}
$$

For neutrons and protons we adopt for V_1 the value given by Eq.(12.11), for deuterons and tritons we take V_1=17 MeV, and for Helium-3 and alpha particles we take V_1=25 MeV. The finite well depth correction for Eq. (12.69) are made using a well depth of

$$
\begin{aligned}
V &= V_1 \left(\frac{2Z}{A}\right) \ \text{ if } \ n_\pi = 0 \\
&= V_1 \ \text{ otherwise.}
\end{aligned}
\tag{12.71}
$$

The second term of Eq. (12.69) allows for transfer of nucleons at the Fermi level. Here, the Heaviside function is merely used to avoid double counting of $\omega(p_\pi, h_\pi, p_\nu, h_\nu, U)$.

12.4.2 Knockout reactions

For $(nucleon, \alpha)$ reactions a knockout contribution is added. The general differential cross section formula for a knockout reaction of the type $A(a,b)B$ is

$$
\begin{aligned}
\frac{d\sigma_{a,b}^{KO}}{dE_b} &= \frac{\sigma_{a,inv}(E_a)}{14}(2s_b + 1)A_b E_b \sigma_{b,inv}(E_b) \\
&\times \ \frac{P_b g_a g_b [U - A_{KO}(p_a, h_b)]}{\sum_{c=a,b}(2s_c + 1)A_c \langle \sigma_c \rangle (E_{max} + 2B_{coul,c})(E_{max} - B_{coul,c})^2 g_a g_b^2 / 6g_c}
\end{aligned}
\tag{12.72}
$$

where P_b is the probability of exciting a b-type particle-hole pair, E_{max} is the maximum emission energy, and $B_{coul,c}$ is the Coulomb barrier for a particle c. The average inverse cross section $\langle \sigma_c \rangle$ is given by

$$\langle \sigma_c \rangle = \int_{B_{coul,c}}^{E_{max}} dE\, \sigma_c(E) \tag{12.73}$$

For the knockout model, the single-particle state density parameters for the cluster degrees of freedom g represent the number of cluster states per unit energy. The relevant values are given by

$$g_n = N/13, \quad g_p = Z/13, \quad g_\alpha = A/208 \text{ MeV}. \tag{12.74}$$

The Pauli correction factor A_{KO} is given by

$$A_{KO}(p_a, h_b) = \frac{1}{2g_a^2} - \frac{1}{2g_b^2} \tag{12.75}$$

The probabilities for exciting the various particle-hole pairs are

$$
\begin{aligned}
P_n &= \frac{N_A - \phi Z_A}{A_A - 2\phi Z_A + \phi Z_A/2} \\
P_p &= \frac{Z_A - \phi Z_A}{A_A - 2\phi Z_A + \phi Z_A/2} \\
P_\alpha &= \frac{\phi Z_A/2}{A_A - 2\phi Z_A + \phi Z_A/2}
\end{aligned} \tag{12.76}
$$

The factors ϕ are a kind of pre-formation parameters [109]. The following values are adopted

$$
\begin{aligned}
N_A &\leq 116 &:& \quad \phi = 0.08 \\
116 \leq N_A &< 126 &:& \quad \phi = 0.02 + 0.06(126 - N_A)/10 \\
126 \leq N_A &< 129 &:& \quad \phi = 0.02 + 0.06(N_A - 126)/3 \\
129 &\leq N_A &:& \quad \phi = 0.08
\end{aligned}
$$

$$\tag{12.77}$$

12.4.3 Break-up reactions

For reactions induced by complex particles, break-up may play an important role. This holds especially for weakly bound projectiles like deuterons. Break-up is here defined as having a projectile fragment emerge from the reaction in a relatively narrow peak centered close to the beam velocity and strongly directed toward forward angles. For deuterons only, a simple model by Kalbach has been included [110]. This leads to an extra contribution in the (d,n) and (d,p) channels.

The centroid energy of the breakup peak, in MeV, is given by

$$\varepsilon_0 = \frac{A_b}{A_a}\left(\varepsilon_a - B_{a,b} - \frac{Z_a Z_A}{9.5}\right) + \frac{Z_b Z_B}{9.5}, \tag{12.78}$$

where ε_a represents the channel energy (the energy of both the emitted particle and the recoiling nucleus in the center of mass), and $B_{a,b}$ is the binding energy in the projectile for the indicated breakup channel (2.224 MeV for deuterons). The peak is assumed to be described by a Gaussian line shape with a width parameter of

$$\Gamma = 1.15 + 0.12 E_a - \frac{A_A}{140}, \tag{12.79}$$

where E_a is the laboratory energy of the incident deuteron, and the width parameter is given in MeV. The break-up cross section is assumed to be

$$\sigma_{BU} = K_{d,b} \frac{(A_A^{1/3} + 0.8)^2}{1 + \exp(\frac{13 - E_a}{6})}, \tag{12.80}$$

where the normalization factors are

$$
\begin{aligned}
K_{d,n} &= 18, \\
K_{d,p} &= 21.
\end{aligned}
\tag{12.81}
$$

Finally, the differential break-up cross section is given by

$$\frac{d\sigma_{a,b}^{BU}}{dE_b} = \sigma_{BU} \frac{1}{\Gamma\sqrt{2\pi}} \exp\left(-\frac{(\varepsilon_0 - E_b)^2}{\Gamma^2} \right). \tag{12.82}$$

In the output, we have stored the break-up contribution in the column "knockout" (which is normally only used for nucleon-induced reactions with alpha particles as ejectiles).

> **Options 12.4.1** With **preeqcomplex** (p. 601) the various complex particle pre-equilibrium contributions can be enabled. The stripping, pick-up, break-up and knock-out contributions can be adjusted with the **Cstrip** (p. 621), **Cbreak** (p. 623) and **Cknock** (p. 622) keywords.

12.5 Angular distribution systematics

A sound pre-equilibrium theory should, besides the angle-integrated spectra, also describe the smooth forward peaked angular distributions in the continuum. A physics method to do so has been included in TALYS (multi-step direct reactions, but only as a global collective-like method). Semi-classical models, such as the exciton model, have always had some problems to describe angular distributions (essentially because it is based on a compound-like concept instead of a direct one [111]). A powerful phenomenological method is given by Kalbach [112]. It is based on experimental information only and the insight that in general, a pre-equilibrium process consists of a forward peaked part (multi-step direct) and an isotropic part (multi-step compound), and that the angular distributions are fairly structureless and all look alike. The Kalbach formula for the double-differential cross section for a projectile a and an ejectile b is

$$\frac{d^2\sigma_{a,xb}}{dE_b d\Omega} = \frac{1}{4\pi} \left[\frac{d\sigma^{\text{PE}}}{dE_b} + \frac{d\sigma^{comp}}{dE_b} \right] \frac{a}{\sinh(a)} [\cosh(a\cos\Theta) + f_{MSD}(E_b)\sinh(a\cos\Theta)] \tag{12.83}$$

where $\frac{d\sigma^{\text{PE}}}{dE_b}$ and $\frac{d\sigma^{comp}}{dE_b}$ are the angle-integrated pre-equilibrium and compound spectra, respectively, and f_{MSD} is the so-called multi-step direct or pre-equilibrium ratio:

$$f_{MSD}(E_b) = \frac{d\sigma^{\text{PE}}}{dE_b} \bigg/ \left[\frac{d\sigma^{\text{PE}}}{dE_b} + \frac{d\sigma^{comp}}{dE_b} \right] \tag{12.84}$$

which thus increases from practically 0 at very low emission energy to 1 at the highest emission energies. Hence, once the angle-integrated spectra are known, the parameter a determines the

angular distribution. Kalbach parameterized it as

$$
\begin{aligned}
a(e'_a, e'_b) &= 0.04\frac{E_1 e'_b}{e'_a} + 1.8 \times 10^{-6}(\frac{E_1 e'_b}{e'_a})^3 + 6.7 \times 10^{-7} M_a m_b (\frac{E_3 e'_b}{e'_a})^4, \\
E_1 &= \min(e'_a, 130\text{MeV}) \\
E_3 &= \min(e'_a, 41\text{MeV}) \\
e'_b &= E_b + S_b \\
e'_a &= E_a + S_a. \\
M_a &= 1 \text{ for neutrons, protons, deuterons, tritons and Helium} - 3 \\
&= 0 \text{ for alpha's} \\
m_b &= 1 \text{ for protons, deuterons, tritons and Helium} - 3 \\
&= \frac{1}{2} \text{ for neutrons} \\
&= 2 \text{ for alpha's} \\
S_b &= 15.68(A_C - A_B) - 28.07\left[\frac{(N_C - Z_C)^2}{A_C} - \frac{(N_B - Z_B)^2}{A_B}\right] \\
&\quad - 18.56(A_C^{2/3} - A_B^{2/3}) + 33.22\left[\frac{(N_C - Z_C)^2}{A_C^{4/3}} - \frac{(N_B - Z_B)^2}{A_B^{4/3}}\right] \\
&\quad - 0.717\left[\frac{Z_C^2}{A_C^{1/3}} - \frac{Z_B^2}{A_B^{1/3}}\right] + 1.211\left[\frac{Z_C^2}{A_C} - \frac{Z_B^2}{A_B}\right] - I_b \\
I_d &= 2.225 \\
I_t &= 8.482 \\
I_h &= 7.718 \\
I_\alpha &= 28.296,
\end{aligned}
\tag{12.85}
$$

Here, E_a and E_b are the incident and the outgoing energy, respectively. The number M_a represents the incident particle, while m_b represents the outgoing particle, C is a label for the compound nucleus, B for the final nucleus and the Myers and Swiatecki mass formula [29] for spherical nuclides should be used here to determine the separation energy S. Finally I_b is the energy required to break the emitted particle up into its constituents.

Since we calculate the pre-equilibrium and compound cross sections explicitly (and actually only use f_{MSD} for ENDF-6 data libraries), Eq. (12.83) can be reduced to a formula for the double-differential pre-equilibrium cross section

$$
\frac{d^2\sigma_{a,xb}^{\text{PE}}}{dE_b d\Omega} = \frac{1}{4\pi}\frac{d\sigma^{\text{PE}}}{dE_b}\frac{a}{\sinh(a)}\exp(a\cos\Theta),
\tag{12.86}
$$

to which the isotropic compound angular distribution can be added. In sum, given the angle-integrated spectrum $\frac{d\sigma^{\text{PE}}}{dE_b}$ by some physics model, the double-differential cross section is returned quite simply and reasonably accurate by Eq. (12.86).

Sample case 12.1 **Continuum spectra at 63 MeV for Bi(n,xp)...Bi(n,xα)**
In this sample case, we calculate angle-integrated and double-differential particle spectra for 63 MeV neutrons on ^{209}Bi, see Ref. [113].

Case a: Default calculation

The following input file is used

```
#
# n-Bi209-preeq
#
# General
#
projectile n
element bi
mass 209
energy 63.
#
# Output
#
outpreequilibrium y
ddxmode 2
filespectrum n p d t h a
fileddxa p 20.
fileddxa p 70.
fileddxa p 110.
fileddxa d 20.
fileddxa d 70.
fileddxa d 110.
fileddxa t 20.
fileddxa t 70.
fileddxa t 110.
fileddxa h 20.
fileddxa h 70.
fileddxa h 110.
fileddxa a 20.
fileddxa a 70.
fileddxa a 110.
```

Note that we request that angle-integrated spectra for all particles are written on separate files through *filespectrum n p d t h a*. At 20, 70 and 110 degrees, we also ask for the double-differential spectrum for protons up to alpha-particles. The resulting files *pspec063.000.tot*, *pddx020.0.deg*, etc. are presented, together with experimental data, in Figs. 12.2 and 12.3.

The default results of case (a) for the proton spectra are a bit high. Therefore, as a second version of this sample case, we adjust a pre-equilibrium parameter and add the following to the input above:

```
#
# Parameters
#
M2constant 0.80
```
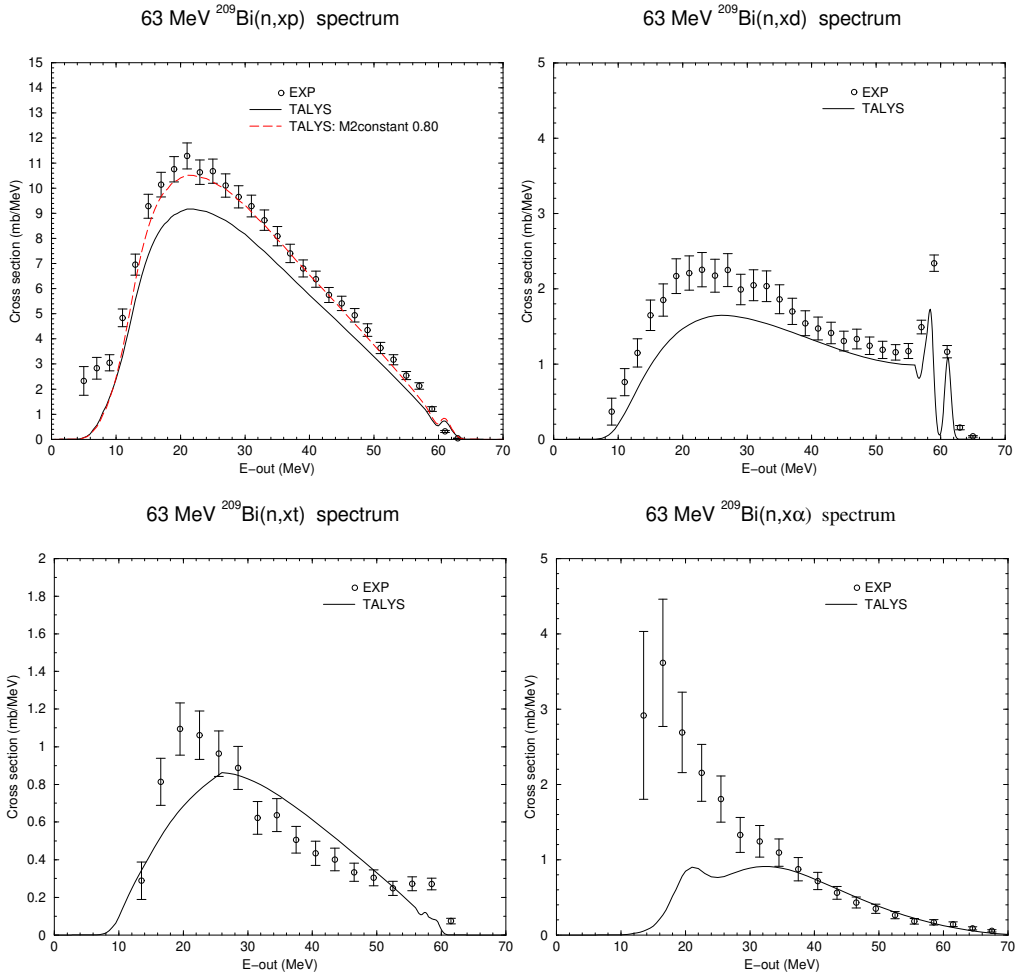
Figure 12.2: Angle-integrated proton, deuteron, triton and alpha emission spectra for 63 MeV neutrons on ^{209}Bi. The experimental data are from [113].

By decreasing **M2constant** by 20% (which is a common and acceptable deviation from the average), we favor the pre-equilibrium emission rate over the rate rate, leading to a harder spectrum. The result is shown in Fig. 12.2 for the proton spectrum.

■

Sample case 12.2 Pre-equilibrium angular dist. and multiple pre-equilibrium emission

At high incident energies, multiple pre-equilibrium reactions play a significant role. In this sample case, we show the results for this mechanism in the output file. Also, as an alternative to the previous sample case, we present another way of producing double-differential cross sections, namely as a function of angle at a fixed outgoing energy. With the following input file, the reaction of 120 MeV protons incident on ^{90}Zr is simulated:

```
#
# p-Zr090-preeq
#
```
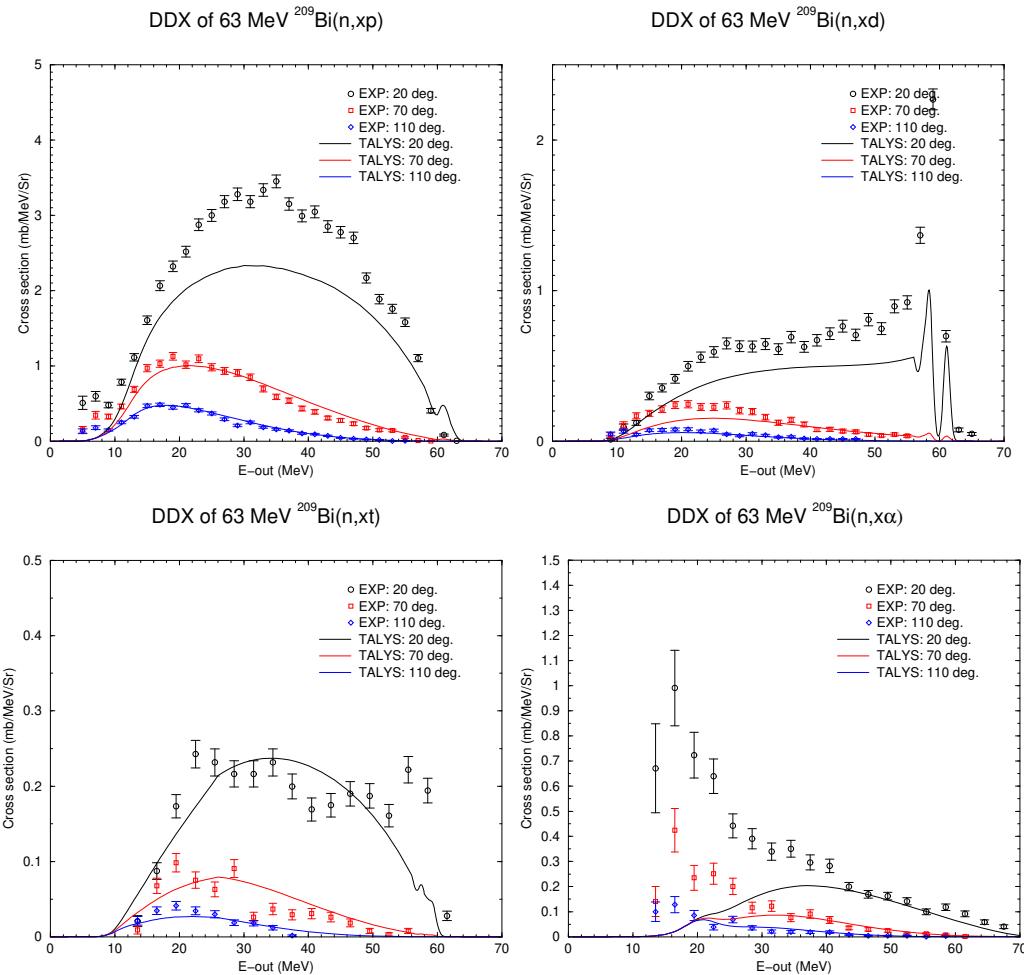
Figure 12.3: Double-differential proton, deuteron, triton and alpha emission spectra for 63 MeV neutrons on ^{209}Bi. The experimental data are from [113].

```
# General
#
projectile p
element zr
mass 90
energy 120.
#
# Output
#
outpreequilibrium y
outpopulation y
ddxmode 1
filespectrum n p
fileddxe p 20.
fileddxe p 40.
fileddxe p 60.
fileddxe p 80.
fileddxe p 100.
```

The results are presented in Figs. 12.4 and 12.5. For this sample case, since **outpopulation y**, after each print of the population for each residual nucleus (as already described in the first sample case), a block with multiple pre-equilibrium decay information is printed. This output block begins with

```
 Multiple preequilibrium emission from Z= 41 N= 49 ( 90Nb):


                                                          Feeding terms from

  bin    Ex  Mpe ratio  neutron    proton   1 1 0 0   0 0 1 1   1 0 0 1   0 1 1 0
                        emission  emission

   11    2.208 0.00000 0.000E+00 0.000E+00 0.000E+00 0.000E+00 5.287E-01 0.000E+00
   12    4.980 0.00000 0.000E+00 0.000E+00 0.000E+00 0.000E+00 1.249E+00 0.000E+00
   13    7.752 0.00000 0.000E+00 0.000E+00 0.000E+00 0.000E+00 1.961E+00 0.000E+00
   14   10.524 0.00001 0.000E+00 4.343E-05 0.000E+00 0.000E+00 2.645E+00 0.000E+00
   15   13.296 0.00555 3.214E-04 1.999E-02 0.000E+00 0.000E+00 3.300E+00 0.000E+00
   16   16.067 0.04999 5.901E-03 2.049E-01 0.000E+00 0.000E+00 3.928E+00 0.000E+00
   17   18.839 0.10870 2.305E-02 5.024E-01 0.000E+00 0.000E+00 4.527E+00 0.000E+00
   18   21.611 0.17335 5.014E-02 8.952E-01 0.000E+00 0.000E+00 5.098E+00 0.000E+00
.....................................
```

For each continuum bin, with excitation energy E_x, we print the fraction of the population that is emitted as multiple pre-equilibrium. Also the total neutron and proton emission per residual nucleus is printed, as well as the feeding terms from previous particle-hole configurations. With this input file, files *nspec120.000.tot* and *pspec120.000.tot* are created through the *filespectrum n p* keyword. The results are displayed in Fig. 12.4. Also, the combination of **ddxmode 1** and the various **fileddxe** keywords generate the *pddx100.0.mev*, etc. files that are compared with experimental data in Fig. 12.5.
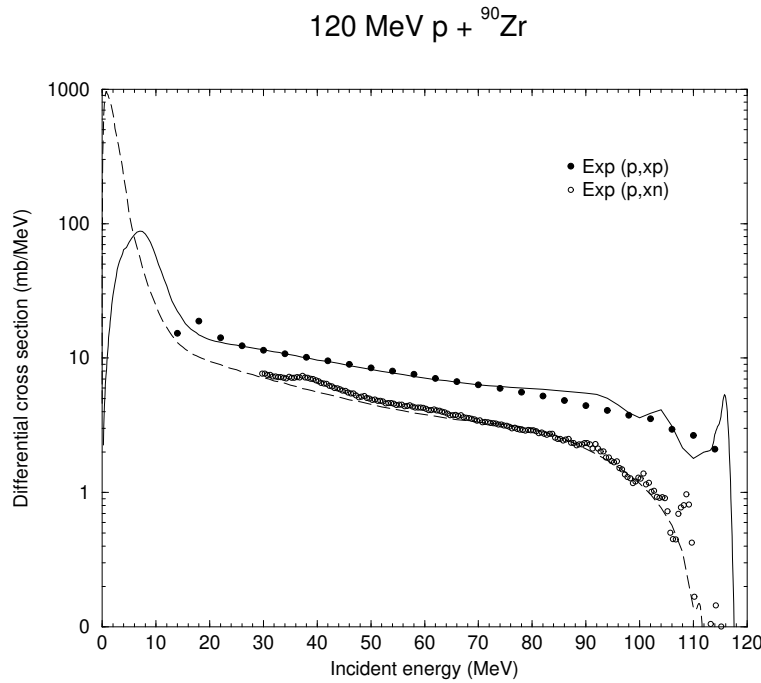
120 MeV p + ^{90}Zr

Figure 12.4: Angle-integrated (p,xn) and (p,xp) spectra for 120 MeV protons on ^{90}Zr. Experimental data are taken from [114, 115]

^{90}Zr(p,xp) at 120 MeV
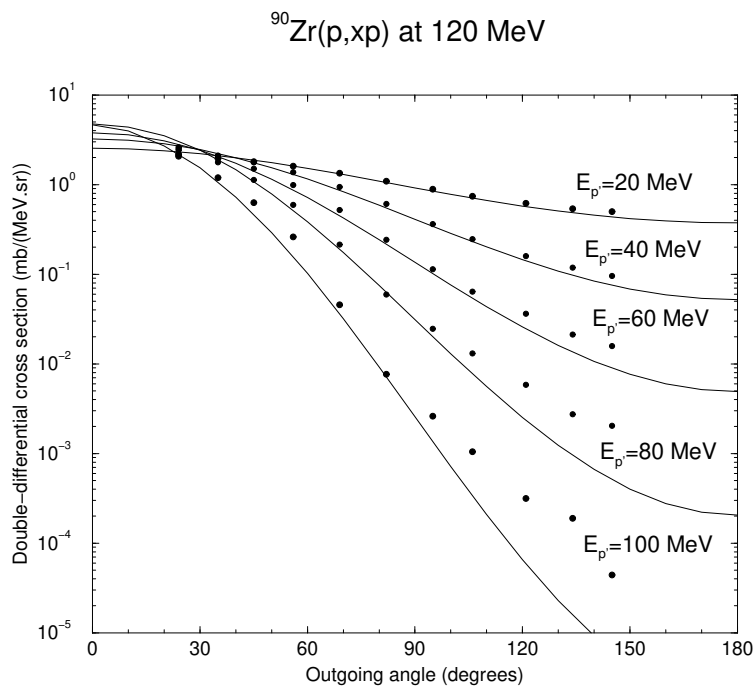
Figure 12.5: Double-differential (p,xp) spectra for 120 MeV protons on ^{90}Zr. Experimental data are taken from [114]

Sample case 12.3 **Calculations up to 500 MeV for p + ^{209}Bi**

In TALYS, the maximum allowed incident energy has formally been extended to 1 GeV. The term 'formally' means that the code seems to produce reasonable results, without crashing, while we are well aware that the physics beyond about 200 MeV is different from that at lower energies. The question is at which energy the "low-energy" models will start to fail. To investigate this, the extension to 1 GeV has been made. In this sample case we perform calculations for p + ^{209}Bi at 5 different energies,

```
#
# p-Bi209-500MeV
#
# General
#
projectile p
element bi
mass 209
energy 500.
bins 60
#
# To get excitation curves, create an energy range
# at the expense of longer computer times.
#
```

■

13. Compound reactions

The term compound nucleus reaction is commonly used for two different mechanisms: (i) the process of the capture of the projectile in the target nucleus to form a compound nucleus, which subsequently emits a particle or gamma, (ii) the multiple emission process of highly excited residual nuclei formed after the binary reaction. The latter, which is known as multiple compound emission, will be explained in Section 14. We first treat the binary compound nucleus reaction that plays a role at low incident energy. It differs from the multiple compound emission at two important points: (a) the presence of width fluctuation corrections and (b) non-isotropic, though still symmetric, angular distributions.

13.1 Binary compound cross section and angular distribution

In the compound nucleus picture, the projectile and the target nucleus form a compound nucleus with a total energy E^{tot} and a range of values for the total spin J and parity Π. The following energy, angular momentum and parity conservation laws need to be obeyed,

$$
\begin{aligned}
E_a + E_x + S_a &= E_{a'} + E_{x'} + S_{a'} = E^{tot} \\
s + I + l &= s' + I' + l' = J \\
\pi_0 \Pi_0 (-1)^l &= \pi_f \Pi_f (-1)^{l'} = \Pi.
\end{aligned}
\tag{13.1}
$$

The compound nucleus formula for the binary cross section is given by

$$
\begin{aligned}
\sigma_{\alpha\alpha'}^{comp} &= D^{comp} \frac{\pi}{k^2} \sum_{J=mod(I+s,1)}^{l_{max}+I+s} \sum_{\Pi=-1}^{1} \frac{2J+1}{(2I+1)(2s+1)} \sum_{j=|J-I|}^{J+I} \sum_{l=|j-s|}^{j+s} \sum_{j'=|J-I'|}^{J+I'} \sum_{l'=|j'-s'|}^{j'+s'} \\
&\times \ \delta_\pi(\alpha)\delta_\pi(\alpha') \frac{T_{\alpha l j}^{J}(E_a)\left\langle T_{\alpha'l'j'}^{J}(E_{a'})\right\rangle}{\sum_{\alpha'',l'',j''}\delta_\pi(\alpha'')\left\langle T_{\alpha''l''j''}^{J}(E_{a''})\right\rangle} W_{\alpha l j\alpha'l'j'}^{J},
\end{aligned}
\tag{13.2}
$$

In the above equations, the symbols have the following meaning:

$E_a =$ projectile energy

$s =$ spin of the projectile

$\pi_0 =$ parity of the projectile

$l =$ orbital angular momentum of the projectile

$j =$ total angular momentum of the projectile

$\delta_\pi(\alpha) =$ 1, if $(-1)^l \pi_0 \Pi_0 = \Pi$ and 0 otherwise

$\alpha =$ channel designation of the initial system of projectile and target nucleus:

$\quad\quad \alpha = \{a, s, E_a, E_x, I, \Pi_0\}$, where a is the projectile type

E_x excitation energy of the target nucleus (usually zero)

$l_{max} =$ maximum l-value for projectile

$S_a =$ separation energy

$E_{a'} =$ ejectile energy

$s' =$ spin of the ejectile

$\pi_f =$ parity of the ejectile

$l' =$ orbital angular momentum of the ejectile

$j' =$ total angular momentum of the ejectile

$\delta_\pi(\alpha') =$ 1, if $(-1)^{l'} \pi_f \Pi_f = \Pi$ and 0 otherwise

$\alpha' =$ channel designation of the final system of ejectile and residual nucleus:

$\quad\quad \alpha' = \{a', s', E_{a'}, E_{x'}, I', \Pi_f\}$, where a' is the ejectile type

$E_{x'}$ excitation energy of the residual nucleus

$I =$ spin of the target nucleus

$\Pi_0 =$ parity of the target

$I' =$ spin of the residual nucleus

$\Pi_f =$ parity of the residual nucleus

$\Pi =$ parity of the compound system

$J =$ total angular momentum of the compound system

$D^{comp} =$ depletion factor to account for direct and pre-equilibrium effects

$k =$ wave number of relative motion

$T =$ transmission coefficient

$W =$ width fluctuation correction (WFC) factor, see the next Section.

In order to let Eq. (13.2) represent the general case, we have denoted the outgoing transmission coefficient by $\left\langle T^J_{\alpha'l'j'} \right\rangle$. For this, two cases can be distinguished. If the excitation energy $E_{x'}$, that is implicit in the definition of channel α', corresponds to a discrete state of the final nucleus, then we simply have

$$\left\langle T^J_{\alpha'l'j'}(E_{a'}) \right\rangle = T^J_{\alpha'l'j'}(E_{a'}) \tag{13.3}$$

and $E'_{a'}$ is exactly determined by Eq. (13.1). For α' channels in which $E_{x'}$ is in the continuum, we have an effective transmission coefficient for an excitation energy bin with width $\Delta E_{x'}$,

$$\left\langle T^J_{\alpha'l'j'}(E_{a'}) \right\rangle = \int_{E_{x'}-\frac{1}{2}\Delta E_{x'}}^{E_{x'}+\frac{1}{2}\Delta E_{x'}} dE_{x''}\rho(E_{x''},J,\Pi)T^J_{\alpha'l'j'}(E_{a'}) \tag{13.4}$$

where ρ is the level density, see Chapter 8, and T is evaluated at an emission energy $E_{a'}$ that corresponds to the middle of the excitation energy bin, i.e. $E_{a'} = E^{tot} - E_{x'} - S_{a'}$. Hence, both transitions to discrete states and transitions to the whole accessible continuum are covered by the

sum over α' in Eq. (13.2). The normalization factor D^{comp} is

$$D^{comp} = [\sigma_{reac} - \sigma^{disc,direct} - \sigma^{PE}]/\sigma_{reac} \tag{13.5}$$

This indicates that in TALYS we assume that direct and compound contributions can be added incoherently. This formula for D^{comp} is only applied for weakly coupled channels that deplete the flux, such as contributions from DWBA or pre-equilibrium. In the case of coupled-channels calculations for the discrete collective states, the transmission coefficients of Eq. (13.2) are automatically reduced by ECIS-06 to account for direct effects and TALYS only subtracts the direct cross section for the weakly coupled levels (DWBA), i.e. if

$$\sigma^{disc,direct} = \sigma^{disc,cc} + \sigma^{disc,DWBA} \tag{13.6}$$

then

$$D^{comp} = [\sigma_{reac} - \sigma^{disc,DWBA} - \sigma^{PE}]/\sigma_{reac} \tag{13.7}$$

TALYS also computes the compound nucleus formula for the angular distribution. It is given by

$$\frac{d\sigma_{\alpha\alpha'}^{comp}(\theta)}{d\Omega} = \sum_L C_L^{comp} P_L(\cos\Theta), \tag{13.8}$$

where P_L are Legendre polynomials. The Legendre coefficients C_L^{comp} are given by

$$
\begin{aligned}
C_L^{comp} &= D^{comp}\frac{\pi}{k^2}\sum_{J,\Pi}\frac{2J+1}{(2I+1)(2s+1)}\sum_{j=|J-I|}^{J+I}\sum_{l=|j-s|}^{j+s}\sum_{j'=|J-I'|}^{J+I'}\sum_{l'=|j'-s'|}^{j'+s'} \\
&\times\ \delta_\pi(\alpha)\delta_\pi(\alpha')\frac{T_{\alpha l j}^J(E_a)\left\langle T_{\alpha'l'j'}^J(E_{a'})\right\rangle}{\sum_{\alpha'',l'',j''}\delta_\pi(\alpha'')\left\langle T_{\alpha''l''j''}^J(E_{a''})\right\rangle}W_{\alpha l j\alpha'l'j'}^J A_{Il jI'l'j';L}^J,
\end{aligned}
\tag{13.9}
$$

where the Blatt-Biedenharn factor A is given by

$$
A_{Il jI'l'j';L}^J = \frac{(-1)^{I'-s'-I+s}}{4\pi}(2J+1)(2j+1)(2l+1)(2j'+1)(2l'+1)
$$
$$
(ll00|L0)\,\mathcal{W}(JjJj;IL)\mathcal{W}(jjll;Ls)\,(l'l'00|L0)\,\mathcal{W}(Jj'Jj';I'L)\mathcal{W}(j'j'l'l';Ls'), \tag{13.10}
$$

where $(\ \ |\ )$ are Clebsch-Gordan coefficients and $\mathcal{W}$ are Racah coefficients.

Formulae (13.2) and (13.8-13.10) show that the width fluctuation correction factors and the angular distribution factors depend on all the angular momentum quantum numbers involved, and thus have to be re-evaluated each time inside all the summations. We generally need these formulae for relatively low incident energy, where the WFC has a significant impact and where the compound nucleus cross section to each individual discrete state is large enough to make its angular distribution of interest. For projectile energies above several MeV (we generally take the neutron separation energy for safety), the width fluctuations have disappeared, meaning that $W_{\alpha l j\alpha'l'j'}^J = 1$ for all channels. Then for the angle-integrated compound cross section, instead of performing the full calculation, Eq. (13.2) can be decoupled into two parts that represent the incoming and outgoing reaction flux, respectively. It simplifies to

$$\sigma_{\alpha\alpha'}^{comp} = \sum_{J=mod(I+s,1)}^{l_{max}+I+s}\sum_{\Pi=-1}^{1}\sigma_{J\Pi}^{CF}(E^{tot})\frac{\Gamma_{\alpha'}(E^{tot},J,\Pi\longrightarrow E_{x'},I',\Pi_f)}{\Gamma^{tot}(E^{tot},J,\Pi)} \tag{13.11}$$

where $\sigma_{J\Pi}^{CF}$ is the compound formation cross section per spin and parity:

$$\sigma_{J\Pi}^{CF}(E^{tot}) = D^{comp}\frac{\pi}{k^2}\frac{2J+1}{(2I+1)(2s+1)}\sum_{j=|J-I|}^{J+I}\sum_{l=|j-s|}^{j+s} T_{\alpha l j}^J(E_a)\delta_\pi(\alpha) \quad (13.12)$$

which itself obeys

$$\sum_{J=mod(I+s,1)}^{l_{max}+I+s}\sum_{\Pi=-1}^{1}\sigma_{J\Pi}^{CF}(E^{tot}) = D^{comp}\sigma_{reac} \quad (13.13)$$

The partial decay widths are

$$\Gamma_{\alpha'}(E^{tot},J,\Pi\longrightarrow E_{x'},I',\Pi_f) = \frac{1}{2\pi\rho(E^{tot},J,\Pi)}\sum_{j'=|J-I'|}^{J+I'}\sum_{l'=|j'-s'|}^{j'+s'}\delta_\pi(\alpha')\left\langle T_{\alpha'l'j'}^J(E_{a'}')\right\rangle \quad (13.14)$$

and the total decay width is

$$\Gamma^{tot}(E^{tot},J,\Pi) = \sum_{\alpha''}\Gamma_{\alpha''}(E^{tot},J,\Pi\longrightarrow E_{x'},I'',\Pi_f) \quad (13.15)$$

where we sum over all possible states in the residual nuclides through the sum over α''. Note that the term with the compound nucleus level density, $2\pi\rho$, is present in both Eq. (13.14) and Eq. (13.15) and therefore does not need to be calculated in practice for Eq. (13.11). A formula similar to Eq. (13.11) is used for multiple emission, see Section 14.

In sum, we use Eqs. (13.2) and (13.9) if either width fluctuations (**widthfluc y**, (p. 573) or compound angular distributions (**outangle y**, (p. 558) are to be calculated and Eq. (13.11) if they are both not of interest.

A final note to make here is that the formulae of this whole Section can also be applied for excited (isomeric) target states.

13.2 Width fluctuation correction factor

The WFC factor W accounts for the correlations that exist between the incident and outgoing waves. From a qualitative point of view, these correlations enhance the elastic channel and accordingly decrease the other open channels. Above a few MeV of projectile energy, when many competing channels are open, the WFC factor can be neglected and the simple Hauser-Feshbach model is adequate to describe the compound nucleus decay. To explain the WFC factors, we now switch to a more compact notation in which we leave out J and define $a = \{\alpha, l, j\}$ and $b = \{\alpha', l', j'\}$. With such a notation the compound nucleus cross section can be written in the compact form

$$\sigma_{ab} = \frac{\pi}{k_a^2}\frac{T_a T_b}{\sum_c T_c}W_{ab} \quad (13.16)$$

for each combination of a and b. In general, the WFC factor may be calculated using three different expressions, which have all been implemented in TALYS: The Hofmann-Richert-Tepel-Weidenmüller (HRTW) model [116, 117, 118], the Moldauer model [119, 120], and the model using the Gaussian Orthogonal Ensemble (GOE) of Hamiltonian matrices [121]. A comparison between the three models is given by Hilaire et al. [122].

For each expression, flux conservation implies that

$$T_a = \sum_b \frac{T_a T_b}{\sum_c T_c}W_{ab} \quad (13.17)$$

This equation can be used to check the numerical accuracy of the WFC calculation (see the **flagcheck** keyword in Part III).

13.2.1 The HRTW method

The simplest approach is the HRTW method. It is based on the assumption that the main effect of the correlation between incident and outgoing waves is in the elastic channel. In that case, it is convenient to express the compound nucleus cross section (13.16) as

$$\sigma_{ab} = \frac{\pi}{k^2} \frac{V_a V_b}{\sum_c V_c} \left[1 + \delta_{ab}(W_a - 1) \right], \tag{13.18}$$

where the V_i's are effective transmission coefficients that take into account the correlations.

This expression means that only the elastic channel enhancement is described since for $a = b$, Eq. (13.18) becomes

$$\sigma_{aa} = \frac{\pi}{k_a^2} \frac{V_a^2}{\sum_c V_c} W_a \tag{13.19}$$

while for $a \neq b$,

$$\sigma_{ab} = \frac{\pi}{k_a^2} \frac{V_a V_b}{\sum_c V_c} \tag{13.20}$$

An expression for the V_i values can be determined from the flux conservation condition

$$\sum_b \sigma_{ab} = \frac{\pi}{k_a^2} T_a, \tag{13.21}$$

which yields using Eq. (13.18)

$$T_a = V_a + (W_a - 1) \frac{V_a^2}{\sum_c V_c}, \tag{13.22}$$

or

$$V_a = \frac{T_a}{1 + \frac{(W_a - 1)V_a}{\sum_c V_c}}. \tag{13.23}$$

The only required information is thus the expression for W_a, which can be derived from an analysis using random matrix calculations. In TALYS, the expression of Ref. [118] is used. It reads

$$W_a = 1 + \frac{2}{1 + T_a^F} + 87 \left(\frac{T_a - \overline{T}}{\sum_c T_c} \right)^2 \left(\frac{T_a}{\sum_c T_c} \right)^5, \tag{13.24}$$

with $\overline{T} = \dfrac{\sum_c T_c^2}{\sum_c T_c}$ and the exponent $F = \dfrac{4\dfrac{\overline{T}}{\sum_c T_c}\left(1 + \dfrac{T_a}{\sum_c T_c}\right)}{1 + \dfrac{3\overline{T}}{\sum_c T_c}}.$

The result for V_a is obtained after iterating Eq. (13.23) several times, starting from the initial value

$$V_a(i = 0) = \frac{T_a}{1 + (W_a - 1)\dfrac{T_a}{\sum_c T_c}} \tag{13.25}$$

and calculating $V_a(i+1)$ using

$$V_a(i+1) = \frac{T_a}{1 + (W_a - 1)\dfrac{V_a(i)}{\sum_c V_c(i)}} \tag{13.26}$$

until $V_a(i+1) \approx V_a(i)$. In a calculation, a few tens of iterations are generally required to reach a stable result.

For each J and Π, expressions (13.23)-(13.26) only need to be evaluated once. This is done in *hrtwprepare.f*, before all the loops over l, j, l' and j', etc. quantum numbers are performed. For the calculation of $W^J_{\alpha l j \alpha' l' j'}$ in Eq. (13.2), which takes place inside all loops, the correct V_a and V_b are then addressed. The WFC factor can then be derived from Eqs. (13.16) and (13.18),

$$W_{ab} = \frac{V_a V_b}{\sum_c V_c} [1 + \delta_{ab}(W_a - 1)] \frac{\sum_c T_c}{T_a T_b} \tag{13.27}$$

which is calculated in *hrtw.f*.

13.2.2 Moldauer expression

This is the default option for the WFC in TALYS. Moldauer's expression for W_{ab} is based on the assumption that a χ^2 law with ν degrees of freedom applies for the partial widths Γ, which can be calculated from a Porter-Thomas distribution. These are associated with transmission coefficients as

$$T = \frac{2\pi \langle \Gamma \rangle}{D} \tag{13.28}$$

provided $\langle \Gamma \rangle << D$, where D is the mean level spacing. The WFC factor W_{ab} reads

$$W_{ab} = \left(1 + \frac{2\delta_{ab}}{\nu_a}\right) \int_0^{+\infty} \prod_c \left(1 + \frac{2T_c x}{\nu_c \sum_i T_i}\right)^{-(\delta_{ac} + \delta_{bc} + \nu_c/2)} dx \tag{13.29}$$

Moldauer has parameterised ν using Monte Carlo calculations, giving

$$\nu_a = 1.78 + \left(T_a^{1.212} - 0.78\right) \exp\left(-0.228 \sum_c T_c\right) \tag{13.30}$$

In TALYS, the integral in Eq. (13.29) is evaluated numerically. For this, the Gauss-Laguerre method has been chosen and we find that 40 integration points are enough to reach convergence, the criterion being the flux conservation of Eq. (13.17). As for the HRTW model, the calculation can be split into parts dependent and independent of the channel quantum numbers. First, in *molprepare.f*, for each J and Π, we calculate Eq. (13.30) for all channels and the product $\prod_c \left(1 + \frac{2T_c x}{\nu_c \sum_i T_i}\right)^{-\nu_c/2}$ that appears in Eq. (13.29). Inside all the loops, we single out the correct a and b channel and calculate Eq. (13.29) in *moldauer.f*.

Eq. (13.29) involves a product over all possible open channels. When the number of channels is large, the product calculation drastically increases the time of computation, forcing us to consider another method. Many open channels are considered for capture reactions and reactions to the continuum.

A. Capture reactions

If the projectile is captured by the target nucleus, the compound nucleus is formed with an excitation energy at least equal to the projectile separation energy in the compound system. Since the γ transmission coefficient calculation involves all the possible states to which a photon can be emitted from the initial compound nucleus state, the number of radiative open channels is almost infinite, but each has a very small transmission coefficient. Following Ref. [123], the product over the radiative channels in Eq. (13.29) can be transformed as

$$
\prod_{c \in \gamma} \left(1 + \frac{2T_c x}{v_c \sum_i T_i} \right)^{-v_c/2} \approx \lim_{v_\gamma \to +\infty} \left(1 + \frac{2T_\gamma x}{\bar{v}_\gamma \sum_i T_i} \right)^{-\bar{v}_\gamma/2} = \exp \left(-\frac{T_\gamma^{eff} x}{\sum_i T_i} \right) \tag{13.31}
$$

where T_γ^{eff} is given by the procedure sketched in Section 9. The derivation is based on the hypothesis that all the individual T_γ are almost identical to 0. Therefore, to calculate W_{ab} when b denotes the gamma channel, we set $T_b = 0$ in Eqs. (13.29) and use Eqs. (13.31) to calculate the product for γ channels.

B. Continuum reactions

For high excitation energies, it is impossible to describe all the open channels individually. It is then necessary to introduce energy bins to discretize the continuum of levels and define continuum (or effective) transmission coefficients as

$$
T_{eff}(U) = \int_{E_{min}}^{E_{max}} \rho(\varepsilon) T(\varepsilon) d\varepsilon, \tag{13.32}
$$

where U is generally taken as the middle of the interval $[E_{min}, E_{max}]$ and ρ is the density of levels under consideration. This effective transmission coefficient corresponds to an effective number of channels $N_{eff}(U)$, given by

$$
N_{eff}(U) = \int_{E_{min}}^{E_{max}} \rho(\varepsilon) d\varepsilon. \tag{13.33}
$$

Calculating the product term in Eq. (13.29) is tedious, unless one assumes that the energy variation of $T(\varepsilon)$ is smooth enough to warrant that each of the $N_{eff}(U)$ channels has the same average transmission coefficient

$$
T_{mean}(U) = \frac{T_{eff}(U)}{N_{eff}(U)}. \tag{13.34}
$$

Then, the product over the channels c belonging to such a continuum bin in the Moldauer integral Eq. (13.29) can be replaced by a single term, i.e.

$$
\prod_c \left(1 + \frac{2T_c}{v_c \sum_i T_i} x \right)^{-v_c/2} \approx \left(1 + \frac{2T_{mean}(U)}{v_{mean} \sum_i T_i} x \right)^{-N_{eff}(U) v_{mean}/2}, \tag{13.35}
$$

where

$$
v_{mean} = 1.78 + \left(T_{mean}^{1.212} - 0.78 \right) \exp \left(-0.228 \sum_c T_c \right) \tag{13.36}
$$

C. Fission reactions

The fission reaction is treated as one global channel, regardless of the nature of the fission fragments that result from fission. In Chapter 15, it is explained how the global fission transmission coefficient is calculated. It is however important to state here that the fission transmission coefficient is generally greater than 1 since it results from a summation over several fission paths and can therefore be defined as

$$T_{fis}(U) = \int_{E_{min}}^{E_{max}} \rho_{fis}(\varepsilon) T_f(\varepsilon) d\varepsilon. \tag{13.37}$$

Of course, one has $0 \leq T_f(\varepsilon) \leq 1$, but one can not assume that T_f is constant over the whole integration energy range as in the case of continuum reactions. To bypass this problem, instead of using a global fission transmission coefficient, we have grouped the various components of Eq. (13.37) according to their values. Instead of dealing with a global fission transmission coefficient, we use N different global transmission coefficients (where N is an adjustable parameter) such that

$$T_{fis}(U) = \sum_{i=0}^{N} T_{fis}(i,U) \tag{13.38}$$

where

$$T_{fis}(i,U) = \int_{E_{min}}^{E_{max}} \rho_{fis}(\varepsilon) T_f(\varepsilon) \delta_{i,N} d\varepsilon \tag{13.39}$$

and $\delta_{i,N} = 1$ is $i/N \leq T_f(\varepsilon) \leq (i+1)/N$ and 0 otherwise.

In this case one can define, as for continuum reactions, an effective number of channels $N_{fis}(i,U)$, and use N average fission transmission coefficients defined by

$$T_{fismean}(i) = \frac{T_{fis}(i,U)}{N_{fis}(i,U)}. \tag{13.40}$$

If N is large enough, these N average coefficients can be used for the width fluctuation calculation without making a too crude approximation.

13.2.3 The GOE triple integral

The two previously described methods to obtain W_{ab} are readily obtained since both are relatively simple to implement. However, in each case, a semi-empirical parameterisation is used. The GOE formulation avoids such a parameterisation, in which sense it is the more general expression. In the GOE approach, W_{ab} reads

$$W_{ab} = \frac{\sum_c T_c}{8} \int_0^{+\infty} d\lambda_1 \int_0^{+\infty} d\lambda_2 \int_0^1 d\lambda \ f(\lambda_1,\lambda_2,\lambda) \prod_c (\lambda_1,\lambda_2,\lambda) \ g_{ab}(\lambda_1,\lambda_2,\lambda) \tag{13.41}$$

with

$$f(\lambda_1,\lambda_2,\lambda) = \frac{\lambda(1-\lambda)|\lambda_1 - \lambda_2|}{\sqrt{\lambda_1 \lambda_2 (1+\lambda_1)(1+\lambda_2)}(\lambda+\lambda_1)^2(\lambda+\lambda_2)^2}, \tag{13.42}$$

$$\prod_c(\lambda_1, \lambda_2, \lambda) = \prod_c \frac{1 - \lambda \, T_c}{\sqrt{(1 + \lambda_1 T_c)(1 + \lambda_2 T_c)}}, \tag{13.43}$$

and

$$g_{ab} \; (\lambda_1, \lambda_2, \lambda) = \delta_{ab}(1 - T_a)\left(\frac{\lambda_1}{1 + \lambda_1 T_a} + \frac{\lambda_2}{1 + \lambda_2 T_a} + \frac{2\lambda}{1 - \lambda T_a}\right)^2 + (1 + \delta_{ab})$$
$$\times \left[\frac{\lambda_1(1 + \lambda_1)}{(1 + \lambda_1 T_a)(1 + \lambda_1 T_b)} + \frac{\lambda_2(1 + \lambda_2)}{(1 + \lambda_2 T_a)(1 + \lambda_2 T_b)} + \frac{2\lambda(1 - \lambda)}{(1 - \lambda T_a)(1 - \lambda T_b)}\right] \tag{13.44}$$

The numerical method employed to compute this complicated triple integral is explained by Hilaire et al. [122].

Also here, a particular situation exists for the capture channel, where we set

$$\prod_{c \in \gamma} \frac{1 - \lambda \, T_c}{\sqrt{(1 + \lambda_1 T_c)(1 + \lambda_2 T_c)}} \approx \exp\left[-(2\lambda + \lambda_1 + \lambda_2)\, T_\gamma^{eff}/2\right] \tag{13.45}$$

and for the continuum, for which we set

$$\prod_c(\lambda_1, \lambda_2, \lambda) = \prod_{c \in continuum} \frac{(1 - \lambda \, \bar{T}_c)^{N_c}}{\sqrt{(1 + \lambda_1 \bar{T}_c)^{N_c}(1 + \lambda_2 \bar{T}_c)^{N_c}}}. \tag{13.46}$$

Again, for each J and Π, the multiplications that do not depend on a or b are first prepared in *goeprepare.f*, while the actual WFC calculation takes place in *goe.f*.

Options 13.2.1 With **widthfluc** (p. 573 the WFC calculation can be enabled and disabled. The various WFC models can be set with **widthmode** (574).

Sample case 13.1 **Comparison of compound nucleus WFC models: 10 keV n + ^{93}Nb**
In this sample case, we demonstrate the difference between the various models for the width fluctuation correction in compound nucleus reactions, as discussed extensively in Ref. [122]. As sample case, we take 10 keV neutrons incident on ^{93}Nb and we ask for various compound nucleus models to calculate cross sections and angular distributions (**outangle y**), and to put the result for the elastic scattering angular distribution on a separate file, called *nn000.010ang.L00*. Since the GOE calculation (**widthmode 3**) is rather time-consuming, we reduce the number of bins to 20 for all cases. We wish to check whether the flux is conserved in the compound nucleus model for the various WFC models, so we set **outcheck y**. This means that for each set of quantum numbers, unitarity is checked by means of Eq. (13.17).

This sample case illustrates the capabilities of TALYS to simulate photonuclear reactions. We calculate the (γ,n) reaction on ^{90}Zr as a function of incident energy, with default model parameters, and compare the result to experimental data. The following input file is used

```
#
# n-Nb093-HF
#
# General
#
projectile n
element nb
mass 93
```

Model	$\sigma^{comp-el}$
Hauser-Feshbach	2410.89 mb
Moldauer	2617.22 mb
HRTW	2752.25 mb
GOE	2617.12 mb

Table 13.1: Compound elastic cross section for 4 different compound nucleus models for 10 keV neutrons incident on ^{93}Nb.

```
energy 0.01
#
# Parameters
#
bins 20
widthmode 0
#
# Output
#
outcheck y
outangle y
fileelastic y
```

This only new output block, i.e. not discussed before, is

```
++++++++++ CHECK OF FLUX CONSERVATION OF TRANSMISSION COEFFICIENTS ++++++++++
Hauser-Feshbach model

Parity=-  J= 3.0  j= 1.5  l= 1  T(j,l)= 7.98822E-03  Sum over outgoing channels
Parity=-  J= 4.0  j= 0.5  l= 1  T(j,l)= 4.54100E-03  Sum over outgoing channels
Parity=-  J= 4.0  j= 1.5  l= 1  T(j,l)= 7.98822E-03  Sum over outgoing channels
Parity=-  J= 5.0  j= 0.5  l= 1  T(j,l)= 4.54100E-03  Sum over outgoing channels
Parity=-  J= 5.0  j= 1.5  l= 1  T(j,l)= 7.98822E-03  Sum over outgoing channels
Parity=-  J= 6.0  j= 1.5  l= 1  T(j,l)= 7.98822E-03  Sum over outgoing channels
....................................
```

in which the aforementioned unitarity is checked. For the Moldauer model the above input file has **widthmode 1** For the HRTW model the above input file has **widthmode 2**. For the GOE model the above input file has **widthmode 3**.

Table 13.1 lists the obtained compound nucleus elastic cross section for the 4 cases.

Fig. 13.1 displays the elastic angular distribution for the 4 models. Results like these made us conclude in Ref. [122] that Moldauer's model, which is closest to the exact GOE result, is the one to use in practical applications, especially when considering the long calculation time of the GOE model. Obviously, this sample case can be extended to one with various incident energies, so that the differences between excitation functions can be studied, see also Ref. [122].
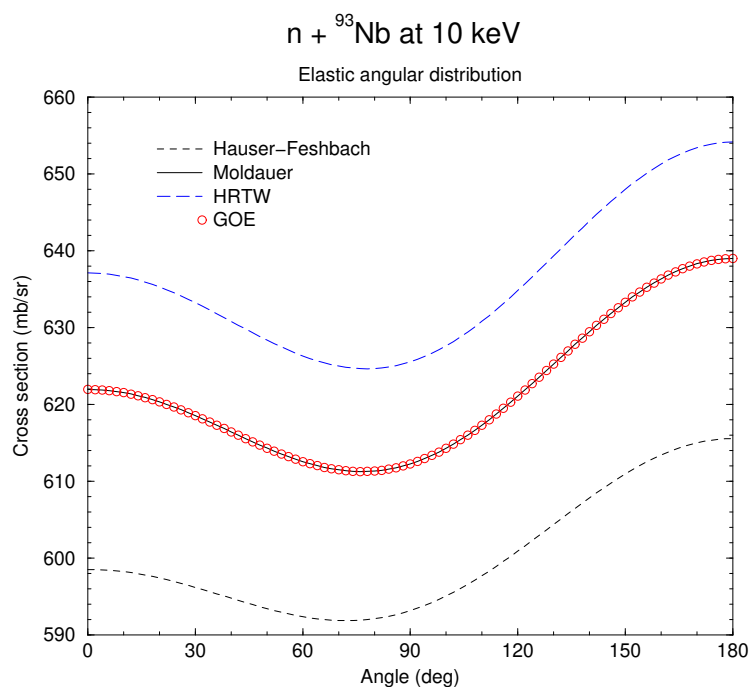
Figure 13.1: Total elastic angular distribution for 4 different compound nucleus models for 10 keV neutrons incident on ^{93}Nb.

14. Multiple emission

At incident energies above approximately the neutron separation energy, the residual nuclides formed after the first binary reaction are populated with enough excitation energy to enable further decay by particle emission or fission. This is called multiple emission. We distinguish between two mechanisms: multiple compound (Hauser-Feshbach) decay, which comes important as soon as the incident energy is higher than the neutron separation energy and multiple pre-equilibrium decay,which becomes important above 30-40 MeV of incident energy.

14.1 Multiple Hauser-Feshbach decay

This is the conventional way, and for incident energies up to several tens of MeV a sufficient way, to treat multiple emission. It is assumed that pre-equilibrium processes can only take place in the binary reaction and that secondary and further particles are emitted by compound emission.

After the binary reaction, the residual nucleus may be left in an excited discrete state i' or an excited state within a bin i' which is characterized by excitation energy $E'_x(i')$, spin I' and parity Π'. The population of this state or set of states is given by a probability distribution for Hauser-Feshbach decay P^{HF} that is completely determined by the binary reaction mechanism. For a binary neutron-induced reaction to a discrete state i', i.e. when $E_{x'}(i'), I'$ and Π' have unique values, the residual population is given by

$$P^{\mathrm{HF}}(Z',N',E_{x'}(i'),I',\Pi') = \sigma_{n,k'}^{i'}(E^{tot},I,\Pi \to E_{x'}(i'),I',\Pi'), \tag{14.1}$$

where the non-elastic reaction cross section for a discrete state $\sigma_{n,k'}^{i'}$ was defined in Section 4.2.3 and where the ejectile k' connects the initial compound nucleus (Z_C,N_C) and the residual nucleus (Z',N'). For binary reactions to the continuum, the residual population of states characterised by

(I', Π') per $E_{x'}(i')$ bin is given by the sum of a pre-equilibrium and a compound contribution

$$P^{\mathrm{HF}}(Z', N', E_{x'}(i'), I', \Pi') = \int dE_{k'} \frac{d\sigma^{comp,cont}}{dE_{k'}}(E^{tot}, I, \Pi \to E_{x'}(i'), I', \Pi')$$
$$+ \quad \mathscr{P}^{\mathrm{pre}}(Z', N', p_\pi^{max}+1, h_\pi^{max}+1, p_\nu^{max}+1, h_\nu^{max}+1, E_{x'}(i')), \qquad (14.2)$$

where the integration range over $dE_{k'}$ corresponds exactly with the bin width of $E_x'(i')$ and $\mathscr{P}^{\mathrm{pre}}$ denotes the population entering the compound stage after primary preequilibrium emission. The expression for $\mathscr{P}^{\mathrm{pre}}$ will be given in Eq. (14.6) of the next section. Once the first generation of residual nuclides/states has been filled, the picture can be generalized to tertiary and higher order multiple emission.

In general, the population P^{HF} before decay of a level i' or a set of states $(I', \Pi', E_{x'}(i'))$ in bin i' of a nucleus (Z', N') in the reaction chain is proportional to the feeding, through the ejectiles k', from all possible mother bins i with an energy $E_x(i)$ in the (Z, N) nuclides, i.e.

$$P^{\mathrm{HF}}(Z', N', E_{x'}(i'), I', \Pi') = \sum_{I,\Pi} \sum_{k'} \sum_{i} [P^{\mathrm{HF}}(Z, N, E_x(i), I, \Pi)$$
$$+ \quad \mathscr{P}^{\mathrm{pre}}(Z, N, p_\pi^{max}+1, h_\pi^{max}+1, p_\nu^{max}+1, h_\nu^{max}+1, E_x(i))]$$
$$\times \quad \frac{\Gamma_{k'}(E_x(i), I, \Pi \to E_{x'}(i'), I', \Pi')}{\Gamma^{tot}(E_x(i), I, \Pi)}. \qquad (14.3)$$

The appearance of the indices p_π^{max} indicates that only the reaction population that has not been emitted via the (multiple) pre-equilibrium mechanism propagates to the multiple compound stage. Similar to Eq. (13.14) the decay widths are given by

$$\Gamma_{k'}(E_x(i), I, \Pi \longrightarrow E_{x'}(i'), I', \Pi') = \frac{1}{2\pi\rho(E_x(i), I, \Pi)} \sum_{j'=|J-I'|}^{J+I'} \sum_{l'=|j'-s'|}^{j'+s'} \delta_\pi(\alpha') \left\langle T^J_{\alpha'l'j'}(E'_{a'}) \right\rangle. \quad (14.4)$$

Again, the term $2\pi\rho$ (compound nucleus level density) of the decay width (14.4) falls out of the multiple emission equation (14.3) and therefore does not need to be calculated in practice. The total decay width is

$$\Gamma^{tot}(E_x(i), I, \Pi) = \sum_{k''} \sum_{I''=mod(J+s,1)}^{J+l_{max}} \sum_{\Pi''=-1}^{1} \sum_{i''} \Gamma_{k''}(E_x(i), I, \Pi \longrightarrow E_{x''}(i''), I'', \Pi''). \qquad (14.5)$$

In sum, the only differences between binary and multiple compound emission are that width fluctuations and angular distributions do not enter the model and that the initial compound nucleus energy E^{tot} is replaced by an excitation energy bin E_x of the mother nucleus. The calculational procedure, in terms of sequences of decaying bins, was already explained in Chapter 4.

Options 14.1.1 With **maxZ** (p. 300) and **maxZ** (p. 300) you can set how many residual nuclides are taken into account.

14.2 Multiple pre-equilibrium emission

At high excitation energies, resulting from high incident energies, the composite nucleus is far from equilibrated and it is obvious that the excited nucleus should be described by more degrees of freedom than just E_x, J and Π. In general, we need to keep track of the particle-hole configurations that are excited throughout the reaction chain and thereby calculate multiple pre-equilibrium emission up to any order. This is accomplished by treating multiple pre-equilibrium emission

within the exciton model. This is the default option for multiple pre-equilibrium calculations in TALYS (selected with the keyword **mpreeqmode 1**). TALYS contains, furthermore, an alternative more approximative model for multiple pre-equilibrium emission (**mpreeqmode 2**), called the *s-wave transmission coefficient method*. Both approaches are discussed below.

14.2.1 Multiple pre-equilibrium emission within the exciton model

We introduce the pre-equilibrium population $\mathscr{P}^{\text{pre}}(Z,N,p_\pi,h_\pi,p_\nu,h_\nu,E_x(i))$ which holds the amount of the reaction population present in a unique (Z,N) nucleus, $(p_\pi,h_\pi,p_\nu,h_\nu)$ exciton state and excitation energy bin $E_x(i)$. A special case is the pre-equilibrium population for a particular exciton state after binary emission, which can be written as

$$
\mathscr{P}^{\text{pre}}(Z',N',p_\pi - Z_{k'},h_\pi,p_\nu - N_{k'},h_\nu,E_{x'}(i')) =
$$
$$
= \sigma^{\text{CF}}(Z_C,N_C,E^{\text{tot}})W_{k'}(Z_C,N_C,E^{\text{tot}},p_\pi,h_\pi,p_\nu,h_\nu,E_{k'})
$$
$$
\times \quad \tau(Z_C,N_C,E^{\text{tot}},p_\pi,h_\pi,p_\nu,h_\nu)P(Z_C,N_C,E^{\text{tot}},p_\pi,h_\pi,p_\nu,h_\nu), \tag{14.6}
$$

where Z_C (N_C) again is the compound nucleus charge (neutron) number and $Z_{k'}$ $(N_{k'})$ corresponds to the ejectile charge (neutron) number. The residual excitation energy $E_x(i')$ is linked to the total energy E^{tot}, the ejectile energy $E_{k'}$, and its separation energy $S(k')$ by $E_x(i') = E^{\text{tot}} - E_{k'} - S(k')$. This $\mathscr{P}^{\text{pre}}$ represents the feeding term for secondary pre-equilibrium emission. Note that for several particle-hole configurations this population is equal to zero.

In general, the pre-equilibrium population can be expressed in terms of the mother nucleus, excitation energy bins, and particle-hole configurations from which it is fed. The residual population is given by a generalization of Eq. (12.1), in which $\sigma^{\text{CF}}(Z_C,N_C,E^{\text{tot}})$ is replaced by the population of the particle-hole states left after the previous emission stage $\mathscr{P}^{\text{pre}}(Z,N,p_\pi^0,h_\pi^0,p_\nu^0,h_\nu^0,E_x(i))$. Since several combinations of emission and internal transitions may lead to the same configuration, a summation is applied over the ejectiles treated in multiple pre-equilibrium (neutrons and protons), over the $(p_\pi^0,h_\pi^0,p_\nu^0,h_\nu^0)$ configurations with which the next step is started and over the mother excitation energy bins:

$$
\mathscr{P}^{\text{pre}}(Z',N',p_\pi',h_\pi',p_\nu',h_\nu',E_{x'}(i')) = \sum_{k'=n,p} \sum_{p_\pi^0=1}^{p_\pi^{\max}} \sum_{h_\pi^0=1}^{h_\pi^{\max}} \sum_{p_\nu^0=1}^{p_\nu^{\max}} \sum_{h_\nu^0=1}^{h_\nu^{\max}}
$$
$$
\sum_i \mathscr{P}^{\text{pre}}(Z,N,p_\pi^0,h_\pi^0,p_\nu^0,h_\nu^0,E_x(i))
$$
$$
W_k(Z,N,p_\pi,h_\pi,p_\nu,h_\nu,E_x(i),E_{k'})\tau(Z,N,p_\pi,h_\pi,p_\nu,h_\nu,E_x(i))
$$
$$
\times \quad P(Z,N,p_\pi,h_\pi,p_\nu,h_\nu,E_x(i)), \tag{14.7}
$$

where the mother and daughter quantities are related by

$$
\begin{aligned}
Z &= Z' + Z_{k'}, \\
N &= N' + N_{k'}, \\
p_\pi &= p_\pi' + Z_{k'}, \\
h_\pi &= h_\pi', \\
p_\nu &= p_\nu' + N_{k'}, \\
h_\nu &= h_\nu', \\
E_x &= E_{x'}(i') + E_{k'} + S_{k'}.
\end{aligned} \tag{14.8}
$$

In the computation, we thus need to keep track of every possible $(Z',N',p_\pi',h_\pi',p_\nu',h_\nu',E_{x'}(i'))$ configuration, which is uniquely linked to a mother exciton state $(Z,N,p_\pi,h_\pi,p_\nu,h_\nu,E_x(i))$ through

the ejectile characterized by $(Z_{k'}, N_{k'}, E_{k'})$. The term $P(Z, N, p_\pi, h_\pi, p_\nu, h_\nu, E_x(i))$ represents the part of the pre-equilibrium cross section that starts in $(Z, N, p_\pi^0, h_\pi^0, p_\nu^0, h_\nu^0, E_x(i))$ and survives emission up to a new particle-hole state $(Z, N, p_\pi, h_\pi, p_\nu, h_\nu, E_x(i))$. Again (see Eq. (12.16)),

$$P(Z, N, p_\pi^0, h_\pi^0, p_\nu^0, h_\nu^0, E_x(i)) = 1, \tag{14.9}$$

and the calculation for each newly encountered $(Z, N, p_\pi, h_\pi, p_\nu, h_\nu, E_x(i))$ configuration proceeds according to Eq. (12.14).

The part of $\mathscr{P}^{\text{pre}}$ that does not feed a new multiple pre-equilibrium population automatically goes to the multiple Hauser-Feshbach chain of Eq. (14.3).

The final expression for the multiple pre-equilibrium spectrum is very similar to Eq.(12.1)

$$
\begin{aligned}
\frac{d\sigma_k^{\text{MPE}}}{dE_{k'}} = {} & \sum_{p_\pi^0=1}^{p_\pi^{\max}} \sum_{h_\pi^0=1}^{h_\pi^{\max}} \sum_{p_\nu^0=1}^{p_\nu^{\max}} \sum_{h_\nu^0=1}^{h_\nu^{\max}} \\
& \sum_i \mathscr{P}^{\text{pre}}(Z, N, p_\pi^0, h_\pi^0, p_\nu^0, h_\nu^0, E_x(i)) \\
& \sum_{p_\pi=p_\pi^0}^{p_\pi^{\max}} \sum_{h_\pi=h_\pi^0}^{h_\pi^{\max}} \sum_{p_\nu=p_\nu^0}^{p_\nu^{\max}} \sum_{h_\nu=h_\nu^0}^{h_\nu^{\max}} W_k(Z, N, p_\pi, h_\pi, p_\nu, h_\nu, E_x(i), E_{k'}) \\
& \times \quad \tau(Z, N, p_\pi, h_\pi, p_\nu, h_\nu, E_x(i)) \, P(Z, N, p_\pi, h_\pi, p_\nu, h_\nu, E_x(i))
\end{aligned}
\tag{14.10}
$$

14.2.2 Multiple pre-equilibrium emission with the s-wave transmission coefficient method

Apart from the exciton model, TALYS offers another, slightly faster, method to determine multiple pre-equilibrium emission by Chadwick et al. [124, 125]. Within this approach the multiple pre-equilibrium spectrum is given by the following expression:

$$
\begin{aligned}
\frac{d\sigma_k^{\text{MPE}}}{dE_{k'}} = {} & \sum_{p_\pi^0=1}^{p_\pi^{\max}} \sum_{h_\pi^0=1}^{h_\pi^{\max}} \sum_{p_\nu^0=1}^{p_\nu^{\max}} \sum_{h_\nu^0=1}^{h_\nu^{\max}} \\
& \sum_i \mathscr{P}^{\text{pre}}(Z, N, p_\pi^0, h_\pi^0, p_\nu^0, h_\nu^0, E_x(i)) \\
& \frac{1}{p_\pi^0 + p_\nu^0} \frac{\omega(Z_{k'}, h_\pi^0, N_{k'}, h_\nu^0, E_{k'} + S_{k'}) \omega(p_\pi^0 - Z_{k'}, h_\pi^0, p_\nu^0 - N_{k'}, h_\nu^0, E_x(i) - E_{k'} - S_{k'})}{\omega(p_\pi^0, h_\pi^0, p_\nu^0, h_\nu^0, E_x(i))} \\
& \times \quad T_s(E_{k'})
\end{aligned}
\tag{14.11}
$$

In this approach each residual particle-hole configuration created in the primary pre-equilibrium decay may have one or more excited particles in the continuum. Each of these excited particles can either be emitted or captured. The emission probability is assumed to be well represented by the s-wave transmission coefficient $T_s(E_{k'})$.

15. Fission

The probability that a nucleus fissions can be estimated by TALYS on both phenomenological and microscopic grounds. Cross sections for (multi-chance) fission can be calculated. For this, various nuclear quantities are required.

15.1 Level densities for fission barriers

The level density formulae given in Section 8 for the ground state of the nucleus can all be applied for the fission barriers. In general, only the ingredients for a few level density expressions change as compared to the non-fissile case. In TALYS, two methods for fission level densities are programmed. The level densities are used in the calculation of fission transmission coefficients.

15.1.1 Explicit treatment of collective effects

Eq. (8.89) for the rotational enhancement also holds for inner barriers with neutron number $N \leq 144$, which are all assumed to be axially symmetric (specified by the keyword **axtype 1**). Inner barriers with $N > 144$, e.g. the Am-isotopes, are taken to be axially asymmetric (**axtype 3**), and in that case the rotational enhancement is

$$K_{rot}(E_x) = K_{rot}^{asym}(E_x, \beta_2) = \max([\sqrt{\frac{\pi}{2}}\sigma_\perp^2(1 - \frac{2\beta_2}{3})\sigma_\parallel - 1]f(E_x) + 1, 1). \tag{15.1}$$

For outer barriers, we apply an extra factor of 2 to $K_{\rm rot}$, due to the mass asymmetry. For all fission barriers, the default parameters for the damping function Eq. (8.90) are $U_f^{bar} = 45$ MeV, $C_f^{bar} = 5$ MeV.

The shell correction is also different: For the inner barrier, $\delta W = 1.5$ MeV for an axially symmetric barrier, and 2.5 MeV otherwise. For the other barriers, we take 0.6 MeV in general.

15.1.2 Effective treatment of collective effects

Despite being of a more "effective" nature than the approach described above, this method (invoked with **colldamp y**) has been more successful in the description of fission cross sections, see e.g. [126]. An essential aspect is that the damping of collective effects are taken into account in a phenomenological way through the level density parameter a. The asymptotic level density parameter $\tilde{a}$, see Eq. (8.13) is damped from its effective limit $A/8$ to its intrinsic limit $A/13$ as follows

$$\tilde{a}^{\text{eff}} = \frac{A}{13} f(E_x) + \tilde{a}(1 - f(E_x)) \tag{15.2}$$

where

$$f(E_x) = \frac{1}{1 + \exp -\left(\frac{E_x - E^{g.s.}_{col}}{d^{g.s.}_{col}}\right)}, \tag{15.3}$$

with the same values as mentioned below Eq. (8.90). Next, the resulting $a(E_x)$ is used in all equations. After this, an extra rotational enhancement needs only to be taken into account for tri-axial barriers (**axtype 2**). Instead of Eq. (8.89), this is taken as

$$K_{rot}(E_x) = \left(\frac{U}{a_{\text{eff}}}\right)^{1/4}(1 - f(E_x)) + f(E_x), \tag{15.4}$$

where $a_{\text{eff}} = 8a/13$ and

$$f(E_x) = \frac{1}{1 + \exp(-\frac{1}{2}(E_x - 18))}, \tag{15.5}$$

For barriers other than tri-axial, $K_{rot} = 1$. There is no vibrational enhancement in this model. For the shell correction, for all barriers $\delta W = \frac{2}{3}|\delta W^{g.s.}|$. Finally, the spin cut-off parameter (8.28) is multiplied by $\left(1 + \frac{\beta_2}{3}\right)$ as done in Eq. (8.86) for the perpendicular spin cut-off parameter.

15.2 Fission transmission coefficients

For fission, the default model implemented in TALYS is based on the transition state hypothesis of Bohr and the Hill-Wheeler expression. This yields transmission coefficients that enter the Hauser-Feshbach model to compete with the particle and photon transmission coefficients.

15.2.1 Transmission coefficient for one fission barrier

The Hill-Wheeler expression gives the probability of tunneling through a barrier with height B_f and width $\hbar\omega_f$ for a compound nucleus with excitation energy E_x. It reads

$$T_f(E_x) = \frac{1}{1 + \exp\left[-2\pi\frac{(E_x - B_f)}{\hbar\omega_f}\right]} \tag{15.6}$$

For a transition state with excitation energy ε_i above the top of the same barrier, one has

$$T_f(E_x, \varepsilon_i) = \frac{1}{1 + \exp\left[-2\pi\frac{(E_x - B_f - \varepsilon_i)}{\hbar\omega_f}\right]} \tag{15.7}$$

which means that the barrier is simply shifted up by ε_i.

For a compound nucleus with excitation energy E_x, spin J, and parity Π, the total fission transmission coefficient is the sum of the individual transmissions coefficients for each barrier through which the nucleus may tunnel, and thus reads in terms of the previously introduced $T_f(E_x, \varepsilon_i)$

$$T_f^{J,\Pi}(E_x) = \sum_i T_f(E_x, \varepsilon_i) f(i, J, \Pi) + \int_{E_{th}}^{E_x} \rho(\varepsilon, J, \Pi) T_f(E_x, \varepsilon) d\varepsilon \qquad (15.8)$$

The summation runs over all discrete transition states on top of the barrier and E_{th} marks the beginning of the continuum. In this equation, $f(i, J, \Pi) = 1$ if the spin and parity of the transition state equal that of the compound nucleus and 0 otherwise. Moreover, $\rho(\varepsilon, J, \Pi)$ is the level density of fission channels with spin J and parity Π for an excitation energy ε. The main difference with the usually employed expressions is that the upper limit in the integration is finite. This expression also enables to define the number of fission channels by replacing $T_f(E_x, \varepsilon_i)$ by 1 in Eq. (15.8). This is needed for width fluctuation calculations where the fission transmission coefficient is treated as a continuum transmission coefficient.

15.3 Transmission coefficient for multi-humped barriers

For double humped barriers, the generally employed expression is based on an effective transmission coefficient T_{eff} defined by

$$T_{eff} = \frac{T_A T_B}{T_A + T_B} \qquad (15.9)$$

where T_A and T_B are the transmission coefficients for barrier A and B respectively, calculated with Eq. (15.8).

If a triple humped barrier needs to be considered, the expression for T_{eff} reads

$$T_{eff} = \frac{T_{AB} T_C}{T_{AB} + T_C} \qquad (15.10)$$

where T_{AB} is given by Eq. (15.9). Consequently, the expression used in TALYS reads

$$T_{eff} = \frac{T_A T_B T_C}{T_A T_B + T_A T_C + T_B T_C} \qquad (15.11)$$

For any number of barrier, the effective number of fission channels is calculated as in the case for one barrier [122].

15.4 Class II/III states

Class II (resp. III) states may be introduced when double (resp. triple) humped barriers are considered. In the particular situation where the excitation energy E_{CN} of the compound nucleus is lower than the barrier heights, fission transmission coefficients display resonant structures which are due to the presence of nuclear excited levels (Class II) in the second, or in the third (Class III) well of the potential energy surface. When such resonant structures occur, the expression for the effective fission transmission coefficient has to be modified (generally enhanced).

The way this resonant effect is determined depends on the number of barriers that are considered.

15.4.1 Double humped fission barrier

In the case where two barriers occur, the effective fission transmission coefficient T_{eff} can be written as

$$
T_{eff} = \frac{T_A T_B}{T_A + T_B} \times F_{AB}(E_{CN})
\tag{15.12}
$$

where $F_{AB}(E_{CN})$ is a factor whose value depends on the energy difference between the excitation energy of the nucleus and that of the a class II state located in the well between barrier A and B. It has been shown [127] that the maximum value of $F_{AB}(E)$ reaches $\frac{4}{T_A + T_B}$ and gradually decreases over an energy interval defined as the width Γ_{II} of the class II state with excitation energy E_{II}. This is accounted for using the empirical quadratic expression

$$
F_{AB}(E) = \frac{4}{T_A + T_B} + \left(\frac{E - E_{II}}{0.5\Gamma_{II}} \right)^2 \times \left(1 - \frac{4}{T_A + T_B} \right)
\tag{15.13}
$$

if $E_{II} - 0.5\Gamma_{II} \leq E \leq E_{II} + 0.5\Gamma_{II}$ and $F_{AB} = 1$ otherwise.

Theoretically, this expression is valid for the tunneling through a single double humped barrier whereas in realistic situations, both T_A and T_B are obtained from a summation over several transition states. One may thus have large T_A and T_B values so that Eq. 15.13 may give $F_{AB}(E) \leq 1$. Such a situation can only occur for high enough excitation energies for which the individual Hill-Wheeler contributions in Eq. (15.8) are large enough. However, in TALYS, we only consider class II states with excitation energies lower than the height of the first barrier. Consequently, the resonant effect can only occur if the compound nucleus energy E_{CN} is (i) lower than the top of the first barrier and (ii) close to a resonant class II state ($E_{II} - 0.5\Gamma_{II} \leq E_{CN} \leq E_{II} + 0.5\Gamma_{II}$). With such requirements, the individual Hill-Wheeler terms are clearly small, and $T_A + T_B \ll 1$.

15.4.2 Triple humped fission barrier

If three barriers A, B and C are considered, the situation is more complicated. In this case, three situations can occur depending on the positions of the class II and class III states. Indeed the enhancement can be due either to a class II state or to a class III state, but on top of that, a double resonant effect can also occur if both a class II and a class III state have an excitation energy close to the compound nucleus energy. For any situation, the enhancement is first calculated for the first and the second barrier giving the transmission coefficient

$$
T_{eff}^{AB} = T_{AB} \times F_{AB}
\tag{15.14}
$$

with F_{AB} given by Eq. (15.13) as in the previous case.

Next, the eventual coupling with a class III state with energy E_{III} of width Γ_{III} is accounted for by generalizing Eq. (15.12) writing

$$
T_{eff}^{ABC} = \frac{T_{eff}^{AB} T_C}{T_{eff}^{AB} + T_C} \times F_{ABC}(E_{CN})
\tag{15.15}
$$

where $F_{ABC}(E_{CN})$ is given by generalizing Eq. (15.13) writing

$$F_{ABC}(E) = \frac{4}{T_{eff}^{AB} + T_C} + \left(\frac{E - E_{III}}{0.5\Gamma_{III}}\right)^2 \times \left(1 - \frac{4}{T_{eff}^{AB} + T_C}\right) \tag{15.16}$$

if $E_{III} - 0.5\Gamma_{III} \leq E \leq E_{III} + 0.5\Gamma_{III}$ and $F_{ABC} = 1$ otherwise.

15.5 Fission barrier parameters

In TALYS several options are included for the choice of the fission barrier parameters:

1. Experimental parameters [6]: collection of a large set of actinide fission barrier heights and curvatures for both the inner and outer barrier based on a fit to experimental data, compiled by V. Maslov. Moreover, this compilation contains head band transition states.
2. Mamdouh parameters [128]: set of double-humped fission barrier heights for numerous isotopes derived from Extended Thomas-Fermi plus Strutinsky Integral calculations.
3. Rotating-Finite-Range Model (RFRM) by Sierk [129]: single-humped fission barrier heights are determined within a rotating liquid drop model, extended with finite-range effects in the nuclear surface energy and finite surface-diffuseness effects in the Coulomb energy.
4. Rotating-Liquid-Drop Model (RLDM) by Cohen *et al* [130].

In the current version of TALYS, the dependence on angular momentum of the fission barriers is discarded. If LDM barriers are employed in the calculation, they are corrected for the difference between the ground-state and fission barrier shell correction energy:

$$B_f^{LDM}(T) = B_f^{LDM}(0) - (\delta W_{groundstate} - \delta W_{barrier}) * g(T) \tag{15.17}$$

This correction gradually disappears with temperature due to the washing out of the shell effects [131]:

$$g(T) = \begin{cases} 1 & for \quad T < 1.65\text{MeV}, \\ g(T) = 5.809 \exp(-1.066\, T) & for \quad T \geq 1.65\text{MeV}. \end{cases} \tag{15.18}$$

Shell corrections on top of the fission barrier are generally unknown. They obviously play an important role for the level density as well. Default values are adopted: for subactinides $\delta W_{barrier} = 0$ MeV, for actinides $\delta W_{barrier,inner} = 2.5$ MeV and $\delta W_{barrier,outer} = 0.6$ MeV [6].

15.6 WKB approximation

As an alternative to the Hill-Wheeler approach, it is also possible to use the WKB approximation to calculate fission transmission coefficients We use an implementation by Mihaela Sin and Roberto Capote and refer to Ref. [10] for the full details of this method. It can be invoked with the keyword **fismodel 5**.

15.7 Fission fragment properties

Since TALYS-1.6, two models for fission fragments are available, the temperature dependent Brosa model, and the GEF model.

15.7.1 GEF model

A fission model has been developed model by Schmidt-Jurado [132]. It is based on the statistical population of states in the fission valleys at the moment of dynamical freeze-out, which is specific to each collective degree of freedom. Three fission channels are considered. The separability principle governs the interplay of macroscopic and microscopic effects. The newly discovered energy-sorting mechanism determines the division of intrinsic excitation energy between the fragments at scission and the creation of a strong even-odd effect at large mass asymmetry. This model gives a new insight into several dynamical times. Most parameters are fixed from independent sources, only about 20 parameters have specifically been adjusted. Since the parameters of the model are closely related to physical properties of the systems, valuable conclusions on the fission process can be deduced. The good reproduction of measured data and the high predictive power of the code make it useful for applications in nuclear technology and complement the use of purely empirical models.

15.7.2 Temperature-dependent Brosa model

The description of fission fragment and product yields follows the procedure outlined in Ref. [133]. The Hauser-Feshbach formalism gives a fission cross section per excitation energy bin for each fissioning system. The fission fragment masses and charges are, subsequently, determined per given excitation energy bin E_x, in a fissioning system FS, characterised by (Z_{FS}, A_{FS}, E_x), for which the fission cross section exceeds some minimum value. The total fragment mass distribution is given by a sum over all contributing bins weighted with the corresponding fission cross sections:

$$\sigma(A_{FF}) = \sum_{Z_{FS}, A_{FS}, E_x} \sigma_f(Z_{FS}, A_{FS}, E_x) Y(A_{FF}; Z_{FS}, A_{FS}, E_x), \tag{15.19}$$

where $Y(A_{FF}; Z_{FS}, A_{FS}, E_x)$ is the relative yield of a fission fragment with mass A_{FF} originating from a fissioning system. Combining this expression with the result of a fission fragment charge distribution calculation yields the final production cross section of a fission fragment with mass A_{FF} and charge Z_{FF}:

$$\begin{aligned} \sigma_{prod}(Z_{FF}, A_{FF}) \;\; = \;\; & \sum_{Z_{FS}, A_{FS}, E_x} \sigma_f(Z_{FS}, A_{FS}, E_x) Y(A_{FF}; Z_{FS}, A_{FS}, E_x) \\ & \times Y(Z_{FF}; A_{FF}, Z_{FS}, A_{FS}, E_x) \end{aligned} \tag{15.20}$$

$Y(Z_{FF}; A_{FF}, Z_{FS}, A_{FS}, E_x)$ is the relative yield of a fission fragment with charge Z_{FF} given its mass A_{FF} and the fissioning system characterised by (Z_{FS}, A_{FS}, E_x).

In general, an excitation energy distribution is connected to these fission *fragment* production cross sections. In theory, this could be used to deduce the fission *product* yields through a full evaporation calculation of the fission fragments. This is not yet possible in TALYS. Instead a rather crude approximation, outlined later in this section, is adopted to estimate the number of post-scission neutrons emitted from each fragment. This procedure leads to relative yields for the fission product masses $Y(A_{FP}; Z_{FS}, A_{FS}, E_x)$ and charges $Y(Z_{FP}; A_{FP}, Z_{FS}, A_{FS}, E_x)$ and, hence, to expressions similar to Eq. (15.19) and Eq. (15.20) for the final fission products.

15.7.3 Fission fragment mass distribution

The fission fragment mass distribution is determined with a revised version of the multi-modal random neck-rupture model (MM-RNRM). The original model has been developed by Brosa to calculate properties of fission fragments at zero temperature [134]. However, fission calculations within TALYS require fragment mass distributions up to higher temperatures.

In the recent version of the model [133] the temperature is added to the calculation of the potential energy landscape of the nucleus. A search for the fission channels in deformation space yields the superlong (SL), standard I (ST I), and standard II (ST II) fission barriers and prescission shapes as a function of temperature. In this manner, the incorporated melting of shell effects naturally gives rise to the vanishing of the asymmetric fission modes ST I and ST II with increasing excitation energies. The obtained temperature-dependent fission barrier and prescission shape parameters serve as input for the fragment mass distribution computations in TALYS.

Each mass distribution is a sum over contributions of the three dominant fission modes FM:

$$Y(A_{FF};Z_{FS},A_{FS},E_x) = \sum_{FM=SL,STI,STII} W_{FM}(Z_{FS},A_{FS},E_x)Y_{FM}(A_{FF};Z_{FS},A_{FS},E_x), \quad (15.21)$$

where $W_{FM}(Z_{FS},A_{FS},E_x)$ denotes the weight of a fission mode, and $Y_{FM}(A_{FF};Z_{FS},A_{FS},E_x)$ is the corresponding mass distribution. $Y(A_{FF};Z_{FS},A_{FS},E_x)$ can then be substituted in Eq. (15.19) to determine the full fission fragment mass distribution for the reaction under consideration. An analogous expression can be written down for $Y(A_{FP};Z_{FS},A_{FS},E_x)$.

Each mass distribution calculation is started by determining the relative contributions of the different fission modes. These are evaluated with the Hill-Wheeler penetrability through inverted parabolic barriers using temperature-dependent barrier parameters and, consequently (the reader is referred to [133] for a detailed explanation), ground-state level densities:

$$T_{f,FM}(Z_{FS},A_{FS},E_x) = \int_0^\infty d\varepsilon \, \rho_{gs}(Z_{FS},A_{FS},\varepsilon) \frac{1}{1+\exp\left[\frac{2\pi(B_{f,FM}(Z_{FS},A_{FS},T(\varepsilon))+\varepsilon-E_x)}{\hbar\omega_{f,FM}(Z_{FS},A_{FS},T(\varepsilon))}\right]}. \quad (15.22)$$

All actinides encounter a double-humped barrier on their way to fission. The effective transmission coefficient can be expressed in terms of the transmission coefficient through the first and second barrier denoted by T_f^A and T_f^B respectively by Eq. (15.9). Since, however, the theoretical inner barrier is much lower than the outer barrier, the relative contribution $W_{FM}(Z_{FS},A_{FS},E_x)$ of the three fission modes may simply be determined by an equation of the following form:

$$W_{SL}(Z_{FS},A_{FS},E_x) = \frac{T_{f,SL}^B}{T_{f,SL}^B + T_{f,STI}^B + T_{f,STII}^B}. \quad (15.23)$$

Equivalent formulas hold for $W_{STI}(Z_{FS},A_{FS},E_x)$ and $W_{STII}(Z_{FS},A_{FS},E_x)$.

For subactinides it is not possible to calculate the competition between symmetric and asymmetric fission modes, since the computed fission channels exhibit rather broad and strangely shaped outer barriers, which makes a parabola fit to these barriers impossible. Hence, the Hill-Wheeler approach cannot be applied. Fortunately, the SL barriers are much lower than the ST barriers. Therefore, in all these calculations the asymmetric fission modes are simply discarded and the dominant symmetric SL mode is solely taken into account for subactinides.

The RNRM is employed to calculate the mass distribution per fission mode. An extensive description of the RNRM may be found in [134]. Here it is merely attempted to communicate its main ideas. In this model, the fission process is regarded as a series of instabilities. After the passage over the barriers, a neck starts to form. If this neck becomes flat its rupture may happen anywhere, which means that the point of future constriction can shift over the neck. This motion of the dent is called the shift instability. In the instant that the Rayleigh instability starts to deepen the dent, the position of the asymmetry is frozen and rupture is taking place. The RNRM translates the effect of both mechanisms into measurable quantities.

In order for the shift instability to do its work, a perfectly flat neck is required. Hence, the so-called flat-neck parameterisation is introduced: (see Fig. 15.1):

$$
\rho(\zeta) = \begin{cases} \left(r_1^2 - \zeta^2\right)^{1/2} & -r_1 \le \zeta \le \zeta_1 \\ r + a^2 c \left(\cosh\left(\frac{\zeta - z + l - r_1}{a}\right) - 1\right) & \zeta_1 \le \zeta \le \zeta_2 \\ \left(r_2^2 - (2l - r_1 - r_2 - \zeta)^2\right)^{1/2} & \zeta_2 \le \zeta \le 2l - r_1. \end{cases} \tag{15.24}
$$

The radius of the nucleus is given by ρ as a function of a parameter ζ in terms of several parameters: the semilength l, the neck radius r, the position z of the dent, the curvature c, the extension of the neck a, the radii of the spherical heads r_1 and r_2, and the transitional points ζ_1 and ζ_2. By requiring continuity and differentiability of the shape, volume conservation and a minimal value of c for a really flat neck, only (l, r, z) remain as independent parameters. Subsequently, the neck radius is eliminated by the Rayleigh criterion, which relates the total length $2l$ of the prescission shape to the neck radius r by $2l = 11r$. The value of z can be transformed into the heavy fragment mass A_h by:

$$
A_h = \frac{3A}{4r_{cn}^3} \int_{-l}^{z} \rho^2(\zeta) d\zeta, \tag{15.25}
$$

where r_{cn} is the compound nucleus radius. The actual values of A_h and l originate from the channel searches and are called the prescission shape parameters. They have been stored in the structure database and are input to the RNRM calculations.

One last ingredient is missing for the computation of the mass distribution, namely the surface tension:

$$
\gamma_0 = 0.9517 \left(1 - 1.7828 \left(\frac{N - Z}{A}\right)^2\right) MeV fm^{-2}. \tag{15.26}
$$

This is taken from the LDM by Myers and Swiatecki [29].

Fluctuations amplified by the shift instability alter the shape slightly and enable the rupture of the nucleus to take place at another point than the most probable point z. In order to determine the fission-fragment mass distribution, the probability of cutting the neck at an arbitrary position z_r has to be calculated. This probability is given by the change in potential energy from z_r to z: $E(z_r) - E(z)$. This is replaced by the energy to cut the nucleus at the two positions: $E_{cut}(z_r) - E_{cut}(z)$, with $E_{cut}(z_r) = 2\pi\gamma_0\rho^2(z_r)$. The rupture probability is now proportional to the Boltzmann factor:

$$
y(A_{FF}) \propto \exp\left(\frac{-2\pi\gamma_0 \left(\rho^2(z_r) - \rho^2(z)\right)}{T}\right). \tag{15.27}
$$

The fragment mass number A_{FF} can be computed according to the analogue of Eq. (15.25):

$$
A_{FF}(z_r) = \frac{3A}{4r_{cn}^3} \int_{-l}^{z_r} \rho^2(\zeta) \, d\zeta. \tag{15.28}
$$

The theoretical yield is finally determined with the following relation in which $Y(A_{FF})$ stands for the normalized fission fragment mass yield:

$$
Y_{FM}(A_{FF}; Z_{FS}, A_{FS}, E_x) = y(A_{FF}) + y(A - A_{FF}). \tag{15.29}
$$

In Eq. (15.27) the temperature of the scissioning nucleus must be provided. All calculations of the PES and the crossing of the fission barriers have been isothermal. However, for the RNRM the
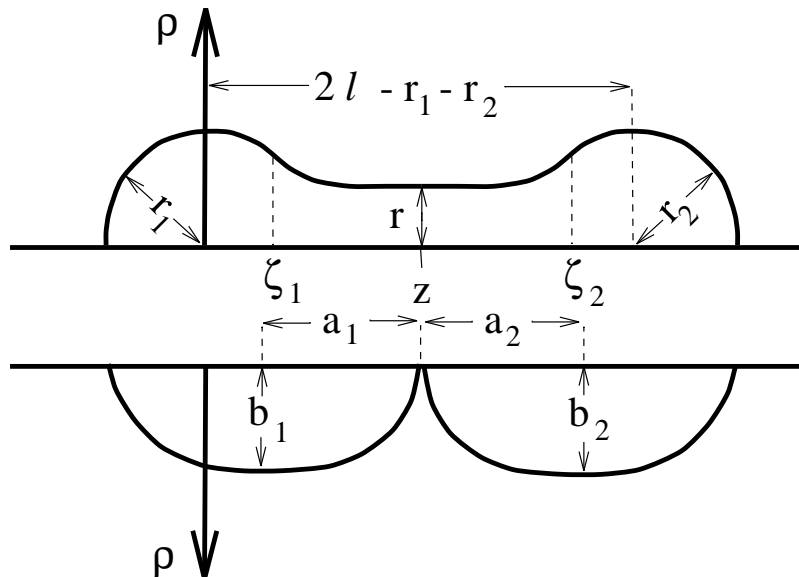
Figure 15.1: The upper part illustrates the flat-neck representation. The lower part contains the embedded spheroids parameterisation.

loss and gain of excitation energy in crossing the barrier is taken into account into a new excitation energy and temperature at scission:

$$E_x^{scission} = E_x^{groundstate} + F_{def,scission}. \tag{15.30}$$

The new excitation energy has two components: the original excitation energy in the ground state $E_x^{groundstate}$ and the deformation energy at scission $F_{def,scission}$. $F_{def,scission}$ is positive for actinides and becomes negative in the subactinide region. The new excitation energy is related to a new temperature $T_{scission}$. However, a new prescission temperature corresponds to a different prescission shape with a somewhat different value for $F_{def,scission}$. Therefore, the temperature $T_{scission}$ has to be determined in a self-consistent manner together with the final prescission shape. If a prescission shape has a high temperature or a very long neck, the mass distribution will be broad. Low temperatures and short necks result in a narrow mass distribution.

15.7.4 Post-scission neutron multiplicities

The mass distribution calculated above belongs to the primary fission fragments. Most fragments, however, are highly excited directly after their creation. They take their share of total excitation energy available at scission (15.30). Moreover, they are strongly deformed, which manifests itself in an extra amount of excitation energy set free when this deformation relaxes towards the ground-state deformation of the fragments by the strong surface tension. The superfluous excitation energy is released during the process of post-scission neutron and gamma emission. The neutron emission is responsible for a shift of the pre-neutron emission mass distribution to somewhat smaller masses.

The total excitation energy in a newly created fragment with mass A_{FF} results from:

$$E_x^{fragment}(A_{FF}) = E_{def,fragment}(A_{FF}) + \frac{A_{FF}}{A} E_x^{scission}. \tag{15.31}$$

$E_{def,fragment}(A_{FF})$ denotes the deformation energy of the fragment, and the second term contains the portion of the thermal energy at scission of the whole fissioning system picked up by the fragment. The assumption is that the fragment receives a share proportional to its mass.

For the calculation of $E_{def,fragment}(A_{FF})$ another shape parameterisation is employed: the embedded spheroids (see Fig. 15.1). The newborn fragments are modeled as two contacting spheroids with major axes a_1 and a_2, which are linked to $2l$ and z_r by:

$$a_1 = \frac{1}{2}(r_1 + z_r), \qquad a_2 = l - \frac{1}{2}(r_1 + z_r). \tag{15.32}$$

The minor axes b_1 and b_2 follow from volume conservation:

$$b_1^2 = \frac{3}{4a_1} \int_{-r_1}^{z_r} \rho^2 d\zeta, \qquad b_2^2 = \frac{3}{4a_2} \int_{z_r}^{2l-r_1} \rho^2 d\zeta. \tag{15.33}$$

The energy difference of the spheroidally deformed and the spherical fragment $E_{def,fragment}(A_{FF})$ is given by:

$$\begin{aligned}
E_{def,fragment}(A_{FF},\varepsilon) &= E_{surf}^{sph}(A_{FF}) \left(\frac{\arcsin(\varepsilon) + \varepsilon\left(1-\varepsilon^2\right)^{1/2}}{2\varepsilon\left(1-\varepsilon^2\right)^{1/6}} - 1 \right) + \\
&\quad E_{Coul}^{sph}(A_{FF}) \left(\frac{\left(1-\varepsilon^2\right)^{1/3}}{2\varepsilon} ln\left(\frac{1+\varepsilon}{1-\varepsilon}\right) - 1 \right).
\end{aligned} \tag{15.34}$$

The eccentricity is defined as:

$$\varepsilon_i = \left(1 - \left(\frac{b_i}{a_i}\right)^2 \right)^{1/2}, \tag{15.35}$$

and $E_{surf}^{sph}(A_{FF})$ and $E_{Coul}^{sph}(A_{FF})$ represent the LDM surface and the Coulomb energy of a spherical nucleus obtained from Ref. [135].

The neutron multiplicity $\nu_{FM}(A_{FF})$ for a fragment with mass A_{FF} is now derived by finding the root of the following relation:

$$E_x^{fragment}(A_{FF}) = \sum_{n=1}^{\nu_{FM}(A_{FF})} (S_n + \eta_n) + E_\gamma. \tag{15.36}$$

The separation energy S_n is calculated from the mass formula [135]. The average kinetic energy of the neutrons is taken to be $\frac{3}{2}$ times the fragment temperature, and the energy carried off by γ-rays E_γ is approximately half the separation energy of the first non-evaporated neutron.

The final fission product mass yield per fission mode is given by:

$$Y_{FM}(A_{FP}; Z_{FS}, A_{FS}, E_x) = Y_{FM}(A_{FF} - \nu_{FM}(A_{FF})) + Y_{FM}(A - A_{FF} - \nu_{FM}(A - A_{FF})). \tag{15.37}$$

15.7.5 Fission fragment charge distribution

Unfortunately, the MM-RNRM only yields information on the mass yields of the fission fragments. Predictions of charge distributions are performed in TALYS within a scission-point-model-like approach (Wilkins *et al.* [136]). Corresponding to each fission fragment mass A_{FF} a charge distribution is computed using the fact that the probability of producing a fragment with a charge Z_{FF} is given by the total potential energy of the two fragment system inside a Boltzmann factor:

$$Y_{FM}(Z_{FF};A_{FF},Z_{FS},A_{FS},E_x) = \frac{\exp\left(\frac{-E(Z_{FF},A_{FF},Z,A)}{T}\right)}{\sum_{Z_{FF_i}} \exp\left(\frac{-E(Z_{FF_i},A_{FF},Z,A)}{T}\right)} \tag{15.38}$$

In the original scission-point model this potential energy is integrated over all deformation space. Within the MM-RNRM, however, fission channel calculations already define the deformation at the scission point. Furthermore, a strong coupling between the collective and single particle degrees of freedom is assumed near the scission point. This means that the nucleus is characterised by a single temperature T.

The potential energy for the creation of one fragment with (Z_{FF},A_{FF}) and a second fragment with $(Z - Z_{FF}, A - A_{FF})$ consists of a sum over the binding energy of the deformed fragments by the droplet model without shell corrections and their mutual Coulomb repulsion energy as well as the nuclear proximity repulsion energy:

$$E(Z_{FF},A_{FF},Z,A) = B(Z_{FF},A_{FF}) + B(Z - Z_{FF}, A - A_{FF}) + E_{Coul} + V_{prox}. \tag{15.39}$$

The single constituents of this formula are defined by the following relations:

$$B(Z_{FF},A_{FF}) = -a_1\left[1 - \kappa\left(\frac{A_{FF} - 2Z_{FF}}{A_{FF}}\right)^2\right]A_{FF} \tag{15.40}$$

$$+a_2\left[1 - \kappa\left(\frac{A_{FF} - 2Z_{FF}}{A_{FF}}\right)^2\right]A_{FF}^{\frac{2}{3}}f(shape)$$

$$+\frac{3}{5}\frac{e^2}{r_0}\frac{Z_{FF}^2}{A_{FF}^{\frac{1}{3}}}g(shape) - \frac{\pi^2}{2}\frac{e^2}{r_0}\left(\frac{d}{r_0}\right)^2\frac{Z_{FF}^2}{A_{FF}} \tag{15.41}$$

$$E_{Coul} = e^2 Z_{FF}(Z - Z_{FF})S_{form}/(a_1 + a_2) \tag{15.42}$$

$$V_{prox} = -1.7817\frac{4\pi\gamma_0 b_1^2 b_2^2}{a_1 b_2^2 + a_2 b_1^2} \tag{15.43}$$

The parameters in the binding energy formula are taken from Ref. [135]. The function $f(shape)$ is the form factor for the Coulomb term whereas $g(shape)$ denotes the form factor for the surface energy. S_{form} is the form factor for the Coulomb interaction energy between two spheroids.

The fission product charge distribution is obtained from the calculated fission fragment charge distribution by shifting the corresponding fragment masses A_{FF} to the fission product masses A_{FP} with the aid of the post-scission neutron multiplicity $\nu_{FM}(A_{FF})$:

$$Y_{FM}(Z_{FP};A_{FP},Z_{FS},A_{FS},E_x) = Y_{FM}(Z_{FF};A_{FF} - \nu_{FM}(A_{FF}),Z_{FS},A_{FS},E_x). \tag{15.44}$$

Since proton evaporation of the fission fragments is neglected, the charge distribution connected with A_{FF} becomes simply linked to the fission product mass A_{FP}.

15.7.6   Fission fragment distribution models

The de-excitation of the fission fragments by the Hauser-Feshbach statistical decay theory is implemented in TALYS (later than version 1.96). The methodology used here is to apply the deterministic technique for primary fission fragment decay calculation similar to the HF^{3}D model. In order to calculate the de-excitation of the fission fragment, input of the initial conditions, namely $Y_{\text{ff}}(Z,A,E_x,J,\Pi)$, are necessary.

Recently, Nordström et al. produced a substantial fission fragment distribution dataset for more than 700 fissionable nuclides for the 0–25 MeV incident neutron energy range for fissionable isotopes ranging from Os to Mc by the GEF code. Including the GEF produced dataset mentioned above, TALYS incorporates three fission fragment distribution parameters dataset produced by GEF, HF^{3}D, and Scission Point Yield (SPY) models, so far. The HF^{3}D model is available for ^{235}U, ^{238}U, and ^{239}Pu. The SPY model is available for Am and Pu isotopes. The covered nuclides are shown in Fig. 15.2. The user can specify the fission fragment model in TALYS input with `ffmodel` keyword. The available models, compound nuclides, and energy ranges are expected to be extended and be
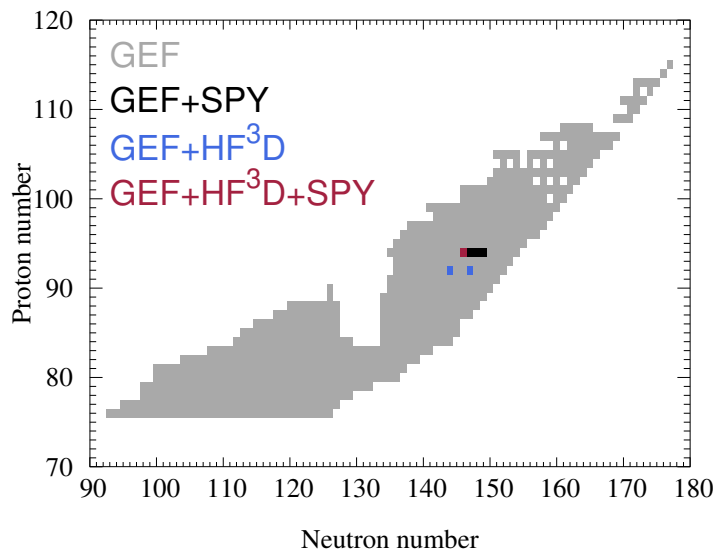
Figure 15.2: Valid range of each model.

updated from time to time. The models are introduced below.

GEF model

The GEF code is the fission modelling code that attempts to provide a general description of fission observables based on benchmarking the model with empirical datasets. The GEF code calculates the fission observables based on the Monte Carlo sampling, which preserves the event-by-event correlation between fission observables, such as fragment yields and kinetic energies and the kinematics of fragments and emitted particles. A macroscopic approach is utilized by deriving global fit parameters to a large set of experimental data such as fission mass and charge yields, prompt fission neutrons, and gamma rays. The code estimates fission barrier heights from the topographic theorem and derives fission fragment yields by utilizing the Brosa model with Gaussian fitting. It estimates the sharing of available energy (Q value) between Total Kinetic Energy (TKE) and Total Excitation Energy (TXE). It further employs statistical mechanics and the law of entropy

to share the excitation energy between the fragments. The TXE partitioning is determined according to a probability distribution that is given by the product of the level densities of the individual fragments.

Nordström et al. used GEF as a fission event generator and performed 1,000,000 random samplings. Then the Python script was used to calculate the average TKE and TXE of the fission fragment pair, and to produce mean and standard deviations, $E_{l,h}$ and $W_{l,h}$, of light and heavy fragments from the list mode output file.

HF³D model

The Hauser-Feshbach fission fragment decay model (HF³D) has been developed based on the full deterministic technique to calculate fission observables. In the HF³D model, the primary fission fragment yield $Y(A)$ and TKE are determined by fitting experimental data with simple analytical functions. In order to generate charge distribution $Y(A, Z)$, Z_P model is employed, and the excitation energy divide is made by the anithothermal model to reproduce $\overline{v}(A)$. For the TALYS fission fragment distribution parameter dataset, 3 compound nuclides, ^{235}U, ^{238}U, and ^{239}Pu, for which some fittable experimental data exist, are provided. The details of the HF³D model are explained below.

The fission fragment mass distribution $Y(A)$ is made of the sum of multi (5 or 7) Gaussian functions.

$$Y(A) = \sum_{i=1}^{5} \frac{Y_i}{\sqrt{2\pi}\sigma_i} \exp\left\{ -\frac{(A - A_m + \Delta_i)^2}{2\sigma_i^2} \right\}, \tag{15.45}$$

where σ_i and Δ_i are the Gaussian parameters, A_m $(= A_c/2)$ is the symmetry point of the mass distribution, and Y_i is the component of yield. Y_i is divided into the principal peak curves $Y_{1,5}$, the inner peak curves $Y_{2,4}$, and the central peak curve Y_3.

Principal curves
> $Y_{1,5}$ are the main component of the mass distribution for high and low energy fission, and The shape of curves depends on the charge of the fissile nuclide Z_F and the precursor excitation energy (the projectile incident energy E_{inc} plus the separation energy S_N)

Inner peak curves
> $Y_{2,4}$ especially affects the shape of mass distribution for $A_h = 130$ and $A_l = A_c - 130$. The large kinetic energies and the small amount of the prompt neutron emission derives in $Y_{2,4}$.

Central peak curve
> The intensity of Y_3 increases with getting the precursor excitation energy bigger.

The Gaussian parameters are determined with the least square method.

Every $Y(A)$ has the charge distribution and Wahl's Z_P model is employed to get yield $Y(A, Z)$ in HF³D model. The Z_P model treats a dispersion of fractional independent yields of primary fission products with Z for each A. In this calculation, this yield is regarded as the fragment yield. Gaussian dispersion, modified for even-odd proton and neutron effects, is assumed. Parameters for the model are determined by the method of least squares from fractional independent and fractional cumulative yield values derived from experimental data. The equations are shown with the error
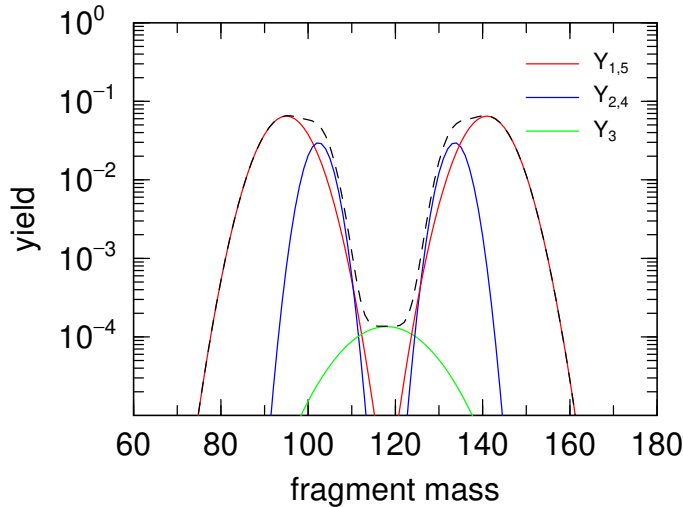
Figure 15.3: Fission fragment yield defined in the HF^{3}D model. Solid lines represent each Gaussian component and the dashed line is the sum of these Gaussians.

function of x, $erf(x)$:

$$
\begin{aligned}
Y(A,Z) &= 0.5F(A)N(A)\{erf(V) - erf(W)\}, \\
V &= \frac{Z(A) - Z_p(A) + 0.5}{\sigma_Z(A)\sqrt{2}}, \\
W &= \frac{Z(A) - Z_p(A) - 0.5}{\sigma_Z(A)\sqrt{2}}, \\
Z_p(A_{l,h}) &= Z_{\text{UCD}}(A_{l,h}) \pm \Delta Z(A_{l,h}), \\
&= A_{l,h} \times Z_c/A_c \pm \Delta Z(A_{l,h}).
\end{aligned}
\tag{15.46}
$$

where $N(A)$ is the normalization factor, and $F(A)$ is the even-odd factor. As shown below, this factor is distinguished by even or odd for neutron and proton numbers. Parameters $\sigma_Z, \Delta Z, F_Z, F_N$

for Z	for N	$F(A)$
even	even	$F_Z(A) \times F_N(A)$
even	odd	$F_Z(A)/F_N(A)$
odd	even	$F_N(A)/F_Z(A)$
odd	odd	$1/\{F_Z(A) \times F_N(A)\}$

Table 15.1: The even-odd factors for the fission fragment yield

and their slopes with respect to A are determined in contiguous regions of A for each fission reaction by the method of least squares. $Z_p(A_{l,h})$ is the most probable charge in the fission fragment. In the UCD (Unchanged Charge Distribution) assumption, $Z_p(A_{l,h})$ is the same charge proportion as its fissile nuclide. However, the actual Z_P seems to be different from Z_{UCD}, the charge from UCD approximation, and the difference between actual one and UCD one is called the charge polarization ΔZ.

The total kinetic energy TKE is given by a Gaussian function:

$$
\begin{aligned}
\text{TKE}(A_h) &= (p_1 - p_2 A_h)\left\{1 - p_3 \exp\left(-\frac{(A_h - A_m)^2}{p_4}\right)\right\} + \varepsilon_{\text{TKE}} \\
&\propto \exp\left(-\frac{(A_h - A_m)^2}{2W_{\text{TKE}}^2}\right)
\end{aligned}
\tag{15.47}
$$

where p_1, p_2, p_3, and p_4 are fitting parameters and ε_{TKE} is a small correction. Both parameters are fitted to agree with evaluated $\overline{\text{TKE}}$. Moreover, TKE is also represented with a width parameter W_{TKE} which is empirically known to be about 8-10 MeV. The total excitation energy TXE which is shared with the light and heavy fragments is shown with this TKE,

$$
\begin{aligned}
\text{TXE}(A_l, Z_l; A_h, Z_l) &= Q_f(A_l, Z_l; A_h, Z_l) - \text{TKE}(A_l, Z_l; A_h, Z_l) \\
&= [M_n(A_c, Z_c) - M_n(A_l, Z_l) - M_n(A_h, Z_h)]c^2 \\
&\quad + E_{inc} + S_n - \text{TKE}(A_l, Z_l; A_h, Z_l),
\end{aligned}
\tag{15.48}
$$

where Q_f is the Q value of the fission reaction, and M_n represents the nuclear mass. The TXE is distributed using the R_T parameter which is defined as the ratio of effective temperatures in the fission fragments,

$$
R_T = \frac{T_l}{T_h} = \sqrt{\frac{E_l}{E_h} \frac{a_h(E_h)}{a_l(E_l)}},
\tag{15.49}
$$

where $a_{l,h}(E_{l,h})$ are the level density parameters related to shell correction at $E_{l,h}$. Therefore, the energies are:

$$
E_h = \text{TXE}\frac{a_h}{R_T^2 a_l + a_h}, \qquad E_l = \text{TXE}\frac{R_T^2 a_l}{R_T^2 a_l + a_h}.
\tag{15.50}
$$

The TXE distribution G is also represented by a Gaussian but the width is different from the width W_{TXE} which propagates from W_{TKE} due to the R_T;

$$
G(E_x) = \frac{1}{\sqrt{2\pi}W_{l,h}} \exp\left\{-\frac{(E_x - E_{l,h})^2}{2W_{l,h}^2}\right\}.
\tag{15.51}
$$

In (15.51), $W_{l,h}$ is

$$
W_{l,h} = \frac{W_{\text{TXE}}}{\sqrt{E_l^2 + E_h^2}} E_{l,h} \qquad (W_{\text{TXE}} = W_{\text{TKE}}).
\tag{15.52}
$$

SPY model

The SPY model is a static and statistical scission-point model that assumes a statistical equilibrium at scission. This model is fully based on microscopic inputs, computed within the constraint Hartree-Fock-Bogoliubov (HFB) mean-field model using the Skyrme BSk27 nucleon-nucleon effective interaction. This interaction can predict all the 2353 experimental masses with a root-mean-square deviation of 0.5 MeV and also describe infinite homogeneous nuclear matter properties. The main advantage of using the HFB model is it can describe nuclear structure properties for a wide range of nuclei without phenomenological parameters apart from those of the effective interaction.

In the SPY model, the scission configuration is defined by the proton density at the scission neck of the fissioning nucleus. The fission fragment yields are obtained by counting the number of

available states at scission for all possible fragmentations. In regard, TKE is defined as the mean value of Coulomb repulsion plus nuclear attraction energy between fragments. TXE is the sum of the deformation energy and the intrinsic energy of the fission fragment pair. As TALYS input, the SPY model provides pre-neutron fission yields of 4 compound nuclei with excitation energies ranging from 0 to 20 MeV with a step of 2 MeV.

15.8 Implementation, options and sample cases

Implementation 15.8.1 The fission parameters are stored in the *talys/structure/fission/* directory. There are various subdirectories: *barrier/*, *states/*, *gef/*, *brosa/*, *mamdouh/*, *hfbpath/*, *firstchance/*, and *ff/*.

First, the experimental fission parameter set can be found in directory *barrier/*. The directory *states/* includes headband transition states for even-even, even-odd, odd-odd, and odd-even nuclides. The parameters are the result of an extensive fit to many experimental fission cross sections, compiled by V. Maslov for the RIPL library. As an example we show the available parameters for the uranium isotopes which are present in the file *barrier/U.bar*. We have stored Z, A, a parameter specifying the symmetry of the inner barrier, height of the inner barrier, curvature of the inner barrier, a parameter specifying the symmetry of the outer barrier, height of the outer barrier, curvature of the outer barrier, the pairing correlation function at the barrier (which is not used in the calculation) and the nuclear symbol with the format (2i4,a5,2f8.3,a5,2f8.3,f9.4,15x,i4,a2).

```
92 231   S    4.40    0.70   MA    5.50    0.50    0.869              231U
92 232   S    4.90    0.90   MA    5.40    0.60    0.848              232U
92 233   S    4.35    0.80   MA    5.55    0.50    0.946              233U
92 234   S    4.80    0.90   MA    5.50    0.60    0.889              234U
92 235   S    5.25    0.70   MA    6.00    0.50    0.803              235U
92 236   S    5.00    0.90   MA    5.67    0.60    0.833              236U
92 237   GA   6.40    0.70   MA    6.15    0.50    0.809              237U
92 238   GA   6.30    1.00   MA    5.50    0.60    0.818              238U
92 239   GA   6.45    0.70   MA    6.00    0.50    0.816              239U
```

In *states*, we have stored files with default head band and class II-states for even-even, even-odd, odd-odd, and odd-even nuclides. An example of a file containing the head band transition states is given below for *states/hbstates.ee*. This file is used for even-even nuclides. We loop over the two barriers. On the first line one finds the barrier number, the number of head band states and the energy at which the continuum starts with the format(2i4,f8.3). Next we loop over the transition states, in which we read the level number, level energy in MeV, spin and parity with the format (i4,f11.6,f6.1,i5).

```
   1   8   0.800
   1   0.000000   0.0    1
   2   0.500000   2.0    1
   3   0.400000   0.0   -1
   4   0.400000   1.0   -1
   5   0.500000   2.0    1
   6   0.400000   2.0   -1
   7   0.800000   0.0    1
```

```
   8   0.800000    0.0    1
   2    4   0.500
   1   0.000000    0.0    1
   2   0.500000    2.0    1
   3   0.200000    0.0   -1
   4   0.500000    1.0   -1
```

We also include the possibility to incorporate the effect of class II states in the calculation. For this purpose we take four parameter sets with class II states for even-even, even-odd, odd-odd, and odd-even nuclides. As an example we show the file *states/class2states.ee*. This file contains the well number, and the number of class II states. Subsequent lines contain the level number, the level energy in MeV, spin and parity with the format (i4,f8.3,f9.1,i5).

```
   1   10
   1    2.700       0.0    1
   2    3.400       0.0   -1
   3    4.100       1.0   -1
   4    4.800       2.0   -1
   5    5.000       1.0    1
   6    5.200       0.0    1
   7    5.400       0.0   -1
   8    5.500       1.0   -1
   9    5.600       2.0   -1
  10    5.700       1.0    1
```

The directory *brosa/* contains three subdirectories: *barrier/*, *groundstate/*, and *prescission/*. In *brosa/barrier/* temperature-dependent fission barrier parameters per fission mode can be found. They are the results of calculations performed within the Brosa model. The extension in the filename reveals the fission mode: sl for superlong, st for standard I, and st2 for standard II. As an example, below are the superlong parameters for several U isotopes taken from *brosa/barrier/U.sl*. Each line gives Z, A, temperature T in MeV, B_F in MeV, $\hbar\omega$ in MeV, and the barrier position in terms of the distance between the fragment centers d in fm. The format is (2i4,4f15.5).

```
  92 240        0.00000      11.40470       3.92020      10.37450
  92 240        0.30000      11.23440       4.18630      10.34980
  92 240        0.60000      11.64780       4.25390      10.44170
  92 240        0.90000       9.58680       2.58900      10.35970
  92 240        1.20000       7.88030       2.36520      10.53400
  92 240        1.60000       5.69890       1.58010      10.43420
  92 240        2.00000       4.17750       1.07010      10.28590
  92 240        2.50000       2.76320       0.47300       9.69080
  92 240        3.00000       1.84230       0.25520       8.57080
  92 238        0.00000      10.88450       4.67530      10.27930
  92 238        0.30000      10.97680       4.87110      10.27090
  92 238        0.60000      10.59680       4.44100      10.29590
  92 238        0.90000       9.31080       3.69600      10.37940
  92 238        1.20000       7.55620       2.32260      10.40990
  92 238        1.60000       5.46180       1.51320      10.33670
  92 238        2.00000       3.98050       0.82730      10.15860
  92 238        2.50000       2.74050       0.43440       9.43930
```

```
92 238          3.00000       1.87030       0.34600          8.62610
```

The ground state energies as a function of temperature are stored in *brosa/barrier/groundstate/*. Each line has the same format: Z, A, T in MeV, and E*groundstate* in MeV (2i4,2f15.5). An example is included for U isotopes, see *brosa/barrier/groundstate/U.fis*.

```
92 240          0.00000      -1811.82104
92 240          0.30000      -1813.38599
92 240          0.60000      -1818.06006
92 240          0.90000      -1825.59497
92 240          1.20000      -1836.26599
92 240          1.60000      -1855.76294
92 240          2.00000      -1881.23901
92 240          2.50000      -1921.08105
92 240          3.00000      -1969.60205
92 238          0.00000      -1800.57996
92 238          0.30000      -1802.16504
92 238          0.60000      -1806.85205
92 238          0.90000      -1814.34302
92 238          1.20000      -1825.23596
92 238          1.60000      -1844.68799
92 238          2.00000      -1870.17004
92 238          2.50000      -1910.02905
92 238          3.00000      -1958.52405
```

The third directory, *brosa/barrier/prescission/*, contains parameters that fix the prescission shape of the nucleus in each fission mode. They mark the end of the fission path found in the same fission channel calculations that resulted in the Brosa barrier parameters. Again each line has the same format: Z, A, T in MeV, A_h the heavy fragment mass in amu, l the nucleus half length in fm, and E*prescission* in MeV (2i4,4f15.5). An example is included for prescission shape parameters in the superlong mode of U isotopes, see *brosa/barrier/prescission/U.sl*,

```
92 240          0.00000      120.45900      21.29700      -1840.84900
92 240          0.30000      120.83730      21.48670      -1826.35022
92 240          0.60000      120.83670      20.74300      -1831.38477
92 240          0.90000      120.30430      20.21950      -1840.12256
92 240          1.20000      120.65520      20.13060      -1854.43555
92 240          1.60000      120.83060      19.56120      -1874.16174
92 240          2.00000      120.74340      19.33610      -1902.75671
92 240          2.50000      120.62800      18.38600      -1945.59497
92 240          3.00000      120.78300      18.45000      -1998.50598
92 238          0.00000      120.00730      21.40630      -1815.46497
92 238          0.30000      119.64770      21.36200      -1816.33203
92 238          0.60000      119.50730      20.50950      -1821.51123
92 238          0.90000      119.27930      20.50120      -1830.13428
92 238          1.20000      119.47550      19.91770      -1842.70630
92 238          1.60000      123.00390      19.23990      -1864.13489
92 238          2.00000      120.49580      19.24370      -1892.63281
92 238          2.50000      119.62200      18.37100      -1935.14502
92 238          3.00000      119.37600      18.38000      -1988.42395
```

In directory *gef*, masses and shell correction energies for the GEF model are stored.

The Mamdouh fission parameter set can be found in directory *mamdouh/*. This parameter set has been derived from Extended Thomas-Fermi plus Strutinsky Integral calculations and comprise double-humped fission barrier heights and curvatures for numerous isotopes. As an example we show the available parameters for the various U isotopes which are present in the file *mamdouh/U.bar*. We have stored Z, A, height of the inner barrier, height of the outer barrier in MeV and the nuclear symbol with the format (i3,i4,2(24x,f8.2),5x,i3,a2).

```
92 230    1.24    0.00    0.00    3.80    1.77   -0.02    0.35    3.90    230U
92 231    1.24    0.01    0.00    4.10    1.83    0.05    0.50    4.30    231U
92 232    1.25    0.02    0.00    4.20    1.83    0.05    0.53    4.20    232U
92 233    1.28    0.05    0.00    4.70    1.84    0.06    0.53    4.40    233U
92 234    1.28    0.03    0.00    4.80    1.83    0.06    0.53    4.40    234U
92 235    1.28    0.04    0.00    5.40    1.63    0.01    0.53    4.10    235U
92 236    1.29    0.04    0.00    5.20    1.64    0.01    0.53    4.00    236U
92 237    1.28    0.04    0.00    5.70    1.63    0.01    0.53    4.30    237U
92 238    1.29    0.03    0.00    5.70    1.91    0.07    0.47    4.90    238U
92 239    1.29    0.03    0.00    6.10    1.81   -0.07    0.35    5.50    239U
92 240    1.29    0.03    0.00    6.00    1.90   -0.04    0.53    6.30    240U
92 241    1.30    0.04    0.00    6.30    1.91   -0.03    0.55    5.70    241U
92 242    1.30    0.04    0.00    5.90    1.90   -0.04    0.53    6.00    242U
```

If we use the WKB approximation to calculate fission transmission coefficients, **fismodel 5**, we need potential energy curves. They can be found in the directory *hfbpath/*. As an example, we show the data for ^{235}U as present in the file *hfbpath/U.fis*. We have stored Z, A, number of fission width values, total energy (not used) with the format (3i4,f12.3). Next, we give the values for the fission width and height with the format (f10.3,20x,f10.3),

```
92 235 100     -1781.682
     0.269     0.000     0.152     0.000
     0.298     0.000     0.180     0.332
     0.326     0.000     0.189     1.047
     0.355     0.000     0.171     1.987
     0.383     0.000     0.216     2.846
     0.412     0.000     0.199     3.921
     0.440     0.000     0.194     4.695
     0.470     0.000     0.158     5.002
     0.501     0.000     0.136     5.391
     0.531     0.000     0.156     5.390
     0.563     0.000     0.173     5.186
```

The fission fragment parameters are stored in the *ff/* directory. Three kinds of ffmodel, GEF, HF3D, and SPY, are stored in, and each fissioning system which is regarded as a compound nucleus is stored in each ffmodel. As an example, the input parameter which is presented in the file *ff/gef/U236/U236_6.55e+00MeV_gef.ff* is given below. The first 5 lines are the information of this input: the charge Z, the mass A of a compound nucleus, the excitation energy E_x which is a sum of incident neutron energy and neutron separation energy of compound nucleus, and the number of fragment pairs $Ntotal$.

```
# Z       =    92
# A       =   236
```

```
# Ex (MeV) = 6.55e+00
# Ntotal   =   868
# Zl  Al Zh  Ah Yield      TKE[MeV]   TXE[MeV]   El[MeV]    Wl[MeV]    Eh[MeV]    Wh[MeV]
  46 118 46 118 3.9358e-03 1.6387e+02 3.5404e+01 1.7702e+01 2.7264e+00 1.7702e+01 2.7264e+00
  45 117 47 119 4.4534e-03 1.6379e+02 3.4714e+01 1.5507e+01 2.2652e+00 1.9207e+01 4.0430e+00
  44 116 48 120 6.9902e-03 1.6453e+02 3.5142e+01 1.4014e+01 1.9368e+00 2.1128e+01 5.5635e+00
  43 115 49 121 1.9397e-03 1.6661e+02 3.2898e+01 1.3628e+01 2.0851e+00 1.9270e+01 6.3823e+00
  42 114 50 122 9.2456e-04 1.7326e+02 2.8813e+01 1.4316e+01 2.8689e+00 1.4496e+01 7.0989e+00
```

There are some pointers on the preparation of user's model files and to read files from TALYS correctly.

Implementation 15.8.2 In currently TALYS (version 1.96), users can use our own fission fragment yields by replacing original yield files. However, there are some cautions;

Format

In the fourth line of the format, the number of fragment pairs is required to run calculations.

Z,A: format must be (13x,i4).

E_x: format must be (13x,e8.2).

Ntotal: format must be (13x,i4).

Column header should be at line 5.

File name

Each fission fragment file includes the sum of the projectile incident energy and the neutron separation energy in the title. TALYS calculates neutron separation energy and refers to the title when TALYS reads fission fragment files. Therefore, we need to pay attention to the title when fission fragment files are prepared.

.E file

Each nuclide directory must have a .E (*i.e.* Energy) file. In this file, available E_x, which is the sum of the neutron separation energy of CN and projectile incident energy should be listed. This file will be used when TALYS reads fission fragment files and interpolates between energies. For the case of the Am243 as CN, the file name must be

```
/talys/structure/fission/ff/user/Am243/Am243_user.E.
```

```
6.53e+00 7.03e+00 7.53e+00 8.53e+00 1.05e+01
1.25e+01 1.65e+01 2.05e+01 2.65e+01
```

Sample case 15.1 **Fission yields for** ^{238}U

In this sample case we compute fission fragment/product mass/isotope yields. The fission fragment mass yield curve is determined for neutrons on ^{238}U at incident energies of 1.6 and 5.5 MeV (these incident energies are given in the file *energies*). The following input file is used:

```
#
# n-U238-fy
#
# General
#
projectile n
element    U
```

```
mass        238
energy      energies
partable y
bins 40
channels y
filechannels y
best y
ecissave y
massdis y
ffevaporation y
#
# For more precise results you may increase bins to 100
# and have a finer grid in the energies file
#
```

The long list of adjustable parameters, not visible here but automatically taken from *talys/structure/best/U238/z092a238n.best* through the **best y** keyword, is mainly needed to give a decent (though not yet perfect) description of the total fission cross section. For completeness, we show the results for ^{238}U we obtained for incident energies of 1, 1.6, 3.5, 5.5, 7.5 and 10 MeV. The TALYS results for the pre-neutron emission mass yields can be found in *yield001.600.fis* and *yield005.500.fis* and are given in the upper plot of Fig. 15.4. The two other plots show a comparison of the normalized yields with experimental data [137].

Since we have added the keyword *ffevaporation y* to the input, we have also calculated the fission product isotope yields. Fig. 15.5 contains the result for the production of the fission products ^{115}Cd and ^{140}Ba. The left plot shows the cumulative yield (obtained after adding the calculated independent yields of all beta-decay precursors). The normalized cumulative yields are compared to experimental data [138, 139] in the other two plots.   ∎

Sample case 15.2 **Neutron multiplicities and fission yields for n + ^{242}Pu**
TALYS contains an implementation of several versions of the GEF code by Karl-Heinz Schmidt and Beatriz Jurado. Part of GEF has been translated by Vasily Simutkin and Michail Onegin into a Fortran subroutine. In this sample case, the prompt neutron multiplicity as a function of mass, $\overline{\nu}(A)$, number of neutrons, $P(\nu)$, and the total average, $\overline{\nu}$, are calculated, as well as the pre- and post-neutron fission yields as a function of N and A. The following input file is used

```
#
# n-Pu242-fy
#
# General
#
projectile n
element     Pu
mass        242
energy      energies
#
```
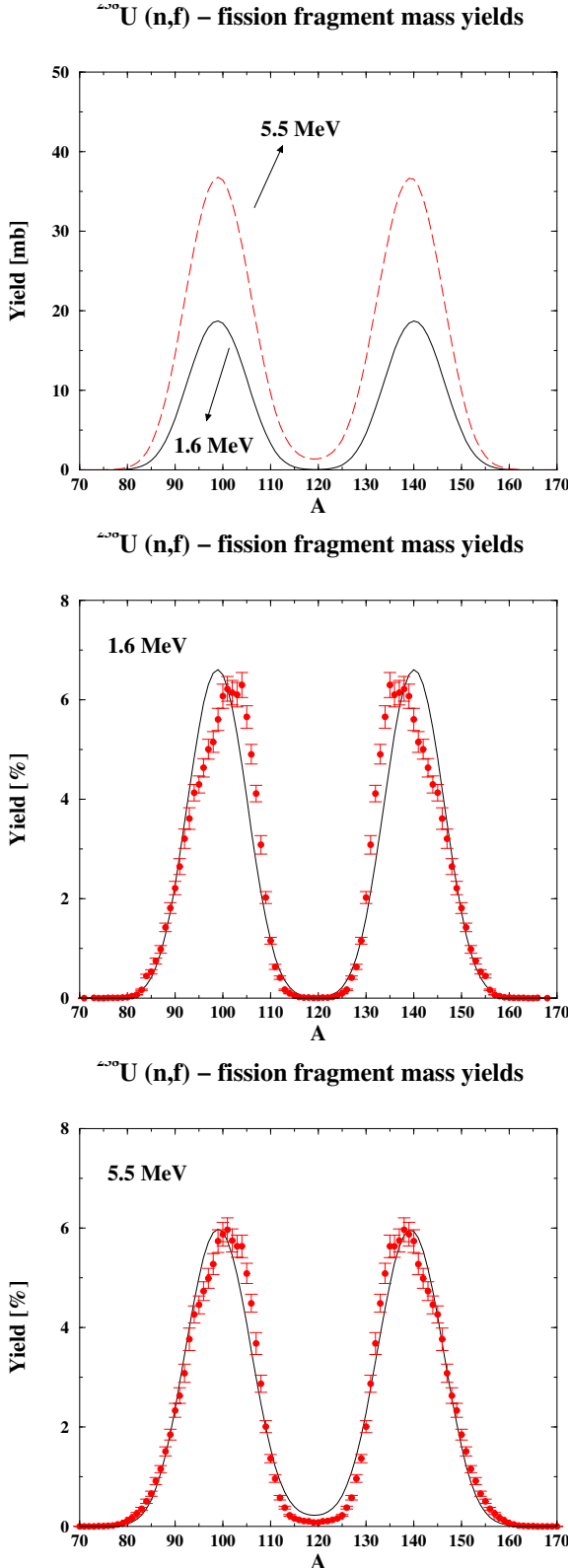
Figure 15.4: Fission fragment mass yield curves as function of the mass number A, produced by 1.6 MeV and 5.5 MeV neutrons on ^{238}U. The upper curve shows the results as they are produced by TALYS and the other two plots contain the comparison with experimental data in terms of normalized yields [137].
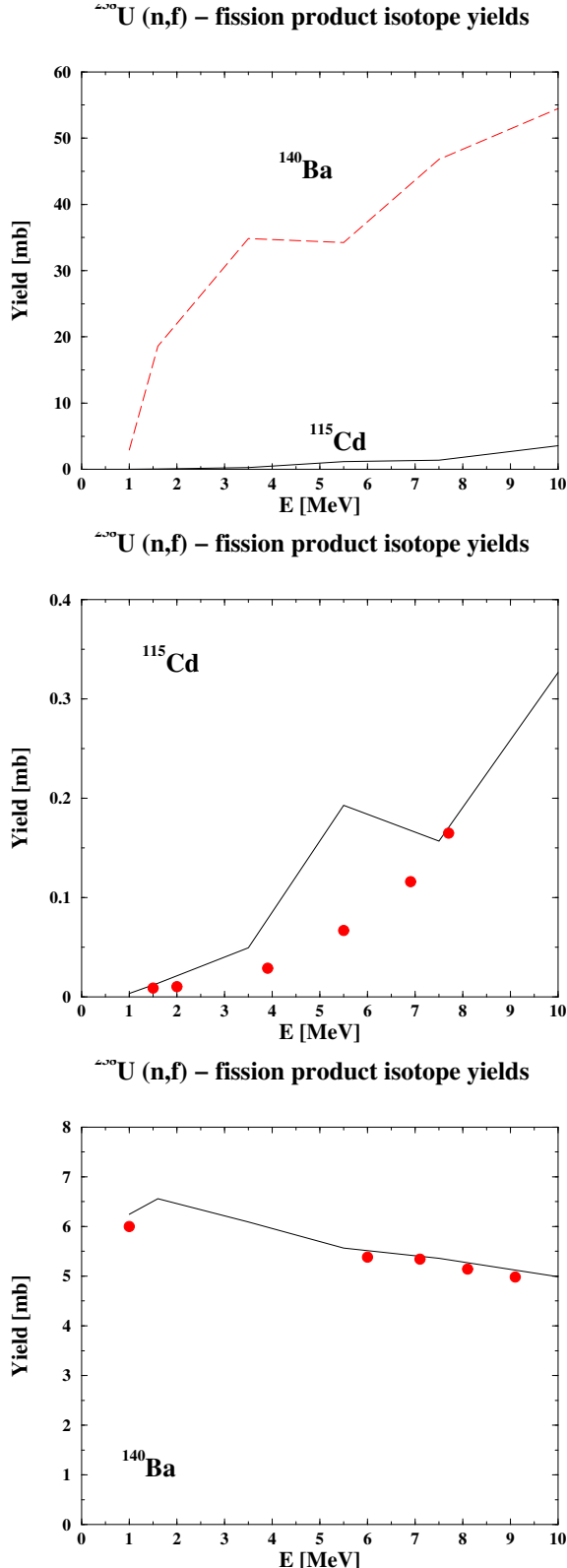
Figure 15.5: Fission product isotope yields produced by neutrons on ^{238}U as function of the mass number A. The upper plot shows the results for ^{115}Cd and ^{140}Ba as they are produced by TALYS and the other two plots contain the comparison with experimental data in terms of normalized yields [138, 139].

```
# Parameters and models
#
maxrot 2
fymodel 2
best y
#
# Output
#
channels y
filechannels y
ecissave y
inccalc y
eciscalc y
massdis y
# In a second run, you may use
# eciscalc n
# inccalc n
# for efficient variations for this input file
```

Note the comment given at the end of the input file. Note also that a hardwired energy grid is used through *n0-20.grid*. The prompt average neutron multiplicity $\bar{\nu}$ is given in the output file *nubar.tot*. Fig. 15.6 shows a comparison with experimental data and some of the world nuclear data libraries. Fig. 15.7 presents the distribution of $\bar{\nu}(A)$ as a function of fission product mass, for an incident energy of 1 MeV. This is given in output file *nuA001.000.fis*. Fig. 15.8 presents the distribution of ν as a function of number of neutrons, for an incident energy of 1 MeV. This is given in output file *Pnu001.000.fis*.   ■

Sample case 15.3 **Fission yields and neutron observables n + ^{239}Pu**

Since 2020, TALYS has the option to start a calculation with a pre-defined fission fragment (FF) distribution and to explicitly calculate the neutron and gamma decay from that, leading to fission product yields (FPY) and various fission neutron observables. In these sample cases for thermal neutrons on ^{239}Pu, 3 different FF models are compared with regards to the resulting FPY and neutron distributions. The prompt neutron multiplicity as a function of mass, $\bar{\nu}(A)$, number of neutrons, $P(\nu)$, the total average, $\bar{\nu}$, and the prompt fission neutron spectrum, are calculated, as well as the fission product yields as a function of Z and A. The following input file for the GEF model is used

```
projectile n
element    Pu
mass       239
energy   2.53e-8
ejectiles g n
massdis y
fymodel 4
ffmodel 1
```
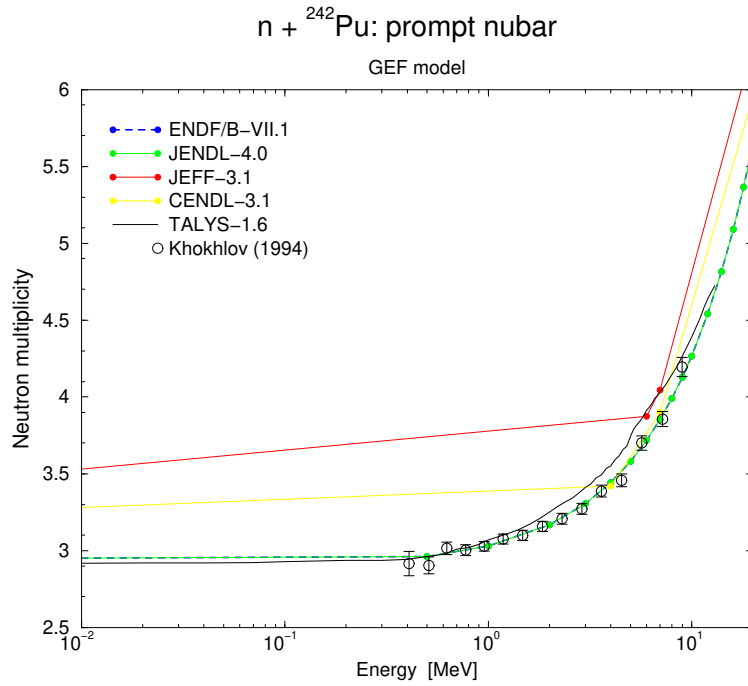
Figure 15.6: Average prompt neutron multiplicity $\overline{\nu}$ for n + ^{242}Pu, with the GEF model, compared with experimental data and nuclear data libraries.
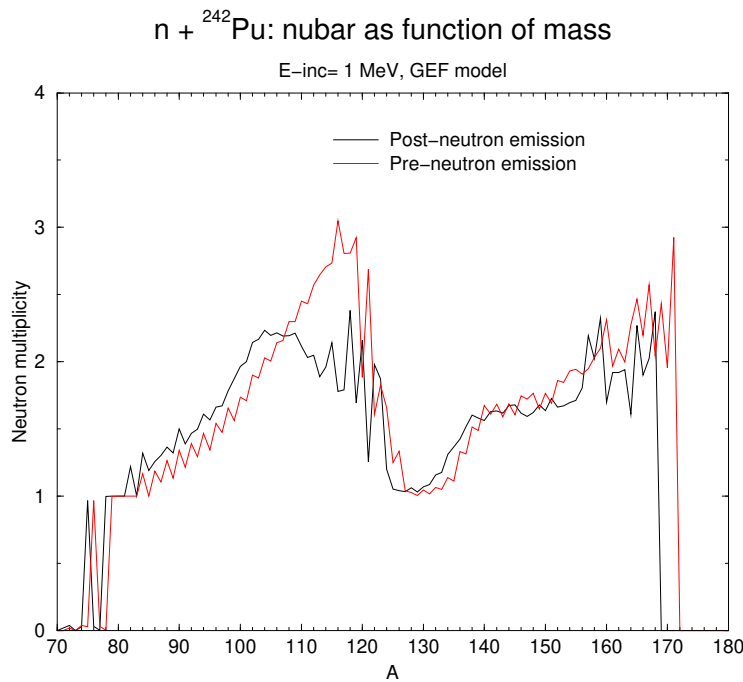

Figure 15.7: Average prompt neutron multiplicity $\overline{\nu}(A)$, as a function of fission product mass, for n + ^{242}Pu, with the GEF model.

n + ^{242}Pu: Prompt neutron multiplicity distribution
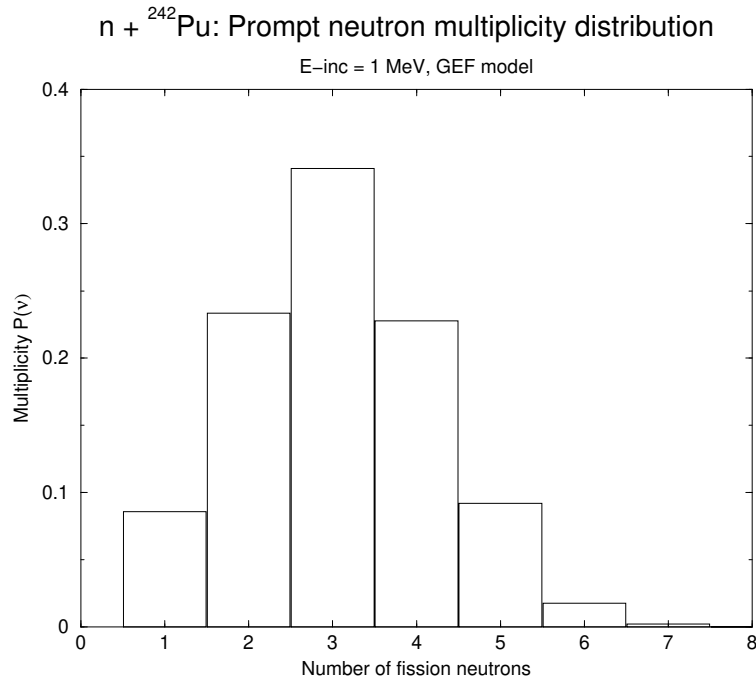
Figure 15.8: Prompt neutron multiplicity distribution $P(\nu)$, as a function of the number of neutrons, for n + ^{242}Pu, with the GEF model.

```
ldmodel 5
Rfiseps 1.e-5
outspectra y
bins 40
channels y
maxchannel 8
#
# For more precise results you may decrease Rfiseps to e.g. 1.e-9 and
# increase bins to 100
#
```

and similarly for the HF3D model (**ffmodel 2**) and SPY model (**ffmodel 3**). The FY calculation can be somewhat time consuming so the sample cases are done only for thermal neutron energy, for 40 bins and for a relative large value of Rfiseps. These values could be altered to get more precise results. Note however that the usual incident energy file can also be used to obtain e.g. $\overline{\nu}$ as a function of incident energy. In Fig. 15.9 the FPY results for the 3 models are plotted together with the FPY from ENDF/B-VIII.0. These FPY as a function of A are given in file *yieldA1.00E-06.fis*. Fig. 15.10 presents the distribution of $\overline{\nu}(A)$ as a function of fission product mass. This is given in output file *nunA1.00E-06.fis*. Fig. 15.11 presents the distribution of ν as a function of number of neutrons, for an incident energy of 1 MeV. This is given in output file *Pnun1.00E-06.fis*. The prompt fission neutron spectrum of Fig. 15.12 is given in file *pfns1.00E-06.fis*. In the addition to the latter case, in *n-Pu239-fy-pfns* we have also done a TALYS run without explicit FY evaporation, which means the phenomenological model of Iwamoto model for PFNS is automatically used.   ∎
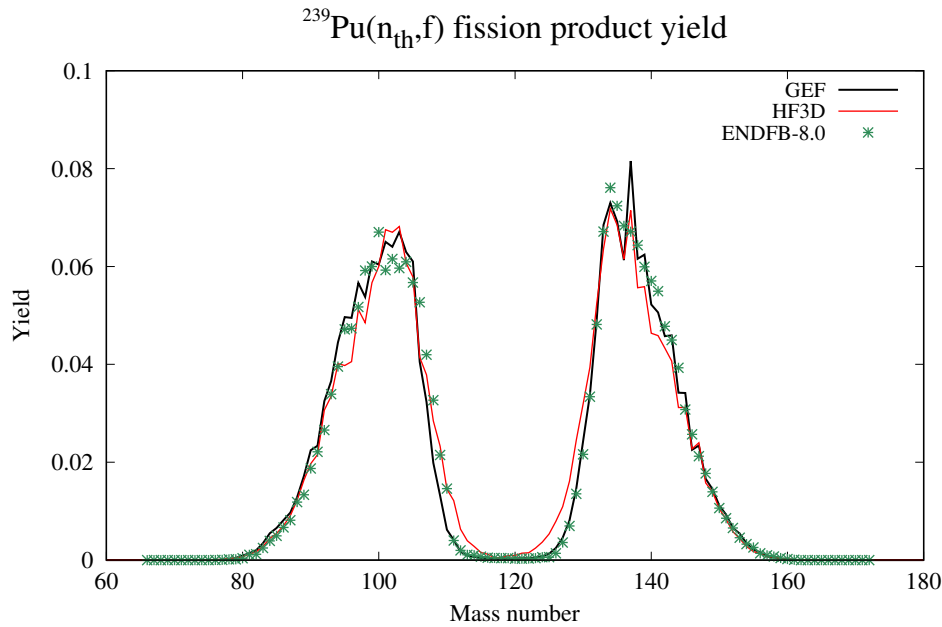
Figure 15.9: Fission product yields for n_{th} + ^{239}Pu, for 3 FF models.
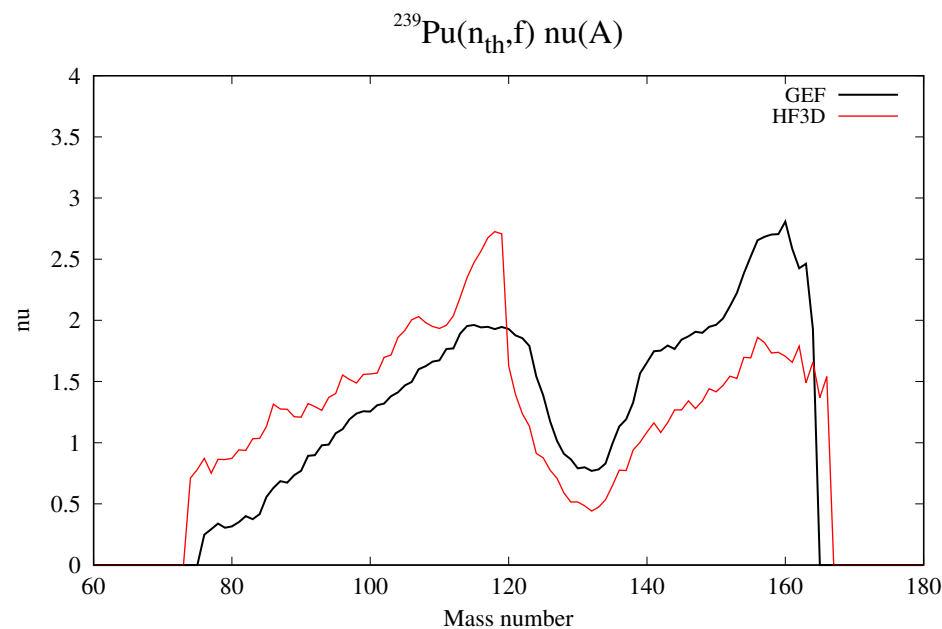
Figure 15.10: Prompt neutron multiplicity $\overline{\nu}(A)$, as a function of fission product mass, for n_{th} + ^{239}Pu, for 3 FF models.
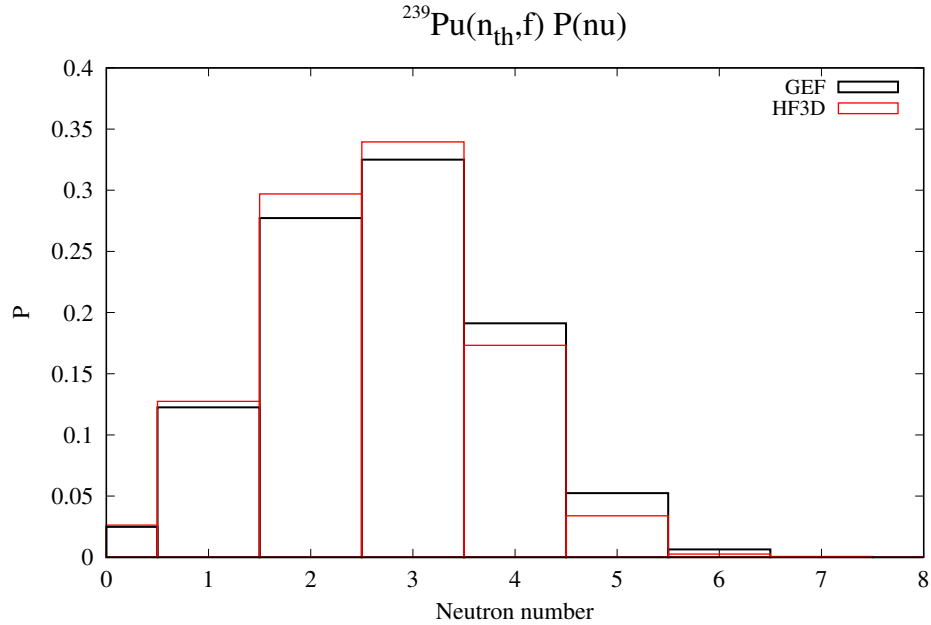
Figure 15.11: Prompt neutron multiplicity distribution $P(\nu)$, for $n_{th} + {}^{239}$Pu, for 3 FF models.
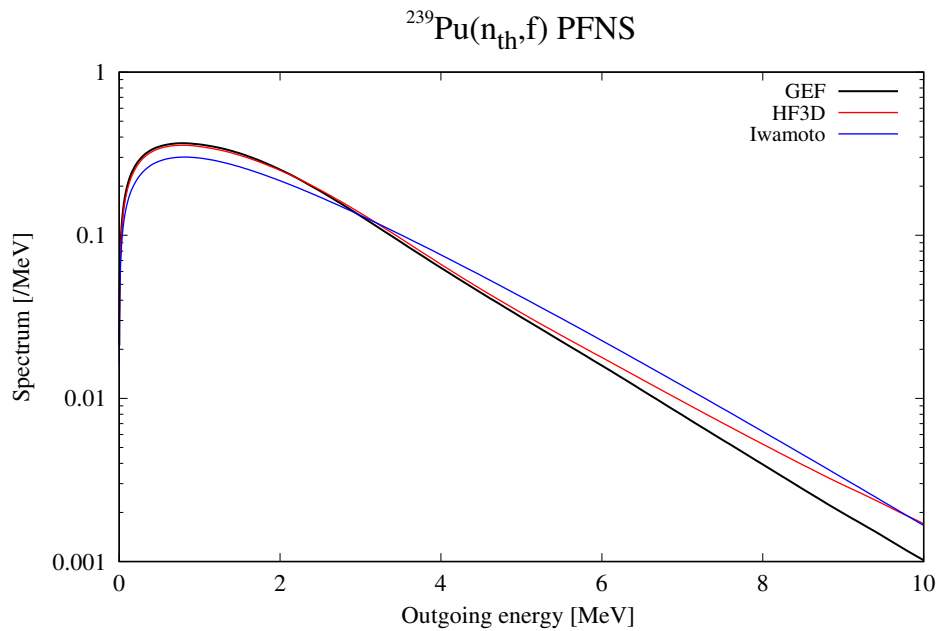
Figure 15.12: Prompt fission neutron spectrum, for $n_{th} + {}^{239}$Pu, for 3 FF models.

16. Thermal reactions

The Introduction states that TALYS is meant for the analysis of data in the 1 keV - 200 MeV energy region. The lower energy of 1 keV should not be taken too literally. More accurate is: above the resolved resonance range. The start of the unresolved resonance range differs from nucleus to nucleus and is related to the average resonance spacing D_0 or, equivalently, the level density at the binding energy. Generally, the starting energy region is higher for light nuclides than for heavy nuclides. Only beyond this energy, the optical and statistical models are expected to yield reasonable results, at least for the non-fluctuating cross sections. The lower energies are the domain of R-matrix theory, which describes the resonances. Nevertheless, it would be useful to have a first-order estimate of the non-threshold reactions, not only for the obvious neutron capture channel, but also for the exothermal (n, p), (n, α) and fission channels. The fact that a nuclear model calculation in TALYS is only performed down to about 1 keV should not prevent us to give at least an estimate of the $1/v$-like behaviour of the excitation function down to 10^{-5} eV (the lower energy limit in ENDF-6 files). In collaboration with J. Kopecky, we constructed a method that provides this.

16.1 Capture channel

First, we decide on the lower energy of validity of a TALYS nuclear model calculation E_L. Somewhat arbitrarily, we set as default $E_L = D_0$ when we wish to construct evaluated data libraries, where D_0 is taken from the nuclear model database or, if not present, derived from the level density. E_L can also be entered as an input keyword (**Elow**). Next, we determine the neutron capture cross section at the thermal energy $E_{th} = 2.53.10^{-8}$ MeV, either from the experimental database, see Chapter 5, or, if not present, from the systematical relation [140]

$$\sigma_{n,\gamma}(E_{th}) = 1.5 \times 10^{-3} a (S_n - \Delta)^{3.5} \quad \text{mb} \tag{16.1}$$
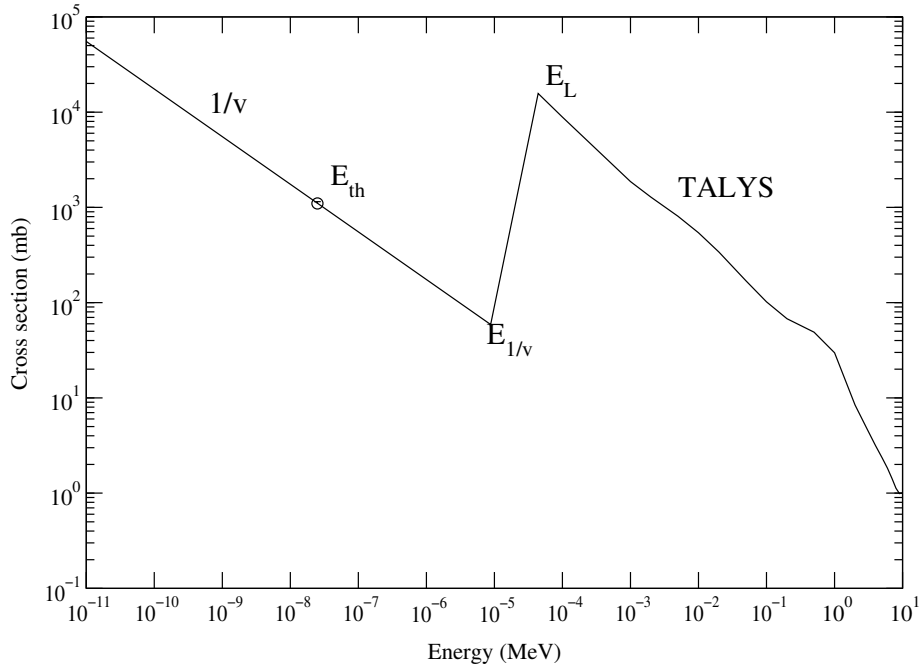
Figure 16.1: Capture cross section at low energies. The origin of the various energy regions are indicated.

with a the level density parameter at the separation energy S_n and Δ the pairing energy. We assign a $1/v$, i.e. $1/\sqrt{E}$, dependence to the cross section from 10^{-5} eV to an upper limit $E_{1/v}$ which we set, again arbitrarily, at $E_{1/v} = 0.2E_L$. The $1/v$ line obviously crosses $\sigma_{n,\gamma}(E_{th})$ at E_{th}. The points at $E_{1/v}$ and E_L are connected by a straight line. The resulting capture cross section then looks like Fig. 16.1. In reality, the region between $E_{1/v}$ and E_L is filled with resolved resonances, the only feature we did not try to simulate.

16.2 Other non-threshold reactions

For other reactions with positive Q-values, such as (n, p) and (n, α), only a few experimental values at thermal energy are available and a systematical formula as for (n, γ) is hard to construct. If we do have a value for these reactions at thermal energy, the same method as for capture is followed. If not, we assume that the ratio between the gamma decay width and e.g. the proton decay width is constant for incident energies up to E_L. Hence, we determine $R_p = \sigma_{n,p}/\sigma_{n,\gamma}$ at E_L, and since we know the thermal (n, γ) value we can produce the (n,p) excitation function down to 10^{-5} eV by multiplying the capture cross section by R_p. A similar procedure is applied to all other non-threshold reactions.

16.3 Implementation, options and sample cases

Implementation 16.3.1 In *talys/structure/thermal/*, the thermal cross sections for (n, γ), (n, p), (n, α) and (n, f) cross sections are stored. The values come from Mughabghab [141] and Kopecky, who has compiled this database for use in the EAF library. In TALYS, we use this to determine cross sections for non-threshold reactions at low energies. For each isotope, we read Z, A, target state (ground state or isomer), final state (ground state or isomer), the thermal

(n, γ) cross section, its error, the thermal (n, p) cross section, its error, the thermal (n, α) cross section, its error, the thermal (n, f) cross section, its error, nuclear symbol. The format is (4i4,8e9.2,7x,i4,a2). As an example, below are the values for the Fe-isotopes from *Fe.ther*.

```
 26  54  0   0 2.25E+03 1.80E+02                      1.00E-02      ...      54Fe
 26  55  0   0 1.30E+04 2.00E+03                      1.70E+05      ...      55Fe
 26  56  0   0 2.59E+03 1.40E+02                                    ...      56Fe
 26  57  0   0 2.48E+03 3.00E+02                                    ...      57Fe
 26  58  0   0 1.32E+03 3.00E+01                                    ...      58Fe
 26  59  0   0 1.30E+04 3.00E+03                      1.00E+04      ...      59Fe
```

Sample case 16.1 **Low energy resonance data for n + ^{89}Y**

TALYS can read in resonance parameters, from various possible sources, and call the RECENT code of Red Cullen's PREPRO package, in TALYS included as a subroutine. Low energy pointwise resonance cross sections will then be added to channels like total, elastic, fission and capture.

Case a: Resonance input file: Standard

The input file is

```
#
# n-Y089-RRR-standard
#
# General
#
projectile n
element Y
mass 89
energy energies
#
# Model
#
resonance y
#
# Output
#
channels y
filechannels y
wtable 39 90 0.82 E1
```

where *n0-2.grid* is the built-in TALYS energy grid for neutrons between 0 and 2 MeV.

Case b: Resonance input file: Temperature broadening

The input file is

```
#
# n-Y089-RRR-temp
```

```
#
# General
#
projectile n
element Y
mass 89
energy energies
#
# Model
#
resonance y
Tres 1200.
#
# Output
#
channels y
filechannels y
wtable 39 90 0.82 E1
```

Case c: Resonance input file: Group structure

The input file is

```
#
# n-Y089-RRR-group
#
# General
#
projectile n
element Y
mass 89
energy energies
#
# Model
#
resonance y
group y
#
# Output
#
channels y
filechannels y
wtable 39 90 0.82 E1
```

The results are depicted in Fig. 16.2. Note the discontinuity between the end of the resonance range and the statistical model energy range of TALYS. Obviously, this needs to be studied case by case. ∎
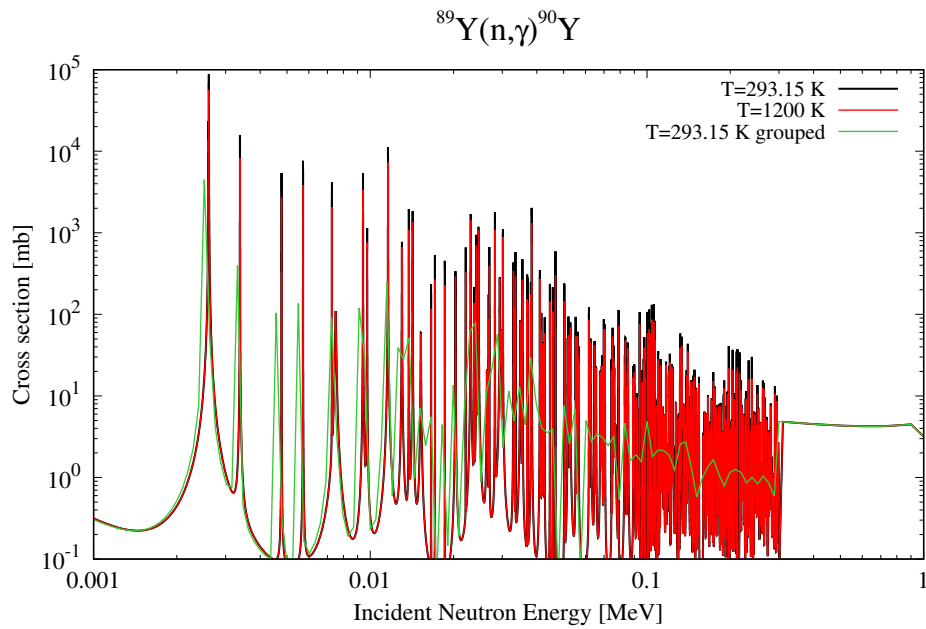
Figure 16.2: ^{89}Y(n,γ) cross section, at 293.15 K, 1200 K, and grouped.

Sample case 16.2 **Unresolved resonance range parameters: n + ^{136}Ba**

With TALYS, parameters for the unresolved resonance range (URR) can be produced. The following input file is used

```
#
# n-Ba136-URR
#
# General
#
projectile n
element    ba
mass       136
energy    energies
#
# Output
#
urr y
```

where the line **urr y** results in a set of URR output files which are described page 576. The top of the general output file *urr.dat* looks as follows:

```
# header:
#   title: Ba136(n,urr) URR parameter at  1.000000E-03 MeV
#   source: TALYS-2.0
#   user: Arjan Koning
#   date: 2023-12-17
```

```
#    format: YANDF-0.1
# target:
#    Z: 56
#    A: 136
#    nuclide: Ba136
# reaction:
#    type: (n,urr)
#    E-incident [MeV]:  1.000000E-03
# parameters:
#    neutron separation energy [MeV]:  6.905644E+00
# observables:
#    thermal capture cross section [mb]:  7.030000E+02
#    potential scattering radius [fm]:  4.397314E+00
# datablock:
#    quantity: URR parameter
#    columns: 13
#    entries: 3
##        l              J              P            D(l)         D(l,J)
##       []             []             []           [eV]          [eV]
     0          5.000000E-01       1          1.200750E+03  1.200750E+03
     1          5.000000E-01      -1          4.147023E+02  1.200750E+03
     1          1.500000E+00      -1          4.147023E+02  6.334905E+02
```

17. Populated initial nucleus

Usually, a TALYS calculation will concern a projectile with a certain incident energy and a target, either in its ground or an excited state. For various reasons, we have introduced the possibility to start the decay from an initial population, i.e. an excited nucleus with a population distributed over excitation energy. An example of an interesting application is the neutron spectrum from fission fragments. One could calculate the fragment distribution from fission, e.g. as described in Section 15.7.3 or from empirical methods, and assume a population per excitation energy and spin, of the excited light and heavy fission fragment (models for such distributions exist, see e.g. Ref. [142]). This distribution can then be the starting point for a TALYS calculation. The initial population enters the Hauser-Feshbach scheme and the compound nucleus calculation proceeds as usual. The emitted neutrons can be recorded as well as the path from fission fragment to fission product. All relevant nuclear structure quantities are available since we simulate the process by a photon-induced reaction, the only difference being that we do not excite a single compound nucleus energy but directly fill the continuum bins and discrete levels according to our specified starting population. TALYS can be used in this mode by simply specifying **projectile 0**, (p. 290), and providing an energy file as input, see **energy** (p. 293). The initial population can be provided at two levels of detail. A full excitation energy-spin-parity population can be given, which is then interpolated on the internal excitation energy scheme of TALYS. Alternatively, only the total population per excitation energy can be given, after which the spin-parity-dependent population is determined by multiplying it with the spin distribution of Eq. (8.8). For the fission neutron spectrum example mentioned above, one could loop over all fission fragments (by writing a clever script), sum the results, and obtain the fission neutron spectrum. There are more applications for this feature, such as coupling a high-energy intranuclear cascade code with TALYS, the latter taking care of the low energy evaporation part including all its quantum-mechanical conservation rules.

18. Astrophysical reaction rates

A complete calculation of astrophysical reaction rates is possible with TALYS. In stellar interiors, nuclides not only exist in their ground states but also in different thermally excited states and a thermodynamic equilibrium holds locally to a very good approximation. Therefore, most of nuclear astrophysics calculations have made use of nuclear reaction rates evaluated within the statistical model [143]. The assumption of a thermodynamic equilibrium combined with the compound nucleus cross sections for the various excited states then allows to produce Maxwellian-averaged reaction rates, which is important input for stellar evolution models. Calculation of stellar reaction rates is obviously not new, but TALYS provides some features which automatically makes the extension to reaction rate calculations very worthwhile. In contrast with existing dedicated astrophysical reaction rate codes, the present Chapter shows that we provide the inclusion of pre-equilibrium reaction mechanism, the detailed competition between all open channels, the inclusion of multi-particle emission (neglected in most astrophysics codes), the inclusion of detailed width fluctuation corrections, the inclusion of parity-dependent level densities, the inclusion of coupled channel description for deformed nuclei, and the coherent inclusion of fission channel. Different prescriptions are also used when normalizing nuclear models on available experimental data, such as level densities on s-wave spacings or E1 resonance strength on photoabsorption data.

The energies of both the targets and projectiles, as well as their relative energies E, obey Maxwell-Boltzmann distributions corresponding to the temperature T at that location (or a black-body Planck spectrum for photons). The astrophysical rate is obtained by integrating the cross section given by Eq. (13.2) over a Maxwell-Boltzmann distribution of energies E at the given temperature T. In addition, in hot astrophysical plasmas, a target nucleus exists in its ground as well as excited states. In a thermodynamic equilibrium situation, the relative populations of the various levels of nucleus with spins I^μ and excitation energies E_x^μ obey a Maxwell-Boltzmann distribution. Hence, in the formulae to follow, it is understood that the definition of the incident α channel, see below Eq. (13.2), now includes an explicit superscript μ to distinguish between the

excited states. The effective stellar rate of $\alpha \to \alpha'$ in the entrance channel at temperature T taking due account of the contributions of the various target excited states is finally expressed as

$$N_A \langle \sigma v \rangle^*_{\alpha\alpha'}(T) = \left(\frac{8}{\pi m}\right)^{1/2} \frac{N_A}{(kT)^{3/2} G(T)} \int_0^\infty \sum_\mu \frac{(2I^\mu + 1)}{(2I^0 + 1)} \times$$
$$\sigma^\mu_{\alpha\alpha'}(E)E \exp\left(-\frac{E + E_x^\mu}{kT}\right) dE, \tag{18.1}$$

where k is the Boltzmann constant, m the reduced mass of the α channel, N_A the Avogadro number, and

$$G(T) = \sum_\mu (2I^\mu + 1)/(2I^0 + 1) \exp(-E_x^\mu/kT) \tag{18.2}$$

the T-dependent normalized partition function. Reverse reactions can also be estimated making use of the reciprocity theorem [143]. In particular, the stellar photodissociation rates are classically derived from the radiative capture rates by

$$\lambda^*_{(\gamma,\alpha)}(T) = \frac{(2I + 1)(2j + 1)}{(2I' + 1)} \frac{G_I(T)}{G_{I'}(T)} \left(\frac{AA_a}{A'}\right)^{3/2} \left(\frac{kT}{2\pi\hbar^2 N_A}\right)^{3/2} \times$$
$$N_A \langle \sigma v \rangle^*_{(\alpha,\gamma)} e^{-Q_{\alpha\gamma}/kT}, \tag{18.3}$$

where $Q_{\alpha\gamma}$ is the Q-value of the $I^0(\alpha,\gamma)I'^0$ capture channel. Note that, in stellar conditions, the reaction rates for targets in thermal equilibrium are usually believed to obey reciprocity since the forward and reverse channels are symmetrical, in contrast to the situation which would be encountered for targets in their ground states only [143]. In TALYS, the total stellar photodissociation rate is determined from

$$\lambda^*_{(\gamma,j)}(T) = \frac{\sum_\mu (2J^\mu + 1) \lambda^\mu_{(\gamma,\alpha)}(T) \exp(-E_x^\mu/kT)}{\sum_\mu (2J^\mu + 1) \exp(-E_x^\mu/kT)}, \tag{18.4}$$

where the photodissociation rate $\lambda^\mu_{(\gamma,\alpha)}$ of state μ with excitation energy E_x^μ is given by

$$\lambda^\mu_{(\gamma,\alpha)}(T) = \int_0^\infty c\, n_\gamma(E,T)\, \sigma^\mu_{(\gamma,\alpha)}(E)\, dE, \tag{18.5}$$

where c is the speed of light, $\sigma^\mu_{(\gamma,j)}(E)$ the photodisintegration cross section at energy E, and n_γ the stellar γ-ray distribution well described by the black-body Planck spectrum at the given temperature T.

Options 18.0.1 In TALYS, if **astro y**, an appropriate incident energy grid for astrophysical calculations is made which overrules any incident energy given by the user. Inclusion of ground state only, or particular excited states can be steered with **astrogs** (p. 673), **nonthermlev** (p. 677) and **astroex** (p. 676). With **astroE** (p. 674) the energy of Maxwellian average can be chosen, which one usually wants to put at 30 keV. Also the temperature can be set with **astroT** (p. 675).

Implementation 18.0.1 The implementation of astrophysical reaction rates takes place in *astro.f*.

Sample case 18.1 **Astrophysical reaction rates : n + ^{187}Os**

With TALYS, astrophysical reaction rates can be calculated. As sample case, we took the work done in Ref.[144] where the ^{187}Os(n,γ) was studied for the derivation of the age of the galaxy withing the Re-Os cosmochronology.

Case a: ^{187}**Os(n,γ) cross section**

First, the calculated ^{187}Os(n,γ) was compared with experimental data, using the following input file

```
#
# n-Os187-astro-ng
#
# General
#
projectile n
element    os
mass       187
energy    energies
channels y
filechannels y
#
# Parameters
#
ldmodel 1
strength 8
wtable        76 188    0.88 e1
```

The results are given in Fig.18.1.

Case b: ^{187}**Os(n,γ) astrophysical reaction rate**

Next, the astrophysical reaction rates for neutrons on ^{187}Os are computed with the following input file

```
#
# n-Os187-astro-rate
#
# General
#
projectile n
element    os
mass       187
energy    1.
#
# Parameters
#
astro y
```

```
astrogs n
partable y
ldmodel 1
strength 8
wtable        76 188    0.88 e1
```

which produces various output files in which the reaction rates as function of temperature are given. The (n, γ) rate as given in the file *astrorate.g* is

```
# header:
#   title: Os187(n,g) reaction rate
#   source: TALYS-2.0
#   user: Arjan Koning
#   date: 2023-12-14
#   format: YANDF-0.1
# target:
#   Z: 76
#   A: 187
#   nuclide: Os187
# reaction:
#   type: (n,g)
#   Q-value [MeV]:  7.989608E+00
#   E-threshold [MeV]:  0.000000E+00
# datablock:
#   quantity: reaction rate
#   columns: 4
#   entries: 30
##      T          reaction rate     MACS          G(T)
##    [10^9 K]       [cm3/mol/s]      [mb]          []
   1.000000E-04   1.255844E+09   5.124098E+05   1.000000E+00
   5.000000E-04   9.040671E+08   1.649672E+05   1.000000E+00
   9.999999E-04   7.231653E+08   9.330813E+04   1.000000E+00
   5.000000E-03   4.264272E+08   2.460604E+04   1.000000E+00
   1.000000E-02   3.303214E+08   1.347778E+04   1.000024E+00
   5.000000E-02   1.845430E+08   3.367398E+03   1.207792E+00
   9.999999E-02   1.470494E+08   1.897340E+03   1.645169E+00
   1.500000E-01   1.335211E+08   1.406650E+03   1.952226E+00
   2.000000E-01   1.263106E+08   1.152409E+03   2.198210E+00
.....................................
```

Similar same numbers can be found in the file for protons, etc. In *astrorate.tot* the rates for all reactions can be found.

■

Sample case 18.2 **Maxwellian averaged cross section at 30 keV: n + ^{138}Ba**
In this sample case, the Maxwellian averaged cross section (MACS) at 30 keV is calculated. The following input file is used

```
#
# n-Ba138-MACS
#
```

^{187}Os(n,γ)^{188}Os
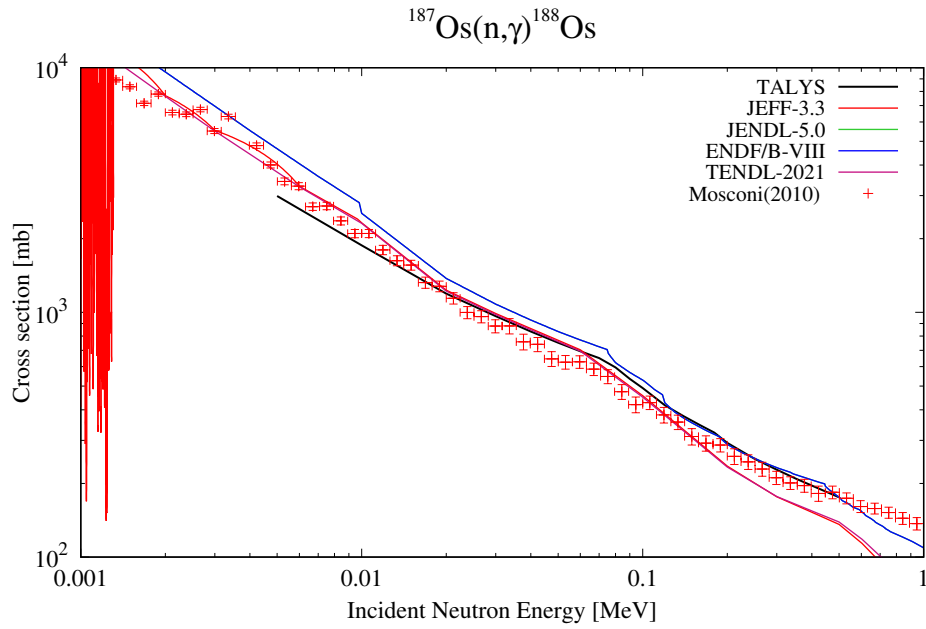
Figure 18.1: ^{187}Os(n,γ) cross section.

```
# General
#
projectile n
element    ba
mass       138
energy   1.
#
# Output
#
astroE 0.030
```

where the line **astroE 0.03** determines the energy in MeV for which the average is calculated. Note that the line **energy 1.** is irrelevant, but must nevertheless be given. The file *astrorate.g* looks as follows:

```
# header:
#   title: Ba138(n,g) reaction rate
#   source: TALYS-2.0
#   user: Arjan Koning
#   date: 2023-12-14
#   format: YANDF-0.1
# target:
#   Z: 56
#   A: 138
#   nuclide: Ba138
# reaction:
#   type: (n,g)
```

```
#   Q-value [MeV]:  4.723434E+00
#   E-threshold [MeV]:  0.000000E+00
#   <E> [MeV]: 3.000000E-02
#   astrogs: y
# datablock:
#   quantity: reaction rate
#   columns: 4
#   entries: 1
##       T         reaction rate      MACS           G(T)
##    [10^9 K]       [cm3/mol/s]       [mb]            []
   3.481369E-01   8.521989E+05   5.887537E+00   1.000000E+00
```

in which the temperature, reaction rate and MACS is given. For this case, the deviation from
a normal 30 keV calculation (which can be obtained by removing the **astroE** line and using
energy 0.03) is small.   ∎

19. Medical isotope production

This section describes the formalism to calculate the production yield of a radioactive nucleus by a nuclear reaction. Starting from the general formalism we will introduce realistic approximations and derive simpler equations that hold in basically all cases of interest. In TALYS we have implemented only analytical solutions to the production and depletion equations. This may be generalized in future versions.

19.1 Production and depletion of isotopes

The most general situation is that of the irradiation of a piece of material, consisting of many different isotopes, which were either present at the start of the irradiation, have been formed, or will be formed during the irradiation, by either the primary flux of particles, by secondary particles, or by radioactive decay. If we have a total of K different isotopes (theoretically K may stand for the the entire nuclide chart) and the number of each isotope k is N_k, then the temporal development of such a system is described by K differential equations:

$$
\begin{aligned}
\frac{dN_1(t)}{dt} &= \sum_{k=1,k\neq 1}^{K} \Lambda_{k\rightarrow 1} N_k(t) - \Lambda_1 N_1(t) \\
&\quad \ldots \\
\frac{dN_i(t)}{dt} &= \sum_{k=1,k\neq i}^{K} \Lambda_{k\rightarrow i} N_k(t) - \Lambda_i N_i(t) \\
&\quad \ldots \\
\frac{dN_K(t)}{dt} &= \sum_{k=1,k\neq K}^{K} \Lambda_{k\rightarrow K} N_k(t) - \Lambda_K N_K(t)
\end{aligned}
\tag{19.1}
$$

In each equation, the first term is a feeding term. In the most general case, various parent nuclides may contribute to the formation of isotope i, hence the summation over parent nuclides k, with

$\Lambda_{k\to i}$ the partial formation rate for any possible parent isotope k to isotope i. Each partial formation rate can be expressed as

$$\Lambda_{k\to i} = \lambda_{k\to i} + R_{k\to i} \tag{19.2}$$

with $\lambda_{k\to i}$ the (partial) radioactive decay rate and $R_{k\to i}$ the (partial) nuclear reaction rate for any possible parent isotope k to isotope i. The second terms of Eq. (19.1) are loss terms due to radioactive decay and nuclear reactions from isotope i to any other isotope. Here the total depletion rate (we interchange "depletion" with "formation" whenever appropriate) for isotope i is

$$\Lambda_i = \lambda_i + R_i \tag{19.3}$$

where the total decay rate for isotope i is

$$\lambda_i = \sum_{k=1, k\neq i}^{K} \lambda_{i\to k}$$

and the total nuclear reaction rate for isotope i is

$$R_i = \sum_{k=1, k\neq i}^{K} R_{i\to k} \tag{19.4}$$

The entire loop over k may run over isotopes in their ground or isomeric states . Theoretically, the sum over reaction rates could include secondary particles (neutrons, photons, alpha particles etc.) formed after the first interaction of the incident beam with the material, over the entire outgoing energy spectrum. Since the number of isotopes i, $N_i(t)$ may appear simultaneously in many equations, due to its possible formation, or depletion, by many different nuclear reactions, it is clear that such a coupled system can only be solved by complicated mathematical and computational techniques. In fact, the most exact simulation would involve a Monte Carlo 3D transport calculation in which all primary and secondary particles are taken into account, including complete cross section libraries for all possible particles, coupled with an activation code that keeps track of the nuclide inventory. If we neglect such thick target transport issues, a system of equations like (19.1) is often solved by methods developed by Bateman [145] for radioactive decay and later generalized for source terms by Rubinson [146].

Fortunately, the situation is often not as complex as sketched above, since very reasonable approximations can be introduced into Eq. (19.1), certainly for charged-particle induced reactions. First, let us start with the common case of the irradiation of a target which contains of only one natural element at the start of the irradiation. This set of equations can be then be separated into a linear combination of contributions by each target *isotope*. Hence, we solve Eq. (19.1) one by one for each target isotope and add these contributions at the end to get the answer for the target material. Then, for such a mono-isotopic target T we have at the start of the irradiation

$$\begin{aligned} t = 0 : N_T &= N_T(0) \\ N_i &= 0 \\ &\cdots \\ N_K &= 0 \end{aligned} \tag{19.5}$$

Since in practice our target isotope is not radioactive, the loss terms reduce to $\Lambda_T = R_T$ in Eq. (19.1) for N_T. Next, if a substantial part of the target is converted into other isotopes, beam particles

may interact with atoms other than the original target atoms. However, this is only a concern for irradiation times of the order of months or longer. For most practical applications, like medical isotope production, we can often assume that the burn-up of the target is small and that the target composition does not change much during the irradiation (this will be confirmed by some of our sample cases). Hence, in addition we will assume there are no nuclear reaction or radioactive decay feeding terms for the *target* isotope T.

This means that the target isotope is described by the following simple equation

$$\frac{dN_T(t)}{dt} = -R_T N_T(t) \tag{19.6}$$

which basically assumes that the only thing that happens to the target material is burn-up through nuclear reactions.

For the isotopes that are produced during the irradiation we can make similar reasonable assumptions. We assume there is no loss of a *produced* isotope of interest through nuclear reactions with beam particles, i.e. we assume nuclides are not hit twice (again, this assumption becomes less accurate at very long irradiation times). This is equivalent to stating that the isotopes of interest are only produced from nuclear reactions on the target isotopes or from decay of other products formed during the irradiation. Also, consistent with the assumption for the target isotope that nuclides are not hit twice, we have $\Lambda_i = \lambda_i$ for the depletion term, and assume that no other nuclear reactions lead to the isotope of interest. Thus for the produced isotopes i we obtain

$$\frac{dN_i(t)}{dt} = \sum_{k=1,k\neq i}^{K} \lambda_{k\to i} N_k(t) + R_{T\to i} N_T(t) - \lambda_i N_i(t) \tag{19.7}$$

Nuclides often have only one or a few radioactive decay modes. Usually, only beta decay to the ground state or an isomer needs to be considered, although in some cases alpha decay may occur as well. If we neglect alpha decay, the summation in the first term above reduces to only one term. Thus, Eq. (19.7) reduces to

$$\frac{dN_i(t)}{dt} = \lambda_{p\to i} N_p(t) + R_{T\to i} N_T(t) - \lambda_i N_i(t) \tag{19.8}$$

where we now use the subscript p for the parent isotope which decays to isotope i. The parent isotope itself is described by the equation,

$$\frac{dN_p(t)}{dt} = R_{T\to p} N_T(t) - \lambda_p N_p(t) \tag{19.9}$$

where for simplicity we have left out a possible feeding term $\lambda_{g\to p} N_g(t)$ from its own parent (i.e. the grandparent of isotope i). It neglects radioactive decay to channels produced by multiple proton emission, e.g. ^{120}Te(p,2p)^{119}Sb and the contribution from its feeding channel ^{120}Te(p,2n)^{119}I + $2\beta^+$. Although the (p,2p) channel is generally smaller and therefore often not relevant for most practical medical isotope production routes, it would be safer that at higher energies feeding from radioactive decay is taken into account. For that a more general solution of Eq. (19.1) would have to be implemented, similar to solutions for neutron-induced problems where processes like e.g. multiple fission yield decay need to be taken into account. For most charged-particle induced reactions of interest, the current approximation is justified.

If we now use the boundary conditions $N_T(t=0) = N_T(0)$ and $N_p(t=0) = N_i(t=0) = 0$, the solutions to these equations are given by:

$$
\begin{aligned}
N_T(t) &= N_T(0)\, e^{-R_T t}, \\
N_p(t) &= N_T(0)\, \frac{R_{T \to p}}{\lambda_p - R_T}\, [e^{-R_T t} - e^{-\lambda_p t}], \\
N_i(t) &= N_T(0)\, \frac{R_{T \to i}}{\lambda_i - R_T}\, [e^{-R_T t} - e^{-\lambda_i t}] + N_T(0)\frac{R_{T \to p}\lambda_{p \to i}}{\lambda_p - R_T}\left[\frac{e^{-R_T t} - e^{-\lambda_i t}}{\lambda_i - R_T} - \frac{e^{-\lambda_p t} - e^{-\lambda_i t}}{\lambda_i - \lambda_p}\right]
\end{aligned}
\tag{19.10}
$$

This is derived in the Appendix.

By setting the derivative of $N_i(t)$ to zero, the irradiation time for which a maximal yield is obtained can be easily derived:

$$
t_{max} = \frac{ln(\lambda_i/R_T)}{\lambda_i - R_T}
\tag{19.11}
$$

The production of i is restrained by its β-decay on the one hand and by the decreasing number of available target atoms on the other hand. Hence, this observable t_{max} depends on the decay constant λ_i and the total production rate R_T.

Now that the analytical formulae for production are set with Eq. (19.10), the remaining ingredients needed to evaluate Eqs.(19.10) and (19.11) are: $N_1(0), \ldots, N_I(0)$, R, and λ, and this will be done in the next two sections.

19.2 Initial condition and stopping power

The number of target atoms at t=0, $N_i(0)$, for $1 \le i \le I$ equals:

$$
N_i(0) = \frac{N_A}{A}\, B_i\, \rho\, V_{tar},
\tag{19.12}
$$

where $N_A = 6.022\ 10^{23}$ is Avogadro's number, A is the mass number, B_i is the abundance of isotope i with $\sum_i^I B_i = 1$, ρ the mass density in [g/cm^3], and V_{tar} the active target volume in [cm^3]. V_{tar} is given by the product of the beam surface S_{beam} in [cm^2] and the effective target thickness in [cm], which can be expressed in terms of the stopping power $\frac{dE}{dx}$,

$$
V_{tar} = S_{beam} \int_{E_{back}}^{E_{beam}} \left(\frac{dE}{dx}\right)^{-1} dE,
\tag{19.13}
$$

where E_{beam} denotes the incident beam energy and E_{back} is the average projectile energy available at the backside of the target. If the projectiles travels through the target, the average projectile beam energy will decrease. The amount of energy loss inside the target is determined by the target thickness and the stopping power. The integration limits E_{beam} and E_{back} are fixed by the requested projectile energy range inside the target, which is determined by the cross section as function of projectile energy (excitation function). This formula neglects the spreading of the beam inside the target.

The stopping power describes the average energy loss of projectiles in the target by atomic collisions as a function of their energy in [MeV/cm]. We use the Bethe-Bloch formula [147]:

$$
\frac{dE}{dx} = 0.1535\, \rho\, \frac{Z}{A}\, \frac{z_p^2}{\beta^2}\, [ln\left(\frac{2m_e\gamma^2 v^2 W_{max}}{I^2}\right) - 2\beta^2],\ \ \text{MeV/cm}
\tag{19.14}
$$

with Z the target charge number, and z_p the projectile charge number, while β represents a beam particle traveling at a relative velocity

$$\beta = \frac{v}{c} = \sqrt{\frac{E_{beam}(E_{beam}+2m_0c^2)}{(E_{beam}+m_0c^2)^2}}, \qquad (19.15)$$

with rest mass m_0. Further, m_e is the electron mass, and $\gamma = \frac{1}{\sqrt{1-\beta^2}}$. The maximum energy transfer in a single collision, W_{max} is given by

$$W_{max} = 2m_ec^2(\beta\gamma)^2, \qquad (19.16)$$

if the incident particle is much heavier than the electron mass. For the mean excitation potential I a semi-empirical formula is adopted:

$$\frac{I}{Z} = 9.76 + 58.8Z^{-1.19} \text{ eV}. \qquad (19.17)$$

This expression is claimed to be tested only if $Z \geq 13$, but we use it for all values.

19.3 Nuclear reaction and decay rates

When the full beam hits the target (i.e., assuming that the beam diameter is smaller than the target dimensions), the production rate in [atoms/s] of isotope i through the nuclear reaction on the target isotope T is given by the following expression

$$R_{T \to i} = \frac{I_{beam}}{z_p\, q_e} \frac{1}{V_{tar}} \int_{E_{back}}^{E_{beam}} \left(\frac{dE}{dx}\right)^{-1} \sigma_i^{rp}(E)\, dE \qquad (19.18)$$

where I_{beam} is the beam current in [A] and q_e is the electron charge. The factor $I_{beam}/(z_p q_e)$ corresponds to the number of projectiles impinging on the target per [s]. The residual production cross section of i in [mb] is denoted by $\sigma_i^{rp}(E)$.

Analogously, the production rate in [s^{-1}] of all reaction channels, from the target, is given by:

$$R_T = \frac{I_{beam}}{z_p\, q_e} \frac{1}{V_{tar}} \int_{E_{back}}^{E_{beam}} \left(\frac{dE}{dx}\right)^{-1} (\sigma_{non}(E) - \sigma_{in}(E))\, dE \qquad (19.19)$$

where $\sigma_{non}(E)$ is the non-elastic cross section and $\sigma_{in}(E)$ is the inelastic cross section of i in [mb], which is nothing else than the residual production cross section $\sigma_i^{rp}(E)$. The difference $\sigma_{non}(E) - \sigma_{in}(E)$ provides the probability to create an isotope different from the original target atom in the nuclear reaction.

The decay rate of i is given by the simple relation

$$\lambda_i = \frac{\ln 2}{T_i^{1/2}}, \qquad (19.20)$$

where $T_i^{1/2}$ is the half-life of isotope i in [s]. The λ_i in the loss term usually feeds only one or two different channels, namely by beta decay to the ground state or isomer of the daughter isotope d,

$$\lambda_i = \lambda_{i \to d} = \lambda_{i \to d}^{g.s.} + \lambda_{i \to d}^{iso}. \qquad (19.21)$$

With this, all ingredients of Eq. (19.10) are defined and we may calculate the nuclide inventory $N_i(t)$ at any time during or after the irradiation process.

19.4   Radioactive activity

With $N_i(t)$ known, the final expression for the activity of the produced isotope i, A_i, as a function of the irradiation time t can now be given by

$$A_i(t) = \lambda_i \, N_i(t). \tag{19.22}$$

For small irradiation times the expression for $N_i(t)$, Eq. (19.10), behaves as:

$$N_i(t) = N_T(0) \, R_{T \to i} \, t, \tag{19.23}$$

and hence the activity of i as

$$A_i(t) = \lambda_i \, N_T(0) \, R_{T \to i} \, t, \tag{19.24}$$

Under these circumstances, the yield scales linearly with the irradiation time t and the production rate $R_{T \to i}$. Only then, the production yield expressed in [MBq/mAh] is a meaningful quantity, which can be used to determine the yield, given a certain irradiation time and beam current.

> **Options 19.4.1** With **production** (p. 680), the calculation of medical isotope production is invoked. Characteristics of the accelerator can be set with **Ebeam** (p. 681), **Eback** (p. 682), **Ibeam** (p. 683), **Area** (p. 684) and **rho** (p. 685). Irradiation parameters are set with **Tirrad** (p. 688), **Tcool** (p. 689), **radiounit** (p. 686), and **yieldunit** (p. 687).

> **Sample case 19.1** **Medical isotope production with p + ^{100}Mo**
> In this sample case, the activity of all the produced isotopes from the reaction p + ^{100}Mo are given, for a 150 μA proton accelerator, as a function of time. The following input file is used
>
> ```
> #
> # p-Mo100-medical
> #
> # General
> #
> projectile p
> element    Mo
> mass       100
> energy     8. 30. 0.5
> #
> # Spherical OMP and adjusted parameters
> #
> spherical y
> rvadjust     p    1.00676
> rwdadjust    p    1.11091
> rvadjust     n    1.04395
> gadjust       43 101    1.22030
> gadjust       43 100    1.04828
> ctableadjust  43  99    1.34123 0
> s2adjust      43  99    0.14784 0
> #
> # Medical isotope production
> ```
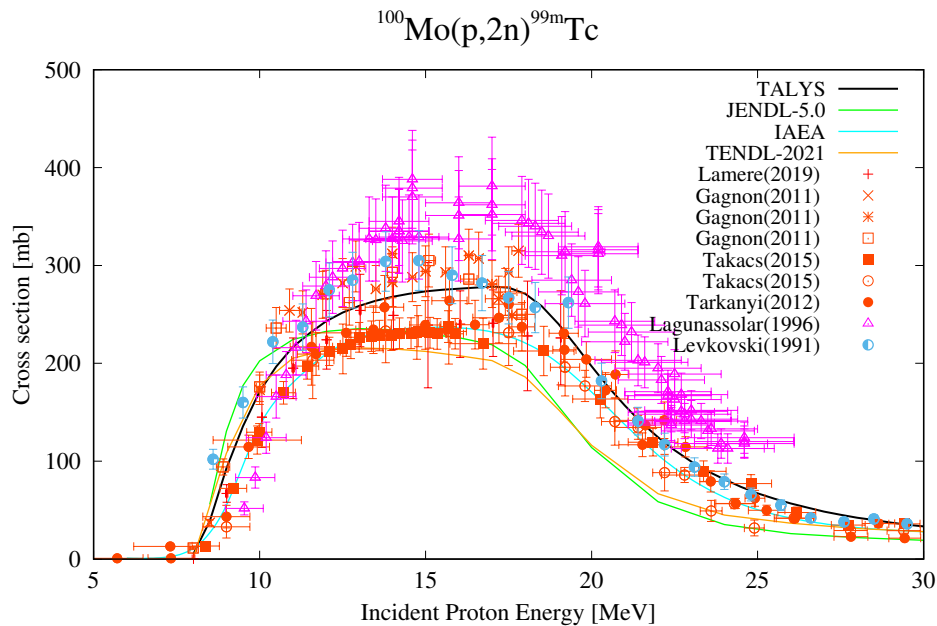
```
#
production y
Ibeam 0.15
Ebeam 24.
Eback 10.
```

Note the use of the **energy** keyword: Cross sections are calculated for incident energies between 8 and 30 MeV with 0.5 MeV energy steps. The keyword **production y** means that activities of all radioactive products as a function of bombarding and/or decay time will be produced in tables. The incident energy of the particle beam is 24 MeV, and the required thickness of the target (which is given in the output) is such that at the back of the target the energy is 10 MeV. Other keywords relevant for isotope production, such as **Tcool**, see page 689, **Tirrad**, see page 688, **rho**, see page 685, **area**, see page 684, **radiounit**, see page 686, **yieldunit**, see page 687, have their default values in this sample case.

We like to point out an efficient option for medical isotope calculations. Suppose one is interested in varying several accelerator options, such as e.g. **Ebeam**. Once the first calculation, like the sample case above, has been done, one may rerun that case and add the extra line **reaction n** to the input file. Then, TALYS will *not* redo the nuclear reaction calculations, but use the various *rpZZZAAA.tot, etc.* cross section output files which are already available in the work directory. Obviously, **Ebeam** and **Eback** must always fall inside the energy grid for which the cross sections are calculated, in this case between 8 and 30 MeV.

Of most interest are probably the files with the produced activity (in Bq or Ci) per isotope. These yields are in files *YZZZAAA.tot* where ZZZ is the charge number and AAA is the mass number in (i3.3) format. For produced isomers, and ground states, there are additional files *pZZZAAA.LMM*, where MM is the number of the isomer (ground state=0) in (i2.2) format. For the above sample case, *Y043099.L02*, i.e. the production of ^{99m}Tc looks as follows:

```
# header:
#   title: Mo100(p,x)Tc99m Isotope production
#   source: TALYS-2.0
#   user: Arjan Koning
#   date: 2023-12-14
#   format: YANDF-0.1
# target:
#   Z: 42
#   A: 100
#   nuclide: Mo100
# reaction:
#   type: (p,x)
# residual:
#   Z: 43
#   A: 99
#   nuclide: Tc99m
# parameters:
#   Beam current [mA]:  1.500000E-01
#   E-Beam [MeV]:  2.400000E+01
#   E-Back [MeV]:  1.000000E+01
#   Initial production rate [s^-1]:  1.961665E-10
#   Decay rate [s^-1]:  3.203675E-05
```

$$^{100}\text{Mo}(p,2n)^{99m}\text{Tc}$$

Figure 19.1: Excitation function of $^{100}\text{Mo}(p,2n)^{99m}\text{Tc}$.

```
#    Initial production yield [GBq/mAh]:  2.119981E-01
#    Total activity at EOI [GBq]:  9.572902E+02
#    Irradiation time:      0 years   1 days  0 hours  0 minutes  0 seconds
#    Cooling time:      0 years   1 days  0 hours  0 minutes  0 seconds
#    Half-life:      0 years   0 days  6 hours  0 minutes 36 seconds
#    Maximum production at:      0 years   3 days 16 hours 36 minutes 54 seconds
# datablock:
#    quantity: Isotope production
#    columns: 5
#    entries: 100
##     Time          Activity         Isotopes          Yield      Isotopic fract.
##      [h]            [GBq]             []              [GBq]           []
    5.000000E-01   5.723950E+01    1.786682E+15    2.119981E-01    9.946191E-02
    1.000000E+00   1.112715E+02    3.473244E+15    2.001184E-01    9.695597E-02
    1.500000E+00   1.622756E+02    5.065295E+15    1.889043E-01    9.452177E-02
    2.000000E+00   2.104216E+02    6.568132E+15    1.783186E-01    9.216321E-02
    2.500000E+00   2.558697E+02    7.986755E+15    1.683262E-01    8.987931E-02
.................................
```

where the final column denotes the fraction of the produced isotope relative to all isotopes of
that element. Fig. 19.2 shows the ^{99m}Tc production as a function of time. Note that the curve is
not a straight line due to the decay of ^{99m}Tc to the ground state. ∎
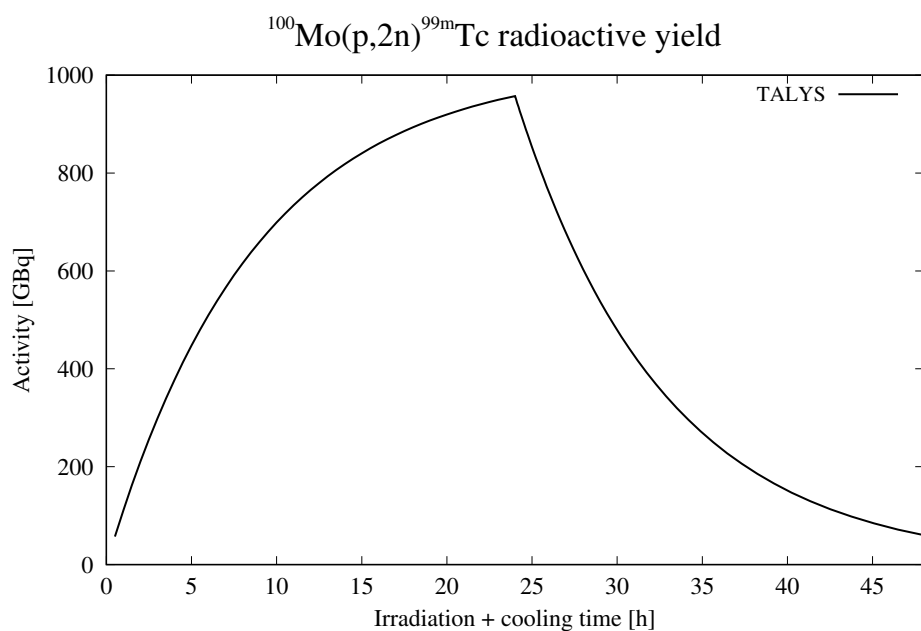
Figure 19.2: Total activity of ^{99m}Tc produced by a 24 MeV proton accelerator of 150 μA and a ^{100}Mo target with an energy of 10 MeV at the back of the target.

20. Verification and validation

TALYS has been tested both formally ("computational robustness") and by comparison of calculational results with experimental data. This will be described in the present Chapter.

20.1 Robustness test with DRIP

One way to test a nuclear model code is to let it calculate results for a huge number of nuclides, and the whole range of projectiles and energies. We have written a little code DRIP, not included in the release, that launches TALYS for complete calculations for all nuclides, from dripline to dripline. Besides checking whether the code crashes, visual inspection of many curves simultaneously, e.g. (n,2n) excitation functions for 50 different targets, may reveal non-smooth behaviour. Various problems, not only in the TALYS source code itself, but also in the nuclear structure database, were revealed with this approach in the initial development stages.

20.2 Robustness test with MONKEY

Part III contains a description of the close to 400 keywords that can be used in a problem for TALYS. Some of them are flags which can only be set to **y** or **n**. Other keywords can be set to a few or several integer values and there are also keywords whose values may cover a quasi-continuous range between the minimum and maximum possible value that we allow for them. Strictly speaking, the total number of possible input files for TALYS is huge (though theoretically finite, because of the finite precision of a computer), and obviously only a small subset of them corresponds to physically meaningful cases. Indeed, as with many computer codes it is not too difficult to bring a TALYS calculation to a formally successful end, i.e. without crashing, with an input file that represents a completely unphysical case. Obviously, there is no way to prevent this - the user is supposed to have full responsibility for what she or he is doing - and we can never anticipate what

input files are made by other users. Nevertheless, to test the robustness of our code, we wrote a program called MONKEY which remotely simulates TALYS in the hands of an evil user: It creates an input file for TALYS, using *all* the keywords, with *random* values, and starts a run with it. Each keyword in this input file has a value that remains within the allowed range as specified in Part III. If TALYS is compiled with all checking options (i.e. array out-of-bounds checks, divisions by zero, other over/underflow errors, etc.) enabled and runs successfully for thousands of such random input files without crashing, we can at least say we have tested *computational* robustness to some extent, and that we *may* have probed every corner of the code. We realize that this is not a full-proof method to test TALYS formally on the Fortran level (if there exists such a test!), but MONKEY has helped us to discover a few bugs during development which otherwise would have come to the surface sooner or later. We think it is better that *we* find them first. The ideal result of this procedure would be that TALYS never crashes or stops without giving an appropriate error message. We emphasize that this test alone does obviously not guarantee any physical quality of the results. For that, much more important are the input files that *are* physically meaningful. These are discussed in the next Section.

20.3   Sample cases

With this manual, we hope to convince you that a large variety of nuclear reaction calculations can be handled with TALYS. To strengthen this statement, we have included many different sample cases throughout this tutorial. In each case, the TALYS input file, the relevant output and, if available, a graphical comparison with experimental data has been presented. The entire collection of sample cases serves as (a) verification of TALYS: our sample output files should coincide, apart from numerical differences of insignificant order, with the output files obtained on your computer, and (b) validation of TALYS: the results should be comparable to experimental data for a widely varying set of nuclear reactions.

It may take a while (about 1-2 hours on a Macbook Pro) before all sample cases have finished. Running the *verify* script included in the TALYS package will be worth the wait however, since a successful execution of all sample cases will put you on safer ground for your own calculations.

Below are the sample cases described in this tutorial and to be found in the *talys/samples* directory. Some of them are split into sub-sample cases with various different options.

- n-Nb093-14MeV: **All results for 14 MeV n + ^{93}Nb**, page 72
- n-Pb208-xs: **Excitation functions: ^{208}Pb (n,n'), (n,2n), (n,p) etc**, page 82
- p-Fe000-rp: **Residual production cross sections for protons on Fe**, page 86
- n-Pb208-nngamma: **Gamma-ray intensities: ^{208}Pb$(n, n\gamma)$ and ^{208}Pb$(n, 2n\gamma)$**, page 89
- n-Bi209-spec: **Inelastic spectra at 20 MeV: Direct + Preeq + GR + Compound**, page 93
- n-Th232-fis-wkb: **Fission cross sections with WKB method: n + ^{232}Th**, page 99
- n-Si028-recoil-exact: **Recoils: 20 MeV n + ^{28}Si**, page 106
- n-Tc099-ld1: **Different level density models : n + ^{99}Tc**, page 145
- g-Zr090-xs: **Photonuclear reactions: g + ^{90}Zr, page**, page 153
- n-Y089-dircap: **Direct neutron capture for n + ^{89}Y**, page 153
- n-Sn120-omp-KD03: **Different optical models : n + ^{120}Sn**, page 166
- a-Ho165-omp1: **Different alpha-particle optical model potentials: alpha + ^{165}Ho**, page 172
- n-Nb093-adjust: **Local parameter adjustment for n + ^{93}Nb**, page 176
- n-Si028-cc: **Coupled-channels rotational model: n + ^{28}Si**, page 180

- n-Ge074-vib: **Coupled-channels vibrational model: n + ^{74}Ge**, page 181
- n-Pb208-omp: **Spherical optical model and DWBA: n + ^{208}Pb**, page 183
- n-Bi209-preeq: **Continuum spectra at 63 MeV for Bi(n,xp)...Bi(n,xα)**, page 207
- p-Zr090-preeq: **Pre-equilibrium angular dist. and multiple pre-equilibrium emission**, page 209
- p-Bi209-500MeV: **Calculations up to 500 MeV for p + ^{209}Bi**, page 211
- n-Nb093-WFC-HF: **Comparison of compound nucleus WFC models: 10 keV n + ^{93}Nb**, page 222
- n-U238-fy: **Fission yields for ^{238}U**, page 249
- n-Pu242-fy: **Neutron multiplicities and fission yields for n + ^{242}Pu**, page 252
- n-Pu239-fy-gef: **Fission yields and neutron observables n + ^{239}Pu**, page 257
- n-Y089-RRR-standard: **Low energy resonance data for n + ^{89}Y**, page 260
- n-Ba136-URR: **Unresolved resonance range parameters: n + ^{136}Ba**, page 262
- n-Os187-astro-ng: **Astrophysical reaction rates : n + ^{187}Os**, page 268
- n-Ba138-MACS: **Maxwellian averaged cross section at 30 keV: n + ^{138}Ba**, page 270
- p-Mo100-medical: **Medical isotope production with p + ^{100}Mo**, page 278

Part Three: Reference Guide

In this part, all TALYS keywords will be described, one per page. The description of each keyword is as follows:

- Name of the keyword
- Explanation
- Examples
- Range of allowed values
- Default value
- Comments (optional), when we feel that some extra warnings or explanation for proper use is appropriate.

In each chapter, the keywords are roughly ordered by importance, rather than alphabetically. This is rather subjective of course, but it may make this part a bit more readable. Hence, it could be that the keywords near the end of certain Chapters are seldom used. In principle, all keywords may be referred to in the other parts of this tutorial, often in the Sections called *Implementation, Options and Sample cases*.

21. Four main keywords

projectile

Eight different symbols can be given as **projectile**, namely **n, p, d, t, h, a, g** representing neutron, proton, deuteron, triton, ^{3}He, alpha and gamma, respectively, and **0**, which is used if instead of a nuclear reaction (projectile + target) we start with an initial population of an excited nucleus.

Examples

> **projectile n**
> **projectile d**
> **projectile 0**

Range

projectile must be equal to **n, p, d, t, h, a, g** or **0**.

Default

None.

element

Either the nuclear symbol or the charge number Z of the target nucleus can be given. Possible values for **element** range from Li (3) to C4 (124).

Examples

> **element pu**
> **element 41**
> **element V**
> **element B9**

Range

$3 \leq$ **element** $\leq$ **124** or **Li** $\leq$ **element** $\leq$ **C4**.

Default

None.

Comments

- To accommodate target nuclides with $Z > 110$ the element names are defined as follows: Rg(111), Cn(112), Nh(113), Fl(114), Mc(115), Lv(116), Ts(117), Og(118), B9(119), C0-4(120-124), which takes as a basis for $Z = 100$ the symbol $A0$, etc. unless an official name has been assigned to it, which is currently the case for $Z \leq 118$. Clearly, if we ever need or wish to go beyond $Z = 124$, there are enough symbols left. Obviously, the symbols for Z above 118 will be changed as soon as official names are assigned to them.

mass

The target mass number A. The case of a natural element can be specified by **mass 0**. Then, a TALYS calculation for each naturally occurring isotope will be performed (see also the **abundance** keyword, p. 333), after which the results will be properly weighted and summed.

Examples

mass 239
mass 0

Range

mass 0 or $5 < \textbf{mass} \leq 339$. The extra condition is that the target nucleus, i.e. the combination of **mass** and **element** must be present in the mass database, which corresponds to all nuclei between the proton and neutron drip lines.

Default

None.

energy

The incident energy in MeV. The user has four possibilities: (1) A single incident energy is specified in the input as a real number, (2) A filename is specified, where the corresponding file contains a series of incident energies, with one incident energy per line. Any name can be given to this file, provided it starts with a character, and it is present in your working directory. Option (2) is helpful for the calculation of excitation functions or for the creation of nuclear data libraries. Option (2) is mandatory if **projectile 0**, i.e., if instead of a nuclear reaction we start with a population of an excited nucleus (see the **Special cases** below). There are an additional 2 options which allows to use a whole range of incident energies without having to make a file for this: (3) A filename that is predefined by TALYS. This contains a hardwired energy grid with for example for neutrons a finer energy grid at low energies and a progressively wider grid at high energies. These have the form *pE1-E2.grid* where *p* is the name of the projectile, and *E1, E2* are the start and end energy in integer form respectively. The *.grid* specifies that this concerns a predefined energy grid. An often used example is *n0-200.grid* which is the neutron energy grid of the TENDL library. More energies are used in the eV and keV range while at high energies automatically a course grid is used. With the file *n0-20.grid* exactly the same incident energy grid is used, but only up to the final energy of 20 MeV. Finally, option (4) is to give after the *energy* keyword 3 numbers: the starting energy, the end energy and the energy step. Next, an equidistant grid is made based on these 3 numbers.

Examples

 energy 140.
 energy 0.002
 energy range (user-defined file *range* with energies)
 energy n0-30.grid (hardwired energy grid for incident neutrons between 0 and 20 MeV)
 energy p10-100.grid (hardwired energy grid for incident protons between 10 and 100 MeV)
 energy 0.5 20. 0.5 (Incident energies: 0.5, 1, 1.5, ...20 MeV)

Range

10^{-11} MeV $\leq$ **energy** $<$ **1000** MeV or a *filename*, whereby the corresponding file contains at least 1 and a maximum of **numenin** incident energies, where **numenin** is an array dimension specified in *talys.cmb*. Currently **numenin=600**.

Default

None.

Using the four main keywords

To summarize the use of the four basic keywords, consider the following input file

```
projectile n
element    pd
mass       110
energy range
```

The file *range* looks e.g. as follows

```
0.1
0.2
0.5
1.
1.5
2.
5.
8.
10.
15.
20.
```

In the source code, the number of incident energies, here 11, is known as **numinc**. For the four-line input given above, TALYS will simulate all open reaction channels for $n + {}^{110}$Pd for all incident energies given in the file *range*, using defaults for all models and parameters. The most important cross sections will automatically be written to the output file.

Special cases

There are two examples for which the **energy** keyword does not represent the incident energy of the projectile.

1. Populated initial nucleus

If **projectile 0**, the user *must* give a filename for the **energy** keyword. This time however, the file does not consist of incident energies but of the excitation energy grid of the initial population, see Section 17. On the first line of the file we read the number of energies (lines), number of spins, and number of parities. The excitation energies that are read represent the middle values of the bins, and are followed by either (a) if the number of spins is zero, the total population in that bin, or (b) if the number of spins is not zero, the population per excitation energy bin and spin, using one column per spin. The values given in the second column represent either a histogram, if **popMeV n** (the default) or spectrum (**popMeV y**). If **popMeV y**, these spectral values are multiplied by the energy bin width and we obtain the population, which has a dimension of millibarns. If the population for only 1 parity is given, the population is equally distributed over both parities. Hence, if we let TALYS determine the spin-parity distribution (case (a)), an example of such a file is

```
    8    0    1
0.25 0.1342
0.75 0.2176
1.25 0.3344
1.75 0.6522
2.25 0.6464
2.75 0.2897
```

```
3.25 0.1154
3.75 0.0653
```

and if we give the full spin-dependent population (case (b)), with equal parity distribution, we could e.g. have

```
    8    3    1
0.25 0.0334 0.0542 0.0112
0.75 0.0698 0.1043 0.0441
1.25 0.1131 0.2303 0.0971
1.75 0.1578 0.3333 0.1143
2.25 0.1499 0.3290 0.1212
2.75 0.1003 0.2678 0.0845
3.25 0.0844 0.1313 0.0661
3.75 0.0211 0.0889 0.0021
```

If in addition the population should be parity-dependent, one would have e.g.

```
    8    3    2
0.25 0.0134 0.0542 0.0112
0.75 0.0298 0.1043 0.0441
1.25 0.0531 0.2303 0.0971
1.75 0.0578 0.3333 0.1143
2.25 0.0599 0.3290 0.1212
2.75 0.0603 0.2678 0.0845
3.25 0.0444 0.1313 0.0661
3.75 0.0111 0.0889 0.0021
0.25 0.0234 0.0142 0.0008
0.75 0.0498 0.0943 0.0141
1.25 0.0666 0.1103 0.0471
1.75 0.0678 0.1333 0.0343
2.25 0.0299 0.1290 0.0512
2.75 0.0403 0.1678 0.0245
3.25 0.0344 0.1013 0.0361
3.75 0.0100 0.0489 0.0011
```

Note that in this case the energy restarts in the middle; first the energy grid for 3 spin values and parity -1 is given, then for parity +1.

2. Astrophysical reaction rates

If **astro y**, (p. 672) for astrophysical reaction rate calculations, the incident energy as given in the input is overruled by a hardwired incident energy grid that is appropriate for the calculation of reaction rates. However, to avoid unnecessary programming complications, the **energy** keyword *must* still be given in the input, and it can have any value. Hence if **astro y** one could e.g. give **energy 1.** in the input file. The adopted incident energies that overrule this value will be given in the output.

Four main keywords: summary

The first four keywords are clearly the most important: they do *not* have a default value while they determine default values for some of the other keywords which, in other words, may be projectile-, energy-, element- or mass-dependent. All the keywords that follow now in this manual have default values and can hypothetically be left out of the input file if you are only interested in a minimal reaction specification. If you want to add keywords, you can enter them one by one in the format

that will be described below. Another way is to go to the top of the output file that is generated by the simple input file given above. You will find all the keywords with their values as adopted in the calculation, either user-specified or as defaults. All nuclear model parameters per nucleus are printed in the file *parameters.dat*, provided **partable y** was set in the input. You can copy this part and paste it into the input file, after which the values can be changed.

22. Keywords for basic and numerical parameters

bins

The number of excitation energy bins in which the continuum of the initial compound nucleus is divided for further decay. The excitation energy region between the last discrete level and the total excitation energy for the initial compound nucleus is divided into **bins** energy bins. The resulting bin width then also determines that for the neighboring residual nuclei, in the sense that for any residual nucleus we ensure that the bins fit exactly between the last discrete level and the maximal possible excitation energy. For residual nuclides far away from the target, a smaller number of bins is automatically adopted. If **bins 0** a simple formula is invoked to take into account the fact that more bins are needed when the incident energy increases. Instead of a constant number of bins, it is then incident energy (E) dependent. More specifically, **nbins 0** means

$$\text{Nbins} = 30 + 50 \frac{E^2}{(E^2 + 60^2)} \tag{22.1}$$

It is obvious that **bins** has a large impact on the computation time.

Examples

   bins 25

Range

bins = **0** or **2** $\leq$ **bins** $\leq$ **numbins**, where **numbins** is specified in the file *talys.cmb*. Currently, **numbins=100**

Default

bins 40

Ltarget

The excited state of the target as given in the discrete level database. This keyword allows to compute cross sections for isomeric targets.

Examples

Ltarget 2

Range

$0 \leq$ **Ltarget** $\leq$ **numlev**, where **numlev** is specified in the file *talys.cmb*. Currently, **numlev=30**

Default

Ltarget 0, i.e. the target is in its ground state.

maxZ

The maximal number of protons away from the initial compound nucleus that is considered in a chain of residual nuclides. For example, if **maxZ 3**, then for a $n + {}^{56}$Fe (Z=26) reaction, the V-isotopes (Z=23) are the last to be considered for further particle evaporation in the multiple emission chain. **maxZ** is normally only changed for diagnostic purposes. For example, if you are only interested in the (n,n'), $(n,2n)$,...(n,xn) residual production cross sections, or the associated discrete gamma ray intensities, **maxZ 0** is appropriate. (Note that in this case, the competition of emission of protons up to alpha particles is *still* taken into account for all the nuclides along the (n,xn) chain, only the decay of the residual nuclides associated with this charged-particle emission are not tracked further).

Examples

maxZ 6

Range

$0 \leq$ **maxZ** $\leq$ **numZ-2**, where **numZ=2+2*memorypar** is specified in the file *talys.cmb*, where **memorypar=5** for a computer with at least 256 Mb of memory.

Default

Continue until all possible reaction channels are closed or until the maximal possible value for **maxZ** is reached (which rarely occurs). By default **maxZ=numZ-2** where the parameter **numZ** is specified in the file *talys.cmb*. This parameter should be large enough to ensure complete evaporation of all daughter nuclei.

maxN

The maximal number of neutrons away from the initial compound nucleus that is considered in a chain of nuclides. For example, if **maxN 3**, then for a $n + {}^{56}$Fe (N=31) reaction, residual nuclei with N=28 (=31-3) are the last to be considered for further particle evaporation in the multiple emission chain. **maxN** is normally only changed for diagnostic or economical purposes.

Examples

> **maxN 6**

Range

$0 \leq$ **maxN** $\leq$ **numN-2**, where **numN=4+4*memorypar** is specified in the file *talys.cmb*, where **memorypar=5** for a computer with at least 256 Mb of memory.

Default

Continue until all possible reaction channels are closed or until the maximal possible value for **maxN** is reached (which rarely occurs). By default **maxN=numN-2** where the parameter **numN** is specified in the file *talys.cmb*. This parameter should be large enough to ensure complete evaporation of all daughter nuclei.

Liso

Level number of isomer. This user assigned value can overrule the one determined from the discrete level file.

Examples

   Liso 2

Range

0 ≤ Liso ≤ numlev, where **numlev** is specified in the file *talys.cmb*.

Default

Liso not given.

isomer

The definition of an isomer in seconds. In the discrete level database, the lifetimes of most of the levels are given. With **isomer**, it can be specified whether a level is treated as an isomer or not. Use **isomer 0.** to treat all levels, with any lifetime, as isomer and use **isomer 1.e38**, or any other number larger than the longest living isomer present in the problem, to include no isomers at all.

Examples

isomer 86400.   (86400 sec.=one day)

isomer 0.1

Range

0. $\leq$ **isomer** $\leq$ **1.e38**

Default

isomer 1. (second)

channels

Flag for the calculation and output of all exclusive reaction channel cross sections, e.g. (n, p), $(n, 2n)$, $(n, 2npa)$, etc. The **channels** keyword can be used in combination with the keywords **outspectra** and **outangle** (see next Section) to give the exclusive spectra and angular distributions.

Examples

> **channels y**
> **channels n**

Range

y or **n**

Default

channels n

partable

Flag to write the all the model parameters used in a calculation on a separate file, *parameters.dat*. This can be a very powerful option when one wishes to vary any nuclear model parameter in the input. The file *parameters.dat* has the exact input format, so it can be easily copied and pasted into any input file. This is helpful for a quick look-up of all the parameters used in a calculation. We have used this ourselves for automatic (random) TALYS-input generators for e.g. covariance data.

Examples

partable y
partable n

Range

y or **n**

Default

partable n

best

Flag to use the set of adjusted nuclear model parameters that produces the optimal fit for measurements of all reaction channels of the nuclide under consideration. TALYS will look in the *talys/structure/best* directory for such a set, see Section 5.4. With the addition of the single line **best y** to the input file, TALYS will automatically use all detailed adjusted parameter fits that are stored in *talys/structure/best*.

Examples

best y
best n

Range

y or **n**

Default

best n

ejectiles

The outgoing particles that are considered in competing reaction channels. By default, all competing channels are included even if one is interested in only one type of outgoing particle. This is necessary since there is always competition with other particles, in e.g. Hauser-Feshbach and pre-equilibrium models, that determines the outcome for the particle under study. Furthermore, reaction Q-values automatically keep channels closed at low incident energies. However, for diagnostic or time-economical purposes, or cases where e.g. one is only interested in high-energy (p, p') and (p, n) multi-step direct reactions, one may save computing time and output by skipping certain ejectiles as competing particles. For neutron-induced reactions on actinides up to 20 MeV, setting **ejectiles g n** is a rather good approximation that saves time. Also comparisons with computer codes that do not include the whole range of particles will be facilitated by this keyword.

Examples

> **ejectiles n**
> **ejectiles g n p a**

Range

ejectiles can be any combination of **g, n, p, d, t, h** and **a**.

Default

Include all possible outgoing particles, i.e. **ejectiles g n p d t h a**

Comments

transpower

A limit for considering transmission coefficients in the calculation. Transmission coefficients T_{lj} smaller than $T_{0\frac{1}{2}} \times 10^{-transpower}/(2l+1)$ are not used in Hauser-Feshbach calculations, in order to reduce the computation time.

Examples

transpower 12

Range

$2 \leq \textbf{transpower} \leq 20$

Default

transpower 5

transeps

A limit for considering transmission coefficients in the calculation. Transmission coefficients smaller than **transeps** are not used in Hauser-Feshbach calculations, irrespective of the value of **transpower**, in order to reduce the computation time.

Examples

transeps 1.e-12

Range

$0. \leq$ **transeps** ≤ 1.

Default

transeps 1.e-8

xseps

The limit for considering cross sections in the calculation, in mb. Reaction cross sections smaller than **xseps** are not used in the calculations, in order to reduce the computation time.

Examples

   xseps 1.e-10

Range

$0. \leq$ **xseps** $\leq$ **1000**.

Default

xseps 1.e-7

popeps

The limit for considering population cross sections in the multiple emission calculation, in mb. Nuclides which, before their decay, are populated with a total cross section less than **popeps** are skipped, in order to reduce the computation time. From **popeps**, also the criteria for continuation of the decay per excitation energy bin (variable **popepsA**) and per (E_x, J, Π) bin (variable **popepsB**) in Hauser-Feshbach calculations are automatically derived.

Examples

popeps 1.e-6

Range

$0. \leq$ **popeps** $\leq$ **1000**.

Default

popeps 1.e-3

popMeV

Flag to use initial population per MeV instead of per histogram, in the case of an excited energy distribution to be used with **projectile 0**. This keyword is given for backward compatibility. It is now seen that it is more natural to input the absolute value of the initial population per continuum bin or level, as histograms.

Examples

popMeV y
popMeV n

Range

y or **n**

Default

popMeV n

Estop

Incident energy above which TALYS stops. This keyword is needed to speed up some uncertainty applications involving random TALYS calculations. No matter which incident energies are given in the input file, TA

Examples

Estop 50.

Range

$1.e-5 \leq$ **Estop** $\leq$ **1000**.

Default

Estop 1000.

endf

Flag for the creation of various output files needed for the assembling of an ENDF-6 formatted file. Apart from the creation of various files that will be discussed for the following keywords, a file *endf.tot* is created which contains the reaction, elastic and total cross sections (calculated by ECIS) on a fine energy grid. Also a file *decay.X* will be created, with X the ejectile symbol in (a1) format, that contains the discrete gamma decay probabilities for the binary residual nuclides. This will be used for gamma-ray production from discrete binary levels. In addition to all the output detailed below, the continuum gamma-ray spectra per residual nucleus and incident energy will be stored in files *gamZZZAAAEYYY.YYY.tot*, where where ZZZ is the charge number and AAA is the mass number in (i3.3) format, and YYY.YYY is the incident energy in (f7.3) format. Setting **endf y** will automatically enable many of the "**file**" keywords given below. All these specific files will be written to output if **endfdetail y**, see the next keyword.

Examples

      endf y
      endf n

Range

y or **n**

Default

endf n

endfdetail

Flag to use specific MT numbers per reaction channel. With **endfdetail**, the corresponding value read from the TALYS output file *endf.inf* can be overruled from **y** to **n**, i.e. even if detailed reaction channel information was provided by TALYS, you may now choose to use a lumped presentation using MT5. Of course, if the corresponding value in *endf.inf* is **n**, then the detailed information was not produced by TALYS, and **endfdetail** can no longer be set to **y**. If you want that, a TALYS run with keyword **endfdetail y** (the default for incident neutrons), should be performed first.

Examples

endfdetail n
endfdetail y

Range

y or **n**

Default

The value of **endfdetail** is adopted from the TALYS output file *tefal.inf*.

angles

Number of emission angles for reactions to discrete states.

Examples

    angles 18

Range

1 $\leq$ angles $\leq$ numang, where **numang** is specified in the file *talys.cmb*. Currently, **numang=90**

Default

angles 90

anglescont

Number of emission angles for reactions to the continuum.

Examples

anglescont 18

Range

$1 \leq$ **anglescont** $\leq$ **numangcont**, where **numangcont** is specified in the file *talys.cmb*. Currently, **numangcont=36**

Default

anglescont 36

maxchannel

Maximal number of outgoing particles in exclusive channel description, e.g. if **maxchannel 3**, then reactions up to 3 outgoing particles, e.g. $(n, 2np)$, will be given in the output. **maxchannel** is only active if **channels y**. We emphasize that, irrespective of the value of **maxchannel** and **channels**, all reaction chains are, by default, followed until all possible reaction channels are closed to determine cumulative particle production cross sections and residual production cross sections.

Examples

    maxchannel 2

Range

$0 \leq$ **maxchannel** $\leq$ **8**,

Default

maxchannel 4

relativistic

Flag for relativistic kinematics.

Examples

relativistic y
relativistic n

Range

y or **n**

Default

relativistic y

reaction

Flag to disable nuclear reaction calculation. This may be helpful if one is e.g. only interested in a level density calculation. A TALYS run will then last only a few hundreds of a second. (This keyword was used for the large scale level density analysis of [22]).

Examples

reaction y
reaction n

Range

y or **n**

Default

reaction y

recoil

Flag to include recoil information.

Examples

recoil n
recoil y

Range

y or **n**

Default

recoil is read from the TALYS output file *endf.inf*. In other words, if *recoil y* was set in the TALYS input file, then this will automatically be used in TEFAL.

labddx

Flag for the calculation of double-differential cross sections in the LAB system. This is only active if **recoil y**. If **labddx n**, only the recoils of the nuclides are computed.

Examples

labddx y
labddx n

Range

y or **n**

Default

labddx n

anglesrec

Number of emission angles for recoiling nuclides. This is only active if **recoil y**.

Examples

anglesrec 4

Range

$1 \leq$ **anglesrec** $\leq$ **numangrec**, where **numangrec** is specified in the file *talys.cmb*. Currently, **numangrec=9**

Default

anglesrec 9 if **labddx y**, **anglesrec 1** if **labddx n**

maxenrec

Number of emission energies for recoiling nuclides. This is only active if **recoil y**.

Examples

maxenrec 4

Range

$1 \leq$ **maxenrec** $\leq$ **numenrec**, where **numenrec** is specified in the file *talys.cmb*. Currently, **numenrec=5*memorypar**, where we suggest **memorypar=5** for a computer with at least 256 Mb of memory.

Default

maxenrec 10

recoilaverage

Flag to consider only one average kinetic energy of the recoiling nucleus per excitation energy bin (instead of a full kinetic energy distribution). This approximation significantly decreases the calculation time. This is only active if **recoil y**.

Examples

recoilaverage y
recoilaverage n

Range

y or **n**

Default

recoilaverage n

channelenergy

Flag to use the channel energy instead of the center-of-mass energy for the emission spectrum.

Examples

channelenergy y
channelenergy n

Range

y or **n**

Default

channelenergy n

equidistant

Flag for adopting an equidistant or non-equidistant (logarithmic) excitation energy grid for the continuum of each residual nucleus. The latter option makes the calculation more efficient since it uses more precision when it is needed.

Examples

equidistant y
equidistant n

Range

y or **n**

Default

equidistant y

equispec

Flag for adopting an equidistant emission energy grid for the evaporation of each residual nucleus. This may be useful for the case of evaporation of fission fragments.

Examples

equispec y
equispec n

Range

y or **n**

Default

equispec n

segment

The number of segments to divide the standard emission energy grid. The basic emission energy grid we use for spectra and transmission coefficient calculations is:

```
 0.001, 0.002, 0.005    MeV
 0.01,  0.02,  0.05     MeV
 0.1-   2 MeV : dE= 0.1 MeV
 2  -   4 MeV : dE= 0.2 MeV
 4  -  20 MeV : dE= 0.5 MeV
20  -  40 MeV : dE= 1.0 MeV
40  - 200 MeV : dE= 2.0 MeV
200 - 300 MeV : dE= 5.0 MeV
above 300 MeV : dE=10.0 MeV
```

This grid is divided into a finer grid by subdividing each interval by **segment**.

Examples

segment 3

Range

$1 \leq$ **segment** ≤ 4. Extra conditions: $1 \leq$ **segment** ≤ 3 if the maximum incident energy is larger than 20 MeV, $1 \leq$ **segment** ≤ 2 if the maximum incident energy is larger than 40 MeV, **segment=1** if the maximum incident energy is larger than 100 MeV. (These rules are imposed due to memory limitations).

Default

segment 1

Elow

Lowest incident energy in MeV for which TALYS performs a full nuclear model calculation. Below this energy, cross sections result from inter- and extrapolation using the calculated values at **Elow** and tabulated values and systematics at thermal energy, see Section 16. This keyword should only be used in the case of several incident energies.

Examples

Elow 0.001

Range

$1.e - 6 \leq$ **Elow** ≤ 1.

Default

Elow=D_0 for data files (**endf y**), **1.e-6** otherwise.

maxZrp

The maximal number of protons away from the initial compound nucleus before new residual evaporation.

Examples

maxZrp 6

Range

$0 \leq$ **maxZ** $\leq$ **numZ-2**, where **numZ=2+2*memorypar** is specified as global parameter.

Default

maxZrp=numZ-2

maxNrp

The maximal number of neutrons away from the initial compound nucleus before new residual evaporation.

Examples

maxNrp 6

Range

$0 \leq$ **maxN** $\leq$ **numN-2**, where **numN=2+2*memorypar** is specified as global parameter.

Default

maxNrp=numN-2

abundance

File with tabulated abundances. The **abundance** keyword is only active for the case of a natural target, i.e. if **mass 0**. By default, the isotopic abundances are read from the structure database, see Chapter 5. It can however be imagined that one wants to include only the most abundant isotopes of an element, to save some computing time. Also, **abundance** may be used to analyze experimental data for targets of a certain isotopic enrichment. On the input line, we read **abundance** and the filename. From each line of the file, TALYS reads Z, A and the isotopic abundance with the format (2i4,f11.6). An example of an abundance file, e.g. *abnew*, different from that of the database, is

```
82 206  24.100000
82 207  22.100000
82 208  52.400000
```

where we have left out the "unimportant" ^{204}Pb (1.4%). TALYS automatically normalizes the abundances to a sum of 1, leading in the above case to 24.44 % of ^{206}Pb, 22.41 % of ^{207}Pb and 53.14 % of ^{208}Pb in the actual calculation.

Examples

   abundance abnew

Range

abundance can be equal to any filename, provided it is present in the working directory.

Default

If **abundance** is not given in the input file, abundances are taken from *talys/structure/abundance* and calculations for all isotopes are performed.

micro

Flag to use microscopic models for all nuclear structure ingredients.

Examples

micro y
micro n

Range

y or **n**

Default

micro n

ompenergyfile

File with incident energies to calculate the total, elastic and reaction cross section on a sufficiently precise energy grid for ENDF-6 file purposes. On the input line, we read **ompenergyfile**, filename.

Examples

ompenergyfile energies.omp

Range

ompenergyfile can be equal to any filename, provided it starts with a character. The incident energies should be in the range 10^{-11} MeV to < 250 MeV, whereby the **ompenergyfile** contains at least 1 and a maximum of **numen6** incident energies, where **numen6** is an array dimension specified in *talys.cmb*. Currently **numen6=10000**.

Default

ompenergyfile is not given in the input file,

bestend

Flag to put the best set of parameters at end of input file, instead of at the beginning. With **bestend n**, the parameters can be overruled later in the input file, while this is no longer possible with **bestend y**. Obviously, this keyword is only relevant if **best y**.

Examples

> **bestend y**
> **bestend n**

Range

y or **n**

Default

bestend n

bestpath

Keyword to enable to use your own collection of "best" TALYS input parameters. This directory should be created under *talys/structure/* after which the current keyword can be used with that directory name. In practice, the user can copy a file from the standard *talys/structure/best/* database to his/her own database and change it. In this way, changes in the "official" database are avoided. See Section 5.4 for the format

Examples

bestpath mybest

For this keyword to work, information needs to be present in the *talys/structure/mybest/* with a format equal to that of the original *talys/structure/best/* directory, see Section 5.4.

Range

bestpath can be equal to any filename, provided it starts with a character. Furthermore, the library must exist in the *talys/structure/* directory. This keyword is only active if **best y**.

Default

bestpath is equal to *talys/structure/best/*.

rescuefile

File with incident energy dependent normalization factors. If TALYS is not able to produce the "ultimate fit", it is possible to invoke a "rescuefile" as a last resort. By giving a table of incident energies and normalization factors, the result of TALYS can be made exactly equal to that of experimental data, an evaluate data set, or any other data set. The contents of the file consist of a simple x-y table with x the incident energy and y the normalization factor. A rescuefile can be used for the reactions (n,n'), (n,γ), (n,f), (n,p), (n,d), (n,t), (n,h), (n,α), (n,2n) and (n,total). To invoke this, the ENDF-6 format for MT numbers representing a reaction channel is used, see the sample cases below. Moreover, a global multiplication factor can be applied. On the input line, we read **rescuefile**, reaction identifier (MT number), global multiplication factor (optional).

Examples

> **rescuefile 0 rescue.001 1.01** (n,total)
> **rescuefile 4 rescue.004** (n,n')
> **rescuefile 16 rescue.016** (n,2n)
> **rescuefile 18 rescue.018 0.995** (n,f)
> **rescuefile 102 rescue.102** (n,γ)
> **rescuefile 103 rescue.103 1.02** (n,p)
> **rescuefile 104 rescue.104** (n,d)
> **rescuefile 105 rescue.105** (n,t)
> **rescuefile 106 rescue.106** (n,h)
> **rescuefile 107 rescue.107** (n,α)

Range

rescuefile can be equal to any filename, provided it starts with a character.

Default

no default.

nulldev

Path for the null device. The null device is a "black hole" for output that is produced, but not of interest to the user. Some ECIS output files fall in this category. To ensure compatibility with Unix, Linux, Windows and other systems a null device string is used, of which the default setting is given in machine.f. With this keyword, extra flexibility is added. If the null device is properly set in machine.f, this keyword is not needed. On the input line, we read **nulldev**, filename.

Examples

> **nulldev /dev/null**
> **nulldev nul**

Range

nulldev can be equal to any appropriate filename, provided it starts with a character.

Default

The default is set in subroutine *machine.f*.

strucpath

Path for the directory with nuclear structure information. With this keyword, extra flexibility is added. Nuclear structure databases other than the default can be invoked with this keyword. If the path name is properly set in machine.f, this keyword is not needed for standard use. On the input line, we read **strucpath**, filename.

Examples

> **strucpath /home/raynal/mon-structure/**

Range

strucpath can be equal to any appropriate directory. The maximum length of the path is 60 characters.

Default

The default is set in subroutine *machine.f*.

user

The current user who produces the result. You may edit the 'user' variable in input_basicpar.f90 and put your own name there. It will appear in the metadata of the various output files. However, you can also use the input keyword.

Examples

user Vlad Avrigeanu

Range

Any string

Default

Arjan Koning

source

The source of the calculations. obviously this is TALYS, but it may be helpful to specify the version such that it appears in the metadata of the many output files. You may edit the 'source' variable variable in input_basicpar.f90 and put your own version there. However, you can also use the input keyword.

Examples

source TALYS-2.01beta3v20240223

Range

Any string

Default

TALYS-2.0

format

The format of the metadata in the output files. It may be helpful to specify the version. You may edit the 'format' variable variable in input_basicpar.f90 and put your own version there. However, you can also use the input keyword.

Examples

format YANDF-0.1beta2

Range

Any string

Default

YANDF-0.1

23. Keywords for masses and deformations

massmodel

Model for nuclear masses. There are 4 theoretical mass models and an analytic formula, see Section 6. They are only used when no experimental mass is available or when **expmass n**.

Examples

      massmodel 0: Duflo-Zuker formula
      massmodel 1: Möller table
      massmodel 2: Goriely HFB-Skyrme table
      massmodel 3: HFB-Gogny D1M table

Range

$0 \leq$ **massmodel** $\leq$ **3**

Default

massmodel 2

expmass

Flag for using the experimental nuclear mass when available. Use **expmass n** to overrule the experimental mass by the theoretical nuclear mass (i.e. the Audi-Wapstra values will not be used). This will then be done for all nuclides encountered in the calculation.

Examples

expmass y
expmass n

Range

y or **n**

Default

expmass y

beta2

Deformation parameter for moment of inertia for the ground state or fission barrier, see Eq. (8.86). On the input line, we read **beta2**, Z, A, value, fission barrier. If the number of the fission barrier is not given or is equal to 0, it concerns the ground state.

Examples

> **beta2 90 232 0.3**
> **beta2 94 239 1.1 2**

Range

$0. \leq$ **beta2** < 1.5

Default

beta2 $Z A$ **0.** for the ground state, **beta2** $Z A$ **0.6** for the first barrier, **beta2 0.8** for the second barrier, and **beta2** $Z A$ **1.** for the third barrier, if present.

massdir

User made directory with nuclear masses. With this keyword, extra flexibility for nuclear masses is added. The directory should be placed under talys/structure/masses, and the individual files should have the same structure as the other mass tables. On the input line, we read **massdir**, directory name.

Examples

massdir hfb69

Range

massdir can be equal to any appropriate directory name. The maximum length of the directory name is 72 characters.

Default

massdir is not used, i.e. the masses are read from an existing mass table.

massnucleus

The mass of the nucleus in amu. Use **massnucleus** to overrule the value given in the mass table. On the input line, we read **massnucleus**, Z, A, value.

Examples

> **massnucleus 41 93 92.12345**
> **massnucleus 94 239 239.10101**

Range

$A - 1 \leq$ **massnucleus** $\leq$ **A+1**, where A is the mass number.

Default

massnucleus 0., i.e. the nuclear mass is read from the mass table.

massexcess

The mass excess of the nucleus in MeV. Use **massexcess** to overrule the value given in the mass table. On the input line, we read **massexcess**, *Z*, *A*, value.

Examples

> **massexcess 41 93 -45.678**
> **massexcess 94 239 39.98765**

Range

$-500. \leq$ **massexcess** $\leq$ **500.**,

Default

massexcess 0., i.e. the mass excess is read from the mass table.

24. Keywords for discrete levels

maxlevelstar

The number of included discrete levels for the *target* nucleus that is considered in Hauser-Feshbach decay and the gamma-ray cascade.

Examples

maxlevelstar 0
maxlevelstar 12

Range

$0 \leq$ **maxlevelstar** $\leq$ **numlev**, where **numlev** is specified in a module. Currently, **numlev=30**

Default

maxlevelstar 30

maxlevelsbin

The number of included discrete levels for the nuclides resulting from *binary* emission that is considered in Hauser-Feshbach decay and the gamma-ray cascade. On the input line we read **maxlevelsbin**, the symbol of the ejectile and the number of levels of the associated residual nucleus.

Examples

>**maxlevelsbin a 8**
>**maxlevelsbin p 12**

Range

$0 \leq$ **maxlevelsbin** $\leq$ **numlev**, where **numlev** is specified in a module. Currently, **numlev=30**

Default

maxlevelsbin g 10, **maxlevelsbin n 10**, **maxlevelsbin p 10**, **maxlevelsbin d 5**, **maxlevelsbin t 5**, **maxlevelsbin h 5**, **maxlevelsbin a 10**.

Comments

- The value for the default of the inelastic channel will always be overruled by the **maxlevelstar** keyword, for the target nucleus, or the value for its default.

maxlevelsres

The number of included discrete levels for all *residual* nuclides that is considered in Hauser-Feshbach decay and the gamma-ray cascade. This keyword is overruled by **maxlevelsbin** and **maxlevelstar** for specified nuclides.

Examples

maxlevelsres 0
maxlevelsres 12

Range

0 ≤ **maxlevelsres** ≤ **numlev**, where **numlev** is specified in a module. Currently, **numlev=30**

Default

maxlevelsres 10

Nlevels

The number of included discrete levels for a *specific residual* nucleus that is considered in Hauser-Feshbach decay and the gamma-ray cascade. On the input line we read **Nlevels**, *Z*, *A*, and the number of levels.

Examples

Nlevels 41 93 8

Range

$0 \leq$ **Nlevels** $\leq$ **numlev**, where **numlev** is specified in a module. Currently, **numlev=30**

Default

Nlevels has the value specified by the defaults of **maxlevelstar**, **maxlevelsbin**, and **maxlevelsres**.

disctable

Keyword to change the used discrete level database. The standard discrete level database from RIPL can be updated with theoretical levels calculated from the microscopic level densities from **ldmodel 5**, for nuclides with no or few experimental levels. Note that **disctable 3** gives the option to perform nuclear reaction calculations using purely theoretically estimated levels.

Examples

disctable 1: RIPL database with experimental levels + theoretical levels added until the 100th level

disctable 2: RIPL database with experimental levels only (the only option until TALYS-1.4)

disctable 3: Theoretical levels for all nuclides

Range

$1 \leq$ **disctable** ≤ 3

Default

disctable 1

levelfile

File with discrete levels. The format of the file is exactly the same as that of the nuclear structure database *talys/structure/levels/*. In practice, the user can copy a file from this database to the working directory and change it. In this way, changes in the "official" database are avoided. Note that even if only changes for one isotope are required, the entire file needs to be copied if for the other isotopes the originally tabulated values are to be used. On the input line, we read **levelfile**, *Z*, filename.

Examples

levelfile 26 Fe.loc

Range

levelfile can be equal to any filename, provided it starts with a character.

Default

If **levelfile** is not given in the input file, the discrete levels are taken from the *talys/structure/levels* database per nucleus.

branch

Branching ratio for discrete level to overrule that given by the discrete level file. With this keyword one can change for example the "guessed" branching ratios put in the discrete level file, or even overwrite those which are supposed to be experimentally known. On the input line we read **branch**, *Z*, *A*, mother level, the number of branching levels Nbr, and next the daughter level and branching ratio for each level up to Nbr.

Examples

branch 38 85 7 2 2 0.7 0 0.3: 70% decay of 7th level of ^{85}Sr to level 2, and 30% to the ground state

branch 38 87 17 1 1 1.: 100% decay of 17th level of ^{87}Sr to level 1.

Range

0 $\leq$ number of levels, mother level, daughter level $\leq$ numlev, where **numlev** is specified in a module.

Default

branch is not given.

Comment

If branching ratios are considered to permanently overrule those of the discrete level file, the keywords as given above can be stored in the talys/structure/levels/branch directory, after which a simple **bestbranch y** (p. 363) is enough to invoke all these adjusted branching ratios.

Risomer

Global adjustable parameter to change the branching ratios between discrete states. This can be helpful as a last resort for fitting isomeric or gamma-ray production cross sections.

Examples

Risomer 0.8

Range

0. $\leq$ Risomer $\leq$ 10.

Default

Risomer 1.

electronconv

Flag for the application of an electron-conversion coefficient on the gamma-ray branching ratios from the discrete level file.

Examples

electronconv y
electronconv n

Range

y or **n**

Default

electronconv y

bestbranch

Flag to use the set of adjusted branching ratios for discrete levels.

Examples

bestbranch y
bestbranch n

Range

y or **n**

Default

bestbranch y

Comment

If branching ratios are considered to permanently overrule those of the discrete level file, the keywords as given by **branch** (p. 360) can be stored in the talys/structure/levels/branch directory, after which a simple **bestbranch y** is enough to invoke all these adjusted branching ratios.

outlevels

Flag for the output of discrete level information for each nucleus. All level energies, spins parities, branching ratios and lifetimes will be printed.

Examples

outlevels y
outlevels n

Range

y or **n**

Default

the same value as **outbasic**: **outlevels n**

fit

Flag to use the set of adjusted nuclear model parameters that produces the optimal fit for all incident channels. With the addition of the single line **fit y** to the input file, TALYS will automatically use all detailed adjusted parameter fits, obtained by automated adjustment, that are stored in *talys/structure/best/fits/*.

Examples

fit y
fit n

Range

y or **n**

Default

fit n

ngfit

Flag to use the set of adjusted nuclear model parameters that produces the optimal fit for (n,γ) cross sections in the fast neutron range. With the addition of the single line **ngfit y** to the input file, TALYS will automatically use all detailed adjusted parameter fits, obtained by automated adjustment, that are stored in *talys/structure/best/fits/ng.par*.

Examples

ngfit y
ngfit n

Range

y or **n**

Default

ngfit n, and **ngfit y** if **fit y**

nffit

Flag to use the set of adjusted nuclear model parameters that produces the optimal fit for (n,f) cross sections. With the addition of the single line **nffit y** to the input file, TALYS will automatically use all detailed adjusted parameter fits, obtained by automated adjustment, that are stored in *talys/structure/best/fits/nf.par*.

Examples

nffit y
nffit n

Range

y or **n**

Default

nffit n, and **nffit y** if **fit y**

nnfit

Flag to use the set of adjusted nuclear model parameters that produces the optimal fit for (n,n'), (n,2n) and (n,p) cross sections. With the addition of the single line **nnfit y** to the input file, TALYS will automatically use all detailed adjusted parameter fits, obtained by automated adjustment, that are stored in *talys/structure/best/fits/nn.par*.

Examples

> **nnfit y**
> **nnfit n**

Range

y or **n**

Default

nnfit n, and **nnfit y** if **fit y**

nafit

Flag to use the set of adjusted nuclear model parameters that produces the optimal fit for (n,α) cross sections. With the addition of the single line **nafit y** to the input file, TALYS will automatically use all detailed adjusted parameter fits, obtained by automated adjustment, that are stored in *talys/structure/best/fits/na.par*.

Examples

nafit y
nafit n

Range

y or **n**

Default

nafit n, and **nafit y** if **fit y**

macsfit

Flag to use the set of adjusted nuclear model parameters that produces the optimal fit for (n,γ) MACS in the fast neutron range. With the addition of the single line **macsfit y** to the input file, TALYS will automatically use all detailed adjusted parameter fits, obtained by automated adjustment, that are stored in *talys/structure/best/fits/macs.par*.

Examples

macsfit y
macsfit n

Range

y or **n**

Default

macsfit n

gamgamfit

Flag to use the set of adjusted nuclear model parameters that produces the optimal fit for (n,γ) average radiative width in the fast neutron range. With the addition of the single line **gamgamfit y** to the input file, TALYS will automatically use all detailed adjusted parameter fits, obtained by automated adjustment, that are stored in *talys/structure/best/fits/gamgam.par*.

Examples

gamgamfit y
gamgamfit n

Range

y or **n**

Default

gamgamfit n

anfit

Flag to use the set of adjusted nuclear model parameters that produces the optimal fit for (α,n) cross sections. With the addition of the single line **anfit y** to the input file, TALYS will automatically use all detailed adjusted parameter fits, obtained by automated adjustment, that are stored in *talys/structure/best/fits/an.par*.

Examples

anfit y
anfit n

Range

y or **n**

Default

anfit n, and **anfit y** if **fit y**

dnfit

Flag to use the set of adjusted nuclear model parameters that produces the optimal fit for (d,n) cross sections. With the addition of the single line **dnfit y** to the input file, TALYS will automatically use all detailed adjusted parameter fits, obtained by automated adjustment, that are stored in *talys/structure/best/fits/dn.par*.

Examples

dnfit y
dnfit n

Range

y or **n**

Default

dnfit n, and **dnfit y** if **fit y**

gnfit

Flag to use the set of adjusted nuclear model parameters that produces the optimal fit for (γ,n) cross sections. With the addition of the single line **gnfit y** to the input file, TALYS will automatically use all detailed adjusted parameter fits, obtained by automated adjustment, that are stored in *talys/structure/best/fits/gn.par*.

Examples

gnfit y
gnfit n

Range

y or **n**

Default

gnfit n, and **gnfit y** if **fit y**

pnfit

Flag to use the set of adjusted nuclear model parameters that produces the optimal fit for (p,n) cross sections. With the addition of the single line **pnfit y** to the input file, TALYS will automatically use all detailed adjusted parameter fits, obtained by automated adjustment, that are stored in *talys/structure/best/fits/pn.par*.

Examples

pnfit y
pnfit n

Range

y or **n**

Default

pnfit n, and **pnfit y** if **fit y**

isofit

Flag to use the set of adjusted nuclear model parameters that produces the optimal fit for isomeric cross sections. With the addition of the single line **fit y** to the input file, TALYS will automatically use all detailed adjusted parameter fits, obtained by automated adjustment, that are stored in *talys/structure/best/fits/*m.par*.

Examples

    isofit y
    isofit n

Range

y or **n**

Default

isofit n

25. Keywords for level densities

ldmodel

Model for level densities. There are 3 phenomenological level density models and 3 options for microscopic level densities, all described in Chapter 8. Since TALYS-1.4, it is possible to choose a level density model per nuclide considered in the reaction.

Examples

> **ldmodel 1**: Constant Temperature + Fermi gas model (CTM)
> **ldmodel 2**: Back-shifted Fermi gas Model (BFM)
> **ldmodel 3**: Generalised Superfluid Model (GSM)
> **ldmodel 4**: Skyrme-Hartree-Fock-Bogolyubov level densities from numerical tables
> **ldmodel 5**: Skyrme-Hartree-Fock-Bogolyubov combinatorial level densities from numerical tables
> **ldmodel 6**: Temperature-dependent Gogny-Hartree-Fock-Bogolyubov combinatorial level densities from numerical tables
> **ldmodel 2 41 93**: Back-shifted Fermi gas Model just for this particular nucleus

Range

$1 \leq$ **ldmodel** ≤ 6

Default

ldmodel 1

Comments

- Note the available flexibility exemplified by the last sample case above. It is possible to use different level density models per nuclide in one and the same TALYS run. Hence, one can e.g. globally use **ldmodel 5** but deviate from that for several nuclides by giving input lines like the **ldmodel 2 41 93** given above in the same input file.

ldmodelCN

Model for level density for the compound nucleus

Examples

> **ldmodelCN 1**: Constant Temperature + Fermi gas model (CTM)
> **ldmodelCN 2**: Back-shifted Fermi gas Model (BFM)
> etc. see definition of **ldmodel**

Range

$1 \leq$ **ldmodelCN** ≤ 6

Default

ldmodelCN = ldmodel

Comments

a

The level density parameter **a** at the neutron separation energy in MeV^{-1}. On the input line, we read **a**, Z, A, value.

Examples

　　a 41 93 11.220
　　a 94 239 28.385

Range

1. $\leq$ **a** $\leq$ **100.**

Default

a is read from the *talys/structure/density/* directory or, if not present, is calculated from systematics, see Eq. (8.12).

aadjust

Multiplier to adjust the level density parameter *a*. On the input line, we read **aadjust**, Z, A and value.

Examples

aadjust 41 93 1.04

Range

$0.5 \leq$ **aadjust** $\leq$ **2**.

Default

aadjust Z A **1.**

Comments

- As a general comment for '**adjust**' keywords: this avoids having to look up the actual parameter value in the TALYS input file, hardwired default value in the source code or this tutorial, or one of the data tables that TALYS uses. One simply multiplies the nominal value with the value given on this keyword line without having to know the actual value.

alimit

The asymptotic level density parameter $\tilde{a}$, for a particular nucleus, in MeV^{-1}, see Eq. (8.12). On the input line, we read **alimit**, Z, A, value.

Examples

    alimit 41 93 10.8
    alimit 94 239 28.010

Range

1. $\leq$ **alimit** $\leq$ **100.**

Default

alimit is determined from the systematics given by Eq. (8.13).

asys

Flag to use all level density parameters from systematics by default, i.e. to neglect the connection between a and the discrete level scheme and D_0, even if experimental values is available for the latter.

Examples

asys y

Range

y or **n**

Default

asys n

deltaW

Shell correction of the mass in MeV, see Eq. (8.12). On the input line, we read **deltaW**, Z, A, value, the ground state or fission barrier to which it applies (optional). If the fission barrier is not given or is equal to 0, TALYS assumes it concerns the ground state of the nucleus.

Examples

deltaW 41 93 0.110
deltaW 94 239 -0.262 1

Range

$-\mathbf{20.} \leq \mathbf{deltaW} \leq \mathbf{20.}$

Default

deltaW is determined from Eq. (8.15).

pair

The pairing correction in MeV. On the input line, we read **pair**, *Z*, *A*, value.

Examples

pair 94 239 0.76

Range

0. $\leq$ **pair** $\leq$ **10.**

Default

pair is determined from Eq. (8.49).

ctable

Constant c of the adjustment function (8.94) for tabulated level densities, per nucleus. On the input line, we read **ctable**, Z, A, value, and (optionally) fission barrier.

Examples

> **ctable 29 65 2.8**
> **ctable 92 234 0.1 1**

Range

-10. $\leq$ **ctable** $\leq$ **10.**

Default

ctable $Z\ A$ **0.**

ctableadjust

Adjustable shift for *ctable* of the adjustment function (8.94) for tabulated level densities, per nucleus. On the input line, we read **ctableadjust**, *Z*, *A*, value, and (optionally) fission barrier.

Examples

> **ctableadjust 29 65 2.8**
> **ctableadjust 92 234 0.1 1**

Range

-10. $\leq$ ctableadjust $\leq$ 10.

Default

ctableadjust *Z A* **0.**

ptable

Constant δ of the adjustment function (8.94) for tabulated level densities, per nucleus. On the input line, we read **ptable**, Z, A, value, and (optionally) fission barrier.

Examples

> **ptable 29 65 -0.6**
> **ptable 92 237 0.2 1**

Range

-10. $\leq$ **ptable** $\leq$ **10.**

Default

ptable Z A **0.**

ptableadjust

Adjustable shift for *ptable* of the adjustment function (8.94) for tabulated level densities, per nucleus. On the input line, we read **ptableadjust**, *Z*, *A*, value, and (optionally) fission barrier.

Examples

ptableadjust 29 65 2.8
ptableadjust 92 234 0.1 1

Range

-10. $\leq$ **ptableadjust** $\leq$ **10.**

Default

ptableadjust *Z A* **0.**

Nlow

Lower level to be used in the temperature matching problem of the Constant Temperature formula. On the input line, we read **Nlow**, Z, A, value, the ground state or fission barrier to which it applies (optional). If the fission barrier is not given or equal to 0, it concerns the ground state of the nucleus.

Examples

Nlow 41 93 4
Nlow 94 239 2 1

Range

$0 \leq$ **Nlow** $\leq$ **200**

Default

Nlow Z A **2**

Ntop

Upper level to be used in the temperature matching problem of the Constant Temperature formula. On the input line, we read **Ntop**, *Z*, *A*, value, the ground state or fission barrier to which it applies (optional). If the fission barrier is not given or equal to 0, it concerns the ground state of the nucleus.

Examples

Ntop 41 93 14
Ntop 94 239 20 1

Range

$0 \leq$ **Ntop** $\leq$ **200**, and **Ntop** $\geq$ **Nlow**.

Default

Ntop is read from the various subdirectories of *talys/structure/density/ground/*. If not present there, **Ntop** is equal to the last discrete level used for the Hauser-Feshbach calculation.

Exmatch

The matching energy between the constant temperature and Fermi gas region in MeV, see Eq. (8.35). On the input line, we read **Exmatch**, *Z*, *A*, value, the ground state or fission barrier to which it applies (optional). If the fission barrier is not given or is equal to 0, TALYS assumes it concerns the ground state of the nucleus.

Examples

> **Exmatch 41 93 4.213**
> **Exmatch 94 239 5.556 2**

Range

$0.1 \leq$ **Exmatch** $\leq 20.$

Default

Exmatch is determined from Eq. (8.42).

Exmatchadjust

Normalisation factor for the matching energy of the four-component formula. This parameter can be used as a relative normalisation instead of the absolute value of **Exmatchadjust**. On the input line, we read **Exmatchadjust**, Z, A, value, the ground state or fission barrier to which it applies (optional). If the fission barrier is not given or is equal to 0, TALYS assumes it concerns the ground state

Examples

> **Exmatchadjust 41 93 0.9**
> **Exmatchadjust 94 239 -1.13 1**

Range

$0.1 \leq$ **Exmatchadjust** $\leq 10.$

Default

Exmatchadjust $Z\,A$ **1.**.

- As a general comment for '**adjust**' keywords: this avoids having to look up the actual parameter value in the TALYS input file, hardwired default value in the source code or this tutorial, or one of the data tables that TALYS uses. One simply multiplies the nominal value with the value given on this keyword line without having to know the actual value.

T

The temperature of the Gilbert-Cameron formula in MeV, see Eq. (8.39). On the input line, we read **T**, *Z*, *A*, value, the ground state or fission barrier to which it applies (optional). If the fission barrier is not given or is equal to 0, TALYS assumes it concerns the ground state of the nucleus.

Examples

T 41 93 0.332
T 94 239 0.673 1

Range

$0.001 \leq \mathbf{T} \leq 10.$

Default

T is determined from Eq. (8.39).

- As a general comment for '**adjust**' keywords: this avoids having to look up the actual parameter value in the TALYS input file, hardwired default value in the source code or this tutorial, or one of the data tables that TALYS uses. One simply multiplies the nominal value with the value given on this keyword line without having to know the actual value.

Tadjust

Normalisation factor for the temperature of the four-component formula. This parameter can be used as a relative normalisation instead of the absolute value of **T**. On the input line, we read **Tadjust**, Z, A, value, the ground state or fission barrier to which it applies (optional). If the fission barrier is not given or is equal to 0, TALYS assumes it concerns the ground state

Examples

Tadjust 41 93 0.9
Tadjust 94 239 -1.13 1

Range

$0.1 \leq$ **Tadjust** $\leq$ **10.**

Default

Tadjust $Z\,A$ **1.**.

- As a general comment for '**adjust**' keywords: this avoids having to look up the actual parameter value in the TALYS input file, hardwired default value in the source code or this tutorial, or one of the data tables that TALYS uses. One simply multiplies the nominal value with the value given on this keyword line without having to know the actual value.

E0

The "back-shift" energy of the four-component formula in MeV, see Eq. (8.36). On the input line, we read **E0**, *Z*, *A*, value, the ground state or fission barrier to which it applies (optional). If the fission barrier is not given or is equal to 0, TALYS assumes it concerns the ground state of the nucleus.

Examples

E0 41 93 0.101
E0 94 239 -0.451 1

Range

$-10. \leq \mathbf{E0} \leq 10.$

Default

E0 is determined from Eq. (8.36).

- As a general comment for '**adjust**' keywords: this avoids having to look up the actual parameter value in the TALYS input file, hardwired default value in the source code or this tutorial, or one of the data tables that TALYS uses. One simply multiplies the nominal value with the value given on this keyword line without having to know the actual value.

E0adjust

Normalisation factor for the "back-shift" energy of the four-component formula. This parameter can be used as a relative normalisation instead of the absolute value of **E0**. On the input line, we read **E0adjust**, Z, A, value, the ground state or fission barrier to which it applies (optional). If the fission barrier is not given or is equal to 0, it concerns the ground state

Examples

E0adjust 41 93 0.9
E0adjust 94 239 -1.13 1

Range

$0.1 \leq$ **E0adjust** $\leq 10.$

Default

E0adjust $Z\,A$ **1.**.

- As a general comment for '**adjust**' keywords: this avoids having to look up the actual parameter value in the TALYS input file, hardwired default value in the source code or this tutorial, or one of the data tables that TALYS uses. One simply multiplies the nominal value with the value given on this keyword line without having to know the actual value.

Pshift

An extra pairing shift for adjustment of the Fermi Gas level density, in MeV. On the input line, we read **Pshift**, Z, A, value.

Examples

Pshift 60 142 0.26

Range

$-\mathbf{10}. \leq \mathbf{Pshift} \leq \mathbf{10.}$

Default

Pshift is determined from Eqs. (8.31), (8.49), or (8.63), depending on the level density model.

Pshiftadjust

Adjustable pairing shift for adjustment of the Fermi Gas level density, in MeV. The difference with **Pshift** is that the default is 0. On the input line, we read **Pshiftadjust**, Z, A, value.

Examples

Pshiftadjust 60 142 -0.13

Range

$-10. \leq$ **Pshift** $\leq$ **10.**

Default

Pshift 0..

- As a general comment for '**adjust**' keywords: this avoids having to look up the actual parameter value in the TALYS input file, hardwired default value in the source code or this tutorial, or one of the data tables that TALYS uses. One simply shifts the nominal value with the value given on this keyword line without having to know the actual value.

Pshiftconstant

Global constant for the adjustable pairing shift in MeV.

Examples

Pshiftconstant 1.03

Range

$-5. \leq$ **Pshiftconstant** $\leq$ **5.**

Default

Pshiftconstant=1.09 for **ldmodel 3** and **Pshiftconstant=0.** otherwise.

Rspincut

Global adjustable constant for spin cut-off parameter. Eq. (8.25) is multiplied by **Rspincut** for all nuclides in the calculation.

Examples

Rspincut 0.8

Range

0. $\leq$ Rspincut $\leq$ 10.

Default

Rspincut 1.

Rspincutff

Global adjustable constant for spin cut-off parameter for fission fragments

Examples

Rspincutff 8.

Range

0. $\leq$ Rspincutff $\leq$ 20.

Default

Rspincutff 4.

s2adjust

Adjustable constant for spin cut-off parameter per nuclide. Eq. (8.25) is multiplied by **s2adjust**. On the input line, we read **s2adjust**, Z, A, value, fission barrier. If the number of the fission barrier is not given or is equal to 0, TALYS assumes it concerns the ground state.

Examples

> **s2adjust 41 93 0.8**
> **s2adjust 94 239 1.1 2**

Range

$0.01 \leq$ **s2adjust** $\leq$ **10.**

Default

s2adjust Z A **1.**

- As a general comment for '**adjust**' keywords: this avoids having to look up the actual parameter value in the TALYS input file, hardwired default value in the source code or this tutorial, or one of the data tables that TALYS uses. One simply multiplies the nominal value with the value given on this keyword line without having to know the actual value.

densfile

Local file with tabulated level densities. The format of the file is exactly the same as that of the nuclear structure database *talys/structure/density/.* In practice, the user can copy a file from this database, e.g. *Fe.tab*, to the working directory and change it. In this way, changes in the "official" database are avoided. Note that even if only changes for one isotope are required, the entire file needs to be copied if for the other isotopes the originally tabulated values are to be used. Note that by default we assume that your table has both a positive and a negative parity part, as in e.g. ldmodel 5. If not, you have to add 'parity n' to the input file. On the input line, we read **densfile**, *Z*, *A*, filename.

Examples

densfile 26 56 Fe.loc

Range

densfile can be equal to any filename, provided it starts with a character.

Default

If **densfile** is not given in the input file, discrete levels are taken from *talys/structure/density/.*

filedensity

Flag to write the level density and associated parameters on a separate file *ldZZZAAA.tot*, where ZZZ is the charge number and AAA is the mass number in (i3.3) format. **filedensity** is only active if **outdensity y**.

Examples

filedensity y
filedensity n

Range

y or **n**

Default

filedensity n

outdensity

Flag for the output of level density parameters and level densities for each residual nucleus.

Examples

outdensity y
outdensity n

Range

y or **n**

Default

The same value as **outbasic**: **outdensity n**

colenhance

Flag to enable or disable explicit collective enhancement of the level density, using the K_{rot} and K_{vib} factors. This keyword can be used in combination with the **ldmodel** keyword. For fission, if **colenhance n**, collective effects for the ground state are included implicitly in the intrinsic level density, and collective effects on the barrier are determined relative to the ground state. It is possible to enable or disable the collective enhancement per nuclide considered in the reaction.

Examples

> **colenhance y**
> **colenhance y 41 93**

Range

y or **n**

Default

colenhance y if **fission y**, **colenhance n** otherwise.

colldamp

Flag for damping of collective effects in effective level density, i.e. in a formulation without explicit collective enhancement. For fission, collective effects for the ground state are included implicitly in the intrinsic level density, and collective effects on the barrier are determined relative to the ground state, see Section 15.1.2.

Examples

colldamp y

Range

y or **n**

Default

colldamp n

- In practice, this option has been used for fission model parameterization as employed in some of the older Bruyeres-le-Chatel actinide evaluations by Pascal Romain. Using it affects also the spin cutoff parameterization.

spincutmodel

Model for spin cut-off parameter for the ground state level densities, see Section 8.1.3. There are 2 expressions.

Examples

spincutmodel 1: $\sigma^2 = c\frac{a}{\tilde{a}}\sqrt{\frac{U}{a}}$

spincutmodel 2: $\sigma^2 = c\sqrt{\frac{U}{a}}$

Range

$1 \leq \textbf{spincutmodel} \leq 2$

Default

spincutmodel 1

shellmodel

Model for liquid drop expression for nuclear mass, to be used to calculate the shell correction. There are 2 expressions.

Examples

shellmodel 1: Myers-Swiatecki
shellmodel 2: Goriely

Range

$1 \leq$ **shellmodel** ≤ 2

Default

shellmodel 1

kvibmodel

Model for the vibrational enhancement of the level density. There are 2 expressions.

Examples

kvibmodel 1: Eq. (8.84)
kvibmodel 2: Eq. (8.78)

Range

$1 \leq$ **kvibmodel** ≤ 2

Default

kvibmodel 2

ctmglobal

Flag to enforce global formulae for the Constant Temperature Model (CTM), see Section 8.1.4. By default, if enough discrete levels are available the CTM will always make use of them for the estimation of the level density at low energies. For an honest comparison with other level density models, and also to test the predictive power for nuclides for which no discrete levels are known, we have included the possibility to perform a level density calculation with a truly global CTM. In practice it means that the matching energy E_M is always determined from the empirical formula (8.45), while T and E_0 are determined from E_M through Eqs.(8.39) and (8.36), respectively. This flag is only relevant if **ldmodel 1**.

Examples

　　　ctmglobal y

Range

y or **n**

Default

ctmglobal n

parity

Flag to enable or disable non-equiparity level densities. At present, this option only serves to average tabulated parity-dependent level densities (**ldmodel 5, 6**) over the two parities (using **parity n**), for comparison purposes.

Examples

parity y

Range

y or **n**

Default

parity n for **ldmodel 1-4**, **parity y** for **ldmodel 5, 6**.

alphald

Constant for the global expression for the asymptotic level density parameter $\tilde{a}$, see Eq. (8.13).

Examples

alphald 0.054

Range

$0.01 \leq$ **alphald** ≤ 0.2

Default

alphald is determined from the systematics given by Table 8.1, depending on the used level density model.

betald

Constant for the global expression for the asymptotic level density parameter $\tilde{a}$, see Eq. (8.13).

Examples

betald 0.15

Range

$-0.5 \leq$ **betald** ≤ 0.5 with the extra condition that if **betald** $< 0.$ then **abs(betald)** $<$ **alphald** (to avoid negative **a** values).

Default

betald is determined from the systematics given by Table 8.1, depending on the used level density model.

gammald

The damping parameter for shell effects in the level density parameter, for a particular nucleus, in MeV^{-1}, see Eq. (8.12). On the input line, we read **gammald**, Z, A, value.

Examples

gammald 41 93 0.051

Range

$0. \leq$ **gammald** $\leq$ **1.**

Default

gammald is determined from either Eq. (8.14) or (8.20).

gammashell1

Constant for the global expression for the damping parameter for shell effects in the level density parameter γ, see Eq. (8.14).

Examples

gammashell1 0.5
gammashell1 0.

Range

$0. \leq$ **gammashell1** $\leq$ **1.**

Default

gammashell1 is determined from the systematics given by Table 8.1.

gammashell2

Constant for the global expression for the damping parameter for shell effects in the level density parameter γ, see Eq. (8.14).

Examples

gammashell2 0.054
gammashell1 0.

Range

$0. \leq$ **gammashell2** $\leq$ **0.2**

Default

gammashell2=0.

pairconstant

Constant for the pairing energy expression in MeV, see Eq. (8.31).

Examples

pairconstant 11.3

Range

$0. \leq$ **pairconstant** $\leq$ **30.**

Default

pairconstant=12.

Krotconstant

Normalization constant for rotational enhancement for the ground state or fission barrier, to be multiplied with the r.h.s. of Eq. (8.87). On the input line, we read **Krotconstant**, Z, A, value, fission barrier. If the number of the fission barrier is not given or is equal to 0, TALYS assumes it concerns the ground state.

Examples

Krotconstant 90 232 0.4
Krotconstant 94 239 1.1 2

Range

$0.01 \leq$ **Krotconstant** $\leq$ **100.**

Default

Krotconstant $Z\,A$ **1.**

Cfermi

Width C_f of the phenomenological Fermi distribution (8.90) for damping of collective effects, in MeV. This can be given for the ground state or for fission barriers.

Examples

Cfermi 92 238 16.
Cfermi 92 236 16. 1

Range

0. $\leq$ **cfermi** $\leq$ **1000.**

Default

Cfermi 5.

Ufermi

Constant U_f of the phenomenological function (8.90) for damping of collective effects, in MeV. This can be given for the ground state or for fission barriers.

Examples

Ufermi 92 238 41.
Ufermi 92 236 41. 1

Range

0. $\leq$ **Ufermi** $\leq$ **1000.**

Default

Ufermi 30. for ground state, **Ufermi 45.** for barriers

Rtransmom

Normalization constant for moment of inertia for transition states, see Eq. (8.86). On the input line, we read **Rtransmom**, Z, A, value, fission barrier. If the number of the fission barrier is not given or is equal to 0, TALYS assumes it concerns the first barrier.

Examples

Rtransmom 90 232 1.15
Rtransmom 94 239 1.1 2

Range

$0.1 \leq$ **Rtransmom** $\leq$ **10.**

Default

Rtransmom 0.6 for the first barrier, **Rtransmom 1.0** for the other barriers.

Rclass2mom

Normalization constant for moment of inertia for class II/III states, see Eq. (8.86). On the input line, we read **Rclass2mom**, Z, A, value, fission barrier. If the number of the fission barrier is not given or is equal to 0, TALYS assumes it concerns the first barrier well.

Examples

Rclass2mom 90 232 1.15
Rclass2mom 94 239 1.1 2

Range

$0.1 \leq$ **Rclass2mom** $\leq$ **10.**

Default

Rclass2mom Z A **1.**

cglobal

Constant c of the adjustment function (8.94) for tabulated level densities, applied for all nuclides at the same time. Individual cases can be overruled by the **ctable** keyword. On the input line, we read **cglobal**, value.

Examples

cglobal 1.5

Range

-10. $\leq$ **cglobal** $\leq$ **10.**

Default

cglobal 0.

pglobal

Constant δ of the adjustment function (8.94) for tabulated level densities, applied for all nuclides at the same time. Individual cases can be overruled by the **ptable** keyword. On the input line, we read **pglobal**, value.

Examples

pglobal 0.5

Range

-10. $\leq$ **pglobal** $\leq$ **10**

Default

pglobal 0.

26. Keywords for gamma emission

gammax

Maximum number of l-values for gamma multipolarity, whereby $l = 1$ stands for M1 and E1 transitions, $l = 2$ for M2 and E2 transitions, etc.

Examples

gammax 1

Range

$1 \leq$ **gammax** ≤ 6

Default

gammax 2

gnorm

Normalisation factor for gamma-ray transmission coefficient. This adjustable parameter can be used to scale e.g. the (n, γ) cross section.

Examples

gnorm 1.6
gnorm -1. (enforce automatic normalization)

Range

0. $\leq$ **gnorm** $\leq$ **100.** or **gnorm -1.**

Default

gnorm is given by the normalization factor of Eq. (9.18) for **strength 1** or **2**.

strength

Model for $E1$ gamma-ray strength function, see Section 9. There are many possibilities.

Examples

> **strength 1** : Kopecky-Uhl generalized Lorentzian
> **strength 2** : Brink-Axel Lorentzian
> **strength 3** : Hartree-Fock BCS tables
> **strength 4** : Hartree-Fock-Bogoliubov tables
> **strength 5** : Goriely's hybrid model [50]
> **strength 6** : Goriely T-dependent HFB
> **strength 7** : T-dependent RMF
> **strength 8** : Gogny D1M HFB+QRPA
> **strength 9** : SMLO
> **strength 10**: Skyrme HFB+QRPA

Range

1 - **10**

Default

strength 9, and **strength 8** if all models are microscopic (**micro y**)

strengthM1

Model for $M1$ gamma-ray strength function. There are various possibilities.

Examples

strengthM1 1 : Use Eq. (9.15)
strengthM1 2 : Normalize the $M1$ gamma-ray strength function with that of $E1$ as $f_{E1}/(0.0588A^{0.878})$.
strengthM1 3 : Spn-flip an scissors mode
strengthM1 8 : Gogny D1M HFB
strengthM1 10: Skyrme HFB

Range

1, 2, 3, 8, 10

Default

strengthM1 3 and **strengthM1 8** if **strength 8**

egr

Energy of the giant dipole resonance in MeV. On the input line, we read **egr**, *Z*, *A*, value, type of radiation (the full symbol, i.e. M1, E1, E2, etc.), number of resonance (optional). If the number of the resonance is not given, it is assumed the keyword concerns the first Lorentzian.

Examples

     egr 41 93 16.2 E1
     egr 94 239 13.7 E1 2

Range

$1. \leq$ **egr** $\leq$ **100.** The optional number of the resonance must be either 1 or 2.

Default

egr is read from the *talys/structure/gamma/* directory. If the value for the first resonance is not present in the directory, it is calculated from systematics, see Section 9. If no parameter for the second resonance is given, this term is omitted altogether.

sgr

Strength of the giant dipole resonance in millibarns. On the input line, we read **sgr**, *Z*, *A*, value, type of radiation (the full symbol, i.e. M1, E1, E2, etc.), number of resonance (optional). If the number of the resonance is not given, it is assumed the keyword concerns the first Lorentzian.

Examples

sgr 41 93 221. E1
sgr 94 239 384. E1 2

Range

0. $\leq$ **sgr** $\leq$ **10000.** The optional number of the resonance must be either 1 or 2.

Default

sgr is read from the *talys/structure/gamma/* directory. If the value for the first resonance is not present in the directory, it is calculated from systematics, see Section 9. If no parameter for the second resonance is given, this term is omitted altogether.

ggr

Width of the giant dipole resonance in MeV. On the input line, we read **ggr**, *Z*, *A*, value, type of radiation (the full symbol, i.e. M1, E1, E2, etc.), number of resonance (optional). If the number of the resonance is not given, it is assumed the keyword concerns the first Lorentzian.

Examples

> **ggr 41 93 5.03 E1**
> **ggr 94 239 4.25 E1 2**

Range

1. $\le$ **ggr** $\le$ **100.** The optional number of the resonance must be either 1 or 2.

Default

ggr is read from the *talys/structure/gamma/* directory. If the value for the first resonance is not present in the directory, it is calculated from systematics, see Section 9. If no parameter for the second resonance is given, this term is omitted altogether.

egradjust

Normalisation factor for the energy of the giant dipole resonance. This parameter can be used as a relative normalisation instead of the absolute value of **egr**.

Examples

egradjust 45 104 0.9

Range

$0.1 \leq$ **egradjust** $\leq$ **10.**

Default

egradjust $Z\,A$ **1.**.

Comments

- As a general comment for '**adjust**' keywords: this avoids having to look up the actual parameter value in the TALYS input file, hardwired default value in the source code or this tutorial, or one of the data tables that TALYS uses. One simply multiplies the nominal value with the value given on this keyword line without having to know the actual value.

sgradjust

Normalisation factor for the strength of the giant dipole resonance. This parameter can be used as a relative normalisation instead of the absolute value of **sgr**.

Examples

  sgradjust 45 104 0.9

Range

$0.1 \leq$ **sgradjust** $\leq$ **10.**

Default

sgradjust $Z\,A$ **1.**.

Comments

- As a general comment for '**adjust**' keywords: this avoids having to look up the actual parameter value in the TALYS input file, hardwired default value in the source code or this tutorial, or one of the data tables that TALYS uses. One simply multiplies the nominal value with the value given on this keyword line without having to know the actual value.

ggradjust

Normalisation factor for the width of the giant dipole resonance. This parameter can be used as a relative normalisation instead of the absolute value of **ggr**.

Examples

ggradjust 45 104 0.9

Range

$0.1 \leq$ **ggradjust** $\leq$ **10.**

Default

ggradjust $Z A$ **1.**.

Comments

- As a general comment for '**adjust**' keywords: this avoids having to look up the actual parameter value in the TALYS input file, hardwired default value in the source code or this tutorial, or one of the data tables that TALYS uses. One simply multiplies the nominal value with the value given on this keyword line without having to know the actual value.

gamgam

The total radiative width, Γ_γ in eV. On the input line, we read **gamgam**, *Z*, *A*, value.

Examples

gamgam 26 55 1.8

Range

0. $\leq$ **gamgam** $\leq$ **10.**

Default

gamgam is read from the *talys/structure/resonances/* directory, or, if not present there, is taken from interpolation, see Section 9.

gamgamadjust

Normalisation factor for the average radiative width Γ_γ. This parameter can be used to scale e.g. the (n, γ) cross section.

Examples

gamgamadjust 45 104 0.9

Range

$0.1 \leq$ **gamgamadjust** $\leq$ **10.**

Default

gamgamadjust $Z\,A$ **1.**.

Comments

- As a general comment for '**adjust**' keywords: this avoids having to look up the actual parameter value in the TALYS input file, hardwired default value in the source code or this tutorial, or one of the data tables that TALYS uses. One simply multiplies the nominal value with the value given on this keyword line without having to know the actual value.

outgamma

Flag for the output of gamma-ray parameters, strength functions, transmission coefficients and reaction cross sections.

Examples

outgamma y
outgamma n

Range

y or **n**

Default

the same value as **outbasic**: **outgamma n**

D0

The s-wave resonance spacing D_0 in keV. On the input line, we read **D0**, Z, A, value.

Examples

D0 26 55 13.

Range

$1.e-6 \leq \textbf{D0} \leq \textbf{10000.}$

Default

D0 is read from the *talys/structure/resonances/* directory.

Rprime

Potential scattering radius.

Examples

Rprime 6.
Rprime 0.3

Range

$0. \leq$ **Rprime** $\leq$ **10.**

Default

Rprime is derived from the OMP.

etable

Constant E_{shift} of the adjustment function (9.17) for tabulated gamma strength functions densities, per nucleus. On the input line, we read **etable**, Z, A, value, type of radiation (the full symbol, i.e. M1, E1, E2, etc.).

Examples

etable 29 65 -0.6 E1

Range

-10. $\leq$ **etable** $\leq$ **10.**

Default

etable Z A **0.**

etableadjust

Adjustable shift for E_{shift} of the adjustment function (9.17) for tabulated gamma strength functions densities, per nucleus. On the input line, we read **etableadjust**, Z, A, value, type of radiation (the full symbol, i.e. M1, E1, E2, etc.).

Examples

     etableadjust 29 65 -0.6 M1

Range

-10. $\leq$ **etableadjust** $\leq$ **10.**

Default

etableadjust Z A **0.**

ftable

Constant f^{nor} of the adjustment function (9.17) for tabulated gamma strength functions densities, per nucleus. On the input line, we read **ftable**, Z, A, value, type of radiation (the full symbol, i.e. M1, E1, E2, etc.).

Examples

ftable 29 65 1.2 E1

Range

0.1 $\leq$ ftable $\leq$ 10.

Default

ftable Z A **1.**

ftableadjust

Adjustable shift for f^{nor} of the adjustment function (9.17) for tabulated gamma strength functions densities, per nucleus. On the input line, we read **ftableadjust**, Z, A, value, type of radiation (the full symbol, i.e. M1, E1, E2, etc.).

Examples

> **ftableadjust 29 65 1.2 M1**

Range

0.1 $\leq$ ftableadjust $\leq$ 10.

Default

ftableadjust Z A **1.**

wtable

Adjustable width of the adjustment function (9.17) for tabulated gamma strength functions densities, per nucleus. On the input line, we read **wtable**, *Z*, *A*, value, type of radiation (the full symbol, i.e. M1, E1, E2, etc.).

Examples

wtable 29 65 1.2 E1

Range

0. $\leq$ **wtable** $\leq$ **10.**

Default

wtable *Z A* **1.**

wtableadjust

Adjustable factor for the width of the adjustment function (9.17) for tabulated gamma strength functions densities, per nucleus. On the input line, we read **wtableadjust**, *Z*, *A*, value, type of radiation (the full symbol, i.e. M1, E1, E2, etc.).

Examples

  wtableadjust 29 65 1.2 E1

Range

0. $\leq$ **wtableadjust** $\leq$ **10.**

Default

wtableadjust *Z A* **1.**

E1file

File with tabulated gamma-ray strength function. The format of the file is the same as that of the nuclear structure database *talys/structure/gamma/hfb/*. On the input line, we read **E1file**, *Z*, *A*, filename.

Examples

E1file 26 56 gam.loc

Range

E1file can be equal to any filename, provided it starts with a character.

Default

If **E1file** is not given in the input file, the default applies.

M1file

File with tabulated gamma-ray strength function. The format of the file is the same as that of the nuclear structure database *talys/structure/gamma/hfb/*. On the input line, we read **M1file**, *Z*, *A*, filename.

Examples

M1file 26 56 gam.loc

Range

M1file can be equal to any filename, provided it starts with a character.

Default

If **M1file** is not given in the input file, the default applies.

filepsf

Flag to write photon strength functions to a separate file.

Examples

filepsf y
filepsf n

Range

y or **n**

Default

filepsf n

psfglobal

Flag to use only global parameterization for PSF, instead of tuned parameters.

Examples

psfglobal y
psfglobal n

Range

y or **n**

Default

psfglobal n

fiso

Correction factor for isospin-forbidden transitions to self-conjugate nuclei [143]. Since isospin-dependent level densities are currently not implemented in TALYS, this is a way to handle transitions to $Z = N$ or $Z = N \pm 1$ nuclei. On the input line, we read **fiso**, particle type value.

Examples

fiso n 2.2

Range

$0.01 \leq$ **fiso** $\leq$ **100.**

Default

If $Z = N$, **fiso 2.** for incident neutrons and protons, **fiso 5.** for incident alpha's. If $Z = N \pm 1$, **fiso 1.5** for incident neutrons, protons and alpha's. In all other cases **fiso 1.**.

fisom

Correction factor for multiple emission for isospin-forbidden transitions to self-conjugate nuclei [143]. Since isospin-dependent level densities are currently not implemented in TALYS, this is a way to handle transitions to $Z = N$ or $Z = N \pm 1$ nuclei. On the input line, we read **fisom**, particle type, value.

Examples

   fisom n 2.2

Range

0.01 $\leq$ fisom $\leq$ 100.

Default

If $Z = N$, **fisom 2.** for incident neutrons and protons, **fisom 5.** for incident alpha's. If $Z = N \pm 1$, **fisom 1.5** for incident neutrons, protons and alpha's. In all other cases **fisom 1.**.

racap

Flag for the inclusion of the direct capture model, for addition to the gamma cross section.

Examples

racap y
racap n

Range

y or **n**

Default

racap n

ldmodelracap

Level density model for direct capture model. There are 3 options.

Examples

ldmodelracap 1: Spin-parity dependent ph-state densities
ldmodelracap 2: Total ph-state densities
ldmodelracap 3: Spin-parity dependent total level densities (**ldmodel 5**)

Range

1 ≤ ldmodelracap ≤ 3

Default

ldmodelracap 1

sfexp

Experimental spectroscopic factor for direct capture reactions. This keyword is only active if **racap y**. On the input line, we read **sfexp**, *Z*, *A*, discrete level, value. The input for *Z*, *A*, discrete level, is optional.

Examples

> **sfexp 20 40 2 0.1**
> **sfexp 2 0.3**
> **sfexp 20 40 0.1**
> **sfexp 0.2**

Range

0. $\leq$ **sfexp** $\leq$ **10.**

Default

sfexp is taken from *talys/structure/levels/spectn*, and if not available there, **sfexp** *Z A level* **0.347**.

sfth

Theoretical spectroscopic factor for direct capture reactions, for levels in the continuum. This keyword is only active if **racap y**. On the input line, we read **sfth**, *Z*, *A*, value. The input for *Z*, *A*, is optional.

Examples

> **sfth 20 40 0.1**
> **sfth 0.3**

Range

0. $\leq$ **sfth** $\leq$ **10.**

Default

sfth *Z A* **0.5**.

epr

Energy of the Pygmy resonance in MeV. On the input line, we read **epr**, *Z*, *A*, value, type of radiation (the full symbol, i.e. M1, E1, E2, etc.), number of resonance (optional). If the number of the resonance is not given, it is assumed the keyword concerns the first Lorentzian.

Examples

> **epr 41 93 10.2 E1**
> **epr 94 239 8.7 E1 2**

Range

$1. \leq$ **epr** $\leq$ **100.** The optional number of the resonance must be either 1 or 2.

Default

no default.

spr

Strength of the Pygmy resonance in millibarns. On the input line, we read **spr**, *Z*, *A*, value, type of radiation (the full symbol, i.e. M1, E1, E2, etc.), number of resonance (optional). If the number of the resonance is not given, it is assumed the keyword concerns the first Lorentzian.

Examples

spr 41 93 21.6 E1
spr 94 239 3.4 E1 2

Range

$0. \leq$ **spr** $\leq$ **10000.** The optional number of the resonance must be either 1 or 2.

Default

no default.

gpr

Width of the Pygmy resonance in MeV. On the input line, we read **gpr**, Z, A, value, type of radiation (the full symbol, i.e. M1, E1, E2, etc.), number of resonance (optional). If the number of the resonance is not given, it is assumed the keyword concerns the first Lorentzian.

Examples

> **gpr 41 93 5.03 E1**
> **gpr 94 239 4.25 E1 2**

Range

$0.1 \leq$ **gpr** ≤ 100. The optional number of the resonance must be either 1 or 2.

Default

no default.

epradjust

Normalisation factor for the energy of the Pygmy resonance. This parameter can be used as a relative normalisation instead of the absolute value of **epr**.

Examples

> **epradjust 45 104 0.9**

Range

$0.1 \leq$ **epradjust** $\leq$ **10.**

Default

epradjust $Z\,A$ **1.**.

Comments

- As a general comment for '**adjust**' keywords: this avoids having to look up the actual parameter value in the TALYS input file, hardwired default value in the source code or this tutorial, or one of the data tables that TALYS uses. One simply multiplies the nominal value with the value given on this keyword line without having to know the actual value.

spradjust

Normalisation factor for the strength of the Pygmy resonance. This parameter can be used as a relative normalisation instead of the absolute value of **spr**.

Examples

spradjust 45 104 0.9

Range

$0.1 \leq$ **spradjust** $\leq$ **10.**

Default

spradjust $Z\,A$ **1.**.

Comments

- As a general comment for '**adjust**' keywords: this avoids having to look up the actual parameter value in the TALYS input file, hardwired default value in the source code or this tutorial, or one of the data tables that TALYS uses. One simply multiplies the nominal value with the value given on this keyword line without having to know the actual value.

gpradjust

Normalisation factor for the width of the Pygmy resonance. This parameter can be used as a relative normalisation instead of the absolute value of **gpr**.

Examples

gpradjust 45 104 0.9

Range

$0.1 \leq$ **gpradjust** $\leq$ **10.**

Default

gpradjust $Z\,A$ **1.**.

Comments

- As a general comment for '**adjust**' keywords: this avoids having to look up the actual parameter value in the TALYS input file, hardwired default value in the source code or this tutorial, or one of the data tables that TALYS uses. One simply multiplies the nominal value with the value given on this keyword line without having to know the actual value.

upbend

Flag to use the low-energy upbend of given multipolarity.

Examples

upbend y
upbend n

Range

y or **n**

Default

upbend n

upbendc

Normalisation factor for the low-energy upbend of the gamma ray strength function.

Examples

upbendc 57 138 1.e-7 M1

Range

$0. \leq$ **upbendc** $\leq$ **1.e-5**

Default

upbendc Z A **0.**.

upbende

Energy-dependent factor for the low-energy upbend of the gamma ray strength function.

Examples

upbende 57 138 1.5 M1

Range

$0. \leq$ **upbende** $\leq$ **10.**

Default

upbende Z A **0..**

upbendf

Normalization factor for the low-energy upbend of the gamma ray strength function.

Examples

upbendf 57 138 1.5 M1

Range

$-10. \leq$ **upbendf** $\leq$ **10.**

Default

upbendf Z A **0.**.

27. Keywords for optical model

rvadjust

Multiplier to adjust the OMP parameter rv of Eq. (10.7). On the input line, we read **rvadjust**, particle symbol, and value.

Examples

   rvadjust t 1.04

Range

$0.1 \leq$ **rvadjust** ≤ 10.

Default

rvadjust *particle* **1.**

Comments

- This keyword can also be used for complex particle potentials.
- As a general comment for '**adjust**' keywords: this avoids having to look up the actual parameter value in the TALYS input file, hardwired default value in the source code or this tutorial, or one of the data tables that TALYS uses. One simply multiplies the nominal value with the value given on this keyword line without having to know the actual value.

avadjust

Multiplier to adjust the OMP parameter av of Eq. (10.7). On the input line, we read **avadjust**, particle symbol, and value.

Examples

avadjust d 0.97

Range

$0.1 \leq$ **avadjust** ≤ 10.

Default

avadjust *particle* **1.**

Comments

- This keyword can also be used for complex particle potentials.
- As a general comment for '**adjust**' keywords: this avoids having to look up the actual parameter value in the TALYS input file, hardwired default value in the source code or this tutorial, or one of the data tables that TALYS uses. One simply multiplies the nominal value with the value given on this keyword line without having to know the actual value.

v1adjust

Multiplier to adjust the OMP parameter v1 of Eq. (10.7). On the input line, we read **v1adjust**, particle symbol, and value.

Examples

v1adjust a 1.12

Range

$0.1 \leq$ **v1adjust** $\leq$ **10**.

Default

v1adjust *particle* **1.**

Comments

- This keyword can also be used for double-folding and complex particle potentials.
- As a general comment for '**adjust**' keywords: this avoids having to look up the actual parameter value in the TALYS input file, hardwired default value in the source code or this tutorial, or one of the data tables that TALYS uses. One simply multiplies the nominal value with the value given on this keyword line without having to know the actual value.

v2adjust

Multiplier to adjust the OMP parameter v2 of Eq. (10.7). On the input line, we read **v2adjust**, particle symbol, and value.

Examples

v2adjust n 0.96

Range

$0.1 \leq$ **v2adjust** ≤ 10.

Default

v2adjust *particle* **1.**

Comments

- This keyword can only be used for a potential of the KD03 form.
- This keyword does not apply to deuterons up to alpha's.
- As a general comment for '**adjust**' keywords: this avoids having to look up the actual parameter value in the TALYS input file, hardwired default value in the source code or this tutorial, or one of the data tables that TALYS uses. One simply multiplies the nominal value with the value given on this keyword line without having to know the actual value.

v3adjust

Multiplier to adjust the OMP parameter v3 of Eq. (10.7). On the input line, we read **v3adjust**, particle symbol, and value.

Examples

     v3adjust p 1.10

Range

$0.1 \leq$ **v3adjust** ≤ 10.

Default

v3adjust *particle* **1.**

Comments

- This keyword can only be used for a potential of the KD03 form.
- This keyword does not apply to deuterons up to alpha's.
- As a general comment for '**adjust**' keywords: this avoids having to look up the actual parameter value in the TALYS input file, hardwired default value in the source code or this tutorial, or one of the data tables that TALYS uses. One simply multiplies the nominal value with the value given on this keyword line without having to know the actual value.

v4adjust

Multiplier to adjust the OMP parameter v4 of Eq. (10.7). On the input line, we read **v4adjust**, particle symbol, and value.

Examples

v4adjust n 0.98

Range

$0.1 \leq$ **v4adjust** ≤ 10.

Default

v4adjust *particle* **1.**

Comments

- This keyword can only be used for a potential of the Koning-Delaroche form.
- This keyword does not apply to deuterons up to alpha's.
- As a general comment for '**adjust**' keywords: this avoids having to look up the actual parameter value in the TALYS input file, hardwired default value in the source code or this tutorial, or one of the data tables that TALYS uses. One simply multiplies the nominal value with the value given on this keyword line without having to know the actual value.

rwadjust

Multiplier to adjust the OMP parameter rw of Eq. (10.7). On the input line, we read **rwadjust**, particle symbol, and value.

Examples

> **rwadjust t 1.04**

Range

$0.1 \leq$ **rwadjust** ≤ 10.

Default

rwadjust *particle* **1.**

Comments

- This keyword can also be used for complex particle potentials.
- As a general comment for '**adjust**' keywords: this avoids having to look up the actual parameter value in the TALYS input file, hardwired default value in the source code or this tutorial, or one of the data tables that TALYS uses. One simply multiplies the nominal value with the value given on this keyword line without having to know the actual value.

awadjust

Multiplier to adjust the OMP parameter aw of Eq. (10.7). On the input line, we read **awadjust**, particle symbol, and value.

Examples

awadjust d 0.97

Range

$0.1 \leq$ **awadjust** ≤ 10.

Default

awadjust *particle* **1.**

Comments

- This keyword can also be used for complex particle potentials.
- As a general comment for '**adjust**' keywords: this avoids having to look up the actual parameter value in the TALYS input file, hardwired default value in the source code or this tutorial, or one of the data tables that TALYS uses. One simply multiplies the nominal value with the value given on this keyword line without having to know the actual value.

w1adjust

Multiplier to adjust the OMP parameter w1 of Eq. (10.7). On the input line, we read **w1adjust**, particle symbol, and value.

Examples

    w1adjust p 1.10

Range

$0.1 \leq$ **w1adjust** $\leq$ **10**.

Default

w1adjust *particle* **1.**

Comments

- This keyword can also be used for double-folding and complex particle potentials.
- As a general comment for '**adjust**' keywords: this avoids having to look up the actual parameter value in the TALYS input file, hardwired default value in the source code or this tutorial, or one of the data tables that TALYS uses. One simply multiplies the nominal value with the value given on this keyword line without having to know the actual value.

w2adjust

Multiplier to adjust the OMP parameter w2 of Eq. (10.7). On the input line, we read **w2adjust**, particle symbol, and value.

Examples

w2adjust n 0.80

Range

$0.1 \leq$ **w2adjust** $\leq$ **10**.

Default

w2adjust *particle* **1.**

Comments

- This keyword can only be used for a potential of the KD03 form.
- This keyword does not apply to deuterons up to alpha's.
- As a general comment for '**adjust**' keywords: this avoids having to look up the actual parameter value in the TALYS input file, hardwired default value in the source code or this tutorial, or one of the data tables that TALYS uses. One simply multiplies the nominal value with the value given on this keyword line without having to know the actual value.

w3adjust

Multiplier to adjust the OMP parameter w3 of Eq. (10.18). On the input line, we read **w3adjust**, particle symbol, and value.

Examples

     w3adjust n 0.80

Range

$0.1 \leq$ **w3adjust** $\leq$ **10**.

Default

w3adjust *particle* **1.**

Comments

- This keyword can only be used for the high-energy extension of the KD03 form.
- This keyword does not apply to deuterons up to alpha's.
- As a general comment for '**adjust**' keywords: this avoids having to look up the actual parameter value in the TALYS input file, hardwired default value in the source code or this tutorial, or one of the data tables that TALYS uses. One simply multiplies the nominal value with the value given on this keyword line without having to know the actual value.

w4adjust

Multiplier to adjust the OMP parameter w4 of Eq. (10.18). On the input line, we read **w4adjust**, particle symbol, and value.

Examples

w4adjust n 0.80

Range

$0.1 \leq$ **w4adjust** ≤ 10.

Default

w4adjust *particle* **1.**

Comments

- This keyword can only be used for the high-energy extension of the KD03 form.
- This keyword does not apply to deuterons up to alpha's.
- As a general comment for '**adjust**' keywords: this avoids having to look up the actual parameter value in the TALYS input file, hardwired default value in the source code or this tutorial, or one of the data tables that TALYS uses. One simply multiplies the nominal value with the value given on this keyword line without having to know the actual value.

rvdadjust

Multiplier to adjust the OMP parameter rvd of Eq. (10.7). On the input line, we read **rvdadjust**, particle symbol, and value.

Examples

rvdadjust d 0.97

Range

$0.1 \leq$ **rvdadjust** $\leq$ **10**.

Default

rvdadjust *particle* **1.**

Comments

- Usually **rvd** and **rvdadjust** are not used.
- This keyword can also be used for complex particle potentials.
- As a general comment for '**adjust**' keywords: this avoids having to look up the actual parameter value in the TALYS input file, hardwired default value in the source code or this tutorial, or one of the data tables that TALYS uses. One simply multiplies the nominal value with the value given on this keyword line without having to know the actual value.

avdadjust

Multiplier to adjust the OMP parameter avd of Eq. (10.7). On the input line, we read **avdadjust**, particle symbol, and value.

Examples

    avdadjust d 0.97

Range

$0.1 \leq$ **avdadjust** $\leq$ **10**.

Default

avdadjust *particle* **1.**

Comments

- Usually **avd** and **avdadjust** are not used.
- This keyword can also be used for complex particle potentials.
- As a general comment for '**adjust**' keywords: this avoids having to look up the actual parameter value in the TALYS input file, hardwired default value in the source code or this tutorial, or one of the data tables that TALYS uses. One simply multiplies the nominal value with the value given on this keyword line without having to know the actual value.

rwdadjust

Multiplier to adjust the OMP parameter rwd of Eq. (10.7). On the input line, we read **rwdadjust**, particle symbol, and value.

Examples

rwdadjust d 0.97

Range

$0.1 \leq$ **rwdadjust** $\leq$ **10**.

Default

rwdadjust *particle* **1.**

Comments

- This keyword can also be used for complex particle potentials.
- As a general comment for '**adjust**' keywords: this avoids having to look up the actual parameter value in the TALYS input file, hardwired default value in the source code or this tutorial, or one of the data tables that TALYS uses. One simply multiplies the nominal value with the value given on this keyword line without having to know the actual value.

awdadjust

Multiplier to adjust the OMP parameter awd of Eq. (10.7). On the input line, we read **awdadjust**, particle symbol, and value.

Examples

awdadjust d 0.97

Range

$0.1 \leq$ **awdadjust** ≤ 10.

Default

awdadjust *particle* **1.**

Comments

- This keyword can also be used for complex particle potentials.
- As a general comment for '**adjust**' keywords: this avoids having to look up the actual parameter value in the TALYS input file, hardwired default value in the source code or this tutorial, or one of the data tables that TALYS uses. One simply multiplies the nominal value with the value given on this keyword line without having to know the actual value.

d1adjust

Multiplier to adjust the OMP parameter d1 of Eq. (10.7). On the input line, we read **d1adjust**, particle symbol, and value.

Examples

   d1adjust d 0.97

Range

$0.1 \leq$ **d1adjust** ≤ 10.

Default

d1adjust *particle* **1.**

Comments

- This keyword can also be used for complex particle potentials.
- As a general comment for '**adjust**' keywords: this avoids having to look up the actual parameter value in the TALYS input file, hardwired default value in the source code or this tutorial, or one of the data tables that TALYS uses. One simply multiplies the nominal value with the value given on this keyword line without having to know the actual value.

d2adjust

Multiplier to adjust the OMP parameter d2 of Eq. (10.7). On the input line, we read **d2adjust**, particle symbol, and value.

Examples

d2adjust n 1.06

Range

$0.1 \leq$ **d2adjust** ≤ 10.

Default

d2adjust *particle* **1.**

Comments

- This keyword can only be used for a potential of the KD03 form.
- This keyword does not apply to deuterons up to alpha's.
- As a general comment for '**adjust**' keywords: this avoids having to look up the actual parameter value in the TALYS input file, hardwired default value in the source code or this tutorial, or one of the data tables that TALYS uses. One simply multiplies the nominal value with the value given on this keyword line without having to know the actual value.

d3adjust

Multiplier to adjust the OMP parameter d3 of Eq. (10.7). On the input line, we read **d3adjust**, particle symbol, and value.

Examples

d3adjust n 1.06

Range

$0.1 \leq$ **d3adjust** $\leq$ **10**. This keyword does not apply to deuterons up to alpha's.

Default

d3adjust *particle* **1.**

Comments

- This keyword can only be used for a potential of the KD03 form.
- This keyword does not apply to deuterons up to alpha's.
- As a general comment for '**adjust**' keywords: this avoids having to look up the actual parameter value in the TALYS input file, hardwired default value in the source code or this tutorial, or one of the data tables that TALYS uses. One simply multiplies the nominal value with the value given on this keyword line without having to know the actual value.

vso1adjust

Multiplier to adjust the OMP parameter vso1 of Eq. (10.7). On the input line, we read **vso1adjust**, particle symbol, and value.

Examples

vso1adjust d 1.15

Range

$0.1 \leq$ **vso1adjust** $\leq$ **10**.

Default

vso1adjust *particle* **1.**

Comments

- This keyword can also be used for complex particle potentials.
- As a general comment for '**adjust**' keywords: this avoids having to look up the actual parameter value in the TALYS input file, hardwired default value in the source code or this tutorial, or one of the data tables that TALYS uses. One simply multiplies the nominal value with the value given on this keyword line without having to know the actual value.

vso2adjust

Multiplier to adjust the OMP parameter vso2 of Eq. (10.7). On the input line, we read **vso2adjust**, particle symbol, and value.

Examples

> **vso2adjust n 1.06**

Range

$0.1 \leq$ **vso2adjust** ≤ 10. This keyword does not apply to deuterons up to alpha's.

Default

vso2adjust *particle* **1.**

Comments

- This keyword can only be used for a potential of the Koning-Delaroche form.
- As a general comment for '**adjust**' keywords: this avoids having to look up the actual parameter value in the TALYS input file, hardwired default value in the source code or this tutorial, or one of the data tables that TALYS uses. One simply multiplies the nominal value with the value given on this keyword line without having to know the actual value.

wso1adjust

Multiplier to adjust the OMP parameter wso1 of Eq. (10.7). On the input line, we read **wso1adjust**, particle symbol, and value.

Examples

wso1adjust d 1.15

Range

$0.1 \leq$ **wso1adjust** ≤ 10.

Default

wso1adjust *particle* **1.**

Comments

- This keyword can also be used for complex particle potentials.
- As a general comment for '**adjust**' keywords: this avoids having to look up the actual parameter value in the TALYS input file, hardwired default value in the source code or this tutorial, or one of the data tables that TALYS uses. One simply multiplies the nominal value with the value given on this keyword line without having to know the actual value.

wso2adjust

Multiplier to adjust the OMP parameter wso2 of Eq. (10.7). On the input line, we read **wso2adjust**, particle symbol, and value.

Examples

   wso2adjust n 1.06

Range

0.**1** $\leq$ **wso2adjust** $\leq$ **10**. This keyword does not apply to deuterons up to alpha's.

Default

wso2adjust *particle* **1.**

Comments

- This keyword can only be used for a potential of the Koning-Delaroche form.
- As a general comment for '**adjust**' keywords: this avoids having to look up the actual parameter value in the TALYS input file, hardwired default value in the source code or this tutorial, or one of the data tables that TALYS uses. One simply multiplies the nominal value with the value given on this keyword line without having to know the actual value.

rvsoadjust

Multiplier to adjust the OMP parameter rvso of Eq. (10.7). On the input line, we read **rvsoadjust**, particle symbol, and value.

Examples

    rvsoadjust d 1.15

Range

$0.1 \leq$ **rvsoadjust** $\leq$ **10**.

Default

rvsoadjust *particle* **1.**

Comments

- This keyword can also be used for complex particle potentials.
- As a general comment for '**adjust**' keywords: this avoids having to look up the actual parameter value in the TALYS input file, hardwired default value in the source code or this tutorial, or one of the data tables that TALYS uses. One simply multiplies the nominal value with the value given on this keyword line without having to know the actual value.

avsoadjust

Multiplier to adjust the OMP parameter avso of Eq. (10.7). On the input line, we read **avsoadjust**, particle symbol, and value.

Examples

     avsoadjust d 1.15

Range

$0.1 \leq$ **avsoadjust** ≤ 10.

Default

avsoadjust *particle* **1.**

Comments

- This keyword can also be used for complex particle potentials.
- As a general comment for '**adjust**' keywords: this avoids having to look up the actual parameter value in the TALYS input file, hardwired default value in the source code or this tutorial, or one of the data tables that TALYS uses. One simply multiplies the nominal value with the value given on this keyword line without having to know the actual value.

rwsoadjust

Multiplier to adjust the OMP parameter rwso of Eq. (10.7). On the input line, we read **rwsoadjust**, particle symbol, and value.

Examples

    rwsoadjust d 1.15

Range

$0.1 \leq$ **rwsoadjust** ≤ 10.

Default

rwsoadjust *particle* **1.**

Comments

- This keyword can also be used for complex particle potentials.
- As a general comment for '**adjust**' keywords: this avoids having to look up the actual parameter value in the TALYS input file, hardwired default value in the source code or this tutorial, or one of the data tables that TALYS uses. One simply multiplies the nominal value with the value given on this keyword line without having to know the actual value.

awsoadjust

Multiplier to adjust the OMP parameter awso of Eq. (10.7). On the input line, we read **awsoadjust**, particle symbol, and value.

Examples

   awsoadjust d 1.15

Range

$0.1 \leq$ **awsoadjust** $\leq$ **10**.

Default

awsoadjust *particle* **1.**

Comments

- This keyword can also be used for complex particle potentials.
- As a general comment for '**adjust**' keywords: this avoids having to look up the actual parameter value in the TALYS input file, hardwired default value in the source code or this tutorial, or one of the data tables that TALYS uses. One simply multiplies the nominal value with the value given on this keyword line without having to know the actual value.

rcadjust

Multiplier to adjust the OMP parameter rc of Eq. (10.7). On the input line, we read **rcadjust**, particle symbol, and value.

Examples

rcadjust d 1.15

Range

$0.1 \leq \textbf{rcadjust} \leq \textbf{10}$.

Default

rcadjust *particle* **1.**

Comments

- As a general comment for '**adjust**' keywords: this avoids having to look up the actual parameter value in the TALYS input file, hardwired default value in the source code or this tutorial, or one of the data tables that TALYS uses. One simply multiplies the nominal value with the value given on this keyword line without having to know the actual value.

dispersion

Flag to invoke the dispersive optical model, see Section 10.2. These potentials are only available as tabulated neutron local potentials. If not available, TALYS will automatically resort to normal OMP's.

Examples

dispersion n

Range

y or **n**

Default

dispersion n.

localomp

Flag to overrule the local, nucleus-specific optical model by the global optical model of Eqs. (10.8) or (10.9). This may be helpful to study global mass-dependent trends.

Examples

localomp n

Range

y or **n**

Default

localomp y, i.e. a nucleus-specific optical model, when available.

deuteronomp

Specific deuteron OMP. The default deuteron optical model coming from standard Watanabe folding does not always perform well. Therefore, we have included various other options:

Examples

deuteronomp 1: Normal deuteron potential [63]
deuteronomp 2: Deuteron potential of Daehnick et al. [65]
deuteronomp 3: Deuteron potential of Bojowald et al.[66]
deuteronomp 4: Deuteron potential of Han et al.[67]
deuteronomp 5: Deuteron potential of Haixia An et al.[68]

Range

$1 \leq$ **deuteronomp** ≤ 5

Default

deuteronomp 1

alphaomp

Specific alpha OMP.

Examples

alphaomp 1: Normal alpha potential[69]
alphaomp 2: Alpha potential of McFadden and Satchler
alphaomp 3: Alpha potential of Demetriou and Goriely [70], table 1.
alphaomp 4: Alpha potential of Demetriou and Goriely [70], table 2.
alphaomp 5: Alpha potential of Demetriou and Goriely [70], dispersive model.
alphaomp 6: Alpha potential of Avrigeanu et al. [72].
alphaomp 7: Alpha potential of Nolte et al. [148].
alphaomp 8: Alpha potential of Avrigeanu et al. [149].

Range

1 $\leq$ alphaomp $\leq$ 8

Default

alphaomp 6

aradialcor

Normalization factor for the shape of the double-folding alpha potential. This keyword is only relevant for **alphaomp** $\geq$ **3**. On the input line, we read **aradialcor** and value.

Examples

aradialcor 1.07

Range

$0.5 \leq$ **aradialcor** ≤ 1.5

Default

aradialcor 1.

adepthcor

Normalization factor for the depth of the double-folding alpha potential. This keyword is only relevant for **alphaomp** $\geq$ **3**. On the input line, we read **adepthcor** and value.

Examples

    adepthcor 1.07

Range

$0.5 \leq$ **adepthcor** ≤ 1.5

Default

adepthcor 1.

pruitt

Flag to use the OMP parameters of Pruitt et al. for the KD03 global OMP.

Examples

pruitt n

Range

y or **n**

Default

pruitt n, i.e. for the global OMP, the KD03 parameters are used.

pruittset

One of the random OMP parameter sample sets of Pruitt et al.

Examples

pruittset 181

Range

$0 \leq$ **pruittset** $\leq$ **416**

Default

pruittset 0, i.e use the average global OMP parameters.

jlmomp

Flag to use the JLM microscopic optical model potential instead of the phenomenological optical model potential, see Section 10.4.

Examples

jlmomp n

Range

y or **n**

Default

jlmomp n, i.e. to use the phenomenological OMP.

jlmmode

Keyword to enable different normalizations for the imaginary potential of the JLM optical model, as explained in Ref. [150] These different normalizations apply to the constant 0.44 in Eq. (10.47). This keyword is only active if 'jlmomp y'.

Examples

jlmmode 0: standard JLM imaginary potential of Eq. (10.47)
jlmmode 1: 0.44 replaced by $1.1 \exp(-0.4E^{1/2})$
jlmmode 2: 0.44 replaced by $1.25 \exp(-0.2E^{1/2})$
jlmmode 3: as jlmmode 2 but with $\lambda_W(E)$ twice as large, recommended for energies below 1 MeV.

Range

$0 \leq$ **jlmmode** ≤ 3

Default

jlmmode 0, i.e. the standard JLM OMP.

lvadjust

Normalization factor for the real central potential for JLM calculations, see Eq. (10.44). On the input line, we read **lvadjust** and value.

Examples

> **lvadjust 1.15**

Range

$0.5 \leq$ **lvadjust** ≤ 1.5

Default

lvadjust 1.

Comments

- As a general comment for '**adjust**' keywords: this avoids having to look up the actual parameter value in the TALYS input file, hardwired default value in the source code or this tutorial, or one of the data tables that TALYS uses. One simply multiplies the nominal value with the value given on this keyword line without having to know the actual value.

lwadjust

Normalization factor for the imaginary central potential for JLM calculations, see Eq. (10.45). On the input line, we read **lwadjust** and value.

Examples

lwadjust 1.15

Range

$0.5 \leq$ **lwadjust** ≤ 1.5

Default

lwadjust 1.

Comments

- As a general comment for '**adjust**' keywords: this avoids having to look up the actual parameter value in the TALYS input file, hardwired default value in the source code or this tutorial, or one of the data tables that TALYS uses. One simply multiplies the nominal value with the value given on this keyword line without having to know the actual value.

lv1adjust

Normalization factor for the real isovector potential for JLM calculations, see Eq. (10.46). On the input line, we read **lv1adjust** and value.

Examples

      lv1adjust 1.15

Range

$0.5 \leq$ **lv1adjust** ≤ 1.5

Default

lv1adjust 1.

Comments

- As a general comment for '**adjust**' keywords: this avoids having to look up the actual parameter value in the TALYS input file, hardwired default value in the source code or this tutorial, or one of the data tables that TALYS uses. One simply multiplies the nominal value with the value given on this keyword line without having to know the actual value.

lw1adjust

Normalization factor for the imaginary isovector potential for JLM calculations, see Eq. (10.47). On the input line, we read **lw1adjust** and value.

Examples

lw1adjust 1.15

Range

$0.5 \leq$ **lw1adjust** ≤ 1.5

Default

lw1adjust 1.

Comments

- As a general comment for '**adjust**' keywords: this avoids having to look up the actual parameter value in the TALYS input file, hardwired default value in the source code or this tutorial, or one of the data tables that TALYS uses. One simply multiplies the nominal value with the value given on this keyword line without having to know the actual value.

lvsoadjust

Normalization factor for the real spin-orbit potential for JLM calculations, see Eq. (10.50). On the input line, we read **lvsoadjust** and value.

Examples

    lvsoadjust 1.15

Range

$0.5 \leq$ **lvsoadjust** ≤ 1.5

Default

lvsoadjust 1.

Comments

- As a general comment for '**adjust**' keywords: this avoids having to look up the actual parameter value in the TALYS input file, hardwired default value in the source code or this tutorial, or one of the data tables that TALYS uses. One simply multiplies the nominal value with the value given on this keyword line without having to know the actual value.

lwsoadjust

Normalization factor for the imaginary spin-orbit potential for JLM calculations, see Eq. (10.51). On the input line, we read **lwsoadjust** and value.

Examples

lwsoadjust 1.15

Range

$0.5 \leq$ **lwsoadjust** ≤ 1.5

Default

lwsoadjust 1.

Comments

- As a general comment for '**adjust**' keywords: this avoids having to look up the actual parameter value in the TALYS input file, hardwired default value in the source code or this tutorial, or one of the data tables that TALYS uses. One simply multiplies the nominal value with the value given on this keyword line without having to know the actual value.

radialmodel

Model for radial matter densities in the JLM optical model. There are two options. This keyword is only active if 'jlmomp y'.

Examples

radialmodel 1: HFB-Skyrme based matter densities
radialmodel 2: HFB-Gogny based matter densities

Range

$1 \leq$ **radialmodel** ≤ 2

Default

radialmodel 2.

radialfile

File with radial matter densities. The format of the file is exactly the same as that of the nuclear structure database *talys/structure/optical/jlm/*. In practice, the user can copy a file from this database to the working directory and change it. In this way, changes in the "official" database are avoided. Note that even if only changes for one isotope are required, the entire file needs to be copied if for the other isotopes the originally tabulated values are to be used. On the input line, we read **radialfile**, *Z*, filename.

Examples

radialfile 26 Fe.loc

Range

radialfile can be equal to any filename, provided it starts with a character.

Default

If **radialfile** is not given in the input, radial matter densities are taken from *talys/structure/optical/jlm*.

Ejoin

Joining energy E_J, in MeV, between the original form of the KD03 OMP and its high-energy extension , see Eq. (10.18). On the input line, we read **Ejoin**, particle symbol, and value.

Examples

Ejoin n 250.

Range

$0. \leq$ **Ejoin** $\leq$ **1000.**.

Default

Ejoin 200.

Vinfadjust

Multiplier to adjust the OMP parameter V_∞ for the real volume potential of Eq. (10.18). On the input line, we read **Vinfadjust**, particle symbol, and value.

Examples

Vinfadjust n 1.10

Range

$0.01 \leq$ **Vinfadjust** $\leq$ **10**.

Default

Vinfadjust *particle* **1.**

Comments

- This keyword can only be used for the high-energy extension of the KD03 form.
- As a general comment for '**adjust**' keywords: this avoids having to look up the actual parameter value in the TALYS input file, hardwired default value in the source code or this tutorial, or one of the data tables that TALYS uses. One simply multiplies the nominal value with the value given on this keyword line without having to know the actual value.

incadjust

Flag to use adjusted optical model parameters for the incident channel *and* exit channels. Disabling this flag allows to use a different OMP for the exit channels than for the incident channel, e.g. using **rvadjust n 1.10** together with **incadjust n** means that the OMP for the incident channel is unaltered, while that for the outgoing channel has an adjust r_V parameter. This can be used to simulate e.g. temperature-dependent OMP effects.

Examples

incadjust n

Range

y or **n**

Default

incadjust y

omponly

Flag to let TALYS perform *only* an optical model calculation. In this way, TALYS acts simply as a driver for ECIS. All non-elastic calculations for the various reaction channels are skipped. This is helpful for systematic, and quick, testing of optical model potentials.

Examples

- **omponly n**
- **omponly y**

Range

y or **n**

Default

omponly n

optmod

File with tabulated phenomenological optical model parameters as a function of energy, see Section 10. This can be helpful if one wishes to use an optical model parameterisation which is not hardwired in TALYS. One could write a driver to automatically generate a table with parameters. On the input line, we read **optmod**, *Z*, *A*, filename, and (optionally) particle type. From the file, TALYS first reads Z, A, and the number of lines to be read with format (3i4). Next, from each line of the file, TALYS reads *E*, *v*, *rv*, *av*, *w*, *rw*, *aw*, *vd*, *rvd*, *avd*, *wd*, *rwd*, *awd*, *vso*, *rvso*, *avso*, *wso*, *rwso*, *awso*, and *rc* in free format.

Examples

optmod 40 90 ompzr90 d
optmod 94 239 omppu239

Range

optmod can be equal to any filename, provided it starts with a character. The particle type must be equal to either **n, p, d, t, h** or **a**. A table of up to **numomp** incident energies (this is set in a module or the input) and associated parameters can be specified.

Default

If the particle type is not given, as in the second example above, neutrons are assumed. If **optmod** is not given in the input file, the optical model parameters are taken from the *talys/structure/optical* database per nucleus or, if not present there, from the global optical model.

optmodfileN

File with the neutron optical model parameters of Eq. (10.7). The format of the file is exactly the same as that of the nuclear structure database *talys/structure/optical/neutron/*. In practice, the user can copy a file from this database, e.g. *n-Fe.omp*, to the working directory and change it. In this way, changes in the "official" database are avoided. Note that even if only changes for one isotope are required, the file for the whole element needs to be copied if for the other isotopes the originally tabulated values are to be used. On the input line, we read **optmodfileN**, *Z*, filename.

Examples

optmodfileN 26 Fe.loc

Range

optmodfileN can be equal to any filename, provided it starts with a character, which should be present in the working directory.

Default

If **optmodfileN** is not given in the input file, the optical model parameters are taken from the *talys/structure/optical/neutron/* database per nucleus or, if not present there, from the global optical model.

optmodfileP

File with the proton optical model parameters of Eq. (10.7). The format of the file is exactly the same as that of the nuclear structure database *talys/structure/optical/proton/*. In practice, the user can copy a file from this database, e.g. *p-Fe.omp*, to the working directory and change it. In this way, changes in the "official" database are avoided. Note that even if only changes for one isotope are required, the file for the whole element needs to be copied if for the other isotopes the originally tabulated values are to be used. On the input line, we read **optmodfileP**, Z, filename.

Examples

      optmodfileP 26 Fe.loc

Range

optmodfileP can be equal to any filename, provided it starts with a character, which should be present in the working directory.

Default

If **optmodfileP** is not given in the input file, the optical model parameters are taken from the *talys/structure/optical/proton/* database per nucleus or, if not present there, from the global optical model.

optmodall

Flag for a new optical model calculation for each compound nucleus in the decay chain. In usual multiple Hauser-Feshbach decay, the transmission coefficients for the first compound nucleus are used for the whole decay chain. When a residual nucleus is far away from the initial compound nucleus, this approximation may become dubious. With **optmodall y**, new optical model calculations are performed for every compound nucleus that is depleted, for all types of emitted particles.

Examples

optmodall y

Range

y or **n**

Default

optmodall n

outomp

Flag for the output of optical model parameters for each particle and energy.

Examples

outomp y
outomp n

Range

y or **n**

Default

the same value as **outbasic**: **outomp n**

outkd

Flag for the output of KD03 OMP parameters for each particle and energy.

Examples

outkd y
outkd n

Range

y or **n**

Default

outkd n

soukho

Flag for the use of Soukhovitskii OMP for actinides instead of KD03.

Examples

> **soukho y**
> **soukho n**

Range

y or **n**

Default

soukho y

Comments

This is currently overruled by RIPL OMP.

riplomp

RIPL OMP number for particle. On the input line, we read **riplomp**, particle type, RIPL OMP number.

Examples

riplomp n 2408
riplomp n 2413

Range

riplomp should exist as a RIPL OMP number.

Default

riplomp is only used as default for incident neutrons on actinides, in which case **riplomp n 2408**.

riplrisk

Flag for using the RIPL OMP outside the specified mass range.

Examples

riplrisk y
riplrisk n

Range

y or **n**

Default

riplrisk n

rvadjustF

Energy-dependent function to adjust the OMP parameter r_V. If physically adequate OMPs fail, such energy-dependent adjustment can be invoked as a last resort. As long as the deviation from the original model is not too large, unpleasant surprises in the various reaction channels are avoided. On the input line, we read **rvadjustF**, particle symbol, begin energy E_b and end energy E_e in MeV, maximal deviation D in % , and variance σ in MeV, of the function. If this keyword is specified, r_V will keep its original constant value for $E < E_b$ and $E > E_e$ while in between these two values if will be multiplied by the function

$$f(E) = 1 + D\exp(-(E - E_m)^2/2\sigma^2) + R \tag{27.1}$$

where $E_m = (E_e + E_b)/2$ and the offset value

$$R = -D\exp(-(E_e - E_m)^2/2\sigma^2) \tag{27.2}$$

ensures continuity at E_b and E_e. Fig. 27.1 shows an example for r_V with an original value of 1.20, which is locally multiplied by the function f with parameters E_b=2, E_e=10, $D = 5$, $\sigma = 2$. Up to 10 energy ranges, i.e. **rvadjustF** keywords, per particle can be used. We suggest however that the keyword **rvadjustF** is now replaced by the method explained in Section 3.2.1 for all parameters. We keep **rvadjustF** and related OMP keywords for backward compat

Examples

    rvadjustF n 2. 10. 5. 2.

Range

The particle symbol should be equal to n, p, d, t, h or a, $\mathbf{0 \leq E_b \leq 250}$, $\mathbf{0 \leq E_e \leq 250}$, $\mathbf{E_b < E_e}$, $\mathbf{-100 \leq D \leq 100}$, $\mathbf{0 \leq \sigma \leq 100}$. If $\sigma = 0$, then the value $\sigma = (E_e - E_m)/2$ will be adopted.

Default

rvadjustF is not applied.
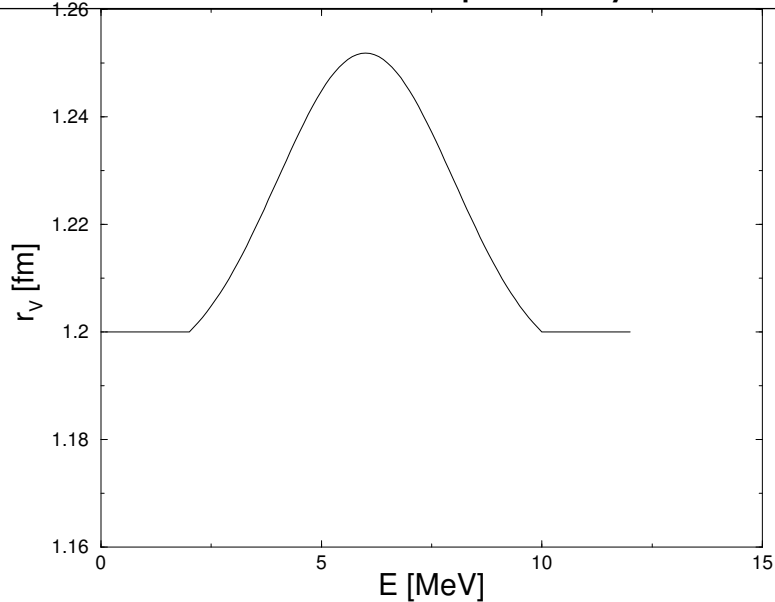
Figure 27.1: Energy-dependent radius r_V obtained with the **rvadjustF** keyword

avadjustF

Energy-dependent function to adjust the OMP parameter a_V. On the input line, we read **avadjustF**, particle symbol, begin energy E_b and end energy E_e in MeV, maximal deviation D in % , and variance σ in MeV, of the function. The same formalism as explained for the **rvadjustF** keyword applies.

Examples

   avadjustF n 2. 10. 5. 2.

Range

See **rvadjustF** keyword.

Default

avadjustF is not applied.

rwadjustF

Energy-dependent function to adjust the OMP parameter a_V. On the input line, we read **rwadjustF**, particle symbol, begin energy E_b and end energy E_e in MeV, maximal deviation D in % , and variance σ in MeV, of the function. The same formalism as explained for the **rvadjustF** keyword applies.

Examples

rwadjustF n 2. 10. 5. 2.

Range

See **rvadjustF** keyword.

Default

rwadjustF is not applied.

awadjustF

Energy-dependent function to adjust the OMP parameter a_V. On the input line, we read **awadjustF**, particle symbol, begin energy E_b and end energy E_e in MeV, maximal deviation D in % , and variance σ in MeV, of the function. The same formalism as explained for the **rvadjustF** keyword applies.

Examples

     awadjustF n 2. 10. 5. 2.

Range

See **rvadjustF** keyword.

Default

awadjustF is not applied.

rvdadjustF

Energy-dependent function to adjust the OMP parameter rvd. On the input line, we read **rvdadjustF**, particle symbol, begin energy E_b and end energy E_e in MeV, maximal deviation D in % , and variance σ in MeV, of the function. The same formalism as explained for the **rvadjustF** keyword applies.

Examples

rvdadjustF n 2. 10. 5. 2.

Range

See **rvadjustF** keyword.

Default

rvdadjustF is not applied.

avdadjustF

Energy-dependent function to adjust the OMP parameter avd. On the input line, we read **avdadjustF**, particle symbol, begin energy E_b and end energy E_e in MeV, maximal deviation D in % , and variance σ in MeV, of the function. The same formalism as explained for the **rvadjustF** keyword applies.

Examples

    avdadjustF n 2. 10. 5. 2.

Range

See **rvadjustF** keyword.

Default

avdadjustF is not applied.

rwdadjustF

Energy-dependent function to adjust the OMP parameter rwd. On the input line, we read **rwdadjustF**, particle symbol, begin energy E_b and end energy E_e in MeV, maximal deviation D in % , and variance σ in MeV, of the function. The same formalism as explained for the **rvadjustF** keyword applies.

Examples

  rwdadjustF n 2. 10. 5. 2.

Range

See **rvadjustF** keyword.

Default

rwdadjustF is not applied.

awdadjustF

Energy-dependent function to adjust the OMP parameter awd. On the input line, we read **awdadjustF**, particle symbol, begin energy E_b and end energy E_e in MeV, maximal deviation D in % , and variance σ in MeV, of the function. The same formalism as explained for the **rvadjustF** keyword applies.

Examples

awdadjustF n 2. 10. 5. 2.

Range

See **rvadjustF** keyword.

Default

awdadjustF is not applied.

rvsoadjustF

Energy-dependent function to adjust the OMP parameter rvso. On the input line, we read **rvsoadjustF**, particle symbol, begin energy E_b and end energy E_e in MeV, maximal deviation D in % , and variance σ in MeV, of the function. The same formalism as explained for the **rvadjustF** keyword applies.

Examples

rvsoadjustF n 2. 10. 5. 2.

Range

See **rvadjustF** keyword.

Default

rvsoadjustF is not applied.

avsoadjustF

Energy-dependent function to adjust the OMP parameter avso. On the input line, we read **avsoadjustF**, particle symbol, begin energy E_b and end energy E_e in MeV, maximal deviation D in % , and variance σ in MeV, of the function. The same formalism as explained for the **rvadjustF** keyword applies.

Examples

> **avsoadjustF n 2. 10. 5. 2.**

Range

See **rvadjustF** keyword.

Default

avsoadjustF is not applied.

rwsoadjustF

Energy-dependent function to adjust the OMP parameter rwso. On the input line, we read **rwsoadjustF**, particle symbol, begin energy E_b and end energy E_e in MeV, maximal deviation D in % , and variance σ in MeV, of the function. The same formalism as explained for the **rvadjustF** keyword applies.

Examples

rwsoadjustF n 2. 10. 5. 2.

Range

See **rvadjustF** keyword.

Default

rwsoadjustF is not applied.

awsoadjustF

Energy-dependent function to adjust the OMP parameter awso. On the input line, we read **awsoadjustF**, particle symbol, begin energy E_b and end energy E_e in MeV, maximal deviation D in % , and variance σ in MeV, of the function. The same formalism as explained for the **rvadjustF** keyword applies.

Examples

    awsoadjustF n 2. 10. 5. 2.

Range

See **rvadjustF** keyword.

Default

awsoadjustF is not applied.

28. Keywords for direct reactions and ECIS

spherical

Flag to enforce a spherical OMP calculation, regardless of the availability of a deformed OMP and a coupling scheme. Direct inelastic scattering will then be treated by DWBA.

Examples

spherical n

Range

y or **n**

Default

spherical n

rotational

Flag to enable or disable the rotational optical model for the various particles appearing in the calculation. This flag is to enable or disable coupled-channels calculations for the inverse channels provided a coupling scheme is given in the deformation database. Using no rotational model at all can be set with another keyword: **spherical y**.

Examples

rotational n
rotational n p a

Range

rotational can be any combination of **n, p, d, t, h** and **a**

Default

rotational n p. Warning: setting e.g. **rotational a** will thus automatically disable the default setting. If this needs to be retained as well, set **rotational n p a**

Tjadjust

Multiplier to adjust the OMP transmission coefficient per l-value. On the input line, we read **Tjadjust**, particle symbol, value and l-value.

Examples

Tjadjust n 0.80 0

Range

$0.001 \leq$ **Tjadjust** ≤ 1000.

Default

Tjadjust *particle* **1.** *l-value*

Comments

- As a general comment for '**adjust**' keywords: this avoids having to look up the actual parameter value in the TALYS input file, hardwired default value in the source code or this tutorial, or one of the data tables that TALYS uses. One simply multiplies the nominal value with the value given on this keyword line without having to know the actual value.

sysreaction

The types of particles for which the optical model reaction cross section is overruled by values obtained from systematics, see Section 10.5. The optical model transmission coefficients will be accordingly normalized.

Examples

sysreaction p
sysreaction d a

Range

sysreaction can be any combination of **n, p, d, t, h** and **a**

Default

sysreaction is disabled for any particle.

ecissave

Flag for saving ECIS input and output files. This has two purposes: (a) if the next calculation will be performed with already existing reaction cross sections and transmission coefficients. This is helpful for time-consuming coupled-channels calculations, (b) to study the ECIS input and output files in detail. **ecissave** *must* be set to **y**, if in the next run **inccalc n** or **eciscalc n** will be used. If not, an appropriate error message will be given and TALYS stops.

Examples

ecissave y
ecissave n

Range

y or **n**

Default

ecissave n

Comments

- Suppose you want to study the effect of changing variables other than for the OMP in a calculation. Then it can be time consuming to repeat complicated coupled-channels calculations while you are only interested in changing e.g. a level density parameter. Then, in the first run you do

```
ecissave y
inccalc y    (the default)
eciscalc y    (the default)
```

while the next runs can all be done with

```
ecissave y
inccalc n
eciscalc n
```

which reads in the previously generated transmission coefficients, cross sections etc. from files.

eciscalc

Flag for the ECIS calculation of transmission coefficients and reaction cross sections for the inverse channels. If this calculation has already been performed in a previous run, and in that previous run **ecissave y** has been set, it may be helpful to put **eciscalc n**, which avoids a new calculation. This saves time, especially in the case of coupled-channels calculations. We stress that it is the responsibility of the user to ensure that the first run of a particular problem is done with **ecissave y**. You also have to make sure that the same energy grid for inverse channels is used.

Examples

eciscalc y
eciscalc n

Range

y or **n**

Default

eciscalc y

Comments

- Suppose you want to study the effect of changing variables other than for the OMP in a calculation. Then it can be time consuming to repeat complicated coupled-channels calculations while you are only interested in changing e.g. a level density parameter. Then, in the first run you do

```
ecissave y
inccalc y    (the default)
eciscalc y    (the default)
```

while the next runs can all be done with

```
ecissave y
inccalc n
eciscalc n
```

which reads in the previously generated transmission coefficients, cross sections etc. from files.

inccalc

Flag for the ECIS calculation of transmission coefficients and reaction cross sections for the incident channel. If this calculation has already been performed in a previous run, and in that previous run **ecissave y** has been set, it may be helpful to put **inccalc n**, which avoids a new ECIS calculation. This saves time, especially in the case of coupled-channels calculations. We stress that it is the responsibility of the user to ensure that the first run of a particular problem is done with **eciscalc y**. If not, an appropriate error message will be given and TALYS stops. You also have to make sure that the same grid of incident energies is used.

Examples

>   **inccalc y**
>   **inccalc n**

Range

y or **n**

Default

inccalc y

Comments

- Suppose you want to study the effect of changing variables other than for the OMP in a calculation. Then it can be time consuming to repeat complicated coupled-channels calculations while you are only interested in changing e.g. a level density parameter. Then, in the first run you do

```
ecissave y
inccalc y    (the default)
eciscalc y    (the default)
```

while the next runs can all be done with

```
ecissave y
inccalc n
eciscalc n
```

which reads in the previously generated transmission coefficients, cross sections etc. from files.

maxrot

Number of excited levels to be included in a rotational band of a deformed nucleus for coupled-channels calculations. For example, use **maxrot 4** if the $0^+ - 2^+ - 4^+ - 6^+ - 8^+$ states need to be included.

Examples

maxrot 4

Range

$0 \leq$ **maxrot** ≤ 10

Default

maxrot 2

maxband

Maximum number of vibrational bands added to the rotational coupling scheme, regardless of the number of bands specified in the deformation database.

Examples

maxband 4

Range

$0 \leq \mathbf{maxband} \leq 10$

Default

maxband 0

autorot

Flag for automatic rotational coupled-channels calculations, see Section 11.1, for $A > 150$. The discrete level database is scanned and an attempt is made to automatically identify the lowest rotational band. Deformation parameters are also read from the database so automated coupled-channels calculations can be performed. This option is possible for the rare earth and actinide region. Note that for all natural isotopes, the coupling scheme is already given in the *talys/structure/deformation* database.

Examples

autorot y

Range

y or **n**

Default

autorot n

outdirect

Flag for the output of the results from the direct reaction calculation of ECIS (DWBA, giant resonances and coupled-channels).

Examples

outdirect y
outdirect n

Range

y or **n**

Default

the same value as **outbasic**: **outdirect n**

outinverse

Flag for the output of particle transmission coefficients and inverse reaction cross sections.

Examples

outinverse y
outinverse n

Range

y or **n**

Default

the same value as **outbasic**: **outinverse n**

outecis

Flag for keeping the various ECIS output files produced during a TALYS run. This is mainly for diagnostic purposes.

Examples

outecis y
outecis n

Range

y or **n**

Default

outecis n

endfecis

Flag for the ECIS calculation of transmission coefficients and reaction cross sections for the ENDF-6 energy grid. If this calculation has already been performed in a previous run, it may be helpful to put **endfecis n**, which avoids a new calculation. This saves time, especially in the case of coupled-channels calculations. We stress that it is the responsibility of the user to ensure that the first run of a particular problem is done with **ecissave y** and **endfecis y**. If not, an appropriate error message will be given and TALYS stops.

Examples

endfecis y
endfecis n

Range

y or **n**

Default

endfecis y

giantresonance

Flag for the calculation of giant resonance contributions to the continuum part of the spectrum. The GMR, GQR, LEOR and HEOR are included.

Examples

giantresonance y
giantresonance n

Range

y or **n**

Default

giantresonance y for incident neutrons and protons, **giantresonance n** otherwise.

elwidth

Width of elastic peak in MeV. For comparison with experimental angle-integrated and double-differential spectra, it may be helpful to include the energy-broadened cross sections for discrete states in the high-energy tail of the spectra. **elwidth** is the width of the Gaussian spreading that takes care of this. **elwidth** is only active if **outspectra y** or if **ddxmode 1, 2** or **3**.

Examples

elwidth 0.2

Range

$1.e-6 \leq$ **elwidth** ≤ 100

Default

elwidth 0.5

outangle

Flag for the output of angular distributions for scattering to discrete states.

Examples

outangle y
outangle n

Range

y or **n**

Default

outangle n

outlegendre

Flag for the output of Legendre coefficients for the angular distributions for scattering to discrete states. **outlegendre** is only active if **outangle y**.

Examples

outlegendre y
outlegendre n

Range

y or **n**

Default

outlegendre n

outdiscrete

Flag for the output of cross sections to each individual discrete state. This is given for both the direct and the compound component.

Examples

outdiscrete y
outdiscrete n

Range

y or **n**

Default

the same value as **outbasic**: **outdiscrete n**

adddiscrete

Flag for the addition of energy-broadened non-elastic cross sections for discrete states to the continuum spectra. **adddiscrete** is only active if **outspectra y**.

Examples

adddiscrete y
adddiscrete n

Range

y or **n**

Default

adddiscrete y

addelastic

Flag for the addition of energy-broadened elastic cross sections to the continuum spectra. This case is treated separately from **adddiscrete**, since sometimes the elastic contribution is already subtracted from the experimental spectrum. **addelastic** is only active if **outspectra y**.

Examples

addelastic y
addelastic n

Range

y or **n**

Default

the same value as **adddiscrete**: **addelastic y**

coulomb

Flag for Coulomb excitation calculation with ECIS, to be used for incident charged particles.

Examples

coulomb y

Range

y or **n**

Default

coulomb y

cpang

Flag for compound angular distribution calculation for incident charged particles.

Examples

cpang y

Range

y or **n**

Default

cpang n

soswitch

Energy switch to on-set deformed spin-orbit calculation and sequential iterations in ECIS. For coupled-channels calculations on rotational nuclei, such a switch needs to be made. On the input line, we read **soswitch**, value.

Examples

soswitch 1.2

Range

$0.1 \leq$ **soswitch** ≤ 10.

Default

soswitch 3. MeV.

statepot

Flag for a different optical model parameterisation for each excited state in a DWBA or coupled-channels calculation. This may be appropriate if the emission energy of the ejectile, corresponding to a large excitation energy, differs considerably from the incident energy.

Examples

statepot y

Range

y or **n**

Default

statepot n

outtransenergy

Flag for the output of transmission coefficients sorted per energy (**y**) or per angular momentum (**n**). **outtransenergy** is only active if **outinverse y**.

Examples

outtransenergy y
outtransenergy n

Range

y or **n**

Default

outtransenergy y

deformfile

File with deformation parameters and coupling schemes. The format of the file is exactly the same as that of the nuclear structure database *talys/structure/deformation/*. In practice, the user can copy a file from this database, e.g. *Fe.def*, to the working directory and change it. In this way, changes in the "official" database are avoided. Note that even if only changes for one isotope are required, the entire file needs to be copied if for the other isotopes the originally tabulated values are to be used. On the input line, we read **deformfile**, Z, filename.

Examples

   deformfile 26 Fe.loc

Range

deformfile can be equal to any filename, provided it starts with a character.

Default

If **deformfile** is not given in the input file, discrete levels are taken from *talys/structure/deformation*.

core

Integer to denote the even-even core for the weak-coupling model for direct scattering of odd-*A* nuclei. A value of -1 means the even-even core is determined by subtracting a nucleon from the target nucleus, while a value of +1 means a nucleon is added.

Examples

core 1

Range

-1 or **1**

Default

core -1

29. Keywords for compound nucleus

compound

Flag for compound nucleus calculation. This keyword can be used to disable compound nucleus evaporation if one is for example only interested in high-energy pre-equilibrium spectra.

Examples

compound y
compound n

Range

y or **n**

Default

compound y

widthfluc

Enabling or disabling width fluctuation corrections (WFC) in compound nucleus calculations, see Section 13.2. For **widthfluc**, the user has 3 possibilities: **y**, **n** or a value for the energy above which WFC's are disabled. The latter option is helpful in the case of a calculation with several incident energies. Then, the user may want to set the width fluctuation off as soon as the incident energy is high enough, in order to save computing time. We have taken care of this by the default, **widthfluc=S**, where S is the projectile separation energy (~ 8 MeV), of the target nucleus. This default is rather safe, since in practice width fluctuation corrections are already negligible for incident energies above a few MeV, because the presence of many open channels reduces the correction to practically zero, i.e. the WFC factors to 1. Note that the disabling of width fluctuations for *any* incident energy can be accomplished by **widthfluc n**, which is equivalent to **widthfluc 0.** or any other energy lower than the (lowest) incident energy. Similarly, **widthfluc y**, equivalent to **widthfluc 20.**, will activate width fluctuations for any incident energy. To avoid numerical problems, width fluctuations are never calculated for incident energies beyond 20 MeV.

Examples

> **widthfluc y**
> **widthfluc n**
> **widthfluc 4.5**

Range

y or **n** or $\mathbf{0. \leq}$ **widthfluc** $< \mathbf{20.}$

Default

widthfluc is equal to the projectile separation energy S, i.e. width fluctuation corrections are only used for incident energies below this value.

widthmode

Model for width fluctuation corrections in compound nucleus calculations, see Section 13.2.

Examples

    widthmode 0: no width fluctuation, i.e. pure Hauser-Feshbach model
    widthmode 1: Moldauer model
    widthmode 2: Hofmann-Richert-Tepel-Weidenmüller model
    widthmode 3: GOE triple integral model

Range

$0 \leq$ **widthmode** ≤ 3

Default

widthmode 1

resonance

Flag for variation of resonance parameters for an ENDF-6 general purpose file, by making a system call to the resonance code TARES.

(Only relevant if **#tmc y**.)

Examples

#resonance n
#resonance y

Range

y or **n**

Default

#resonance y

urr

Flag for the output of unresolved resonance parameters (URR). Since a full compound nucleus model and all its parameters are included in TALYS, it is only a small step to produce the URR parameters in the output. All calculated parameters, per incident energy, are stored in the file *urr.dat*. Energy-dependent tables can be found in the files *urrspacinglj.lLL*, with LL the orbital angular momentum in (i2.2) format, for the l,j-dependent neutron spacing, *urrneustrengthl.l00* for the l-dependent neutron spacing, *urrneuwidth.lLL* for the neutron width, *urrgamwidth.lLL* for the gamma width, *urrfiswidth.lLL* for the fission width, and *urrcomwidth.lLL* for the competitive width, These can be used for evaluated nuclear data files.

Examples

   urr y
   urr n
   urr 8.

Range

y or **n** or energy on-set value in MeV.

Default

urr y

lurr

Maximum orbital angular momentum taken into account for URR calculations. This keyword is only active if **urr y**.

Examples

lurr 1
lurr 4

Range

$0 \leq$ **lurr** $\leq$ **numl**, where *numl* is specified in *talys.cmb* (currently lurr=60).

Default

lurr 2

urrnjoy

Flag for normalization of URR parameters with NJOY method. This keyword is only active if
urr y. In addition to the files mentioned under the **urr** keyword, a few other files are produced:
urrtalys.tot, the cross sections as calculated with the TALYS URR parameters, *urrnjoy.tot*, the cross
sections as calculated with the NJOY URR method, and *urrratio.tot*, containing the ratio between
the aforementioned two.

Examples

    urrnjoy y
    urrnjoy n

Range

y or **n**

Default

urrnjoy y

fullhf

Flag for Hauser-Feshbach calculation using the full j,l coupling. This keyword can be used to enable/disable the loop over total angular momentum of the ejectile j' in Eq. (13.2). If **fullhf n**, the transmission coefficients are averaged over j, reducing the calculation time of the full Hauser-Feshbach model. In practice, the difference with the results from the full calculation is negligible.

Examples

fullhf y
fullhf n

Range

y or **n**

Default

fullhf n

WFCfactor

Model for systematics of the number of degrees of freedom for width fluctuation corrections, see Section 13.2.

Examples

> **WFCfactor 1:** original Moldauer prescription
> **WFCfactor 2:** Ernebjerg and Herman
> **WFCfactor 3:** Kawano

Range

$1 \leq$ **WFCfactor** ≤ 3

Default

WFCfactor 1

eciscompound

Flag for compound nucleus calculation by ECIS-06, done in parallel with TALYS. This keyword is used for checking purposes only and does not influence the TALYS results. An ECIS input file is created that contains the same discrete levels, level density parameters etc., as the TALYS calculation. The compound nucleus results given by ECIS can be compared with the results from TALYS, but are not used in TALYS. The results are written on a separate ECIS output file.

Examples

eciscompound y
eciscompound n

Range

y or **n**

Default

eciscompound n

group

Flag for processing pointwise resonance cross sections into energy groups. This keyword is only relevant if **resonance y**.

Examples

> **group y**
> **group n**

Range

y or **n**

Default

group n

reslib

Choice for the source of the resonance parameters. This keyword is only relevant if **resonance y**.

Examples

reslib default
reslib endfb7.1
reslib jendl4.0
reslib jeff3.2

Range

One of the 4 choices listed above.

Default

reslib default

Tres

Temperature, in Kelvin, for the broadening of resonances. This keyword is only relevant if
resonance y.

Examples

Tres 600.
Tres 0.

Range

0. < **Tres** < **1.e12**

Default

Tres 293.16

skipCN

Flag to skip the decay of a compound nucleus altogether. In this way, for example (n,γn) reactions can be skipped. Furthermore, the flag can be used for debugging purposes or other te

Examples

skipCN 40 91
skipCN 92 239

Range

skipCN Z A.

Default

skipCN not used.

xscaptherm

The thermal capture cross section in millibarn. By default, these are read from the nuclear structure database or taken from systematics. The **xscaptherm** keyword gives the possibility to overwrite this by using the input file.

Examples

    xscaptherm 320.2

Range

$10^{-20} \leq$ **xscaptherm** $\leq 10^{10}$

Default

xscaptherm is read from the nuclear structure database or taken from systematics.

xsalphatherm

The thermal (n, α) cross section in millibarn. By default, these are read from the nuclear structure database or taken from systematics. The **xsalphatherm** keyword gives the possibility to overwrite this by using the input file.

Examples

    xsalphatherm 0.2

Range

$10^{-20} \leq \text{xsalphatherm} \leq 10^{10}$

Default

xsalphatherm is read from the nuclear structure database or taken from systematics.

xsptherm

The thermal (n,p) cross section in millibarn. By default, these are read from the nuclear structure database or taken from systematics. The **xsptherm** keyword gives the possibility to overwrite this by using the input file.

Examples

> **xsptherm 0.2**

Range

$10^{-20} \leq \text{xsptherm} \leq 10^{10}$

Default

xsptherm is read from the nuclear structure database or taken from systematics.

rpevap

Flag to enable evaporation at very high excitation energies by looping over excited residual products.

Examples

rpevap y
rpevap n

Range

y or **n**

Default

rpevap n

30. Keywords for pre-equilibrium reactions

preequilibrium

Enabling or disabling the pre-equilibrium reaction mechanism. For **preequilibrium**, the user has 3 possibilities: **y**, **n** or a value for the starting energy. The latter option is helpful in the case of a calculation with several incident energies. Then, the user may want to set pre-equilibrium contributions on as soon as the incident energy is high enough. We have taken care of this by the default, **preequilibrium=Ex(Nm)**, where Ex(Nm) is the excitation energy of the last discrete level Nm of the target nucleus. This default is very safe, since in practice the pre-equilibrium contribution becomes only sizable for incident energies several MeV higher than Ex(Nm). Note that the disabling of pre-equilibrium for *any* incident energy can be accomplished by **preequilibrium n**. Similarly, **preequilibrium y**, equivalent to **preequilibrium 0.**, will enable pre-equilibrium for any incident energy.

Examples

> **preequilibrium y**
> **preequilibrium n**
> **preequilibrium 4.5**

Range

y or **n** or $0. \leq$ **preequilibrium** $< 250.$

Default

preequilibrium is equal to Ex(NL), i.e. pre-equilibrium calculations are included for incident energies above the energy of the last discrete level of the target nucleus.

preeqmode

Model for pre-equilibrium reactions. There are four possibilities, see Section 12.

Examples

preeqmode 1: Exciton model: Analytical transition rates with energy-dependent matrix element.

preeqmode 2: Exciton model: Numerical transition rates with energy-dependent matrix element.

preeqmode 3: Exciton model: Numerical transition rates with optical model for collision probability.

preeqmode 4: Multi-step direct/compound model

Range

$1 \leq$ **preeqmode** ≤ 4

Default

preeqmode 2

multipreeq

Enabling or disabling multiple pre-equilibrium reaction mechanism. For **multipreeq**, the user has 3 possibilities: **y**, **n** or a value for the starting energy. The latter option is helpful in the case of a calculation with several incident energies. Then, the user may want to set multiple pre-equilibrium contributions on as soon as the incident energy is high enough. We have taken care of this by the default, **multipreeq 20.**. This default is very safe, since in practice the multiple pre-equilibrium contribution becomes only sizable for incident energies a few tens of MeV higher than the default. Note that the disabling of multiple pre-equilibrium for *any* incident energy can be accomplished by **multipreeq n**. Similarly, **multipreeq y**, equivalent to **multipreeq 0.**, will activate multiple pre-equilibrium for any incident energy.

Examples

> **multipreeq y**
> **multipreeq n**
> **multipreeq 40.**

Range

y or **n** or $0. \leq$ **multipreeq** $< 250.$

Default

multipreeq 20., i.e. multiple pre-equilibrium calculations are included for incident energies above this value. TALYS always sets **multipreeq n** if **preequilibrium n**.

mpreeqmode

Model for multiple pre-equilibrium reactions. There are two possibilities, see Section 14.2 for an explanation.

Examples

mpreeqmode 1: Multiple exciton model
mpreeqmode 2: Transmission coefficient method

Range

$1 \leq$ **mpreeqmode** ≤ 2

Default

mpreeqmode 2

preeqspin

Flag to use the pre-equilibrium or compound nucleus spin distribution for the pre-equilibrium population of the residual nuclides. For backward-compatibility with earlier versions of TALYS, the following options are now possible:

Examples

preeqspin n or **preeqspin 1**: the pre-equilibrium spin distribution is made equal to the relative spin-dependent population after compound nucleus emission
preeqspin 2: the spin distribution from total level densities is adopted
preeqspin y or **preeqspin 3**: the pre-equilibrium spin distribution
preeqspin 4: spin distribution from Marc Dupuis: Microscopic description of target spin distribution after inelastic scattering to the continuum Marc Dupuis, Toshihiko Kawano, Maelle Kerveno, Stephane Hilaire EPJ Web of Conf. 284 03003 (2023) DOI: 10.1051/epj-conf/202328403003

Range

y or **n**, or $1 \leq$ **preeqspin** ≤ 4.

Default

preeqspin n

Rspincutpreeq

Global adjustable constant for spin cut-off parameter for particle-hole state density for pre-equilibrium reactions.

Examples

Rspincutpreeq 0.8

Range

0. $\leq$ Rspincutpreeq $\leq$ 10.

Default

Rspincutpreeq 1.

preeqsurface

Flag to use surface corrections in the exciton model.

Examples

preeqsurface y
preeqsurface n

Range

y or **n**

Default

preeqsurface y

outpreequilibrium

Flag for the output of pre-equilibrium parameters and cross sections. **outpreequilibrium** is only active if **preequilibrium y**.

Examples

outpreequilibrium y
outpreequilibrium n

Range

y or **n**

Default

outpreequilibrium n

Esurf

Effective well depth for surface effects in MeV in the exciton model, see Eq. (12.11).

Examples

Esurf 25.

Range

0. $\leq$ **Esurf** $\leq$ **Efermi**, where **Efermi** = 38 MeV is the Fermi well depth.

Default

Esurf is given by Eq. (12.11).

preeqcomplex

Flag to use the Kalbach model for pickup, stripping and knockout reactions, in addition to the exciton model, in the pre-equilibrium region.

Examples

preeqcomplex y
preeqcomplex n

Range

y or **n**

Default

preeqcomplex y

twocomponent

Flag to use the two-component (y) or one-component (n) exciton model.

Examples

twocomponent y
twocomponent n

Range

y or **n**

Default

twocomponent y

pairmodel

Model for pairing correction for pre-equilibrium model.

Examples

pairmodel 1: Fu's pairing energy correction, see Eq. (12.5).
pairmodel 2: Compound nucleus pairing correction

Range

$1 \leq$ **pairmodel** ≤ 2

Default

pairmodel 1

phmodel

Model for particle-hole state densities. There are two possibilities.

Examples

phmodel 1: Phenomenological particle-hole state densities
phmodel 2: Microscopic particle-hole state densities

Range

$1 \leq$ **phmodel** ≤ 2

Default

phmodel 1

Kph

Value for the constant of the single-particle level density parameter, i.e. $g = A/K_{ph}$, or $g_\pi = Z/K_{ph}$ and $g_\nu = N/K_{ph}$

Examples

Kph 12.5

Range

1. $\leq$ **Kph** $\leq$ **100.**

Default

Kph 15.

g

The single-particle level density parameter **g** in MeV^{-1}. On the input line, we read **g**, Z, A, value.

Examples

g 41 93 7.15
g 94 239 17.5

Range

$0.1 \leq \textbf{g} \leq 100.$

Default

$g = A/Kph$

gp

The single-particle proton level density parameter g_π in MeV^{-1}. On the input line, we read **gp**, Z, A, value.

Examples

gp 41 93 3.15
gp 94 239 7.2

Range

$0.1 \leq \text{gp} \leq 100.$

Default

$gp = Z/Kph$

gn

The single-particle neutron level density parameter g_v in MeV^{-1}. On the input line, we read **gn**, Z, A, value.

Examples

gn 41 93 4.1
gn 94 239 11.021

Range

$0.1 \leq$ **gn** $\leq$ **100.**

Default

$gn = N/Kph$

gpadjust

Multiplier to adjust the partial level density parameter g_π. On the input line, we read **gpadjust**, Z, A and value.

Examples

gpadjust 41 93 1.04

Range

$0.5 \leq$ **gpadjust** ≤ 2.

Default

gpadjust $Z\,A$ **1.**

Comments

- As a general comment for '**adjust**' keywords: this avoids having to look up the actual parameter value in the TALYS input file, hardwired default value in the source code or this tutorial, or one of the data tables that TALYS uses. One simply multiplies the nominal value with the value given on this keyword line without having to know the actual value.

gnadjust

Multiplier to adjust the partial level density parameter g_v. On the input line, we read **gnadjust**, Z, A and value.

Examples

   gnadjust 41 93 1.04

Range

$0.5 \leq$ **gnadjust** ≤ 2.

Default

gnadjust $Z A$ **1.**

Comments

- As a general comment for '**adjust**' keywords: this avoids having to look up the actual parameter value in the TALYS input file, hardwired default value in the source code or this tutorial, or one of the data tables that TALYS uses. One simply multiplies the nominal value with the value given on this keyword line without having to know the actual value.

gadjust

Multiplier to adjust the partial level density parameter g. On the input line, we read **gadjust**, Z, A and value.

Examples

gadjust 41 93 1.04

Range

$0.5 \leq$ **gadjust** ≤ 2.

Default

gadjust $Z\,A$ **1.**

Comments

- As a general comment for '**adjust**' keywords: this avoids having to look up the actual parameter value in the TALYS input file, hardwired default value in the source code or this tutorial, or one of the data tables that TALYS uses. One simply multiplies the nominal value with the value given on this keyword line without having to know the actual value.

gshell

Flag to include the damping of shell effects with excitation energy in single-particle level densities. The Ignatyuk parameterisation for total level densities is also applied to the single-particle level density parameters.

Examples

gshell y
gshell n

Range

y or **n**

Default

gshell n

M2constant

Overall constant for the matrix element, or the optical model strength, in the exciton model. The parameterisation of the matrix element is given by Eq. (12.46) for the one-component model, and by Eq. (12.26) for the two-component model. **M2constant** is also used to scale the MSD cross section (preeqmode 4).

Examples

M2constant 1.22

Range

$0. \leq$ **M2constant** $\leq$ **100**.

Default

M2constant 1.

M2limit

Constant to scale the asymptotic value of the matrix element in the exciton model. The parameterisation of the matrix element is given by Eq. (12.46) for the one-component model, and by Eq. (12.26) for the two-component model.

Examples

M2limit 1.22

Range

$0. \leq$ **M2limit** $\leq$ **100**.

Default

M2limit 1.

M2shift

Constant to scale the energy shift of the matrix element in the exciton model. The parameterisation of the matrix element is given by Eq. (12.46) for the one-component model, and by Eq. (12.26) for the two-component model.

Examples

M2shift 1.22

Range

$0. \leq$ **M2shift** $\leq$ **100**.

Default

M2shift 1.

Rnunu

Neutron-neutron ratio for the matrix element in the two-component exciton model, see Eq. (12.24).

Examples

Rnunu 1.6

Range

$0. \leq \textbf{Rnunu} \leq 100$.

Default

Rnunu 1.5

Rnupi

Neutron-proton ratio for the matrix element in the two-component exciton model, see Eq. (12.24).

Examples

Rnupi 1.6

Range

$0. \leq$ **Rnupi** ≤ 100.

Default

Rnupi 1.

Rpipi

Proton-proton ratio for the matrix element in the two-component exciton model, see Eq. (12.24).

Examples

Rpipi 1.6

Range

$0. \leq$ **Rpipi** $\leq$ **100**.

Default

Rpipi 1.

Rpinu

Proton-neutron ratio for the matrix element in the two-component exciton model, see Eq. (12.24).

Examples

Rpinu 1.6

Range

$0. \leq$ **Rpinu** ≤ 100.

Default

Rpinu 1.

Rgamma

Adjustable parameter for pre-equilibrium gamma decay.

Examples

  Rgamma 1.22

Range

0. $\leq$ **Rgamma** $\leq$ **100**.

Default

Rgamma 2.

Cstrip

Adjustable parameter for the stripping or pick-up process, to scale the complex-particle pre-equilibrium cross section per outgoing particle, see Section 12.4. On the input line, we read **Cstrip**, particle symbol, and value.

Examples

Cstrip d 1.3
Cstrip a 0.4

Range

$0. \leq$ **Cstrip** $\leq$ **10**.

Default

Cstrip 1.

Cknock

Adjustable parameter for the knock-out process, to scale the complex-particle pre-equilibrium cross section per outgoing particle, see Section 12.4. In practice, for nucleon-induced reactions this parameter affects only alpha-particles. This parameter is however also used as scaling factor for break-up reactions (such as (d,p) and (d,n)). On the input line, we read **Cknock**, particle symbol, and value.

Examples

Cknock a 0.4

Range

$0. \leq$ **Cknock** $\leq$ **10**.

Default

Cknock 1.

Cbreak

Adjustable parameter for the break-up process, to scale the complex-particle pre-equilibrium cross section per outgoing particle, see Section 12.4. On the input line, we read **Cbreak**, particle symbol, and value.

Examples

Cbreak d 1.3
Cbreak a 0.4

Range

$0. \leq$ **Cbreak** $\leq$ **10**.

Default

Cbreak 1.

breakupmodel

Model for break-up reactions.

Examples

> **breakupmodel 1**: Kalbach model
> **breakupmodel 2**: Avrigeanu model

Range

$1 \leq$ **breakupmodel** ≤ 2

Default

breakupmodel 1

ecisdwba

Flag for DWBA calculations for multi-step direct calculations. If this calculation has already been performed in a previous run, it may be helpful to put **ecisdwba n**, which avoids a new calculation and thus saves time. We stress that it is the responsibility of the user to ensure that the first run of a particular problem is done with **ecisdwba y**. If not, an appropriate error message will be given and TALYS stops.

Examples

ecisdwba y
ecisdwba n

Range

y or **n**

Default

ecisdwba y

outdwba

Flag for the output of DWBA cross sections for the multi-step direct model.

Examples

outdwba y
outdwba n

Range

y or **n**

Default

outdwba n

onestep

Flag for inclusion of *only* the one-step direct contribution in the continuum multi-step direct model. This is generally enough for incident energies up to about 14 MeV, and thus saves computing time.

Examples

onestep y
onestep n

Range

y or **n**

Default

onestep n

msdbins

The number of emission energy points for the DWBA calculation for the multi-step direct model.

Examples

msdbins 8

Range

$2 \leq$ **msdbins** $\leq$ **numenmsd/2-1**, where **numenmsd** is specified in the file *talys.cmb*. Currently, **numenmsd=18**

Default

msdbins 6

Emsdmin

The minimal emission energy in MeV for the multi-step direct calculation.

Examples

Emsdmin 8.

Range

$0. \leq$ **Emsdmin**

Default

Emsdmin is equal to **eninc/5.** where **eninc** is the incident energy.

31. Keywords for fission

fission

Flag for enabling or disabling fission. By default **fission** is enabled if the target mass is above 209. Hence, for lower masses, it is necessary to set **fission y** manually at high incident energies (subactinide fission).

Examples

fission y
fission n

Range

y or **n**. Fission is not allowed for $A \leq 56$

Default

fission y for $A > 209$, **fission n** for $A \leq 209$. The default enabling or disabling of fission is thus mass dependent.

fismodel

Model for fission barriers. **fismodel** is only active if **fission y**. There are 5 possibilities:

Examples

       fismodel 1: "experimental" fission barriers
       fismodel 2: theoretical fission barriers, Mamdouh table
       fismodel 3: theoretical fission barriers, Sierk model
       fismodel 4: theoretical fission barriers, rotating liquid drop
       fismodel 5: WKB approximation for fission path model

Range

$1 \leq$ **fismodel** ≤ 5

Default

fismodel 1

fismodelalt

"Back-up" model for fission barriers, for the case that the parameters of the tables used in **fismodel 1-2** are not available. There are two possibilities:

Examples

       fismodelalt 3 : theoretical fission barriers, Sierk model
       fismodelalt 4 : theoretical fission barriers, rotating liquid drop model

Range

$3 \leq$ **fismodelalt** ≤ 4

Default

fismodelalt 4

axtype

Type of axiality of the fission barrier. There are five options:

    1: axial symmetry
    2: left-right asymmetry
    3: triaxial and left-right asymmetry
    4: triaxial no left-right asymmetry
    5: no symmetry

On the input line, we read **axtype**, Z, A, value, fission barrier. If the number of the fission barrier is not given or is equal to 0, it concerns the first barrier.

Examples

    axtype 90 232 3
    axtype 94 239 1 2

Range

$1 \leq$ **axtype** ≤ 5

Default

axtype 2 for the second barrier and $N > 144$, **axtype 3** for the first barrier and $N > 144$, **axtype 1** for the rest.

fisbar

Fission barrier in MeV. On the input line, we read **fisbar**, *Z*, *A*, value, fission barrier. This keyword overrules the value given in the nuclear structure database. If the number of the fission barrier is not given or is equal to 0, it concerns the first barrier.

Examples

> **fisbar 90 232 5.6**
> **fisbar 94 239 6.1 2**

Range

$0. \leq$ **fisbar** $\leq$ **100.**

Default

fisbar is read from the *talys/structure/fission/* directory, or determined by systematics according to the choice of **fismodel**.

fishw

Fission barrier width in MeV. On the input line, we read **fishw**, *Z*, *A*, value, fission barrier. This keyword overrules the value given in the nuclear structure database. If the number of the fission barrier is not given or is equal to 0, it concerns the first barrier.

Examples

fishw 90 232 0.8
fishw 94 239 1.1 2

Range

$0.01 \leq$ **fishw** $\leq$ **10.**

Default

fishw is read from the *talys/structure/fission/* directory or determined by systematics, according to the choice of **fismodel**.

fisbaradjust

Normalisation factor for the fission barrier. This parameter can be used as a relative normalisation instead of the absolute value of **fisbar**. On the input line, we read **fisbaradjust**, Z, A, value, fission barrier. If the number of the fission barrier is not given or is equal to 0, it concerns the first barrier.

Examples

fisbaradjust 90 232 0.9
fisbaradjust 94 239 1.13 2

Range

$0.1 \leq$ **fisbaradjust** $\leq$ **10.**

Default

fisbaradjust $Z\,A$ **1.**.

Comments

- As a general comment for '**adjust**' keywords: this avoids having to look up the actual parameter value in the TALYS input file, hardwired default value in the source code or this tutorial, or one of the data tables that TALYS uses. One simply multiplies the nominal value with the value given on this keyword line without having to know the actual value.

fishwadjust

Normalisation factor for the fission barrier width. This parameter can be used as a relative normalisation instead of the absolute value of **fishw**. On the input line, we read **fishwadjust**, Z, A, value, fission barrier. If the number of the fission barrier is not given or is equal to 0, it concerns the first barrier.

Examples

fishwadjust 90 232 0.9
fishwadjust 94 239 1.13 2

Range

$0.1 \leq$ **fishwadjust** $\leq$ **10.**

Default

fishwadjust $Z\,A$ **1.**.

Comments

- As a general comment for '**adjust**' keywords: this avoids having to look up the actual parameter value in the TALYS input file, hardwired default value in the source code or this tutorial, or one of the data tables that TALYS uses. One simply multiplies the nominal value with the value given on this keyword line without having to know the actual value.

bdamp

The fission damping parameter. On the input line, we read **bdamp**, *Z*, *A*, value, fission barrier. If the number of the fission barrier is not given or is equal to 0, it concerns the first barrier.

Examples

> **bdamp 90 232 0.9**
> **bdamp 94 239 1.13 2**

Range

$0. \leq$ **bdamp** $\leq$ **50.**

Default

bdamp *Z A* **1.**

bdampadjust

Normalisation factor for the fission damping parameter. This parameter can be used as a relative normalisation instead of the absolute value of **bdamp**. On the input line, we read **bdampadjust**, Z, A, value, fission barrier. If the number of the fission barrier is not given or is equal to 0, it concerns the first barrier.

Examples

bdampadjust 90 232 0.9
bdampadjust 94 239 1.13 2

Range

$0.01 \leq$ **bdampadjust** $\leq$ **100.**

Default

bdampadjust $Z A$ **1.**

fispartdamp

Flag for partial damping in the fission model.

Examples

fispartdamp y
fispartdamp n

Range

y or **n**. **fispartdamp** can only be **y** for **fismodel 5**.

Default

fispartdamp n.

Cbarrier

Global adjustable parameter to change the fission barriers for the RLDM model of Sierk.

Examples

Cbarrier 0.8

Range

$0.1 \leq$ **Cbarrier** $\leq 10.$

Default

Cbarrier 0.85 for subactinides and **Cbarrier 1.2** for actinides.

hbstate

Flag to use head band states in fission.

Examples

> **hbstate y**
> **hbstate n**

Range

y or **n**.

Default

hbstate n.

hbtransfile

File with head band transition states. The format of the file is exactly the same as that of the nuclear structure database *talys/structure/fission/barrier/*. In practice, the user can copy a file from this database, e.g. *hbstates.eo*, to the working directory and change it. In this way, changes in the "official" database are avoided. Note that one file in the working directory can only be used for one isotope. On the input line, we read **hbtransfile**, *Z*, *A*, filename.

Examples

hbtransfile 92 238 u238.hb

Range

hbtransfile can be equal to any filename, provided it starts with a character.

Default

If **hbtransfile** is not given in the input file, the head band transition states are taken from the *talys/structure/fission/states* database.

class2

Flag for the enabling or disabling of class II/III states in fission. **class2** is only active if **fission y**.

Examples

class2 y
class2 n

Range

y or **n**

Default

class2 n

class2width

Width of class II/III states. On the input line, we read **class2width**, *Z*, *A*, value, fission barrier. If the number of the fission barrier is not given or is equal to 0, it concerns the first barrier well.

Examples

class2width 90 232 0.35
class2width 94 239 0.15 2

Range

$0.01 \leq$ **class2width** $\leq$ **10.**

Default

class2width *Z A* **0.2**

class2file

File with class II/III transition states. The format of the file is exactly the same as that of the nuclear structure database *talys/structure/fission/states/*. In practice, the user can copy a file from this database, e.g. *class2states.eo*, to the working directory and change it. In this way, changes in the "official" database are avoided. Note that one file in the working directory can only be used for one isotope. On the input line, we read **class2file**, *Z*, *A*, filename.

Examples

      class2file 92 238 u238.c2

Range

class2file can be equal to any filename, provided it starts with a character.

Default

If **class2file** is not given in the input file, the head band transition states are taken from the *talys/structure/fission/states* database.

betafiscor

Factor to adjust the width of the WKB fission path. (only applies for **fismodel 5**). On the input line, we read **betafiscor**, Z, A, value.

Examples

betafiscor 92 239 1.2

Range

0.1 $\leq$ betafiscor $\leq$ 10.

Default

betafiscor Z A **1.**

vfiscor

Factor to adjust the height of the WKB fission path. (only applies for **fismodel 5**). On the input line, we read **vfiscor**, Z, A, value.

Examples

vfiscor 92 239 0.9

Range

0.1 $\leq$ vfiscor $\leq$ 10.

Default

vfiscor $Z\,A$ **1.**

betafiscoradjust

Adjustable factor for betafiscor, to adjust the width of the WKB fission path. (only applies for **fismodel 5**). On the input line, we read **betafiscoradjust**, Z, A, value.

Examples

betafiscoradjust 92 239 1.2

Range

$0.1 \leq$ **betafiscoradjust** $\leq$ **10.**

Default

betafiscoradjust Z A **1.**

vfiscoradjust

Adjustable factor for vfiscor, to adjust the height of the WKB fission path. (only applies for **fismodel 5**). On the input line, we read **vfiscoradjust**, Z, A, value.

Examples

    vfiscoradjust 92 239 0.9

Range

$0.1 \leq$ **vfiscoradjust** $\leq 10.$

Default

vfiscoradjust Z A **1.**

Rfiseps

Ratio for limit for fission cross section per nucleus. This parameter determines whether the mass distribution for a residual fissioning nucleus will be calculated. Cross sections smaller than **Rfiseps** times the fission cross section are not used in the calculations, in order to reduce the computation time.

Examples

Rfiseps 1.e-5

Range

$0. \leq$ **Rfiseps** $\leq$ **1**.

Default

Rfiseps 1.e-3

fymodel

Model for the calculation of fission yields.

Examples

fymodel 1: Brosa model (the only option until TALYS-1.4)
fymodel 2: GEF model from Schmidt-Jurado [132]
fymodel 3: GEF model from Schmidt-Jurado [132], but evaporation of fission fragments done by Hauser-Feshbach model
fymodel 4: Okumura model - read in yields and excitation energies [151]
fymodel 5: General model - read in full population per fission fragment [151]

Range

$1 \leq$ **fymodel** ≤ 5

Default

fymodel 2

ffmodel

Model for the distribution of fission fragments.

Examples

ffmodel 0: tables by user in subdirectory user/
ffmodel 1: GEF model , fission fragments generated by Ali Al-Adili and Fredrik Nordstroem.
ffmodel 2: Okumura model [151]
ffmodel 3: SPY model [152]
ffmodel 4: Langevin-4D model

Range

$0 \leq$ **ffmodel** ≤ 4

Default

ffmodel 1

pfnsmodel

Model for prompt fission neutron spectra.

Examples

      pfnsmodel 1: Iwamoto model (2007)
      pfnsmodel 2: Explicit decay from fission fragments

Range

$1 \leq$ **pfnsmodel** ≤ 2

Default

pfnsmodel 2 if **massdis y**, **pfnsmodel 1** otherwise.

Fsadjust

Adjustable factor for the number of scission neutrons, for correction of prompt fission neutron spectrum. This works for the Iwamoto model for PFNS, **pfnsmodel 1**. On the input line, we read **Fsadjust**, value.

Examples

Fsadjust 1.2

Range

$0.1 \leq$ **Fsadjust** $\leq$ **10.**

Default

Fsadjust 1.

Tmadjust

Adjustable factor for the temperature of prompt fission neutron spectrum. This works for the Iwamoto model for PFNS, **pfnsmodel 1**. On the input line, we read **Tmadjust**, value.

Examples

Tmadjust 1.2

Range

0.1 $\leq$ Tmadjust $\leq$ 10.

Default

Tmadjust 1.

outfy

Detailed output of fission yields from each excited bin.

Examples

outfy y
outfy n

Range

y or **n**

Default

outfy n

ffspin

Flag to enable a choice between spin dependent excitation functions for excited fission fragments as emerging from GEF, or assignment of spin distributions by TALYS. This only applies to **fymodel 3**.

Examples

ffspin y
ffspin n

Range

y or **n**

Default

ffspin n

gefran

Number of random samples for GEF calculation.

Examples

gefran 18000

Range

$1000 \leq \textbf{gefran} \leq 1000000$

Default

gefran 50000

Cnubar1

Adjustable parameter for the energy-dependent constant of nubar from Wahl's systematics. On the input line, we read **Cnubar1** and value.

Examples

Cnubar1 1.3
Cnubar1 0.4

Range

$0.1 \leq$ **Cnubar1** $\leq$ **10**.

Default

Cnubar1 1.

Cnubar2

Adjustable parameter for the energy-dependent constant of nubar from Wahl's systematics. On the input line, we read **Cnubar2** and value.

Examples

Cnubar2 1.3
Cnubar2 0.4

Range

$0.1 \leq$ **Cnubar2** ≤ 10.

Default

Cnubar2 1.

massdis

Flag for the calculation of the fission-fragment mass distribution.

Examples

massdis y
massdis n

Range

y or **n**

Default

massdis n

outfission

Flag for the output of fission parameters, transmission coefficients and partial cross sections. **outfission** is only active if **fission y**.

Examples

outfission y
outfission n

Range

y or **n**

Default

the same value as **outbasic**: **outfission n**

filefission

Flag to write all the fission cross sections as a function of incident energy on a separate file *fission.tot*. The file contains the incident energy and the total fission cross section. If in addition *filechannels y*, the exclusive fission cross sections will be written to files *fisNPDTHA.tot*, where N is the neutron number of the exclusive channel, P the proton number, etc., in (a1) format. For example, *fis200000.tot* contains the excitation function for $\sigma(n, 2nf)$, also known as the third chance fission cross section. **filefission** is only active if **fission y**.

Examples

filefission y
filefission n

Range

y or **n**

Default

filefission n

ffevaporation

Flag to enable phenomenological correction for evaporated neutrons from fission fragments with the Brosa model.

Examples

ffevaporation y
ffevaporation n

Range

y or **n**

Default

ffevaporation n

yieldfile

File with fission fragment yields per pair, and their respective TXE and TKE values, to be used for evaporation using TALYS. The format of the file is as used by Okumura et al. [151] On the input line, we read **yieldfile**, filename.

Examples

yieldfile fy.dat

Range

yieldfile can be equal to any filename, provided it starts with a character.

Default

If **yieldfile** is not given in the input.

fisfeed

Flag for the output of the fission contribution per excitation energy bin. This allows to couple TALYS with e.g. fission yield software, by using the feeding per bin as input for normalization. The associated files have the name *fisZZZAAA.nex* where ZZZ is the charge number and AAA is the mass number in (i3.3) format.

Examples

fisfeed y
fisfeed n

Range

y or **n**

Default

fisfeed n

32. Keywords for astrophysics

astro

Flag for the calculation of thermonuclear reaction rates for astrophysics, see Section 18.

Examples

> **astro y**
> **astro n**

Range

y or **n**

Default

astro n

astrogs

Flag for treating the target in the ground state only, for astrophysical reaction calculations. In the default case, **astrogs n**, an average between excited target states will be made. This keyword is only active if **astro y**.

Examples

astrogs y
astrogs n

Range

y or **n**

Default

astrogs n

astroE

Energy, in MeV, for thermonuclear reactions around which Maxwellian averaging should take place. This is only active if **astro y**. Actually, specifying this value will automatically activate **astro y** and **astrogs y**. Hence, if you require the Maxwellian averaged 30 keV capture cross section, all you need to give is the input line below. **astroE** may not be specified simultaneously with **astroT9**. The **energy** keyword must still be given in the TALYS input file, but becomes irrelevant since it concerns an average over a large number of incident energies.

Examples

astroE 0.03

Range

$0.00001 \leq$ **astroE** $\leq 1.$.

Default

astroE 0.

astroT

Temperature, in units of 10^9 K, for thermonuclear reactions and Maxwellian averaging. This is only active if **astro y**. Actually, specifying this value will automatically activate **astro y**. **astroT** may not be specified simultaneously with **astroE**. The **energy** keyword must still be given in the TALYS input file, but becomes irrelevant since it concerns an average over a large number of incident energies.

Examples

astroT 0.53

Range

$0.0001 \leq$ **astroT** $\leq$ **10.**.

Default

astroT 0.

astroex

Flag for calculation of astrophysics reaction rate to final long-lived excited states. This extends the calculation of the rate for the ground state only. This keyword is only active if **astro y**.

Examples

astroex y
astroex n

Range

y or **n**

Default

astroex n

nonthermlev

Non-thermalized level in the calculation of astrophysics rate.

Examples

nonthermlev 2

Range

0 $\leq$ **nonthermlev** $\leq$ **numlev**, where **numlev** is specified in the file *talys.cmb*.

Default

nonthermlev is not used.

33. Keywords for medical isotope production

production

Flag to calculate medical isotope production.

Examples

production n
production y

Range

y or **n**

Default

production n

Ebeam

The incident energy of the particle beam in MeV. This keyword in only active if **production y**.

Examples

Ebeam 140.
Ebeam 16.

Range

10^{-11} MeV $\leq$ **Ebeam** $<$ **Emax** MeV, where Emax is the highest incident energy.

Default

None, **Ebeam** must be given if **production y**.

Eback

The lower end of the energy range at the back end of the target in MeV. This energy degradation is directly related to the effective thickness of the target. This keyword in only active if **production y**.

Examples

> **Eback 130.**
> **Eback 12.**

Range

Emin $\leq$ **Eback** $<$ **Ebeam**, where Emin is the lowest incident energy.

Default

Eback = Ebeam - 5 MeV.

Ibeam

Particle beam current in mA. This keyword in only active if **production y**.

Examples

> **Ibeam 0.1**
> **Ibeam 5.**

Range

0 $<=$ Ibeam $<=$ 10000.

Default

Ibeam 1. mA.

Area

Area of the target in cm^2. This keyword in only active if **production y**.

Examples

Area 1.

Range

$0 <=$ **Area** $<=$ **10000**.

Default

Area 10. cm^2.

rho

Material density of the target in g/cm^3. This keyword in only active if **production y**.

Examples

rho 10.

Range

$0 <=$ **rho** $<= 100$.

Default

rho 1. is read from a hardwired material density table.

radiounit

Unit for radioactivity, to be used in the output files for isotope production. This keyword in only active if **production y**.

The following units are possible:

> **radiounit Bq**: Becquerel
> **radiounit kBq**: kiloBecquerel
> **radiounit MBq**: MegaBecquerel
> **radiounit GBq**: GigaBecquerel
> **radiounit Ci**: Curie
> **radiounit mCi**: milliCurie
> **radiounit kCi**: kiloCurie

Range

radiounit should be equal to one of the units above.

Default

radiounit Mbq.

yieldunit

Unit for isotope yield, in weight or number of isotopes. This keyword in only active if **production y**.

The following units are possible:

yieldunit mug: microgram
yieldunit mg: milligram
yieldunit g: gram
yieldunit kg: kilogram
yieldunit num: number of isotopes

Range

yieldunit should be equal to one of the units above.

Default

yieldunit num.

Tirrad

Irradiation time. A general input for the irradiation time has been enabled. On the input line we read integer values and time units, which can be y (years), d (days), h (hours), m (minutes) or s (seconds). These all need to be separated by blanks. This keyword in only active if **production y**.

Examples

Tirrad	**2 d 5 h**
Tirrad	**32 h 30 m**
Tirrad	**1 d 6 h 24 m 12 s**

Range

$0 <=$ **Tirrad** $<=$ **1e6** for every time unit.

Default

Tirrad 1 d.

Tcool

Target cooling time. A general input for the cooling time has been enabled. On the input line we read integer values and time units, which can be y (years), d (days), h (hours), m (minutes) or s (seconds). These all need to be separated by blanks. This keyword in only active if **production y**.

Examples

Tcool	**2 d 5 h**
Tcool	**32 h 30 m**
Tcool	**1 d 6 m 24 m 12 s**

Range

0 $<=$ Tcool $<=$ 1e6 for every time unit.

Default

Tcool 1 d.

34. Keywords for output

outmain

Flag for the main output. The header of TALYS is printed, together with the input variables and the automatically adopted default values. Also the most important computed cross sections are printed.

Examples

> **outmain y**
> **outmain n**

Range

y or **n**

Default

outmain y

outall

Flag to repeat the output of *all* separate output files in the main output.

Examples

outall y
outall n

Range

y or **n**

Default

outall n

outbasic

Flag for the output of *all* basic information needed for the nuclear reaction calculation, such as level/bin populations, numerical checks, optical model parameters, transmission coefficients, inverse reaction cross sections, gamma and fission information, discrete levels and level densities. If **outbasic** is set to **y** or **n**, the keywords **outpopulation**, **outcheck**, **outlevels**, **outdensity**, **outomp**, **outdirect**, **outdiscrete**, **outinverse**, **outgamma** and **outfission** (see below for their explanation) will all be set to the same value automatically. Setting **outbasic y** is generally not recommended since it produces a rather large output file. Less extensive output files can be obtained by enabling some of the aforementioned keywords separately.

Examples

> **outbasic y**
> **outbasic n**

Range

y or **n**

Default

outbasic n

block

Flag to put output data in large data blocks. If the output is activated, exclusive spectra, particle spectra, discrete gamma-ray cross sections, angular distributions and Legendre coefficients are all stored in individual files if **block n**. If **block y**, they are stored in large data blocks.

Examples

> **block y**
> **block n**

Range

y or **n**

Default

block n, though **block y** will be set automatically if **endf y**.

Comments

For example, if **block n**, there could be output files *sp100000E0001.000.tot, sp100000E0002.000.tot* etc. while with **block y**, the data for all incident energies is stored in *sp100000.tot*.

outpopulation

Flag for the output of the population, as a function of excitation energy, spin and parity, of each compound nucleus in the reaction chain before it decays.

Examples

outpopulation y
outpopulation n

Range

y or **n**

Default

the same value as **outbasic**: **outpopulation n**

outcheck

Flag for the output of various numerical checks. This is to check interpolation schemes for the transformation from the emission grid to the excitation energy grid and vice versa, and to test the WFC method by means of flux conservation in the binary compound nucleus calculation. Also, the emission spectra integrated over energy are compared with the partial cross sections, and summed exclusive channel cross sections are checked against total particle production cross sections and residual production cross sections.

Examples

outcheck y
outcheck n

Range

y or **n**

Default

the same value as **outbasic**: **outcheck n**

outdecay

Flag for the output of detailed decay information per excitation bin in the decaying nuclide. Thus flag may give a **HUGE** output and is to be used with care. For every bin in the continuum, there is a detailed table for the decay via all particles to all other bins.

Examples

outdecay y
outdecay n

Range

y or **n**

Default

outdecay n

Comments

Use with care, this can give a huge output file.

outexcitation

Flag for the output of excitation functions, i.e. cross sections as a function of incident energy, such as residual production cross sections, inelastic cross sections, etc.

Examples

outexcitation y
outexcitation n

Range

y or **n**

Default

outexcitation n if only one incident energy is given in the input file, and **outexcitation y** for more than one incident energy.

outspectra

Flag for the output of angle-integrated emission spectra.

Examples

outspectra y
outspectra n

Range

y or **n**

Default

outspectra y if only one incident energy is given in the input file, and **outspectra n** for more than one incident energy.

outbinspectra

Flag for the output of emission spectra per compound nucleus bin. **outbinspectra** is only active if **outspectra y** and **population y**.

Examples

> **outbinspectra y**
> **outbinspectra n**

Range

y or **n**

Default

outbinspectra n.

ddxmode

Option for the output of double-differential cross sections. There are 4 possibilities.

Examples

ddxmode 0: No output.
ddxmode 1: Output per emission energy as a function of angle (angular distributions).
ddxmode 2: Output per emission angle as a function of energy (spectra).
ddxmode 3: Output per emission energy and per emission angle.

Range

$0 \leq$ **ddxmode** ≤ 3

Default

ddxmode 0. If there is a **fileddxe** keyword, , in the input file, **ddxmode 1** will be set automatically . If there is a **fileddxa** keyword, , in the input file, **ddxmode 2** will be set automatically. If both **fileddxe** and **fileddxa** are present, **ddxmode 3** will be set automatically.

outgamdis

Flag for the output of discrete gamma-ray intensities. All possible discrete gamma transitions for all nuclei are followed. In the output they are given in tables per nuclide and for each decay from state to state.

Examples

outgamdis y
outgamdis n

Range

y or **n**

Default

outgamdis n

sacs

Flag for the output of the statistical analysis of cross sections. With this flag the maximum cross section and the corresponding energy per excitation function are printed on a file.

Examples

sacs y
sacs n

Range

y or **n**

Default

sacs n

integral

Keyword to calculate the effective cross section for integral activation measurements, by folding the excitation functions by an experimental spectrum. In *talys/structure/integral/spectra*, we have stored more than 40 spectra, coming from the EASY package [16], which have been used in past activation benchmarks. Obviously, this keyword does not produce a reliable answer for low energies, since TALYS does not cover the resonance range. On the input line, we read **integral**, and optionally the cross section filename and the name of the experimental spectrum. The latter should be equal to the extension of the *spectrum.* files in *talys/structure/integral/spectra*.

Examples

integral xs010000.L01 tud_cucrzr
integral xs200000.tot cf252_flux
integral y

Range

y or **n** or name of cross section and spectrum

Default

integral n

fileelastic

Flag to write the elastic angular distribution on a separate file *XXYYY.YYYang.L00*, where XX is the particle symbol in (2a1) format (e.g. *nn* for elastic scattering), and YYY.YYY the incident energy in (f7.3) format. The file contains the angle, and 3 columns containing the total, shape elastic, and compound elastic angular distribution, respectively. If in addition **outlegendre y**, the elastic scattering Legendre coefficients will be written on a file *XXYYY.YYYleg.L00*. This file contains the *L*-value, and 4 columns containing the total, direct, compound and normalized Legendre coefficient. **fileelastic** is only active if **outangle y**.

Examples

fileelastic y, giving files *nn014.000ang.L00*, and (if **outlegendre y**) *nn014.000leg.L00*, for an incident energy of 14 MeV.

fileelastic n

Range

y or **n**

Default

fileelastic n

fileangle

Designator for the output of the non-elastic angular distribution of one specific level on a separate file *PXYYY.YYYang.LMM*, where P and X are the particle symbols in (a1) format for the projectile and ejectile, respectively, YYY.YYY is the incident energy in (f7.3) format, and MM is the level number in (i2.2) format. The file contains the angle and 3 columns with the total inelastic, direct inelastic and compound inelastic angular distribution to the specified level. On the input line we read the level number. The **fileangle** keyword can appear more than once in an input file, one for each level that one is interested in. It will automatically produce files for all ejectiles. If in addition **outlegendre y**, the non-elastic scattering Legendre coefficients will be written on a file *PXYYY.YYYleg.LMM*. This file contains the *L*-value, and 4 columns containing the total, direct, compound and normalized Legendre coefficient. **fileangle** is only active if **outdiscrete y** and **outangle y**.

Examples

> **fileangle 2**, giving files *np014.000ang.L02* and (**outlegendre y**) *np014.000leg.L02*, for the (n, p) reaction to the second discrete level and an incident energy of 14 MeV, and similarly for the other ejectiles.

Range

0 < **fileangle** < **numlev**. Currently, **numlev=30**

Default

fileangle not active.

filediscrete

Designator for the output of the excitation function of one specific non-elastic level on a separate file *PX.LMM*, where P and X are the particle symbols in (a1) format for the projectile and ejectile, respectively, and MM is the level number in (i2.2) format. The file contains the incident energy and 3 columns with the total inelastic, direct inelastic and compound inelastic cross section to the specified level. On the input line we read the level number. The **filediscrete** keyword can appear more than once in an input file, one for each level that one is interested in. It automatically produces a file for each ejectile. **filediscrete** is only active if **outdiscrete y**.

Examples

> **filediscrete 2** , giving files *nn.L02*, *np.L02*, etc. for the excitation functions of (inelastic and other) neutron scattering to the second discrete level.

Range

0 < **filediscrete** < **numlev**. Currently, **numlev=30**

Default

filediscrete not active.

filechannels

Flag to write the exclusive channel cross sections as a function of incident energy on separate files. The files will be called *xsNPDTHA.tot*, where N is the neutron number of the exclusive channel, P the proton number, etc., in (a1) format. For example *xs210000.tot* contains the excitation function for $\sigma(n,2np)$, if the incident particle was a neutron. The files contain the incident energy and 3 columns with the exclusive cross section, the associated gamma-ray production cross section, and the fraction of this cross section relative to the total residual production cross section. If in addition isomers can be produced, files called *xsNPDTHA.LMM* will be created with MM the isomeric level number in (i2.2) format. If **filechannels y**, the exclusive binary continuum cross sections, such as continuum inelastic scattering, will also be written to files *PX.con*, where P and X are the particle symbols in (a1) format for the projectile and ejectile, respectively. If *outspectra y*, the exclusive channel spectra will be written on files *spNPDTHAEYYY.YYY.tot* where YYY.YYY is the incident energy in (f7.3) format. The files contain the incident energy and 6 columns, with the spectra per outgoing particle type. **filechannels** is only active if **channels y**.

Examples

filechannels y
filechannels n

Range

y or **n**

Default

filechannels n

filespectrum

Designator for the output of the composite particle spectrum for a specific particle type on a separate file. On the input line we read the particle symbols. This will result in files *XspecYYY.YYY.tot*, where X is the outgoing particle symbol in (a1) format, and YYY.YYY the incident energy in (f7.3) format. The file contains the emission energy and 5 columns with the total, direct, pre-equilibrium, multiple pre-equilibrium and compound spectrum, respectively. **filespectrum** is only active if **outspectra y**.

Examples

filespectrum n p a, giving files *nspec014.000.tot*, *pspec014.000.tot* and *aspec014.000.tot*, for an incident energy of 14 MeV.

Range

n p d t h a

Default

filespectrum not active.

fileddxe

Designator for the output of double-differential cross sections per emission energy for a specific particle type. On the input line we read the particle type and the emission energy. This will result in files *XddxYYY.Y.mev*, where X is the particle symbol in (a1) format and YYY.Y the emission energy in (f5.1) format. The file contains the emission angle and 5 columns with the total, direct, pre-equilibrium, multiple pre-equilibrium and compound spectrum, respectively. The **fileddxe** keyword can appear more than once in an input file, one for each outgoing energy that one is interested in. If there is at least one **fileddxe** keyword in the input **ddxmode**, see p. 702, will automatically be enabled.

Examples

fileddxe n 60. (giving a file *nddx060.0.mev*).

Range

n p d t h a for the particles and **0. -** E_{inc} for outgoing energies.

Default

fileddxe not active.

fileddxa

Designator for the output of double-differential cross sections per emission angle for a specific particle type. On the input line we read the particle type and the emission angle. This will result in files *XddxYYY.Y.deg*, where X is the particle symbol in (a1) format and YYY.Y the emission angle in (f5.1) format. The file contains the emission energy and 5 columns with the total, direct, pre-equilibrium, multiple pre-equilibrium and compound spectrum, respectively. The **fileddxa** keyword can appear more than once in an input file, one for each outgoing angle that one is interested in. If there is at least one **fileddxa** keyword in the input **ddxmode**, see p. 702, will automatically be enabled.

Examples

　　　　fileddxa n 30. (giving a file *nddx030.0.deg*).

Range

n p d t h a for the particles and **0. - 180.** for outgoing angles.

Default

fileddxa not active.

filegamdis

Flag to write the discrete gamma-ray intensities as a function of incident energy to separate files. This will result in files *gamZZZAAALYYLMM.tot*, where ZZZ is the charge number and AAA is the mass number in (i3.3) format, YY is the number of the initial discrete state and MM the number of the final discrete state. **filegamdis** is only active if **outgamdis y**.

Examples

filegamdis y
filegamdis n

Range

y or **n**

Default

filegamdis n

filetotal

Flag to write all the total cross sections as a function of incident energy on a separate file *all.tot*. The file contains the incident energy, and 9 columns containing the non-elastic, total elastic, total, compound elastic, shape elastic, reaction, compound non-elastic, direct and pre-equilibrium cross section. In addition, the total particle production cross sections will be written on files *Xprod.tot*, with X the particle symbol in (a1) format. Finally, separate x-y tables will be made for the total cross section, on *total.tot*, the total elastic cross section, on *elastic.tot*, and the total nonelastic cross section, on *nonelastic.tot*. **filetotal** is only active if **outexcitation y** or **endf y**.

Examples

> **filetotal y**
> **filetotal n**

Range

y or **n**

Default

filetotal n

fileresidual

Flag to write all the residual production cross sections as a function of incident energy on separate files. The files for the total (i.e. the sum over ground state + isomers) residual production cross sections have the name *rpZZZAAA.tot* where ZZZ is the charge number and AAA is the mass number in (i3.3) format. If a residual nuclide contains one or more isomeric states, there are additional files *rpZZZAAA.LMM*, where MM is the number of the isomer (ground state=0) in (i2.2) format. The files contain the incident energy and the residual production cross section. **fileresidual** is only active if **outexcitation y** or **endf y**.

Examples

fileresidual y
fileresidual n

Range

y or **n**

Default

fileresidual n

filerecoil

Flag to write the recoil spectra of the residual nuclides as a function of incident energy on separate files. The files for the recoil spectra have the name *recZZZAAAspecYYY.YYY.tot* where ZZZ is the charge number and AAA is the mass number in (i3.3) format and YYY.YYY the incident energy in (f7.3) format. If in addition **flagchannels y**, there are additional files *spNPDTHAEYYY.YYY.rec*, where N is the neutron number of the exclusive channel, P the proton number, etc. The files contain the incident energy and the recoil.

Examples

filerecoil y
filerecoil n

Range

y or **n**

Default

filerecoil n

components

Flag to write the direct, pre-equilibrium and compound components of the cross sections in the various output files.

Examples

components y
components n

Range

y or **n**

Default

components n

35. Keywords of TALYS

Table 35.1: The keywords of TALYS.

Keyword	Range	Default	Page
a	1. - 100.	table or systematics	380
aadjust	0.5 - 2.	1.	381
abundance	filename	no default	333
adddiscrete	y,n	y	561
addelastic	y,n	y	562
adepthcor	0.5 - 1.5	1.	503
alimit	1. - 100.	systematics	382
alphald	0.01 - 0.2	systematics	414
alphaomp	1 - 8	6	501
anfit	y,n	n	372
angles	1-numang	90	316
anglescont	1-numangcont (36)	36	317
anglesrec	1-numangrec (9)	9	323
aradialcor	0.5 - 1.5	1.	502
area	0. - 10000.	1.	684
astro	y,n	n	672
astroE	0.00001-1.	0.	674
astroex	y,n	n	676
astrogs	y,n	n	673
astroT	0.0001-10.	0.	675
asys	y,n	n	383
autorot	y,n	n	551
avadjust	0.5 - 2.	1.	471
avadjustF	-100 - 100	no default	530
avdadjust	0.5 - 2.	1.	483
avdadjustF	-100 - 100	no default	534
avsoadjust	0.5 - 2.	1.	494
avsoadjustF	-100 - 100	no default	538
awadjust	0.5 - 2.	1.	477
awadjustF	-100 - 100	no default	532
awdadjust	0.5 - 2.	1.	485
awdadjustF	-100 - 100	no default	536
awsoadjust	0.5 - 2.	1.	496
awsoadjustF	-100 - 100	no default	540
axtype	1-5	1 and 2,3 for $N > 144$	635
bdamp	0. - 50.	0.01	640
bdampadjust	0.01 - 100.	1.	641
best	y,n	n	306
bestbranch	y,n	y	363
bestend	y,n	n	336

Continuation of **Table 35.1.**

Keyword	Range	Default	Page
bestpath	pathname	no default	337
beta2	0. - 1.5	0.-1. (barrier dep.)	348
betafiscor	0.1 - 10.	1.	649
betafiscoradjust	0.1 - 10.	1.	651
betald	0. - 0.5	systematics	415
bins	0, 2 - numbins (100)	40	298
block	y,n	n	695
branch	0 - numlev	no default	360
breakupmodel	1 - 2	1	624
Cbarrier	0.1 - 10.	0.85 or 1.20	643
Cbreak	0. - 10.	1.	623
Cfermi	0. - 1000.	5.	421
cglobal	-10. - 10.	1.	425
channelenergy	y,n	n	326
channels	y,n	n	304
Cknock	0. - 10.	1.	622
class2	y,n	n	646
class2file	filename	no default	648
class2width	0.01 - 10.	0.2	647
Cnubar1	0.1 - 10.	1.	662
Cnubar2	0.1 - 10.	1.	663
colenhance	y,n [Z,A]	n	407
colldamp	y,n	n	408
components	y,n	n	717
compound	y,n	y	572
core	-1,1	-1	569
coulomb	y,n	y	563
cpang	y,n	n	564
Cstrip	0. - 10.	1.	621
ctable	-10. - 10.	1.	386
ctableadjust	-10. - 10.	1.	387
ctmglobal	y,n	n	412
D0	1.e-6 - 10000.	table	441
d1adjust	0.2 - 5.	1.	486
d2adjust	0.2 - 5.	1.	487
d3adjust	0.2 - 5.	1.	488
ddxmode	0 - 3	0	702
deformfile	filename	no default	568
deltaW	-20. - 20.	calculated	384
densfile	filename	no default	404

Continuation of **Table 35.1.**

Keyword	Range	Default	Page
deuteronomp	1 - 5	1	500
disctable	1 - 3	1	358
dispersion	y,n	n	498
dnfit	y,n	n	373
E0	-10. - 10.	calculated	396
E0adjust	0.1 - 10.	1.	397
E1file	filename	no default	449
Eback	0. - Ebeam	Ebeam - 5.	682
Ebeam	0. - Ein	no default	681
eciscalc	y,n	y	547
eciscompound	y,n	n	581
ecisdwba	y,n	y	625
ecissave	y,n	n	546
egr	1. - 100.	table or systematics	432
egradjust	0.1 - 10.	1.	435
ejectiles	g n p d t h a	g n p d t h a	307
Ejoin	0. - 1000.	200.	516
electronconv	y,n	n	362
element	3 - 124 or Li - C4	no default	291
Elow	1.e-6 - 1.	D_0	330
elwidth	1.e-6 - 100.	0.5	557
Emsdmin	>0.	Eninc/5.	629
endf	y,n	n	314
endfdetail	y,n	y for n,g; n otherwise	315
endfecis	y,n	y	555
energy	1.e-11 - 250.	no default	293
epr	1. - 100.	no default	459
epradjust	0.1 - 10.	1.	462
equidistant	y,n	y	327
equispec	y,n	n	328
Estop	1.e-5 - 1000.	1000.	313
Esurf	0. - 38.	systematics	600
etable	-10. - 10.	0.	443
etableadjust	-10. - 10.	0.	444
Exmatch	0.1 - 20.	calculated	392
Exmatchadjust	0.1 - 10.	1.	393
expmass	y,n	y	347
ffevaporation	y,n	n	667
ffmodel	1 - 2	1	655
ffspin	y,n	n	660

Continuation of **Table 35.1.**

Keyword	Range	Default	Page
fileangle	0 - numlev	no default	707
filechannels	y,n	n	709
fileddxa	n,...,a 0. - 180.	no default	712
fileddxe	n,...,a 0. - energy	no default	711
filedensity	y,n	n	405
filediscrete	0 - numlev	no default	708
fileelastic	y,n	n	706
filefission	y,n	n	666
filegamdis	y,n	n	713
filepsf	y,n	n	451
filerecoil	y,n	n	716
fileresidual	y,n	n	715
filespectrum	g n p d t h a	no default	710
filetotal	y,n	n	714
fisbar	0. - 100.	table or systematics	636
fisbaradjust	0.1 - 10.	1.	638
fisfeed	y,n	n	669
fishw	0.01 - 10.	table or systematics	637
fishwadjust	0.1 - 10.	1.	639
fismodel	1 - 5	1	633
fismodelalt	3 - 4	4	634
fiso	0.01 - 100.	1.5, 2 or 5 (nuc-dep)	453
fisom	0.01 - 100.	1.5, 2 or 5 (nuc-dep)	454
fispartdamp	y,n	n	642
fission	y,n,$A \geq 56$	y for mass> 209, n for mass≤ 209	632
fit	y,n	n	365
format	format name	YANDF	343
Fsadjust	0.1 - 10.	1.	657
ftable	0.1 - 10.	1.	445
Ftableadjust	0.1 - 10.	1.	446
fullhf	y,n	n	579
fymodel	1 - 5	2	654
g	0.1-100.	systematics	606
gadjust	0.5 - 2.	1.	611
gamgam	0. - 10.	table or systematics	438
gamgamadjust	0.1 - 10.	1.	439
gamgamfit	y,n	n	371
gammald	0.01 - 1.	systematics	416
gammashell1	0. - 1.	systematics	417
gammashell2	0. - 0.2	0.	418

Continuation of **Table 35.1.**

Keyword	Range	Default	Page
gammax	1 - 6	2	428
gefran	1000 - 1000000	50000	661
ggr	1. - 100.	table or systematics	434
ggradjust	0.1 - 10.	1.	437
giantresonance	y,n	y for n,p; n otherwise	556
gn	0.1 - 100.	systematics	608
gnadjust	0.5 - 2.	1.	610
gnfit	y,n	n	374
gnorm	0. - 100. or -1.	calculated	429
gp	0.1 - 100.	systematics	607
gpadjust	0.5 - 2.	1.	609
gpr	1. - 100.	no default	461
gpradjust	0.1 - 10.	1.	464
group	y,n	n	582
gshell	y,n	n	612
hbstate	y,n	n	644
hbtransfile	filename	no default	645
Ibeam	0. - 10000.	1.	683
incadjust	y,n	y	518
inccalc	y,n	y	548
integral	filenames	no default	705
isofit	y,n	n	376
isomer	0. - 1.e38	1.	303
jlmmode	0 - 3	1	507
jlmomp	y,n	n	506
Kph	1. - 100.	15.	605
Krotconstant	0.01 - 100.	1.	420
kvibmodel	1 - 2	2	411
labddx	y,n	n	322
ldmodel	1 - 6 [Z,A]	1	378
ldmodelCN	1 - 6	ldmodel	379
ldmodelracap	1 - 3	1	456
levelfile	filename	no default	359
Liso	0 - numlev	no default	302
localomp	y,n	y	499
Ltarget	0 - numlev	0	299
lurr	1 - numl	2	577
lv1adjust	0.5 - 1.5	1.	510
lvadjust	0.5 - 1.5	1.	508
lvsoadjust	0.5 - 1.5	1.	512

Continuation of **Table 35.1.**

Keyword	Range	Default	Page
lw1adjust	0.5 - 1.5	1.	511
lwadjust	0.5 - 1.5	1.	509
lwsoadjust	0.5 - 1.5	1.	513
M1file	filename	no default	450
M2constant	0. - 100.	1.	613
M2limit	0. - 100.	1.	614
M2shift	0. - 100.	1.	615
macsfit	y,n	n	370
mass	0, 5 - 339	no default	292
massdir	filename	no default	349
massdis	y,n	n	664
massexcess	-500. - 500.	mass table	351
massmodel	1 - 3	3	346
massnucleus	A-0.5 - A+0.5	mass table	350
maxband	0 - 100	0	550
maxchannel	0 - 8	4	318
maxenrec	0 - numenrec (25)	10	324
maxlevelsbin	0 - numlev	10 (g,n,p,a) and 5 (d,t,h)	355
maxlevelsres	0 - numlev	10	356
maxlevelstar	0 - numlev	20	354
maxN	0 - numN-2	22	301
maxNrp	0 - numN-2	22	332
maxrot	0 - 10	2	549
maxZ	0 - numZ-2	10	300
maxZrp	0 - numZ-2	10	331
micro	y,n	n	334
mpreeqmode	1 - 2	1	595
msdbins	2 - numenmsd/2-1 (8)	6	628
multipreeq	y,n or 0.001 - 250.	20.	594
nafit	y,n	n	369
nffit	y,n	n	367
ngfit	y,n	n	366
Nlevels	0 - numlev	equal to maxlevelsres	357
Nlow	0 - 200	2	390
nnfit	y,n	n	368
nonthermlev	0 - numlev	not used	677
Ntop	0 - 200	table or equal to Nlevels	391
nulldev	filename	no default	339
ompenergyfile	filename	no default	335
omponly	y,n	n	519

Continuation of **Table 35.1.**

Keyword	Range	Default	Page
onestep	y,n	n	627
optmod	filename	no default	520
optmodall	y,n	n	523
optmodfileN	filename	no default	521
optmodfileP	filename	no default	522
outall	y,n	n	693
outangle	y,n	y for one energy, n for many	558
outbasic	y,n	n	694
outbinspectra	y,n	n	701
outcheck	y,n	equal to outbasic	697
outdecay	y,n	n	698
outdensity	y,n	equal to outbasic	406
outdirect	y,n	equal to outbasic	552
outdiscrete	y,n	equal to outbasic	560
outdwba	y,n	n	626
outecis	y,n	n	554
outexcitation	y,n	n for one energy, y for many	699
outfission	y,n	equal to outbasic	665
outfy	y,n	n	659
outgamdis	y,n	n	703
outgamma	y,n	equal to outbasic	440
outinverse	y,n	equal to outbasic	553
outkd	y,n	n	525
outlegendre	y,n	n	559
outlevels	y,n	equal to outbasic	364
outmain	y,n	y	692
outomp	y,n	equal to outbasic	524
outpopulation	y,n	equal to outbasic	696
outpreequilibrium	y,n	n	599
outspectra	y,n	y for one energy, n for many	700
outtransenergy	y,n	y	567
pair	0. - 10.	systematics	385
pairconstant	0. - 30.	12.	419
pairmodel	1 - 2	1	603
parity	y,n	n	413
partable	y,n	n	305
pfnsmodel	1 - 2	1	656
pglobal	-10. - 10.	0.	426
phmodel	1 - 2	1	604
pnfit	y,n	n	375

Continuation of **Table 35.1.**

Keyword	Range	Default	Page
popeps	0. - 1000.	1.e-3	311
popMeV	y,n	n	312
preeqcomplex	y,n	y	601
preeqmode	1 - 4	2	593
preeqspin	y,n or 1-3	n	596
preeqsurface	y,n	y	598
preequilibrium	y,n or 0.001 - 250.	Ex(NL)	592
production	y,n	n	680
projectile	n,p,d,t,h,a,g,0	no default	290
psfglobal	y,n	n	452
Pshift	-10. - 10.	systematics	398
Pshiftadjust	-10. - 10.	systematics	399
Pshiftconstant	-5. - 5.	0. or 1.09	400
pruitt	y,n	n	504
pruittset §	0 - 416	0	505
ptable	-10. - 10.	0.	388
ptableadjust	-10. - 10.	1.	389
racap	y,n	n	455
radialfile	filename	no default	515
radialmodel	1 - 2	2	514
radiounit	(k,M,G)Bq, (m,k)Ci	Gbq	686
rcadjust	0.5 - 2.	1.	497
Rclass2mom	0.1 - 10.	1.	424
reaction	y,n	y	320
recoil	y,n	n	321
recoilaverage	y,n	n	325
relativistic	y,n	y	319
rescuefile	filename	no default	338
reslib	library name, default	default	583
resonance	y,n	n	575
Rfiseps	0. - 1.	1.e-3	653
Rgamma	0. - 100.	2.	620
rho	0. - 100.	from table	685
riplomp	in RIPL table	2408 for actinides	527
riplrisk	y,n	n	528
Risomer	0. - 10.	1.	361
Rnunu	0. - 100.	1.	616
Rnupi	0. - 100.	1.	617
rotational	n p d t h a	n p	543
rpevap	y,n	n	589

Continuation of **Table 35.1.**

Keyword	Range	Default	Page
Rpinu	0. - 100.	1.	619
Rpipi	0. - 100.	1.	618
Rprime	0. - 10.	not given	442
Rspincut	0. - 10.	1.	401
Rspincutff	0. - 20.	9.	402
Rspincutpreeq	0. - 10.	1.	597
Rtransmom	0.1 - 10.	1.	423
rvadjust	0.5 - 2.	1.	470
rvadjustF	-100 - 100	no default	529
rvdadjust	0.5 - 2.	1.	482
rvdadjustF	-100 - 100	no default	533
rvsoadjust	0.5 - 2.	1.	493
rvsoadjustF	-100 - 100	no default	537
rwadjust	0.5 - 2.	1.	476
rwadjustF	-100 - 100	no default	531
rwdadjust	0.5 - 2.	1.	484
rwdadjustF	-100 - 100	no default	535
rwsoadjust	0.5 - 2.	1.	495
rwsoadjustF	-100 - 100	no default	539
s2adjust	0.01 - 10.	1.	403
sacs	y,n	n	704
segment	1 - 4	1	329
sfexp	0. - 10.	table or 0.347	457
sfth	0. - 10.	table or 0.5	458
sgr	0. - 10000.	table or systematics	433
sgradjust	0.1 - 10.	1.	436
shellmodel	1 - 2	1	410
skipCN	[Z,A]	no default	585
soswitch	0.1 - 10.	3.	565
soukho	y,n	y	526
source	name of source	TALYS-2.0	342
spherical	y,n	n	542
spincutmodel	1 - 2	1	409
spr	0. - 10000.	table or systematics	460
spradjust	0.1 - 10.	1.	463
statepot	y,n	n	566
strength	1 - 10	9	430
strengthM1	1 - 10	3	431
strucpath	filename	no default	340
sysreaction	n p d t h a	d t h a	545

Continuation of **Table 35.1.**

Keyword	Range	Default	Page
T	0.001 - 10.	calculated	394
Tadjust	0.1 - 10.	1.	395
Tcool	0. - 1.e6	1 d	689
Tirrad	0. - 1.e6	1 d	688
Tjadjust	0.001 - 1000.	1.	544
Tmadjust	0.1 - 10.	1.	658
transeps	0. - 1.	1.e-8	309
transpower	2 - 20	5	308
Tres	0. - 1.e12	293.16	584
twocomponent	y,n	n	602
Ufermi	0. - 1000.	30. or 45.	422
upbend	y,n	n	465
upbendc	0. - 1.e-5	0.	466
upbende	0. - 10.	0.	467
upbendf	-10. - 10.	0.	468
urr	y,n, 0.-20.	n	576
urrnjoy	y,n	y	578
user	your name	no default	341
v1adjust	0.2 - 5.	1.	472
v2adjust	0.2 - 5.	1.	473
v3adjust	0.2 - 5.	1.	474
v4adjust	0.2 - 5.	1.	475
vfiscor	0.1 - 10.	1.	650
vfiscoradjust	0.1 - 10.	1.	652
Vinfadjust	-200. - 0.	-30.	517
vso1adjust	0.2 - 5.	1.	489
vso2adjust	0.2 - 5.	1.	490
w1adjust	0.2 - 5.	1.	478
w2adjust	0.2 - 5.	1.	479
w3adjust	0.2 - 5.	1.	480
w4adjust	0.2 - 5.	1.	481
WFCfactor	1 - 3	1	580
wso1adjust	0.2 - 5.	1.	491
wso2adjust	0.2 - 5.	1.	492
widthfluc	y,n or 0.001 - 20.	S(n)	573
widthmode	0 - 3	1	574
wtable	0. - 10.	1.	447
wtableadjust	0. - 10.	1.	448
xsalphatherm	$10^{-20} - 10^{10}$	table or systematics	587
xscaptherm	$10^{-20} - 10^{10}$	table or systematics	586
xseps	0. - 1000.	1.e-7	310
xsptherm	$10^{-20} - 10^{10}$	table or systematics	588
yieldfile	filename	no default	668
yieldunit	num, mug, mg, g or kg	num	687

IV

Part Four: Miscellaneous

36. Development of TALYS

(Beta) versions of TALYS have been available since 2005, and since thene the possibilities of the code have grown. For several users, who may revisit the code every now and then, it may be useful to see what has been added to the code since they last used it. Therefore, from the previous TALYS-1.x manuals we have copied the temporary development in terms of features and keywords.

36.1 From TALYS-1.0 to TALYS-1.2

On December 21, 2007 the first official version of the code, TALYS-1.0, was released. Since then, the code has undergone changes that fall in the usual two categories: significant extensions and corrections that may affect a large part of the user community, and several small bug fixes. As appendix to this manual, we add the full log file of changes since the release of TALYS-1.0. Here we list the most important updates:

- Further unification of microscopic structure information from Hartree-Fock-Bogoliubov (HFB) calculations. Next to masses, HFB deformation parameters are now also provided. The latest HFB-based tabulated level densities for both the ground state and fission barriers were included in the structure database. Another new addition is a database of microscopic particle-hole densities for preequilibrium calculations.
- Introduction of more keywords for adjustment. Often, these are defined relative to the default values, and thus often have a default value of 1. This is convenient since one does not have to look up the current value of the parameter if it is to be changed by a certain amount. Instead, giving e.g. **aadjust 41 93 1.04** means multiplying the built-in value for the level density parameter *a* by 1.04. Such keywords are now available for many parameters of the optical model, level density, etc., enabling easy sensitivity and covariance analyses with TALYS.
- An alternative fission model has been added, or more precisely, revived. Pascal Romain and colleagues of CEA Bruyeres-le-Chatel has been more successful to fit actinide data with

older TALYS options for fission (present in versions of the code before the first released beta version TALYS-0.64) using effective level densities, than with the newer options with explicit collective enhancement for the level densities[153, 154]. Therefore we decided to re-include that option again, through the **colldamp** keyword. Also his corrections for the class-II states were adopted. We generally use this option now for our actinide evaluations, until someone is able to do that with the newer fission models built in the code.

- Average resonance parameters for the unresolved resonance range are calculated.

- More flexibility has been added for cases where TALYS fails to fit experimental data. It is now possible to normalize TALYS directly to experimental or evaluated data for each reaction channel. This is not physical, but needed for several application projects.

- Perhaps the most important error was found by Arjan Plompen and Olivier Bersillon. In the discrete level database of TALYS-1.0, the internal conversion coefficients were wrongly applied to the gamma-ray branching ratios. A new discrete level database has been generated and internal conversion is now correctly taken into account. In some cases, this affects the production of discrete gamma lines and the cross section for isomer production.

- TALYS can be turned into a "pure" optical model program with the keyword **omponly y**. After the optical model calculation and output it then skips the calculation for all nonelastic reaction channels. In this mode, TALYS basically becomes a driver for ECIS.

- It is now possible to save and use your best input parameters for a particular isotope in the structure database (helpful for data evaluation). With the **best** keyword these parameter settings can automatically be invoked. We include part of our collection in the current version.

- Pygmy resonance parameters for gamma-ray strength functions can be included.

To accommodate all this, plus other options, the following new keywords were introduced: **aadjust**, see page 381, **rvadjustF**, see page 529, **avadjustF**, see page 530, **rvdadjustF**, see page 533, **avdadjustF**, see page 534, **rvsoadjustF**, see page 537, **avsoadjustF**, see page 538, **best**, see page 306, **colldamp**, see page 408, **coulomb**, see page 563, **epr**, see page 459, **fiso**, see page 453, **gamgamadjust**, see page 439, **gnadjust**, see page 610, **gpadjust**, see page 609, **gpr**, see page 461, **hbstate**, see page 644, **jlmmode**, see page 507, **micro**, see page 334, **ompenergyfile**, see page 335, **omponly**, see page 519, **phmodel**, see page 604, **radialmodel**, see page 514, **rescuefile**, see page 338, **s2adjust**, see page 403, **soswitch**, see page 565, **spr**, see page 460, **strengthM1**, see page 431, **urr**, see page 576, **xsalphatherm**, see page 587, **xscaptherm**, see page 586, **xsptherm**, see page 588.

36.2 From TALYS-1.2 to TALYS-1.4

On December 23, 2009 the second official version of the code, TALYS-1.2, was released. Since then, the code has undergone changes that fall in the usual two categories: significant extensions and corrections that may affect a large part of the user community, and several small bug fixes. As appendix to this manual, we add the full log file of changes since the release of TALYS-1.2. Here we list the most important updates:

- A new phenomenological model for break-up reactions by Connie Kalbach was included. This model is documented in an unpublished report to the FENDL-3 meeting at the IAEA, December 2010, and resolves some of the cross section prediction problems that were observed in earlier versions of TALYS. The contribution can be scaled by a normalization factor (**Cbreak** keyword).

- The alpha double-folding potential by Demetriou et al[70] was added as an option.
- Several deuteron OMP's were added to provide a better prediction of deuteron reaction cross sections and transmission coefficients.
- As part of the output of the binary reaction information, the compound nucleus formation cross section as a function of spin and parity is now also printed.
- TALYS is now able to produce unresolved resonance range (URR) parameters with a higher quality than that of TALYS-1.2, thanks to modelling and programming help by Gilles Noguere, CEA-Cadarache, and testing by Paul Koehler, ORNL.
- We increased the flexibility of using level densities. Up to TALYS-1.2, it was possible to choose between 5 level density models, which were then used for *all* nuclides in the calculation. It is now possible to choose one of these 5 level density models *per nuclide*, e.g. the Constant Temperature model for the target nucleus and the Backshifted Fermi Gas model for the compound nucleus. The **ldmodel** and **colenhance** keywords have been extended with (optional) Z,A identifiers.
- We have added the possibility to print the direct, pre-equilibrium and compound components of each cross section in the output files, in order to check which reaction mechanism is responsible for different parts of the excitation function. This can be enabled with the new **components** keyword.
- It is now possible to calculate the Maxwellian averaged cross section (MACS) at a user-defined energy. By using the **astroE** keyword, one can for example compare TALYS with experimental 30 keV averaged capture cross sections.
- We have included the possibility to calculate the so-called effective cross section for integral activation measurements, by folding the excitation functions by an experimental flux. In *talys/structure/flux*, we have stored more than 40 spectra which have been used in past activation benchmarks.

For TALYS-1.4 the following new keywords were introduced: **Cbreak**, see page 623, **deuteronomp**, see page 500, **rwadjustF**, see page 531, **awadjustF**, see page 532, **rwdadjustF**, see page 535, **awdadjustF**, see page 536, **rwsoadjustF**, see page 539, **awsoadjustF**, see page 540, **integral**, see page 705, **urrnjoy**, see page 578, **components**, see page 717, **astroE**, see page 674, **astroT**, see page 675, while the possibilities of **alphaomp**, see page 501, **ldmodel**, see page 378, **colenhance**, see page 407, were extended.

It is worthwhile to mention here that the structure database has almost not changed since the release of version 1.2. The only exceptions are the *structure/mass/hfb* directory, which contains the latest Hartree-Fock-Bogoliubov + Skyrme-based theoretical masses, and the *structure/flux* directory, which contains a collection of experimental neutron spectra for the calculation of effective integral cross sections.

36.3 From TALYS-1.4 to TALYS-1.6

On December 28, 2011 the third official version of the code, TALYS-1.4, was released. Since then, the code has undergone changes that fall in the usual two categories: significant extensions and corrections that may affect a large part of the user community, and several small bug fixes. As appendix to this manual, we add the full log file of changes since the release of TALYS-1.4. Here we list the most important updates:

- The activity of all residual products can be given in the output. This means that TALYS can now directly be used for medical isotope production with accelerators through the use of

the **production keyword**. For this the decay data library is added to the TALYS structure database. Excitation functions are thus automatically transferred into isotope production rates in MBq or Ci, as a function of time. Various extra keywords for this are included for flexibility.

- Part of the GEF code for fission yields, by Schmidt and Jurado, has been translated into FORTRAN and into a TALYS subroutine by Vasily Simutkin and Michail Onegin. This now allows the calculation of fission yields and fission neutron multiplicities as a function of Z, N, A and the number of emitted neutrons, while the calculation of fission neutron spectra will be done in a future version of TALYS. GEF is designed to produce this information starting from an excited state of a fissile system. Hence, the TALYS-GEF combination can now give estimates for these fission quantities in the case of multi-chance fission.

- Non-equidistant binning for the excitation energy grid was introduced. The excitation energies can now be tracked on a logarithmic grid, and has now become the default. It allows to use less excitation energy bins while not losing precision. The old situation of TALYS-1.4 and before can be invoked with the new **equidistant** keyword, but from now on the default will be **equidistant n**. Especially for cross sections above 100 MeV the improvement is significant in terms of smoothness and more reliable absolute values.

- Thanks to the previous improvement, TALYS can now technically be used up to 1 GeV. For this, the Koning-Delaroche OMP was extended as well.

- A radiative capture model for the direct capture cross section was added.

- An extra option for the pre-equilibrium spin distribution was included, see the **preeqspin** keyword.

- The **energy** keyword has been made more flexible, avoiding long files with energy values to be constructed by the user.

- About 70 keywords can now have energy-dependent values. After the keyword and its value are given in the input, an energy range can be specified over which the corresponding model parameter is altered. Hence, it is for example possible to have a (usual) constant value for the optical model radius r_V, but to increase its value between e.g. 6 and 10 MeV, through a simple addition on the input line.

For TALYS-1.6 the following new keywords were introduced: **equidistant**, see page 327, **disctable**, see page 358, **Tjadjust**, see page 544, **branch**, see page 360, **racap**, see page 455, **sfexp**, see page 457, **sfth**, see page 458, **ldmodelracap**, see page 456, **Vinfadjust**, see page 517, **Ejoin**, see page 516, **w3adjust**, see page 480, **w4adjust**, see page 481, **incadjust**, see page 518, **Liso**, see page 302, **fisfeed**, see page 669, **production**, see page 680, **Ebeam**, see page 681, **Eback**, see page 682, **Tcool**, see page 689, **Tirrad**, see page 688, **rho**, see page 685, **Ibeam**, see page 683, **Area**, see page 684, **radiounit**, see page 686, **yieldunit**, see page 687, **cpang**, see page 564, **egradjust**, see page 435, **ggradjust**, see page 437, **sgradjust**, see page 436, **epradjust**, see page 462, **gpradjust**, see page 464, **spradjust**, see page 463, **E0adjust**, see page 397, **Exmatchadjust**, see page 393, **Tadjust**, see page 395, **fisbaradjust**, see page 638, **fishwadjust**, see page 639, **fymodel**, see page 654, **outfy**, see page 659, **gefran**, see page 661, while the possibilities of **preeqspin**, see page 596, **ldmodel**, see page 378, were extended.

36.4 From TALYS-1.6 to TALYS-1.8

On December 23, 2013 the fourth official version of the code, TALYS-1.6, was released. Since then, the code has undergone changes that fall in the usual two categories: significant extensions

and corrections that may affect a large part of the user community, and several small bug fixes. As appendix to this manual, we add the full log file of changes since the release of TALYS-1.6. Here we list the most important updates:

- Low energy resonance cross sections were added to the output. For this, the resonance keyword was introduced. If **resonance y**, TALYS will read in resonance parameters, from various possible sources, and call the RECENT code of Red Cullen's PREPRO package[155]. Low energy pointwise resonance cross sections are added to channels like total, elastic, fission and capture. Choices for adoption of resonance parameters from various libraries can be made with the **reslib** keyword, which can be equal to default, endfb7.1, jeff3.1, jendl4.0. In addition, use can be made of Cullen's SIGMA1 code, for resonance broadening, and GROUPIE, for groupwise cross sections.
- The stand-alone Fortran version of the GEF code was added as a subroutine to enable, in principle, the evaporation of fission fragments by TALYS. For this, TALYS "loops over itself"", i.e. it is restarted internally for every excited fission fragment. The results are not yet good however. The option for this is **fymodel 3**. In principle, quantities like the neutron spectrum for evaporated fission fragments, nubar etc. are available now.
- The range of elements that is allowed in the input is extended up to Z=124, with nuclear symbols Rg(111), Cn(112), Nh(113), Fl(114), Mc(115), Lv(116), Ts(117), Og(118), B9(119), C0-4(120-124).
- More models (**strength 6, 7, 8** for gamma-ray strength functions are added.
- More models (**alphaomp 6, 7, 8** for the alpha optical model potential are added. *alphaomp 6*, i.e. of Avrigeanu et al [72] is now the default alpha OMP potential.

For TALYS-1.8 the following new keywords were introduced: **pshiftadjust**, see page 399, **resonance**, see page 575, **Tres**, see page 584, **group**, see page 582, **reslib**, see page 583, **bestend**, see page 336, **E1file**, see page 449, **Estop**, see page 313, **popMeV**, see page 312, **bestbranch**, see page 363, **breakupmodel**, see page 624, **outbinspectra**, see page 701, **ffspin**, see page 660, **skipCN**, see page 585, while the possibilities of **strength**, see page 430, **element**, see page 291, **alphaomp**, see page 501, **fymodel**, see page 654, were extended.

36.5 From TALYS-1.8 to TALYS-1.9

On December 28, 2015 the fifth official version of the code, TALYS-1.8, was released. Since then, the code has undergone changes that fall in the usual two categories: significant extensions and corrections that may affect a large part of the user community, and several small bug fixes. As appendix to this manual, we add the full log file of changes since the release of TALYS-1.8. Here we list the most important updates:

- More flexibility for gamma-ray strength functions, such as the possibility to read in M1 strength function tables.
- Extension of astrophysical reaction rate calculations to excited states.

For TALYS-1.9 the following new keywords were introduced: **M1file**, see page 450, **massdir**, see page 349, **upbendc**, see page 466, **upbende**, see page 467, **astroex**, see page 676, **nonthermlev**, see page 677, while the possibilities of **etable**, see page 443, **ftable**, see page 445, were extended.

36.6 From TALYS-1.9 to TALYS-1.95

On December 23, 2017 the sixth official version of the code, TALYS-1.9, was released. Since then, the code has undergone changes that fall in the usual two categories: significant extensions and

corrections that may affect a large part of the user community, and several small bug fixes. As appendix to this manual, we add the full log file of changes since the release of TALYS-1.9. Here we list the most important updates:

- More, and better, options for the photon strength functions (PSF). New D1M/QRPA based M1 tables are provided, including so called 'upbend' formula to scale low-energy behavior, as well as improved E1 data tables and the Simplified Modified Lorentzian (SMLO), allowing better default predictions of the PSF. This impacts both neutron capture cross sections and photonuclear data.
- For fission, a model for partial damping (so far only full damping was included) was added, including extra flexibility for damping parameters.

For TALYS-1.95 the following new keywords were introduced: **bdamp**, see page 640, **bdampadjust**, see page 641, **ctableadjust**, see page 387, **ptableadjust**, see page 389, **etableadjust**, see page 444, **ftableadjust**, see page 446, **wtable**, see page 447, **wtableadjust**, see page 448, **outkd**, see page 525, **filepsf**, see page 451, **psfglobal**, see page 452, **maxNrp**, see page 332, **maxZrp**, see page 331, **outdecay**, see page 698, **Rprime**, see page 442, **sacs**, see page 704, **upbend**, see page 465, **upbendf**, see page 468, while the possibilities of **strength**, see page 430, were extended.

36.7 From TALYS-1.95 to TALYS-1.96

On December 30, 2019 the seventh official version of the code, TALYS-1.95, was released. Since then, the code has undergone changes that fall in the usual two categories: significant extensions and corrections that may affect a large part of the user community, and several small bug fixes. As appendix to this tutorial, we add the full log file of changes since the release of TALYS-1.95. Here we list the most important updates:

- Capability to read in the distribution of excited fission fragments, per fragment pair, after which TALYS calculated the fission product yield as well as all neutron observables such as nu(A), nubar, PFNS etc. Currently, three models for excited fission fragments are included: HF3D, GEF and SPY.
- Reading of the OMP for actinides from the Reference Input Parameter Library. These OMP's are now the default for neutrons incident on actinides.
- An improved deuteron break-up model by Marilena Avrigeanu.
- Change of the default of Hauser-Feshbach binning from **equidistant n** to **equidistant y**, which improves high energy excitation functions.
- Change of the default for subactinide fission. Now **fismodel 3** is used for charged-particle induced reactions on all targets and for neutrons on subactinides, which gives a dramatic improvement for the fission cross sections.
- Change in the default adjustment parameters for break-up and stripping/pick-up reactions to improve charged-particle induced cross sections.
- Changed the default in TALYS for photon strength functions into **strength 9** (SMLO), and **strengthm1 3** with **upbend y**. This is applied for all incident particles, improving the default prediction for (n,g), (g,n), (p,g), (a,g) considerably. Automatic **wtable** parameters are read in for adjustment to capture cross sections in the fast neutron range.
- Phenomenological models for nubar (Wahl) and PFNS (Iwamoto).

For TALYS-1.96 the following new keywords were introduced: **betafiscoradjust**, see page 651, **block**, see page 695, **Cnubar1**, see page 662, **Cnubar2**, see page 663, **ffmodel**, see page 655, **fisom**, see page 454, **fispartdamp**, see page 642, **Fsadjust**, see page 657, **gadjust**, see page 611,

ldmodelCN, see page 379, **ngfit**, see page 366, **nnfit**, see page 368, **nafit**, see page 369, **pfnsmodel**, see page 656, **riplomp**, see page 527, **riplrisk**, see page 528, **Rspincutff**, see page 402, **soukho**, see page 526, **Tmadjust**, see page 658, **vfiscoradjust**, see page 652, **yieldfile**, see page 668, while the possibilities of **fymodel**, see page 654, were extended.

37. Outlook and conclusions

This manual describes TALYS-1.97/2.0, a nuclear reaction code. After several years of development, and application in various areas, by many users, we decided that after the previous (TALYS-0.64, TALYS-0.72) beta releases, the first official Version 1.0 of the code could be released at the end of 2007. After the release of TALYS-1.2 in December 2009, TALYS-1.4 in December 2011, TALYS-1.6 in December 2013, TALYS-1.8 in December 2015, TALYS-1.9 in December 2017, TALYS-1.95 in December 2019, TALYS-1.96 in December 2021, TALYS-1.97/TALYS-2.0 is the next update of that release.

We note that various extensions are possible for the physics included in TALYS, and some will be mentioned below. Obviously, we can not guarantee that these will be included in a future release (if any). This depends on the required effort, future careers of the authors, your willingness to share your extensions with us, our willingness to implement them, and in the case of significant extensions, financial input from research programs that require nuclear data.

- extension of the nuclear structure database with more tables based on microscopic nuclear structure calculations. Through trivial changes in the TALYS code, the impact of these ingredients on reaction calculations can immediately be tested.
- further development of the capability to predict reactions up to 1 GeV. Right now, a simple extension of the OMP beyond 200 MeV is included which is not based on the correct physics. In addition the first derivative of the cross sections around 200 MeV is not continuous. A semi-microscopic OMP would have to be implemented to improve this. After that, the (multiple) preequilibrium models are supposed to cover the first stages of the interaction. Obviously, at some point the omission of pion production will have an impact on the results.
- extension of TALYS to become a heavy-ion code. A double-folding OMP would have to be implemented to define the first stage of the reaction. After that, pre-equilibrium and Hauser-feshbach processes would cover the prediction of the various reaction channels.
- a few direct reaction items, such as the deformed JLM OMP developed by Eric Bauge,

accounting for discrete state transitions in (d,p) and (d,n) reactions a la FRESCO, and the prediction of the Isobaric Analogue State.

- a general analysis of all actinides simultaneously should result in a stable, ready-to-use fission database. It is clear that the theoretical fission models themselves are also not yet mature, even though microscopic fission paths are now included.

- concerning continuum reactions, there exists a microscopic multi-step direct code, MINGUS, for quantum-mechanical pre-equilibrium calculations (MSD/MSC) [156], which still needs to be merged with TALYS.

- including direct capture, discrete state gamma-ray transitions as available in the EGAF database.

As for computational possibilities, the current day computer power enables to use nuclear model codes in ways that were previously thought impossible. Applications that have already proven to be possible are the generation of nuclear-model based covariances with Monte Carlo methods, automatic multi-parameter fitting of all partial cross sections to the existing experimental data, and dripline-to-dripline generation of all cross sections over the entire energy and projectile range, see e.g. the TENDL link on our website. The applications range from basic science (e.g. astrophysics) to the production of nuclear data libraries for existing and future nuclear technologies.

There are two important satellite codes for TALYS that have appeared in the literature: TAS-MAN [157], for determining nuclear model based covariances and automatic optimization to experimental data, and TEFAL [157], for translating the results of TALYS into ENDF-6 data libraries. These are released as separate packages.

The development of TALYS has always followed the "first completeness, then quality" principle. This merely means that, in our quest for completeness, we tried to divide our effort equally among all nuclear reaction types. We think that, with the exception of a few issues the code is indeed *complete* in terms of predicted quantities. We now hope that TALYS also qualifies for "completeness and quality". Nevertheless, it is certain that future theoretical enhancements as suggested above are needed to bring our computed results even closer to measurements.

Bibliography

[1] P.G. Young, E.D. Arthur, and M.B. Chadwick. "The GNASH nuclear model code". In: *Workshop on Computation and Analysis of Nuclear Data Relevant to Nuclear Energy and Safety, edited by M.K. Mehta and J.J. Schmidt, Feb. 10 - March 13 1992, Trieste, Italy* (1993), p. 622.

[2] M. Blann. "Recent progress and current status of pre-equilibrium reaction theories and computer code ALICE". In: *Workshop on Computation and Analysis of Nuclear Data Relevant to Nuclear Energy and Safety, edited by M.K. Mehta and J.J. Schmidt, Feb. 10 - March 13 1992, Trieste, Italy* (1993), p. 622.

[3] M. Uhl and B. Strohmaier. "Computer code for particle induced activation cross sections and related quantities". In: *IRK Vienna report* 76/01 (1976).

[4] M. Herman et al. "EMPIRE: Nuclear Reaction Model Code System for Data Evaluation". In: *Nucl. Data Sheets* 108 (2007), p. 2655.

[5] J. Raynal. "Notes on ECIS94". In: *CEA Saclay Report* CEA-N-2772 (1994).

[6] R. Capote et al. "RIPL - Reference Input Parameter Library for Calculation of Nuclear Reactions and Nuclear Data Evaluations". In: *Nucl.Data Sheets* 110 (2009), p. 3107.

[7] R. Michel et al. "Cross sections for the production of residual nuclides by low- and medium-energy protons from the target elements C, N, O, Mg, Al, Si, Ca, Ti, V, Mn, Fe, Co, Ni, Cu, Sr, Y, Zr, Nb, Ba and Au". In: *Nuclear Instruments and Methods in Physics Research Section B: Beam Interactions with Materials and Atoms* 129 (1997), pp. 153–193. DOI: 10.1016/S0168-583X(97)00213-9.

[8] H. Vonach et al. "^{207,208}Pb(n,xnγ) reactions for neutron energies from 3 to 200 MeV". In: *Phys. Rev. C* 50 (4 1994), pp. 1952–1963. DOI: 10.1103/PhysRevC.50.1952. URL: https://link.aps.org/doi/10.1103/PhysRevC.50.1952.

[9]   A. Marcinkowski et al. "Neutron emission cross sections on ^{93}Nb and ^{209}Bi at 20 MeV
      incident energy". In: *Nuclear Physics A* 530 (1991), pp. 75–93. DOI: 10.1016/0375-
      9474(91)90756-V.

[10] M. Sin et al. "Fission of light actinides: ^{232}Th(n,f) and ^{231}Pa(n,f) reactions". In: *Phys.
      Rev. C* 74 (1 July 2006), p. 014608. DOI: 10.1103/PhysRevC.74.014608. URL: https:
      //link.aps.org/doi/10.1103/PhysRevC.74.014608.

[11] S. Goriely, S. Hilaire, and A. J. Koning. "Improved Predictions of Nuclear Reaction
      Rates with the TALYS Reaction Code for Astrophysical Applications". In: *Astronomy &
      Astrophysics* 487.2 (2008), pp. 767–774. ISSN: 0004-6361. DOI: 10.1051/0004-6361:
      20078825.

[12] A.M. Baldin. "Kinematics of Nuclear Reactions, Oxford University Press". In: (1961).

[13] M. B. Chadwick et al. "Cross-Section Evaluations to 150 MeV for Accelerator-Driven
      Systems and Implementation in MCNPX". In: *Nuclear Science and Engineering* 131.3
      (1999), pp. 293–328. DOI: 10.13182/NSE98-48. URL: https://doi.org/10.13182/
      NSE98-48.

[14] M.B. Chadwick et al. "High Energy Nuclear Data Libraries for Accelerator-Driven Tech-
      nologies: Calculational Method for Heavy Recoils". In: *Second International Conference
      on Accelerator-Driven Transmutation Technologies and Applications, Kalmar, Sweden,
      June 3-7 1996* (1996), p. 483.

[15] J.-C. Sublet et al. "EASY-II(12): modern modelling of n, d, p, g, a activation and trans-
      mutation processes". In: *Proceedings of the 12th Intewrnational conference on Radiation
      Shielding, Sep 2-7 2012, Nara, Japan, Progress in Nuclear Science and Technology* (2013).

[16] R.A. Forrest and J. Kopecky. "EASY-2005: Validation and new tools for data checking".
      In: *Fusion Engineering and Design* 82.15 (2007). Proceedings of the 24th Symposium on
      Fusion Technology, pp. 2471–2477. ISSN: 0920-3796. DOI: https://doi.org/10.1016/
      j.fusengdes.2007.04.032. URL: https://www.sciencedirect.com/science/
      article/pii/S0920379607001779.

[17] W.J. Huang et al. "The AME2016 atomic mass evaluation (I)". In: *Chinese Physics* C41, 3
      (2017), p. 030002.

[18] S. Goriely, N. Chamel, and J. M. Pearson. "Skyrme-Hartree-Fock-Bogoliubov Nuclear
      Mass Formulas: Crossing the 0.6 MeV Accuracy Threshold with Microscopically Deduced
      Pairing". In: *Phys. Rev. Lett.* 102 (15 Apr. 2009), p. 152503. DOI: 10.1103/PhysRevLett.
      102.152503. URL: https://link.aps.org/doi/10.1103/PhysRevLett.102.
      152503.

[19] S. Goriely et al. "The Gogny-Hartree-Fock-Bogoliubov nuclear-mass model". In: *European
      Physical Journal A* 52 (2016), p. 202.

[20] P. Moller et al. "Nuclear ground-state masses and deformations: FRDM(2012)". In: *Chinese
      Physics* 109 (2016), pp. 1–204.

[21] J. Duflo and A.P. Zuker. "Microscopic mass formulas". In: *Phys. Rev. C* 52 (1 July 1995),
      R23–R27. DOI: 10.1103/PhysRevC.52.R23. URL: https://link.aps.org/doi/10.
      1103/PhysRevC.52.R23.

[22] A.J. Koning, S. Hilaire, and S. Goriely. "Global and local level density models". In: *Nuclear Physics A* 810.1 (2008), pp. 13–76. ISSN: 0375-9474. DOI: https://doi.org/10.1016/j.nuclphysa.2008.06.005. URL: https://www.sciencedirect.com/science/article/pii/S0375947408005903.

[23] T. Ericson. "The statistical model and nuclear level densities". In: *Adv. Phys.* 9 (1960), pp. 425–511.

[24] A. Gilbert and A.G.W. Cameron. "A composite nuclear-level density formula with shell corrections". In: *Can. J. Phys.* 43 (1965), pp. 1446–1496.

[25] W. Dilg et al. "Level density parameters for the Back-Shifted Fermi gas model in the mass range 40 < A < 250". In: *Nuclear Physics A* 217.2 (1973), pp. 269–298. ISSN: 0375-9474. DOI: https://doi.org/10.1016/0375-9474(73)90196-6. URL: https://www.sciencedirect.com/science/article/pii/0375947473901966.

[26] H. Baba. "A shell-model nuclear level density". In: *Nuclear Physics A* 159.2 (1970), pp. 625–641. ISSN: 0375-9474. DOI: https://doi.org/10.1016/0375-9474(70)90862-6. URL: https://www.sciencedirect.com/science/article/pii/0375947470908626.

[27] A.V. Ignatyuk, G.N. Smirenkin, and A.S. Tishin. "Phenomenological description of energy dependence of the level density parameter". In: *Sov. J. Nucl. Phys.* 21, no. 3 (1975), p. 255.

[28] A. Mengoni and Y. Nakajima. "Fermi-Gas Model Parametrization of Nuclear Level Density". In: *J. Nucl. Sci. Techn.* 31 (1994), pp. 151–162.

[29] William D. Myers and Wladyslaw J. Swiatecki. "Nuclear masses and deformations". In: *Nuclear Physics* 81.1 (1966), pp. 1–60. ISSN: 0029-5582. DOI: https://doi.org/10.1016/0029-5582(66)90639-0. URL: https://www.sciencedirect.com/science/article/pii/0029558266906390.

[30] S. Goriely. "A new nuclear level density formula including shell and pairing correction in the light of a microscopic model calculation". In: *Nuclear Physics A* 605.1 (1996), pp. 28–60. ISSN: 0375-9474. DOI: https://doi.org/10.1016/0375-9474(96)00162-5. URL: https://www.sciencedirect.com/science/article/pii/0375947496001625.

[31] S. Hilaire. In: *PhD thesis, unpublished* (1997).

[32] S. F. Mughabghab and C. Dunford. "Nuclear Level Density and the Effective Nucleon Mass". In: *Phys. Rev. Lett.* 81 (19 Nov. 1998), pp. 4083–4086. DOI: 10.1103/PhysRevLett.81.4083. URL: https://link.aps.org/doi/10.1103/PhysRevLett.81.4083.

[33] M.K. Grossjean and H. Feldmeier. "Level density of a Fermi gas with pairing interactions". In: *Nuclear Physics A* 444.1 (1985), pp. 113–132. ISSN: 0375-9474. DOI: https://doi.org/10.1016/0375-9474(85)90294-5. URL: https://www.sciencedirect.com/science/article/pii/0375947485902945.

[34] P. Demetriou and S. Goriely. "Microscopic nuclear level densities for practical applications". In: *Nuclear Physics A* 695.1 (2001), pp. 95–108. ISSN: 0375-9474. DOI: https://doi.org/10.1016/S0375-9474(01)01095-8. URL: https://www.sciencedirect.com/science/article/pii/S0375947401010958.

[35] A.V. Ignatyuk, K.K. Istekov, and G.N. Smirenkin. "The role of collective effects in the systematics of nuclear level densities". In: *Sov. J. Nucl. Phys.* 29, no. 4 (1979), p. 450.

[36] A. V. Ignatyuk et al. "Density of discrete levels in ^{116}Sn". In: *Phys. Rev. C* 47 (4 Apr. 1993), pp. 1504–1513. DOI: 10.1103/PhysRevC.47.1504. URL: https://link.aps.org/doi/10.1103/PhysRevC.47.1504.

[37] O.T. Grudzevich et al. "Consistent Systematics of Level Density for Medium and Heavy Nuclei". In: *Proc. Nuclear Data for Science and Technology (Mito, JAERI)* (1988), p. 187.

[38] A.S. Iljinov et al. "Phenomenological statistical analysis of level densities, decay widths and lifetimes of excited nuclei". In: *Nuclear Physics A* 543.3 (1992), pp. 517–557. ISSN: 0375-9474. DOI: https://doi.org/10.1016/0375-9474(92)90278-R. URL: https://www.sciencedirect.com/science/article/pii/037594749290278R.

[39] A.R. Junghans et al. "Projectile-fragment yields as a probe for the collective enhancement in the nuclear level density". In: *Nuclear Physics A* 629.3 (1998), pp. 635–655. ISSN: 0375-9474. DOI: https://doi.org/10.1016/S0375-9474(98)00658-7. URL: https://www.sciencedirect.com/science/article/pii/S0375947498006587.

[40] G. Hansen and A.S. Jensen. "Energy dependence of the rotational enhancement factor in the level density". In: *Nuclear Physics A* 406.2 (1983), pp. 236–256. ISSN: 0375-9474. DOI: https://doi.org/10.1016/0375-9474(83)90459-1. URL: https://www.sciencedirect.com/science/article/pii/0375947483904591.

[41] S. Goriely, F. Tondeur, and J.M. Pearson. In: *Atom. Data Nucl. Data Tables* 77 (2001), p. 311.

[42] S. Goriely, S. Hilaire, and A. J. Koning. "Improved microscopic nuclear level densities within the Hartree-Fock-Bogoliubov plus combinatorial method". In: *Phys. Rev. C* 78 (6 Dec. 2008), p. 064307. DOI: 10.1103/PhysRevC.78.064307. URL: https://link.aps.org/doi/10.1103/PhysRevC.78.064307.

[43] S. Hilaire et al. "Temperature-dependent combinatorial level densities with the D1M Gogny force". In: *Phys. Rev. C* 86 (6 Dec. 2012), p. 064317. DOI: 10.1103/PhysRevC.86.064317. URL: https://link.aps.org/doi/10.1103/PhysRevC.86.064317.

[44] V.A. Plujko et al. "Giant dipole resonance parameters of ground-state photoabsorption: Experimental values with uncertainties". In: *At. Data Nucl. Data Tables* 123 (2018), p. 1.

[45] S. Goriely et al. "Reference Database for Photon Strength Functions". In: *Eur. Phys. J. A* 55 (2019), p. 172.

[46] D.M. Brink. "Individual particle and collective aspects of the nuclear photoeffect". In: *Nuclear Physics* 4 (1957), pp. 215–220. ISSN: 0029-5582. DOI: https://doi.org/10.1016/0029-5582(87)90021-6. URL: https://www.sciencedirect.com/science/article/pii/0029558287900216.

[47] Peter Axel. "Electric Dipole Ground-State Transition Width Strength Function and 7-MeV Photon Interactions". In: *Phys. Rev.* 126 (2 Apr. 1962), pp. 671–683. DOI: 10.1103/PhysRev.126.671. URL: https://link.aps.org/doi/10.1103/PhysRev.126.671.

[48] J. Kopecky and M. Uhl. "Test of gamma-ray strength functions in nuclear reaction model calculations". In: *Phys. Rev. C* 41 (5 May 1990), pp. 1941–1955. DOI: 10.1103/PhysRevC.41.1941. URL: https://link.aps.org/doi/10.1103/PhysRevC.41.1941.

[49] J. Kopecky, M. Uhl, and R. E. Chrien. "Radiative strength in the compound nucleus ^{157}Gd". In: *Phys. Rev. C* 47 (1 Jan. 1993), pp. 312–322. DOI: 10.1103/PhysRevC.47.312. URL: https://link.aps.org/doi/10.1103/PhysRevC.47.312.

[50] S. Goriely. "Radiative neutron captures by neutron-rich nuclei and the r-process nucleosynthesis". In: *Physics Letters B* 436.1 (1998), pp. 10–18. ISSN: 0370-2693. DOI: `https://doi.org/10.1016/S0370-2693(98)00907-1`. URL: `https://www.sciencedirect.com/science/article/pii/S0370269398009071`.

[51] S. Goriely and E. Khan. "Large-scale QRPA calculation of E1-strength and its impact on the neutron capture cross section". In: *Nuclear Physics A* 706.1 (2002), pp. 217–232. ISSN: 0375-9474. DOI: `https://doi.org/10.1016/S0375-9474(02)00860-6`. URL: `https://www.sciencedirect.com/science/article/pii/S0375947402008606`.

[52] S Goriely, E Khan, and M Samyn. "Microscopic HFB + QRPA predictions of dipole strength for astrophysics applications". In: *Nuclear Physics A* 739.3 (2004), pp. 331–352. ISSN: 0375-9474. DOI: `https://doi.org/10.1016/j.nuclphysa.2004.04.105`. URL: `https://www.sciencedirect.com/science/article/pii/S0375947404006578`.

[53] I. Daoutidis and S. Goriely. "Large-scale continuum random-phase approximation predictions of dipole strength for astrophysical applications". In: *Phys. Rev. C* 86 (3 Sept. 2012), p. 034328. DOI: `10.1103/PhysRevC.86.034328`. URL: `https://link.aps.org/doi/10.1103/PhysRevC.86.034328`.

[54] S. Goriely et al. "Gogny-HFB+QRPA dipole strength function and its application to radiative nucleon capture cross section". In: *Phys. Rev. C* 98 (1 July 2018), p. 014327. DOI: `10.1103/PhysRevC.98.014327`. URL: `https://link.aps.org/doi/10.1103/PhysRevC.98.014327`.

[55] B. L. Berman et al. "Photoneutron Cross Sections for Zr^{90}, Zr^{91}, Zr^{92}, Zr^{94}, and Y^{89}". In: *Phys. Rev.* 162 (4 Oct. 1967), pp. 1098–1111. DOI: `10.1103/PhysRev.162.1098`. URL: `https://link.aps.org/doi/10.1103/PhysRev.162.1098`.

[56] D.G. Gardner. "Neutron Radiative Capture". In: (1984), p. 62.

[57] M. B. Chadwick et al. "Pauli-blocking in the quasideuteron model of photoabsorption". In: *Phys. Rev. C* 44 (2 Aug. 1991), pp. 814–823. DOI: `10.1103/PhysRevC.44.814`. URL: `https://link.aps.org/doi/10.1103/PhysRevC.44.814`.

[58] Yi Xu and Stephane Goriely. "Systematic study of direct neutron capture". In: *Phys. Rev. C* 86 (4 Oct. 2012), p. 045801. DOI: `10.1103/PhysRevC.86.045801`. URL: `https://link.aps.org/doi/10.1103/PhysRevC.86.045801`.

[59] A.J. Koning and J.P. Delaroche. "Local and global nucleon optical models from 1 keV to 200 MeV". In: *Nuclear Physics A* 713.3 (2003), pp. 231–310. ISSN: 0375-9474. DOI: `https://doi.org/10.1016/S0375-9474(02)01321-0`. URL: `https://www.sciencedirect.com/science/article/pii/S0375947402013210`.

[60] A.J. Koning, D. Rochman, and S.C. van der Marck. "Extension of TALYS to 1 GeV". In: *Nuclear Data Sheets* 118 (2014), pp. 187–190. ISSN: 0090-3752. DOI: `https://doi.org/10.1016/j.nds.2014.04.033`. URL: `https://www.sciencedirect.com/science/article/pii/S0090375214000635`.

[61] S. Typel, O. Riedl, and H.H. Wolter. "Elastic proton-nucleus scattering and the optical potential in a relativistic mean field model". In: *Nuclear Physics A* 709.1 (2002), pp. 299–318. ISSN: 0375-9474. DOI: `https://doi.org/10.1016/S0375-9474(02)01031-X`. URL: `https://www.sciencedirect.com/science/article/pii/S037594740201031X`.

[62] Satoshi Chiba et al. "The isovector/isoscalar ratio of the imaginary part of the intermediate-energy nucleon optical model potential studied by the quantum molecular dynamics". In: *Spec. Meet. on the nucleon nucleus optical model up to 200 MeV, Bruyeres-le-Chatel* (1996).

[63] Shigueo Watanabe. "High energy scattering of deuterons by complex nuclei". In: *Nuclear Physics* 8 (1958), pp. 484–492. ISSN: 0029-5582. DOI: `https://doi.org/10.1016/0029-5582(58)90180-9`. URL: `https://www.sciencedirect.com/science/article/pii/0029558258901809`.

[64] D.G. Madland. "Recent results in the development of a global medium-energy nucleon-nucleus optical model potential". In: *Proceedings of a Specialists' Meeting on preequilibrium nuclear reactions, Semmering, Austria, February 10-12 1988* (), p. 103.

[65] W. W. Daehnick, J. D. Childs, and Z. Vrcelj. "Global optical model potential for elastic deuteron scattering from 12 to 90 MeV". In: *Phys. Rev. C* 21 (6 June 1980), pp. 2253–2274. DOI: `10.1103/PhysRevC.21.2253`. URL: `https://link.aps.org/doi/10.1103/PhysRevC.21.2253`.

[66] J. Bojowald et al. "Elastic deuteron scattering and optical model parameters at energies up to 100 MeV". In: *Phys. Rev. C* 38 (3 Sept. 1988), pp. 1153–1163. DOI: `10.1103/PhysRevC.38.1153`. URL: `https://link.aps.org/doi/10.1103/PhysRevC.38.1153`.

[67] Yinlu Han, Yuyang Shi, and Qingbiao Shen. "Deuteron global optical model potential for energies up to 200 MeV". In: *Phys. Rev. C* 74 (4 Oct. 2006), p. 044615. DOI: `10.1103/PhysRevC.74.044615`. URL: `https://link.aps.org/doi/10.1103/PhysRevC.74.044615`.

[68] Haixia An and Chonghai Cai. "Global deuteron optical model potential for the energy range up to 183 MeV". In: *Phys. Rev. C* 73 (5 May 2006), p. 054605. DOI: `10.1103/PhysRevC.73.054605`. URL: `https://link.aps.org/doi/10.1103/PhysRevC.73.054605`.

[69] Lynne McFadden and G.R. Satchler. "Optical-model analysis of the scattering of 24.7 MeV alpha particles". In: *Nuclear Physics* 84.1 (1966), pp. 177–200. ISSN: 0029-5582. DOI: `https://doi.org/10.1016/0029-5582(66)90441-X`. URL: `https://www.sciencedirect.com/science/article/pii/002955826690441X`.

[70] P. Demetriou, C. Grama, and S. Goriely. "Improved global alpha-optical model potentials at low energies". In: *Nuclear Physics A* 707.1 (2002), pp. 253–276. ISSN: 0375-9474. DOI: `https://doi.org/10.1016/S0375-9474(02)00756-X`. URL: `https://www.sciencedirect.com/science/article/pii/S037594740200756X`.

[71] J. Glorius et al. "Experimental cross sections of ^{165}Ho$(\alpha,n)^{168}$Tm and ^{166}Er$(\alpha,n)^{169}$Yb for optical potential studies relevant for the astrophysical γ process". In: *Phys. Rev. C* 89 (6 2014), p. 065808. DOI: `10.1103/PhysRevC.89.065808`. URL: `https://link.aps.org/doi/10.1103/PhysRevC.89.065808`.

[72] V. Avrigeanu, M. Avrigeanu, and C. Mihaelescu. "Further explorations of the α-particle optical model potential at low energies for the mass range A$\approx$ 45–209". In: *Phys. Rev. C* 90 (4 2014), p. 044612. DOI: `10.1103/PhysRevC.90.044612`. URL: `https://link.aps.org/doi/10.1103/PhysRevC.90.044612`.

[73] E. Bauge, J. P. Delaroche, and M. Girod. "Lane-consistent, semimicroscopic nucleon-nucleus optical model". In: *Phys. Rev. C* 63 (2 Jan. 2001), p. 024607. DOI: 10.1103/PhysRevC.63.024607. URL: https://link.aps.org/doi/10.1103/PhysRevC.63.024607.

[74] F. Maréchal et al. "Proton scattering by short lived sulfur isotopes". In: *Phys. Rev. C* 60 (3 Aug. 1999), p. 034615. DOI: 10.1103/PhysRevC.60.034615. URL: https://link.aps.org/doi/10.1103/PhysRevC.60.034615.

[75] H. Scheit et al. "Proton scattering by the unstable neutron-rich isotopes ^{42,44}Ar". In: *Phys. Rev. C* 63 (1 Dec. 2000), p. 014604. DOI: 10.1103/PhysRevC.63.014604. URL: https://link.aps.org/doi/10.1103/PhysRevC.63.014604.

[76] E. Khan et al. "Proton scattering from the unstable nuclei 30S and 34Ar: structural evolution along the sulfur and argon isotopic chains". In: *Nucl. Phys* A694 (2001), p. 103.

[77] E. Bauge et al. "Neutron scattering from the ^{155,156,157,158,160}Gd isotopes: Measurements and analyses with a deformed, semimicroscopic optical model". In: *Phys. Rev. C* 61 (3 Feb. 2000), p. 034306. DOI: 10.1103/PhysRevC.61.034306. URL: https://link.aps.org/doi/10.1103/PhysRevC.61.034306.

[78] J.P Jeukenne, A Lejeune, and C Mahaux. "Many-body theory of nuclear matter". In: *Physics Reports* 25.2 (1976), pp. 83–174. ISSN: 0370-1573. DOI: https://doi.org/10.1016/0370-1573(76)90017-X. URL: https://www.sciencedirect.com/science/article/pii/037015737690017X.

[79] J. -P. Jeukenne, A. Lejeune, and C. Mahaux. "Optical-model potential in nuclear matter from Reid's hard core interaction". In: *Phys. Rev. C* 10 (4 Oct. 1974), pp. 1391–1401. DOI: 10.1103/PhysRevC.10.1391. URL: https://link.aps.org/doi/10.1103/PhysRevC.10.1391.

[80] J. -P. Jeukenne, A. Lejeune, and C. Mahaux. "Microscopic calculation of the symmetry and Coulomb components of the complex optical-model potential". In: *Phys. Rev. C* 15 (1 Jan. 1977), pp. 10–29. DOI: 10.1103/PhysRevC.15.10. URL: https://link.aps.org/doi/10.1103/PhysRevC.15.10.

[81] J.-P. Jeukenne, A. Lejeune, and C. Mahaux. "Optical-model potential in finite nuclei from Reid's hard core interaction". In: *Phys. Rev. C* 16 (1 July 1977), pp. 80–96. DOI: 10.1103/PhysRevC.16.80. URL: https://link.aps.org/doi/10.1103/PhysRevC.16.80.

[82] E. Bauge, J. P. Delaroche, and M. Girod. "Semimicroscopic nucleon-nucleus spherical optical model for nuclei with A > 40 at energies up to 200 MeV". In: *Phys. Rev. C* 58 (2 Aug. 1998), pp. 1118–1145. DOI: 10.1103/PhysRevC.58.1118. URL: https://link.aps.org/doi/10.1103/PhysRevC.58.1118.

[83] Robert R. Scheerbaum. "Spin-orbit splitting in nuclei near closed shells: (I). Contribution of the two-body spin-orbit interaction". In: *Nuclear Physics A* 257.1 (1976), pp. 77–108. ISSN: 0375-9474. DOI: https://doi.org/10.1016/0375-9474(76)90476-0. URL: https://www.sciencedirect.com/science/article/pii/0375947476904760.

[84] R.K. Tripathi, F.A. Cucinotta, and J.W. Wilson. In: *NASA technical paper 3621* (1997).

[85]   Taro Tamura. "Analyses of the Scattering of Nuclear Particles by Collective Nuclei in Terms of the Coupled-Channel Calculation". In: *Rev. Mod. Phys.* 37 (4 Oct. 1965), pp. 679–708. DOI: 10.1103/RevModPhys.37.679. URL: https://link.aps.org/doi/10.1103/RevModPhys.37.679.

[86]   J.P. Delaroche. "Use of coupled-channel optical model calculations in nuclear data evaluations for incident energies up to 1 GeV". In: *Proceedings of the International Symposium on Nuclear Data Evaluation Methodology, ed. C.L. Dunford, October 12-16 1992, Brookhaven, USA* (1992), p. 347.

[87]   N. Olsson, E. Ramström, and B. Trostell. "Neutron elastic and inelastic scattering from Mg, Si, S, Ca, Cr, Fe and Ni at En = 21.6 MeV". In: *Nuclear Physics A* 513 (1990), pp. 205–238. DOI: 10.1016/0375-9474(90)90096-5.

[88]   B.V. Carlsson. "Optical model calculations with the code ECIS95". In: *Workshop on Nuclear Reaction Data and Nuclear Reactors: Physics, Design and Safety, edited by N. Paver, M. Herman and A. Gandini, March 13 - April 14 2000, Trieste Italy* (2001), p. 61.

[89]   Efrem Sh Soukhovitskii et al. "Global coupled-channel optical potential for nucleon-actinide interaction from 1 keV to 200 MeV". In: *Journal of Physics G: Nuclear and Particle Physics* 30.7 (May 2004), p. 905. DOI: 10.1088/0954-3899/30/7/007. URL: https://dx.doi.org/10.1088/0954-3899/30/7/007.

[90]   P. P. Guss et al. "Optical model description of the neutron interaction with ^{116}Sn and ^{120}Sn over a wide energy range". In: *Phys. Rev. C* 39 (2 Feb. 1989), pp. 405–414. DOI: 10.1103/PhysRevC.39.405. URL: https://link.aps.org/doi/10.1103/PhysRevC.39.405.

[91]   G.R. Satchler. "Direct Nuclear Reactions, Clarendon Press". In: (1983).

[92]   P.E. Hodgson. "Nuclear Reactions and Nuclear Structure". In: *Clarendon Press, Oxford* (1971).

[93]   A. van der Woude. "Electric and Magnetic Giant Resonances in Nuclei". In: (1991), pp. 99–232.

[94]   C. Kalbach. "Surface and collective effects in preequilibrium reactions". In: *Phys. Rev. C* 62 (4 Sept. 2000), p. 044608. DOI: 10.1103/PhysRevC.62.044608. URL: https://link.aps.org/doi/10.1103/PhysRevC.62.044608.

[95]   A.J. Koning and M.C. Duijvestijn. "A global pre-equilibrium analysis from 7 to 200 MeV based on the optical model potential". In: *Nuclear Physics A* 744 (2004), pp. 15–76. ISSN: 0375-9474. DOI: https://doi.org/10.1016/j.nuclphysa.2004.08.013. URL: https://www.sciencedirect.com/science/article/pii/S037594740400870X.

[96]   H. Gruppelaar, P. Nagel, and P.E. Hodgson. "Pre-Equilibrium Processes in Nuclear Reaction Theory". In: *Riv. Nuovo Cimento* 9, No. 7 (1986), p. 1.

[97]   E. Gadioli and P.E. Hodgson. "Pre-equilibrium nuclear reactions". In: (1992).

[98]   C. Kalbach. "Two-component exciton model: Basic formalism away from shell closures". In: *Phys. Rev. C* 33 (3 Mar. 1986), pp. 818–833. DOI: 10.1103/PhysRevC.33.818. URL: https://link.aps.org/doi/10.1103/PhysRevC.33.818.

[99] C.K. Cline and M. Blann. "The pre-equilibrium statistical model: Description of the nuclear equilibration process and parameterization of the model". In: *Nuclear Physics A* 172.2 (1971), pp. 225–259. ISSN: 0375-9474. DOI: https://doi.org/10.1016/0375-9474(71)90713-5. URL: https://www.sciencedirect.com/science/article/pii/0375947471907135.

[100] J. Dobeš and E. Běták. "Two-component exciton model". In: *Zeit. Phys.* A310 (1983), p. 329.

[101] E. Běták and J. Dobeš. "The finite depth of the nuclear potential well in the exciton model of preequilibrium decay". In: *Zeit. Phys.* A279 (1976), p. 319.

[102] C.Y. Fu. "Implementation of on Advanced Pairing Correction for Particle-Hole State Densities in Precompound Nuclear Reaction Theory". In: *Nucl. Sci. Eng.* 86 (1984), p. 344.

[103] C. Kalbach. "Surface effects in the exciton model of preequilibrium nuclear reactions". In: *Phys. Rev. C* 32 (4 Oct. 1985), pp. 1157–1168. DOI: 10.1103/PhysRevC.32.1157. URL: https://link.aps.org/doi/10.1103/PhysRevC.32.1157.

[104] C. Kalbach. "Two-component exciton model: Basic formalism away from shell closures". In: *Phys. Rev. C* 33 (3 Mar. 1986), pp. 818–833. DOI: 10.1103/PhysRevC.33.818. URL: https://link.aps.org/doi/10.1103/PhysRevC.33.818.

[105] C. Kalbach-Cline. "Residual two-body matrix elements for pre-equilibrium calculations". In: *Nuclear Physics A* 210.3 (1973), pp. 590–604. ISSN: 0375-9474. DOI: https://doi.org/10.1016/0375-9474(73)90296-0. URL: https://www.sciencedirect.com/science/article/pii/0375947473902960.

[106] Frederick C. Williams. "Particle-hole state density in the uniform spacing model". In: *Nuclear Physics A* 166.2 (1971), pp. 231–240. ISSN: 0375-9474. DOI: https://doi.org/10.1016/0375-9474(71)90426-X. URL: https://www.sciencedirect.com/science/article/pii/037594747190426X.

[107] J.M. Akkermans and H. Gruppelaar. "Analysis of continuum gamma-ray emission in precompound-decay reactions". In: *Physics Letters B* 157.2 (1985), pp. 95–100. ISSN: 0370-2693. DOI: https://doi.org/10.1016/0370-2693(85)91524-2. URL: https://www.sciencedirect.com/science/article/pii/0370269385915242.

[108] H. Gruppelaar. "Level density in unified preequilibrium and equilibrium models". In: *IAEA Advisory Group Meeting on Basic and Applied Problems on Nuclear Level Densities, (Brookhaven National Laboratory report, Report BNL-NCS-51694)* (1983), p. 143.

[109] C. Kalbach. "Preequilibrium reactions with complex particle channels". In: *Phys. Rev. C* 71 (3 Mar. 2005), p. 034606. DOI: 10.1103/PhysRevC.71.034606. URL: https://link.aps.org/doi/10.1103/PhysRevC.71.034606.

[110] C. Kalbach. "Phenomenological model for light-projectile breakup". In: *Phys. Rev. C* 95 (1 Jan. 2017), p. 014606. DOI: 10.1103/PhysRevC.95.014606. URL: https://link.aps.org/doi/10.1103/PhysRevC.95.014606.

[111] A.J Koning and J.M Akkermans. "Randomness in multi-step direct reactions". In: *Annals of Physics* 208.1 (1991), pp. 216–250. ISSN: 0003-4916. DOI: https://doi.org/10.1016/0003-4916(91)90345-9. URL: https://www.sciencedirect.com/science/article/pii/0003491691903459.

[112] C. Kalbach. "Systematics of continuum angular distributions: Extensions to higher energies". In: *Phys. Rev. C* 37 (6 1988), pp. 2350–2370. DOI: 10.1103/PhysRevC.37.2350. URL: https://link.aps.org/doi/10.1103/PhysRevC.37.2350.

[113] E. Raeymackers et al. "Light charged particle production in the interaction of fast neutrons (25-65 MeV) with uranium nuclei". In: *Phys.Rev. C* 68 (2003), p. 024604.

[114] A. A. Cowley et al. "Preequilibrium proton emission induced by 80 and 120 MeV protons incident on ^{90}Zr". In: *Phys. Rev. C* 43 (2 1991), pp. 678–686. DOI: 10.1103/PhysRevC.43.678. URL: https://link.aps.org/doi/10.1103/PhysRevC.43.678.

[115] W. Scobel et al. "Preequilibrium (p,n) reaction as a probe for the effective nucleon-nucleon interaction in multistep direct processes". In: *Phys. Rev. C* 41 (5 1990), pp. 2010–2020. DOI: 10.1103/PhysRevC.41.2010. URL: https://link.aps.org/doi/10.1103/PhysRevC.41.2010.

[116] J.W. Tepel, H.M. Hofmann, and H.A. Weidenmueller. "Hauser-Feshbach formulas for medium and strong absorption". In: *Physics Letters B* 49.1 (1974), pp. 1–4. ISSN: 0370-2693. DOI: https://doi.org/10.1016/0370-2693(74)90565-6. URL: https://www.sciencedirect.com/science/article/pii/0370269374905656.

[117] H.M Hofmann et al. "Direct reactions and Hauser-Feshbach theory". In: *Annals of Physics* 90.2 (1975), pp. 403–437. ISSN: 0003-4916. DOI: https://doi.org/10.1016/0003-4916(75)90005-6. URL: https://www.sciencedirect.com/science/article/pii/0003491675900056.

[118] H.M. Hofmann et al. "Hauser-Feshbach calculations in the presence of weakly absorbing channels with special reference to the elastic enhancement factor and the factorization assumption". In: *Zeit. Phys.* A297 (1980), p. 153.

[119] P. A. Moldauer. "Evaluation of the fluctuation enhancement factor". In: *Phys. Rev. C* 14 (2 Aug. 1976), pp. 764–766. DOI: 10.1103/PhysRevC.14.764. URL: https://link.aps.org/doi/10.1103/PhysRevC.14.764.

[120] P.A. Moldauer. "Statistics and the average cross section". In: *Nuclear Physics A* 344.2 (1980), pp. 185–195. ISSN: 0375-9474. DOI: https://doi.org/10.1016/0375-9474(80)90671-5. URL: https://www.sciencedirect.com/science/article/pii/0375947480906715.

[121] J.J.M. Verbaarschot, H.A. Weidenmueller, and M.R. Zirnbauer. "Grassmann integration in stochastic quantum physics: The case of compound-nucleus scattering". In: *Physics Reports* 129.6 (1985), pp. 367–438. ISSN: 0370-1573. DOI: https://doi.org/10.1016/0370-1573(85)90070-5. URL: https://www.sciencedirect.com/science/article/pii/0370157385900705.

[122] S. Hilaire, Ch. Lagrange, and A.J. Koning. "Comparisons between various width fluctuation correction factors for compound nucleus reactions". In: *Annals of Physics* 306.2 (2003), pp. 209–231. ISSN: 0003-4916. DOI: https://doi.org/10.1016/S0003-4916(03)00076-9. URL: https://www.sciencedirect.com/science/article/pii/S0003491603000769.

[123] H. Gruppelaar and G. Reffo. "Some Properties of the Width Fluctuation Factor". In: *Nuclear Science and Engineering* 62.4 (1977), pp. 756–763. DOI: 10.13182/NSE77-A15219. URL: https://doi.org/10.13182/NSE77-A15219.

[124] M. B. Chadwick et al. "Multiple preequilibrium emission in Feshbach-Kerman-Koonin analyses". In: *Phys. Rev. C* 50 (2 Aug. 1994), pp. 996–1005. DOI: 10.1103/PhysRevC.50.996. URL: https://link.aps.org/doi/10.1103/PhysRevC.50.996.

[125] A. J. Koning and M. B. Chadwick. "Microscopic two-component multistep direct theory for continuum nuclear reactions". In: *Phys. Rev. C* 56 (2 Aug. 1997), pp. 970–994. DOI: 10.1103/PhysRevC.56.970. URL: https://link.aps.org/doi/10.1103/PhysRevC.56.970.

[126] P Romain, B Morillon, and AJ Koning. "Neutron actinides evaluations with the TALYS code". In: *NEMEA-3 Neutron Measurements, Evaluations and Applications* 25 (2006), p. 113.

[127] E.V. Gai et al. "Two-bump barrier and the neutron-induced nuclear fission". In: *Physics and Chemistry of Fission, IAEA, Vienna* (1969), p. 337.

[128] A. Mamdouh et al. "Fission barriers of neutron-rich and superheavy nuclei calculated with the ETFSI method". In: *Nuclear Physics A* 679.3 (2001), pp. 337–358. ISSN: 0375-9474. DOI: https://doi.org/10.1016/S0375-9474(00)00358-4. URL: https://www.sciencedirect.com/science/article/pii/S0375947400003584.

[129] Arnold J. Sierk. "Macroscopic model of rotating nuclei". In: *Phys. Rev. C* 33 (6 June 1986), pp. 2039–2053. DOI: 10.1103/PhysRevC.33.2039. URL: https://link.aps.org/doi/10.1103/PhysRevC.33.2039.

[130] S. Cohen, F. Plasil, and W.J. Swiatecki. "Equilibrium configurations of rotating charged or gravitating liquid masses with surface tension". In: *Annals of Physics* 82.2 (1974), pp. 557–596. ISSN: 0003-4916. DOI: https://doi.org/10.1016/0003-4916(74)90126-2. URL: https://www.sciencedirect.com/science/article/pii/0003491674901262.

[131] A. D'Arrigo et al. "Semi-empirical determination of the shell correction temperature and spin dependence by means of nuclear fission". In: *Journ. Phys. G* 20 (1994), pp. 365–376.

[132] Karl-Heinz Schmidt and Beatriz Jurado. "Thermodynamics of nuclei in thermal contact". In: *Phys. Rev. C* 83 (1 Jan. 2011), p. 014607. DOI: 10.1103/PhysRevC.83.014607. URL: https://link.aps.org/doi/10.1103/PhysRevC.83.014607.

[133] M. C. Duijvestijn, A. J. Koning, and F.-J. Hambsch. "Mass distributions in nucleon-induced fission at intermediate energies". In: *Phys. Rev. C* 64 (1 June 2001), p. 014607. DOI: 10.1103/PhysRevC.64.014607. URL: https://link.aps.org/doi/10.1103/PhysRevC.64.014607.

[134] Ulrich Brosa, Siegfried Grossmann, and Andreas Müller. "Nuclear scission". In: *Physics Reports* 197.4 (1990), pp. 167–262. ISSN: 0370-1573. DOI: https://doi.org/10.1016/0370-1573(90)90114-H. URL: https://www.sciencedirect.com/science/article/pii/037015739090114H.

[135] W.D. Myers and W.S. Swiatecki. In: *Ark. Fysik* 36 (1967), p. 593.

[136] B. D. Wilkins, E. P. Steinberg, and R. R. Chasman. "Scission-point model of nuclear fission based on deformed-shell effects". In: *Phys. Rev. C* 14 (5 Nov. 1976), pp. 1832–1863. DOI: 10.1103/PhysRevC.14.1832. URL: https://link.aps.org/doi/10.1103/PhysRevC.14.1832.

[137] F. Vivès et al. "Investigation of the fission fragment properties of the reaction ^{238}U (n,f) at incident neutron energies up to 5.8 MeV". In: *Nuclear Physics A* 662 (2000), pp. 63–92. DOI: 10.1016/S0375-9474(99)00413-3.

[138] S. Nagy et al. "Mass distributions in monoenergetic-neutron-induced fission of ^{238}U". In: *Phys. Rev. C* 17 (1 1978), pp. 163–171. DOI: 10.1103/PhysRevC.17.163. URL: https://link.aps.org/doi/10.1103/PhysRevC.17.163.

[139] T. C. Chapman et al. "Fission product yields from 6-9 MeV neutron-induced fission of ^{235}U and ^{238}U". In: *Phys. Rev. C* 17 (3 1978), pp. 1089–1097. DOI: 10.1103/PhysRevC.17.1089. URL: https://link.aps.org/doi/10.1103/PhysRevC.17.1089.

[140] J. Kopecky et al. "Revisions and extensions of neutron capture cross-sections in the European Activation File EAF-3". In: *ECN-C–92-051, July 1992* (1992).

[141] S.F. Mughabghab. "Atlas of Neutron Resonances, 5th edition, Elsevier Publisher". In: (2006).

[142] S. Lemaire et al. "Monte Carlo approach to sequential neutron emission from fission fragments". In: *Phys. Rev. C* 72 (2 Aug. 2005), p. 024601. DOI: 10.1103/PhysRevC.72.024601. URL: https://link.aps.org/doi/10.1103/PhysRevC.72.024601.

[143] J.A. Holmes et al. In: *At. Data Nucl. Data Tables* 18 (1976), p. 306.

[144] M. Segawa et al. "Neutron capture cross sections of ^{186}Os, ^{187}Os, and ^{189}Os for the Re-Os chronology". In: *Phys. Rev. C* 76 (2 Aug. 2007), p. 022802. DOI: 10.1103/PhysRevC.76.022802. URL: https://link.aps.org/doi/10.1103/PhysRevC.76.022802.

[145] H. Bateman. In: *Proc. Cambridge Phil. Soc.* 15 (1910), p. 423.

[146] W. Rubinson. In: *J. Chem. Phys.* 17 (1949), p. 542.

[147] W. R. Leo. "Techniques for Nuclear and Particle Physics Experiments". In: *Springer Verlag, Berlin* (1994).

[148] M. Nolte, H. Machner, and J. Bojowald. "Global optical potential for α particles with energies above 80 MeV". In: *Phys. Rev. C* 36 (4 Oct. 1987), pp. 1312–1316. DOI: 10.1103/PhysRevC.36.1312. URL: https://link.aps.org/doi/10.1103/PhysRevC.36.1312.

[149] V. Avrigeanu, P. E. Hodgson, and M. Avrigeanu. "Global optical potentials for emitted alpha particles". In: *Phys. Rev. C* 49 (4 Apr. 1994), pp. 2136–2141. DOI: 10.1103/PhysRevC.49.2136. URL: https://link.aps.org/doi/10.1103/PhysRevC.49.2136.

[150] S. Goriely and J.-P. Delaroche. "The isovector imaginary neutron potential: A key ingredient for the r-process nucleosynthesis". In: *Physics Letters B* 653.2 (2007), pp. 178–183. ISSN: 0370-2693. DOI: https://doi.org/10.1016/j.physletb.2007.07.046. URL: https://www.sciencedirect.com/science/article/pii/S0370269307009069.

[151] Shin Okumura et al. "235U(n,f) Independent fission product yield and isomeric ratio calculated with the statistical Hauser-Feshbach theory". In: *Journal of Nuclear Science and Technology* 55 (2018), pp. 1009–1023.

[152] J.-F. Lemaitre et al. "Fully microscopic scission-point model to predict fission fragment observables". In: *Phys. Rev. C* 99 (3 Mar. 2019), p. 034612. DOI: 10.1103/PhysRevC.99.034612. URL: https://link.aps.org/doi/10.1103/PhysRevC.99.034612.

[153] M.J. Lopez Jimenez, B. Morillon, and P. Romain. "Triple-humped fission barrier model for a new 238U neutron cross-section evaluation and first validations". In: *Annals of Nuclear Energy* 32.2 (2005), pp. 195–213. ISSN: 0306-4549. DOI: `https://doi.org/10.1016/j.anucene.2004.08.005`. URL: `https://www.sciencedirect.com/science/article/pii/S0306454904001525`.

[154] B. Morillon, H. Duarte, and P. Romain. "New BRC Neutron Evaluations of Actinides with the TALYS code : Modelization and First Validation Tests". In: *Proceedings of the 4th International Workshop on Nuclear Fission and Fission-Product Spectroscopy, Cadarache, France, May 13-16, AIP Conference Proceedings, A. Chatillon, H. Faust, G. Fioni, D. Goutte, H. Goutte [Eds]* (2009), p. 79.

[155] D.E. Cullen. "PREPRO 2021 - ENDF/B6 Pre-processing codes". In: *Technical report IAEA-NDS-0238, IAEA* (2021).

[156] A. J. Koning and M. B. Chadwick. "Microscopic two-component multistep direct theory for continuum nuclear reactions". In: *Phys. Rev. C* 56 (2 Aug. 1997), pp. 970–994. DOI: `10.1103/PhysRevC.56.970`. URL: `https://link.aps.org/doi/10.1103/PhysRevC.56.970`.

[157] A.J. Koning et al. "TENDL: Complete Nuclear Data Library for innovative Nuclear Science and Technology". In: *Nuclear Data Sheets* 155 (2019), p. 1.

A. Yet Another Nuclear Data Format: YANDF

YANDF stands for 'Yet Another Nuclear Data Format'. As it name suggests, it is inspired by the YAML markup language, as YAML is the serialization format which in my view is closest to being human and computer readable at the same time. YANDF is an attempt to unify the nuclear data structure for data sets which come from either TALYS, ENDF nuclear data libraries or EXFOR. The format is aimed to be relatively simple. Once data are stored in YANDF, processing can be done independently from the particular source of the data into JSON, ENDF, GNDS etc. data formats. This may be useful for processing of data from any of these categories for numerical operations, plotting, ML applications etc. The main reason for its construction was a consistent output for the TALYS nuclear model code to enable easier processing towards various applications, but at the same time we took ENDF and EXFOR along in the process. The serialization of YANDF has a key-value schema which is not as non-descriptive as ENDF and not as heavy as GNDS. It aims to give a compact yet complete description of a nuclear reaction in terms of metadata. The source of the data, TALYS, ENDF or EXFOR may give rise to some keywords which are different, but in general the structure is the same for each of these categories. The metadata and associated keywords are supposed to be a direct classification of a nuclear reaction as defined by nuclear physics, such as found in textbooks or journal articles. This means that nuclear reaction observables are leading in the description, and not the ENDF format with its MF/MT numbers and secondary relative distributions and neither the EXFOR format with its emphasis on experimental methods and details. As the role of a nuclear model code is to provide an estimate of all nuclear reaction observables as commonly defined in nuclear physics, we have taken TALYS as the basis for the schema. As EXFOR stores experimental observables, the step from EXFOR to YANDF is almost only a format change: the main keywords are the same as the one of TALYS and all experimental details are stored in their original format for the moment. (The main challenge for EXFOR is to determine *which* EXFOR entries correspond to the reaction channels as defined in ENDF or in TALYS output files. Several different EXFOR categories of data may have to be included or

excluded.) In ENDF libraries, only some data are observables (cross sections, nubar), but most of the data need to be processed into observables using operations on data in different parts of the data file. (Some codes for this exist, like Dece, we have used ENDFtables.)

Before we describe the format in more detail we give 3 examples of a typical YANDF file, for the same nuclear reaction ^{235}U(n,f). This is the file coming from TALYS

```
# header:
#   title: U235(n,f) cross section
#   source: TALYS-2.0
#   user: Arjan Koning
#   date: 2023-11-24
#   format: YANDF-0.1
# target:
#   Z: 92
#   A: 235
#   nuclide: U235
# reaction:
#   type: (n,f)
#   ENDF_MF: 3
#   ENDF_MT: 18
# datablock:
#   quantity: cross section
#   columns: 2
#   entries: 24
##        E              xs
##      [MeV]           [mb]
   1.000000E-11   0.000000E+00
   2.530000E-08   0.000000E+00
   2.000000E-07   0.000000E+00
   1.000000E-06   3.049857E+05
   1.000000E-05   9.592149E+04
.....
```

This is the file for the ENDF-B/VIII.0 data library

```
# header:
#   title: U235(n,f) cross section
#   source: ENDF
#   user: Arjan Koning
#   date: 2023-11-26
#   format: YANDF-0.1
# endf:
#   library: endfb8.0
#   author: IAEA CIELO Collaboration
#   year: 2017
# target:
#   Z: 92
#   A: 235
```

```
#    nuclide: U235
# reaction:
#    type: (n,f)
#    Q-value [MeV]:  1.934054E+02
#    E-threshold [MeV]:  1.000000E-11
#    ENDF_MF: 3
#    ENDF_MT: 18
# datablock:
#    quantity: cross section
#    columns: 4
#    entries: 333
##        E              xs            xslow           xsup
##      [MeV]           [mb]           [mb]            [mb]
    1.000000E-11   0.000000E+00   0.000000E+00   0.000000E+00
    2.250000E-03   0.000000E+00   0.000000E+00   0.000000E+00
    2.250000E-03   2.634378E+03   2.397892E+03   2.870864E+03
    2.250014E-03   2.668097E+03   2.428584E+03   2.907610E+03
    2.250056E-03   2.769988E+03   2.521328E+03   3.018648E+03
....
```

This is the file for one of the experimental data sets in EXFOR

```
# header:
#    title: U235(n,f) cross section
#    source: EXFOR
#    user: Arjan Koning
#    date: 2023-09-18
#    format: YANDF-0.1
# exfor:
#    author: Moore
#    year: 1978
#    subentry: 10629004
#    X4 reaction: 92-U-235(N,F),,SIG
#    X4 source: IAEA-NDS C5 file, database version 2023-07-18
#    X4 link: https://nds.iaea.org/EXFOR/10629004
# target:
#    Z: 92
#    A: 235
#    nuclide: U235
# reaction:
#    type: (n,f)
#    ENDF_MF: 3
#    ENDF_MT: 18
# datablock:
#    quantity: cross section
#    columns: 5
#    entries: 3777
```

```
##        E                dE              xs              dxs          Normalization
##      [MeV]            [MeV]            [mb]            [mb]              []
    1.625000E-06    0.000000E+00    1.304000E+04    1.539000E+02    1.000000E+00
    1.675000E-06    0.000000E+00    1.256000E+04    1.510000E+02    1.000000E+00
    1.725000E-06    0.000000E+00    1.270000E+04    1.549000E+02    1.000000E+00
    1.775000E-06    0.000000E+00    1.226000E+04    1.527000E+02    1.000000E+00
.....
```

Obviously, for EXFOR we have several files which in metadata only differ in the **exfor** keyword. The metadata in the above files completely defines the U235(n,f) reaction.

A.1 Format

The YANDF format is almost equal to the well-known YAML format. If the '#' is removed from the first columns of the metadata header of the above file, we almost have a YAML file. The difference is that we do not quote strings and that the data are given in multi-column format. This means that indentation of the key-value pairs is essential, which is the price that YAML pays for not having to include computational symbols such as '', '[', ',' as in e.g. JSON The above files show the most general keywords without any indentation, while sub-keywords are indented by two spaces, subsub-keywords by 4 spaces, etc. As there are many users who want to use numerical data directly from the file, as in gnuplot or other software, we have chosen to use a '#' at the start of every metadata line. We assume it will not be difficult to remove the '#' and parse the above file to JSON, with either your own script or a patched yaml2json converter.

A YANDF file only contains what is relevant. For example, in the above case there is no specification of any isomeric level in either the target or residual nucleus. Hence, we have decided to leave all 'inactive' metadata out. Parsers will have to take this feature into account.

A.2 Keywords and values

The main keywords should be general enough to describe nuclear reaction observables from at least TALYS, ENDF or EXFOR, but also for additional quantities such as e.g. level densities, photon strength functions, radioisotope yields, etc. as written by TALYS to output files.

A.2.1 header

All YANDF files start with the same keywords:
- **header**: the header of the file describing the main metadata,
    - **title**: the title, generally constructed from the other metadata, enabling the user to see directly which nuclear reaction this concerns
    - **source**: the source of the datafile, this is usually TALYS, ENDF or EXFOR. If calculated uncertainties and covariance data are available, this can also be another source, like e.g. TASMAN
    - **user**: the name of the person who produced this file (e.g. in TALYS you can change the hard-wired name into your own)
    - **date**: the date of the production of this file in yyyy-mm-dd format
    - **format**: version of the YANDF format

A.2.2 endf

When the source is an ENDF library, we have the keywords

- **endf**: specific information from an ENDF file
  - **library**: one of the NDL's such as ENDFB8.0, JENDL5.0, JEFF3.3, TENDL-2021, CENDL3.2 etc,
  - **author**: the author of the evaluation as extracted from the ENDF file
  - **year**: the year of the evaluation as extracted from the ENDF file

A.2.3 exfor

When the source is EXFOR, we have the keywords

- **exfor**: specific information of an experimental data set from EXFOR
  - **author**: first author of the experimental work
  - **year**: the year of the publication of the measurement
  - **subentry**: the EXFOR subentry number
  - **X4 reaction**: the particular EXFOR reaction code as extracted from EXFOR, for checking purposes
  - **X4 source**: the version of EXFOR, and the specific computational form of starting database
  - **X4 link**: the https link to the EXFOR subentry, for all experimental details

A.2.4 target

The first part of a nuclear reaction specification is the target nucleus.

- **target**: the target nucleus
  - **Z**: the charge number
  - **A**: the mass number
  - **nuclide**: the nuclide name

The above keywords are always present. In addition, isomeric level information can be provided by the **level** keywords described below.

A.2.5 reaction

The nuclear reaction may have several keywords for a complete description.

- **reaction**: the nuclear reaction
  - **type**: the nuclear reaction channel
  - **Q-value [MeV]**: the Q-value (only specified when appropriate)
  - **E-threshold [MeV]**: the incident energy threshold (only specified when appropriate)
  - **ENDF_MF**: the ENDF MF number for specification of the type of data
  - **ENDF_MT**: the ENDF MT number for specification of the reaction channel

A.2.6 residual

Often, but not always, a nuclear reaction leads to a well-defined residual nucleus.

- **residual**: the residual nucleus
  - **Z**: the charge number
  - **A**: the mass number
  - **nuclide**: the nuclide name

The above keywords are always present when **residual** is present. In addition, isomeric level information can be provided by the **level** keyword described below.

A.2.7 datablock

Before we read the data, we need to know what we are reading and in what format.

- **datablock**: Description of the data block that follows below.
  - **quantity**: the physical quantity that we are reading
  - **columns**: the number of columns
  - **entries**: the number of entries

Below these keywords always follow 2 lines starting with '##', one with the quantities and the other one with the units.

A.2.8 Keyword: level

The **level** keyword describes the data of a discrete level. It can appear as an keyword under

- **target**, when the target is in an isomeric state
- **reaction**, for scattering off a discrete level
- **residual**, when the residual nuclide is in an isomeric state, or for gamma-ray transitions between discrete states

It is described by

- **level**: Description of discrete level
  - **isomer**: the isomeric number
  - **number**: the level number
  - **energy [MeV]**: the level energy
  - **spin**: the level spin
  - **parity**: the level parity
  - **half-life [sec]**: the half life

In general, the indentation for **level** is 2 spaces, i.e. one below the main keyword, but for discrete level gamma-ray transitions the final level is specified at 4 spaces.

A.2.9 parameters

This is a TALYS-specific keyword. It contains the nuclear models and parameters used in the calculation. It starts with

- **parameters**:

after which various parameters can be given. Here is an example for a level density output file

```
# parameters:
#   ldmodel keyword: 5
#   level density model: Hilaire-Goriely tables
#   Nlow: 8
#   Ntop: 17
#   ctable: -1.621100E-01
#   ptable: -5.763700E-01
```

A.2.10 observables

This is a TALYS-specific keyword. It contains the observables estimated by TALYS used in the calculation. It starts with

- **observables**:

after which various observables can be given. Here is an example for a level density output file

```
# observables:
#    experimental D0 [eV]:  1.200000E+01
#    experimental D0 unc. [eV]:  1.300000E+00
#    theoretical D0 [eV]:  1.245919E+01
#    Chi-2 D0:  1.247688E-01
#    C/E D0:  1.038266E+00
```

B. Log file of changes since TALYS-1.0

```
Development of TALYS since release of TALYS-1.0

- December 21, 2007

********** Release of TALYS-1.0 **********

- January 11, 2008

Repaired little bug for angular distributions in isomeric reactions in
angleout.f, discovered by Neil Summers, LLNL

- January 17 2008

Added protection for average radiative width in resonancepar.f
gamgam is never larger than 10.
Only required for extreme cases.

- January 22 2008

Suggestion from Stephane Goriely:
Added HFB deformations, consistent with the HFB masses
Added keyword deformmodel to choose between Moeller deformations
(deformmodel 1) and HFB deformations (deformmodel 2)

- March 4 2008

Suggestion by Emmeric Dupont: small format change for writing D0
```

in partable.f

- March 4 2008

Advice of Stephane Goriely:
Removed unphysical behavior of pre-equilibrium gamma emission for
extremely neutron rich nuclides. Changed emissionrate.f, emissionrate2.f
and preeqtotal.f

- March 4 2008

Added very small preequilibrium contribution to inelastic cross
section, in preeqcorrect.f, to prevent discontinuous inelastic
cross sections.

- March 11 2008

Emmeric Dupont spotted a small omission in partable.f for
the second GDR Lorentzian. Solved.

- March 13 2008

Removed an error for Kopecky-Uhl gamma-ray strength functions
They are now computed at every incident energy since the model
is incident energy dependent.

- March 29 2008

Introduced keywords aadjust, gnadjust, gpadjust, gamgamadjust
(all default 1.)
to make relative changes to level density and other parameters.
This avoid looking up the default values of a, etc. and changing
them.

- April 8 2008

Stephane Hilaire found an important initialization problem for the
case 'projectile 0'; the maximum l-value was zero instead of gamma. This
is repaired in densprepare.f

- April 18 2008

Changed a few 0 energies in the file hbstates.eo by energy 0.01 as
given in Maslov's report. This was pointed out by Emmeric Dupont.

- May 5 2008

Error with 'segment' variable in spectra.f. Found by Ian Thompson.

- May 19 2008

Added extra if statement for calculation of radiative widths
in nuclides.f. Test case 9 crashed for Vittorio Zecca.

- May 24, 2008

Corrected gamma-ray branching ratios with electron conversion, following
advice of Olivier Bersillon and Arjan Plompen.
Default is now 'electronconv y'.
Also the branching ratios in the levels database have changed.

- June 20 2008

Pascal Romain found a problem with indexing optical model files,
for cases where more than 1 external potential per particle is given.
Therefore, the array index for omlines has been enlarged to
3 dimensions.

- June 30 2008

Small normalization problem solved for pre-equilibrium. The
pre-equilibrium cross section could be slightly negative, and this is
repaired in preeq.f, preeqtot.f and binary.f. Found by Stephane Hilaire.

-July 29 2008

Solved a bug found by Arnd Junghans. Small change in basicinitial.f
where lmax is set to gamma for gamma's. This caused problems for
calculations with ompall y.

- August 1 2008

Added the possibility to use microscopic particle-hole configurations, as
generated from Stephane Hilaire's HFB software. A directory
structure/density/ph has been added in the nuclear structure database,
which contains 2-component particle-hole state densities for many
configurations per nuclide. A new keyword has been introduced,
phmodel, where phmodel 1 is used for the (default) analytical densities
and phmodel 2 is used for the tabulated densities.
Various subroutines were generalized to accommodate the choice between
these different types of ph-densities. A subroutine phdensitytable.f was
added to read in the values from the structure database.

Inside phdens.f and phdens2.f there is now a choice for the model.

- August 4 2008

Added a keyword endfecis, similar to inccalc and eciscalc, such that
calculations for a more precise ENDF-6 energy grid can be kept from a
previous run.

- August 14 2008

Added a keyword omponly, so that Talys runs can be done in which
ONLY an optical model calculation is done, i.e. Talys simply acts as
a driver for ECIS.

- August 20 2008

Stephane Goriely sent a table with ground state and spins predicted by
HFB calculations. This has now been added to the nuclear structure
database. If the ground state spin and/or parity is not know
experimentally, we now take it from the HFB table instead of a
simple 0+ (even) or 0.5+ (odd) assignment.

- August 20 2008

A keyword jlmmode has been added to enable different normalizations for
the imaginary potential, as explained in
''The isovector imaginary neutron potential:
A key ingredient for the r-process nucleosynthesis'',
S. Goriely, , J.-P. Delaroche, Physics Letters B 653 (2007) 178
Obviously, this keyword only works if 'jlmomp y'.

- August 20 2008

On advice of Stephane Goriely, the possibility to include Pygmy
resonance parameters for gamma-ray strength functions was included.
Three new keywords 'epr', 'gpr' and 'tpr' were defined.

- September 6 2008

Repaired small error with nbins in input2.f

- September 11 2008

Added correction factor for gamma-ray strength function to take into
account isospin -forbidden transitions, and the associated fiso keyword.
Also included strength function model 5 for Goriely's hybrid strength

model.
Added a keyword micro to do a completely microscopic calculation, i.e.
without any phenomenological models or adjustment

- September 21 2008

Added a keyword 'best' to adopt a set of adjusted best parameters for a
particular reaction. Such parameter sets can be stored in the
structure/best directory.

- October 17 2008

Added the flexibility to use user-defined thermal capture, (n,p),
and (n,alpha) cross sections. Also created a new subroutine thermalxs.f
to handle these values there.

- November 1 2008

Changed the default for multiple preequilibrium reactions,
i.e. mpreeqmode 2 is now the default. This means that the transmission
coefficient method of Chadwick is used instead of multiple exciton model.
This may increase the speed of TALYS at higher energies by
several factors.

- November 17 2008

Corrected small database reading bug for strength=5 in gammapar.f.
Discovered by Stephane Goriely.

Stephane Goriely discovers a Lab/CM bug in his stellarrate subroutine
which may be non-negligible for light nuclides.
Corrected version adopted.

- December 1 2008

Solved a problem encountered by Arjan Plompen for JLM based exciton model
transitions in bonetti.f (fluctuating behaviour at low
outgoing energies). For negative energies, the JLM results are
normalized to the phenomenological imaginary potential.
This only applies if 'preeqmode 3' and 'jlmomp y'.

- December 2 2008

External optical model input files can now also be made adjustable
through the rvadjust, etc. keywords. Changed opticaln.f,...opticala.f
for this.

- December 16 2008

Implemented several corrections and options by Pascal Romain for
fission calculations:
- Increased maximum possible number of rotational levels to 20 in
checkvalue.f
- Possibility to read in head band and class2 states for 3 barriers
in fissionpar.f
- Increased maximum number of incident energies to 500 in talys.cmb
- Increased maximum number of rotational states to 700 in talys.cmb
- Updated the subroutine tfission.f with improved equations for the
  treatment of class-II states.
- Re-introduced the keyword colldamp. If 'colldamp y' fission
  calculations according to the method of Pascal Romain of
  CEA Bruyeres-le-Chatel are performed. This means different options
  for the spin cutoff parameter and the collective enhancement.
  Also different defaults for some level density parameters are used.

- January 13 2009

TALYS can now produce a table with average resonance parameters,
for the description of the Unresolved Resonance Range (URR).
A keyword 'urr' has been added. If 'urr y', a file called urr.dat
will be produced, which for each incident energy contains the
relevant neutron and gamma strength functions S, mean level
spacings D(J,l) and decay widths Gn(J,l) and Gg(J,l).
To enable this, the subroutines radwidtheory.f and spr.f are
now called for every incident neutron energy.

- February 9 2009

Amir A Bahadori found a problem for emission spectra in a natural
element calculation. The emission energy grids for the various isotopes
were out of sync. I revised the subroutine natural.f to solve this.

- February 20 2009

Added the possibility to normalize certain reaction channels in TALYS
directly to experimental or evaluated data. A new subroutine
normalization.f was written and the keyword 'rescuefile' was added.
With a "rescue file" normalization factors can be given on an incident
energy grid, after which the cross sections are normalized. The
difference is then corrected for in the elastic cross section.
Use with care.

- March 20 2009

Change default of including class 2 states. The default is now class2 y.

- March 20 2009

Corrected little error in densityout.f. The name of the nucleus was
written incorrectly to the ld* files

- April 1 2009

Change the default for deformed OMP calculations: If the incident
particle is a neutron or a proton, only for that particle (as projectile
and ejectile) a deformed OMP is adopted. The default for the other
particle is set to false. As usual this can all be overwritten with the
'rotational' keyword.

- April 6 2009

Ian Thompson found unphysical oscillatory behavior for Al26(n,n')
excitation functions. The cause of this lies in a too large
pre-equilibrium alpha contribution. Therefore, I changed some
C/A terms in preeqcomplex.f into C/(max(A,40)).

- April 9 2009

Added isotopic specification for natural targets, for recoil output
files on advice of Reto Trappitsch. Changed recoilout.f and natural.f.

- April 14 2009

For very short-lived target nuclei the definition of 'isomer' is
overwritten with the lifetime of the target level.
This means that if e.g. the lifetime of the target nucleus is 1 ms,
then all other levels with a lifetime longer than 1 ms will be treated
as "isomer". This overwrites the isomer default or value given in
the input. Change made in levels.f.

- April 16 2009

Changed maximum value of eninclow in grid.f to prevent array overflow.
Only relevant for very exotic nuclei.

- April 23 2009

Updated preeqcomplex.f after discussions with Connie Kalbach on complex

particle pre-equilibrium emission. Changed lab energy into CM energy at
a few formula's

- April 23 2009

Made a correction in recoilinit.f. For reactions with very large
Q-values, e.g. Li-7(d,n) the recoil energy grid was not well defined.
Problem encountered by Markus Lauscher.

- April 29 2009

Added the latest mass and deformation tables from Stephane Goriely,
as published in Phys Rev Lett 102, 152503 (2009).

- April 29 2009

Included default normalization factors for microscopic fission
calculations as published in Goriely et al Phys Rev C79, 024612 (2009).

- April 29 2009

Introduced logarithmic interpolation for tabulated level densities,
instead of linear. Changed densitot.f and phdens.f, phdens2.f.

- May 5 2009

Updated preeqcomplex.f after discussions with Connie Kalbach: included
pairing correction

- May 5 2009

Generalized nuclear mass, deformation and discrete level tables.
Nuclear masses are now read from different subdirectories instead of
from one file. This will allow easier addition of alternative mass
models in the future.
Also the number of theoretical deformation parameter databases is
extended. For both masses and deformation parameters, HFB calculations
based on the Gogny D1M force are now also an option.
For discrete levels, HFB based ground state spins and parities are
added to the discrete level database for nuclides for which no
experimental information exists.
The nuclear structure database, masses.f deformation.f and levels.f
were changed for this.

- May 10 2009

Further changes to the masses, deformation, and ground state property
tables. I removed the 'deformmodel' keyword again (introduced after the
release of TALYS-1.0, so no problems with angry users). It is obvious
that theoretical deformation parameters should be taken from the same
model as that of the masses. The structure/deformation directory is
also cleaned. It now only consists of the subdirectory exp/ where the
coupling schemes for coupled channels (and possibly deformation
parameters) are given. The theoretical deformation parameters are now
found in the mass tables. However, they can be overruled by other
values in the deformation/exp files. In most cases however, only the
coupling scheme and vibrational deformation parameters (from Raman and
Kibedi) remain.
For all (or at least most) stable nuclides above Z=30 and actinides a
coupling scheme is provided in deformation/exp. This will soon be
finalized for all nuclides, enabling default coupled-channel
calculations.

I also changed the numbering of the massmodels.
0: Duflo-Zuker (analytical formula for the masses, no deformation and
   ground state spins, instead, take these from 'massmodel 2'
1: Moller
2: HFB-17 (Skyrme force): this is the default when exp data is
   not available
3: HFBD1M (Gogny force)

- May 11 2009

The keywords "addelastic" and "adddiscrete", to fold in direct peaks in
secondary spectra, for easy comparison with experiment, have been made
energy dependent, similar to that of e.g. the "preequilibrium" keyword.
Possibilities are now e.g.
addelastic y
addelastic n
addelastic 25.

and similarly for adddiscrete.

- May 18 2009

After one year, I ran the monkey code again, and included all new
keywords for testing. This means running Talys with random input files
with bout 300 keywords, and the requirement that it does not crash,
run out of array boundaries etc. A few minor problems were solved in
several
subroutines.

- May 19 2009

Introduced new keyword strengthM1, to vary between M1 strength functions.
The default is strengthM1 = 2 (RIPL-2 prescription) while a value
of 1 corresponds to the older prescription of RIPL-1.

- May 22 2009

Adopted the Duflo-Zuker formula from 1996 (from the RIPL-2 website)
and replaced the older version. This is only used for masses outside
the masstables.

- May 22 2009

Adopted the suggestion of David Perticone to use the longest-lived
nuclide as default for natural element calculations for elements
without stable isotopes. In other words 'element Tc' in combination with
'mass 0' will no longer give an error message but instead A=98 will
be adopted.

- May 22 2009

Added the isotope number to double-differential spectra in the case
of natural targets. David Perticone discovered that this was missing.

- June 9 2009

Added the possibility to give 'nbins 0' in the input. In this case,
TALYS tries to adopt a clever number of bins, depending on the incident
energy, rather than a constant number of bins (the default).

- June 9 2009

Since all theoretical deformations are now in the mass directory,
there is only one set of data left in the structure/deformation/,
the subdirectory exp/ is therefore removed, and the
structure/deformation/ directory now merely contains the coupling
schemes. Added many coupling schemes in this directory

- June 9 2009

Removed an input inconsistency for D0. Both in the input and from the
structure database they are now read in keV.

- August 5 2009

Improved some of the ECIS flags for low incident energies for
deformed nuclides, according to suggestions of Pascal Romain.
Also introduced the keyword 'soswitch' to set the energy where
deformed spin-orbit calculations and sequential iterations begin.

Introduced the keyword 'coulomb' to (de-)activate Coulomb excitation
calculations by ECIS

Reprogrammed the energy dependence of fstrength.f (again!), after
discussion with Pascal Romain and Roberto Capote.

- August 24 2009

Solved a problem with angular distributions for reactions on isomeric
states. Incorrect levels were read in (in other words, elastic and
inelastic angular distributions were mixed.)

- October 28 2009

Included new thermal cross section database of Mughabghab in structure
database. This will change the low energy extension down to thermal
energies.

- December 1 2009

Added new keywords rvadjustF, avadjustF, to enable energy-dependent
geometry parameters for the optical model. This is useful for local
optimization of the optical model. We can now slightly deviate from
constant values, in a smooth manner, and for a restricted energy
range given by the user.

- December 11 2009

Added a keyword bestpath to allow a different directory to store input
files with best TALYS input parameters

- December 17 2009

Smoothened microscopical particle-hole states read from table.

C. Log file of changes since TALYS-1.2

```
Development of TALYS since release of TALYS-1.2


- December 23, 2009


********** Release of TALYS-1.2 **********


- January 6, 2010


Changed some of the defaults for 'micro y' (fully microscopic option).
Among others, the phmodel is kept to 1. Also 'strength 4' if 'micro y'.


- January 8, 2010


Tiny correction by Stephane Goriely
in levels.f, line 153
     if (massmodel.ne.2) then
has been changed into
     if (massmodel.le.1) then


since in the case of D1M (massmodel=3), a spin and parity is
also assigned.


- January 21, 2010


Solved a problem with Elow (eninclow in the source code) found by Dimitri
Rochman: If the highest incident energy is smaller that Elow, Elow is set
to zero (otherwise there would be no output of cross sections).
```

- February 1, 2010

Corrected an indexing problem for exclusive channels in channels.f
For exotic nuclei sometimes the exclusive channel does not open up
at the right moment, so the idnum index is incorrect. This caused
a wrong extrapolation at thermal energies for Th-150(n,n')

Added a small output extension for the branching ratios of
residual products

- February 24 2010

Added a correction for the indexing of exclusive channels
(see also Feb 1). In the case of using 'rescue' files the capture
channel may appear to be closed while the (n,gf) channel, which is
not normalized, remains open. Variables chanopen, in channels.f,
and chanexist, in strucinitial.f, are now reinitialized to true
for the capture channel.

Nikolaj Filatov found a few small bugs, or potential problems,
in the Brosa subroutines. for fission yield calculations.
These have now been corrected

- March 2 2010

Solved a precision problem in molprepare.f for width fluctuation
calculations Very small numbers were multiplied with very large numbers,
leading to NaN's in some cases.

The thermal (n,a) cross section in the thermal database was a factor a
million too high. This is corrected.

- March 7 2010

Erich Ormand found a Bug in Fu's pairing correction, important if
pairmodel 1 (the default is pairmodel 2). The formula contains a factor
(U/delta)**0.68 and not (U/delta**0.68) as coded. Formula corrected.

- March 11 2010

Solved an old problem, first mentioned by Arjan Plompen and now also by
Alexander Konobeyev: Different compilers produce different answers for
the gamma spectrum at low energies. This was visible in sample case 6.
Solved this by a small correction in specemission.f and compemission.f.

After advice of Yan Shengquan, I added a print of the compound nucleus
formation cross section per spin and parity value. This will only be
done if flagcheck y.

- March 12 2010

On the advice of Stephane Hilaire, S(Zcomp,Ncomp,1) was changed into
S(Zcomp,Ncomp,k0) in the Kopecky-Uhl generalized Lorentzian part
of fstrength.f

- March 26 2010

Separated subroutine preeqcomplex into subroutines stripping, knockout
and breakup.

- March 28 2010

Implemented Kalbach's new model for break-up reactions, documented
in a FENDL-3 report (March 2010). For this, the Cbreak keyword was
introduced, similar to Cknock and Cstrip. The new model is in
subroutine breakup.

- March 30 2010

After a problem discovered by Mihai Horoi, and on the advice of
Stephane Goriely, the limits to take transmission coefficients and
cross sections (popeps, etc.) into account are lowered for
astrophysical calculations.

- April 9 2010

Repaired a problem found by Tak Pui Lou. If 'compound n', as in
sample case 9, no subroutine or function calculating gamma ray
strength functions should be called. This was ensured by changing
an if statement near the end of incident.f

- April 14 2010

Erich Ormand found a bug for the exciton model emission rates for
the use of pairmodel=1 (Fu's pairing correction). The exciton number
of the residual system should be taken in preeqpair, when appropriate.
Changed emissionrate.f and emissionrate2.f for this.

- May 20 2010

Added the recoil flag to the endf.inf file, for ENDF evaluations

- June 25 2010

Ronald Murphy discovered an error for angular distributions to
discrete states for reactions other than inelastic scattering.
This problem occurs for low incident energies of complex particles
such as alpha's. Subroutine angdis.f was corrected for this.

- June 28 2010

Ronald Murphy discovered another error for continuum angular
distributions. An if statement was removed from spectra.f

- September 2 2010

Generalized input of characters: filenames and other strings can
now also be given in uppercase

- December 7 2010

An input file of Mahdi Bakhtiari and Mahdi Sadeghi led me to a problem
on interpolation of (input) tabulated OMP parameters with the
optmod keyword. Solved in subroutine omppar.f.
Also, they spotted an error in the manual on the outexcitation
keyword that I corrected, and it TALYS now stops if a microscopic
level density model (ldmodel 4,5) is used in combination with
colenhance y (which only works for phenomenological models).

- December 27 2010

On the advice of Stephane Goriely, I wiped a problem with the JLM
OMP under the carpet: for very neutron-rich nuclides the JLM potential
by Bauge and Delaroche may produce negative reaction cross sections.
Instead of stopping the TALYS calculation directly, we now set
the reaction cross section to zero. Changed incidentread.f and
directread.f for this.

- December 29 2010

Adopted Stephane Goriely's double folding alpha potential.
A new subroutine foldalpha.f was added, and now alphaomp runs from 1
to 5. The default for the alpha OMP remains unchanged.

- January 3 2011

Extended the flexibility for using level densities. It is now possible,

in one and the same calculation, to use different level density models
for different nuclides. If the input file contains e.g.
ldmodel 5
ldmodel 24 52 1
ldmodel 24 53 2
then ldmodel 5 will be used for all nuclides, with the exception of
Cr-52 and Cr-53 for which ldmodel 1 and 2, respectively, will be used.
The level density model thus becomes an adjustable parameter of integer
type.

- January 5 2011

Changed the meaning of the keyword adddiscrete. For (n,p)...(n,alpha)
reactions discrete state cross sections are now always added to the
energy spectrum of the cumulative (n,xp)...(n,xa) spectra.

- January 10 2011

Changed a small cross section limit in preeqcorrect.f to allow
calculation of very small alpha-induced cross sections of
astrophysical interest

- February 3 2011

Solved an error in the extrapolation of partial (n,p) cross sections
to thermal values.

- February 22 2011

Solved a consistency error in the GSM in densitypar.f,
found by Heedong Choi. After determination of the critical
level density parameters, the global l.d. alimit should not be
redefined.

- April 13 2011

Changed the lower input boundary for the Pygmy resonance width to
0.1 MeV, due to a problem found by Samantha Hammond.

- May 10 2011

Added 4 global deuteron OMP's, since the default model coming from
standard Watanabe folding does not perform well. A keyword 'deuteronomp'
has been made to make a choice between the models:
deuteronomp 1 --> Watanabe potential
deuteronomp 2 --> Daehnick potential

```
deuteronomp 3 --> Bojowald potential
deuteronomp 4 --> Han potential
deuteronomp 5 --> Haixia An potential
```

- May 11 2011

Added flexibility in the OMP adjustment factors. If necessary, all
geometrical parameters can now be independently varied (e.g. we no longer
necessarily have rw=rv, etc.)

- May 11 2011

Adopted new egridastro.f subroutine from Stephane Goriely for a finer
energy grid in astrophysical calculations

- June 27 2011

On the advice of Kevin Kelley, I allowed the combination 'ecissave y'
and 'eciscalc n'. TALYS now checks whether transmission coefficients are
available from a previous run. If not, it will create them.

- June 30 2011

Corrected the treatment of the URR: there was an error in the rules
for possible angular momentum combinations in urr.f, discovered by
Paul Koehler. I also included the calculation of the average gamma
width for the URR in the correct place, as suggested by Gilles Noguere.
All URR related actions in TALYS can now be found by searching for
the variable flagurr.

- July 1 2011

Included the possibility to calculate the effective cross section
for integral activation measurements, by folding the excitation
functions by an experimental flux. In talys/structure/flux, we have
stored more than 40 spectra, coming from the EASY package, which
have been used in past activation benchmarks. Such benchmark activities
should eventually be performed using (processed) nuclear data libraries,
especially for reactions containing a low energy resonance range, but it
is helpful to get an idea of the performance directly with TALYS as well.
A new keyword 'integral' has been introduced for this.

- September 19 2011

Adopted Gilles Noguere's subroutines for the calculation of
unresolved resonance parameters. The urr keyword now acts like the

widthfluc keyword: it can be y, n or a value between 0 and 20 MeV
for the on-set of the URR calculations. For more flexibility,
also the keyword lurr (maximal l-value for URR calculations)
and urrnjoy (to normalize capture and fission widths according
to the NJOY URR method). The URR subroutines are urr.f, urrout.f,
csunr2.f, unfac.f, gnrl.f and strengthfunc.f

- September 19 2011

In addition to making ldmodel nuclide-dependent, the same was done
for the colenhance keyword, i.e. for every nuclide in the
chain the collective enhancement for the level density can be turned
on and off.

- November 17 2011

Added the possibility to print the direct, pre-equilibrium and compound
components of each cross section in the output files. This can be
enabled with a new keyword: components

- December 22 2011

Added the possibility to calculate Maxwellian averaged cross sections
(MACS). This was already implicitly available for the calculation of
astrophysical reaction rates, but now with the keywords 'astroE' and
'astroT' the MACS can be calculated at a user-specified energy,
e.g. 30 keV, or temperature.

D. Log file of changes since TALYS-1.4

```
Development of TALYS since release of TALYS-1.4

- December 28, 2011

********** Release of TALYS-1.4 **********

- December 30, 2011

Introduced non-equidistant binning for the excitation energy grid.
The excitation energies can now be given on a logarithmic grid,
and this has also become the default. It allows to use less excitation
energy bins while not losing precision. The old situation, of TALYS-1.4
and before, can be invoked with the new 'equidistant' keyword, but
from now on the default will be 'equidistant n'.
Especially for cross sections above 100 MeV the improvement is
significant: smoothness and more reliable absolute values.
TALYS can now technically be used up to 600 MeV, though I did
not validate that with experimental data yet.

- January 2, 2012

Added the extra MT numbers 152-200, introduced in the ENDF-6 format
in 2010, in the normalization subroutine.

- January 9, 2012

Multiplied the normalization factor for stripping reactions for
```

helions with a factor of 5 to better fit (n,h) data.

- January 16, 2012

Added the statement "Positive parity" to the level density output
file in case of parity-dependent level densities, on the advice
of Goran Arbanas.

- January 17, 2012

Solved a problem reported by Patric Granholm.
At energies far below the Coulomb Barrier, some excitation functions
showed discontinuities. This was due to a too strict choice of
pre-equilibrium spin distributions in subroutine binary.f.
A popepsA constant is now added.

- January 17, 2012

Turned a few TALYS-errors into warnings (TALYS no longer stops) in
integral.f. Also changed the naming of the associated data into
talys/structure/integral in which experimental data and fluxes
can be found.

- January 21, 2012

Patric Granholm's problem of jan 17 motivated me to extend the
'preeqspin' keyword. There are now 3 possibilities:
preeqspin 1 (equivalent to the old 'preeqspin n'): the pre-eq spin
  distribution is made equal to the relative spin-dependent population
  after compound nucleus emission
preeqspin 2: the spin distribution from total level densities is adopted
preeqspin 3 (equivalent to the old 'preeqspin y'): the pre-eq spin
  distribution is based on particle-holr state densities
The input is backward compatible, i.e.
preeqspin y is transformed into preeqspin 3
preeqspin n is transformed into preeqspin 1
Total number of possibilities: preeqspin can be equal to y,n,1,2,3

- February 1, 2012

Added more adjustment flexibility. With the tljadjust keyword the
transmission coefficients for the outgoing channel can be changed in a
certain energy range.

- February 3, 2012

Added more adjustment flexibility. With the 'branch' keyword the
branching ratio for any discrete level in the database can easily be
overwritten in the user input. This may be necessary to adjust isomeric
cross sections.

- February 13, 2012

Corrected a bug found by Yuki Watanabe: for charged-particle elastic
and inelastic scattering the compound components are not written to
output. Corrected angdis.f for this.

- February 13, 2012

Fixed a problem with the calculation of D0 for the case of incident
photons, (used for level density studies) found by Stephane Goriely.
I changed dtheory.f for this.

- February 14, 2012

Removed a bug in rldm.f, introduced just before the release of
TALYS-1.4: A min() function was introduced to prevent an array running
out of bounds. However, this gives huge fission cross sections for
neutrons on subactinides (or any other case where the RLDM is needed),
as discovered by Stephane Goriely.

- February 16, 2012

On the advice of Stephane Goriely, I made a change in fissionpar.f: if
no fission barriers are found in the tables with phenomenological
values, first the tables of Mamdouh (fismodel 2) are scanned for
values, before an analytical model is used.

- February 20, 2012

After a question by Yuki Watanabe, I decided to introduce the
'cpang' keyword, to enable the calculation of discrete level
compound nucleus angular distributions for incident charged particles

- February 25, 2012

Changed the order of reading lines from files of the best/ directory
such that the "best" parameters are now also used for natural targets.

- March 6, 2012

Added radiative capture model for direct and semi-direct capture cross

section. For this the 'racap' keyword was made. By default, 'racap n'.

- March 11, 2012

Added new microscopic level densities, this time generated from
temperature-dependent HFB calculations and the Gogny D1M nucleon force.
This option is now 'ldmodel 6'

- March 27, 2012

Automatically increased the number of included discrete levels for a
highly excited isomer.

- March 27, 2012

To increase fitting flexibility I added the keywords egradjust,
ggradjust, sgradjust, epradjust, gpradjust, spradjust, E0adjust,
Exmatchadjust, Tadjust, fisbaradjust and fishwadjust, all with a
default value of 1.

- March 27, 2012

About 70 keywords can now have energy-dependent values. After the
keyword and its value are given in the input, an energy range can
be specified over which the corresponding model parameter is altered.

- March 29, 2012

Incident energies can now be given in any order, not necessarily in
ascending order. They will be sorted first. Also double energy points
will be removed. TALYS will thus no longer stop when this is provided.

- April 11 2012

Solved an output bug found by Mahdi Baktiari. At energies far below
the Coulomb barrier the direct elastic angular distribution for charged
particles is not copied into the total column.

- April 21 2012

Changed nexout into nexout2 in do loop around line 70 in specemission.f
That error has been there for several years.

- April 26 2012

Generalized a few energy grids, so that TALYS can be used up to 600 MeV.

- May 7 2012

Vivian Demetriou found a problem in the alpha folding potential
which I corrected.

- August 12 2012

Added keyword 'production' for (medical) isotope production.
Added decay data subroutine.

- August 15 2012

Extended nucleon OMP to 1 GeV. For this the keywords Vinf, Ejoin,
w3adjust and w4adjust give some extra flexibility. TALYS can now
technically be used up to 1 GeV.

- August 28 2012

Added all other routines for medical isotope production. With
the 'production' keyword, excitation functions are automatically
transferred into isotope production rates in MBq. Various
extra keywords are included for flexibility.

- September 11 2012

Corrected an error for particle multiplicities found by Pedro Arce.
The yields should be defined relative to the nonelastic cross section
and not to the reaction cross section. This makes a difference at
low energies and will change charged-particle nuclear data libraries,
which use this information.

- September 15 2012

Added possibility to locally adjust the OMP parameters for outgoing
channels only, with the keyword 'incadjust'. If 'incadjust n' then OMP
adjustments are not performed for the incident channel. This gives more
fitting flexibility. Physical argument is that the magnitude of the
approximation to regard inverse channels as occurring from the ground
state, it unknown. (temperature dependent OMP). The default is however
still 'incadjust y'.

- September 15 2012

Arnd Junghans discovered a reading error in the RIPL file for S0.
Some of the values do not have a decimal point, resulting in a factor

of 100 difference for some nuclides. Fortunately S0 is not used,
apart from reference, but the error is now corrected anyway. At his
advice, I also removed the printing of the neutron strength function
at the wrong place (it was in the middle of the gamma data).

- October 6 2012

Introduced a keyword Liso to enforce the isomeric number of the target
(by default it is determined from the discrete level database).

- October 15 2012

Added a keyword fisfeed to output the fission per excitation energy bin.
This allows to couple TALYS with a fission yields code, like GEF.
To enable this, a few outlets in multiple.f had to be made.

- December 10 2012

Changed a statement in the output about level densities. The 'total'
column is given per parity. (issue discovered by Paul Koehler).

- December 21 2012

Revised the direct radiative capture model together with Stephane
Goriely. Three new keywords were introduced:
ldmodelracap, sfexp and sfth.

- December 21 2012

The resulting intermediate code version is called TALYS-1.50

- March 19 2013

Complemented RIPL discrete level database with levels calculated from
microscopic densities. A new keyword 'disctable' was introduced to
include or exclude such additions. The default is now 'disctable 1',
i.e. RIPL discrete levels file + levels added up to level number 100
if missing from RIPL.

- April 27 2013

Changed 'ecis06' into 'ecis' for filenames etc., to make
the filenames independent of the version of ECIS.

- May 18 2013

Increased boundaries for keyword massexcess from 0.500 to 0.600 a.m.u.

- May 20 2013

Put an if statement around loop 150 in comptarget.f to solve an NaN
problem found by Satoshi Chiba for astrophysical calculations.

- May 21 2013

Enforced that the non-elastic cross section is non-negative by
putting a max around xsnonel in binary.f

- May 21 2013

Changed an .lt. into an .le. in tripathi.f which solves a strange ifort
compilation problem.

- May 27 2013

Problem found by Mahdi Bakhtiari for elastic scattering angular
distributions for natural targets. For charged particles these
were not summed to the natural value. Corrected natural.f

- June 4 2013

Wrote more parameters to parameters.dat file

- June 24 2013

Corrected two problems found by Peter Mohr: if cpang y then the
charged-particle compound elastic angular distribution should
be anisotropic (though symmetric). Corrected angdis.f for this.
Also, for incident charged particles, direct discrete
contributions are not taken into account if a coupling scheme
is given. The default for the 'spherical' keyword is changed for this.

- June 30 2013

Added call for GEF subroutine, created by Vasily Simutkin and
Michail Onegin, to massdis.f to use the Schmidt-Jurado model for
fission observables. Introduced the fymodel keyword to choose FY
model fymodel 1= Brosa, fymodel 2 = GEF.
fymodel 1 is now also the default.

- August 18 2013

As requested by Paul Koehler, added the average alpha and proton widths
in the output of the URR subroutines.

- August 22 2013

Disabled the renormalization of the URR by the NJOY method, as a
default at least, to avoid unstable results for the competitive width.

- September 24 2013

Added radiounit and yieldunit keywords to specify units for medical
isotope production

- October 11 2013

Repaired an error in optical model adjustment, discovered by Vlad and
Marilena Avrigeanu, the Coulomb radius was not adjusted with rcadjust.

- December 1 2013

Added new version of GEF subroutine, created by Vasily Simutkin and
Michail Onegin, called geftalys.f. Fission yields, P(nu), nubar, and nu
as function of Z and A are added to the output. Introduced two extra
keywords: outfy, to give detailed output of the GEF calculation,
and gefran, for the number of random events to be fed to GEF.

E. Log file of changes since TALYS-1.6

Development of TALYS since release of TALYS-1.6

- December 23, 2013

********** Release of TALYS-1.6 **********

- January 10, 2014

Stephane Goriely found an error in densitytable.f where for ldmodel=6
no parity-dependence was included. This is corrected.

- January 23, 2014

Introduced extra adjustment to pairing shift with keyword Pshiftadjust.
This works for the Backshifted Fermi Gas model and avoids looking up
the actual value for Pshift for adjustment.

- January 26, 2014

Extended the range of gamgamadjust. Lower limit is now 0.01.

- February 10, 2014

Fixed a problem for FY calculation spotted after calculating a test case
for Charlotte Duchemin.
An extra check is done in massdis.f to speed up the FY calculations

considerably. Charlotte also noted that not al FP files are present.
A correction in massdisout.f was made. In addition, total FP cross
sections per A (cumulative cross section) are now given.

- February 13, 2014

Re-introduced the possibility to fit average radiative width for masses
below A=40. This is now performed if the gamgamadjust keyword is
explicitly given in the input.

- February 21, 2014

Added low energy resonance cross sections to the output. For this, the
keyword 'resonance' was introduced. If resonance y, TALYS will read in
resonance parameters, from various possible sources, and call the
RECENT code of Red Cullen's PREPRO package, which is included as a
subroutine. Low energy pointwise
resonance cross sections will be added to channels like total,
elastic, fission and capture.
Choices for various libraries can be made with the reslib keyword,
which can be equal to default, endfb7.1, jeff3.1, jendl4.0

- March 10, 2014

Extended the resonance option with the SIGMA1 code, for resonance
broadening, and GROUPIE, for groupwise cross sections, of the PREPRO
package.
Introduced the new keywords 'Tres' and 'group' for this. Giving e.g.
Tres 100.
group y
will produce groupwise cross sections at 100 Kelvin Doppler broadening.

- April 1, 2014

Sort of solved an indexing problem for exclusive channels, found after a
crash (indeed!) of TALYS with an input case of Arjen van Vliet.
When maxchannel is high, e.g. 8, so many channels are open that an
indexing problem occurs. The ultimate correction has not been found but
a small change in channels.f, when we jump out of the loop if the
index reaches numchantot-10, seems to do the trick.

- April 1, 2014

Solved a problem discovered by Ismail Sarpun. The GSM model was
insensitive to variations of the level density parameter a in the input.
This is because the GSM model contains a critical level density parameter

a_crit that is solved by iteration.
Now 'a' from the input is set equal to alimit.

- May 29, 2014

Solved a problem for medical isotope production found by Will Webster.
TALYS was not protected against using a very fine incident energy.
This has now been solved and up to 2000 incident energies can be used.
Also some indices for the radioactive decay chain were wrongly assigned,
which is solved now.

- June 21, 2014

Added the absorption cross section to the output. This was missing so
far. The absorption cross section is the sum of all partial cross
sections that do not have the initial particle (usually a neutron) in
the exit channel.
While it is not needed for any application, EXFOR contains some data sets
that can be compared with this.

- July 7, 2014

Added a keyword bestend to insert a structure/best file at the end of
the input file instead of at the beginning. This gives more flexibility
for overruling parameter values.

- July 14, 2014

Replaced HFB masses by HFB24.

- July 14, 2014

Replaced microscopic ph-densities by latest version from
Stephane Hilaire.

- July 14, 2014

Added strength 6,7,8 models for gamma-ray strength functions. Added a
new keyword E1file to read in user-defined gamma-ray strength functions.

- July 29, 2014

Added keyword Estop to stop calculation if incident energy gets above
Estop (while not changing the file with incident energies which may go
beyond Estop).

- August 6, 2014

Changed acceptable range for aadjust, gnadjust and gpadjust into
0.1 - 10. Also extended a few other ranges to accommodate random
variations for TASMAN.

- August 8, 2014

Continue calculation if number of built rotational or class2 states
exceeds numrot (currently 700). Instead of an error message we simply
stop building more states.

- August 18, 2014

Solved a problem for medical isotope production found by Ismail Sarpun.
The wrong lifetime is read from the decay data file for the ground
state if a nuclide has more than 1 isomer. Solved this in decaydata.f.

- August 27, 2014

Extended the range of elements up to Z=124, with nuclear symbols Rg(111),
Cn(112), Fl(114) and Lv(116), B3(113), B5(115), B7-9(117-119),
C0-4(120-124)

- August 28, 2014

Unified the output in separate files a bit more. Everything is now in
1p,e12.5 format. This makes processing by TEFAL and TASMAN easier.

- September 8, 2014

Added the stand-alone Fortran version of the GEF code as a subroutine to
enable, in principle, the evaporation of fission fragments by TALYS.
For this, TALYS "loops over itself", i.e. it is restarted internally
for every excited fission fragment. The option for this is fymodel 3.

- October 8, 2014

Added extra security in compound.f to prevent division by zero in the
case of fission. A rare NaN by TALYS was found for 160 MeV helions on
Bi-203.

- October 22, 2014

Re-indexed the excitation energies in case of an incident population
grid. This was corrected before but not written down.

Olivier Delaune pointed me to that error of TALYS-1.6.
Created a new keyword popMeV. If popMeV y, the population grid is given
as a spectrum per MeV (like before). If popMeV n (the default), the
table represents pure histograms.

- November 25, 2014

Added alpha global OMP by Avrigeanu et al and Nolte et al.
The range for alphaomp has now been extended to 8.

- December 21, 2014

Added keyword bestbranch to enable the adoption of adjusted branching
ratios from the structure/levels/branch/ directory, for better
description of isomeric cross sections and gamma-ray cross sections.

- April 13 2015

Corrected an error in the manual, the default GSF is Kopecky-Uhl for
incident neutrons only, otherwise it is Brink-Axel. Found by David Walz.

- May 1 2015

Started implementing breakup model by Marilena Avrigeanu. There is now
a keyword breakupmode which can have the values 1 (Kalbach) or
2 (Avrigeanu). The implementation is not yet complete.

- May 7 2015

On the advice of Stefan Buller, I added a keyword outbinspectra, which
prints the emission spectra per compound nucleus bin. Obviously, the
default is outbinspectra n, since it generates a lot of output.

- September 6 2015

Solved a problem for astrophysical reaction rates, found by Stylianos
Nikas. The non-equidistant binning of excitation energies was not
properly coded in partfunc.f leading to wrong astrophysical reaction
rates, especially for high temperatures.

- September 24 2015

Defined deltaEx(0) to be half the energy of the first discrete level.
It used to be zero.

- October 3 2015

Added keyword ffspin to enable a choice between spin dependent
excitation functions for excited fission fragments as emerging from GEF,
or assignment of spin distributions by TALYS

Added keyword skipCN to skip the decay of a compound nucleus altogether.

- October 10 2015

Generalized GSM for fission according to suggestions of Michael Onegin.
Various level density parameters for the GSM now have an extra fission
barrier index.

F. Log file of changes since TALYS-1.8

```
Development of TALYS since release of TALYS-1.8


- December 28, 2015


********** Release of TALYS-1.8 **********


- January 21, 2016


Dimitri Rochman managed to crash TALYS, a rare feat indeed!
For ldmodel 6, it was possible to have an undefined value for D0,
leading to possible incident energies of 0 MeV, which crashes ECIS.
Therefore a minimum value for eninclow, 1.e-11 MeV, was set in grid.f


- February 12, 2016


Solved an error found by Vlad Avrigeanu. Contrary to what is stated in
the manual, alphaomp was NOT yet the default in TALYS-1.8.
To use the best alpha OMP, you have to explicitly put alphaomp 6.
This is solved now in input4.f


- June 1, 2016


Implemented the possibility to read external files for M1 strength
functions, and also the possibility to scale them with the etable and
ftable keywords.
Changes were suggested by Stephane Goriely. etable and ftable are now
extended, e.g. etable 40 93 1.2 M1
```

A new keyword m1file was introduced.

- June 2, 2016

Replace RECENT, SIGMA1 and GROUPIE subroutines of PREPRO-2013 to
PREPRO-2015.

- July 9, 2016

Revised Kalbach parameterization for break up reactions, according to
the latest draft of her Phys Rev C paper.

- July 16, 2016

Added keyword massdir to add your own masstables to the
talys/structure/mass/ directory

- September 7, 2016

Corrected an error in the deformed OMP for actinides of Soukhovitskii et
al, after a problem was reported by Fabio Zeisler. The Fermi energy in
the OMP definition was taken from the global KD03 formula, while the
Soukhovitskii OMP uses specific Fermi energies per nucleus.

- September 19, 2016

Corrected an error found by Bernard Erasmus: medical isotope production
Results were different for a second run in which the TALYS results were
already precalculated. Solved this by initializing the discrete levels
for non-binary channels (this was omitted when 'reaction n').

- November 2, 2016

Stephane Goriely added 2 new keywords upbendc and upbende to adjust
gamma-ray strength functions at low energy.

- November 8, 2016

Stephane Goriely added 2 new keywords astroex and nonthermlev to account
for cross sections to excited states.
To accommodate this I introduced variables MaxZastro and MaxNastro to
keep the memory for astro arrays under control.

- November 16, 2016

Solved a problem for low lying 0+ states. ECIS seems to produce

inelastic cross sections larger than the reaction cross section.
In case of a weakcoupling model, if the first discrete level is a 0+
we replace it by 2+.

- November 28, 2016

Added a loop over astrophysical temperatures in resonance.f.
Low energy resonance capture is now broadened by prepro at various
temperatures to obtained physically more realistic reaction rates.

- December 8, 2016

Introduced the trim() option everywhere for characters so the length of
pathnames no longer needs to be recorded, a nasty F77 feature.

- December 15, 2016

Added p-wave radiative width and D1, on the advice of Stephane Goriely.

- March 12 2017

Renamed the files of the entire structure/ directory. Instead of using
e.g. z010.dat it is now called Ne.lev for the discrete levels (Ne for
the element, .lev for the extension) and similarly in all other
databases. The filenaming is now consistent all over the TALYS code
and its satellite codes.

- April 3, 2017

Improved the output of isomeric fission yield ratios, on the advice of
Satoshi Chiba.

- May 3, 2017

Repaired a bug found by Ann-Cecilie Larsen and solved by Stephan Goriely
on equidistant energy grid in astrophysical calculations in partfunc.f

- May 5, 2017

Must repair bug found by Dmitry Smychko: adopt ENDSF suggested spin in
all cases.
Must repair bug found by Steven Gardiner: K39 has even spin levels,
maybe more general problem

- September 22, 2017

Separated quasi-deuteron calculation in separate subroutine

- November 11, 2017

Replaced PREPRO subroutines by 2017 versions.

G. Log file of changes since TALYS-1.9

```
Development of TALYS since release of TALYS-1.9

- December 21, 2017

********** Release of TALYS-1.9 **********

- January 30, 2018

Imported new PSF D1M + QRPA M1 data tables in structure directory.
Adopted two keywords, 'upbend' to enable or disable the low-energy upbend
formula of the PSF (default n) by Stephane Goriely. Also introduced the
'upbendf' parameter for this formula.
The upbendc, upbende and upbendf parameters now have a default,
which are likely to change in the near future.

- February 2, 2018

Removed a few redundant quantities from massdis.f and ffevap.f,
like pre-neutron nubar (which is nonsense)

- February 13, 2018

Corrected an error found by Stephane Goriely. Due to a trim() error in
densitytable.f tables for elements with only one symbol, like U, are not
read for ldmodel 4, 5 and 6.
Corrected that. I expect more comments about this one!
```

- March 14, 2018

Solved a few errors in medical isotope production, found by Jiri Ulrich.
The Tcool keyword was not working properly. Solved that in input5.f
Also some suggestions on time steps and the use of natural targets
were adopted.

- April 13, 2018

Error found by Dimitri Rochman, the combination expmass n,
massmodel 0 did not work. Solved in masses.f

- July 6, 2018

Expanded the output for decay from each continuum and discrete bin.
If outpopulation y, which is automatically enabled when outbasic y, then
an extra keyword can be given 'outdecay y', which will output the
precise Ex,J,pi dependent decay from each mother state in the CN decay.
This was added on the advice of Stephane Goriely to better study
reactions used by the Oslo group for the determination of PSF's.

- March 12, 2019

Added SMLO PSF tables from Stephane Goriely and Vladimir Plujko.
Also changed some of the default parameter for upbend formula for PSF.
strength 9 now added for SMLO.

- March 15, 2019

Added the fission width average fission lifetime, and fission level
density to the specific output of the fission transmission coefficients.

- April 7, 2019

Corrected an error found by Stephane Goriely on the calculation of the
average emission energy.
The discrete levels were not properly taken into account.
This quantity was only printed in the basic output of TALYS (and not
used for anything). Now, however, when 'outspectra y', files like
Eaverage.n will be created containing the average emission energy
per particle.

- April 9, 2019

With 'filedensity y' TALYS now also prints the level density tables
exactly in the form as they are used as input from the nuclear structure

data tables, these files are called e.g. nld041093.tab.

- May 28, 2019

Solved an error in levels.f: if the isomer of a residual nucleus is
above the maximum level included it is brought down to that maximum
level. So far this was only implemented for the target nucleus,
i.e. inelastic scattering.

- June 9 2019

Added normalization of average number of neutrons to massdis.f

- June 23 2019

Solved a bug discovered by Rob Hoffman. In input5, for the gp parameter
(single particle state density for protons) gn was read instead of gp.
Since for fitting we often use gpadjust this bug got unnoticed for years!

- June 23 2019

Added a new keyword 'psfglobal' to use only global photon strength
functions and parameters. By default 'psfglobal n' meaning that the best
GDR parameters, tuned PSF tables etc are used.
This keyword was especially introduced for two tables for the SMLO model,
one optimized and one global, but is applicable in general.

- August 13 2019

Included fission partial damping model constructed by Guillaume Scamps
and Stephane Goriely. This should bring TALYS closer to the capabilities
of EMPIRE for fission prediction. For this, the keywords, fispartdamp,
bdamp and bdampadjust were added.

- December 16 2019

Included parameters wtable and wtableadjust to change the width of a
tabulated PSF.

H. Log file of changes since TALYS-1.95

Development of TALYS since release of TALYS-1.95

- December 30, 2019

********** Release of TALYS-1.95 **********

- January 4, 2020

Added keyword 'soukho' to allow disabling of Soukhovitskii OMP for
actinides. Now parameters relative to KD03 can be given.

- January 16, 2020

Implemented Okumura model for fission yields and subsequent particle
evaporation for fission neutrons. Keyword fymodel has been extended
with option '4' for this model. Also added fymodel 5 which allows to
enter FF population tables.

- February 5, 2020

Introduced keyword 'yieldfile' to allow input of fission fragment
yields per pair, and their respective TXE and TKE values. This serves
as input for the Okumura model to evaporate each excited fission
fragment individually.

- March 2, 2020

Improved the calculation for a populated nucleus, needed after tests
done with Toshihiko Kawano on the depletion of fission products. The
flux of the populated nucleus is now better mapped onto the decay
scheme. Subroutine excitation.f was changed for that. The number of
energy bins can now also be equal to 1, for one starting excited level.

- March 23, 2020

Changed the default to 'equidistant y' after binning problems observed
by Sandor Sudar at high energy proton reactions.

- March 27, 2020

Added keyword gadjust as 1-component version of gnadjust and gpadjust.
This can be used for consistent variation of gn and gp for the
2-component exciton model.

- May 24, 2020

Removed a bug in the reading of an external, tabulated optical model
file. The first line of that file should contain Z, A, number of lines
and (optional) Fermi energy. This did not hurt the sample case for
n + U238 which is why the error got unnoticed for so long.

- May 27, 2020

TALYS can now read RIPL OMP, which is for sure necessary for actinides
and probably helpful for other cases as well. The initial version has
been tested for important actinides.

- May 31, 2020

Extended isospin forbidden transitions for multiple emission using
'fisom' keyword on advice of Stephane Goriely.

- Aug 17, 2020

Reprogrammed the isospin transition cases by making a new subroutine
isotrans.f.

- Sep 27, 2020

Improved the output of level densities after suggestions by
Khashane Malatji: the total parity-dependent level densities were not
properly tabulated. Made a new subroutine densitytotP for this, which
only affects the level density output, not the reaction calculations.

- Oct 19, 2020

On the advice of Jean-Francois Lemaire, revised various subroutines for
the FY and PFNS calculations, There was an error in the CM to LAB
integration boundaries and the FY and spin distribution normalizations.

- Dec 22, 2020

Added a 'block' keyword to write large amount of output data in output
blocks instead of individual files. With 'block n' the old situation is
retained: All spectra, angular distributions etc are stored in an
individual file per incident energy. We use 'block y' now to create
ENDF files, as it does not produce a huge amount of files.

- Feb 1, 2021

Corrected more coding on FY, PFNS and nubar etc. in massdis.f and
ffevap.f on the advice of Jean-Francois Lemaire.

- Feb 15, 2021

Include Marilena Avrigeanu's deuteron break-up model. For this,
the structure/ database was extended with the TENDL neutron and
protons cross sections.

- March 1, 2021

Corrected pre-neutron FY table on advice of Ali Al-Adili. Also added
average gamma and neutron energy per FF in the output.

- April 26, 2021

Changed the default for subactinide fission. Now fismodel 3 is used for
charged-particle induced reactions on all targets and for neutrons
on subactinides, which gives a dramatic improvement of the fission
cross sections.

- April 28, 2021

Added the option to read in fission fragment distributions from the
structure database, after the provision of FF distributions from
Ali Al-Adili and Fredrik Nordstroem.
Added the keyword 'ffmodel' to chose between models of FF distribution.

- June 6, 2021

Updated the resonance parameter files in talys/structure/resfiles.
Now resonance parameters can be read for tendl.2019 (default),
endfb8.0, jeff3.3, cendl3.2 and jendl4.0.

- July 13, 2021

Changed default parameters for break-up reactions for (d,p) and
stripping reactions for (alpha,n) to improve the global quality
of the cross section fits. This extra adjustment is done at the top of
breakup.f.

- August 23, 2021

Added a subroutine for Wahl systematics for nubar, which is now
written to output by TALYS also without an explicit FF to FY
calculation. Separated some of the calculation of nubar for total
and nu(A) for that in nudisout.f and nubarout.f. Made keywords
Cnubar1 and Cnubar2 to alter systematic value for nubar.

- September 1, 2021

Enabled the reading in of so called wtable parameters to change the
width of tabulated photon-strength functions.

- September 6, 2021

Changed the default in TALYS for photon strength functions after
testing with Stephane Goriely. The default is now strength 9 (SMLO),
strengthm1 3 with 'upbend y'. This is applied for all incident
particles, improving the default prediction for (n,g), (g,n), (p,g),
(a,g) considerably. Automatic wtable parameters are read in for
adjustment to capture cross sections in the fast neutron range.

- September 9, 2021

Added new keyword 'ldmodelCN' to assign a particular level density
model to the compound nucleus only. So e.g. ldmodelCN 1 and ldmodel 2,
simultaneously in the input file will use CTM for the CN and BFM for
all other nuclides in the calculation. The same can be achieved by e.g.
ldmodel 1 26 57   and ldmodel 2, but the new option avoids having to
specify the Z,A of the compound nucleus.

- September 28, 2021

Added keywords 'ngfit', 'nnfit', 'nafit', by default disabled,

to use fitted nuclear model parameters. If 'best y' then
'ngfit y' by default.

- November 4, 2021

Added Iwamoto model for PFNS, which is a variant of the Los Alamos
model. Added the keyword 'pfnsmodel' to enable it instead of PFNS coming
from explicit FF evaporation. Also added the keywords 'Tmadjust' and
'Fsadjust' to adjust the temperature and number of scission neutrons
in this model.

- December 29, 2021

Added keywords vfiscoradjust and betafiscoradjust to enable changes
relative to vfiscor and betafiscor.

I. Log file of changes since TALYS-1.96

```
Development of TALYS since release of TALYS-1.96

- December 30, 2021

********** Release of TALYS-1.96 **********

- January 6, 2022

Solved a few out-of-bound cases for exotic input files in wkb.f

- January 16, 2022

Corrected an 'open' error for DDX files in ddxout.f.
Silently uploaded a revised TALYS-1.96.

- February 14, 2022

Removed the extra A-dependent break-up adjustment for (d,p)
reactions due to bad results in TENDL-2021 for (d,n)

- February 15, 2022

Added keyword 'nffit' to get automatically good neutron-induced
fission cross sections

- February 20, 2022
```

Prevented input of excited level 'Ltarget' in case of natural targets

- February 21, 2022

Corrected a bug in natural.f: the natural files for total cross
sections were not produced from the isotopic ones.

- March 15, 2022

Introduced keyword 'Risomer' to manually change branching ratios for
isomeric production. Changed levels.f for this.

- March 20, 2022

Write more output to separate PSF files, including the Gamma_gamma

- March 27, 2022

Changed the default of the 'rotational' keyword. Now, all inverse
reactions are done for a spherical OMP. In the past, when a
coupled-channel OMP was used for a deformed nuclide, the same was done
for the inverse channels, needed for Hauser-Feshbach. Apart from a waste
of computer time, we also think this is physically unjustified.

- March 28, 2022

Solved an initialization problem in basicinitial.f for lmax variable.

- April 3, 2022

Added Z, A indices to Ufermi, Cfermi
This means these keywords are not backward compatible since they
could only get global values for all nuclides.
Also, Cfermibf and Ufermibf were dropped since we now simply add the
fission barrier to the end of Cfermi and Ufermi.

- April 4, 2022

Removed the spline interpolation for Gamma_gamma by Kopecky. When an
experimental average radiative width is not available, it is more
reliable to use the calculated values from the PSF + LD.
I also replaced the 'gnorm' keyword. It is now equal to 'y' or 'n',
and enabling means that the PSF and thus gamma-ray transmission
coefficient is normalized to Gamma_gamma. Numerical adjustment to
the PSF can be done with (preferably) wtable, etable or ftable.
This means gnorm is not backward compatible (as it used to be equal

to a value for normalization). Normalization to Gamma_gamma with
'gnorm y' is now done in radwidththeory.f. It can
still be done with 'gamgamadjust'.

- April 7, 2022

Solved a bug for reading experimental MACS in astroout.f

- April 9, 2022

Added the possibility to have particle decay from a discrete level.
For some strange reason, this was never enabled in TALYS: discrete
levels could only decay by gamma's. Now, if the energy of the discrete
level is above the minimum separation energy (often neutron, proton of
alpha) the Hauser-Feshbach loop is invoked. Used the Smin variable in
multiple.f for this.

- April 15, 2022

Changed the storage of 'best' fit parameters. For every model
combination, the best model parameters are now in
talys/structure/best/fits.

- May 5, 2022

Imposed a default for M! PSF on the basis of the E1 PSF. If strength 8
(QRPA PSF) then automatically strengthM1 8 (QRPA). If strength 9 or
any other value than strengthM1 3

- May 13, 2022

Solved a bug found by Marc Dupuis, RIPL OMP's were not used when
explicitly asked for in the input. Put flagriplomp=.true. in
input, when a RIPL OMP is requested.

- June 11, 2022

Activated ctableadjust and ptableadjust in densitypar.f.
They were inactive. Added keyword ftableadjust.

- June 19, 2022

Solved a problem found by Ross Allen. For economical Hauser-Feshbach
calculations, if there is an isomeric level higher than the maximum
number of included discrete states, the level number is renumbered to
that maximum in the HF calculations. However, it is better to use the

original level of the isomeric state in the output and filename
extension.

- June 26, 2022

Assigned wtable values for projectile 0 or gamma-induced reactions
equal to those of neutron-induced reactions. This ensures that the
same PSF are used in both cases. Also removed k0.gt.0 in fstrength.f
as restriction for calculating the gamma energy for PSF.
Now the PSF are equal for photon induced and neutron induced
reactions when the same parameters are used.

- July 6, 2022

Corrected the assignment of spin distribution for fission fragment
calculations. The adjustable parameters Rspincutff is now only used for
the spin population of the initial FF distribution, while Rspincut is
used, as usual, for the spin distribution of the level density.

- August 2, 2022

Corrected a term for the Maxwell ratio calculation for PFNS. The
exponent of the Maxwell should be -E/(2/3*Eav) instead of -E/Eav.

- August 6, 2022

Changed the default deuteron OMP to that of Han et al, deuteronomp 4.
This was already used for all TENDL etc calculations but not yet
set as the default in TALYS.

- September 1, 2022

Reinstalled the maximum number of included levels for each nuclide to
the value of the level density matching table, as it should be

- September 24, 2022

Added a keyword WFCfactor to have several options for systematics of the
number of degrees of freedom for width fluctuation corrections.
Now, WFCfactor 1 (the default) is the original Moldauer prescription,
WFCfactor 2 is that of Ernebjerg and Herman and WFCfactor 3 that of
Kawano. WFCfactor 1 and 2 apply to both Moldauer (widthmode 1) and HRTW
(widthmode 2) models.

- September 30, 2022

Introduced keyword flagequispec to use equidistant bins for emission spectra. This may be helpful for fission yield calculations.

- October 21, 2022

Added more fitting keywords: fit (to set the global capability to use fitted parameters), ngfit, nafit, nnfit, pnfit, gnfit, dnfit, anfit.

- October 26, 2022

Applied keyword s2adjust now also to tabulated level densities to adjust the spin distribution

- November 6, 2022

Replaced old FRDM mass model from RIPL, FRDM1998, by FRDM2012

- November 21, 2022

Solved a normalization error found by Marc Dupuis: the total continuum inelastic cross section was wrong in preeqtotal.f leading to a too high (n,gamma n) cross section. The error emerged with 'preeqspin y'.

- December 6, 2022

Added total ground state and isomeric file for natural element reactions. Naohiko Otsuka discovered these were missing.

- December 7, 2022

Added pre-equilibrium spin distribution model 'preeqspin 4' from Marc Dupuis inferred from JLM/QRPA calculations. Also added keyword 'Rspincutpreeq' to adjust pre-equilibrium spin cutoff parameter.

- December 14, 2022

Changed first coupled level in structure/deformation/Os.lev for Os187 from 1 to 2. Also changed number of coupled levels for Ag109.

- December 18, 2022

Enforced 'spherical y' if 'jlmomp y', after problem found by Stephane Goriely

- December 18, 2022

Added 'strength 10' model in gammapar.f.

- February 10, 2023

Introduced keyword densfile to read in local level density file

- March 10, 2023

Changed default for fission into 'class2 n' and 'hbstate n'
since all automated fitting is based on that.

- March 17, 2023

Updated the integral activation calculations by including the cleaned
up data base for neutron spectra and integral activation cross sections
from the CONDERC webpage. This is active with 'integral y'

- March 20, 2023

Added a subroutine 'arraysize'. If 'check y' then TALYS will print the
size of some of the largest arrays used in TALYS. This can be consulted
in case of optimization of the code.

- March 21, 2023

Solved an error in medical isotope production found by Asif Amin.
Made TALYS more equal to the subroutines used in the ISOTOPIA code.
There was an error in time conversion from seconds to hours in
prodyield.f.

- April 16, 2023

Enabled flagrpevap for evaporation of residual products at high
incident energies.

- June 1, 2023

Introduced the YANDF format in the entire source code
(TALYS-2 version only)

- June 3, 2023

Introduced keyword outall to have all output of separate files
concatenated in main output.

- June 6, 2023

Introduced keywords source, user and format to specify origin of
the calculation (TALYS-2 only)

- June 12, 2023

Changed total.tot into all.tot.
Changed totalxs.tot into total.tot.
These are more logical filenames.

-June 21, 2023

Yi Xu found some bugs in racap.f and racapcalc.f. Solved.

-June 28, 2023

Introduced keywords gamgamfit and macsfit to automatically fit
Gamma_gamma and MACS.

- July 9, 2023

Changed WFC default for incident charged particles to HRTW, after
Vivian Dimitriou found discontinuities at separation energy
for Moldauer model.

- July 14, 2023

Introduced keyword Cbarrier to multiply the fission barriers given
by Sierks prescription.

- August 15, 2023

In densitypar, took Nlast as the minimum of Ntop and nlev, after an
error discovered by Stephane Goriely.

- August 17, 2023

Changed the MACS database which is now a combination of ASTRAL
(first priority) and KADONIS.

- September 5, 2023

Added Langevin-4D option for excited fission fragments. This is
'ffmodel 4'.

- October 5, 2023

Corrected a bug found by Pierre Chau in densprepare.f which ensures
that transmission coefficients are interpolated at all energies
and lmaxhf is not 0.

- October 29, 2023

For incident photons and neutrons and A > 215, i.e. actinides,
changed the default fission model into fismodel 5 and default
level density model into ldmodel 5.

- November 26, 2023

Replaced PREPRO subroutines by the 2023 versions.

- December 2, 2023

Added loop for second peak in Pygmy resonance in fstrength.f90,
omission found by Vetle Ingeberg.

- December 7, 2023

Added new radial matter densities for JLM calculations from Univ.
Brussels, Goriely and Ryssen. Also renamed the directories in
talys/structure/optical/jlm/ which are now called bskg3 and d1m
respectively.

- December 11, 2023

OMP parameters rwsoadjust and awsoadjust were missing in the
parameters.dat output files. Problem found by Aaron Stott.

J. Derivation of isotope production equations

Here we derive the solutions (19.10) of the differential equations (19.6)-(19.9). Eq. (19.10) has been implemented in ISOTOPIA.

For the target nuclide we have

$$\frac{dN_T(t)}{dt} = -R_T N_T(t).$$ (J.1)

This is easily integrated to give

$$N_T(t) = N_T(0)\,e^{-R_T t}.$$ (J.2)

For every parent nuclide we have

$$\frac{dN_p(t)}{dt} = R_{T\to p} N_T(t) - \lambda_p N_p(t).$$ (J.3)

Multiplying both sides with $e^{\lambda_p t}$ gives

$$e^{\lambda_p t}\frac{dN_p(t)}{dt} = e^{\lambda_p t}\left[R_{T\to p} N_T(t) - \lambda_p N_p(t)\right],$$ (J.4)

or,

$$e^{\lambda_p t}\frac{dN_p(t)}{dt} + e^{\lambda_p t}\lambda_p N_p(t) = e^{\lambda_p t} R_{T\to p} N_T(t),$$ (J.5)

or,

$$\frac{d[e^{\lambda_p t} N_p(t)]}{dt} = e^{\lambda_p t} R_{T\to p} N_T(t).$$ (J.6)

Integrating this, after insertion of Eq. (J.2), gives

$$
\begin{aligned}
e^{\lambda_p t} N_p(t) &= N_T(0)R_{T\to p}\int dt e^{(\lambda_p - R_T)t} \\
&= \frac{N_T(0)R_{T\to p}}{\lambda_p - R_T}e^{(\lambda_p - R_T)t} + C,
\end{aligned}
\tag{J.7}
$$

or,

$$
N_p(t) = \frac{N_T(0)R_{T\to p}}{\lambda_p - R_T}e^{-R_T t} + Ce^{-\lambda_p t}.
\tag{J.8}
$$

Inserting the initial condition $N_p(t=0) = 0$ gives

$$
0 = \frac{N_T(0)R_{T\to p}}{\lambda_p - R_T} + C,
\tag{J.9}
$$

giving the solution for the parent nuclide,

$$
N_p(t) = \frac{N_T(0)R_{T\to p}}{\lambda_p - R_T}\left[e^{-R_T t} - e^{-\lambda_p t}\right].
\tag{J.10}
$$

For every isotope i, directly produced by a nuclear reaction on the target isotope or from decay of the parent nuclide, we have

$$
\frac{dN_i(t)}{dt} = \lambda_{p\to i}N_p(t) + R_{T\to i}N_T(t) - \lambda_i N_i(t).
\tag{J.11}
$$

Multiplying both sides with $e^{\lambda_i t}$ gives analogous to Eqs. (J.4)-(J.6),

$$
\frac{d[e^{\lambda_i t}N_i(t)]}{dt} = e^{\lambda_i t}\left[\lambda_{p\to i}N_p(t) + R_{T\to i}N_T(t)\right],
\tag{J.12}
$$

or, after insertion of the solutions for N_T, Eq. (J.2), and N_p, Eq. (J.10),

$$
\frac{d[e^{\lambda_i t}N_i(t)]}{dt} = e^{\lambda_i t}\left[\lambda_{p\to i}\frac{N_T(0)R_{T\to p}}{\lambda_p - R_T}(e^{-R_T t} - e^{-\lambda_p t}) + N_T(0)R_{T\to i}e^{-R_T t}.\right]
\tag{J.13}
$$

Integrating this gives

$$
\begin{aligned}
e^{\lambda_i t}N_i(t) &= \frac{N_T(0)\lambda_{p\to i}R_{T\to p}}{\lambda_p - R_T}\left[\int dt e^{(\lambda_i - R_T)t} + \int dt e^{(\lambda_i - \lambda_p)t}\right] \\
&+ N_T(0)R_{T\to i}\int dt e^{(\lambda_i - R_T)t} + C,
\end{aligned}
\tag{J.14}
$$

or,

$$
\begin{aligned}
N_i(t) &= \frac{N_T(0)\lambda_{p\to i}R_{T\to p}}{\lambda_p - R_T}\left[\frac{e^{-R_T t}}{\lambda_i - R_T} + \frac{e^{-\lambda_p)t}}{\lambda_i - \lambda_p}\right] \\
&+ \frac{N_T(0)R_{T\to i}}{\lambda_i - R_T}e^{-R_T t} + Ce^{-\lambda_i t}.
\end{aligned}
\tag{J.15}
$$

Inserting the initial condition $N_i(t=0) = 0$ gives

$$
0 = \frac{N_T(0)\lambda_{p\to i}R_{T\to p}}{\lambda_p - R_T}\left[\frac{1}{\lambda_p - R_T} + \frac{1}{\lambda_i - \lambda_p}\right] + \frac{N_T(0)R_{T\to i}}{\lambda_i - R_T} + C,
\tag{J.16}
$$

so we finally obtain

$$
N_i(t) = N_T(0)\frac{R_{T\to i}}{\lambda_i - R_T}\left[e^{-R_T t} - e^{-\lambda_i t}\right] + N_T(0)\frac{\lambda_{p\to i}R_{T\to p}}{\lambda_p - R_T}\left[\frac{e^{-R_T t} - e^{-\lambda_i t}}{\lambda_i - R_T} - \frac{e^{-\lambda_p t} - e^{-\lambda_i t}}{\lambda_i - \lambda_p}\right].
\tag{J.17}
$$

The three solutions of interest are thus given by Eqs. (J.2), (J.10), and (J.17).